15

USAAVRADCOM-TR-80-D-11

AD A085290

LEVEL II

(12)

HEAVY LIFT HELICOPTER -- PROTOTYPE TECHNICAL SUMMARY

Boeing Vertol Company
P.O. Box 16858
Philadelphia, Pennsylvania 19142

April 1980

Final Report for Period January 1973 - August 1975

Approved for public release;
distribution unlimited.

Prepared for

APPLIED TECHNOLOGY LABORATORY
U.S. ARMY RESEARCH AND TECHNOLOGY LABORATORIES (AVRADCOM)
Fort Eustis, Va. 23604

APPLIED TECHNOLOGY LABORATORY POSITION STATEMENT

Due to the termination of the HLH program, reports summarizing the strides made in many of the supporting technology programs were not published under contract. In order to make as much of this information available as possible, selected draft reports prepared under contract prior to termination were edited, converted to the DOD format, and published by the Applied Technology Laboratory. This report, which is the final in this series, summarizes the status of each of the major HLH prototype system/subsystem areas when the program was terminated. The bibliography of this report will be useful in locating more detailed information pertaining to specific HLH technology areas.

UNCLASSIFIED

SECURITY CLASSIFICATION OF THIS PAGE (When Data Entered)

REPORT DOCUMENTATION PAGE

READ INSTRUCTIONS BEFORE COMPLETING FORM

1. REPORT NUMBER: 18 19 USAAVRADCOM TR-80-D-11
2. GOVT ACCESSION NO.: AD-A085 210
3. RECIPIENT'S CATALOG NUMBER
4. TITLE (and Subtitle): 6 HEAVY LIFT HELICOPTER - PROTOTYPE TECHNICAL SUMMARY
5. TYPE OF REPORT & PERIOD COVERED: 9 Final Rep[redacted]t, Jan [redacted]73 — Aug [redacted]75
6. PERFORMING ORG. REPORT NUMBER: 14 D301-10323-1
7. AUTHOR(s)
8. CONTRACT OR GRANT NUMBER(s): 15 DAAJ01-71-C-0840 (P6A)
9. PERFORMING ORGANIZATION NAME AND ADDRESS: Boeing Vertol Company, P. O. Box 16858, Philadelphia, Pennsylvania 19142 — 403682
10. PROGRAM ELEMENT, PROJECT, TASK AREA & WORK UNIT NUMBERS: 12 358
11. CONTROLLING OFFICE NAME AND ADDRESS: U. S. Army Aviation Research and Development Command, P. O. Box 209, St. Louis, Missouri 63166
12. REPORT DATE: 11 Apr[redacted]80
13. NUMBER OF PAGES: 356
14. MONITORING AGENCY NAME & ADDRESS (if different from Controlling Office): Applied Technology Laboratory, U. S. Army Research and Technology Laboratories (AVRADCOM), Fort Eustis, Virginia 23604
15. SECURITY CLASS. (of this report): Unclassified

15a. DECLASSIFICATION/DOWNGRADING SCHEDULE

16. DISTRIBUTION STATEMENT (of this Report)

Approved for public release; distribution unlimited.

17. DISTRIBUTION STATEMENT (of the abstract entered in Block 20, if different from Report)

18. SUPPLEMENTARY NOTES

19. KEY WORDS (Continue on reverse side if necessary and identify by block number)

HELICOPTERS	PROPULSION SYSTEMS	HYDRAULIC EQUIPMENT
CARGO HANDLING	ROTOR BLADES (ROTARY WINGS)	TRANSMISSIONS
AIRFRAMES	CONTROL SYSTEMS	HUBS
HONEYCOMB STRUCTURES	FLIGHT CONTROL SYSTEMS	LOGISTICS PLANNING
LANDING GEAR	ELECTRICAL EQUIPMENT	FLIGHT CREWS

20. ABSTRACT (Continue on reverse side if necessary and identify by block number)

This report summarizes the Heavy Lift Helicopter (HLH) Prototype program, ~~conducted from 1973 through 1975.~~ The program was designed to demonstrate, in the actual flight environment, the capabilities of HLH components previously developed by Boeing Vertol under the Advanced Technology Components (ATC) effort. Design, fabrication, and assembly of one prototype HLH was 90 percent completed. An advanced aluminum honeycomb airframe, landing gear, and subsystems not included in the ATC effort were designed and fabricated. Limited laboratory tests

next page

DD FORM 1 JAN 73 1473 EDITION OF 1 NOV 65 IS OBSOLETE

UNCLASSIFIED

SECURITY CLASSIFICATION OF THIS PAGE (When Data Entered)

403682 slt

Item 19 (Cont)

PERFORMANCE (ENGINEERING)
EXPERIMENTAL DESIGN
WEIGHT
LABORATORY TESTING

Item 20 (Cont)

were conducted to assure airworthiness of the prototype aircraft. Mockups were constructed of the crew compartment and aft pylon area. A description of the aircraft, discussion of the tests conducted, and weight and performance data are presented. A list of references containing detailed documentation of the program is appended.

SUMMARY

The United States Army Aviation Systems Command awarded a contract to the Boeing Vertol Company in July 1971 to conduct an Advanced Technology Component (ATC) program for the Heavy Lift Helicopter (HLH). The ATC components consisted of the rotor blades, hub and upper control system, drive system, flight control system, and cargo handling system. In January 1973, when the ATC design was complete and development of components well under way, a contract was awarded to the Boeing Vertol Company for the construction of one prototype heavy lift helicopter. The purpose of the prototype was to demonstrate the advanced technology components in the actual flight environment.

The prototype program accomplishments included design and fabrication of an advanced aluminum honeycomb airframe, landing gear, and subsystems not included in the ATC effort. Limited laboratory tests were conducted to assure airworthiness of the prototype aircraft. Mockups were constructed of the crew compartment and aft pylon area.

Procurement, fabrication, and assembly of the prototype aircraft were 95 percent complete when the program was terminated on 1 August 1975. Approximately 3 months of final assembly and checkouts remained to be accomplished prior to rollout and installation of the aircraft in a tie-down rig for preflight testing.

TABLE OF CONTENTS

TABLE OF CONTENTS (Continued)

LIST OF ILLUSTRATIONS

LIST OF ILLUSTRATIONS (Continued)

LIST OF ILLUSTRATIONS (Continued)

LIST OF ILLUSTRATIONS (Continued)

LIST OF ILLUSTRATIONS (Continued)

LIST OF ILLUSTRATIONS (Continued)

LIST OF TABLES

LIST OF TABLES (Continued)

INTRODUCTION

The Heavy Lift Helicopter is designed to provide a vertical airlift capability for large and heavy loads, not available in the free world today. It permits deployment and retrieval of tactical and logistic loads rapidly and without dependence on roads, bridges, railways, docks, landing craft, runways, or other surface facilities.

The HLH is designed to transport a 22-1/2-ton external payload, with fuel for two 25-nautical-mile-radius sorties, on a sea level 95°F day. A 35-ton payload can be transported for shorter distances at the maximum alternate gross weight of 148,000 pounds.

Following the design and development of critical advanced technology components (blade, hub, upper controls, drive system, flight control system, cargo handling system), a one-aircraft prototype program was authorized by the U.S. Army Aviation Systems Command with the purpose of demonstrating the advanced components in a flight environment.

The aircraft is a tandem-rotor shaft-driven helicopter powered by three Detroit Diesel Allison XT701-AD-700 gas turbine powerplants rated at 8000 hp each. The aircraft design gross weight is 118,000 pounds, with a maximum alternate gross weight of 148,000 pounds. Diameter of each four-bladed rotor is 92 feet and the airframe length is 89 feet, 3 inches. The crew compartment accommodates a pilot, copilot, flight engineer, and aft-facing load controlling crewman. Aft of the crew compartment is a combination troop/light cargo compartment with accommodations for a crew chief and 12 troops. The center fuselage contains two longitudinally disposed cargo handling hoists, each with 100 feet of cable. The aft fuselage and pylon area contain the combining transmission, aft transmission, and powerplants. Fuel is contained in the stub wings, which also support the main struts of the tricycle landing gear. The airframe is entirely constructed of bonded aluminum honeycomb panels in sizes up to 4 feet by 32 feet.

Rotor blades are constructed with a multiple loadpath D-section spar with a Nomex honeycomb composite skin trailing edge fairing. Blade chord is 40 inches. Pendulum-type vibration absorbers are incorporated. Each blade is retained by an elastomeric bearing which permits pitch, flap, and lag motion of the blade. The titanium hub and upper controls are designed to be fail-safe, through use of multiple load paths,

low failure progression rates, and failure warning systems. Upper controls consist of rotating and stationary swashplates, pitch links, drive scissors, and centering mechanism, supported by three electrohydraulic actuators. Swashplates are hollow bonded aluminum assemblies with boron stiffening rings, approximately 5 feet in outside diameter. The drive system, rated at 18,133 hp at 157 rpm rotor speed, consists of a forward, aft, and combining transmission, together with interconnecting shafting. High contact ratio gears of Vasco X2 steel are utilized and housings are an improved magnesium alloy. Each transmission incorporates an integral lubrication system. A rotor brake is installed on the combining transmission.

The prototype aircraft incorporates a full fly-by-wire flight control system as successfully developed and flown on the Boeing Vertol 347 Chinook derivative helicopter. A multiple redundant primary system is used plus an automatic flight control system which provides improved flying qualities as well as automatic flight path control, hover hold, and provisions for a precision hover sensor and external load stabilization.

The cargo handling system is composed of two hoists, with a capacity of 28 tons at a load factor of 2.5g. Either single point or two point suspension of loads may be used. The winches are pneumatically powered and may be controlled independently or in unison. Design loads may be hoisted at a rate of 60 fpm.

Electrical power system includes two transmission-mounted 60 KVA oil-cooled main AC generators and independent flight control system generators. Transformer-rectifier units are provided for DC power. Pneumatic power is supplied by engine bleed or ground power units. Transmission-driven hydraulic pumps provide power for the swashplate actuators, nose gear steering, and main gear brakes. A separate electrically driven pump powers the rotor brake actuation system.

A minimum of communication-navigation equipment is installed in line with the austere approach to the prototype program.

The prototype aircraft was representative of a production aircraft dimensionally, aerodynamically, and structurally. In order to minimize prototype program costs, subsystem variations from the production requirements were incorporated where the program objectives would not be compromised. These included:

a. Conventially constructed landing gear rather than incorporation of advanced composite materials.

b. Omission of the static electricity dissipator, auxiliary power unit, precision hover sensor, automatic approach to hover mode and load stabilization sensor, visual augmentation system, tactical navigation and communication equipment, blade deicing, windshield and engine inlet anti-icing, armor, armament, IR suppression devices, engine air particle separator, automatic diagnostic systems, searchlight, formation lights, hoisting fittings, fuel dumping, onboard refueling system, auxiliary tanks, and ferry fuel tank.

c. Modification of the hydraulic, pneumatic, fuel and environmental control systems to use existing components and simplify due to subsystem deletions.

Weight empty of the prototype, based on actual weights of 70% of the aircraft, is estimated to be 66,263 pounds. Primary mission weight equals 127,535 pounds, including a 22-1/2-ton external payload, 1342 pounds fixed useful load, and 3554 pounds of instrumentation. Fuel weight for this mission is 11,376 pounds.

The prototype HLH can hover at sea level standard at 132,000 pounds gross weight and at 4000 feet 95°F at 125,200 pounds gross weight. Cruise speed with external payload is 134 knots at sea level 95°F conditions.

Because of the ATC program testing of major subsystems and maximum use of previously qualified items, minimum testing of components was required to assure airworthiness of the aircraft. Structural tests of honeycomb airframe panels, joints, and fasteners verified predicted structural properties, including peel and sonic fatigue. Blade, hub, and upper controls fatigue and endurance tests were conducted to substantiate configuration improvements that were incorporated on the prototype components. The nose and main landing gear struts were drop tested and met design requirements. Environmental, performance, and integration tests were conducted on the generators, environmental control unit, swashplate actuator, flight control system components, brakes, fuel cells, hydraulic modules, engine bleed air manifold, and engine control quadrant. The flight control system integration test stand was completed and testing was started. A load run stand for forward transmission endurance testing was designed and fabricated.

The design, test, and hardware status at program termination is shown in Table 1.

TABLE 1. HLH PROTOTYPE STATUS AT TERMINATION

COMPONENT	DESIGN STATUS	TEST STATUS COMPLETED	TEST STATUS REMAINING	HARDWARE AVAILABILITY
Rotor Blades	Complete	Whirl Test 125% Overspeed Fatigue Test Lightning Survivability	Static Proof Load Pendulum Absorber Fatigue Tests	2 Aft Blades + Subassemblies for 3 more aft and 5 Forward Available
Rotor Hub	Complete	Hub Fatigue Pitch Housing Fatigue	Loop Fatigue	Major Components Completed. Install & Bore Bushings & Assembly still to do.
Lag Dampers	Complete	Temperature, Vibration Limit Load	Endurance and Fatigue Tests	All Hardware Available at Vendor.
Upper Controls	Complete	250-Hr. Swashplate Endurance Drive Scissors Fatigue Pitch Link Fatigue	Swashplate Ring Fatigue Gimbal Fatigue	Major Components Completed. Install & Bore Bushings & Assembly still to do.
Swashplate Actuators	90% Complete	Fatigue Test - 1 Specimen	2nd Fatigue Specimen Temperature, Vibration, Humidity, Limit Load	Six Assembled/Acceptance Tested Parts for Six more Available.
DRIVE SYSTEM Aft Transmission	Complete	Static Strain Survey	Retest with Repatterened Gears 150-Hr. Endurance Test	First Assembly in House Second Available in 2 Months Major Items Available for 2 more
Combiner Transmission	Spiral Bevel Gear Redesign Required	Static Strain Survey	Retest with Redesigned Spiral Bevel Gears 150-Hr. Endurance Test	New Spiral Bevel Gears Required
Forward Transmission	Complete	- -	Static Strain Survey	First Assembly In House Second Available in 2 Months Major Items Available for 2 More
Shafting	Complete	Torsional Fatigue & Ultimate Tests	None	Major Items Available Except Steel Sync Shaft Adapters (in-process when program cancelled).

20

TABLE 1. (Continued)

		TEST STATUS		
COMPONENT	DESIGN STATUS	COMPLETED	REMAINING	HARDWARE AVAILABILITY
Airframe	90% Complete	Honeycomb Structural Tests	Rerun Cockpit Vibration Isolation Test with Redesigned Isolators. LCC vibration Isolation Test	Primary Structure Fabrication 99% Complete, Installation 97%Complete; Secondary Struct. Fabrication 75% Complete, Installation 50%Complete
Landing Gear	Complete	Drop Tests Damping Tests Steering T Wheels & Brakes	None	Main & Nose Gears Complete Main Gear Bottoming Springs, Aft, Side Brace, & Misc. Items still to do.
ENGINE INSTALLATION Mounts	Complete	- -	None (Flight Strain Survey Req'd	100% Available, 50% Installed
Air Inlet	Complete	Prel. Pressure Survey of #1 Engine Inlet	None (Flight Pressure Survey Req'd	100% Available, 50% Installed
Exhaust	Complete	- -	None	100% Available, 0% Installed
Fuel System	Complete	All Component Tests	None	95% Available, 50% Installed
Fire Detection	Complete	- -	None	100% Available, 0% Installed
Engines	Complete	30-Hr. & 60-Hr. Endurance Tests Complete PFRT (Equivalent) Status	Vibration Abusive Test Sand & Dust Ingestion	3 Engines Delivered to Boeing 1 Spare Engine Complete 2nd Spare Engine - Parts Available
FLIGHT CONTRO Direct Elec. Link.	Complete	Temperature, Humidity, Vibration, Dust & Shock on Control Unit Panels	System Integration Test (60%) Complete Salt & Fog	All Hardware Delivered
Automatic Flight Control System	Complete	Temperature, Humidity, & Vibration on Computer Input/Output Panels	Hardware Integration (80% Comp.) Software Validation (20%Comp.) Airspeed Transducer Temp.,Humidity & Vibration	First Set Delivered, Second Set Ready Airspeed Transducer Units in Acceptance at Program Termination

TABLE 1. (Continued)

COMPONENT	DESIGN STATUS	TEST STATUS: COMPLETED	TEST STATUS: REMAINING	HARDWARE AVAILABILITY
SUBSYSTEMS:				
Electrical	Wiring Release	Master Caution & Warning Fire Detection Generator Control Unit Current Transformer	Engine, Transmission, & Rotor Instruments (50% Complete) Generator (60% Complete) Flight Control Generator (70% Complete) Generation & Distribution Sys. Tests (50% Complete)	All Components/Parts Available Some Minor Mods Required.
Hydraulics	Complete	Temperature, Vibration & Endurance	Transmission Driven Pump	All Hardware Available
Avionics	Complete	- -	None	All Major Items G.F.E.
Pneumatics	Complete	- -	None	All Hardware Available
Environmental Control Unit	Complete	- -	None	One Unit Complete & Parts Available for 2nd Unit.
Engine Power Management	Complete	Safety-of-Flight System	None	One Engine Control Quadrant Complete. Second Available but Yet to Incorporate Mods.
Cockpit Controls Force/Feel	Complete	Temperature, Vibration & Proof Load	System Integration Test	All Hardware Delivered
Cargo Handling	Complete	All ATC Tests	Cable Cutter Test	All Components Available. Some minor component modifications based on ATC tests yet to be done.

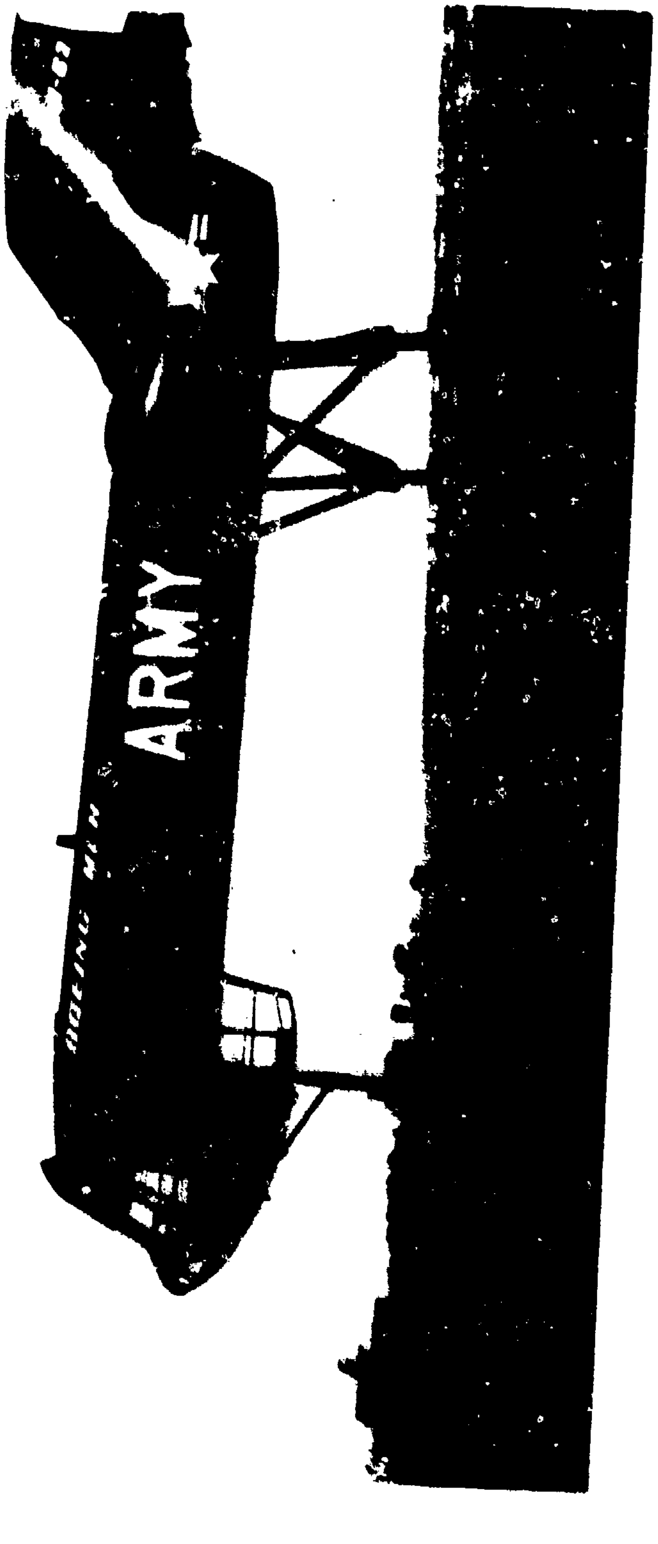

Figure 1. Prototype Heavy Lift Helicopter.

1.0 PROGRAM DESCRIPTION

1.1 SCOPE AND OBJECTIVES

The United States Army Aviation Systems Command awarded a contract to the Boeing Vertol Company in July of 1971 to develop Advanced Technology Components (ATC) for the Heavy Lift Helicopter (HLH). The ATC components consisted of the rotor blades, hub and upper control system, drive system, flight control system, and cargo handling system. In January 1973, when the ATC design was complete and fabrication of components well underway, a contract was awarded to the Boeing Vertol Company for the construction of one prototype Heavy Lift Helicopter designated the XCH-62 (Boeing Model 301).

The purpose of the prototype program was to:

a. Demonstrate vertical lift and air transport of 22.5-ton payload.

b. Demonstrate successful integration and performance of ATC program developed components in the actual flight environment.

c. Provide a first flight at the earliest possible date and at the least Government cost exposure.

d. Demonstrate resolution of major technical problems and cost uncertainties prior to decision to enter engineering development.

e. Demonstrate maintainability design improvements.

f. Provide user assessment of the HLH concept against the material need through actual flight demonstration.

The prototype program included design and fabrication of an advanced aluminum honeycomb airframe, landing gear, and subsystems not included in the ATC effort. Limited laboratory tests were conducted to assure airworthiness of the prototype aircraft. Mockups were constructed of the crew compartment and aft pylon area.

Procurement, fabrication, and assembly of the prototype aircraft was 95% complete when the program was terminated on 1 August 1975 by action of the United States Congress. Approximately three months of final assembly and checkouts remained to be accomplished prior to roll-out and installation of the aircraft in a tie-down rig for pre-flight testing.

1.2 MANAGEMENT

The HLH prototype program was managed by the United States Army Aviation SystemsCommand, St. Louis, Missouri, with technical support by the United States Army Aviation Materiel Research and Development Laboratories at Ft. Eustis, Virginia.

The program was conducted by the Boeing Vertol Company and associated subcontractors. The powerplant was developed and provided by the Detroit Diesel Allison Division of General Motors Corporation.

The Boeing Cost and Schedule Control System validated by the Government during the ATC phase of the program was utilized as the prime management system. The HLH Branch organization established for the ATC program conducted the prototype program.

Quarterly meetings were conducted to review technical, cost, and schedule status. These meetings were attended by all interested Government agencies. Systems Requirements Reviews, Specification Reviews, Preliminary Design Reviews, Critical Design Reviews, and a Crew Compartment Mockup Review were held as the design progressed. During the 2-1/2-year program, a total of 1649 Government representatives visited Boeing Vertol for HLH discussions.

1.3 MILESTONES AND SCHEDULES

Contract milestones were established as shown in Figure 1. This figure shows the original planned milestones plus the dates that each milestone was actually accomplished.

Figure 2 is the master phasing schedule for the program. This figure portrays the engineering, procurement, manufacturing, logistic, and test functions for each subsystem. Original plans are shown plus the actual accomplishment dates.

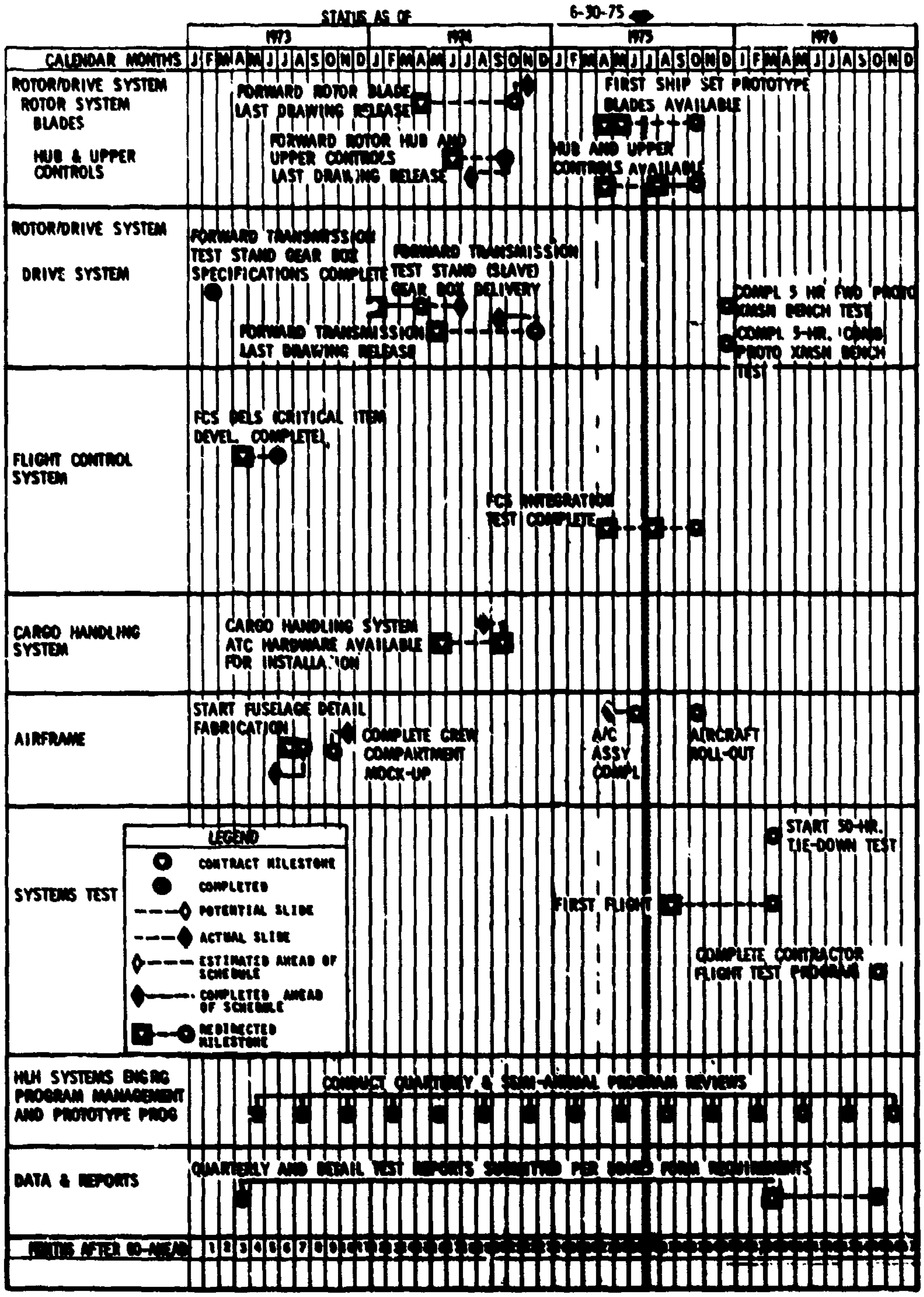

Figure 1. Contract milestones.

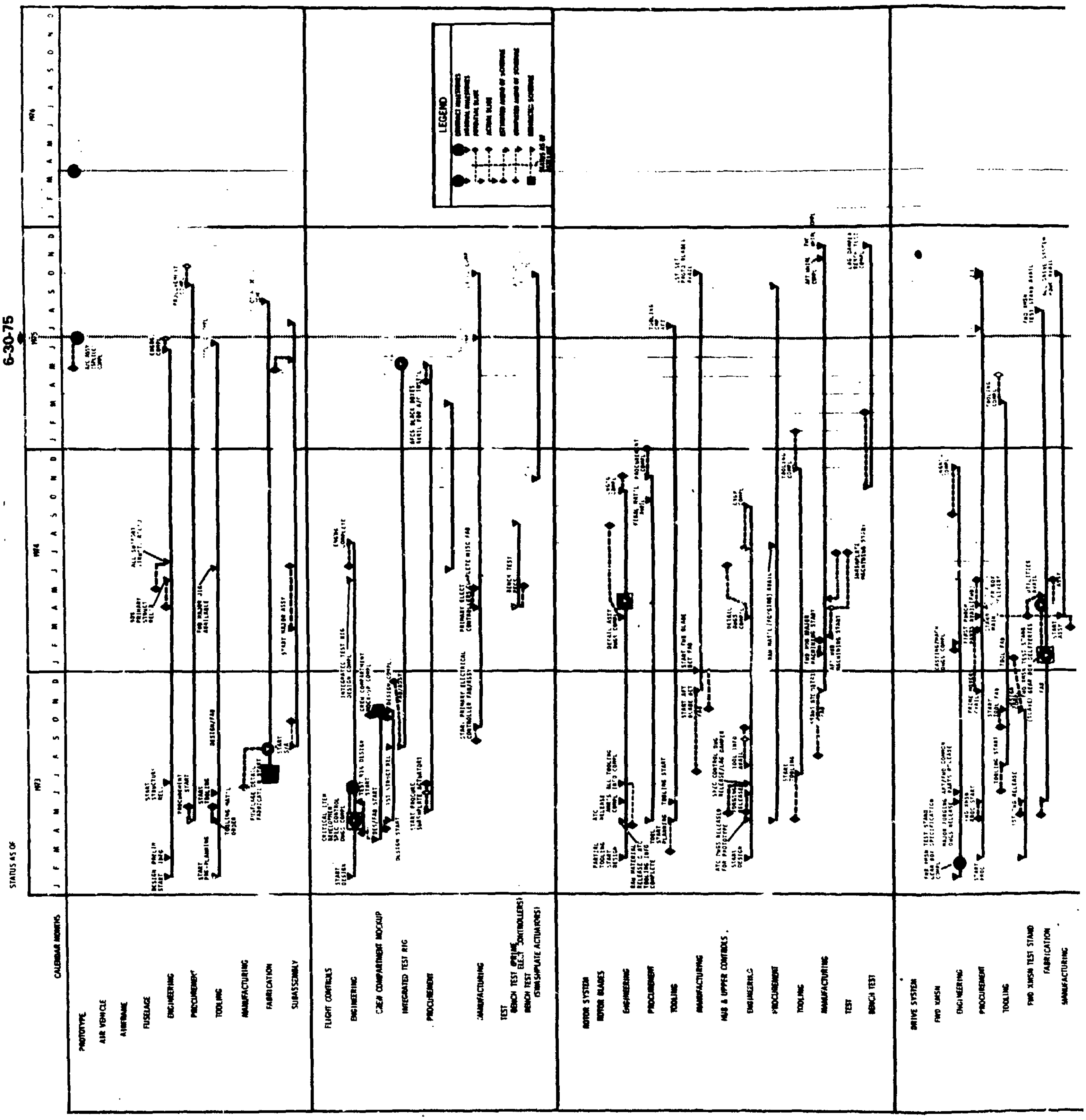

Figure 2. Master phasing schedule.

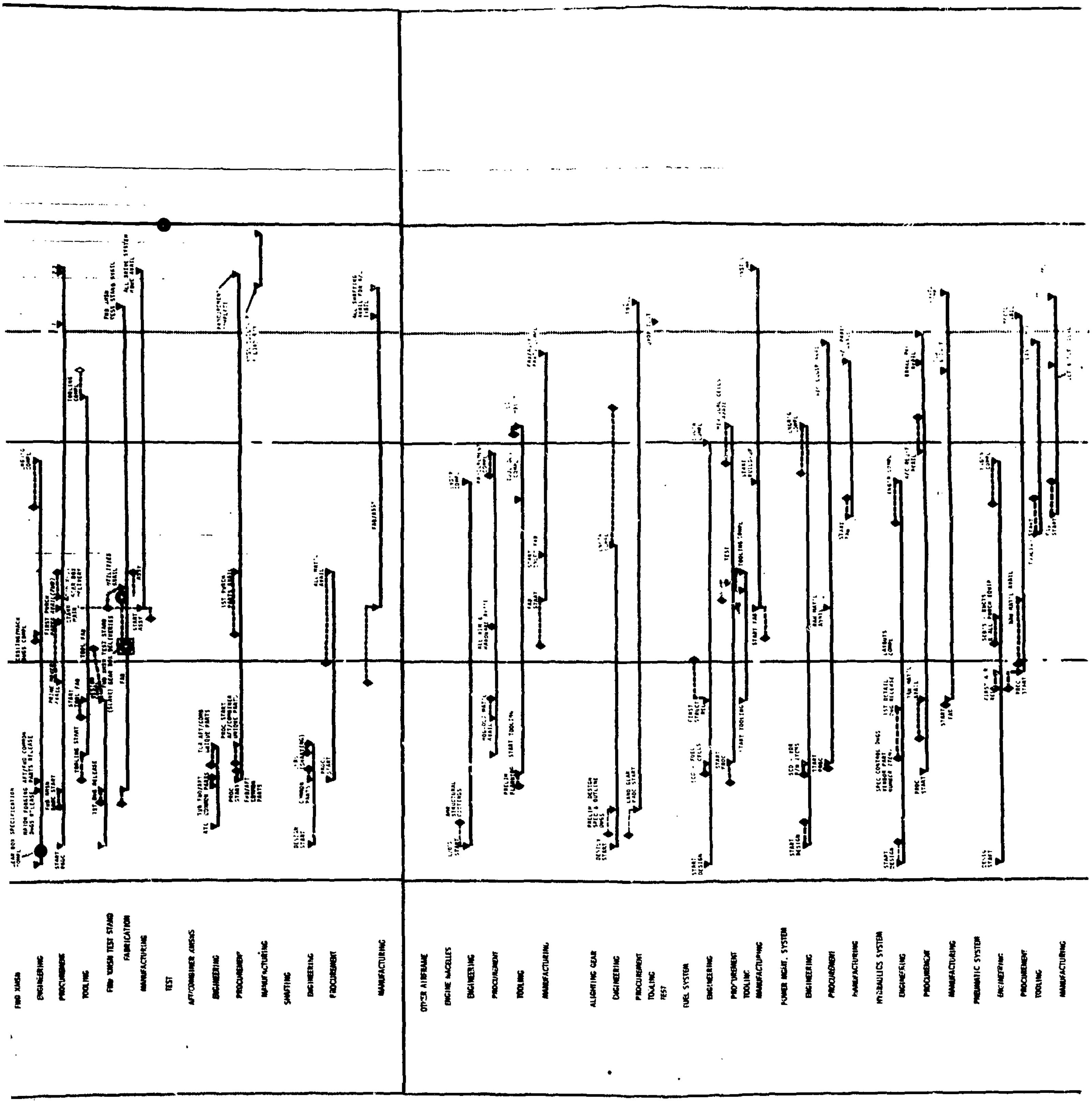
FWD XMSN
ENGINEERING
PROCUREMENT
TOOLING
FWD XMSN TEST STAND
FABRICATION
MANUFACTURING
TEST
AFT/COMBINER XMSNS
ENGINEERING
PROCUREMENT
MANUFACTURING
SHAFTING
ENGINEERING
PROCUREMENT
MANUFACTURING
OTHER AIRFRAME
ENGINE NACELLES
ENGINEERING
PROCUREMENT
TOOLING
MANUFACTURING
ALIGHTING GEAR
ENGINEERING
PROCUREMENT
TOOLING
TEST
FUEL SYSTEM
ENGINEERING
PROCUREMENT
TOOLING
MANUFACTURING
POWER MGMT. SYSTEM
ENGINEERING
PROCUREMENT
MANUFACTURING
HYDRAULICS SYSTEM
ENGINEERING
PROCUREMENT
MANUFACTURING
PNEUMATIC SYSTEM
ENGINEERING
PROCUREMENT
TOOLING
MANUFACTURING

2

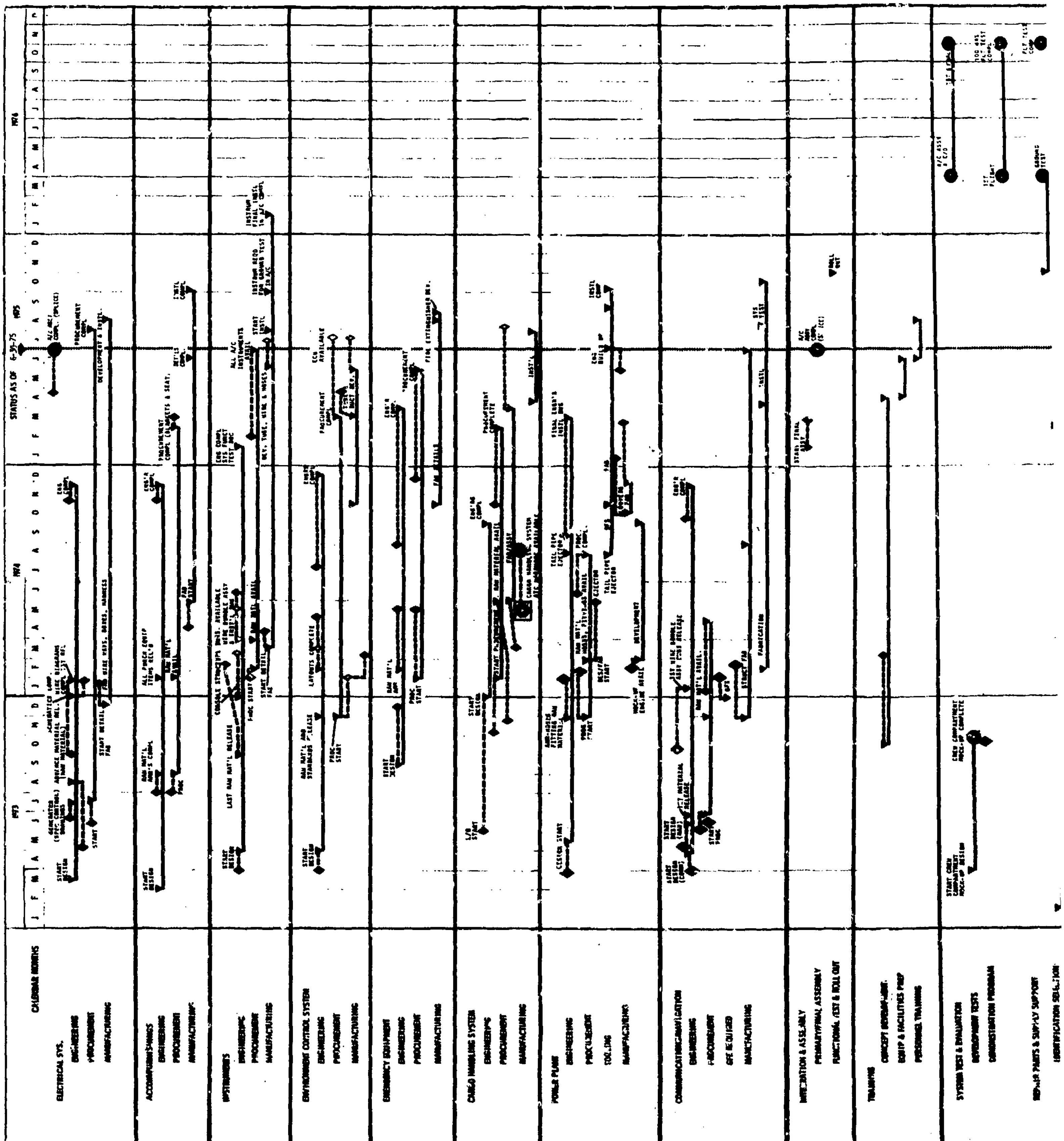

Figure 2. (Continued)

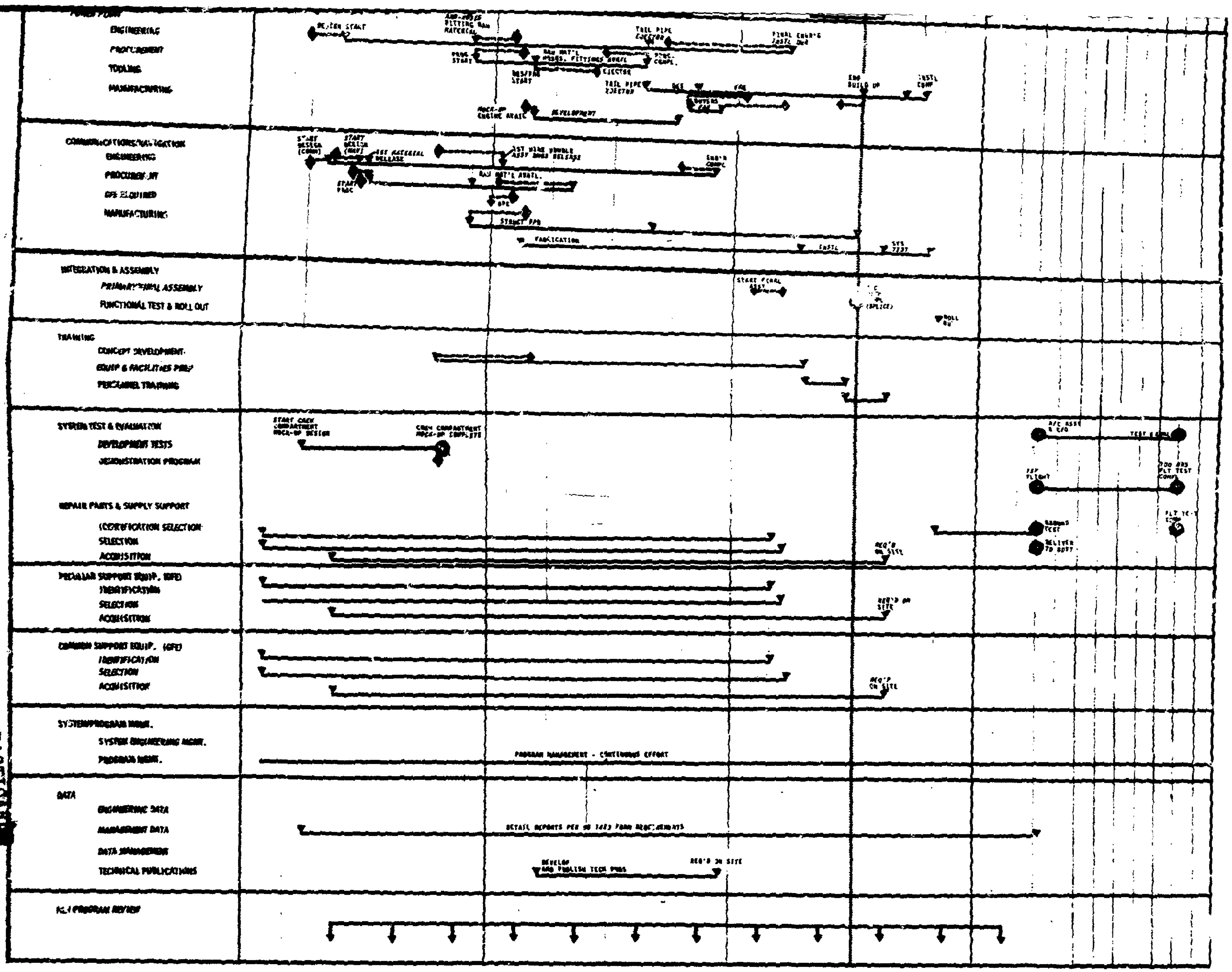
ENGINEERING
TOOLING
MANUFACTURING
INTEGRATION & ASSEMBLY
FUNCTIONAL TEST & ROLL OUT
TRAINING
CONCEPT DEVELOPMENT
EQUIP & FACILITIES PREP
PERSONNEL TRAINING
SYSTEM TEST & EVALUATION
DEVELOPMENT TESTS
DEMONSTRATION PROGRAM
REPAIR PARTS & SUPPLY SUPPORT
SELECTION
ACQUISITION
PECULIAR SUPPORT EQUIP. (GFE)
IDENTIFICATION
SELECTION
ACQUISITION
COMMON SUPPORT EQUIP. (GFE)
IDENTIFICATION
SELECTION
ACQUISITION
SYSTEM/PROGRAM MGMT.
SYSTEM ENGINEERING MGMT.
PROGRAM MGMT.
PROGRAM MANAGEMENT - CONTINUOUS EFFORT
DATA
ENGINEERING DATA
MANAGEMENT DATA
DATA MANAGEMENT
TECHNICAL PUBLICATIONS

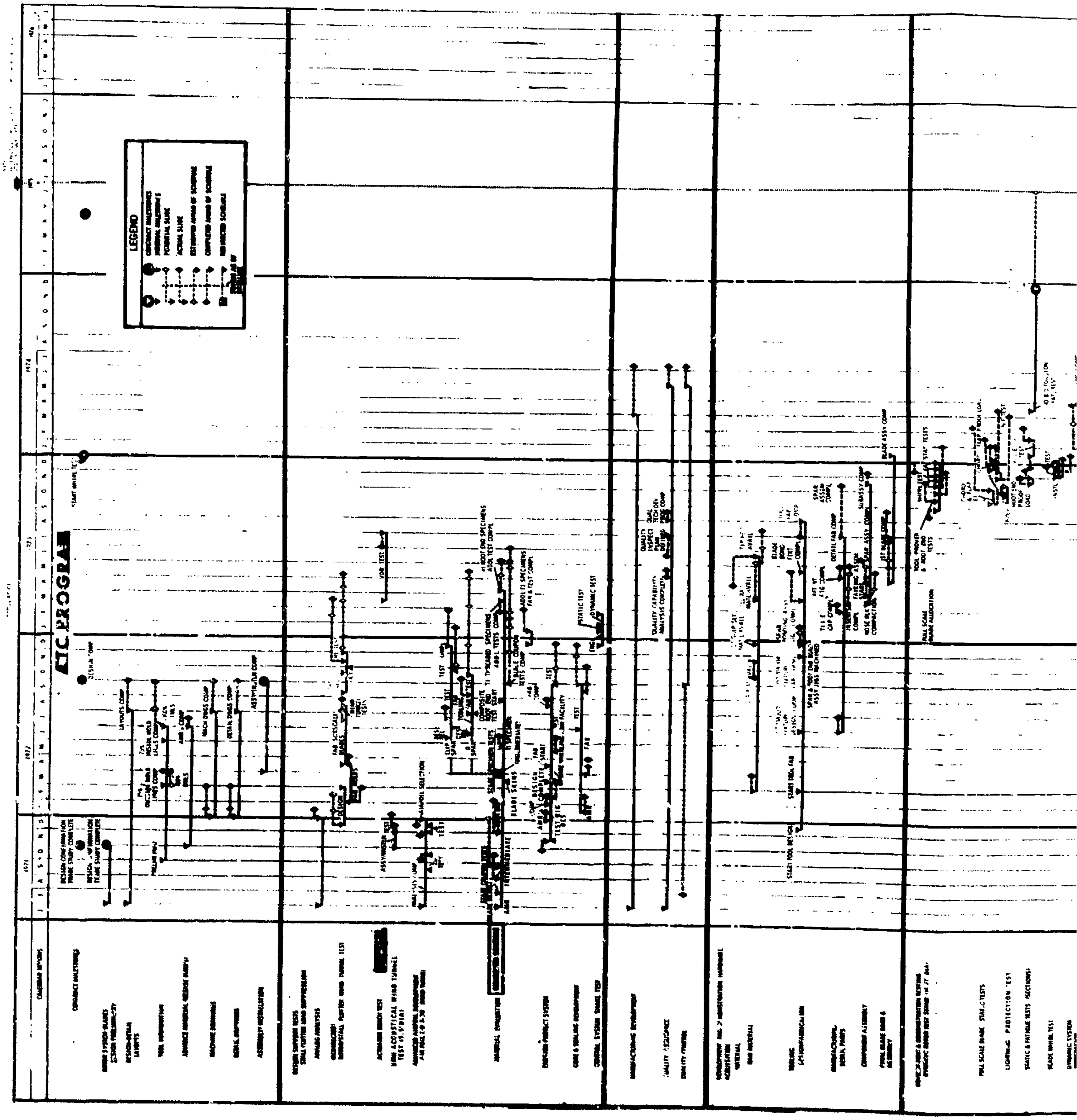

Figure 3. Rotor blade interface phasing.

THIS PAGE
FROM COPY

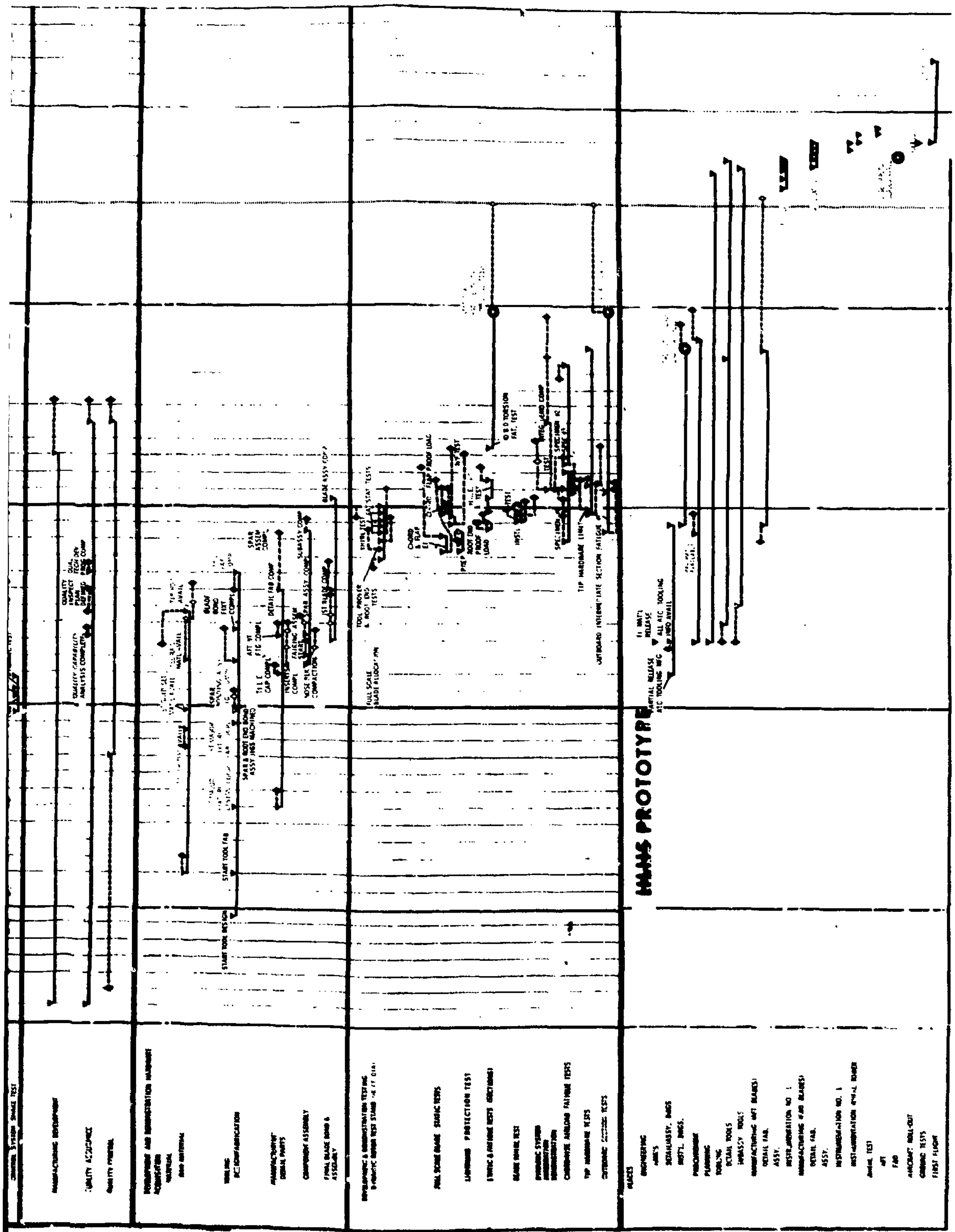

g.

2

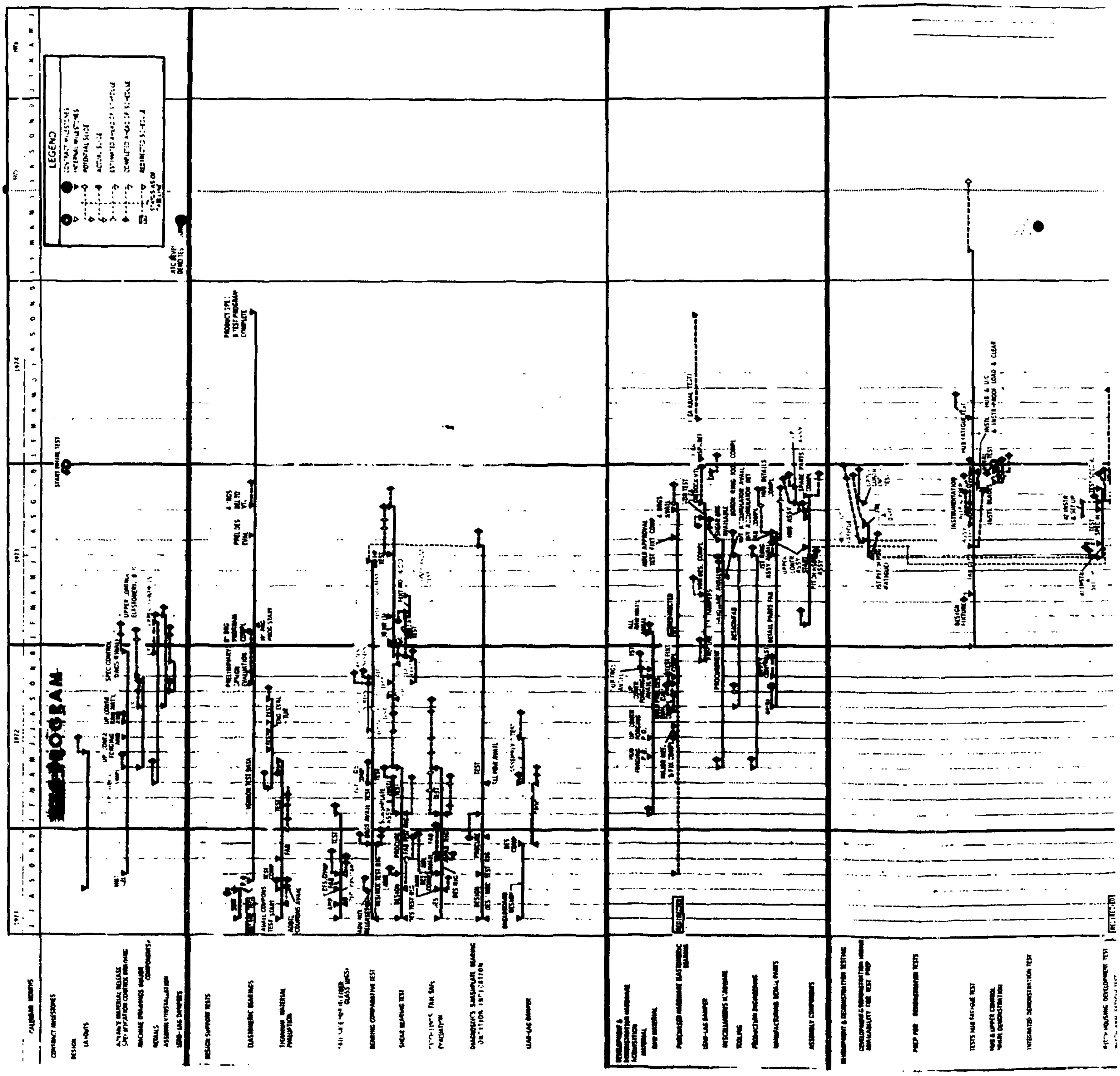

Figure 4. Hub/upper control interface phasing.

THIS PAGE IS
FROM COPY FU

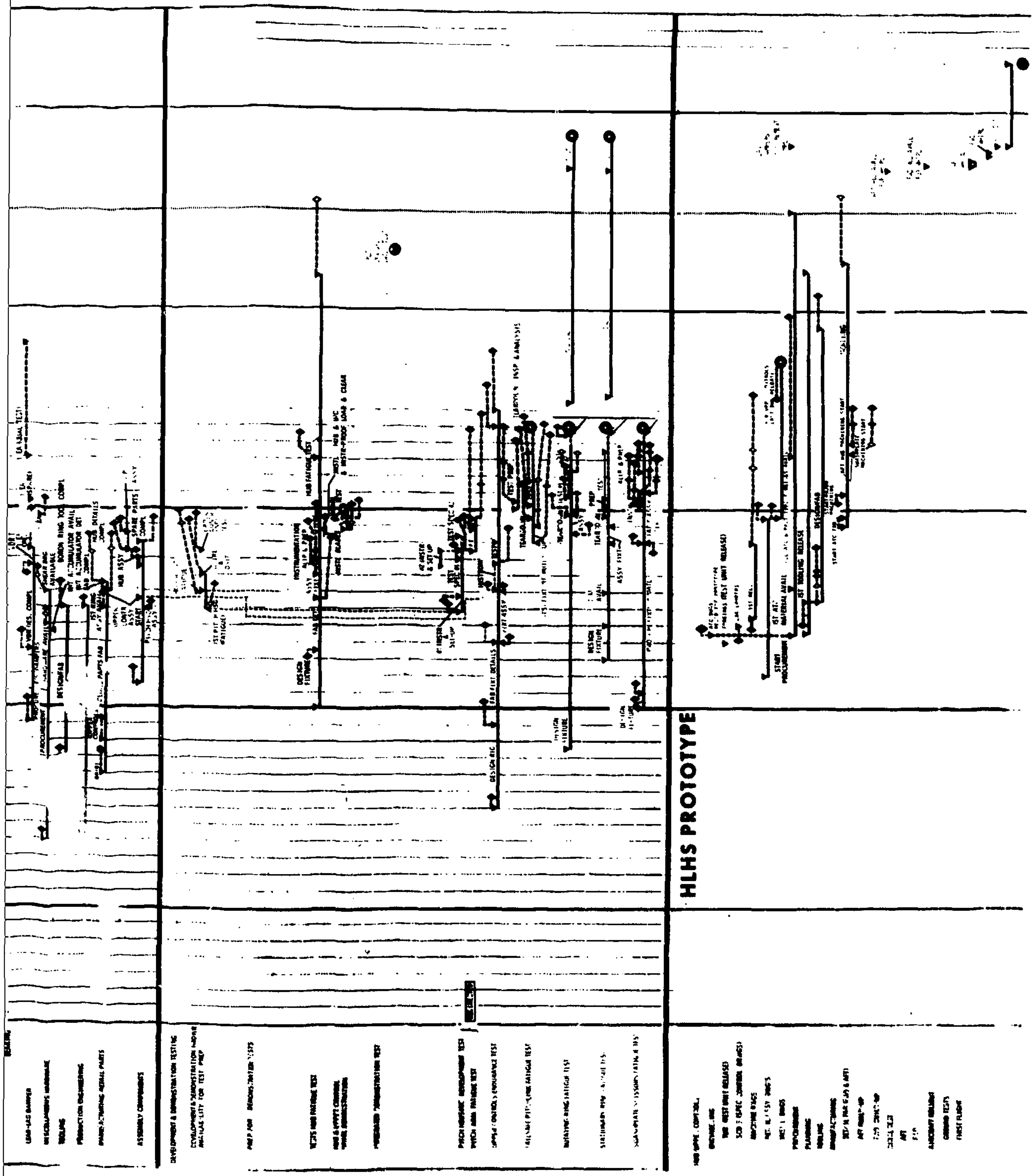

2

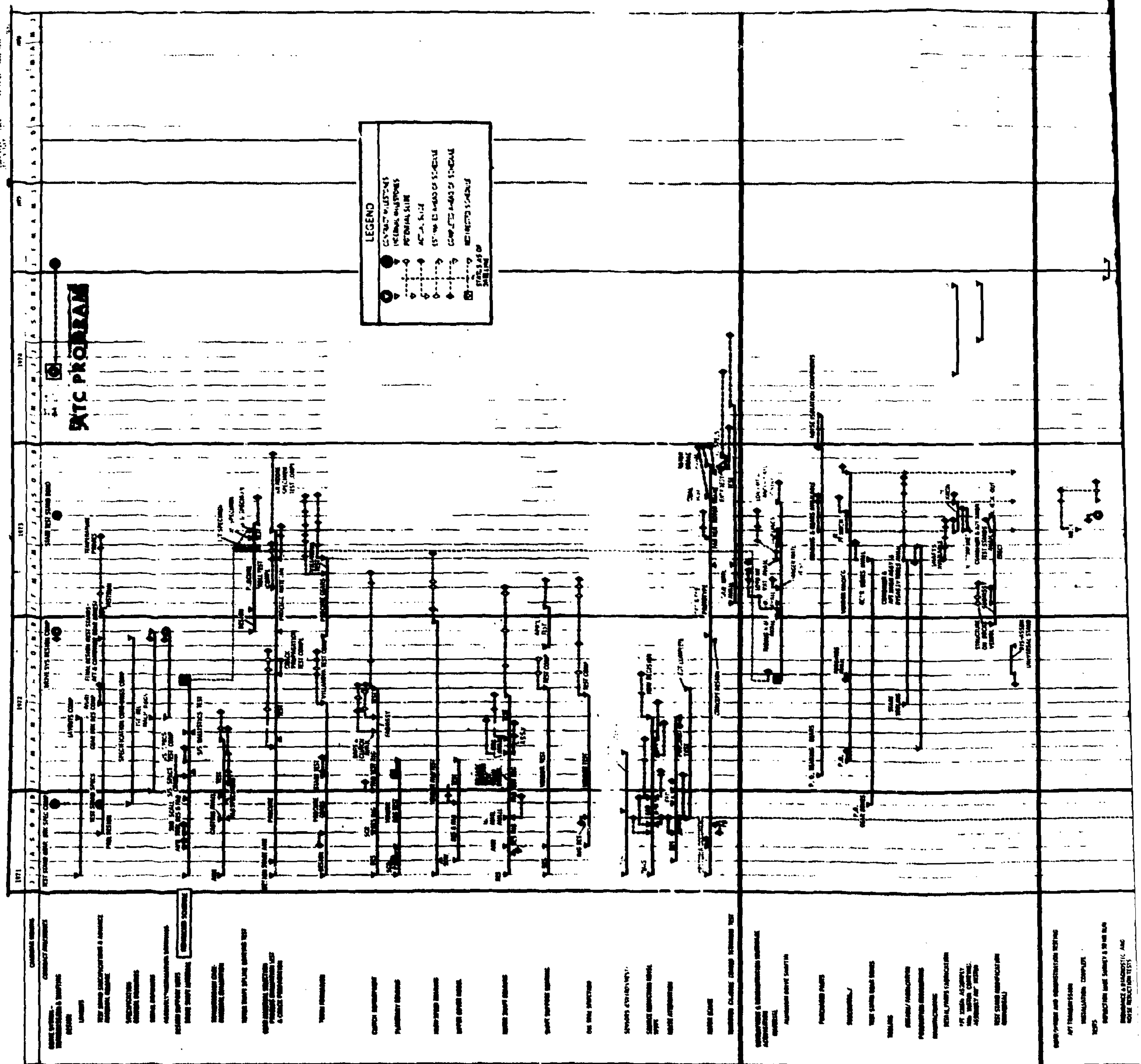

Figure 5. Drive system interface phasing.

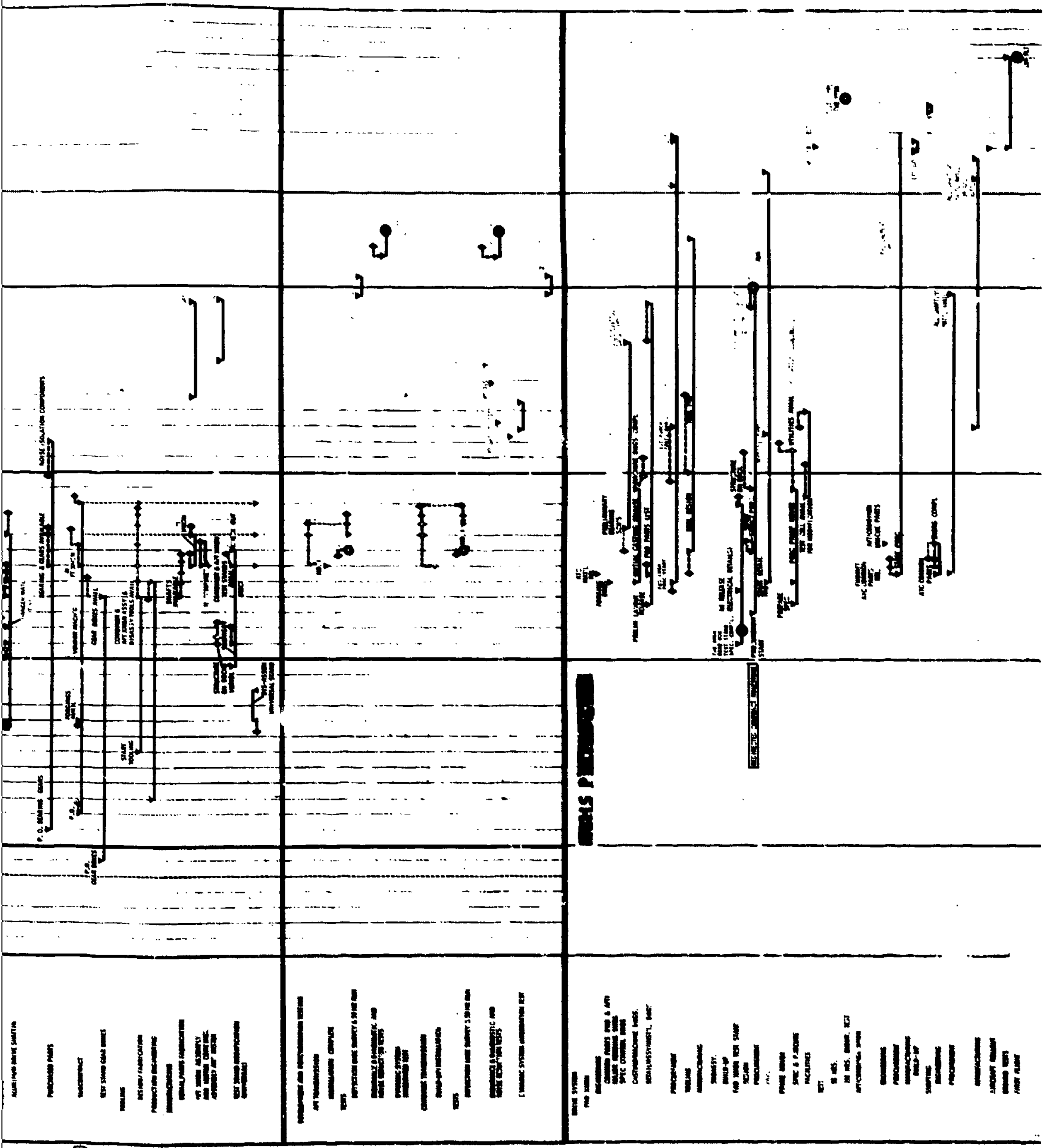

2

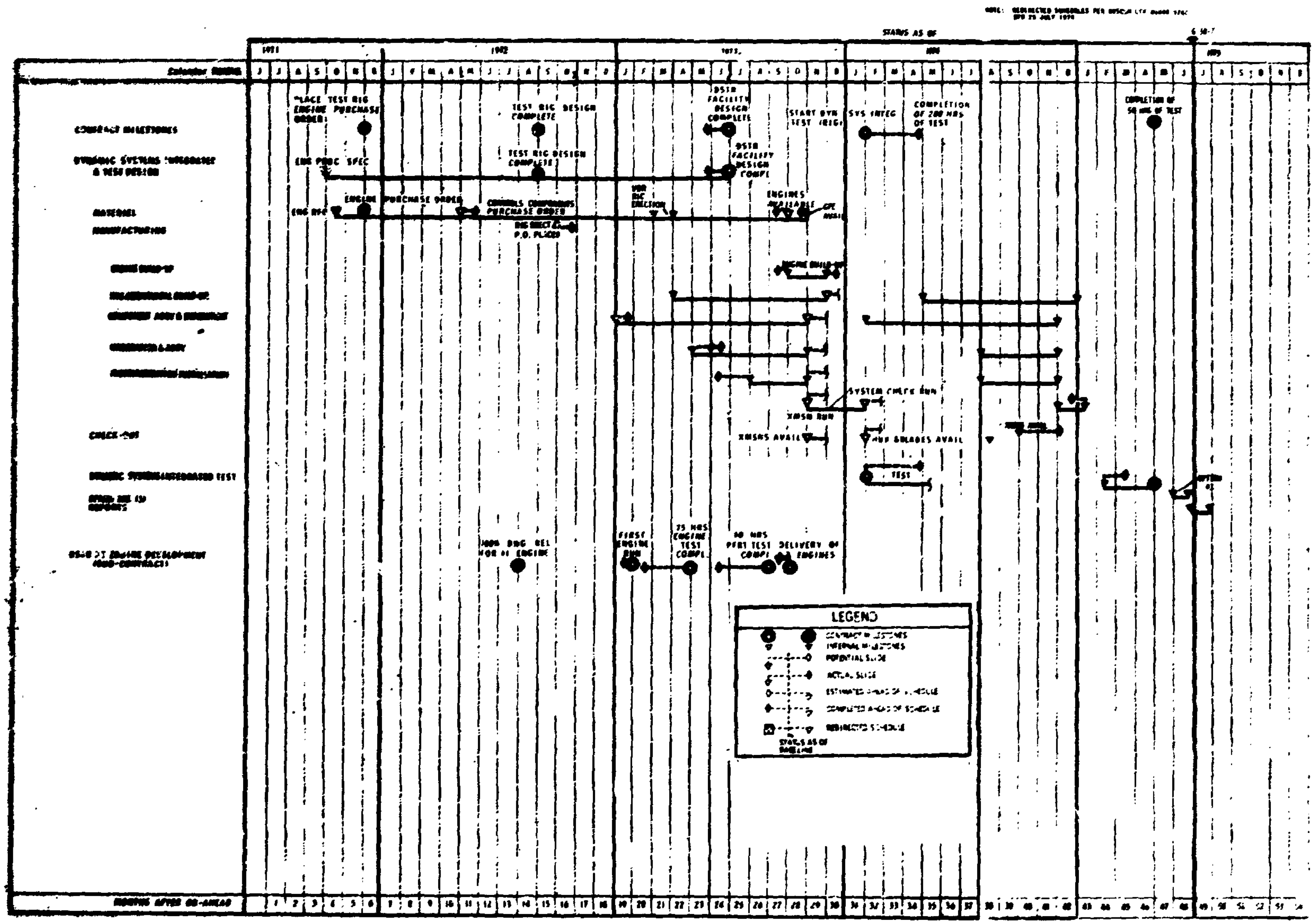

Figure 5A. Integrated rotor/drive system demonstration tests.

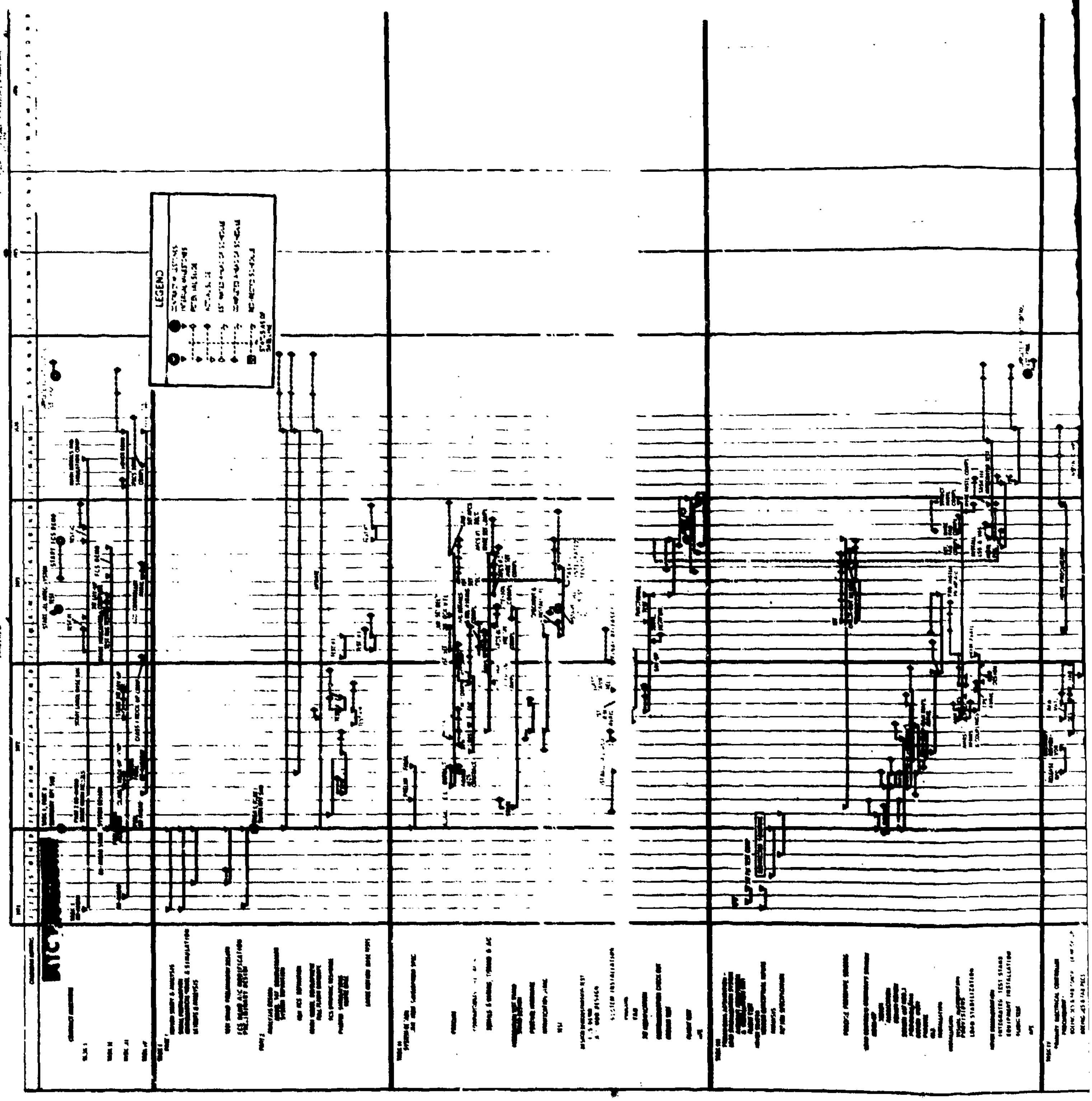

Figure 6. Flight control system interface phasing.

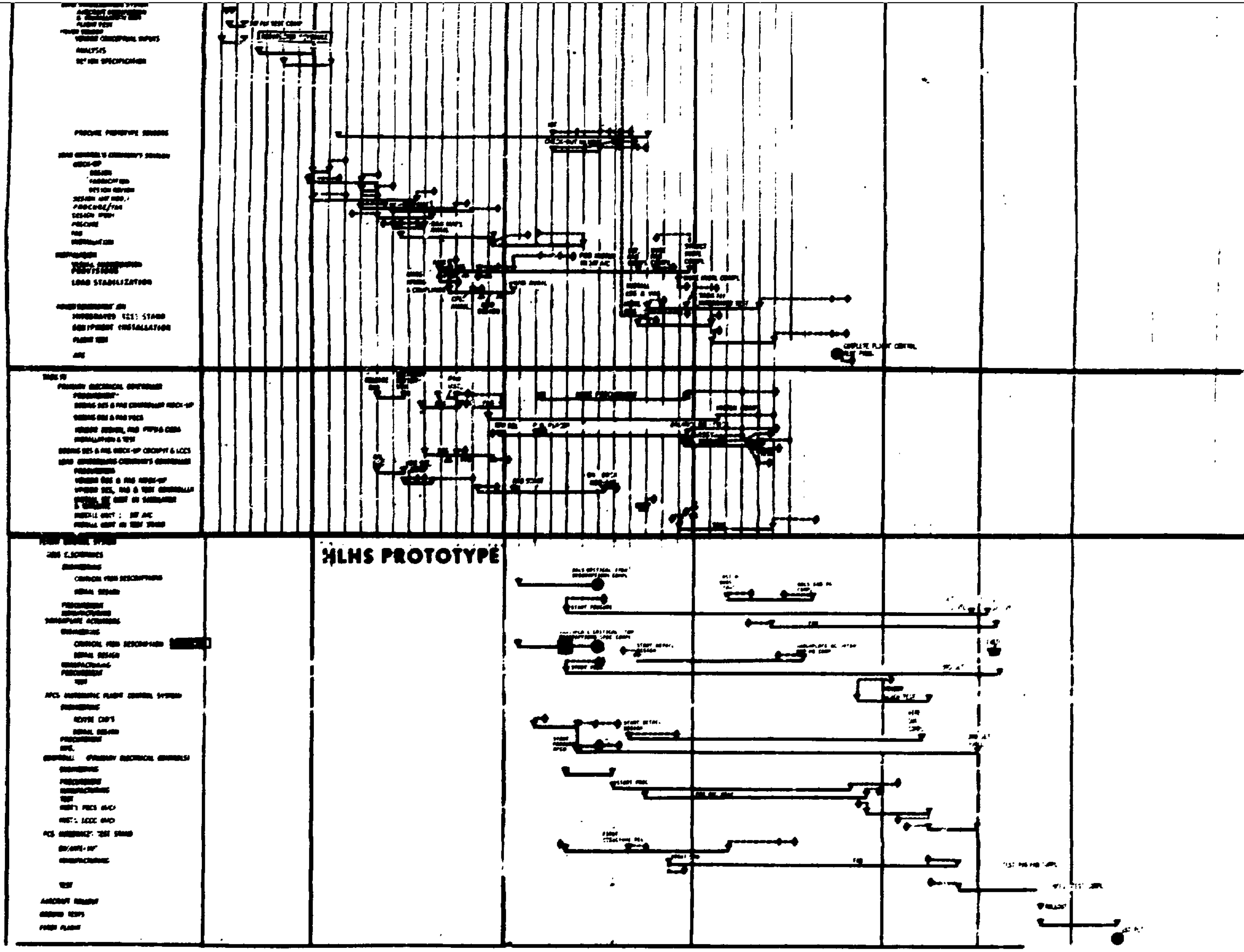
HLHS PROTOTYPE
ANALYSIS
LOAD STABILIZATION
EQUIPMENT INSTALLATION
CRITICAL ITEM DESCRIPTION
REVISE CDR'S
COMPLETE FLIGHT CONTROL

2

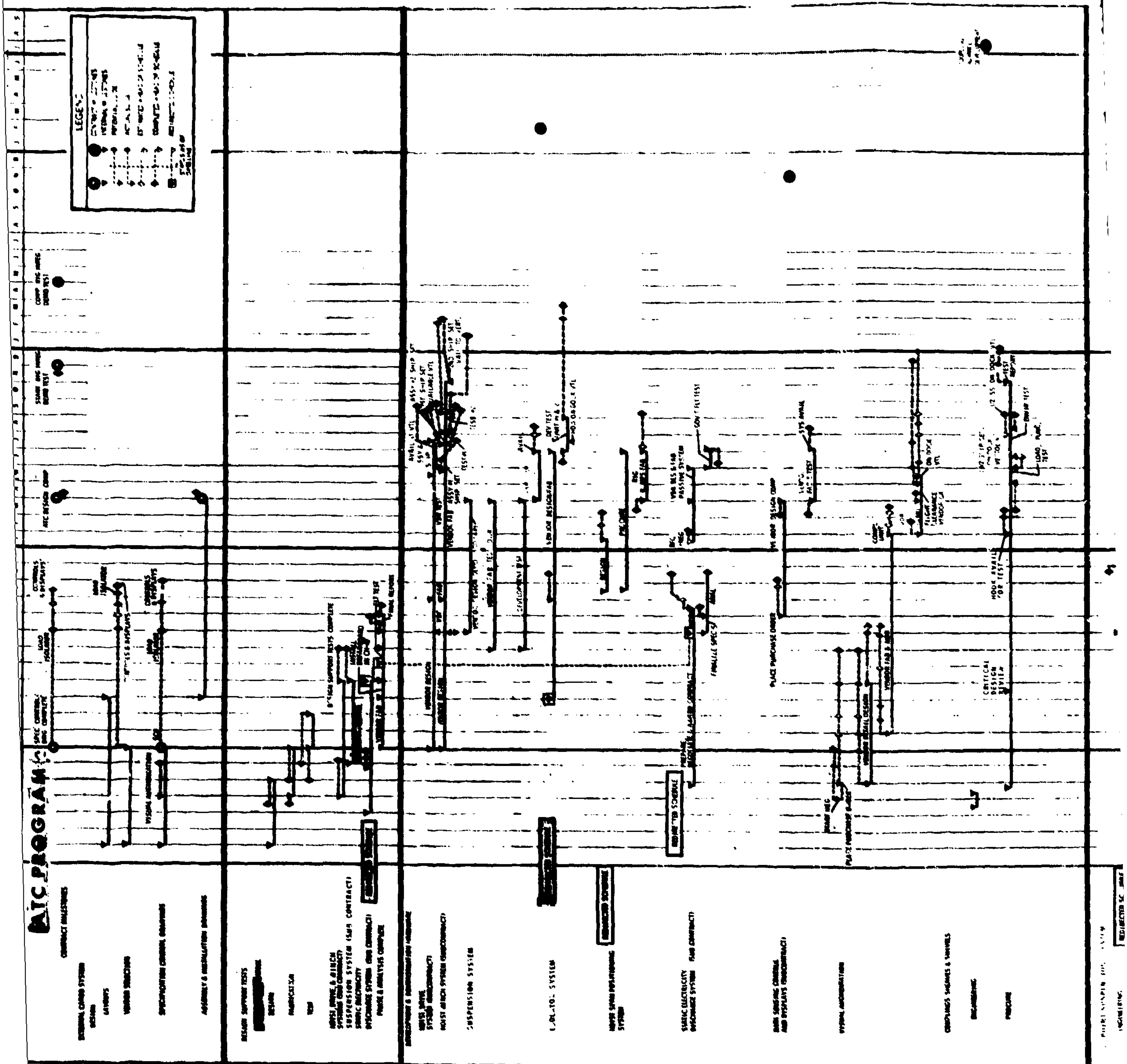

Figure 7. Cargo handling system interface phasing.

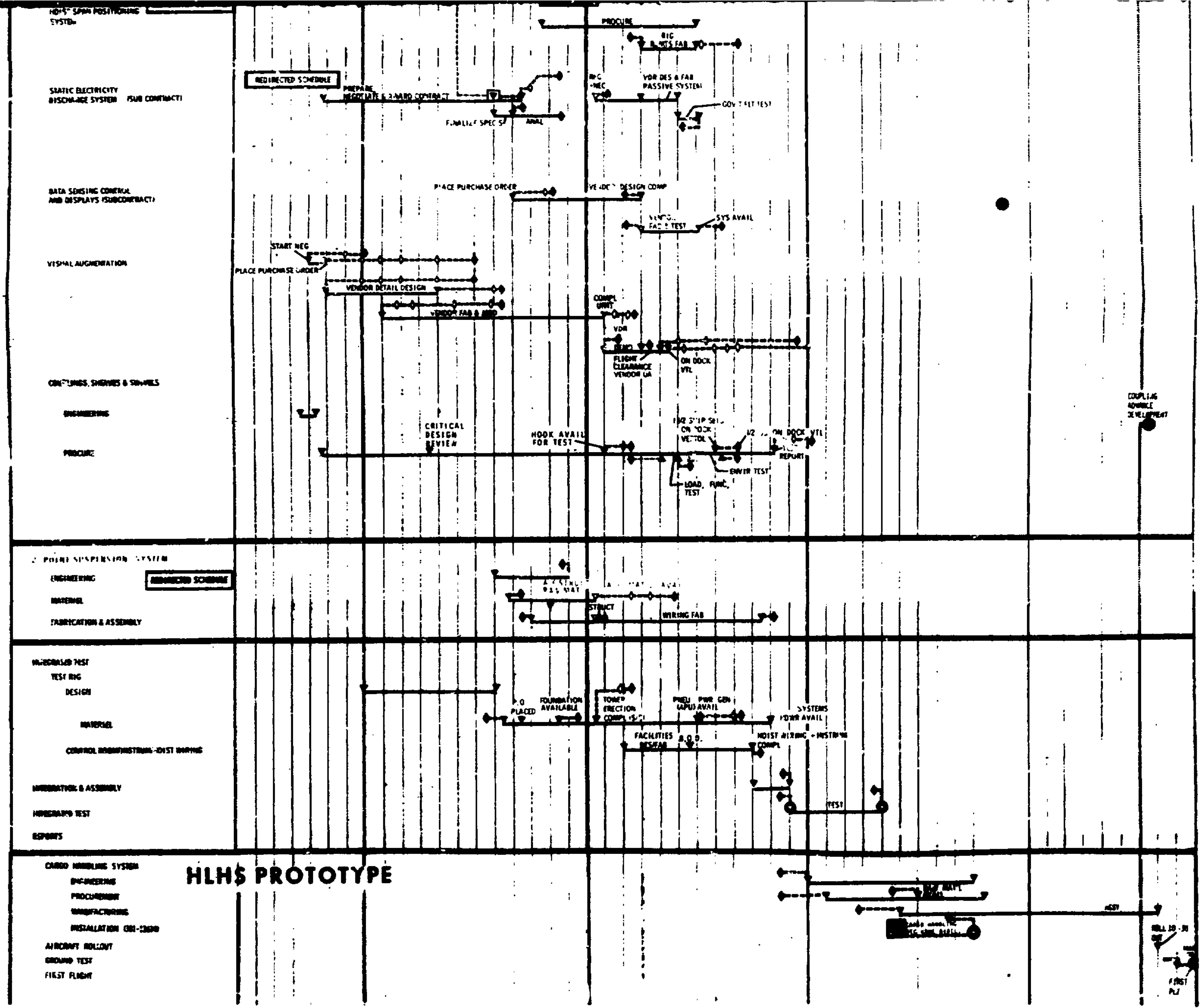

STATIC ELECTRICITY DISCHARGE SYSTEM (SUB CONTRACT)
REDIRECTED SCHEDULE
PREPARE, NEGOTIATE & AWARD CONTRACT
PROCURE
VOR DES & FAB PASSIVE SYSTEM
DATA SENSING CONTROL AND DISPLAYS (SUBCONTRACT)
PLACE PURCHASE ORDER
SYS AVAIL
VISUAL AUGMENTATION
START NEG
PLACE PURCHASE ORDER
VENDOR DETAIL DESIGN
FLIGHT CLEARANCE
ON DOCK VTL
ENGINEERING
PROCURE
CRITICAL DESIGN REVIEW
HOOK AVAIL FOR TEST
ENVIR TEST
LOAD, FUNC, TEST
COUPLING ADVANCE DEVELOPMENT
ENGINEERING
MATERIAL
FABRICATION & ASSEMBLY
STRUCT
WIRING FAB
TEST RIG
DESIGN
MATERIAL
P.O PLACED
FOUNDATION AVAILABLE
TOWER ERECTION
SYSTEMS
FACILITIES
INTEGRATION & ASSEMBLY
REPORTS
TEST
HLHS PROTOTYPE
CARGO HANDLING SYSTEM
ENGINEERING
PROCUREMENT
MANUFACTURING
AIRCRAFT ROLLOUT
GROUND TEST
FIRST FLIGHT

2

The "redirected" milestones or schedules in Figures 1 and 2 were the result of transmission development problems in the ATC phase. In order to incorporate changes for resolution of gear resonance problems and retest the ATC transmissions prior to fabrication of prototype aircraft hardware, the prototype schedule was extended approximately six months. With the exception of this program redirection in mid-1974, no significant schedule variation occurred during the program.

1.4 ATC/PROTOTYPE PROGRAM INTERFACES

Figures 3, 4, 5, 5A, 6, and 7 show the relationship of the ATC program and the prototype program for each of the ATC subsystems (blade, hub, upper controls, drive system, flight control system, and cargo handling system). Since the design and development of these systems was included in the ATC program, the prototype phase included only the following activities:

Blade - The ATC program included only the aft blade. Under the prototype program, the opposite hand forward blade design was accomplished, together with the pendulum vibration absorbers design and development. Design improvements for producibility were also incorporated in prototype blades.

Hub and Upper Controls - The prototype program included the opposite hand forward hub and upper controls design and some design improvements resulting from ATC program testing.

Drive System - The prototype program included the opposite rotation forward transmission design and verification testing. Although the gear train in the forward transmission is identical to the aft transmission, the input shaft angle, housing, and integral oil cooler design is unique. Also a new forward transmission test stand was required due to the shaft angle and rotation direction differences. Synchronizing shafting between the combiner transmission and the forward transmission was not included in the ATC program design and development.

Flight Control System - The flight control system for the prototype aircraft is, in principle, similar to the ATC demonstration system. The major subsystems are a direct electrical linkage system (DELS) and an automatic flight control system (AFCS).

Physically, the prototype DELS differs from the ATC demonstration DELS mainly in the configuration of the output actuators.

In the prototype HLH, the swashplates are supported by three swashplate servoactuators. Swashplate servoactuators are a two-stage integrated design. They have a triplex control stage interfaced with a dual power stage. In addition, the actuators will incorporate a stall flutter damping feature whereby the actuators are made soft to absorb stall flutter loads at the four per revolution frequency.

The prototype AFCS utilizes the flight control computers, input/output processors, a number of sensors, and certain of the control and display panels developed for the Model 347 demonstration program.

The prototype AFCS provides stability and control augmentation functions similar to the Model 347 ATC system except in low-speed flight.

Also, certain of the outer loop selectable modes provided in the Model 347 ATC are deleted in the prototype aircraft to reduce cost. These include: load stabilization, precision hover hold, and automatic approach to hover quidance. The principal equipment changes associated with these model differences are:

Inertial Measurement Units - Reduced from 2 to 1

Three Attitude Reference Systems - Increased from 1 to 3

Load Stabilization Sensors - Deleted	)	Space and
	)	power pro-
Precision Hover Sensing System - Deleted	)	visions only
	)	in
Flight Director Indicator - Deleted	)	prototype.

Cargo Handling System - The prototype cargo handling system was identical to the ATC system except that the longitudinal hoist positioning feature was deleted. Initially, it was planned to conduct the prototype program without operable winches to reduce cost and a winch locking device was designed. The hoists fabricated for the ATC program were used in the prototype.

A general background of the ATC program activities can be derived from Figures 3 thru 7; however, for a complete understanding of the ATC phase, see final reports, References 4 through 9.

2.0 SYSTEMS DEVELOPMENT

2.1 REQUIREMENTS

The Heavy Lift Helicopter system requirements were specified in the ATC phase RFQ, Reference 10 , and the ASRD, Reference 11 . During the ATC phase, the production HLH specification was prepared and periodically updated (see Reference 12). A derivative of this specification was prepared for the prototype aircraft to reflect deletions of unneccssary subsystems and equipments (Reference 1).

The prototype aircraft was representative of the production aircraft dimensionally and aerodynamically. Structural capability was equivalent to the production aircraft.

In order to minimize prototype program costs, subsystem variations from the production requirements were incorporated where the program objectives were not compromised. These included:

a. Conventional construction landing gear rather than incorporation of advanced composite materials.

b. Omission of the static electricity dissipator, auxiliary power unit, precision hover sensor, automatic approach to hover mode and load stabilization sensor, visual augmentation system, tactical navigation and communication equipment, blade deicing, windshield and engine inlet anti-icing, armor, armament, IR suppression devices, engine air particle separator, automatic diagnostic systems, searchlight, formation lights, hoisting fittings, fuel dumping, onboard refueling system, auxiliary tanks, and ferry fuel tank.

c. Modification of the electrical, hydraulic, pneumatic, fuel and environmental control systems to use existing components and simplify due to subsystem deletions.

At the termination of the prototype program, the PIDS Revision B plus SCNs 1, 2, 3, 4, 5, 7, 8, and 9 specified the current requirements for the prototype aircraft.

2.2 CONFIGURATION DEFINITION

The HLH configuration and major characteristics at the time of the prototype proposal submitted in late 1972 is shown in Figure 8.

After contract award, a series of System Requirements Reviews were held during March 1973. Detail level requirements were established and revisions to the preliminary PIDS were defined.

Early in the program, trade studies were conducted in several major areas, including the following:

- Honeycomb sandwich versus conventional aluminum skin and stringer airframe construction
- Fuel pod shape and structure
- Fixed span versus variable span cargo hoists
- Landing gear height and landing gear design criteria
- Flight engineer's station - side facing versus forward facing
- Crew vision study (windshield configuration)
- Nacelle geometry
- DELS swashplate actuator arrangement
- Aft pylon structure and lines

These trade studies resulted in the selection of honeycomb airframe construction, stub wing type fuel pods, 14-foot height fixed landing gear, fixed-position winches with an 18-foot span, a forward-facing flight engineer's station, a reconfigured windshield and nacelle, a three-channel driver-boost swashplate actuator arrangement, a widened aft pylon to accommodate the actuators, and an improved pylon structural arrangement.

The final configuration of the aircraft is shown in Figures 9 and 10.

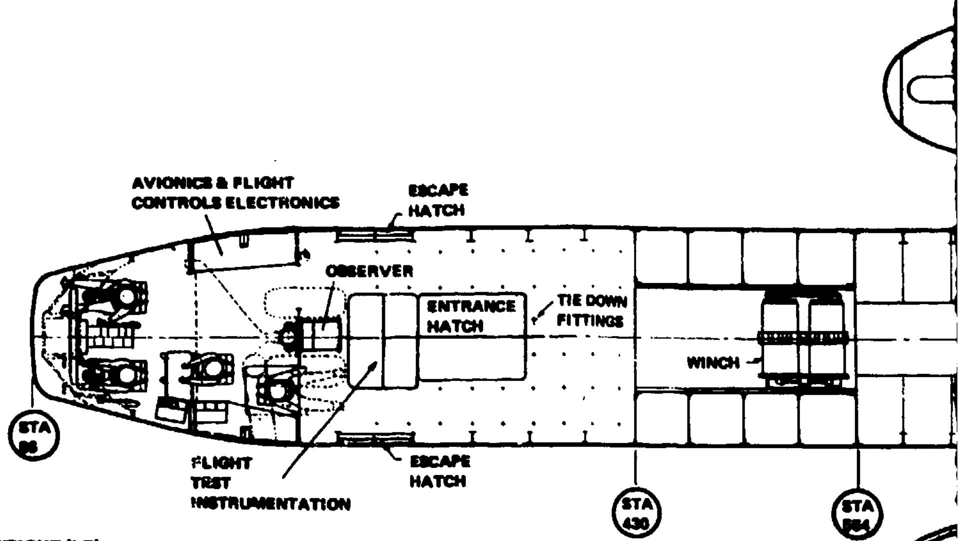

MAJOR CHARACTERISTICS

ROTOR

DIAMETER (FT)	92.0
TIP SPEED (FPS)	750.0
DISC LOADING (PSF) AT DGW	8.9
BLADE AREA (8 AT 153 SQ FT)	1224.0
GEOMETRIC SOLIDITY RATIO	.08226
GEOMETRIC DISC AREA (2 AT 6647.6 SQ FT)	13,295.0

PROPULSION

NUMBER OF ENGINES/TYPE	ALLISON 501-M62C (3) TURBOSHAFT
TRANSMISSION RATING (HP)	17,700
MAX SINGLE ENGINE RATING (HP)	8,080
INTEGRAL FUEL CAPACITY (GAL)	3,092
INTEGRAL FUEL CAPACITY (LB)	20,100

GROUND ANGLES (DEGREES)

TURNOVER (WT. EMPTY)	25.5°
TIP BACK (WT. EMPTY)	19.0°

CONTROL MOVEMENTS

	ROTOR BLADE FORWARD	ROTOR BLADE AFT
COLLECTIVE PITCH	0° TO 17.5°	6° TO 16.0°
DIFFERENTIAL COLLECTIVE PITCH	±5.0°	±3.0°
LONGITUDINAL CYCLIC PITCH	+13.4 −3.8	+8.7 −5.5
DIFFERENTIAL LATERAL CYCLIC PITCH	±11.3°	±10.3°
LATERAL CYCLIC PITCH	± 9.5	± 8.5

LANDING GEAR

NOSE – WHEEL/TIRE SIZE	14 PLY RATING	15:00-20
MAIN – WHEEL/TIRE SIZE		TYPE III

WEIGHT (LB)

DESIGN GROSS WEIGHT, LF = 2.5	118,000
MAX ALTERNATE GROSS WEIGHT, LF = 2.0	148,000
MISSION PAYLOAD – EXTERNAL	45,000
PROTOTYPE MISSION FUEL	11,397
FIXED USEFUL LOAD (INCLUDES 5 MAN CREW)	1,372
FLIGHT TEST INSTRUMENTATION	3,500
PROTOTYPE WEIGHT EMPTY	90,041
PROTOTYPE MISSION GROSS WEIGHT	121,400

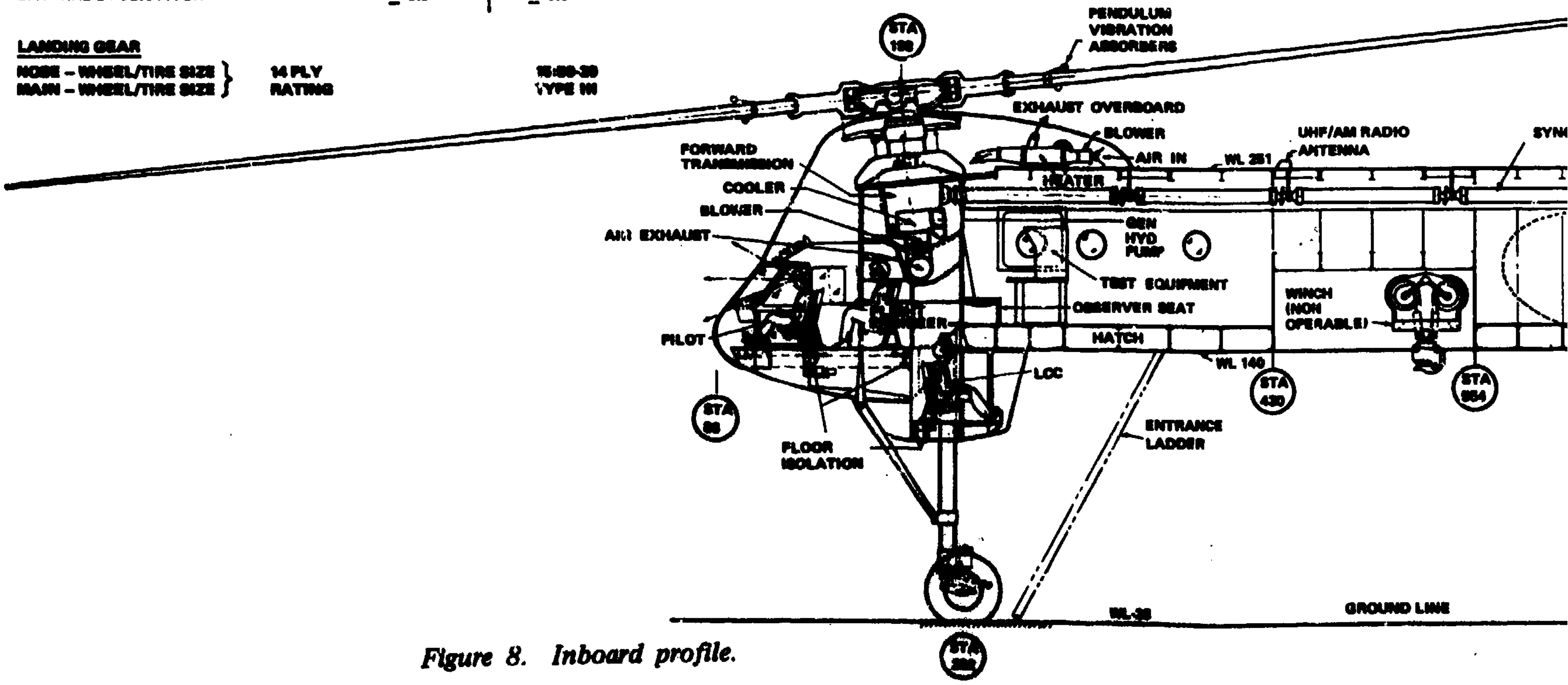

Figure 8. Inboard profile.

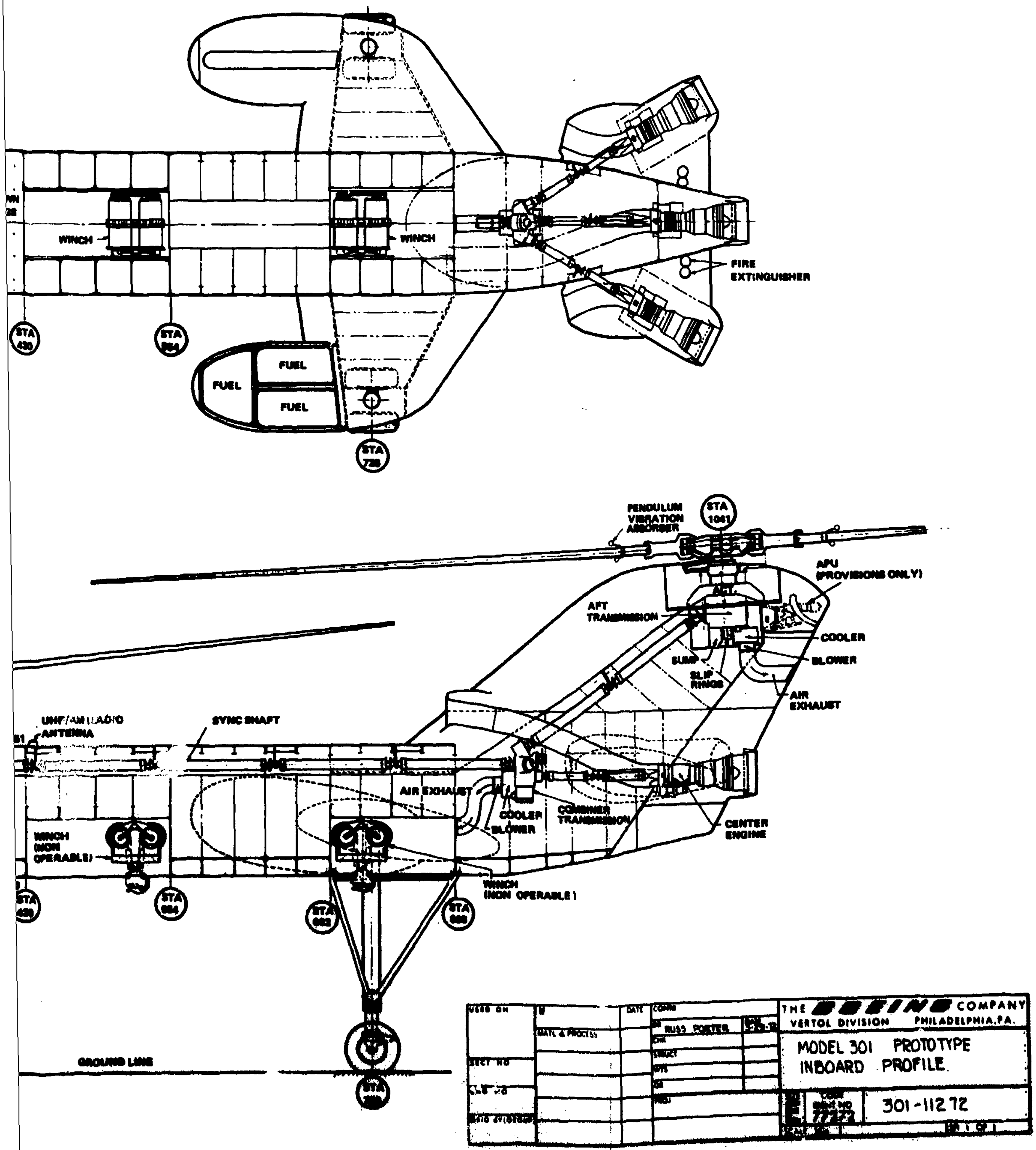

WINCH
WINCH
FIRE EXTINGUISHER
STA 430
STA 564
FUEL
FUEL
FUEL
PENDULUM VIBRATION ABSORBER
STA 1041
APU (PROVISIONS ONLY)
AFT TRANSMISSION
COOLER
SUMP
BLOWER
SLIP RINGS
AIR EXHAUST
UHF/AM RADIO ANTENNA
SYNC SHAFT
AIR EXHAUST
COOLER
BLOWER
COMBINER TRANSMISSION
CENTER ENGINE
WINCH (NON OPERABLE)
WINCH (NON OPERABLE)
STA 430
STA 564
GROUND LINE
USED ON
DATE
MAT'L & PROCESS
RUSS PORTER
THE BOEING COMPANY
VERTOL DIVISION PHILADELPHIA, PA.
MODEL 301 PROTOTYPE
INBOARD PROFILE
301-11272

2

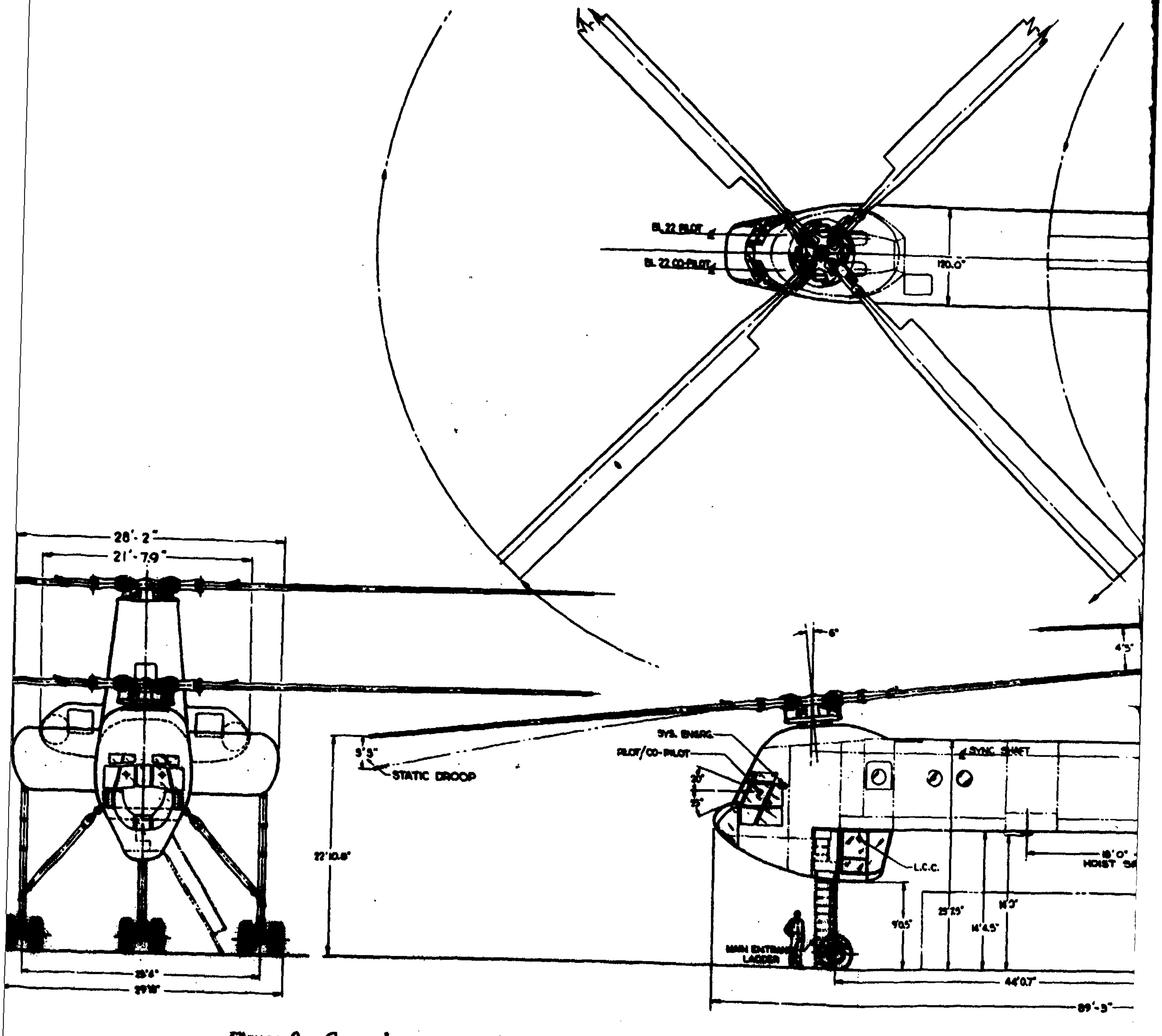

Figure 9. General arrangement.

10

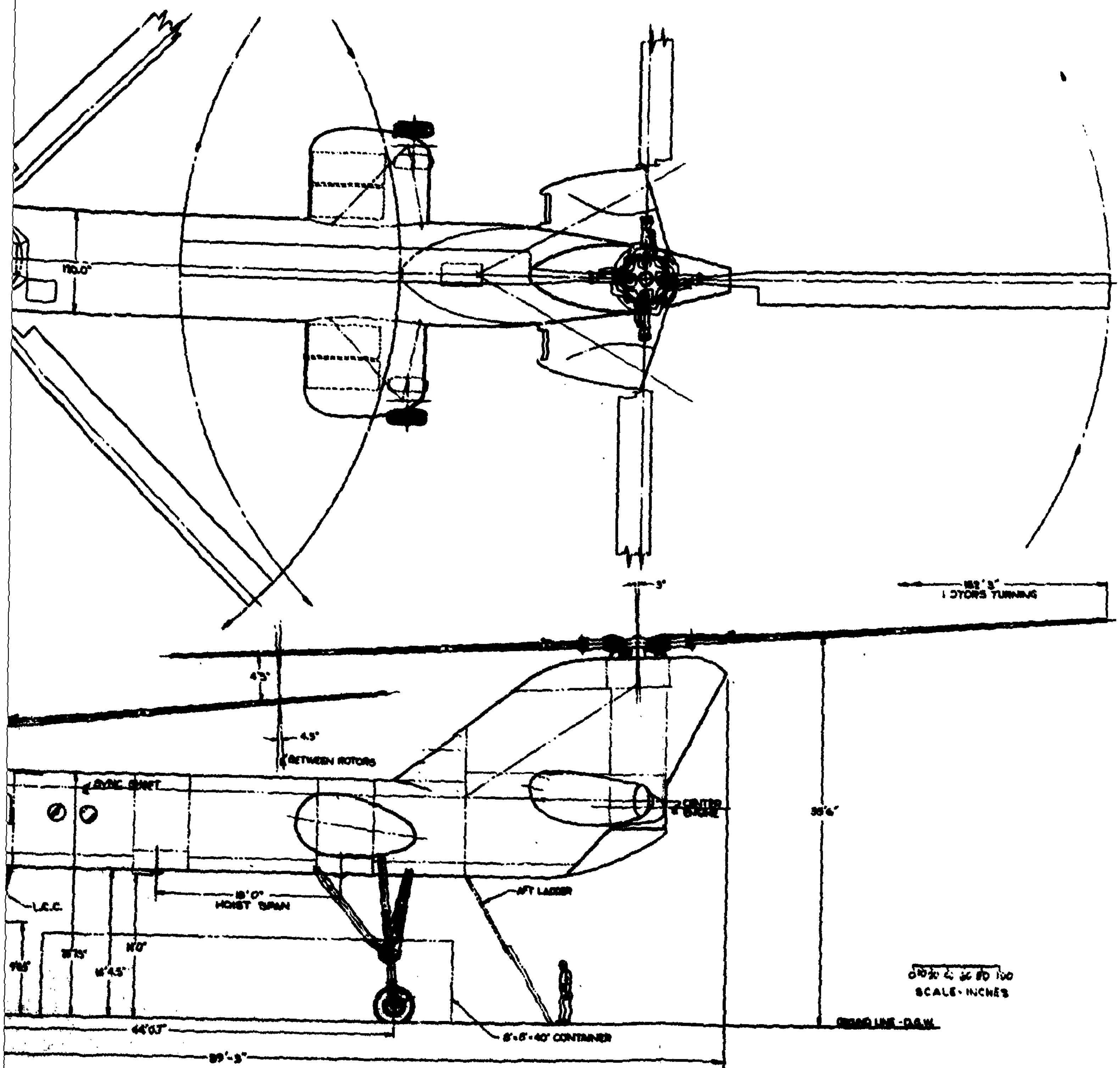

110.0"
3"
4.5"
BETWEEN ROTORS
19'0"
HOIST SPAN
AFT LADDER
38'6"
SCALE - INCHES
8'x8'x40' CONTAINER
99'-3"

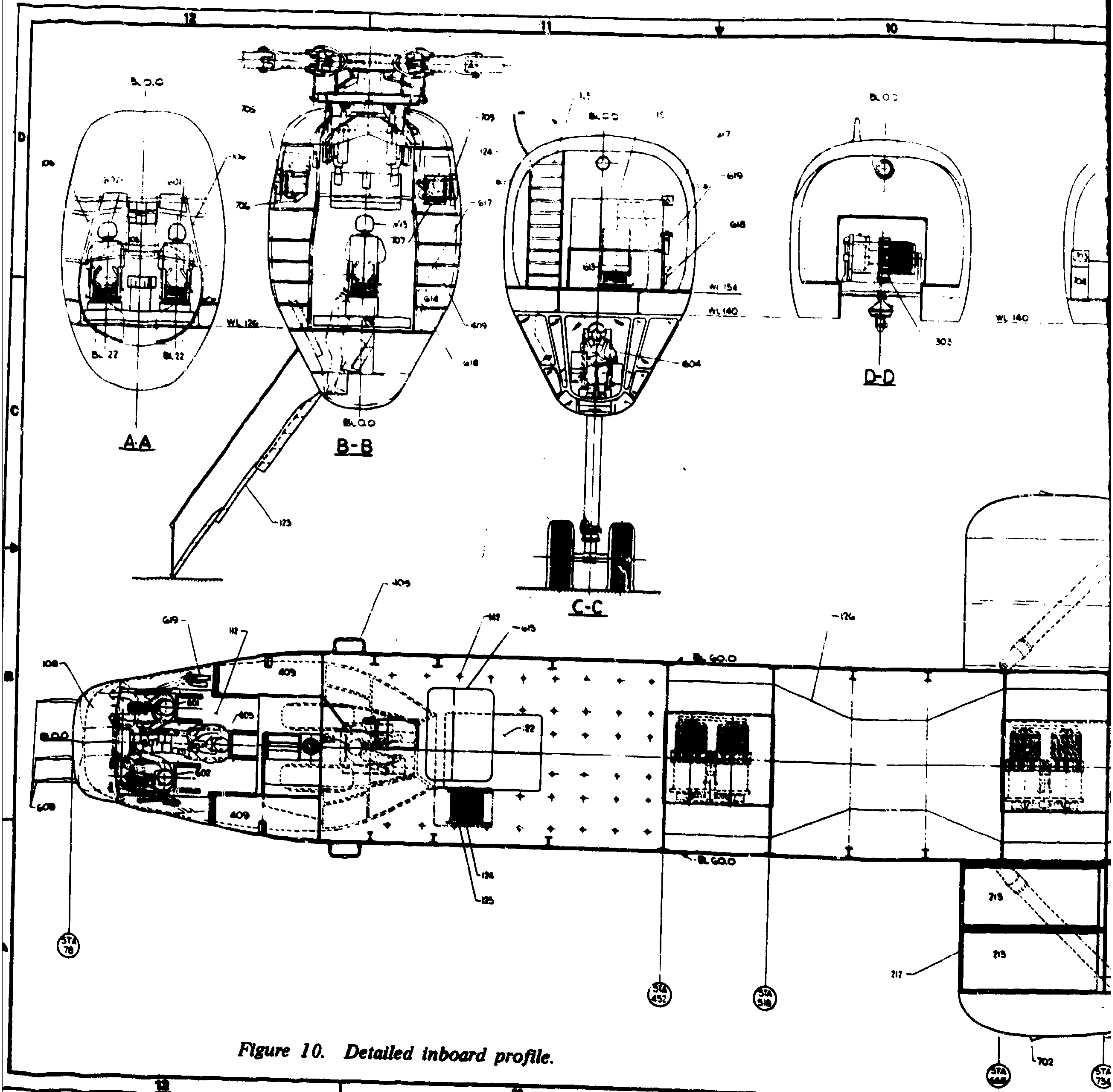

Figure 10. Detailed inboard profile.

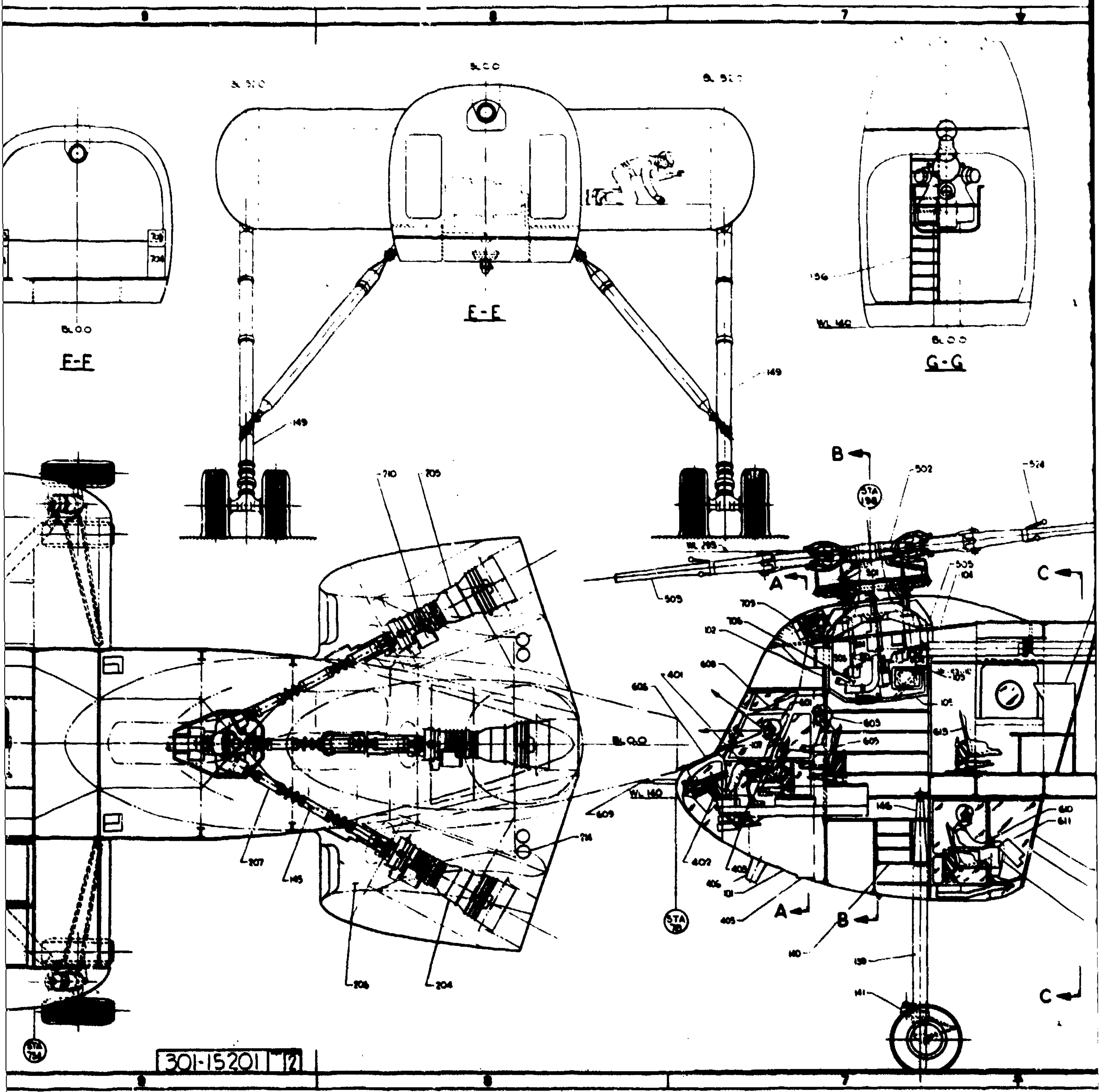

2

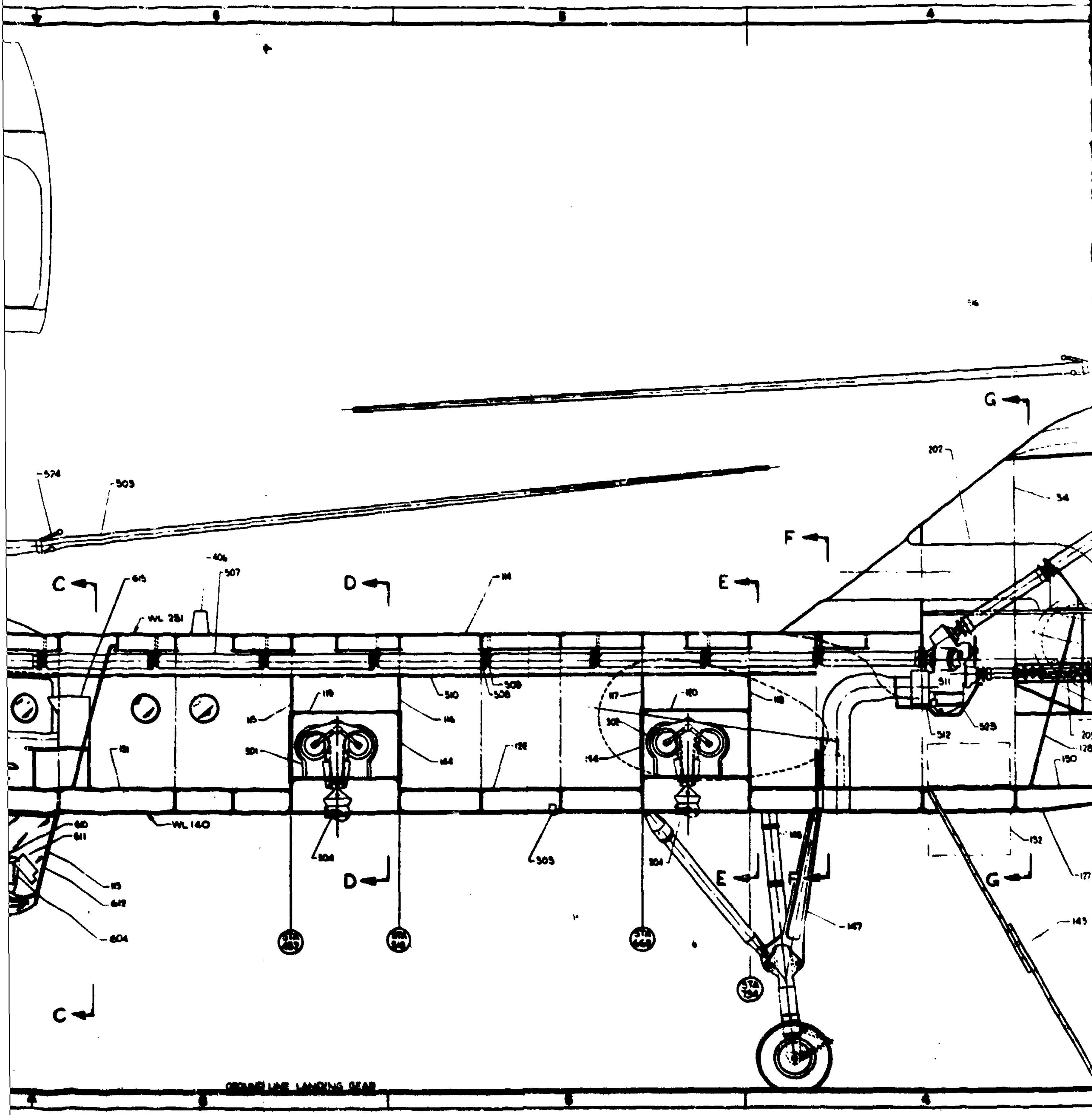

3

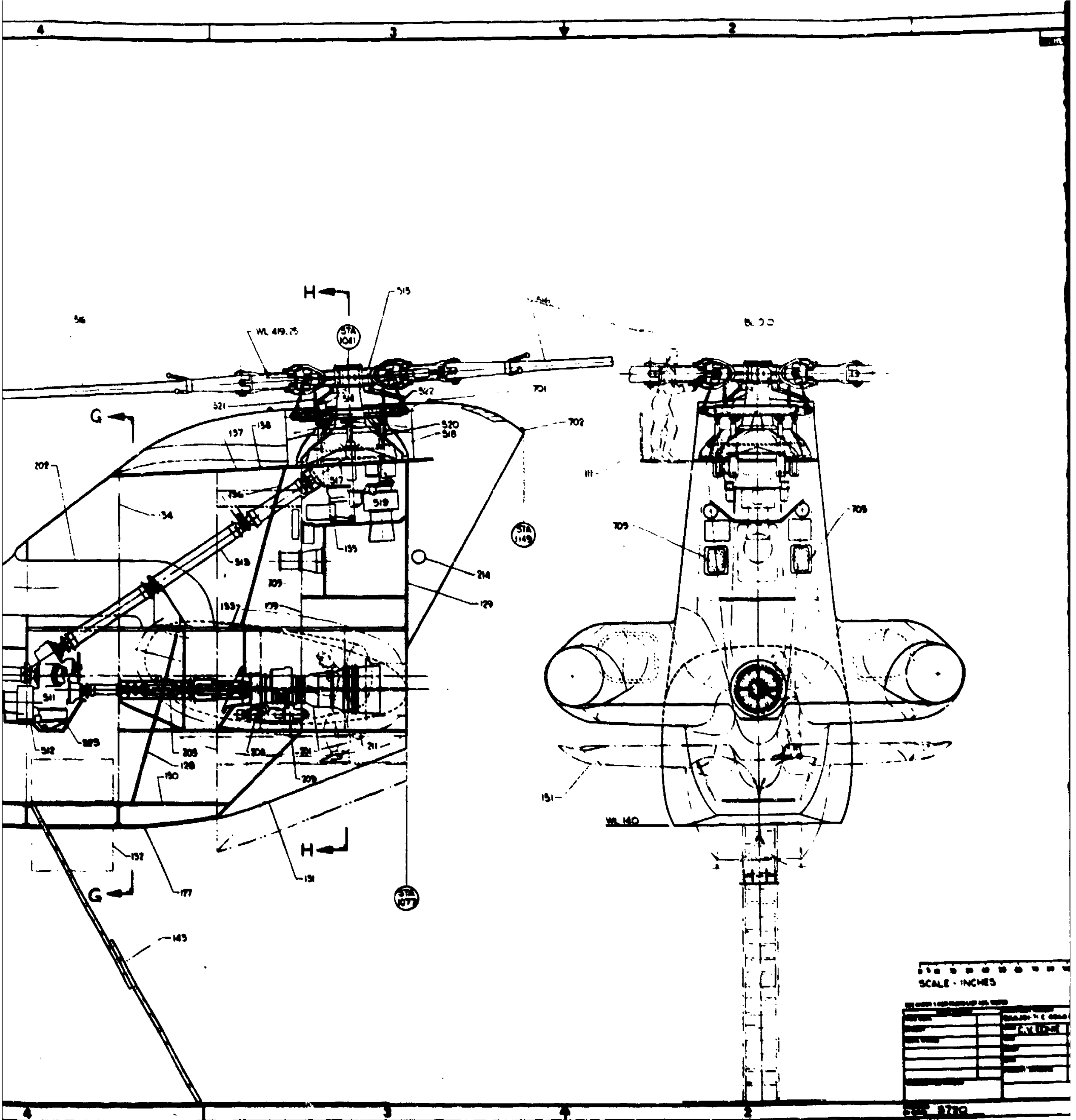

4

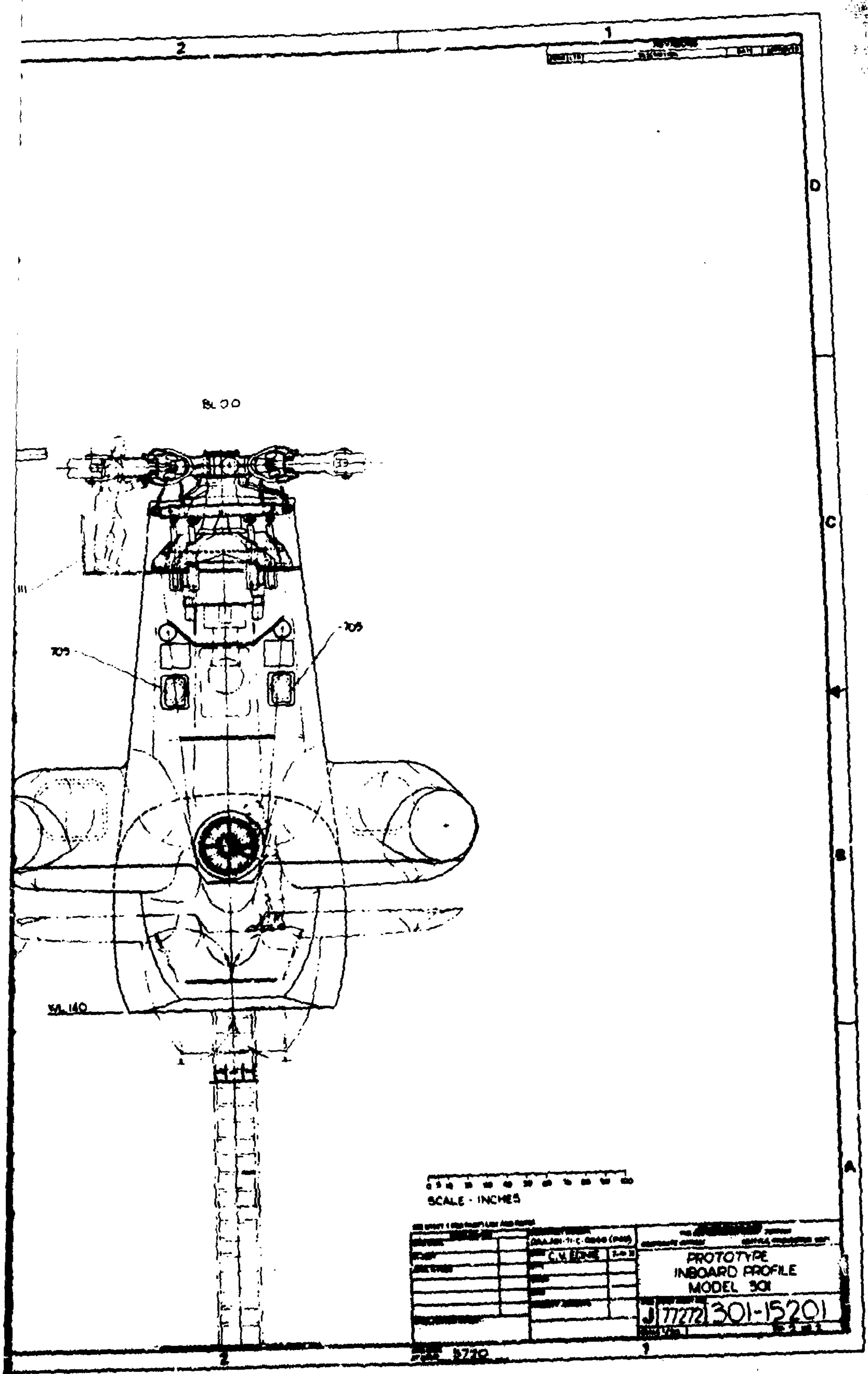
2
1
D
C
B
A
BL 0.0
111
709
709
WL 140
SCALE - INCHES
C.V. EDNIE
PROTOTYPE
INBOARD PROFILE
MODEL 301
J
77272
301-15201
8720

4

5

PROTOTYPE

BOEING MODEL 301

INBOARD PROFILE LEGEND

AIRFRAME AND LANDING GEAR

101 Forebody Structure Sta. 83 to Sta. 236
102 Transmission Support Bulkhead Sta. 170 (Fwd)
103 Transmission Support Bulkhead Sta. 236 (Aft)
104 Transmission Mounting Deck
105 Transmission Compartment Insulation Panels and Drip Pan
106 Windshield
107 Side Vision Transparent Panel
108 Fwd Vision Transparent Panel
109 Transmission Support Bulkhead Sta. 1011 (Fwd)
110 Emergency Exit Hatch (2) Pilot and Copilot

111 Work Platform Aft Transmission and Rotor
112 Flight Deck
113 Load Controlling Crewman Enclosure
114 Constant Section Mid-Body Structure Sta. 236 to Sta. 840
115 Forward Hoist Support Bulkhead Sta. 452
116 Forward Hoist Support Bulkhead Sta. 518
117 Aft Hoist Support Bulkhead Sta. 668
118 Aft Hoist Support Bulkhead Sta. 734
119 Forward Hoist Bay Removable Cover
120 Aft Hoist Bay Removable Cover

121 Troop/Cargo Deck (Floor)
122 Cargo Hatch
123 Stowable Entrance Stairs (Fwd)
124 Overhead Ditching Hatch
125 Ditching Exit Integral Ladder (Stowable)
126 Mid-Body Walkway Flooring
127 Afterbody Structure Sta. 840 to Sta. 1077
128 WL 262 Deck Access Ladder
129 Aft Bulkhead and Transmission Support Sta. 1077
130 Aft Cargo Deck Floor
131 Engine Work Platform
132 Rear Entrance Hatch
133 Deck WL 262
134 Upper Aft Pylon Structure
135 Drip Pan Aft Transmission
136 Xmsn Deck Access Ladder
137 Aft Transmission Mounting Deck
138 Xmsn Deck Access Hatch
139 Forward Landing Gear Assembly
140 WL 98 Deck

141 Nose Gear Steering Unit
142 Tie Down Fittings
143 Stowable Extension Ladder (Aft)
144 Hoist Removable Covers (2) Fwd and Aft
145 WL 262 Deck Access Hatch (Overhead)
146 Strut (Nose)
147 Drag Brace (Main)
148 Main Landing Gear Assembly (2)
149 Strut (Main)

PROPULSION AND FUEL SYSTEM

201 Center Engine Installation
202 Center Engine Air Induction System
203 Center Engine Drive Shafting
204 Left Outboard Engine Installation
205 Right Outboard Engine Installation
206 Outboard Engine Air Induction System
207 Outboard Engine Drive Shafting
208 Accessory Drive Gearbox
209 Starter Unit
210 Engine Oil Tank

211 Firewall
212 Fuel Tank Shell Structure
213 Crashworthy Fuel Cell (4)
214 Fire Detection and Extinguishing System

CARGO HANDLING

301 Forward Hoist Assembly
302 Aft Hoist Assembly
303 Cable Cutter
304 Coupling Assembly
305 External Cargo Optical Sensor

FLIGHT CONTROLS AND AVIONICS

401 Cyclic Control Stick
402 Yaw Control Pedals
403 Collective/Power Control Lever
404
405 Radar Altimeter Antenna (2)
406 VHF-UHF Antenna (2)
407
408 VOR-Localizer Antenna (2)
409 Avionics and Flight Control Equipment

DYNAMIC SYSTEM

501 Forward Rotor
502 Forward Rotor Hub
503 Forward Rotor Blades
504 Forward Rotor Transmission
505 Forward Transmission Mount
506 Forward Transmission Oil Cooler
507 Longitudinal Synchronizing Shaft (9 sections)
508 Sync/Shaft Couplings
509 Sync/Shaft Hangers
510 Sync/Shaft Shroud

511 Combining Transmission
512 Combining Transmission Oil Cooler
513 Slant Shaft (3 sections)
514 Aft Rotor
515 Aft Rotor Hub
516 Aft Rotor Blades
517 Aft Rotor Transmission
518 Aft Transmission Mount
519 Aft Transmission Oil Cooler
520 Control Actuator/Upper Rotor Controls

521 Pitch Link/Upper Rotor Controls
522 Swashplate/Upper Rotor Controls
523 Drip Pan Combiner
524 Pendulum Absorbers

CREW STATIONS AND EQUIPMENT

601 Pilot
602 Copilot
603 Systems Engineer
604 Load Controlling Crewman
605 Crash Attenuation Seat (4)
606 Instrument Display Panel
607 Center Instrument Pedestal
608 Overhead Instrument Panel
609 Pitot Tube (3)
610 Load Controlling Crewman Side Stick Controls

611 Visual Augmentation Display Panel (L.C.C.)
612 Load Controlling Crewman Emergency Exit Panel
613 Observer Crash Attenuation Seat
614 Miscellaneous Equipment Storage Locker
615 Flight Test Instrumentation
616
617 First Aid Kit (2)
618 Fire Axe (2)
619 Fire Extinguisher

HYDRAULICS, PNEUMATICS, ELECTRICAL AND ENVIRONMENTAL [illegible]

701 Flasher/Anti-Collision Light (2)
702 Navigation Light (3)
703 [illegible] Panel
704 Electrical [illegible]
705 Hydraulic Oil Cooler [illegible]
706 Air Turbine Motor
707 Environmental Control Unit

Figure 10. (Continued)

2.3 PERFORMANCE

2.3.1 Definitions. The aircraft performance capabilities are estimated on the basis of key values shown in Table 2, which were derived from estimates of the parasite drag of the HLH prototype, and full-scale tests conducted under the HLH/ATC program. The performance characteristics presented in this section are further based on the following definitions and assumptions.

a. Reference to "Without Payload" in forward flight indicates a parasite drag value of the basic aircraft with no external load.

b. Reference to "With Payload" in forward flight indicates a parasite drag value of the basic aircraft plus 100 square feet of parasite drag (equivalent flat plate) area.

c. Reference to "Without Payload" in hover or vertical flight indicates a vertical drag value of the basic aircraft with no external load.

d. Reference to "With Payload" in hover or vertical flight indicates a vertical drag value of the basic aircraft plus the drag of an 8'x8'x20' rectangular container in the most adverse position.

e. Engine characteristics are based upon Allison Engine Model Specification 844 for the XT701-AD-700 engine. The XT701-AD-700 engine to be used in the prototype shall provide rated powers (uninstalled) as shown in the referenced engine specification. The fuel consumption of the XT701-AD-700 engine may exceed that of the MQT engine by 5%, and the aircraft performance shown reflects this increase. An additional 5% increase in s.f.c. has been applied to the data in accordance with MIL-C-5011.

f. Cruise speed is at highest speed for 99 percent best range, except as limited by maximum continuous power, transmission power rating, or except as noted.

g. Maximum speed (V_{max}) is the power-limited speed at maximum continuous power or transmission power rating, whichever is less.

h. In-ground-effect hover performance is based upon a hover wheel height of 10 feet.

i. Initial fuel: fuel load at initial gross weight condition. Includes starting, warm-up, and taxi fuel.

j. Mission fuel: fuel load at mission gross weight condition. Excludes starting, warm-up, and taxi fuel.

k. Initial gross weight: gross weight at engine start-up. Includes starting, warm-up, and taxi fuel.

l. Mission gross weight: gross weight at critical mission performance condition. Generally, it is the highest gross weight achieved while performing the mission profile.

m. Maximum payload at alternate gross weights is limited by the hoist capacity at 2.0 g of 35 tons plus the equivalent of 12 troops in the cabin at 240 pounds each. Total maximum payload is 72,880 pounds, or 36.44 tons.

n. Abbreviations:

AEO	- All Engines Operative
OEI	- One Engine Inoperative
OGE	- Out of Ground Effect
IGE	- In Ground Effect (10-foot wheel ht)
MCP	- Maximum Continuous Power
INTP	- Intermediate Power (30-minute use)
XMSN P	- Transmission Power Rating

TABLE 2. HLH PROTOTYPE PERFORMANCE BASIS

Rotor Performance

Based on results of full-scale whirl tests performed on the ATC HLH rotor and 14-ft model rotor tests of HLH airfoils, twist, and planform, corrected to full scale HLH rotor characteristics.

Figure of Merit at SL 95°, at Design Gross Weight	.767
L/De at SL std temp, 130 knots, at Design Gross Weight	7.980
Flying Qualities Boundary (% Improvement in C_T/σ over Chinook Rotor) at 150 knots	10.3%
at 90 knots	9.4%
Stall Flutter Boundary (% Improvement in C_T/σ over Chinook Rotor)	5%*

Aircraft Characteristics (Based upon current estimates.)

Aircraft Parasite Drag Area (Fuselage Angle of Attack 4° Nose Down)	154.3 sq ft,
Vertical Download (With Payload, OGE)	6.7% Gross Weight
(Without Payload, OGE)	5.2% Gross Weight
Accessory Power Loss	286 HP
Transmission Loss	680 HP

*Model scale data - not corrected for Reynolds Number.

2.3.2 Performance Summary. Table 3 is prototype estimated performances. For estimated performance on production aircraft; see Reference 12.

TABLE 3. ESTIMATED PERFORMANCE

PERFORMANCE SHOWN IS AT DESIGN GROSS WEIGHT (118,000 POUNDS) WITH PAYLOAD EXCEPT AS OTHERWISE NOTED.

ITEM	UNITS	TEMPERATURE 95°F	STD.
Speed at SL			
Cruise Speed	Knots	134	127
Cruise Speed (without P/L) (1)	Knots	143	133
Max. Speed (XMSN P)	Knots	152	146
Hover Ceiling			
AEO (OGE) at INT PWR	Feet	5520	9000
OEI (IGE) at INT PWR	Feet	2050	4930
OEI (OGE) at INT PWR	Feet	(2)	920
Rate of Climb at SL			
Best R/C, AEO at XMSN P	FPM	2290	2290
Vert. R/C, AEO at INT PWR	FPM	1220	1400
Best R/C, OEI at INT PWR	FPM	1220	1700
Gross Weight			
Max. Hover (OGE at SL)	Pounds	132,000	134,600
Max. Hover (OGE at 4000')	Pounds	125,200	129,200
Payload (3)			
Max. Hover G.W. (OGE at SL)	Tons	24.9	26.2
Max. Hover G.W (OGE at 4000')	Tons	21.8	23.8

NOTES: (1) At "No-Load" Gross Weight of 82,000 pounds.

(2) Max. G.W. For OEI (OGE) Hover at SL/95° is 112,200 pounds.

(3) External payload for two 25-naut mi sorties per primary mission description in addition to 3500 pounds of flight test instrumentation. Weight empty =65,823 pounds.

2.3.3 Mission Definition and Performance

The primary mission is shown below.

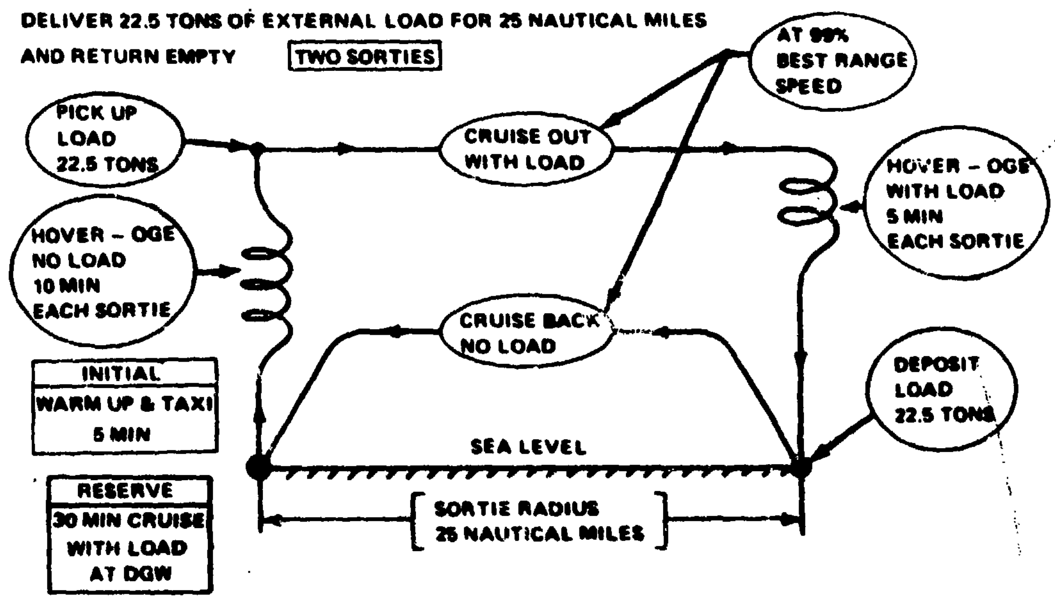

Mission performance for the primary mission is presented in Table 3A. Mission fuel is based upon performing the mission at sea level/95°F since it is more critical than sea level standard. Warm-up and take-off fuel is equivalent to five minutes of hover IGE, at design gross weight, and is considered to be burned off prior to critical hover performance required at mission gross weight. The stipulated payload is carried externally and does not include 3500 pounds of flight test equipment, which is considered to be part of the fixed useful load.

2.3.4 Payload - Radius

Endurance capabilities of the prototype HLH are presented in Figure 11 in terms of payload, total mission radius, and total hover time at sea level standard conditions for design gross weight and maximum hover OGE gross weight. Mission endurance consists of a 40%-60% split between hover and cruise, respectively, which relates to the proportions of hover and cruise for the primary mission.

TABLE 3A. PRIMARY MISSION LOADING TABLE

MISSION CONDITIONS		
T/O Cond. (Altitude/Temperature)	SL/95°F	
Payload (lb)	45000	
Radius (naut mi)	25	
Number of Sorties	2	
MISSION WEIGHTS (lb)		
Gross Weight (Initial)	82710	
Gross Weight (Mission)	127064	
Weight Empty	65823	(1)
Initial Fuel (Int.)	11991	
Mission Fuel (Int.)	11345	
Initial Fuel (Aux.)	0	
Mission Fuel (Aux.)	0	
Payload	45000	(2)
Fixed Useful Load	1342	
MISSION FUEL SEGMENTS (lb)		
Warm-up and Taxi	646	
Hover Fuel with P/L	1450	
Hover Fuel no P/L	1893	
Cruise Fuel with P/L	2928	
Cruise Fuel no P/L	2114	
Reserve Fuel	2960	

NOTES:

(1) Includes 3554 lb of Flight Test Instrumentation

(2) External Payload

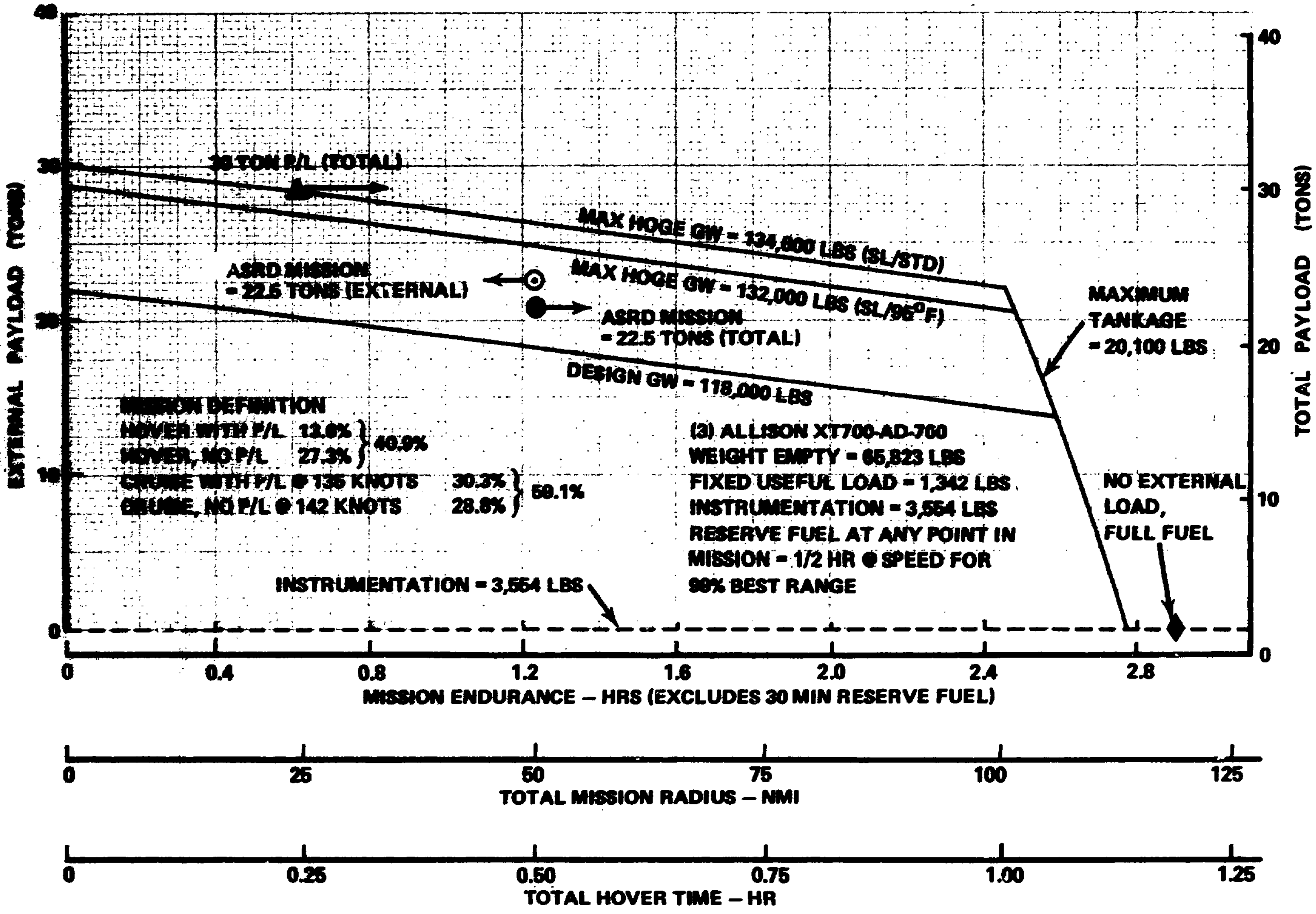

Figure 11. Prototype endurance.

2.3.5 Cruise Performance. Power required and specific range data are presented in Figures 12 and 13 for both the basic aircraft and for an additional parasite drag of 100 square feet, assumed for the drag of the external load. Data shown is for sea level/95°F ambient (Figure 12) and sea level, standard temperature (Figure 13).

2.3.6 Hover power required. Hover power required without vertical drag of the payload for standard temperature and 95°F ambients are shown in Figure 14 as a function of gross weight. These data are shown for hover OGE and hover IGE at a wheel height of 10 feet. Comparable power required for hover with external load may be computed by increasing indicated power by 2.15% for out-of-ground effect hover only. No increase is required for hover in ground effect.

2.3.7 Airspeed limits. Airspeed capability is shown in Figure 15 for both standard atmosphere and 95°F temperature as a function of altitude at design gross weight with external load. These data include the fatigue endurance rotor limit (stall flutter with pitch damping), flying qualities (1.15 g) limit, MAX CONT PWR limit, transmission power limit, and airframe structural limit. Also shown is speed for best climb and highest speed for 99% best range.

2.3.8 Hover Ceiling. Hovering ceiling data for 95°F and standard atmosphere is shown in Figure 16. Performance is shown for all engines operating and with one engine inoperative for OGE and IGE hover at INT PWR.

2.3.9 Rate of climb. Vertical and best (forward flight) rate of climb capabilities are shown in Figure 17.

2.3.10 Engine characteristics. Installed engine shaft horsepower available and installed fuel flow characteristics are shown in Figures 18, 19, and 20. The aircraft transmission power limits are also indicated.

Installed engine characteristics presented include a 1.4% inlet pressure loss and losses due to engine air bleed for the cargo hoist and environmental control system. No losses are included for infrared suppression devices or air particle separators.

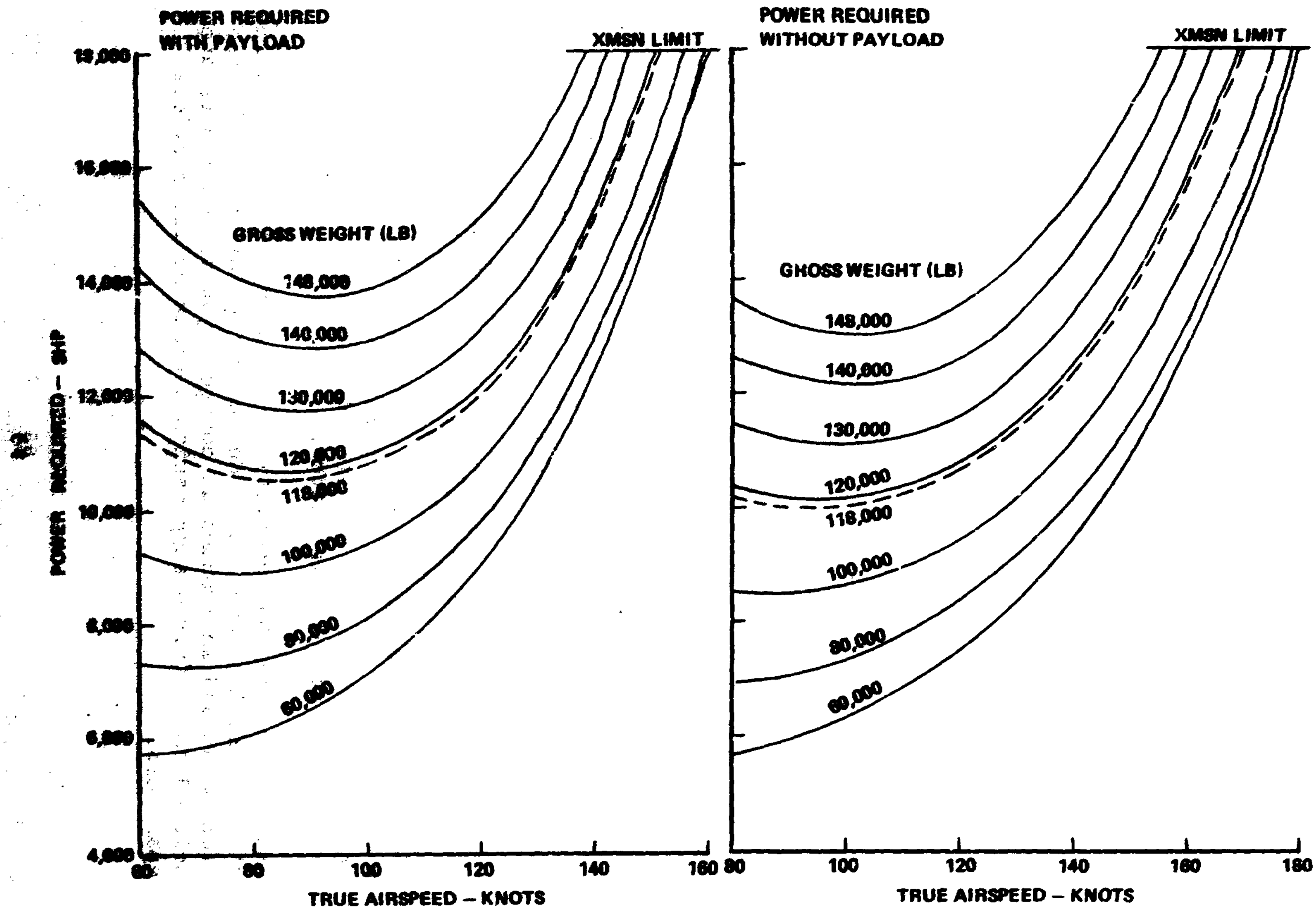

Figure 12. Power required and specific range at sea level – 95°F.

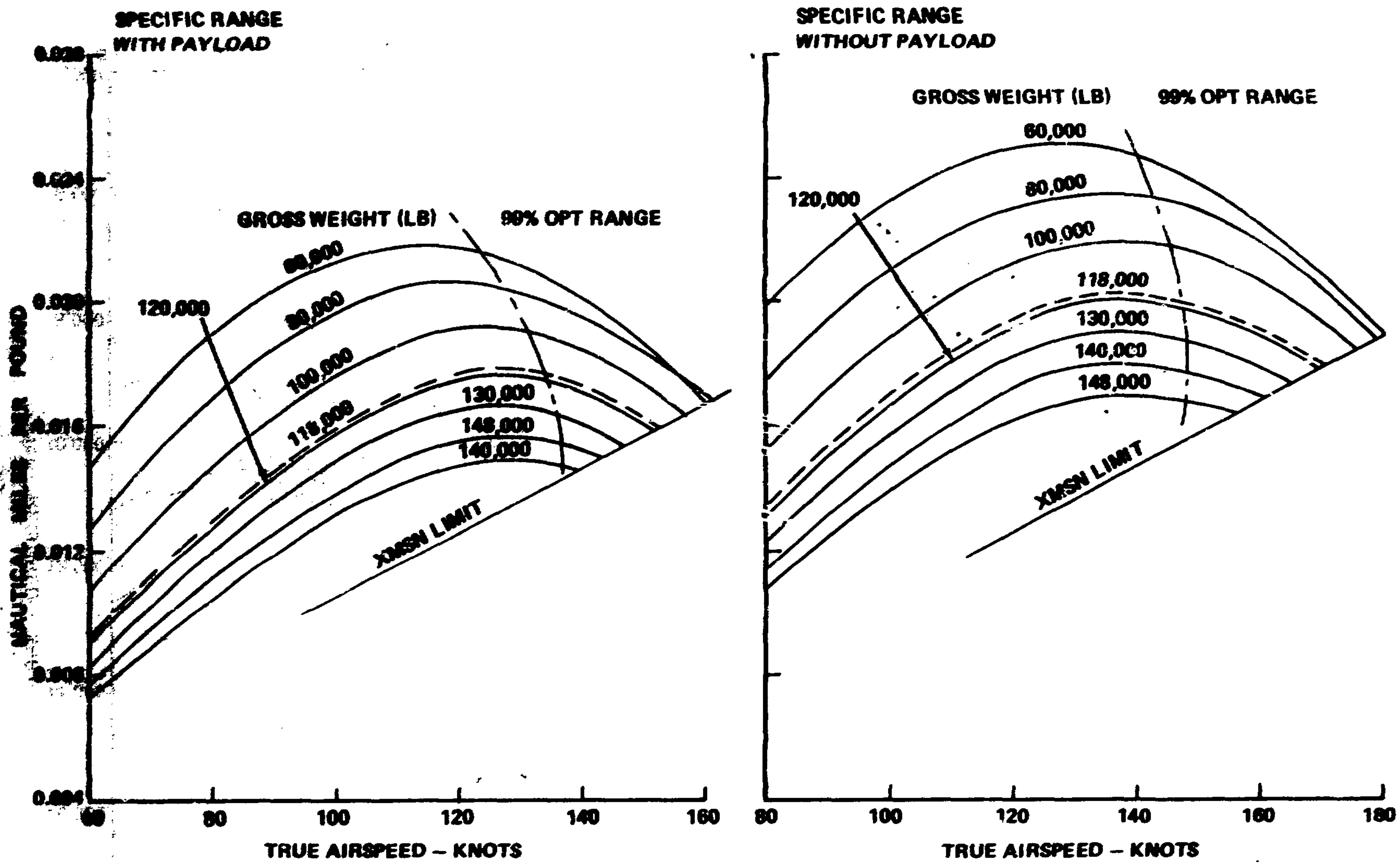

Figure 12. (Continued)

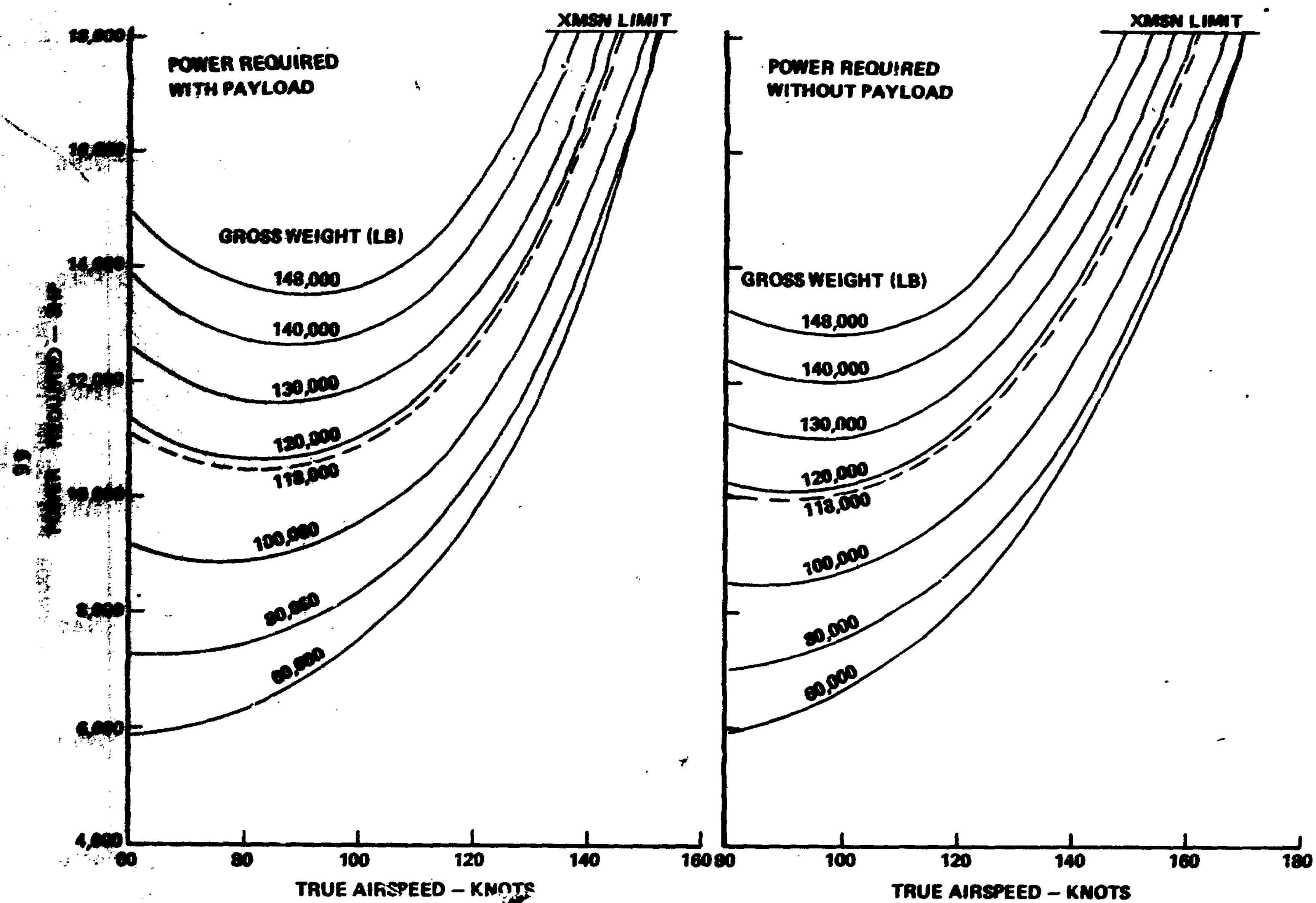

Figure 13. Power required and specific range at sea level – standard day.

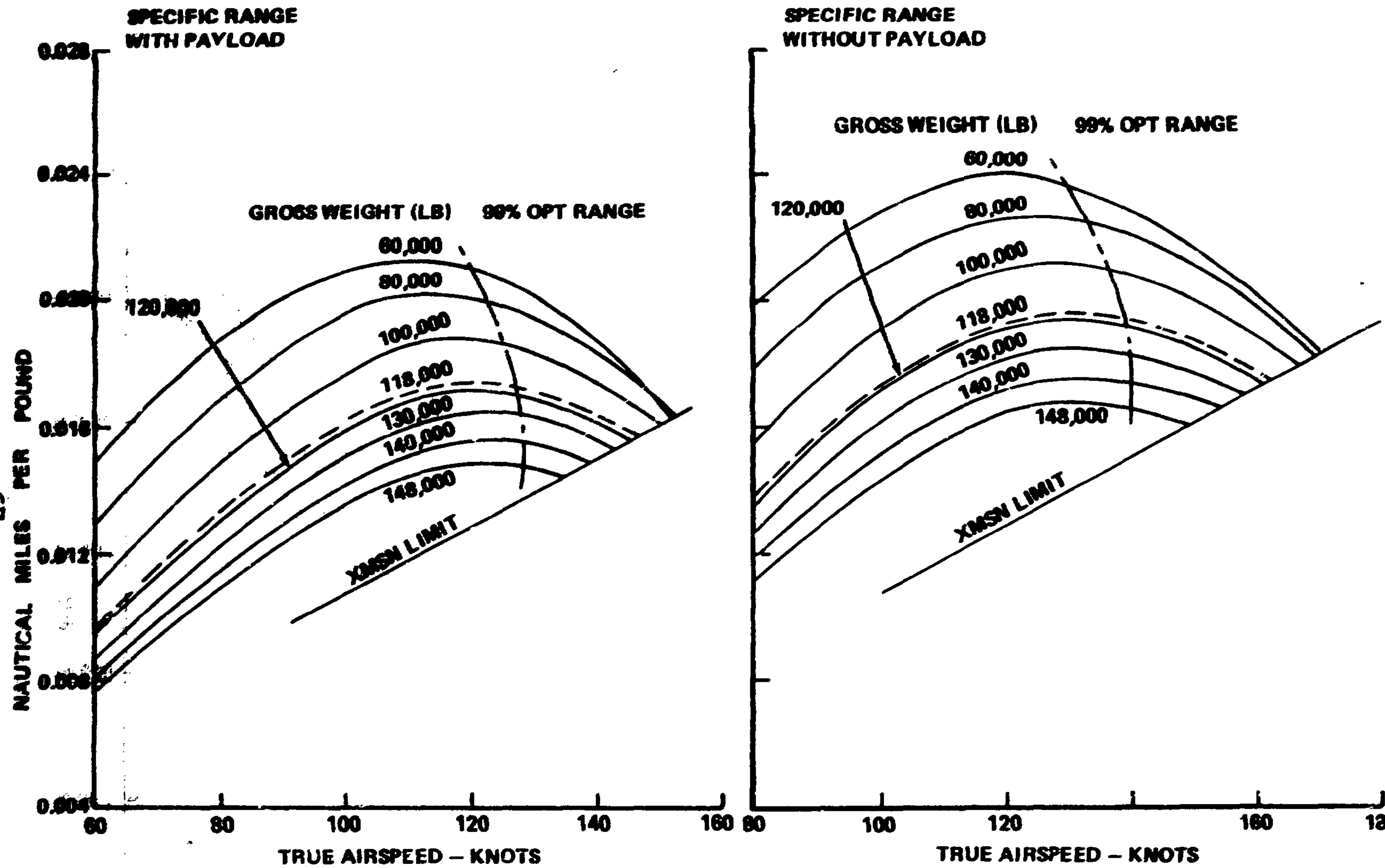

Figure 13. (Continued)

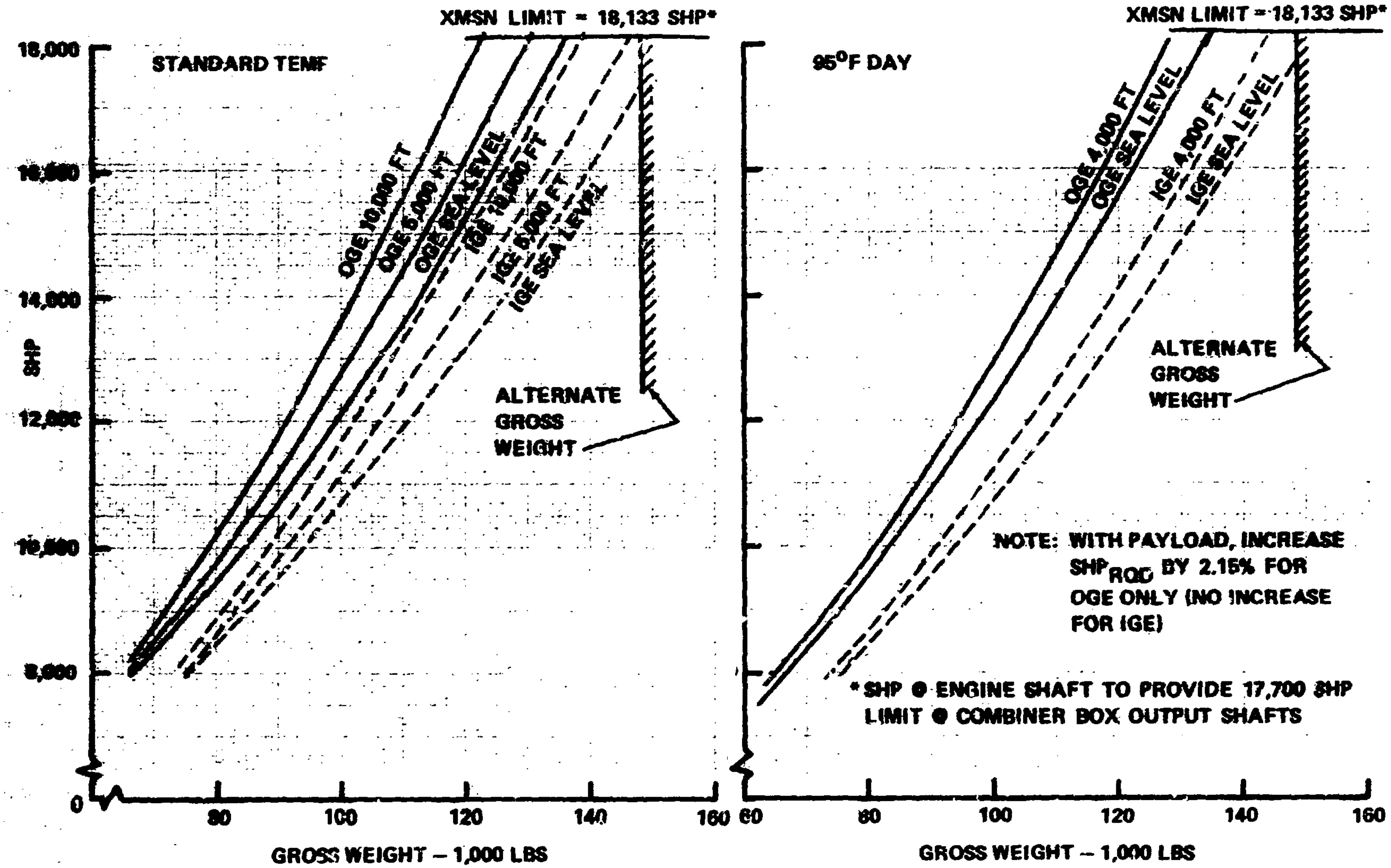

Figure 14. Hover power polars without vertical drag of payload.

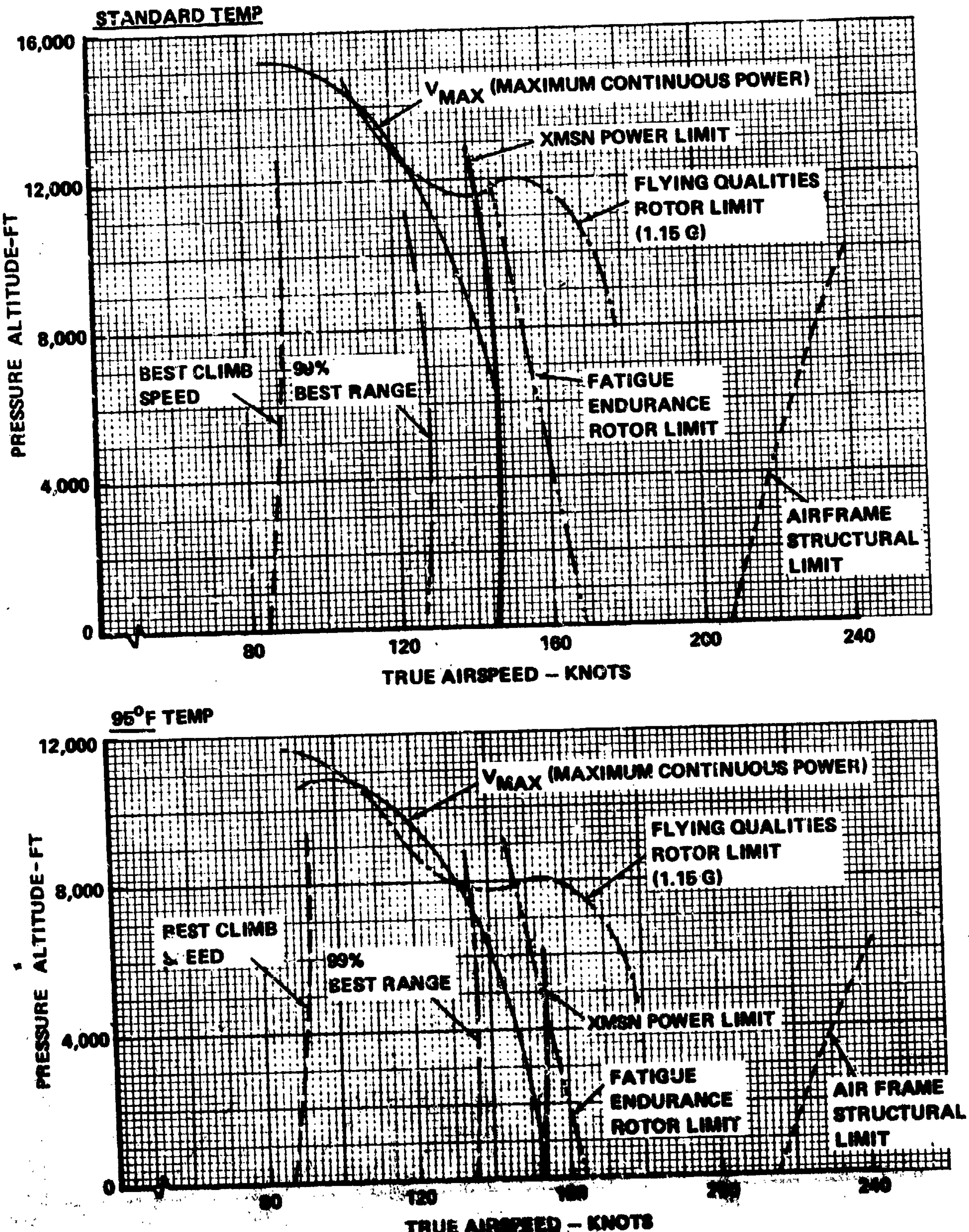

Figure 15. Airspeed limits at design gross weight with external load.

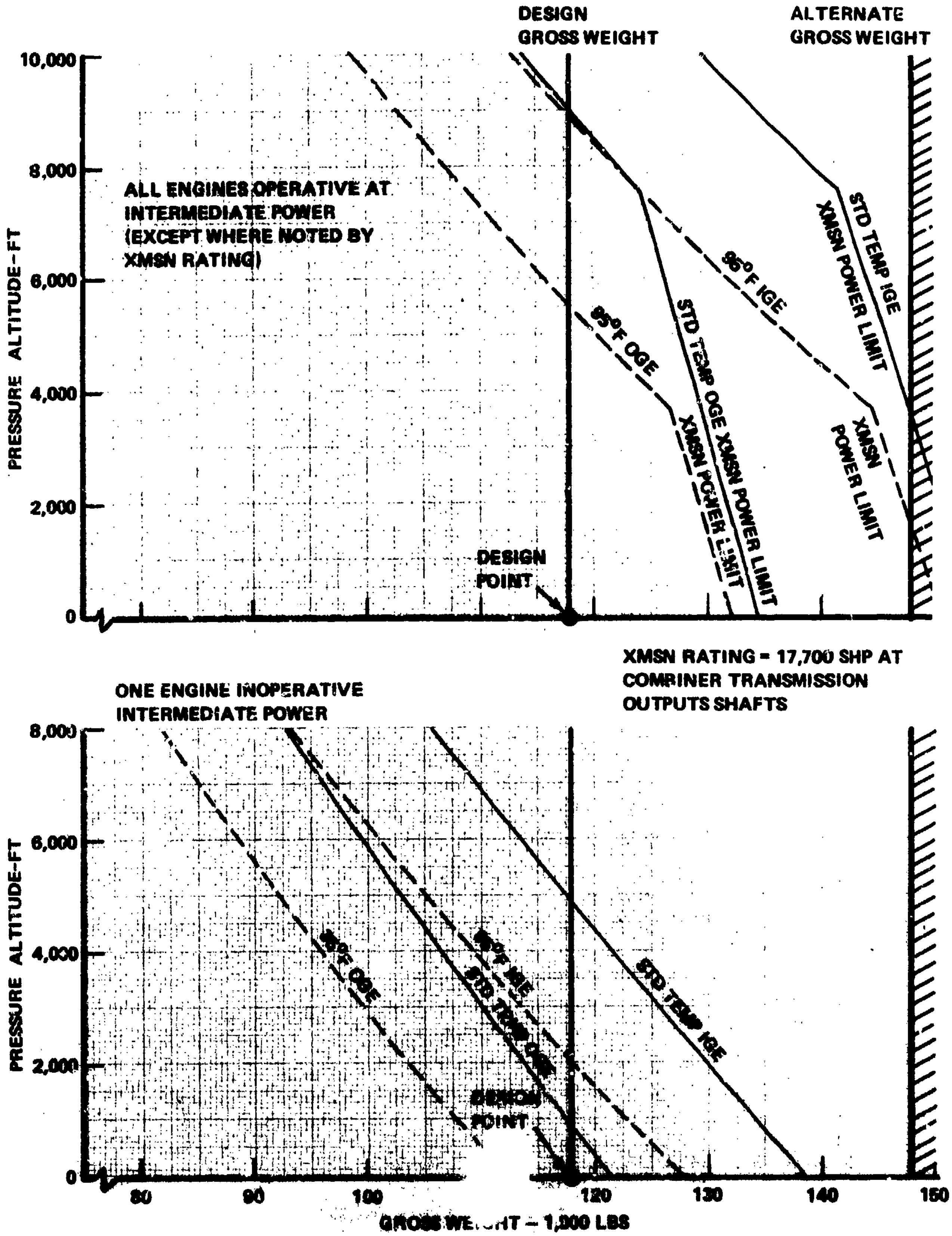

Figure 16. Hover ceiling.

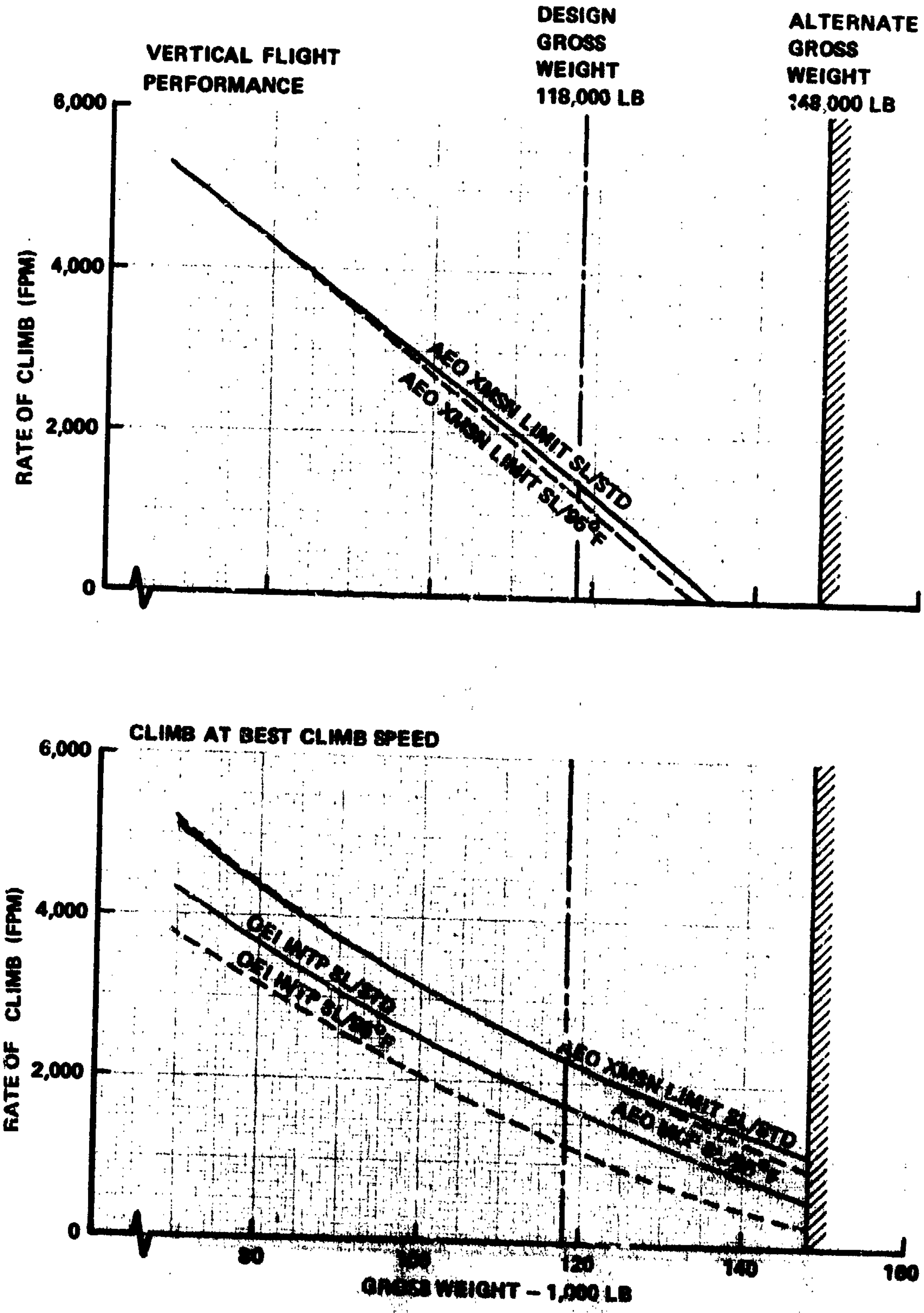

Figure 17. Climb performance.

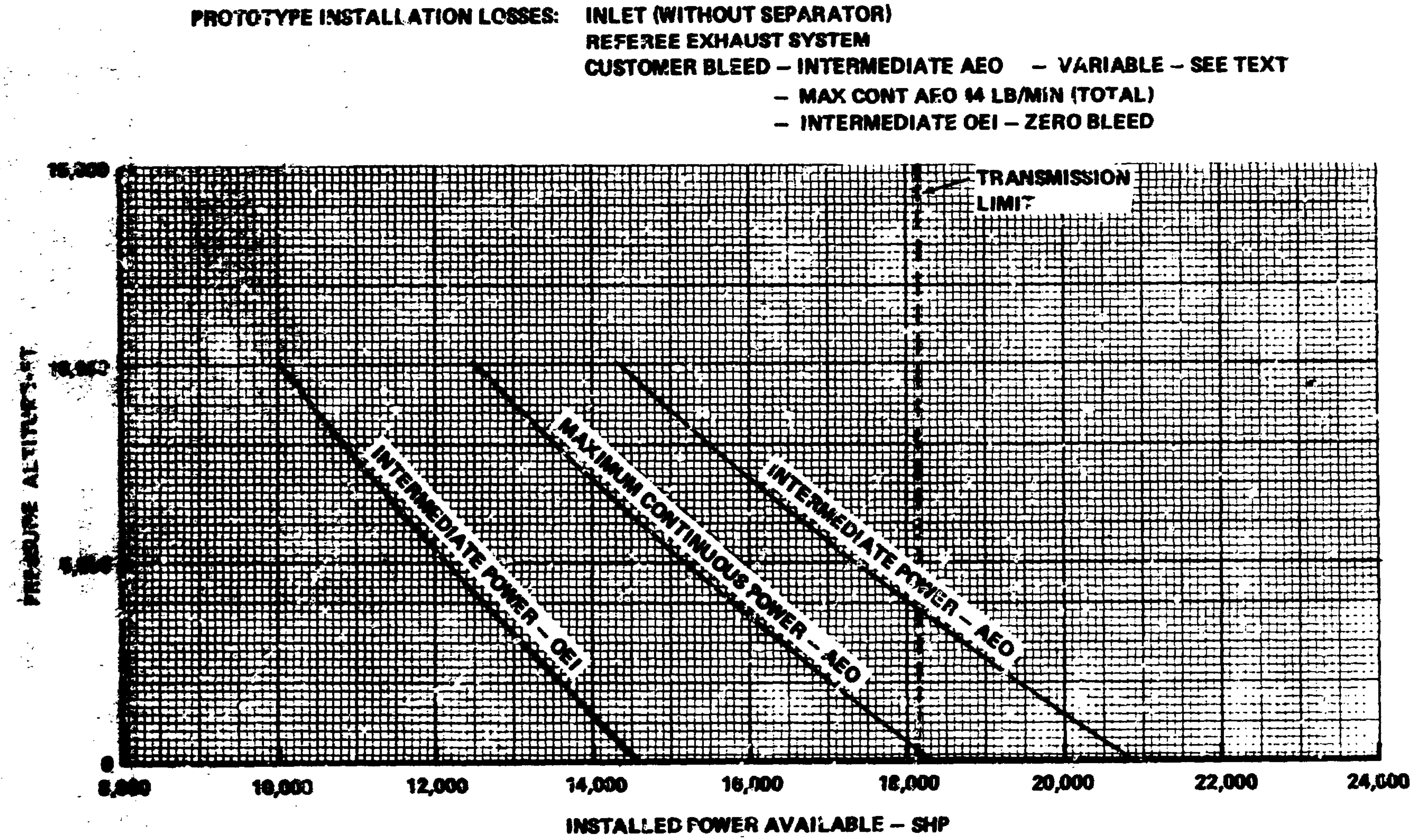

Figure 18. XT701-AD-700 engine static installed power – 95°F, zero to 10,000 feet.

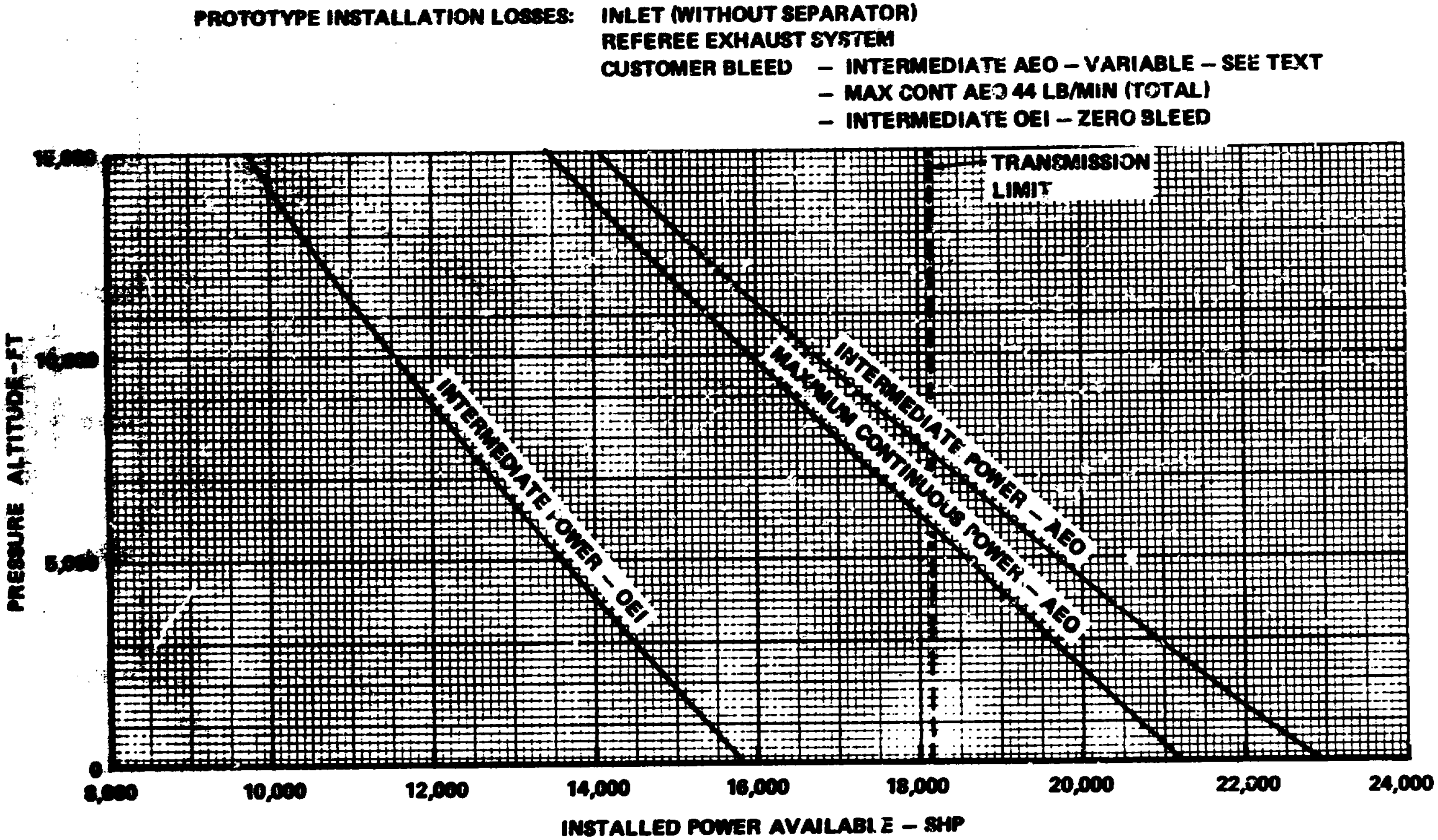

Figure 19. XT701-AD-700 engine static installed power – standard day, zero to 15,000 feet.

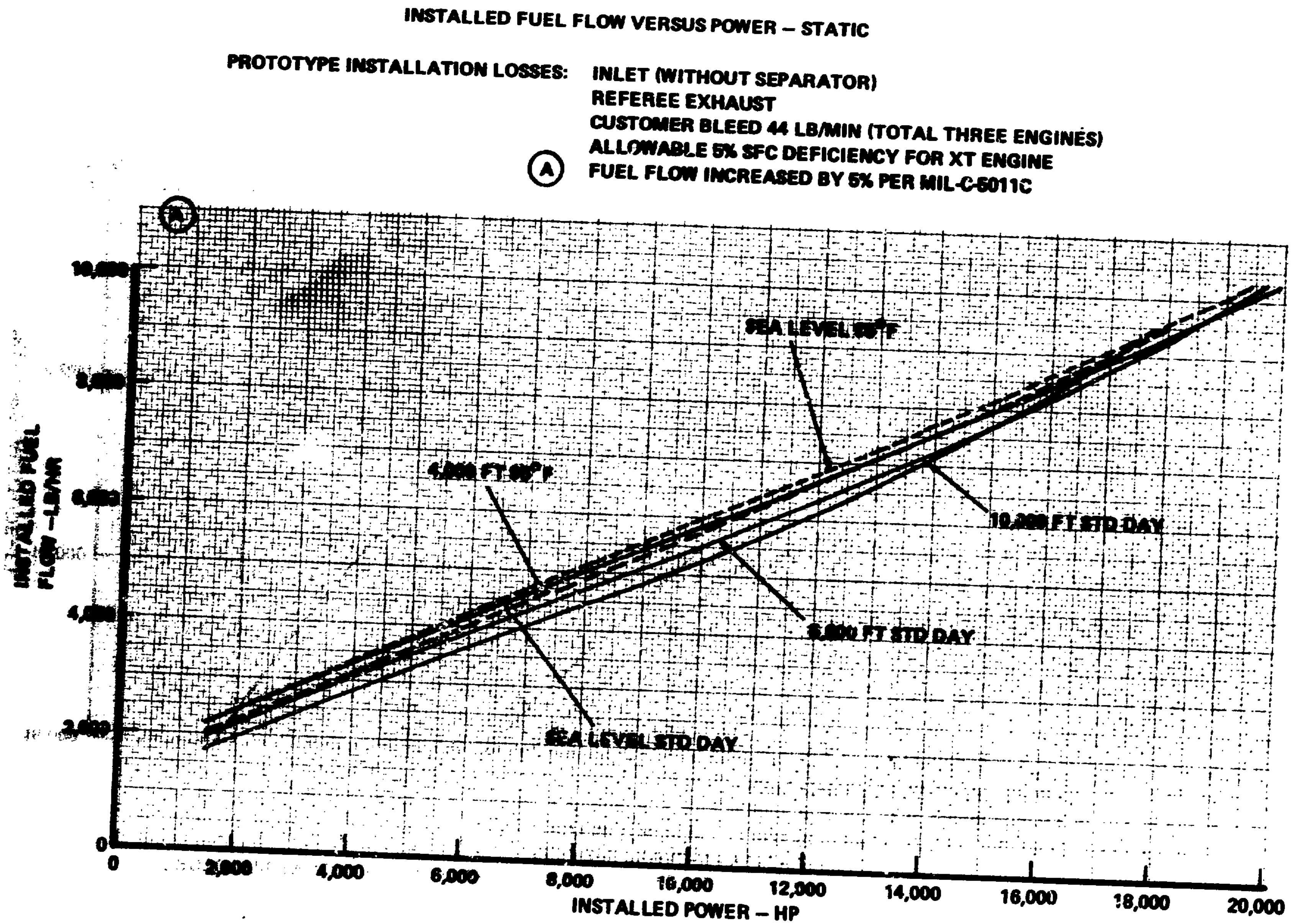

Figure 20. XT701-AD-700 engine (three engines) installed fuel flow versus power.

2.4 WEIGHT AND BALANCE

2.4.1 Classification. The weight and balance classification as defined in MIL-W-25140 is 1B.

2.4.2 Weight and balance summary. A summary of center of gravity locations for pertinent aircraft loading conditions is presented in Table 4.

2.4.3 Weight. A summary weight statement, in the format of MIL-STD-451, Part I, is presented in Table 5. The last status report prior to cancellation of the contract is also presented.

2.4.4 Center of gravity envelope. The center of gravity limits permissible in flight are as follows:

Gross Weight	Extreme Fwd.	Extreme Aft.
112,000 pounds	Sta. 559.5	Sta. 659.5
118,000 pounds	Sta. 566.5	Sta. 659.5
120,000 pounds	Sta. 569.5	Sta. 658.5
148,000 pounds	Sta. 574.5	Sta. 649.5

The C.G. design limits are shown in Figure 21.

The C.G. envelope is based on the maximum HOGE (SL/STD) Gross Weight. The loading condition is as follows:

a. Winches at fixed distance apart (Sta. 480 and 696)

b. Instrumentation allowance 3500 pounds

c. Fuel - 10,555 pounds

d. Cargo - 56,500 pounds- split 60/40 forward and 40/60 aft

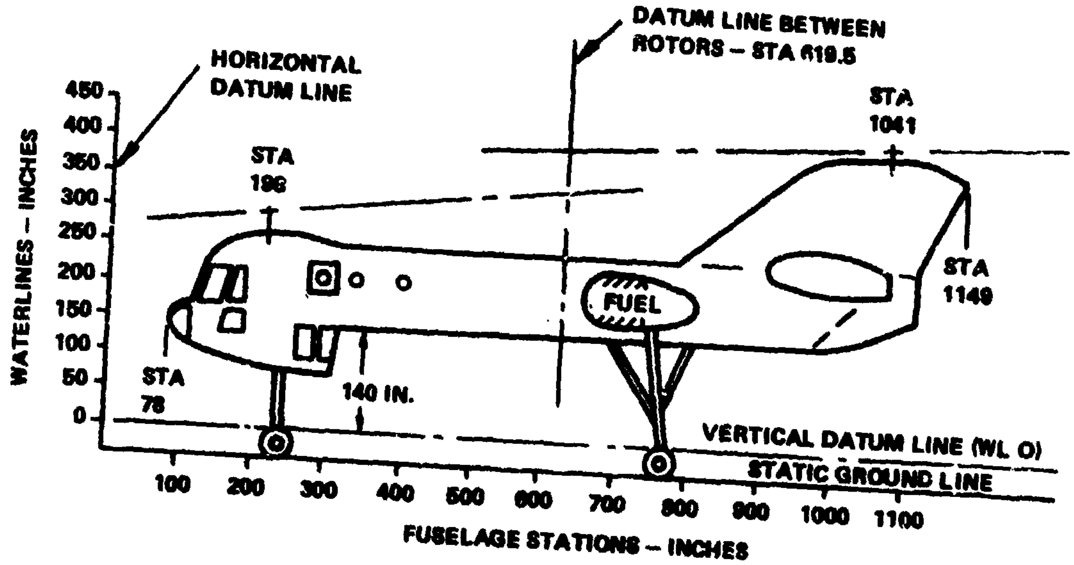

TABLE 4 . DIMENSIONAL DATA AND WEIGHT AND CG SUMMARY

LOAD CONDITION	WEIGHT (LB)	HORIZONTAL CG		VERT CG
		STATION	FWD (–) ON AFT (+) OFF REF LINE BETWEEN ROTORS (IN.)	WATERLINE
WEIGHT EMPTY – STATIC GROUND LINE	60,165	631.3	+ 11.8	244.0
MINIMUM FLYING WEIGHT	66,240	608.2	– 11.3	238.4
DESIGN GROSS WEIGHT MISSION	118,000	607.7	– 11.8	214.4
PRIMARY ASRD MISSION	121,087	607.2	– 12.3	213.8
GROSS WEIGHT – MAX FUEL NO PAYLOAD	86,104	626.3	+ 6.8	231.2
GROSS WEIGHT – MAX HOGE SL/STD	124,000	606.9	– 12.6	210.8
– MOST FWD CG	122,740	589.0	–30.5	212.4
– MOST AFT CG	134,000	615.9	– 3.6	210.6

TABLE 5. WEIGHT STATEMENT

01							
02	ROTOR GROUP						14679.7
03	FLARE ASSEMBLY					7419.9	
04	HUB					2012.0	
05	HINGE AND BLADE RETENTION					5247.8	
06	- FLAPPING				109.0		
07	- LEAD LAG				1571.8		
08	- PITCH				3285.0		
09	- FOLDING				282.0		
10	WING GROUP						
11	WING PANELS-BASIC STRUCTURE						
12	CENTER SECTION-BASIC STRUCTURE						
13	INTERMEDIATE PANEL-BASIC STRUCTURE						
14	OUTER PANEL-BASIC STRUCTURE-INCL TIPS			LBS			
15	SECONDARY STRUCT-INCL FOLD MECH			LBS			
16	AILERONS - INCL BALANCE WTS			LBS			
17	FLAPS						
18	-TRAILING EDGE						
19	-LEADING EDGE						
20	SLATS						
21	SPOILERS						
22							
23	TAIL GROUP						
24	TAIL ROTOR						
25	- BLADES						
26	- HUB						
27	STABILIZER - BASIC STRUCTURE						
28	FINS - BASIC STRUCTURE - INCL DORSAL			LBS			
29	SECONDARY STRUCTURE - STABILIZER AND FINS						
30	ELEVATOR - INCL BALANCE WEIGHT			LBS			
31	RUDDER - INCL BALANCE WEIGHT			LBS			
32							
33	BODY GROUP						9144.9
34	FUSELAGE OR HULL - BASIC STRUCTURE					5979.9	
35	BOOMS - BASIC STRUCTURE						
36	SECONDARY STRUCTURE - FUSELAGE OR HULL					1065.0	
37	- BOOMS						
38	- DOORS, PANELS & MISC					2100.0	
39							
40							
41	ALIGHTING GEAR - LAND TYPE						6432.0
42	LOCATION	*ROLLING	STRUCT	CONTROLS			
43		ASSEMBLY					
44	MAIN	1024.0	3733.0	65.0		4865.0	
45	AUXILIARY	462.0	961.0	144.0		1567.0	
46							
47							
48							
49							
50	ALIGHTING GEAR GROUP - WATER TYPE						
51	LOCATION	FLOATS	STRUTS	CONTROLS			
52							
53							
54							
55							
56							
57							

* WHEELS, BRAKES, TIRES, TUBES AND AIR

TABLE 5. (Continued)

01							
02							
03							
04	INSTRUMENT AND NAVIGATIONAL EQUIPMENT GROUP						296.0
05	INSTRUMENTS					296.0	
06	NAVIGATIONAL EQUIPMENT						
07							
08							
09	HYDRAULIC AND PNEUMATIC GROUP						243.0
10	HYDRAULIC						
11	PNEUMATIC					243.0	
12							
13							
14	ELECTRICAL GROUP						655.0
15	A C SYSTEM					483.6	
16	D C SYSTEM					171.4	
17							
18							
19	ELECTRONICS GROUP						366.0
20	EQUIPMENT					118.0	
21	INSTALLATION					248.0	
22							
23							
24	ARMAMENT GROUP - INCL GUNFIRE PROTECTION				LBS		
25							
26	FURNISHINGS AND EQUIPMENT GROUP						1188.2
27	ACCOMMODATIONS FOR PERSONNEL					573.0	
28	MISCELLANEOUS EQUIPMENT X INCL				LBS BALLASTX	103.5	
29	FURNISHINGS					413.7	
30	EMERGENCY EQUIPMENT					98.0	
31							
32							
33							
34	AIR CONDITIONING AND ANTI-ICING EQUIPMENT						219.0
35	AIR CONDITIONING					211.0	
36	ANTI-ICING					8.0	
37							
38							
39	PHOTOGRAPHIC GROUP						
40	EQUIPMENT						
41	INSTALLATION						
42							
43	AUXILIARY GEAR GROUP						4155.0
44	AIRCRAFT HANDLING GEAR					139.0	
45	LOAD HANDLING GEAR					4016.0	
46	ATO GEAR						
47							
48							
49							
50							
51							
52							
53							
54	MANUFACTURING VARIATION						
55							
56							
[illegible]							60167.5

TABLE 5. (Continued)

01							
02	FLIGHT CONTROLS GROUP						5271.0
03	COCKPIT CONTROLS					271.0	
04	AUTOMATIC STABILIZATION					949.0	
05	SYSTEM CONTROLS - ROTOR - NON ROTATING					2613.1	
06	- ROTATING					1437.9	
07	- FIXED WING						
08							
09							
10	ENGINE SECTION OR NACELLE GROUP						750.0
11	INBOARD						
12	CENTER					114.0	
13	OUTBOARD					404.0	
14	DOORS, PANELS AND MISC					232.0	
15							
16	PROPULSION GROUP						16717.7
17			X AUXILIARY	XX	MAIN	X	
18	ENGINE INSTALLATION					3564.0	
19	ENGINE				3564.0		
20	TIP BURNERS						
21	LOAD COMPRESSOR						
22	REDUCTION GEAR BOX, ETC						
23	ACCESSORY GEAR BOXES AND DRIVES						
24	SUPERCHARGER-FOR TURBOS						
25	AIR INDUCTION SYSTEM					228.0	
26	EXHAUST SYSTEM					90.0	
27	COOLING SYSTEM						
28	LUBRICATING SYSTEM					30.0	
29	TANKS						
30	BACKING BD,TANK SUP & PADDING						
31	COOLING INSTALLATION						
32	PLUMBING, ETC				30.0		
33	FUEL SYSTEM					2584.2	
34	TANKS - UNPROTECTED						
35	- PROTECTED				1735.0		
36	BACKING BD,TANK SUP & PADDING				215.0		
37	PLUMBING, ETC				634.2		
38	WATER INJECTION SYSTEM						
39	ENGINE CONTROLS					89.0	
40	STARTING SYSTEM					131.0	
41	PROPELLER INSTALLATION						
42	DRIVE SYSTEM					10001.5	
43	GEAR BOXES				7907.8		
44	LUBE SYSTEM				951.7		
45	CLUTCH AND MISC				183.0		
46	TRANSMISSION DRIVE				959.1		
47	ROTOR SHAFT						
48	JET DRIVE						
49							
50							
51							
52	AUXILIARY POWER PLANT GROUP						50.2
53							
54							
55							
56							
57							

TABLE 5. (Continued)

01	LOAD CONDITION			MAX HOGE	DGW	PRIMARY	MAX. FUEL
02				GW	MISSION	ASRD	NO. P/L
03	CREW - NO. 5/5/5/5			1200	1200	1200	1200
04	PASSENGERS - NO.						
05	FUEL ▷ LOCATION	TYPE	GALS				
06	UNUSABLE	JP-4	13/13/13/13	84	84	84	84
07	INTERNAL	JP-4	2006 / 1675	13036	10887		
08	INTERNAL	JP-4	1688 / 3092			10973	20100
09							
10							
11	EXTERNAL-AUX. SIDE FUS.						--
12							
13	-FERRY BOT. FUS.						--
14							
15	BOMB BAY						
16							
17							
18							
19	OIL						
20	UNUSABLE	MIL-L23699	2.10	16	16	16	16
21	ENGINE	MIL-L-23699	5.4	42	42	42	42
22	AUXILIARY FUEL TANKS						--
23	FERRY FUEL TANKS						--
24	AERIAL REFUEL PROBE INSTL.						--
25	BAGGAGE						
26	CARGO			56500	△ 42049	⊙ 45000	--
27	FLIGHT TEST EQUIPMENT			3554	3554	3554	3554
28	ARMAMENT						
29	GUNS-LOCATION	TYPE**	QUANTITY CALIBER				
30							
31	△ TOTAL PAYLOAD 45603 POUNDS						
32	⊙ EXTERNAL PAYLOAD ONLY						
33							
34	AMM						
35							
36							
37							
38	BOMB INSTL*						
39	BOMBS						
40							
41	TORPEDO INSTL*						
42	TORPEDOES						
43							
44	ROCKET INSTL*						
45	ROCKETS						
46							
47	EQUIPMENT-PYROTECHNICS						
48	-PHOTOGRAPHIC						
49							
50	-*OXYGEN						
51							
52	-MISCELLANEOUS						
53							
54							
55	USEFUL LOAD						
56	WEIGHT EMPTY			60168	60168	60168	60168
57	GROSS WEIGHTS - PAGES 2-5			[illegible]	118000	121037	[illegible]

* IF NOT SPECIFIED AS WEIGHT EMPTY ** FIXED, FLEXIBLE, ETC.

▷ NO WARM UP AND TAXI FUEL INCLUDED IN FUEL TOTALS

MIL-STD- 1 PART III

WEIGHT AND BALANCE STATUS — ROTORCRAFT

MODEL XCH-62
ENGINE ALLISON XT701-AD-700
CONTRACT NUMBER DAAJ01-71-C-0840(P6A)
DATE 15 AUGUST 1974
ISSUE STATUS NO. 4

		ORIGINAL GUAR OR ORIGINAL SPEC NO. D301-10115-1 DATED 10/31/73	GOVT RESPON-SIBILITY CHANGES AUTH. PENDING, & GFAE VARIA-TIONS	REVISED GUAR OR PROPOSED SPEC SUM COLUMNS 2 & 3	TOTAL CON-TRACTOR RESPON-SIBILITY CHANGES VARIA-TIONS COLUMN 6 MINUS COLUMN 4	CURRENT STATUS SUM COLUMNS 4 & 5 AND SUM COLUMNS 7, 8 & 9	LAST STATUS D301-10115-2.3 DATED 4-22-74 ISSUE 3	CHANGE BETWEEN LAST & CURRENT STATUS REPORTS: TOTAL GOVT RESPON-SIBIL-ITY CHANGES GFAE VARIA-TIONS	CHANGE BETWEEN LAST & CURRENT STATUS REPORTS: TOTAL CON-TRACTOR RESPON-SIBIL-ITY CHANGES	BASIS FOR CURRENT DATA PERCENTAGE: EST	BASIS FOR CURRENT DATA PERCENTAGE: CALC	BASIS FOR CURRENT DATA PERCENTAGE: ACT
	1	2	3	4	5	6	7	8	9	10	11	12
1	ROTOR GROUP	14680		14680	-553	14127	14108		+19	3.5	21.0	75.5
2	BLADE ASSEMBLY+ PENDULUM ABSORB.	7420		7420	-754	6666	6647		+19	0.0	11.7	88.3
3	HUB	2012		2012	- 48	1964	1964			0.7	3.9	95.4
4	HINGE AND BLADE RETENTION	5248		5248	+249	5497	5497			8.7	38.5	52.8
5												
6	WING GROUP	--		--		--	--					
7	WING PANELS-BASIC STRUCTURE											
8	SECONDARY STRUCT-INCL FOLD											
9	AILERONS											
10	FLAPS											
11	SLATS											
12	SPOILERS											
13												
14	TAIL GROUP	--		--		--	--					
15	TAIL ROTOR											
16	STABILIZER-BASIC STRUCTURE											
17	FINS-BASIC STRUCTURE											
18	SECONDARY STRUCT-STAB & FINS											
19	ELEVATOR-INCL BALANCE WEIGHT											
20	RUDDER-INCL BALANCE WEIGHT											
21												
22	BODY GROUP	9145		9145	+1769	10914	10687		+227	29.1	64.4	6.5
23	FUSELAGE OR HULL-BASIC STRUC	5980		5980	+2328	8308	7962		+346	20.0	72.2	7.8
24	BOOMS-BASIC STRUCTURE											
25	SECONDARY STRUCTURE-FUSELAGE	1065		1065	-58	1007	1046		- 39	28.5	65.8	5.7
26	-BOOMS											
27	-DOORS, PANELS, MISC.	2100		2100	-501	1599	1679		- 80	76.5	23.4	0.1
28												
29	ALIGHTING GEAR-LAND TYPE	6432	+187	6519	+673	7292	7216	0	+76	55.9	41.4	2.7
30	MAIN LANDING GEAR	4865	+149	5014	+706	5720	5641	0	+79	55.0	43.0	2.0
31	AUX. LANDING GEAR	1567	+ 38	1605	- 33	1572	1575		-3	59.2	35.5	5.3
32	-WATER TYPE											
33												
34												
35	FLIGHT CONTROLS	5271	-54	5217	+1019	6236	6293	+15	-72	53.6	34.0	12.4
36												
37	ENGINE SECT. OR NACELLE GROUP	750		750	+1102	1852	1362		+490	50.5	45.4	4.1
38												
39	PROPULSION GROUP	16718	-49	16669	+683	17308	17256	+44	+ 8	6.4	69.5	24.1
40	ENGINE INSTALLATION	3564	- 96	3468		3468	3468			0.0	100.0	0.0
41	ENGINES											
42	TIP BURNERS											
43	LOAD COMPRESSOR											
44	REDUCTION GEAR BOX, ETC.											
45	ACCESSORY GEAR BOXES & DRIVE											
46	SUPERCHARGER-FOR TURBOS											
47	AIR INDUCTION SYSTEM	228		228	+ 93	321	273		+48	22.8	77.2	0.0
48	EXHAUST SYSTEM	90		90	+ 26	116	70		+46	4.2	95.1	0.7
49	COOLING SYSTEM	-		-		-	-					
50	LUBRICATING SYSTEM	30		30	- 20	10	30		-20	100.0	0.0	0.0
51	FUEL SYSTEM	2584		2584	- 41	2543	2611		-68	14.4	84.8	0.8
52	WATER INJECTION SYSTEM	-		-		-	-					
53	ENGINE CONTROLS	89	+3	92	- 24	68	68			77.0	22.9	0.1
54	STARTING SYSTEM	131	+44	175	+ 28	159	115	+44		19.5	80.5	0.0
55	PROPELLER INSTALLATION	-		-		-	-			-	-	-
56	DRIVE SYSTEM	10002		10002	+621	10623	10621		+2	5.4	55.5	39.1
57	GEAR BOXES	7908		7908	+557	8465	8482		-17	4.3	61.8	34.0
58	LUBRICATION SYSTEM	952		952	+37	989	993		- 4	18.1	33.0	48.9
59	CLUTCH & MISCELLANEOUS	183		183	+ 1	184	184			13.0	59.1	27.9
60	TRANSMISSION DRIVE	959		959	+26	985	962		+2[illegible]	0.3	23.8	75.9
61	ROTOR SHAFT											
62	JET DRIVE											
63												

37	ENGINE SECT. OR NACELLE GROUP	750		750	+1102	1852	1362		+490	50.5	45.4	4.1
38												
39	PROPULSION GROUP	16718	-49	16669	+683	[illegible]	17256	+44	+ 8	6.4	[illegible]	74.1
40	ENGINE INSTALLATION	3564	- 96	3468		3468	3468			0.0	100.0	0.0
41	ENGINES											
42	TIP BURNERS											
43	LOAD COMPRESSOR											
44	REDUCTION GEAR BOX, ETC.											
45	ACCESSORY GEAR BOXES & DRIVE											
46	SUPERCHARGER-FOR TURBOS											
47	AIR INDUCTION SYSTEM	228		228	+ 93	321	273		+48	22.8	77.2	0.0
48	EXHAUST SYSTEM	90		90	+ 26	116	70		+46	4.2	95.1	0.7
49	COOLING SYSTEM	-		-		-	-					
50	LUBRICATING SYSTEM	30		30	- 20	10	30		-20	100.0	0.0	0.0
51	FUEL SYSTEM	2584		2584	- 41	2543	2611		-68	14.4	84.8	0.8
52	WATER INJECTION SYSTEM	-		-		-	-					
53	ENGINE CONTROLS	89	+3	92	- 24	68	68			77.0	22.9	0.1
54	STARTING SYSTEM	131	+44	175	+ 28	159	115	+44		19.5	80.5	0.0
55	PROPELLER INSTALLATION	-		-		-	-			-	-	-
56	DRIVE SYSTEM	10002		10002	+621	10623	10621		+2	5.4	55.5	39.1
57	GEAR BOXES	7908		7908	+557	8465	8482		-17	4.3	61.8	34.0
58	LUBRICATION SYSTEM	952		952	+37	989	993		- 4	18.1	33.0	48.9
59	CLUTCH & MISCELLANEOUS	183		183	+ 1	184	184			13.0	59.1	27.9
60	TRANSMISSION DRIVE	959		959	+26	985	962		+23	0.3	23.8	75.9
61	ROTOR SHAFT											
62	JET DRIVE											
63												
64	AUXILIARY POWER PLANT GROUP	50		50	- 50	0	0			0.0	0.0	0.0
65	INSTR & NAV EQUIPMENT GROUP	296	-10	286	- 65	221	216		+5	78.8	20.8	0.4
66	~~HYDRAULIC~~ & PNEUMATIC GROUP	243		243	- 52	191	203		-12	57.5	42.5	0.0
67	ELECTRICAL GROUP	655		655	- 83	572	586		-14	52.4	47.4	0.2
68	ELECTRONICS GROUP	366	- 3	363	- 82	281	282		- 1	50.6	47.8	1.6
69	ARMAMENT GROUP	0		0		0	0			0.0	0.0	0.0
70	FURNISHINGS & EQUIPMENT GROUP	1188	-20	1168	+ 44	1212	1247	0	-35	40.0	56.9	3.1
71	AIR COND & ANTI-ICING GROUP	219		219	+26	245	246		- 1	60.0	39.2	0.8
72	PHOTOGRAPHIC GROUP	--				--	--					
73	AUXILIARY GEAR GROUP	3901	-56	3845	-13	3832	3856		-24	4.4	2.8	92.8
74												
75	TOTAL-CONTRACTOR CONTROLLED	49775	+652	50427	+4374	54801	53483	+652	+669	26.4	43.2	30.4
76	TOTAL-GFAE	10139	-657	9482		9482	10075	-593		2.0	60.7	37.3
77	TOTAL-WEIGHT EMPTY	59914	- 5	59909	+4374	[illegible]	63558	+ 59	-666	22.8	45.5	31.4
78										SEE		
79	CREW (5)	1200		1200		[illegible]	[illegible]			INSTRUCTIONS		
80	PASSENGERS OR TROOPS									PAGES 2 & 3		
81	FUEL-UNUSABLE @ 6.5 LBS/GAL	84		84		84	84			MAC DATA		
82	-INTERNAL	11653	- 2	11653	+ 100	11751	11718	+ 3	+ 30	REF DATUM TO		
83	-EXTERNAL									L.E. MAC		
84	-BOMB BAY									INCHES		
85	OIL-UNUSABLE	16		16		16	16			MAC LENGTH		
86	-ENGINE	42		42		42	42			INCHES		
87										ROTOR DATA		
88										REF DATUM TO		
89										C ROTOR OR C		
90										BET ROTORS		
91	BAGGAGE									619.5 INCHES		
92	CARGO Δ {	41591	- 47	41544	-4474	37070	37828	- 62	-696			
93	FLIGHT TEST EQUIPMENT	3500	+ 54	3554		3554	3554					
94	ARMAMENT											
95												
96												
97	Δ TOTAL PAYLOAD	(45091)		(45098)		(40624)	(41382)					
98												
99	EQUIPMENT											
100	PYROTECHNICS											
101	PHOTOGRAPHIC											
102	OXYGEN											
103	MISCELLANEOUS											
104												
105	TOTAL-USEFUL LOAD	58086	+ 5	58091	-4374	53717	54442	- 59	-666			
106	GROSS WEIGHT	118000		118000		118000	118000					

CENTER OF GRAVITY DATA-INCHES FROM REFERENCE DATUM OR % M.A.C.

107	WEIGHT EMPTY - WHEELS DOWN	631.8	0.0	631.8	+ 3.9	635.7	634.9	-0.4	+1.2
108	GROSS WEIGHT - WHEELS DOWN	608.5	0.1	608.5	+ 3.9	612.4	611.6	-0.2	+1.0
109	GROSS WEIGHT - WHEELS UP	--	--	--	--	--	--	--	--
110	MOST FWD - WHEELS ~~UP~~-DOWN*	601.0	*DELETE INAPPLICABLE			605.6	604.7		
111	MOST AFT - WHEELS ~~UP~~-DOWN*	616.2	WHEEL POSITION			619.1	618.5		

RECOMMENDED CENTER OF GRAVITY LIMITS...MOST FWD-WH UP-DWN* %M.A.C. MOST AFT-WH UP-DWN* %M.A.C.
RECMD C.G.LIMITS.MOST FWD-WH ~~UP~~-DWN*60.0 INS.FROM REF.DATUM.MOST AFT-WH ~~UP~~-DWN*40.0 INS.FROM REF. DATUM
STATE SOURCE OF DATA IN INITIAL ISSUE, AND WHENEVER LIMITS ARE REVISED

2

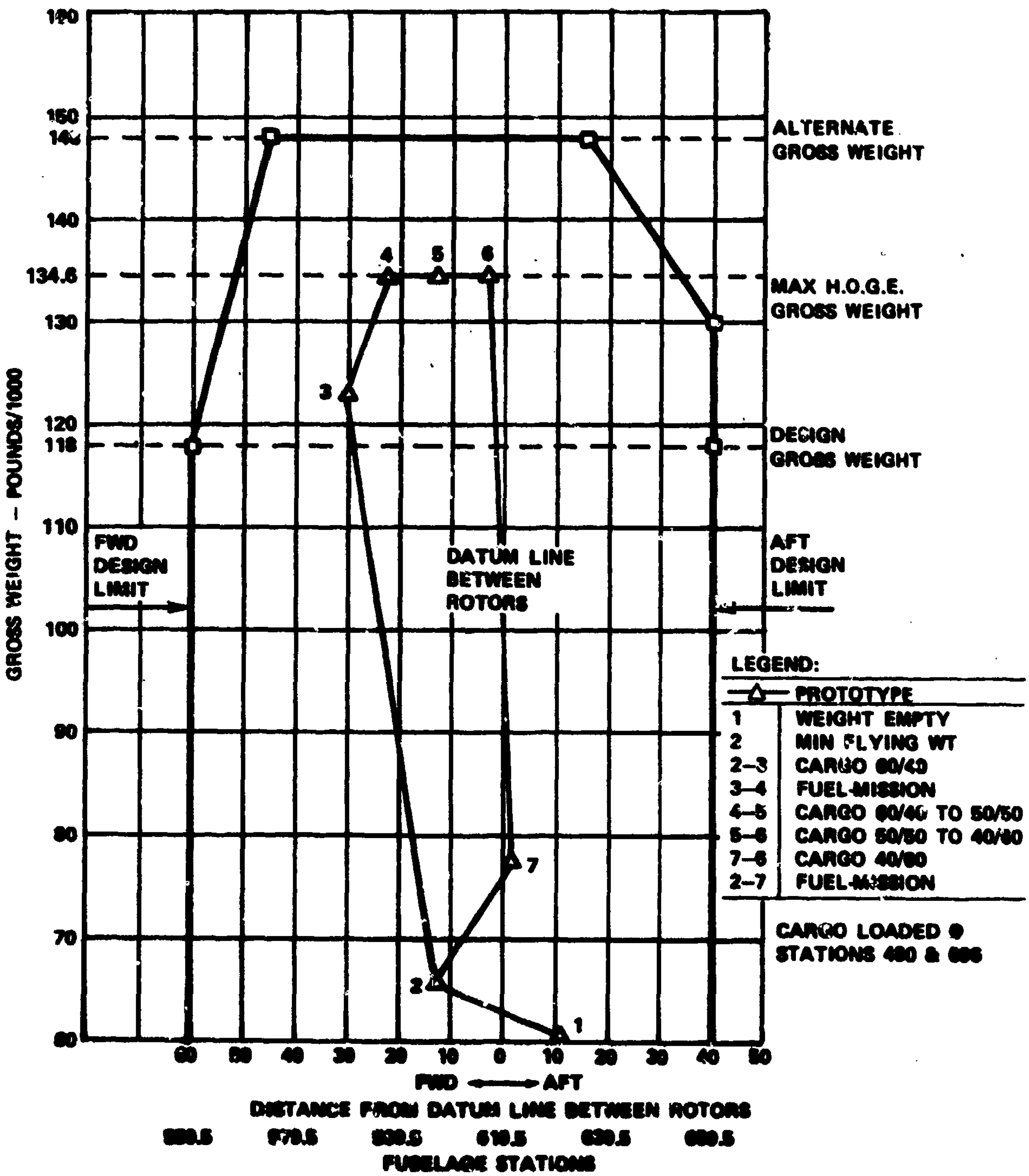

Figure 21. Center of gravity envelope and locations.

2.5 DESIGN DEVELOPMENT

2.5.1 General

The XT701-AD-700 Detroit Diesel Allison (DDA) engine was developed under separate contract with AVSCOM. Engine characteristics are specified in Specification 844B. The power management system was also developed by DDA as defined by Specification 845A.

Design reviews were held covering all subsystems of the prototype aircraft on 15, 16, 17, and 18 October and 5 December, 1973. The meetings were well attended by Government personnel and the interchange was constructive. Minutes were prepared and submitted to AVSCOM.

The Crew Station Mockup Review was held on 25 and 26 October 1973, attended by approximately 45 Government representatives. A total of 137 chits were prepared and 52 were approved for incorporation on the prototype, with 11 more assigned for study. Minutes were prepared and submitted to AVSCOM 16 November 1973.

A Prime Item Development Specification (PIDS) review was held on 30 and 31 October 1973. Minutes of the meeting and a revised PIDS incorporating the decisions of the meeting were submitted on 14 December 1973, and subsequently approved by the Government.

2.5.2 Design to Cost

The initial design-to-cost activities consisted of the development of a design-to-cost plan and identification of configuration features that, if eliminated or modified, would reduce system costs. The design-to-cost plan includes establishment of design-to-cost targets, tracking concepts, schedules for accomplishment, and documentation requirements. Figure 22 shows the design-to-cost program schedule. Table 6 shows the production aircraft cost estimates at the time of contract award, together with the original design-to-cost target.

Lower Level Targets

Targets were established at responsible engineer level and to the lower levels of the Work Breakdown Structure. Table 7 is a summary of the rotor system targets showing the responsible engineer and the target costs to the lowest level of the Work Breakdown Structure (8th level). Similar targets and responsibilities were established for all subsystems.

Monitor Costs

This element of the design-to-cost plan was a continuing effort. Cost tracking and visibility methodology was established for all subsystems. The airframe methodology of establishing part count targets was established at the detail drawing level. Table 8 is a summary sheet of the report issued on 1 April 1974, and Table 9 shows the differences from the previous report on 15 March 1974. Table 10 is an example of the detail visibility given to the responsible engineer.

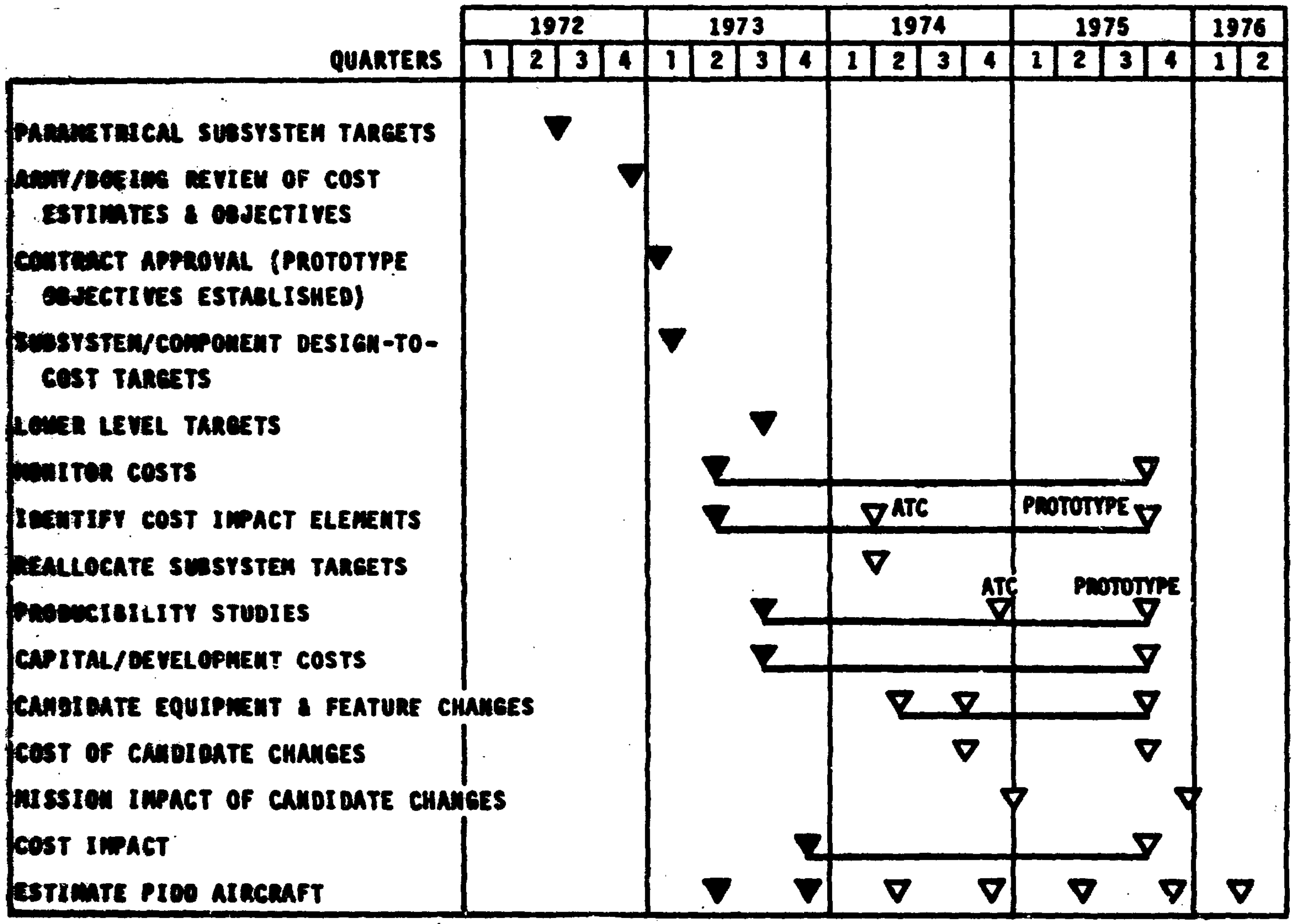

Figure 22. Design-to-cost program schedule.

TABLE 6. AIR VEHICLE PRICE

(Contractor Furnished Equipment)

FY 73 DOLLARS IN MILLIONS

	AVERAGE ESTIMATED PRICE
ROTOR/DRIVE	$1.468
CARGO	.472
FLIGHT CONTROLS	.614
FUSELAGE & LANDING GEAR	1.548
OTHER SUBSYSTEMS	.692
POWER PLANT	.095
COMMUNICATION/NAVIGATION	.018
INTEGRATION & ASSEMBLY	.961
TOTAL	$5.868
DESIGN-TO-COST OBJECTIVE	$5.105

TABLE 7. HLH DESIGN-TO-COST DETAIL TARGETS AND RESPONSIBILITY

	RESPONSIBLE ENGINEFR			TARGET PER/AC
ROTOR/DRIVE	R. Titus			$1,223,959
Rotor System	R. Titus			$ 771,559
Rotor Hub Assembly	F. Mamrol			$ 383,400
Rotor Hub	F. Mamrol		$ 83,754	
Loop Assembly	F. Mamrol		30,251	
Cross Beam	F. Mamrol		32,927	
Pitch Housing	F. Mamrol		116,938	
Elastomeric Bearing	F. Mamrol		31,820	
Accumulators	F. Mamrol		17,254	
Lag Dampers	F. Mamrol		27,226	
Misc. Assembly	F. Mamrol		43,230	
Upper Controls	F. Mamrol			$ 109,300
Drive Collar & Arm Assy	F. Mamrol		$ 16,859	
Scissor Assembly	F. Mamrol		8,645	
Pitch Links	F. Mamrol		15,847	
Swashplate Assembly	F. Mamrol		63,299	
Misc. Assembly	F. Mamrol		4,650	
Rotor Blade	T. Scarpati			$ 262,000
Spar Assembly	T. Scarpati		$ 66,094	
Blade Assembly	T. Scarpati		29,109	
Blade Final Assembly	T. Scarpati		21,464	
Pendulum Absorber	T. Scarpati		7,374	
Material	T. Scarpati		108,158	
Raw Materials	T. Scarpati	$85,090		
ISIS	T. Scarpati	2,400		
De-ice Blankets	T. Scarpati	15,687		
Misc. Parts	T. Scarpati	4,801		

TABLE 8. WEIGHT AND PART COUNT SUMMARY

FUSELAGE SECTION	TARGET		CALCULATED		DELTA		PROJECTED ADDN'L. WEIGHT	TOTAL WEIGHT
	WEIGHT	PARTS	WEIGHT	PARTS	WEIGHT	PARTS		
FORWARD	4080.0	3,798	4640.5	3,409	+ 560.5	- 389	+ 82.0	4,722.5
CENTER	2823.0	2,057	3370.4	1,760	+ 547.4	- 297	+ 89.9	3,459.4
STUB WING	2109.0	1,539	2059.0	1,358	- 50.0	- 181	8	2,067.0
AFT	3787.9	3,113	4205.4	3,427	+ 417.5	+ 314	+161.0	4,366.4
TOTALS use	12,799.9 12,800	10,507 ——	14,275.3 14,275	9,954 ——	+1475.4 +1475	- 553 ——	+340.0 +340	14,615.3 14,615

TABLE 9. WEIGHT AND PART COUNT SUMMARY CHANGES

FUSELAGE SECTION	15 MARCH 1974 DELTA		1 APRIL 1974 DELTA		CHANGES SINCE 15 MARCH 1974	
	WEIGHT	PARTS	WEIGHT	PARTS	WEIGHT	PARTS
FORWARD	+ 393.5	- 677	+ 560.5	- 389	+ 167.0	+ 288
CENTER	+ 529.2	- 362	+ 547.4	- 297	+ 18.2	+ 65
STUB WING	- 92.1	- 225	- 50.0	- 181	+ 42.1	+ 44
AFT	+ 161.4	+ 113	+ 417.5	+ 314	+ 256.11	+ 201
TOTAL	+ 992.0	-1151	+1475.4	- 553	+ 483.4	+ 598

TABLE 10. DRAWING TREE, HLH PROTOTYPE

	TARGET		CALCULATED		DELTA	
	WEIGHT	PART CNT.	WEIGHT	PART CNT.	WEIGHT	PART CNT.
[illegible] - FORWARD FUSELAGE INSTALLATION - V. MURRAY	4080.0	3798	4640.5	3409	+560.5	- 389
20406 - Frame Assembly - Sta. 108 Bottom	14.1	13	74.1	28	+60.0	+15
20407 - Frame Assembly - Sta. 127 Bottom	23.9 (20.3)	22 (19)	21.00	30	- 2.9	+ 8
20834 - Fitting	(3.6)	(3)	(3.46)	(2)	(- .14)	(- 1)
20303 - Frame Assembly - Sta. 170 Top	114.0 (31.0)	106 (29)	116.3	27	+ 2.3)	-79
20800 - Fitting Sta. 170 Xmsn Support	(73.0)	(68)	(73.38)	(2)	(+.38)	(-66)
20824 - Fitting Sta. 170 Cooler Provisions	(10.0)	(9)	(9.79)	(1)	(-.21)	(- 8)
20201 - Frame Assembly - Sta. 170 Side	103.0	96	103.2	42	+.2	-54
20401 - Frame Assembly - Sta. 170 Bottom	65.0 (28.0)	60 (26)	63.9	13	-1.1	-47
20826 - Fitting - Assembly - Sta. 170 Bottom	(37.0)	(34)	(36.45)	(1)	(-.65)	(-33)
20205 - Frame Assembly - Sta. 200 Side	8.5	8	11.3	14	+2.8	+ 6
20403 - Frame Assembly - Sta. 200 Bottom	23.3	21	30.7	42	+7.4	+21
20302 - Frame Assembly - Sta. 236 Top	142.1 (39.1)	132 (36)	122.4	30	-19.7	-102
20801 - Fitting Sta. 236 Xmsn Support	(103.0)	(96)	(84.28)	(2)	(-18.72)	(-94)
20200 - Frame Assembly - Sta. 236 Side	80.0	73	79.8	32	- .2	-41
20400 - Frame Assembly - Sta. 236 Bottom	203.3 (137.3)	189 (128)	210.1	64	+6.8	-125
20802 - Fitting - Sta. 236 - L/G Support	(63.8)	(59)	(64.92)	(1)	(+1.12)	(-58)
20828 - Bushing - Sta. 236 - L/G Support	(2.2)	(2)	(1.32)	(4)	(-.88)	(+ 2)
20304 - Frame Assembly - Sta. 266 Top	35.0	33	30.0	21	-5.0	-12
20202 - Frame Assembly - Sta. 266 Side	18.0	17	15.9	18	-2.1	+ 1
20402 - Frame Assembly - Sta. 266 Bottom	25.8	23	22.6	17	-3.2	- 6
20204 - Frame Assembly - Sta. 308/380 Side	170.0	158	238.2	112	+68.2	-46
20404 - Frame Assembly - Sta. 308/380 Bottom	45.4	43	75.8	20	+30.4	-23
20301 - Frame Assembly - Sta. 344 Crown	2.7	2	3.3	2	+ .6	---

Identify Cost Impact Elements

This element of the design-to-cost plan was also a continuing effort. All responsible engineers identified the high cost impact elements.

Table 11 is a sheet from the combiner transmission design cost and weight visibility by part. This methodology gave the responsible engineer the ability to identify high cost elements from which he could take action to reduce costs.

Reallocate Subsystem Targets

The Design-to-Cost Plan called for targets to be reallocated, if required. A revised estimate and reallocation of targets was completed in May 1974, as shown in Table 12.

Producibility Studies

Trade studies were conducted at the detail part level to determine the most cost effective design approach. Table 13 is a typical example of this type of producibility study.

Candidate Equipment and Feature Changes

A list of design features and Army requirements that could be deleted was identified and presented at the First Quarterly Review in May 1973. This list was updated throughout the program. The final tabulation is shown in Table 14.

2.5.3 Subsystem Design

The prototype subsystem design development is described in the following sections, 2.6 through 2.18. Each of the subsystems is discussed in a generally chronological sequence. Time reference points given in quarters refers to calendar quarters following contract award, relating to the Quarterly Summary Reports (References 2 and 3) issued throughout the program.

TABLE 11. HLH DESIGN TO COST - COMBINER TRANSMISSION COST ELEMENTS

QTY P/ASSY	PART NO.	PART NAME	SUPPLIER	UNIT PRICE	WT/XMSN	DOLLARS/POUND
1	301-10601-1	Gear, Eng. Dr.	Speco	$10,500.31	83.0	127.00
1	301-10602-2	Screen	Westholt	216.55	.2	1,083.00
1	301-10602-3	Screen	Westholt	112.75	.1	1,127.00
3	301-10602-4	Screen	Westholt	58.45	.5	350.00
1	301-10603-1	End Cap	Speco	445.39	3.3	134.97
1	301-10605-1	Support Assy	Speco	1,016.13	15.8	64.31
1	301-10606-1	Housing Assy	Speco	2,155.40	[illegible]	124.59
1	301-10608-1	Housing, Main	Speco	16,459.38	24[illegible]	66.45
1	301-10609-1	Plug, Lube	Speco	108.48	.1	1,084.00
1	301-10609-2	Plug, Lube	Speco	116.67	.3	388.00
1	301-10610-1	Gear, Slant Shaft	Speco	6,521.25	51.0	127.87
1	301-10612-1	Bearing, Slant Shaft	Timken	2,989.09	37.9	78.87
1	301-10613-1	Housing, Support	Speco	2,491.67	26.4	94.38
1	301-10615-1	Spacer, Bearing	Speco	228.28	3.1	73.64
1	301-10615-2	Spacer, Bearing	Speco	132.56	.6	220.00
2	301-10615-3	Spacer, Bearing	Speco	148.16	1.6	185.20
1	301-10615-7	Spacer, Bearing	Speco	172.24	.6	287.00
2	301-10615-8	Spacer, Bearing	Speco	127.38	.9	282.00
1	301-10616-1	Bearing	Timken	2,885.94	17.8	162.13
1	301-10617-1	Retainer, Bearing	Speco	240.85	.2	1,204.00
1	301-10617-2	Retainer, Bearing	Speco	135.63	.1	1,356.00
1	301-10617-3	Retainer, Bearing	Speco	133.90	.1	1,339.00
1	301-10617-4	Retainer, Bearing	Speco	244.76	.1	2,447.00

TABLE 12. HLH DESIGN-TO-COST SUMMARY

	250 AIRCRAFT, AVERAGE COST STATUS	
	MAY 1974	REALLOCATED TARGET
Fuselage	$ 740,560	$ 710,000
Landing Gear	240,600	215,000
Rotor Blades	343,468	295,000
Upper Controls	209,884	170,000
Rotor Hub	540,228	476,000
Drive	640,600	555,200
Cargo Handling	448,894	318,000
Flight Controls	677,480	457,300
Elec/Comm Nav/Instr	257,133	244,300
Hydraulic	110,677	96,600
Pneumatic	122,334	108,600
Fuel	114,797	109,000
Powerplant	205,335	167,200
Accommodations/Furnishings	77,479	72,300
Integration	685,437	642,100
Fee	463,700	463,700
TOTAL	$5,878,606	$5,100,300

TABLE 13. TRADE STUDY - FORWARD TRANSMISSION DECK

TYPE	*PARTS COUNT	WEIGHT (LBS)	FASTENER COUNT	RECURRING COST
Forged	2	146	Equal	1.0
Forged + Honeycomb (Combination)	14	141	Equal	1.18

NOTES: Forged deck adds 5 lbs

Combination deck costs $588 extra

Forged deck saves 12 parts

*Does not include splice plate.

TABLE 14. PRODUCTION HLH COST SAVING ITEMS

ITEM	APPROX. COST PER A/C COST ($)	MALF. RATE PER 1000 HOURS	MMH/FH (1)	WEIGHT (LBS.)
1. a. Delete differential landing gear requirement.	$ 35,000	-47.000	-.250	-1100
b. Reestablish length of landing gear. (14' vs 8'-8")				- 392 (2) - 588 (3)
2. Visual Augmentation System	$180,000	- .500	-.024	- 290
3. Longitudinal winch positioning feature - one fixed position.	$ 20,000	- .682	-.005	- 440
4. Precision Hover System	$ 55,000	-28.694	-.0250	- 135
5. Blade deicing (including slip-rings, two deicing alternators).	$ 25,000	- 2.978	-.138	- 240
6. Substitute single load path pitch links for dual load path pitch links.	$ 12,800	Neg.	Neg.	- 12
7. Eliminate CBR filter in crew and troop compartment ECS and substitute provisions for a kit installation.	$ 2,000	- 1.670	-.0065	- 97
8. Eliminate secondary air ventilation.	$ 2,500	- 4.190	-.0075	- 37
9. Eliminate engine air particle separator and substitute provisions for a kit installation.	$75,000	- 2.187	-.0096	- 363

TABLE 14. (Continued)

ITEM	APPROX. COST PER A/C COST ($)	MALF. RATE PER 1000 HOURS	MMH/FH (1)	WEIGHT (LBS.)
10. Eliminate bird-proof windshield.	$ 500	Neg.	Neg.	- 49
11. Eliminate flight engineer station, including seat, belts, table, panels, instruments, and controls.	$ 18,000	-26.000	-.011	- 242WE - 240UL
12. Eliminate auxiliary tank self-sealing and breakaway valves.	$ 10,000	.107	.0007	- 59WE - 648UL
13. C5A Splice	$ 26,000	Neg.	Neg. (4)	- 180
14. IR Suppression		-21.000 (5)	-.0147	- 482
15. Structural provisions for in-flight refueling.	$ 10,000	Neg.	Neg.	- 65
16. Self Refueling Reel/Hose	$ 30,000	- 2.000	-.002	- 252
17. Bleed Air Cooling	$ 3,250	- .873	-.0017	- 22
18. Force Feel	$ 2,000	Slight reduction	Slight decrease	10
19. AFCS Redundancy				

TABLE 14. (Continued)

ITEM	APPROX. COST PER A/C COST ($)	MALF. RATE PER 1000 HOURS	MMH/FH (1)	WEIGHT (LBS.)
20. Eliminate integral fuel dumping provisions.				
21. Eliminate converter in elect. power supply system.				- 6
22. Vapor Inerting System.				- 90
23. Add standby ATM pump and remove two transfer units and valves/each head.				- 60

NOTES: (1) MMH/FH are "worldwide" and include organizational, direct support, and general support levels. (Based on use of auxiliary tanks 10% of hours flown)

(2) Based on 118,000 lb design gross weight.

(3) Based on 81,000 lb design gross weight.

(4) Affects C-5A transportability.

(5) When kit is installed.

2.6 AIRFRAME

2.6.1 Design

Design criteria for the prototype aircraft were established during the first quarter and reviewed in the Systems Requirements Review Meeting. This review included: Design load factors, design loading conditions, design rpms, and design criteria to satisfy requirements for vibration characteristics, ground resonance, and air resonance. The prototype design criteria are identical to those of the production aircraft and consistent with the requirements of AR-56 as modified by the ASRD in all areas except vibration levels where a deviation from the mixed frequency environment in the crew areas is being taken. The prototype vibration treatment includes blade-mounted pendulum flap absorbers tuned to attenuate 4/rev vertical shear and provisions for 4/rev moment. These absorbers, together with fundamental design considerations in the tuning (or detuning) of the airframe, are expected to provide very acceptable vibration levels in the prototype aircraft. Passive isolation of the crew area module also provides attenuation of 4/rev vibration by means of DAVI isolator units. Retuning of these units to the 2/rev frequency is also possible in the event 2/rev would be a problem.

A joint engineering/operations study was completed to determine the applicability of bonded honeycomb structure to the HLH prototype. Since the production aircraft structural weight bogies were based on the use of bonded structure, it was considered highly desirable to fabricate the prototype airframe in the same manner so that verification of weights, cost, and the associated parts count reductions can be accomplished without production program pressures.

The detailed trade study was conducted based on preliminary layout design covering approximately one-third of the HLH primary structure. Trends established by this study compared favorably with studies previously performed at the Boeing Commercial Airplane Company.

Conclusions drawn from the trade study point to weight reduction of 22%, parts count reduction of 23%, and fastener count reduction of 86%, when honeycomb construction is used. Correspondingly, reductions in costs and manhours associated with fewer fabricated parts and fewer assembly fasteners are achieved. Figure 23 illustrates the comparison of actual construction in honeycomb and in skin and stringer. Figure 24 shows the weight and parts count study results.

Interior View of CH-47 Chinook Fuselage Skin-Stringer Construction

Interior View of HLH Prototype Fuselage Bonded Honeycomb Construction

Figure 23. Structural comparisons – skin/stringer versus honeycomb.

DESCRIPTION	TOTAL NUMBER OF PARTS	WEIGHT (LB)	SPEC WEIGHT (LB)	NO. OF SKIN FASTENERS	TOTAL CURRENT SPEC STRUCT WT (LB)	PERCENT OF AIRCRAFT WEIGHED
HONEYCOMB	1,009	2,672	3,371	13,300 PROTO 5,200 PROD	10,180	33.3
SHEETMETAL	1,307	3,311	3,371	38,500	10,180	33.3
CH-47	1,205	1,026	1,026		3,856	26.6

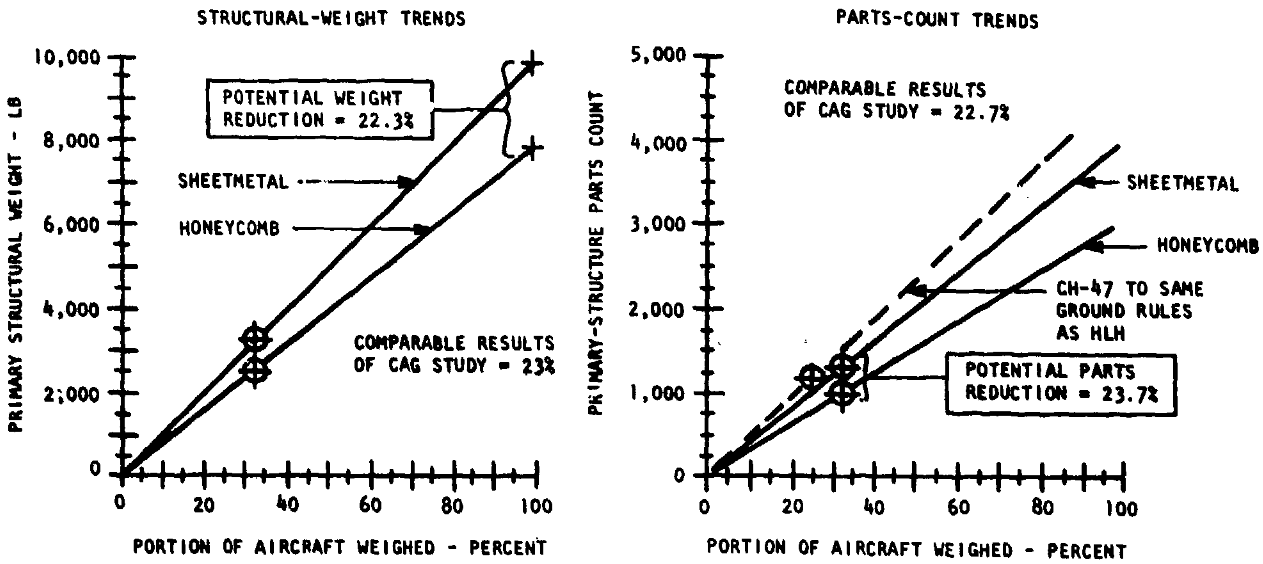

Figure 24. Trade-off study of skin/stringer versus honeycomb.

Table 15 shows the results of the trade study with respect to the expected improvements in reliability and maintainability of honeycomb construction over conventional skin and stringer.

TABLE 15. COMPARISON OF SKIN-AND-STRINGER AND BONDED-HONEYCOMB CONSTRUCTION FOR RELIABILITY AND MAINTAINABILITY

Experience Base

Company data on CH-47 repair	Boeing commercial transport data
Air Force data on C-130 and C141	UH-1 field experience (STRAAD eng)

Reliability Prediction

	Conventional Skin-and-Stringer	Bonded-Honeycomb Sandwich
Estimated malfunction rate per 1,000 hr/lb	0.0516	0.0357
Estimated HLH weight (pounds)	11,700	9,100
Total Malfunction rate/1,000 hours	603.954	324.961
Maintainability Prediction		
Average MH/repair (adjusted for combat environment)	3.88	2.646
MMH/FH for repair (worldwide, organizational, direct, and general support)	2.35	0.859
MMH/FH for inspection (worldwide)	0.059	0.055

Fleet-Maintenance Saving

1.491 MMH/FH x 600 aircraft hr/yr x 10 yr x 100 aircraft x $8.20/hr = $7.33 million savings

Table 16 compares parts per pound and manufacturing manhours per pound for conventional skin-and-stringer construction with bonded honeycomb.

TABLE 16. MANHOURS PER POUND

	CONVENTIONAL Based on CH47	HONEYCOMB Prediction For HLH
Parts per pound	1.69	.79
Manhours per pound (at A/C #1)	19.9	13.3

A firm decision was made at the end of the first quarter to proceed with this concept. A briefing was made on this subject to the Project Manager, AVSCOM, and conceptual layouts and trade studies of the forward, aft, and combining transmission support structure, forward and main landing gear attachment, troop compartment structure, stub wing and fuel cavity structure, winch support structure, and engine support structure were begun during this period. The study shows a reduction in structural weight of 223 pounds based on trend curves, and a subsystem weight reduction of 217 pounds in the winch and pneumatic systems.

The basic loft lines of the constant section and aft fuselage were established and inserted into the master dimensioning system. Loft lines for the nacelle and stub wing were finalized to agree with static wind tunnel test results (ATC program) and fuel volume requirements. Geometry is shown in Figure 25.

During the second quarter, conceptual layouts and major structural components were completed, and design reviews and trade studies conducted. The following major decisions resulted from these reviews:

A shear joint was selected (stub wing/fuselage interface) in lieu of a tension joint. The landing gear attachment points were frozen following AVSCOM confirmation of the landing gear height. A flat windshield arrangement was selected instead of the curved CH-47 windshield. The aft pylon structure was completely revised; the front spar was eliminated, and the frame stations were relocated to provide a more efficient structural arrangement.

The location of the outboard engines required the interruption of primary fuselage members in order to provide an adequate engine inlet airflow with a resulting local structural arrangement and improved maintenance characteristics in the engine area. There was no effect on performance.

A study of engine work platform concepts resulted in a single simplified work platform. This arrangement, shown in Figure 26, eliminated three separate work platforms and provided one platform which can be opened and adjusted for simultaneous access and work area for all three engines. This

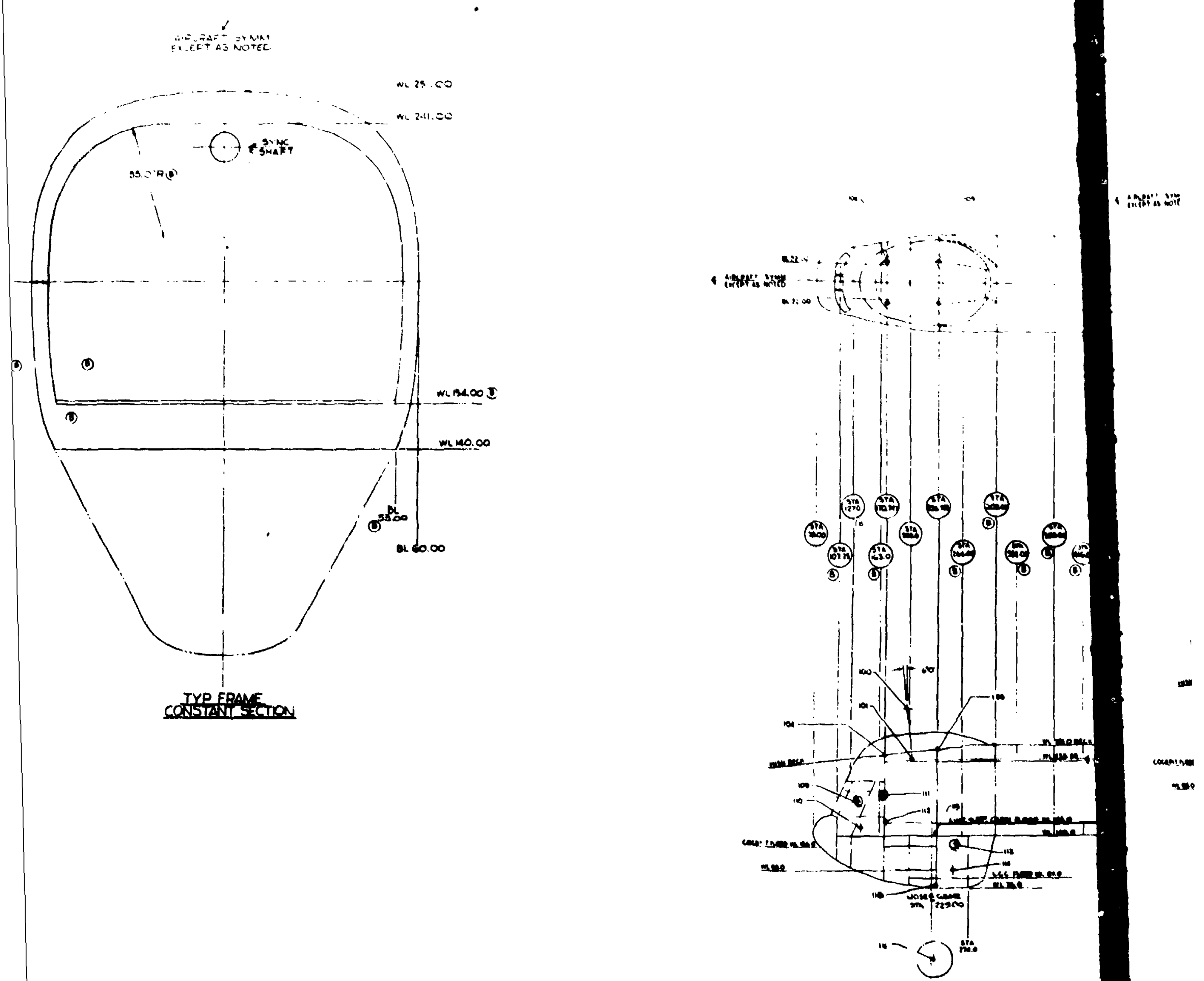

igure 25. Aircraft geometry – basic points and frame locations.

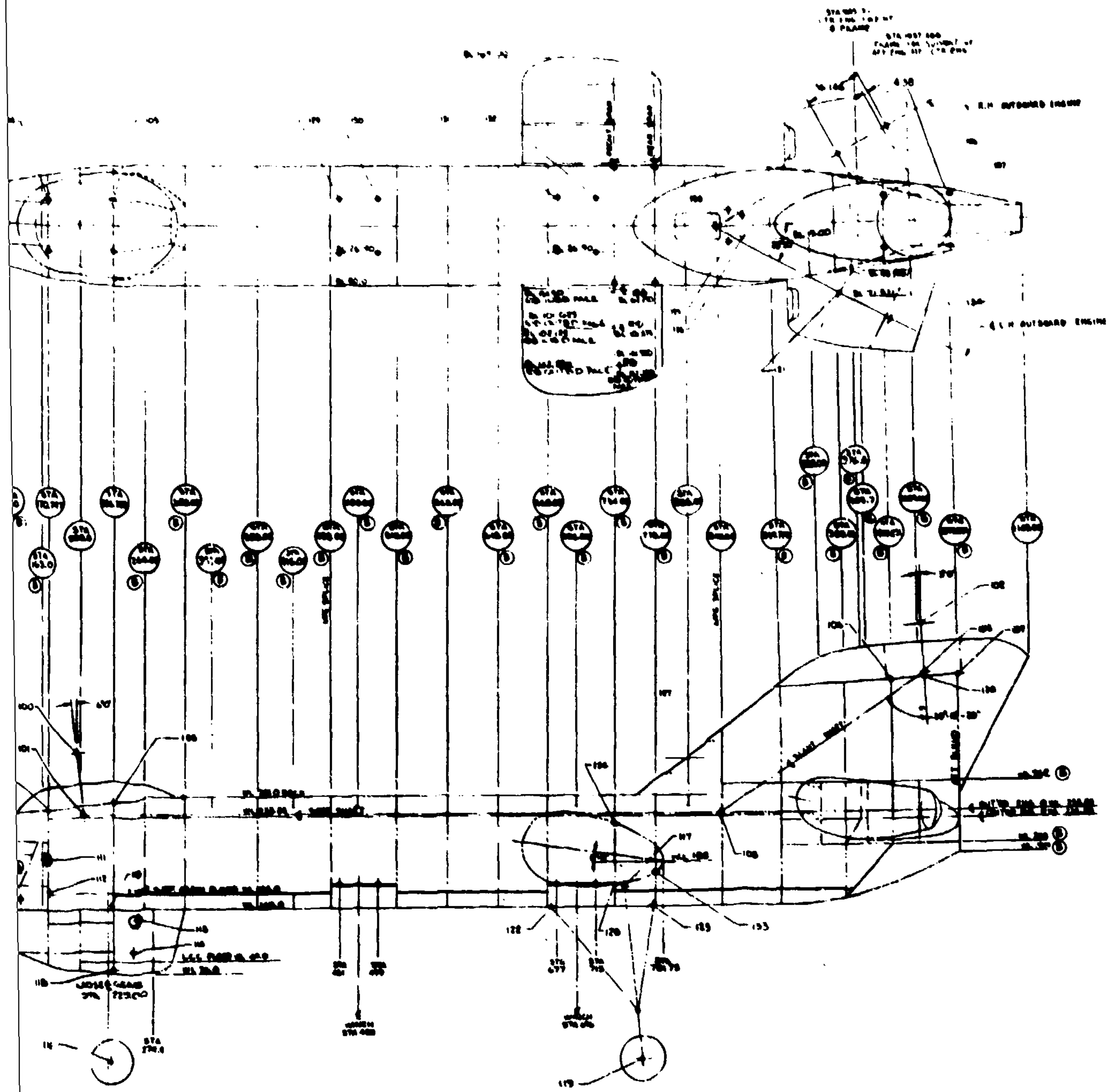

a

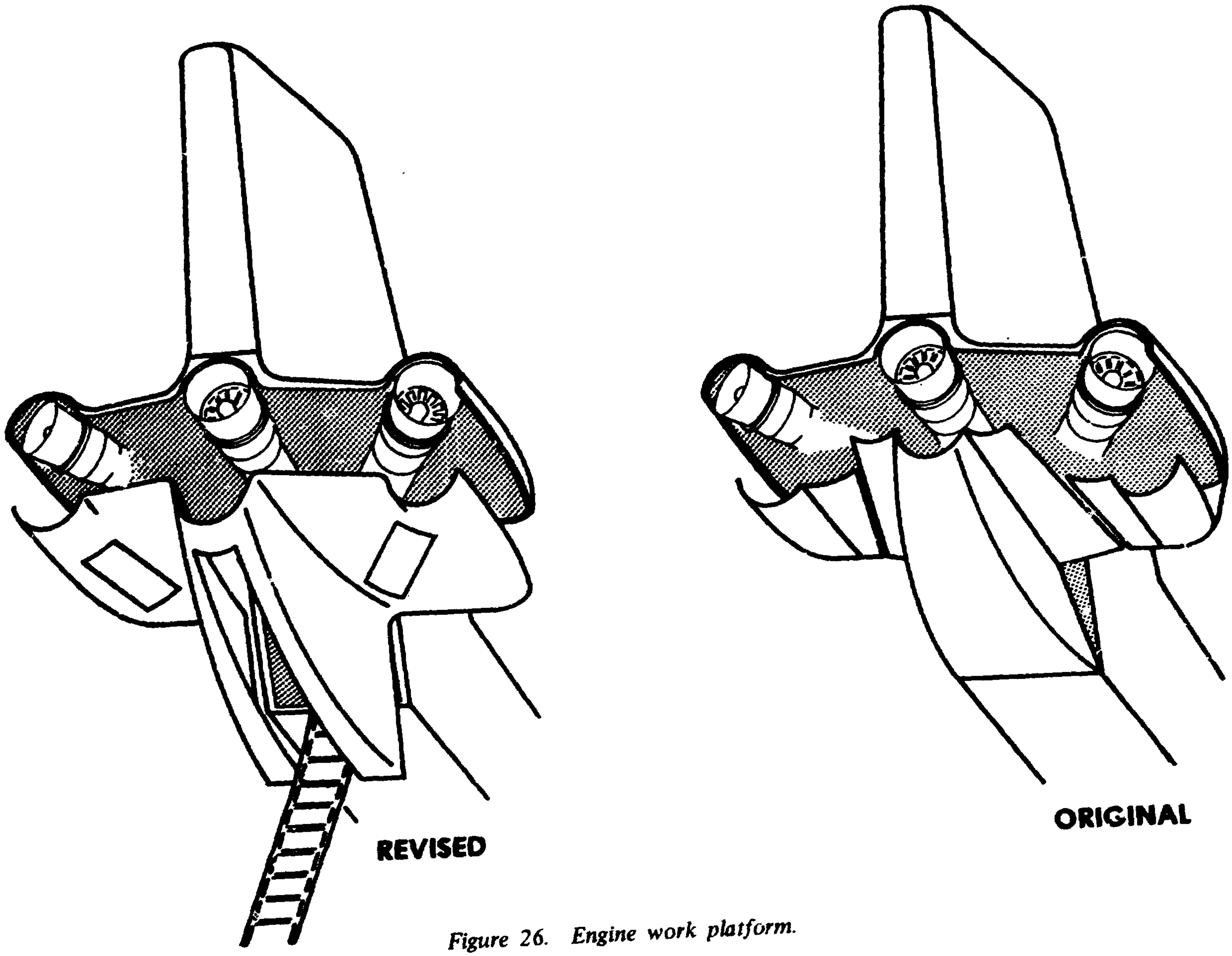

Figure 26. Engine work platform.

concept resulted in a more efficent and cost effective design with little weight penalty. Engine work platform design was modified to provide latching restraint to minimize flight deflections, thereby effecting a significant weight reduction. A modification was made on the trailing edge to accommodate common ejector pipes for all three engines.

Sizing of the fuselage structural elements by manual analytical methods was started while formulating the NASTRAN finite-element program. Properties of all structural members in the NASTRAN model were incorporated in the program, and the finite-element model geometry was verified by using the plotting capability of the program to give a visual representation of the model. Flight loads were developed for the full range of the flight envelope, and approximately 400 maneuver conditions were run on a separate program to determine which of them were critical for fuselage loading. This program has an input of external loads and fuselage mass distribution. The output is a station-by-station compilation of fuselage shear, axial bending, torsion loading, and mass inertia loading. The program also prints out the maximum and minimum of these loadings at each station and the maneuver conditions which generate them. These conditions were selected as the critical loading cases for the NASTRAN program input. By this method, the original 400 conditions were reduced to 37.

The first cut at formulation of the NASTRAN finite-element program model of the fuselage was completed, checked out, and run on the computer. The model is comprised of 3000 structural elements, 1179 grid points, 240 mass degrees of freedom for dynamic analysis, and 400 mass degrees of freedom for stress analysis.

The distribution of the primary modes of the fuselage in the frequency domain is shown in Figure 27.

Aeromechanical stability considerations require the frequency of the lowest fuselage mode to be at or above 1.6/rev (4.15 Hz). The first vertical bending mode falls below this frequency and must be raised. The second vertical bending mode is just below the dominant excitation frequency of 4/rev (10.4 Hz), thus experiencing an amplification in excess of 2.

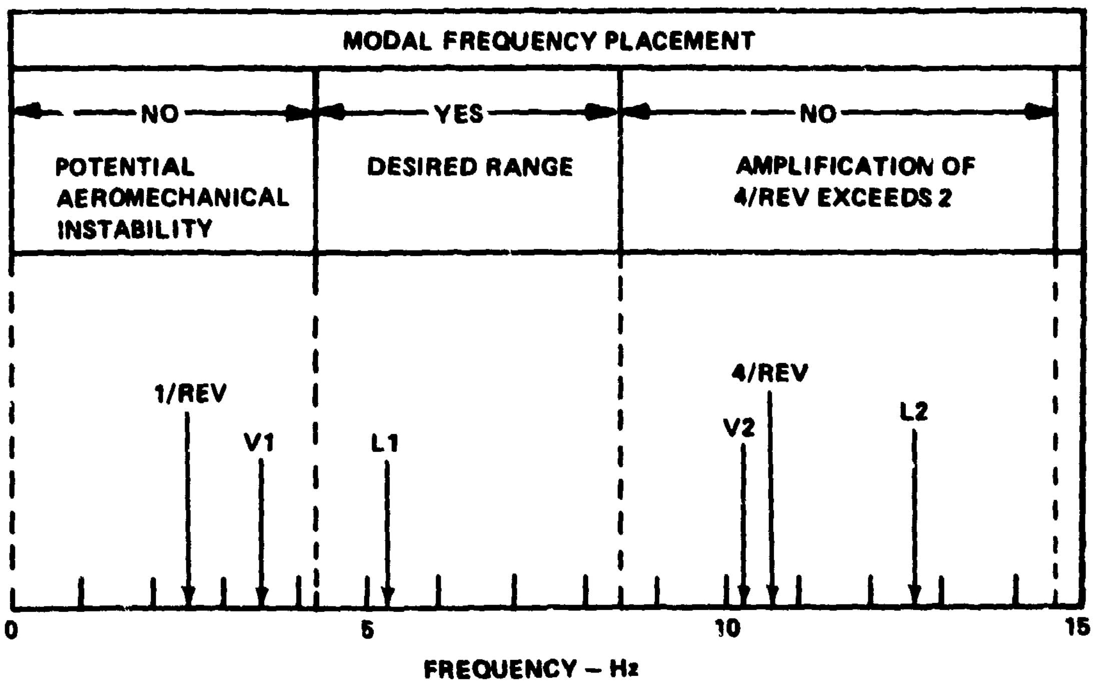

LEGEND

V1 1ST VERTICAL, 3.51 HZ
V2 2ND VERTICAL, 10.04 HZ
L1 1ST LATERAL, 5.05 HZ
L2 2ND LATERAL, 12.47 HZ

Figure 27. Modal frequency placement chart.

Intensive parametric trade studies were conducted to define the most feasible method of raising the first vertical mode to 4.15 Hz and, simultaneously, either lowering the second vertical mode to 8.5 Hz or raising it above 14.7 Hz in order to remove it from the frequency band which has an amplification greater than 2 to 4/rev rotor excitation.

The first lateral bending mode is within the desired frequency (above 4.15 Hz but below 8.5Hz). The second lateral mode was above 4/rev, but within an undesired frequency band. Since tuning the vertical modes will affect the lateral modes also, the second lateral mode was not addressed directly; however, its frequency was carefully monitored as the vertical modes were tuned.

Updating of the NASTRAN model to reflect the current prototype configuration and prediction of in-flight vibration levels was accomplished.

Two alternatives were investigated as a means of achieving a shift in second vertical bending response away from the 4/rev rotor frequency. These alternatives were stiffening or softening of the fuselage shell between stations 236 and 452.

Figure 28 reflects the initial structural arrangement of the forward fuselage. Hatch locations are shaded. Correction of the second vertical bending mode problem was not simple. Using the D-29 stick computer model, stiffening to a level of approximately 6 x strength requirements resulted in only a change of approximately 2 Hz (to approximately 12.5 Hz), still far from the 14.8 cps necessary to achieve the transmissibility criteria of 2. Stiffening was then abandoned as a viable option.

Design studies were conducted to determine a practical approach to softening the forward fuselage, while still meeting strength requirements. The optimum configuration which met softening, structural, and functional requirements was determined to be an opening of 67" x 67" in both sides of the fuselage between stations 308 and 380. For vertical bending, this change altered the elastic bending characteristics sufficiently to lower the second bending mode natural

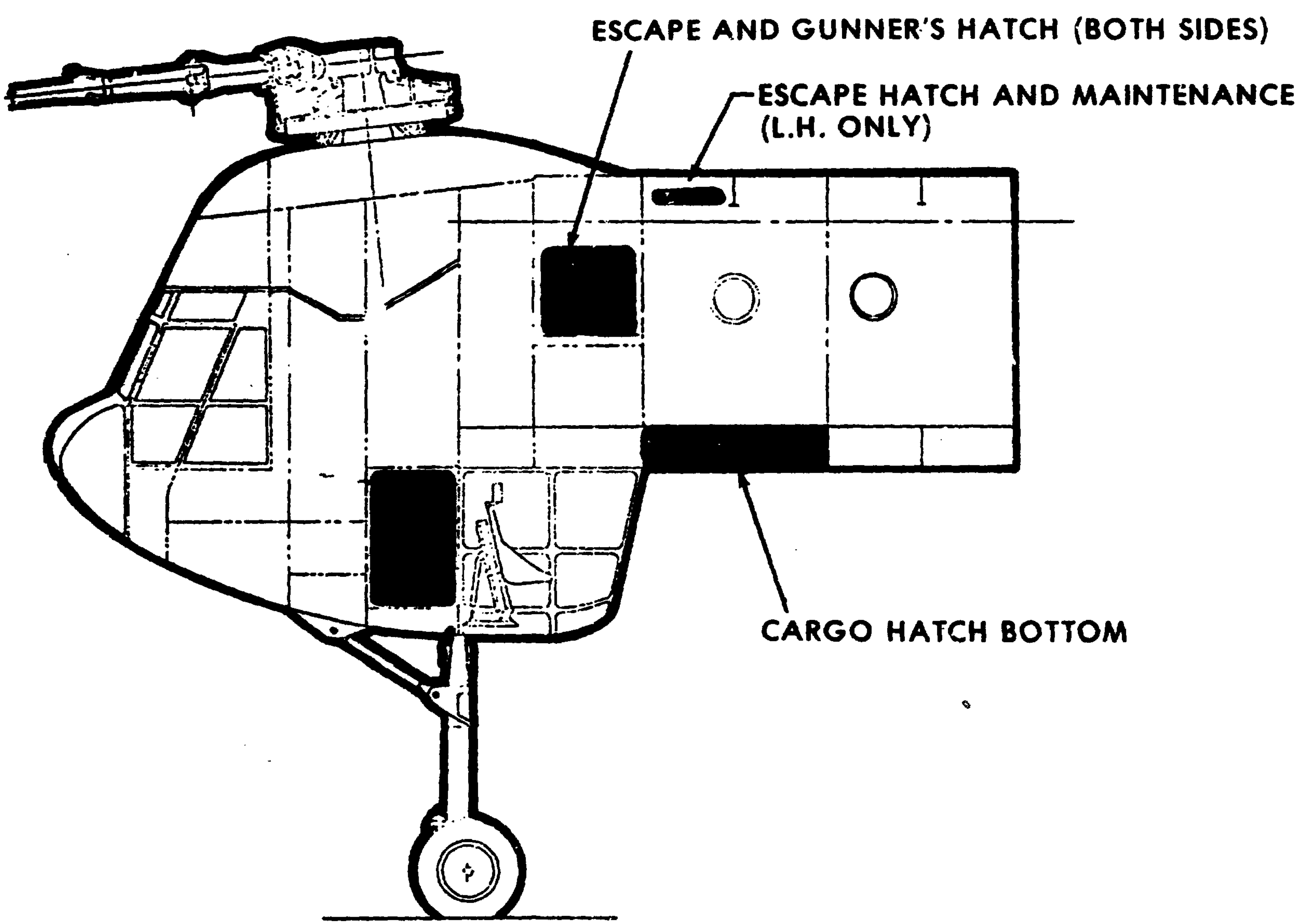

Figure 28. Initial structural arrangement.

frequency to 8.5 Hz, which meets the transmissibility requirement. An evaluation was made of reducing airframe cutouts (2 escape/gunner's hatches, one rollover escape and maintenance hatch, and a bottom cargo hatch) to a minimum. If the number of cutouts could be minimized without compromising functions (ingress/egress, gunner's station maintenance, or cargo handling) a more optimum structural design should be achievable. Alternative arrangements were reviewed. The resulting final arrangement is shown in Figure 29. To satisfy the softening requirements the large cutout of 67" x 67" was added to both sides. The lower cargo door and the overhead maintenance/escape hatch were eliminated. A gunner's hatch/escape panel is included within the non-structural panels. Figure 30 shows cross-sectional views of the concept. The sections are viewed looking aft. The section on the right side of the chart shows the left panel hinged up as a cargo hatch, while the section on the left shows the right hand panel folding out and down with a built-in ladder for maintenance access to the crown of the aircraft. A rollover excape hatch is provided in the floor at the center of the aircraft just forward of the winch bay where structural framing already exists.

In addition, the entry door and airstair forward of station 236 were eliminated to minimize the weight impact of softening, since the new large cargo door can now be used for crew and troop ingress and egress.

Forward fuselage softening resulted in rescheduling of internal engineering releases, which had an effect on major jig loading, but did not impact prototype rollout.

Experience with the CH-47 Chinook helicopter led to the establishment of HLH design criteria for cabin crown frames subjected to vibratory rotor downwash pressures. To meet these criteria, HLH prototype frames were first sized for all static and vibratory loading cases; then using these properties, a dynamic analysis was conducted to establish the required sizing to determine the cabin-crown bending mode away from 8/rev. As a result, the bending stiffness of several frames was increased to give a bending mode at 24.7 Hz (19% above 8/rev).

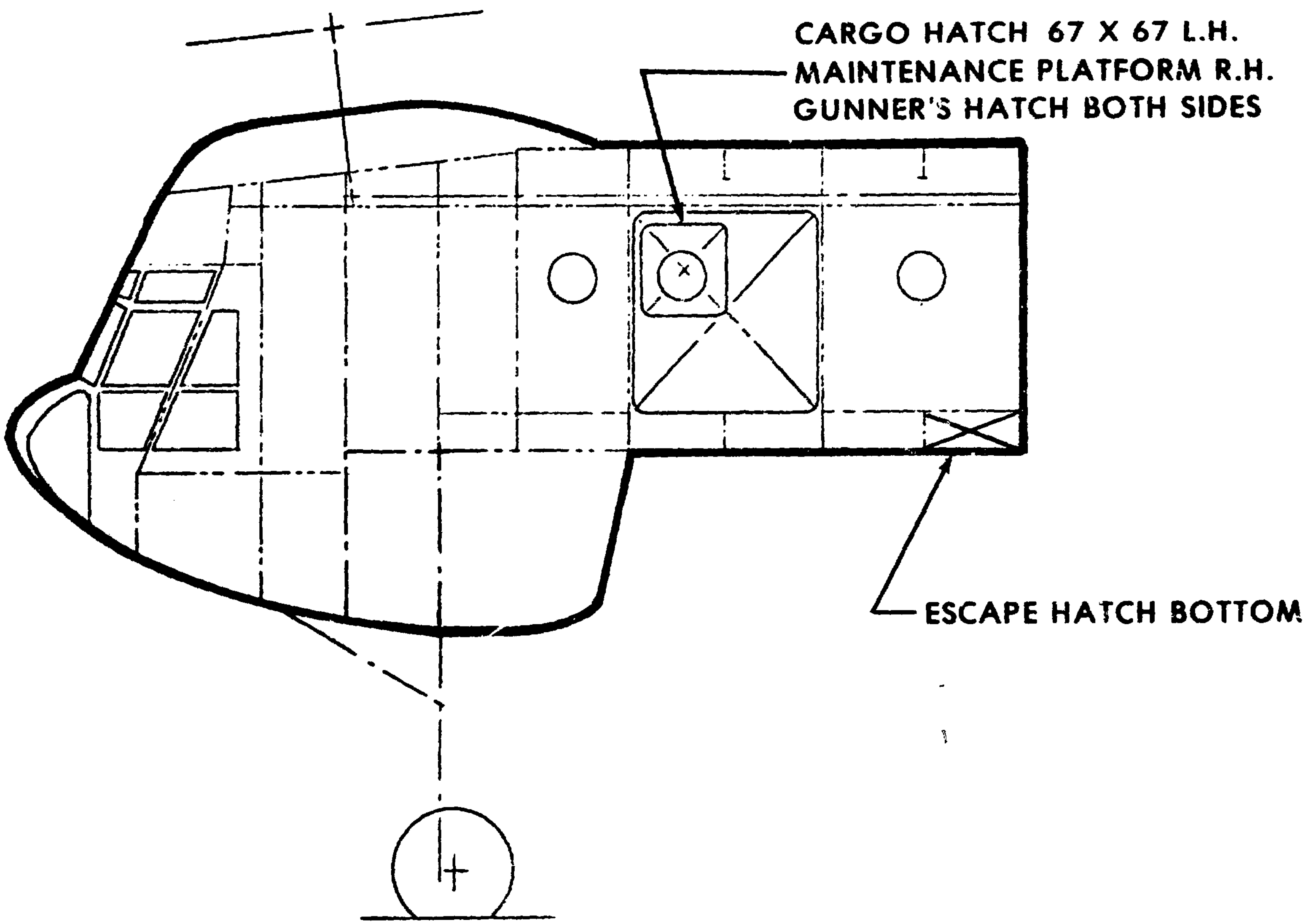

Figure 29. Final structural arrangement.

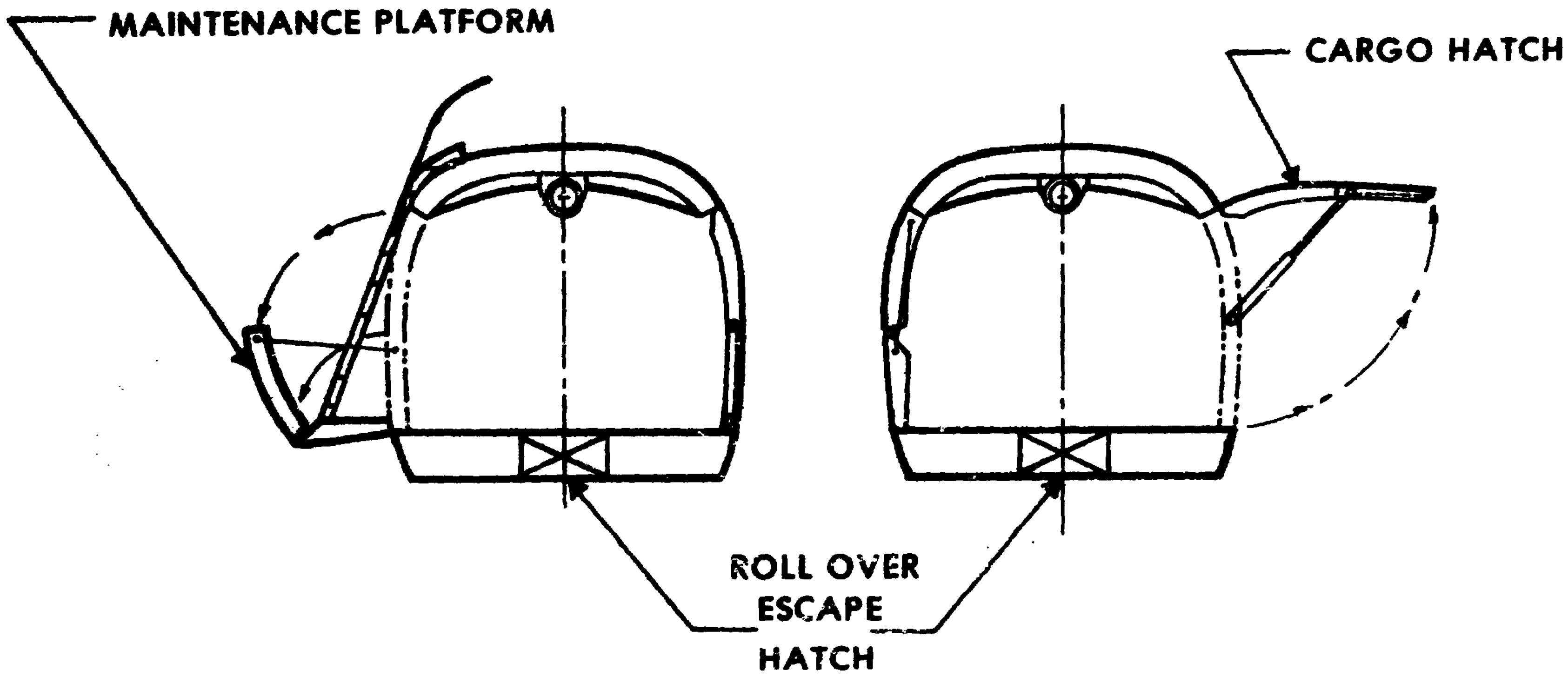

Figure 30. Configuration changes – structural tuning.

Provisions were made in the crew areas to permit utilization of a crew isolation system incorporating the Dynamic Anti-resonance Vibration Isolator (DAVI) concept developed by Kaman Aircraft Corporation. Both DAVI and sine spring concepts were considered and the DAVI was selected as the lowest risk concept which could be employed in the crew area to provide further reduction in the vibration levels beyond that anticipated with the rotor-mounted pendulum absorbers. The DAVI is a single-frequency device and will be tuned to 4/rev to attenuate both vertical forces and pitching and rolling moments. While the sine spring will no longer be considered for application in the prototype, continued development of that concept is desirable, since it can attenuate all frequencies down to and including 1/rev. A detailed analysis of the cockpit area was developed using the NASTRAN finite-element program to evaluate local airframe loads and vibration levels and the effect of isolation between the cockpit floor and the airframe support structure, as well as the use of fixed tuned vibration absorbers which were considered as a backup approach.

Final NASTRAN vibration predictions of the basic untreated (no vibration reduction treatment) fuselage were completed. Fuselage natural frequencies and mode shapes were identified; all basic fuselage modes are well placed for minimizing response. The lowest fuselage bending modes are predicted to meet the 1.6/rev (4.16 Hz) objective for air resonance avoidance by judicious use of composite stiffening of cabin longerons. Basic fuselage modes near 4/rev (10.4 Hz) were found to be acceptable from a modal forced response analysis (modal contributions). A rotor hub forced response analysis was also performed and will be required in analyzing the effectiveness of pendulum absorbers. A local roll resonance of the pilot and copilot seats on the cockpit floor was found and has the effect of amplifying the lateral vibration level from .1g on the floor to .4g on the seat cg. This local mode problem will be confirmed in the planned cockpit crew platform shake test. The 4/rev vibration response predictions throughout the fuselage are shown in Figure 31.

Design of the fuel cell cavity included consideration of lightening damage protection, since the construction is basically fiberglass and/or PRD 49 fibers. The fuel cell cavity structure is protected from the possibility of lightning damage by:

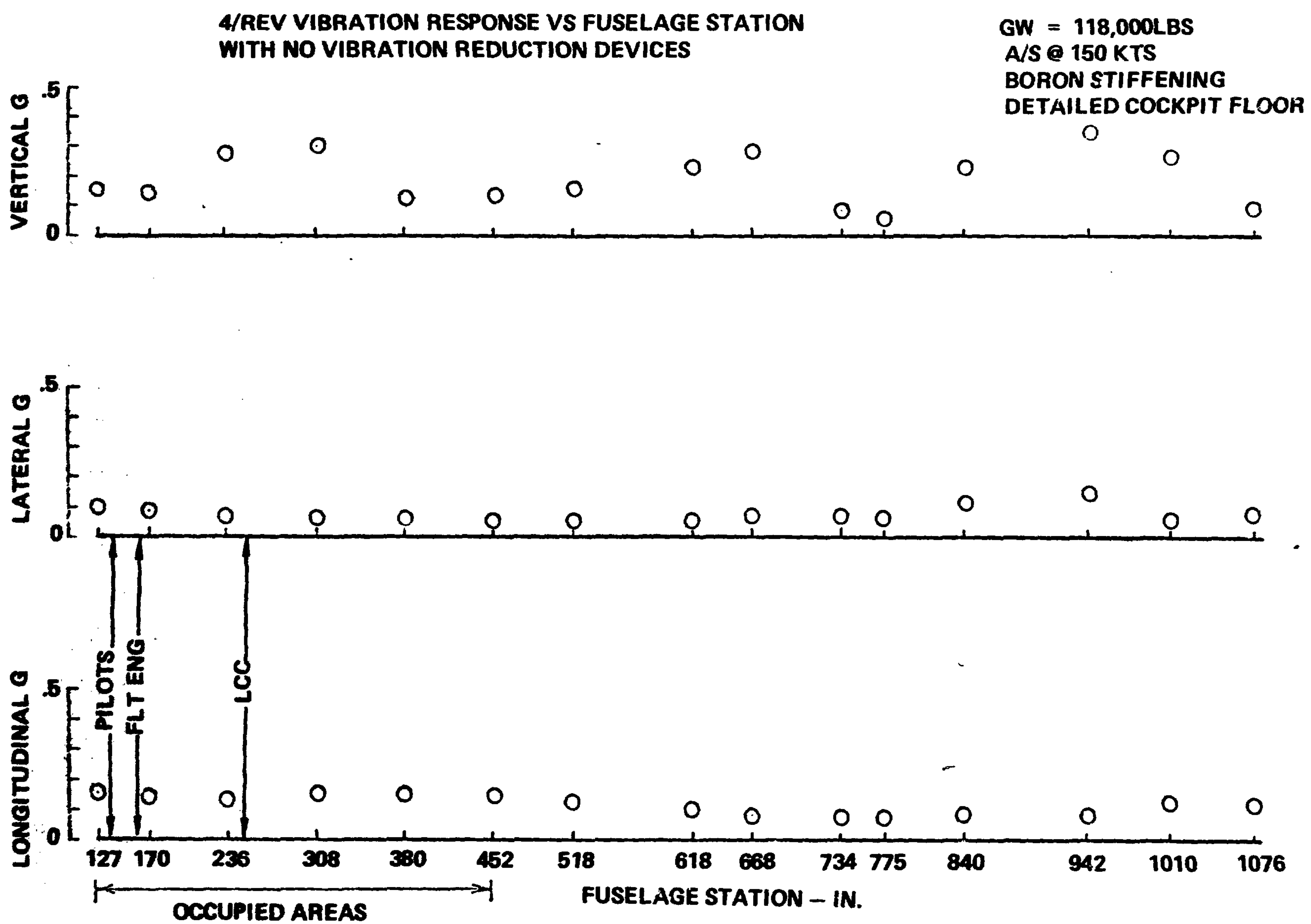

Figure 31. Fuselage vibration prediction.

The general configuration of the aircraft with large-diameter tandem rotors above the stub wing.

Lightning diverter straps, on the structure exterior, which would direct the electrical energy away from the fuel compartment.

Candidate materials and methods of providing a conductive surface to the entire exterior surface of the fiberglass L.E. section of the stub wing included: 200 x 200 2-mil aluminum wire mesh, 5 oz. knitted aluminum fabric, conductive paints, and sprayed aluminum coatings.

Trade studies considered producibility, weight, electrical and structural characteristics, and adaptability for electrical bonding to the aluminum torque box section of the stub wing. None of these approaches appeared attractive, particularly after reviewing the HLH general arrangement and identifying possible direction of lightning strikes.

The more effective lightning protection technique for the stub wing is the use of a peripheral metal strap extending along the leading edge, around the tip, and continuing to the metal portion of the wing. Additional diversion of the lightning strikes is provided by longitudinal fairing strips covering the gaps between the fuel cell structure assemblies and adjacent structure, and extending from the leading edge diverter strap to the aluminum front spar. All interior metal parts (drain fittings, probe supports, manhole flange, etc.) are electrically bonded to the external diverter straps by use of 0.005" thick x 3" wide 1100-H19 aluminum foil adhesively bonded to the fiberglass structure. Metal-to-metal contact surfaces are free of primer or paint to assure conductivity; sealants are provided to assure corrosion protection.

Also in the stub wing area, a decision was made to provide access to the stub interior through a hinged panel on top of the torque box which reached from the fuselage crown walkway rather than through the highly loaded fuselage side skins, as shown in Figure 32. A simple wooden mockup was constructed and evaluated. The mockup resulted in proper placement of safety belt attachment points, finalization of opening size, door hinge location, and adequate foot rests to permit maintenance ingress and egress.

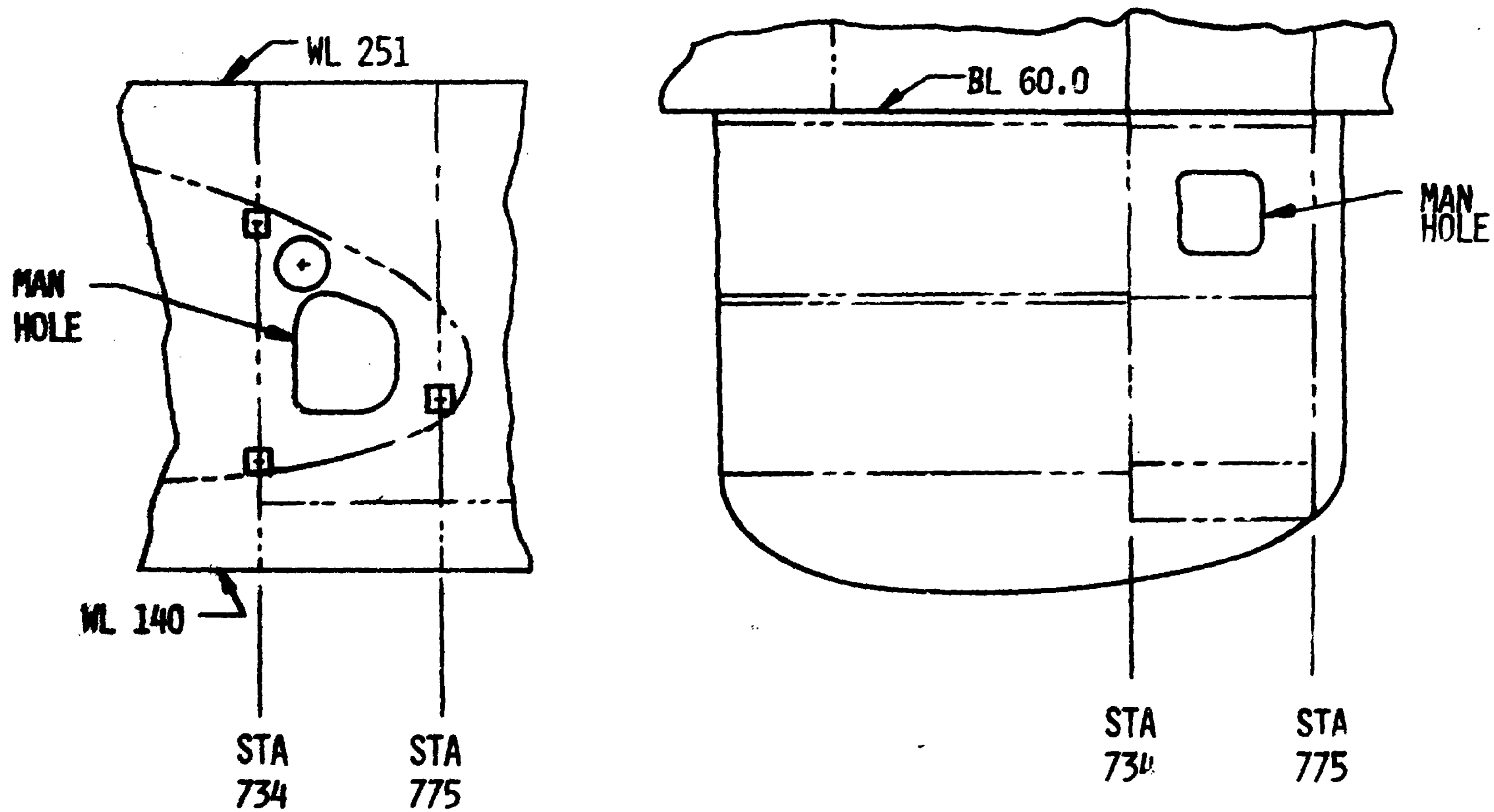

Figure 32. Stub wing configuration alternates.

A foam core mockup of the center engine compartment and associated structure was fabricated to evaluate clearances and to provide a visual tool toward designing the heat/fire shield for the center engine.

A study was conducted on the air flow and temperature levels from all heat sources in the aft fuselage in order to finalize adhesive bonding considerations and major structural cutouts.

A design problem concerning the longitudinal intercostal members was identified. The longitudinal intercostals are functionally needed to provide stability for the edges of the large outer shell (skin) panels, and in turn stabilize the frames. The problem concerned the detail design of the inner chords of the intercostal beams, which can be designed as either continuous or discontinuous.

If these members are designed as discontinuous, an advantage of light weight is achieved since they only pick up low axial loads, but have the disadvantage that "soft ends" at each frame make it difficult to insure stability of the inner frame caps. Thus, adequate stabilizing of the frames may not be achieved.

If these members are designed as continuous they have the advantage of being more stable, but a disadvantage in that they "pick up" a larger axial load, which tends to size the member. The continuous configuration was selected as the best solution for stabilizing the outer shell panels and the frames at the least risk.

A trade study was conducted to determine the best form for the inner chords. The main objective was to configure the member for maximum column allowable at the lowest weight. The study included extruded shapes, hollow shapes, bonded sandwich, and roll-formed shapes. In conjunction with selecting the shape for these members, a design review was conducted to determine an optimum relationship between this structural requirement and that of providing supports for the long runs of hydraulic and electrical subsystems. It was found desirable to combine the structural requirement with support of the electrical wiring, such that the final configuration will serve a dual function.

The resulting intercostal configuration is shown in Figure 33.

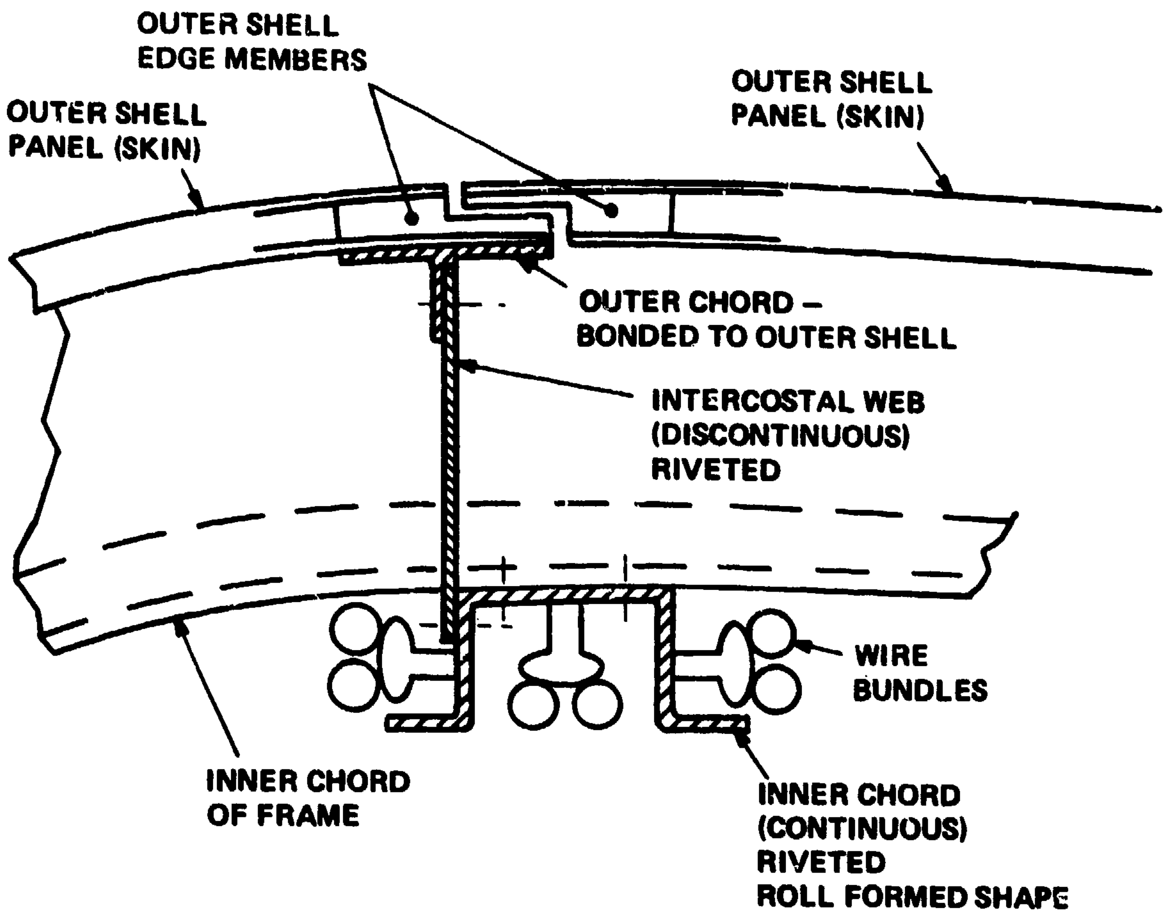

Figure 33. Typical section through longitudinal "intercostal" members.

2.6.2 Honeycomb Panel Development

Preliminary honeycomb panel fastener feasibility specimens were fabricated for design evaluation (Figure 34). A honeycomb skin test panel and a panel bonding tool were fabricated for proving the bonding tool concept, panel joining, design evaluations, and quality assurance inspection techniques (Figure 35).

The panel assembly included built-in defects as specified, in order to confirm and define quality assurance inspection techniques. The panel assembly is shown in Figure 36.

The panel bonding tool demonstrated its capability for bonding acceptable panel assemblies. Evaluation of the fabrication of this concept of tooling indicates a potential cost improvement over past fabrication methods.

Additional bonded honeycomb panel specimens were fabricated for evaluation of joining and splicing techniques. A wave edge panel specimen was fabricated in order to evaluate and demonstrate the effect of honeycomb panel contour tolerance on fit-up. The tolerance effect which could be experienced on joining two panel assemblies is the short pitch waviness characteristic of joints between frames and the honeycomb skin panels. To demonstrate this effect, a panel .625" thick by 20" wide by 48" long was fabricated. The panel consisted of 2.3 lb/ft^3 aluminum face sheets, 0.20" aluminum doublers, and 12 lb/ft^3 aluminum core along one edge.

The panel was then fastened to a heavy aluminum angle which had been fabricated with several waves of approximately 20" pitch and wave depths up to .045". Hi-Loc fasteners 3/16" in diameter and hex head bolts 3/16" in diameter were used with a .050" splice strap for fastening. The honeycomb panel was "pulled" into fit-up with the heavy waved angle. The completed panel shows no visibly detectable effects from the forced fit-up (Figure 37).

Several other specimens were also fabricated to evaluate and demonstrate methods, techniques, and structural integrity. A fabricated 4'x8' aluminum honeycomb panel was representative of the oven bonding of large panel areas under pressure without a bleed path for air escape. Ultrasonic inspection revealed no voids between honeycomb and the outer skins. Peel tests, beam shear, and fatigue tensile tests showed well within allowable limits (Figure 38).

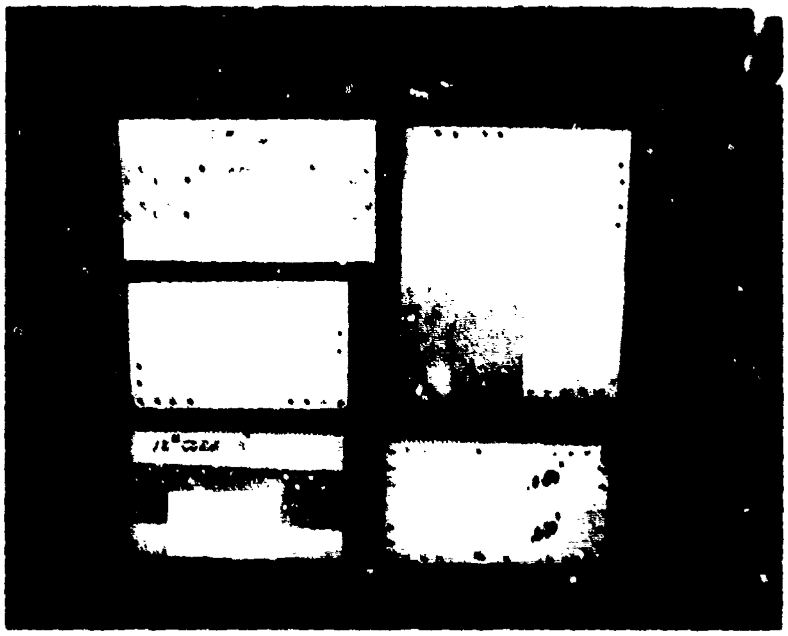

Figure 34. Honeycomb fastener specimens.

Figure 35. Bonding assembly jig for aluminum honeycomb skin panels.

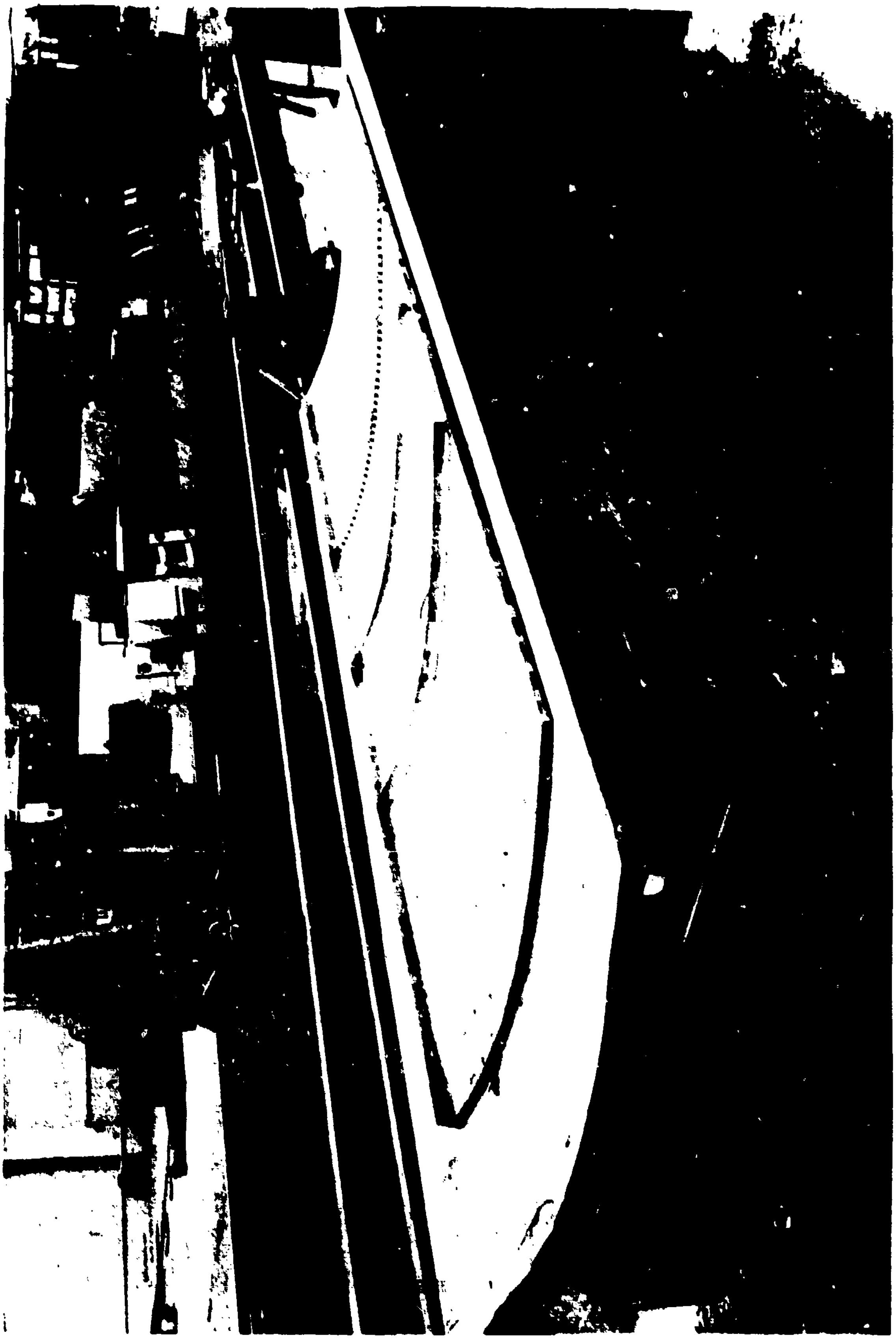

Figure 36. Bonded honeycomb panel – tool prover.

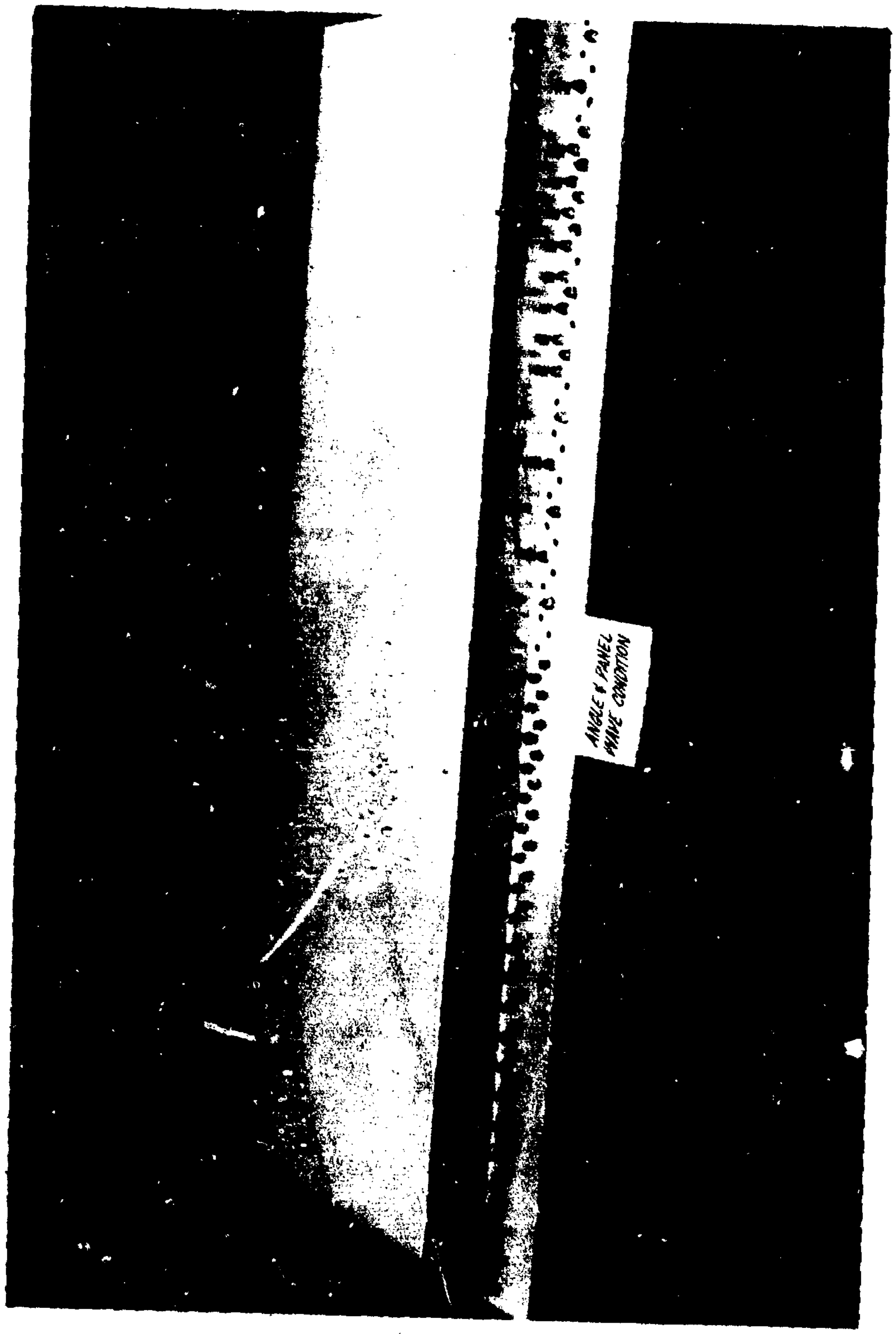

Figure 37. Bonded honeycomb panel specimen with wave condition.

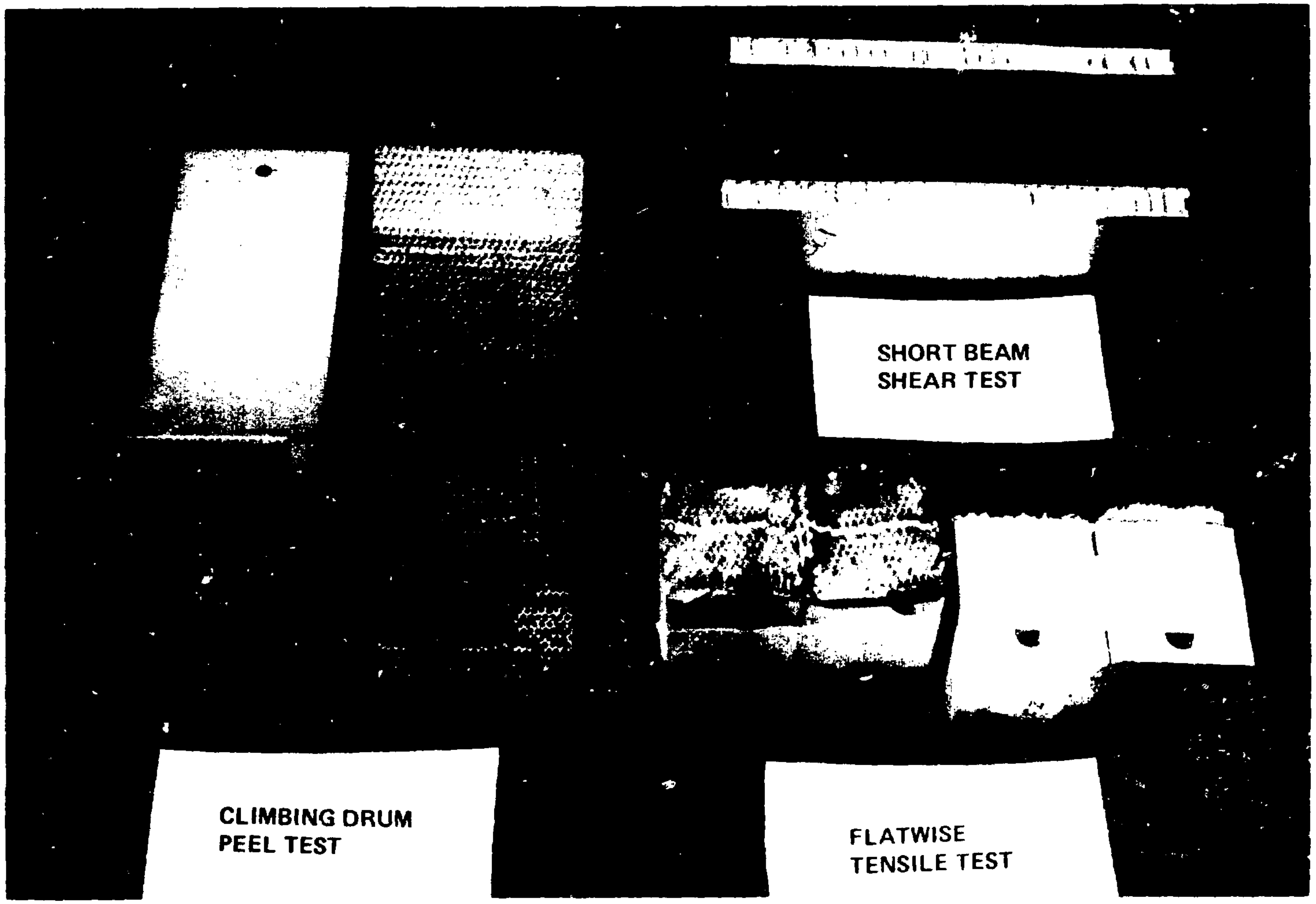

Figure 38. Oven bonded 4 x 8-foot test panel specimen.

A summary of evaluations, specimens and development tests accomplished is shown in Table 17.

A sample compound curved panel, SK301-11715, was fabricated, assembled, and bonded (Figures 39 and 40). The panel was assembled using aluminum flexcore bonded with .020" stretch-formed skins. The panel assembly was visually inspected and accepted, and turned over to Quality Assurance for bond evaluation and verification of inspection procedures. This sample was used to verify the concept of forming both the inner and outer skin on a single forming tool.

Three flatwise tensile specimens, frame attachment SK301-11728, were fabricated, bonded, and tested successfully.

An evaluation using polyvinyl chloride (PVC) film as a method to verify correct dimensional tolerances on compound contoured panels was conducted. The method proved to be successful.

An inspection plan was prepared for the structural bonded assemblies. This plan breaks down the inspection functions required through the build-up, assembly, and bonding of the panels.

Non-destructive test (NDT) procedures were developed for use on full-sized prototype bonded panels. Sections from the structural honeycomb bonded tooling test panel SK301-11679 and the compound curved panel SK301-11715 were used in this evaluation. Results of the SK301-11715 compound curved panel show questionable areas at the foam adhesive core splices using a hand scan test with both Sondicator and Harmonic Bond Test equipment. No other questionable areas were found when this panel was inspected again using immersion through-transmission ultrasonic inspection.

The panel was weighed prior to and following immersion in the ultrasonic tank to determine moisture absorption using this NDT technique. The result was 2.2% weight increase after 12 hours immersion time. An x-ray evaluation of the SK301-11715 panel for the extent of moisture penetration was completed (Figures 41 and 42). The dark areas indicate the presence of liquid and are found in the periphery, foam splice, and densified core area. It must be noted that this panel did not have the edges sealed.

All questionable areas indicated by NDT methods were destructively evaluated for confirmation and identification.

TABLE 17. SUMMARY HLH PROTOTYPE HONEYCOMB PANEL DEVELOPMENT PROGRAM

ITEM	PURPOSE	NUMBER OF SPECIMENS
1. LONGITUDINAL PLANK SPLICE (SK301-11648)	DETERMINE PROPER FABRICATION TECHNIQUE FOR JOINING TWO PANELS WITH MECHANICAL FASTENERS (BUTT JOINT-HIGH DENSITY CORE EDGES).	1
2. FASTENER FEASIBILITY (SK301-11667)	DETERMINE EFFECT OF USING VARIOUS TYPE MECHANICAL FASTENERS ON HONEYCOMB PANEL ASSEMBLIES WITH VARIOUS DENSITIES, SKIN THICKNESS AND EDGE DOUBLERS.	5
3. MISMATCH INNER/OUTER SPLICE STRAPS (SK301-11703)	DETERMINE COMPATABILITY OF JOINING TWO PANELS WITH WAVED SURFACES.	2
4. A/C-BORON REINFORCEMENT (SK301-11704)	TO DETERMINE FABRICATION TECHNIQUES REQUIRED TO REINFORCE PANELS WITH BORON.	2
5. MISMATCH SHIP LAP STYLE (SK301-11706)	DETERMINE FEASIBILITY OF USING THIS JOINT FOR PROTOTYPE.	1
6. MISMATCH FLUSH SHINGLE STYLE (SK301-11707)	DETERMINE FEASIBILITY OF USING THIS JOINT FOR PROTOTYPE.	1
7. CONTOURED PANEL - COMPOUND CURVE (SK301-11715)	MAKE TOOLS AND FABRICATE COMPOUND CURVED PANEL ASSEMBLY (18' x 24") TO DETERMINE MANUFACTURING PROBLEMS.	1
8. AFT PYLON LE SKIN PANEL	EVALUATE FABRICATION PROBLEMS IN LAYING UP PROTOTYPE AFT PYLON LEADING EDGE BONDED ASSEMBLY (APPROXIMATELY 4' x 8').	1
9. HONEYCOMB SPECIMENS FOR WATER RESISTANCE IN JOINTS (SK301-11723)	DETERMINE RESISTANCE OF HONEYCOMB JOINTS TO WATER PENETRATION.	1
10. FUSELAGE - QUALITY ASSURANCE TEST PANELS	ESTABLISH NONDESTRUCTIVE TESTING TECHNIQUES AND PARAMETERS (24" x 24").	1
11. LONGITUDINAL SKIN SPLICE - BONDED JOINT	DETERMINE MANUFACTURING FEASIBILITY FOR FORMING AND BONDING EDGE MEMBER.	1
12. BONDED HONEYCOMB FUSELAGE PANEL TEST PROGRAM	TEST SPEC FROM EXISTING MFG. PANEL AND NEW TEST SPECIMENS (REF. WPD #421001, TEST PLAN D301-10250-1).	40

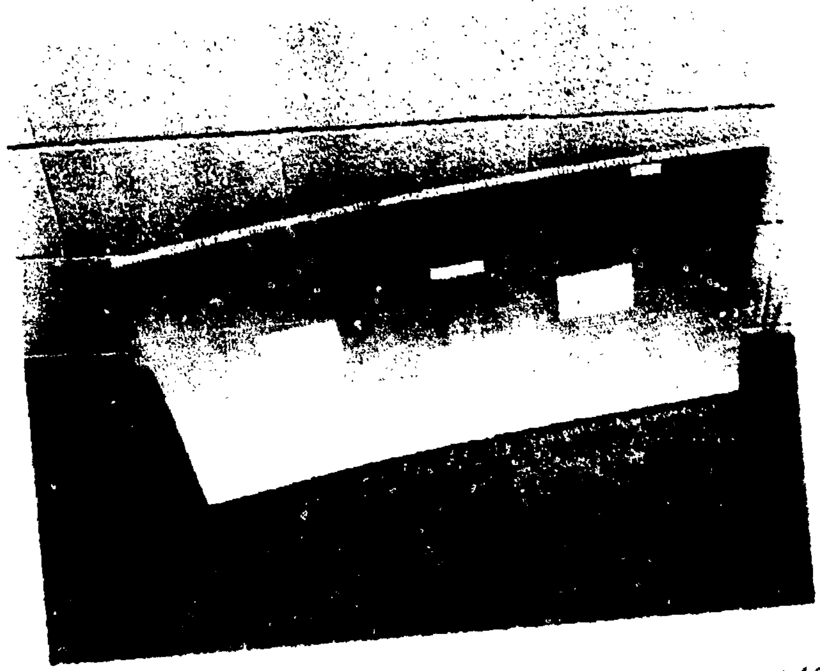

Figure 39. Bonded honeycomb compound contour test panel (front).

Figure 40. Bonded honeycomb compound contour test panel (back).

Figure 41. X-ray of SK301-11715 panel, showing moisture penetration.

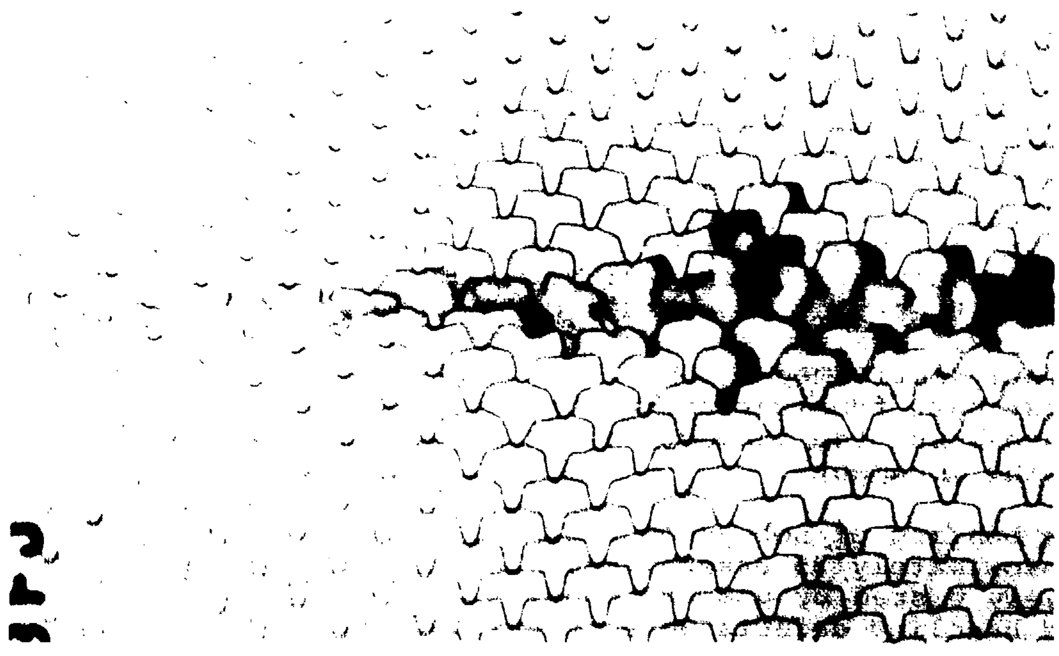

Figure 42. X-ray of SK301-11715 panel, showing moisture penetration in additional area.

The compound curved panel SK301-11715 (non-destructively tested) was further evaluated and found to have anomalies only in the foam splice areas as indicated in Figure 43 .

Evaluation of commercially available ultrasonic test equipment for inspection of prototype panel assemblies was completed. The MKII Harmonic Bond Tester manufactured by Shurtronics Corporation was chosen for the bonded panel assembly inspection.

Advantages of the Harmonic Bond Tester over other equipment are: (1) It requires no liquid coupler (i.e. water or oil) for inspection, eliminating the need for subsequent cleaning of parts. (2) Redundant defect alarm systems (light and buzzer). Light alarm was in the scanning probe eliminating the need for the operator to monitor a meter or oscilloscope. (3) Fast scanning capability which allows for automation. (4) Suitable for operation on a variety of composite structures and materials. Four units were ordered and received in-house. Inspection personnel were trained in the use of this equipment (Figure 44).

A quality standard reference panel with built-in defects, P/N 8-5800-2-94-X900, was fabricated. The defects were evaluated using the Harmonic Bond Tester and found to be an acceptable reference standard.

HLH Quality Assurance personnel reviewed Boeing Wichita's bond and inspection capabilities.

HLH Quality Assurance personnel also participated in the capability survey of the Lockheed Georgia Company, Charleston, South Carolina. This survey established that the facility had the capability to produce good quality bonded assemblies. Minor variations between Lockheed and Boeing specifications were resolved. Quality Procurement accomplished a system survey to review Lockheed's Documentation and Operating Procedures. Quality Assurance personnel and Quality Procurement jointly performed a technical audit of Lockheed during the first part fabrication. This audit included the fabrication process and the inspection techniques as applicable to the Boeing documents.

The bonding of honeycomb structures in-house was completed on approximately 35 assemblies. These assemblies were nondestructively tested by use of the Harmonic MKII Bond Tester. Bonding and handling defects were identified and reworked.

HLH Quality Assurance personnel witnessed the prefit and bonding of the 301-25500 crown panel at Wichita. This was the first large contoured panel (32 ft long) to be bonded.

Figure 43. Compound curved panel showing anomalies in foam splice areas.

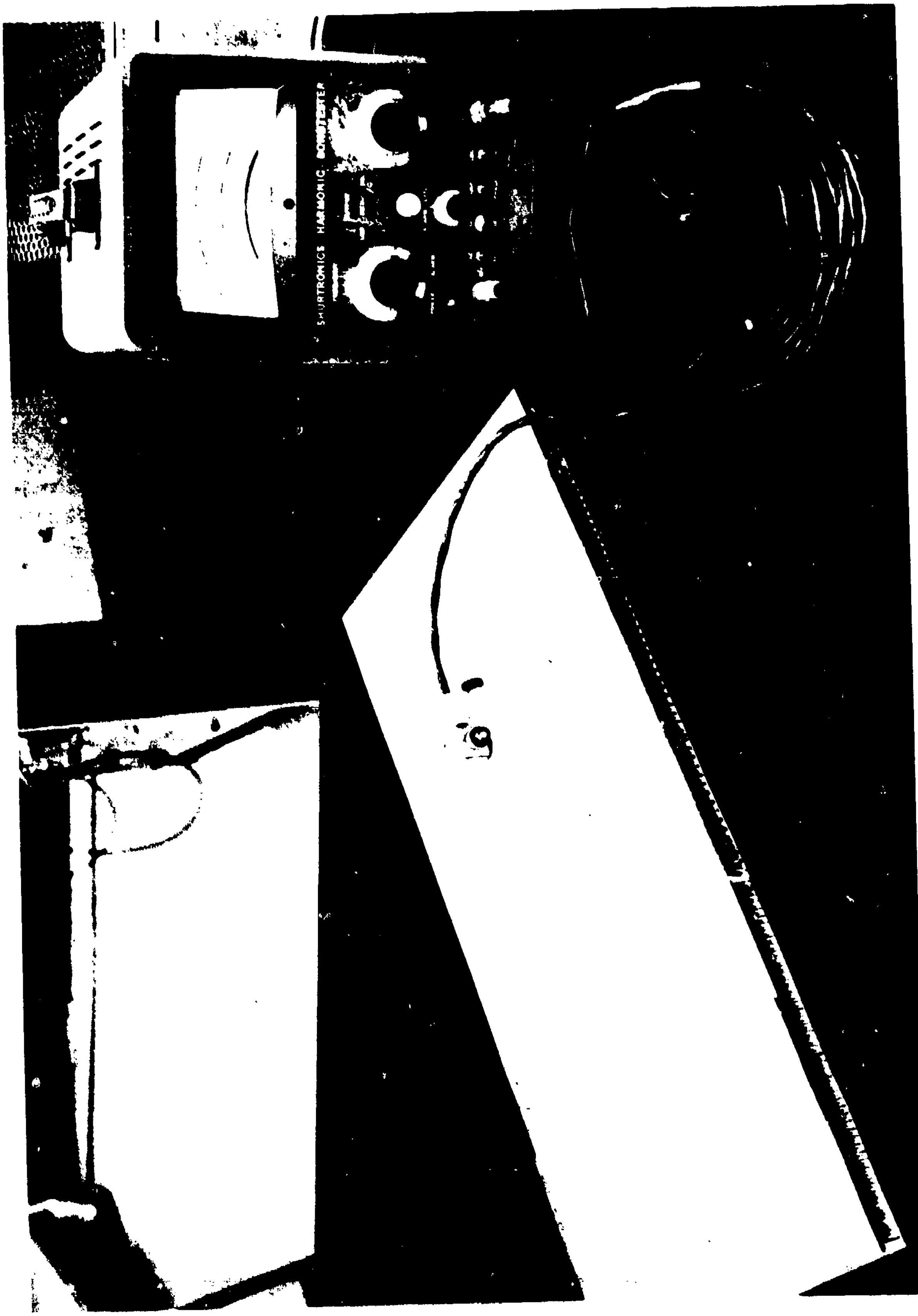

Figure 44. Harmonic bond tester Mk II.

HLH Quality Assurance personnel participated in off-load meetings with Kaman Aircraft. The off-load assemblies involved bonding both fiberglass and aluminum honeycomb assemblies. Kaman prepared specimens for qualification to bond per Boeing Document D-16538, "Bonding Structural Reinforced Plastic Parts" and D-16925, "Structural Bonding Metallic Parts". A survey of Kaman's facility was performed by Quality Assurance Technical Support and Quality Procurement personnel for compliance to Boeing requirements.

HLH Quality Assurance reviewed and approved Lockheed's specification variances. Lockheed submitted samples and data which met the requirements for qualification to D-16925 for structural bonding. The first prefit of detail parts at Lockheed was witnessed by Quality Assurance.

All major bonded assemblies from Boeing Wichita were received, visually inspected, and minor shipping defects documented and dispositioned. All bonded honeycomb panels were completed by Lockheed, Charleston, S.C. and received in-house.

Qualification specimens have been evaluated from Kaman Aerospace Company and Quality Assurance has taken part in facilities survey of Kaman facilities (Broomfield and Moosup, Conn.). Required process deviations were handled by specification revisions and Kaman was added as an approved honeycomb bond vendor.

Quality Assurance and Quality Technology personnel performed a correlation between Boeing Vertol NDT equipment (Harmonic Bond Tester) and techniques and Lockheed's equipment (Sperry 715) and technique. Lockheed constructs a standard test panel for each configuration. Boeing Vertol has one test panel only (for calibration). This analysis showed Boeing Vertol methods could find all bond anomalies reported by Lockheed and, if required, substantiate the area upon receipt of the assembly inhouse.

A reliable method has been developed to allow inspection of assembled panels for the detection of materials such as peel ply or backing paper, inadvertently left in the panel during processing. This involves drilling a small (1/8" diam) hole in the suspect area and examining the chips under magnification and black light. Along with this, nondestructive inspection using ultrasonics is performed to determine unbonds.

Final joining of the HLH fuselage sections was accomplished on 21 April 1975 at Boeing Vertol. The previously joined aft and center fuselage assembly was removed from jig restraints, the aft fuselage jig disassembled, and the fuselage jacked approximately five feet to permit insertion of support

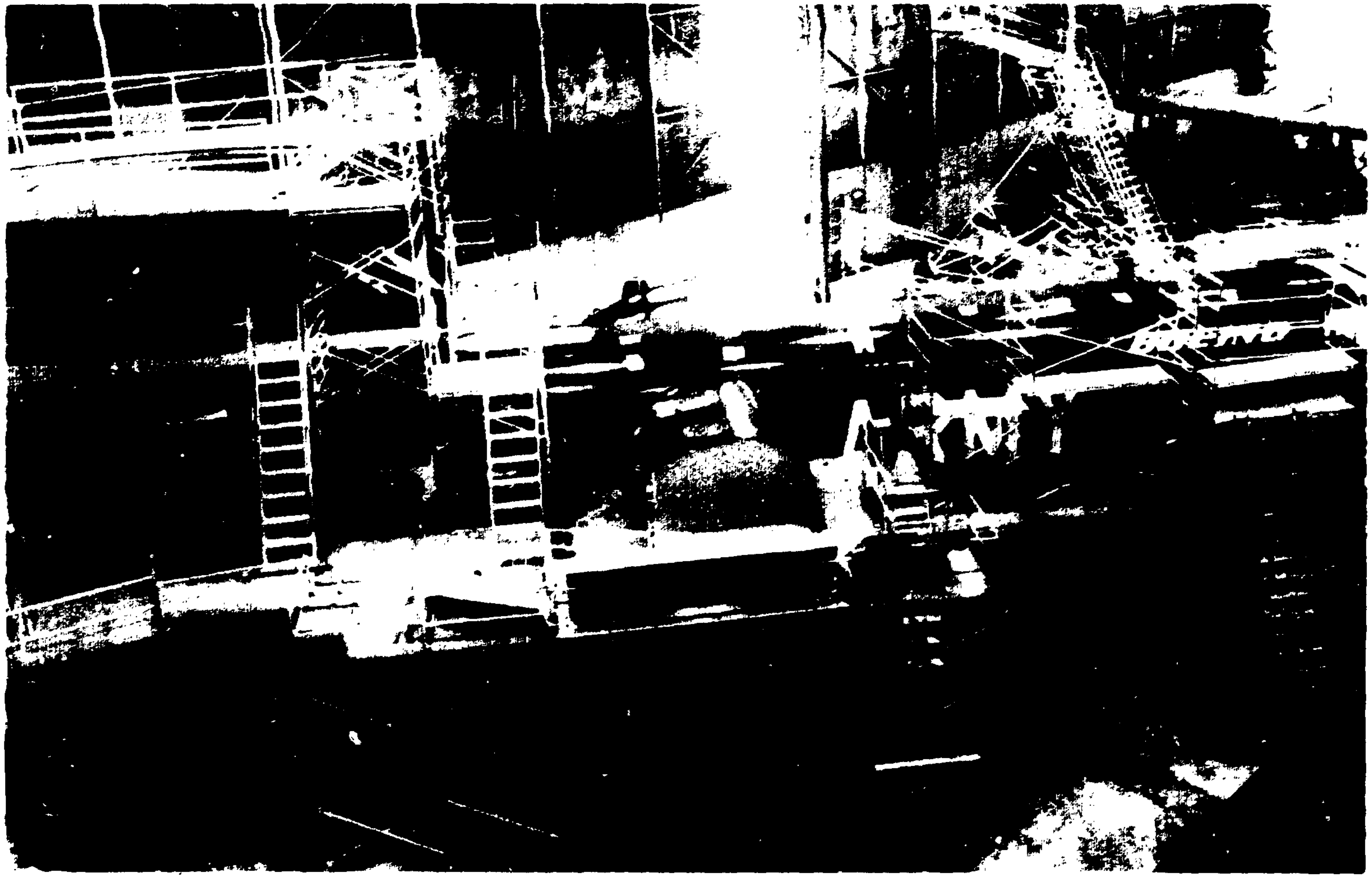

Figure 45. Primary assembly - July 1975.

tooling beneath. The entire assembly was then rolled forward on previously positioned tracks and successfully joined to the forward fuselage. All mismatches at this join were minimal and well within the .040" mismatch experienced at the previous join of the 52-foot center fuselage to the aft fuselage, accomplished in March.

The achievement of little or no mismatch at splice is evidence of significant technical advance in design and tooling concepts, when it is realized that contoured bonded skin panels and their associated tooling were fabricated by four different manufacturing facilities: Boeing Vertol, Ridley Park, Pa.; Boeing Wichita, Kansas; Lockheed Marietta, Georgia and Charleston, S.C.; and Kaman Aerospace, Bloomfield and Moosup, Connecticut.

All tooling information as well as basic lines for non-dimensioned engineering drawings were extracted from the Boeing-developed Master Dimensioning (M.D.) system, a computerized mathematical lofting system first used extensively on the 747 program. Extractions from the M.D. system were made by each manufacturer independently, bypassing the need for tooling masters.

Besides providing contour information for fabrication of bonding tools, which were also of advanced concept, M.D. extractions were also used to supply the input for numerical tape-controlled machining of contours on large fittings and for manufacturing of form blocks for those few areas on the HLH where double curvature skins exist.

Fuselage tuning, i.e. adjusting the natural frequency of the strength-configured airframe, is accomplished by the addition of high strength/high modulus unidirectional composite graphite/ epoxy strips to the axially loaded (longeron) edge members of the honeycomb skin panels.

Low vibration environment for the cockpit and the load controlling crewman station is provided by the isolated module concept. Crew seats, flight controls, instrument panels, and consoles are all mounted to a common structural base to form a module package. Each module assembly is mounted to the airframe via four DAVI (Dynamic Anti-resonant Vibration Isolator) units, which isolate the module from the vibratory characteristics of the basic structure.

The engine work platform is a unique maintenance feature of the HLH. The entire lower section of the fuselage and the outboard engine pods, below the center line of the engines, is a separate unit which, when lowered by the electrically powered lift system, provides a walk-around service platform for access to the three engines. Operation of the lift system is controlled from an operator's control panel located in the fuselage just forward of the work platform. The lift system consists of a centrally located power pack connected to two ball-screw linear actuators. The power pack and the fixed end of the actuators are mounted to basic structure. The lower end of the extendable actuators are connected to the movable work platform. The power pack consists of an electric motor driving a speed reduction "tee" gear box. The two outputs from the power pack are connected to the actuators by torsion drive shafts. The two actuators each consist of an angle drive gear box, the circulating ball housing, and the extendable threaded shaft. The gear box and housing is mounted to basic structure in a fixed relationship. The lower end of the threaded shaft is connected to the work platform with a self-aligning attachment. Longitudinal and lateral positioning of the work platform in all vertical positions is maintained by an extensible scissors mechanism located at each of the vertical actuators.

A review of the weight and parts count status in May 1974 is shown in Table 18. These data indicated that initial estimates were being achieved for the prototype and that further reductions could be attained for the production configuration.

TABLE 18. FUSELAGE PARTS COUNT & WEIGHT SUMMARY

MAY 28,1974 REVISION

FUSELAGE SECTION	CURRENT PROTOTYPE RELEASED			PROTOTYPE ESTIMATE AT COMPLETION			PRODUCTION ESTIMATE			
	PARTS	WT.	PARTS/#	PARTS	WT.	PARTS/#	PARTS	WT.	PARTS/#	% REDUCTION FROM PROTO
FWD.	2,612	3,488	.749	4,143	4,933	.84	3,712	4,415	.84	10.0%
CENTER	1,678	3,129	.536	2,349	3,559	.66	2,100	3,175	.66	11.0%
STUB WING	1,358	2,059	.66	1,364	2,067	.66	1,221	1,845	.66	10.0%
AFT	2,082	2,532	.82	3,368	4,490	.75	3,015	4,015	.75	10.0%
TOTAL	7,730	11,208	.69	11,224	15,049	.75	10,048	13,450	.75	10%

2.6.3 Final Configuration Description. The final primary structure design utilizes sandwich panel bonded aluminum honeycomb construction for the entire outer skin. In addition, the transmission decks, the transmission load path frames, the landing gear load path frames, the fuel pods and engine pods load path frames, and the external cargo hoist support beams are also constructed of bonded aluminum honeycomb (flat) sandwich structures.

Longitudinal beams, which provide edge support for the longitudinal joints between honeycomb panels and stabilize the axially loaded edge members of the panels, as well as fuselage frames other than the major load path frames, are designed as conventional sheet metal structure.

The primary structure section of the fuel pod is a two-spar torque box with four ribs on each side of the aircraft. The spars and ribs are bonded aluminum honeycomb (flat) sandwich panels. The upper and lower skin panels are single-curvature bonded aluminum honeycomb.

The engine pod support structure is a two-spar torque box constructed of bonded aluminum honeycomb panels.

Non-metal bonded honeycomb construction is utilized extensively for secondary structures.

The leading edge of the fuel pod, which forms the cavity structure for the crash resistant fuel cells, consists of sandwich structure ribs and skin panels. The skin panels consist of non-metal cores with fiberglass-reinforced plastic skins. The ribs, which are designed to a stiffness criteria, consist of non-metal cores with Kevlar (PRD-49) reinforced plastic skins.

The center engine shroud, which forms the firewall enclosure, is a bonded sandwich construction using non-metal core and glass-reinforced faces of polyimide resin system producing a panel which meets the specification requirement for engine compartment firewalls.

Fiberglass-reinforced plastic-faced honeycomb skin panels are used exclusively in pylon fairings, pylon work platforms, engine work platform outer skin, and pylon leading and trailing edge components.

All primary structure was released by the first week in May 1974 and the concentration of manpower shifted to the design and release of secondary structure such as forward and aft pylon fairings and work platforms, engine work platform, doors, hatches, and ladders.

2.7 LANDING GEAR

The HLH landing gear is a tricycle type with dual wheels on each strut, differential braking on the main gears only, and power steering on the nose gear. Conventional materials were used for the prototype gear rather than advanced composites.

Early in the prototype program, design-to-cost trade studies were conducted. These studies examined the impact of weight, recurring cost, maintenance, reliability, and load acquisition as a function of landing gear height, kneeling features, and design point (landing gross weight). The results were presented to the HLHS PMO on 30 March 1973 and at the Systems Requirements Review meetings held at Boeing Vertol.

The production HLH landing gear as originally conceived provides for differential kneeling of the main and nose gear to allow for a 10- to 15-degree slope landing. In addition, the landing gear is configured to allow operations with fuselage clearance and also in a "high" configuration with 14' ground-to-fuselage clearance. The latter position, 14' clearance, enables the helicopter to taxi over an 8' high load supported on a dolly. The load-controlling crewmember is equipped with controls and brakes to position the helicopter over such a load.

A review of the landing capability of the HLH indicated that there is ample rotor control to provide for a 10- to 12-degree slope landing with fixed length gear (no differential kneeling). Removal of the kneeling requirement from the present landing gear provides an estimated savings of 1100 pounds and $44,000 recurring cost per aircraft (based on 250 aircraft). There is a reduction in malfunction rate of 47 per 1000 manhours which results in a reliability improvement of .25 maintenance manhours per flight hour.

The design analysis also included an examination of the weight, cost, and performance as a function of landing gear height (ground-to-fuselage clearance). The landing gear height was varied from a maximum of 14' fuselage clearance to provide

taxi capability over an external load to a minimum height of 8'-8" fuselage clearance. Table 19 summarizes the weight and cost comparisons.

TABLE 19. LANDING GEAR HEIGHT TRADE STUDY

FUSELAGE TO GROUND CLEARANCE	LANDING GEAR	WEIGHT (LB)	COST REDUCTION BASED ON 250 A/C
8'-8"	Non-Kneeling	5877	$18,000
14"	Non-Kneeling	6389	Baseline

The above table shows a weight savings of 382 pounds and a cost savings of $14,000 per aircraft (over 250 aircraft) by reducing the clearance height from 14' to 8'-8" which is the minimum height required to accommodate the LCC station. There is no measurable improvement in reliability and maintainability in going from 14' clearance to 8'8" clearance.

The results of an analysis of landing design gross weights is shown in Table 20. The aircraft design gross weight condition (118,000 pounds) is compared to a no-external-load condition (81,000 pounds landing gross weight).

TABLE 20. LANDING WEIGHT TRADE STUDY

GEAR DESIGNED TO GROSS WEIGHT	FUSELAGE CLEARANCE	SINK RATE/ GROSS WEIGHT	LOAD FACTOR	TAXI WEIGHT	LOAD FACTOR	GEAR WEIGHT	COST RED. BASED ON 250 A/C	WEIGHT REDUC.
81,000	14'	16.9 at 81,000	2.25	148,000	2.0	6,389	--------	*
		12.0 at 118,000	2.00					
	8'8"	8.0 at 148,000	----			5,627	$21,000	588
118,000	14'	17.7 at 81,000	2.25	146,000	2.0	6,389	--------	---
		16.9 at 118,000	2.00					
	8'8"	8.0 at 148,000	----			5,877	$14,000	392

*There is some reduction in airframe support structure weight, estimated to be under 100 pounds.

Cost and weight reductions for kneeling, gear height, and design point are additive; thus elimination of kneeling, reduction in gear height to approximately 8'-8", and reduction in design point from 118,000 pounds to approximately 81,000 pounds would result in a weight reduction of 1,688 pounds per aircraft and cost saving of $65,000 per aircraft based on 250 aircraft.

As a result of these analyses, the following recommendations were made for the HLH production and prototype configurations in the interest of cost and weight reduction:

a. Delete the requirement for landing gear kneeling (landing gear to be fixed).

b. If there is a firm operational requirement for over-the-load taxi, retain the 14' fuselage clearance.

c. If the over-the-load taxi requirement is "soft", the 8'-8" fuselage clearance is the most cost effective configuration.

d. Design either the tall or short gear to 92,000-pound gross weight, which is an ample margin over weight empty plus fixed useful load, 12 troops, full fuel, and an allowance of 6,000 pounds for a universal top lift adaptor. In the interest of conservatism, either gear designed to a 92,000-pound gross weight is recommended in lieu of the 81,000 pounds used in the trade studies.

The decision was made by AVSCOM to retain the 14-foot height gear for the prototype in order to allow a service evaluation of this feature. Kneeling was deleted and a 93,000-pound landing gross weight was established.

The procurement specification was released and a vendor (Menasco) was selected to design and fabricate the landing gear. A decision was made to use hydraulic power for the nose gear steering actuator after studies of pneumatic versus hydraulic systems were completed.

As a result of a crashworthiness review in July 1973, the nose landing gear was redesigned to improve crash survivability in the crew compartment. The attachment to the fuselage has been revised to provide a predictable breakaway path for the nose strut away from the crew compartment in the event of a crash landing.

A weight problem of 350 pounds per ship set of landing gear was identified, and was addressed by the vendor and Boeing Vertol engineering.

The landing gear design was subjected to an intensive weight review for optimization of each detail.

In February and March the main gear side brace design underwent a critical evaluation to optimize its weight; however, cost considerations did not permit a design change for the prototype aircraft.

Approval of vendor drawings began in January. The critical design review was held at Boeing Vertol on February 5-6, 1974.

Design of the landing gears and power steering system was completed in June 1974 together with specifications, materials, and processes, and spares requirements.

Qualification testing of the wheels and brakes was conducted by Goodyear Tire and Rubber Company in late 1974. The original test objectives were achieved except in the three areas discussed below. However, it was determined that the wheel and brake assembly was adequate for use on the prototype aircraft for the following reasons:

Static Torque (Hot): Insufficient pressure was applied during this test. Since 3000 psi was available in the aircraft braking system, it was not considered a problem. Also there was no plan in the test program to park the aircraft on a 20° slope.

R.T.O. Requirement: This requirement was based on stoping a 148,000-lb aircraft. Since it was not planned to take off or land at this gross weight, the 20 stops at 93,000 lb gross weight plus what was achieved during the R.T.O. stop was considered adequate.

Structural Torque: This test would normally have been performed after the R.T.O. stop but due to damaged test parts could not be performed. However, this test had been run earlier on a similar part and was successfully completed. This test was considered adequate, based on similarity.

Ground Resonance Test. The main landing gear was tested to determine ground resonance damping qualities. Tests to determine friction forces in the strut of the gear due to axial loading and side loading were conducted and the lateral stiffness of the gear was ascertained.

The damping test covered a range of strut mean loads and a range of amplitudes of oscillation for each strut load. Tests were conducted for a gear with two inflated tires; also in some cases, for a gear with only one inflated tire to simulate a burst tire condition. In the one inflated tire condition, tests included increase of strut air inflation pressure to 120% of normal.

In order to simulate partial airborne conditions of the aircraft, the tests performed at lower strut loads had gear at a cant angle in compliance with the 3° nose up attitude. For higher strut loads the angle was that for the normal, non-airborne attitude, i.e., 6° from vertical.

The damping characteristics of the main landing gear obtained from the damping test were considered to be acceptable. The orifice size was found to be the optimum for lightly loaded and fully extended gear positions.

The equivalent linear damping (Ceq) requirements were exceeded according to test results, for all cases except for amplitudes higher than 1.3 inches at the fully extended and 1" off bottoming spring positions, and 1.5-inch amplitide at the 8.6-inch strut closure position. The reason for these exceptions is the cavitation effect for which there is very little that can be done that would result in a significant improvement above that already accomplished, apart from increasing strut charge pressures.

Results for one inflated tire were obtained and a decrease in damping was required.

By comparing results obtained using table displacement with those of strut movement at a point in the mid-range of the test, it was concluded that the contributions of tire damping to the total Ceq value is about 50 lb. sec./in. Thus the majority of damping, in all cases, is due to the orifice in the strut.

Friction affects the gear by delaying the strut oscillation at small tire amplitudes but after break-out of the strut the effect of friction is to cause a peak in damping coefficient. This effect is reduced after tire amplitudes of approximately .5 inches.

The effect of changing tire pressures could be seen from the graphical results. The Ceq increases significantly when the tire pressures are increased from 94 psi to 134 psi. The reason for this is that increasing the tire pressure increases the tire stiffness. As predicted in the analysis prior to testing, the tire stiffness has a great influence on the damping characteristics of the gear and the higher the stiffness, the higher the Ceq.

The main reason that the initial Ceq measurements with tires at 94 psi were too low is that the tire stiffness was approximately 25% lower than predicted.

Drop Tests. The following series of tests were performed on the main landing gear. Since the test unit was a flying article, no testing beyond limit conditions was permitted.

Leakage Test. The shock strut was fully serviced and mounted in the upright position in the drop test tower. The piston tube was then cycled six times over 9.0 inches from the fully extended position. There was no evidence of leakage during or at the end of the test. The excursion of the piston was smooth and free from chattering or binding.

Static Airspring Curve. The isothermal pressure of the air chamber was measured over the entire piston travel, with the gear installed in the drop test tower. The actual airspring curve is superimposed on the predicted curve in Figure 46.

Drop Testing. A summary of drop tests and test conditions that were performed is given in Table 21. In the three cases that slightly exceeded the specification requirements, the vertical loads in combination with the drag loads did not prove to be a critical design condition.

TABLE 21. SUMMARY OF DROP TESTS AND TEST CONDITIONS - MAIN GEAR

TEST NO.	WEIGHT	Vv FPS	V_H KNOTS	LANDING ATTITUDE	LIMIT VERT LOAD Spec Req't	LIMIT VERT LOAD Test Result
1	BSDGW	12	60	LEVEL 3 PT	58,350	65,500
2	DAGW	8	60	LEVEL 3 PT	61,000	58,700
3	BSDGW	12	0	LEVEL 3 PT	58,350	57,300
4	DAGW	8	0	LEVEL 3 PT	61,000	49,500
5	BSDGW	12	40	20° NOSE UP	68,100	72,000
6	DAGW	8	40	20° NOSE UP	73,100	61,750
7	BSDGW	12	0	20° NOSE UP	68,100	74,000
8	DAGW	8	0	20° NOSE UP	73,100	58,500

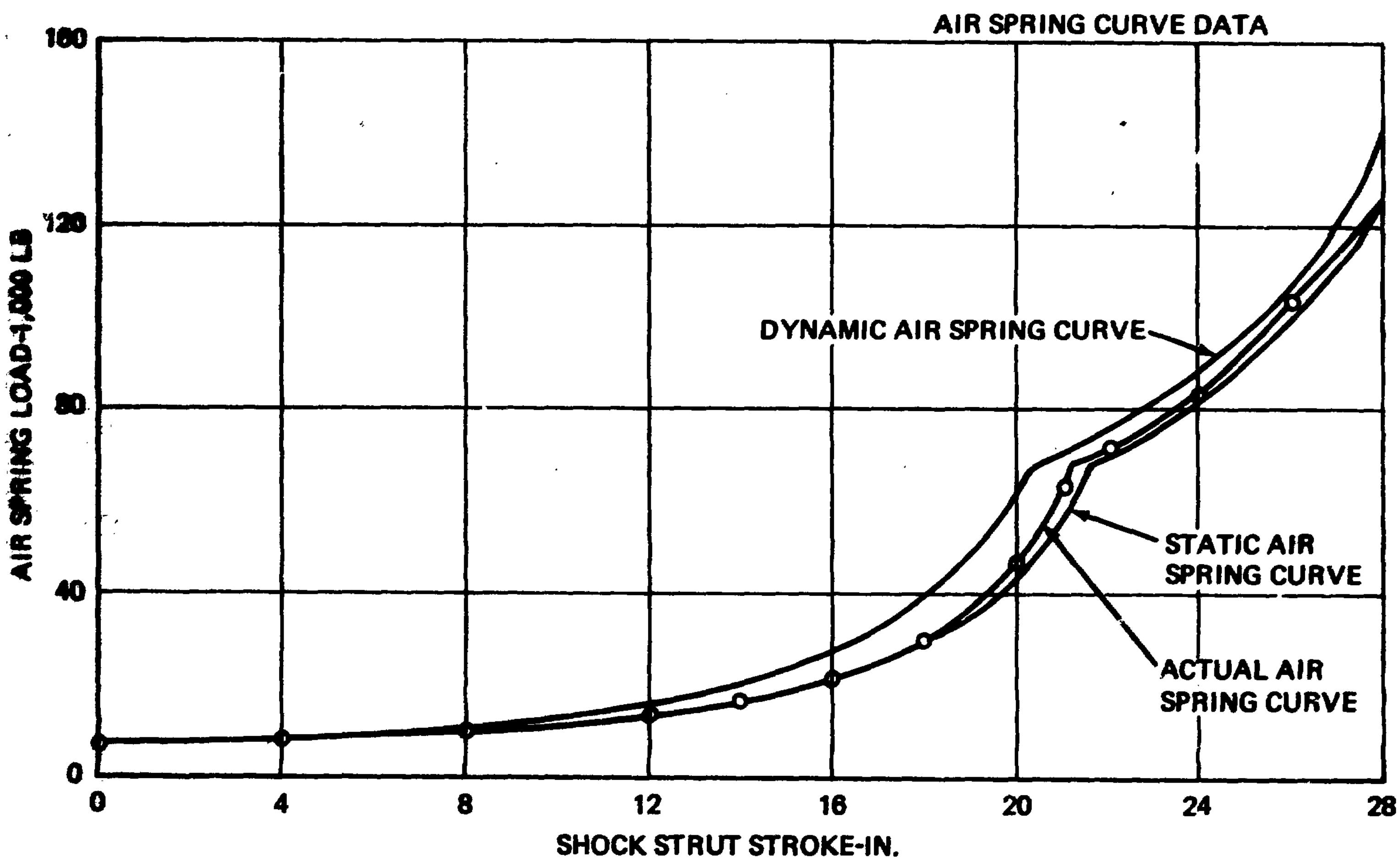

Figure 46. Predicted and actual airspring curves - main gear.

Nose Landing Gear - Qualification Testing.

The following series of tests were performed on the nose landing gear. Since the test unit was a flying article no drop testing beyond limit conditions was permitted. During the steering testing functional tests were performed for a limited number of cycles to give a reasonable confidence level in the design.

Leakage Test. The shock strut was fully serviced and mounted in the upright position in the drop test tower. The piston tube was then cycled six times over 6.5 inches from the fully extended position. There was no evidence of leakage during or at the end of the test. The excursion of the piston was smooth and free from chattering or binding.

Static Air Spring Curve. The fully serviced shock strut was mounted in upright position in the drop test tower. The piston was compressed incrementally from zero stroke to fully compressed and the shock strut load was measured at each increment. The actual airspring curve is superimposed on the predicted curve in Figure 47.

Steering Tests. The following tests were carried out with the Nose Gear installed in the drop test carriage.

a. With the strut deflated and the axle supported in the static stroke position by a low friction rotary table (no external load applied), the steering unit was operated clockwise and counter-clockwise for 100 full-stroke steering cycles. Supply pressure was allowed to build up to 3000 PSIG at the end of each excursion.

b. Additional cycles under load were conducted as described below.

Minimum Steering Pressure. With the strut fully serviced, tires installed and the weight over the gear adjusted to collapse the strut to it's "static" position, the minimum pressure required to maintain motion (near stall) of the scrubbing tires was measured with the following results:

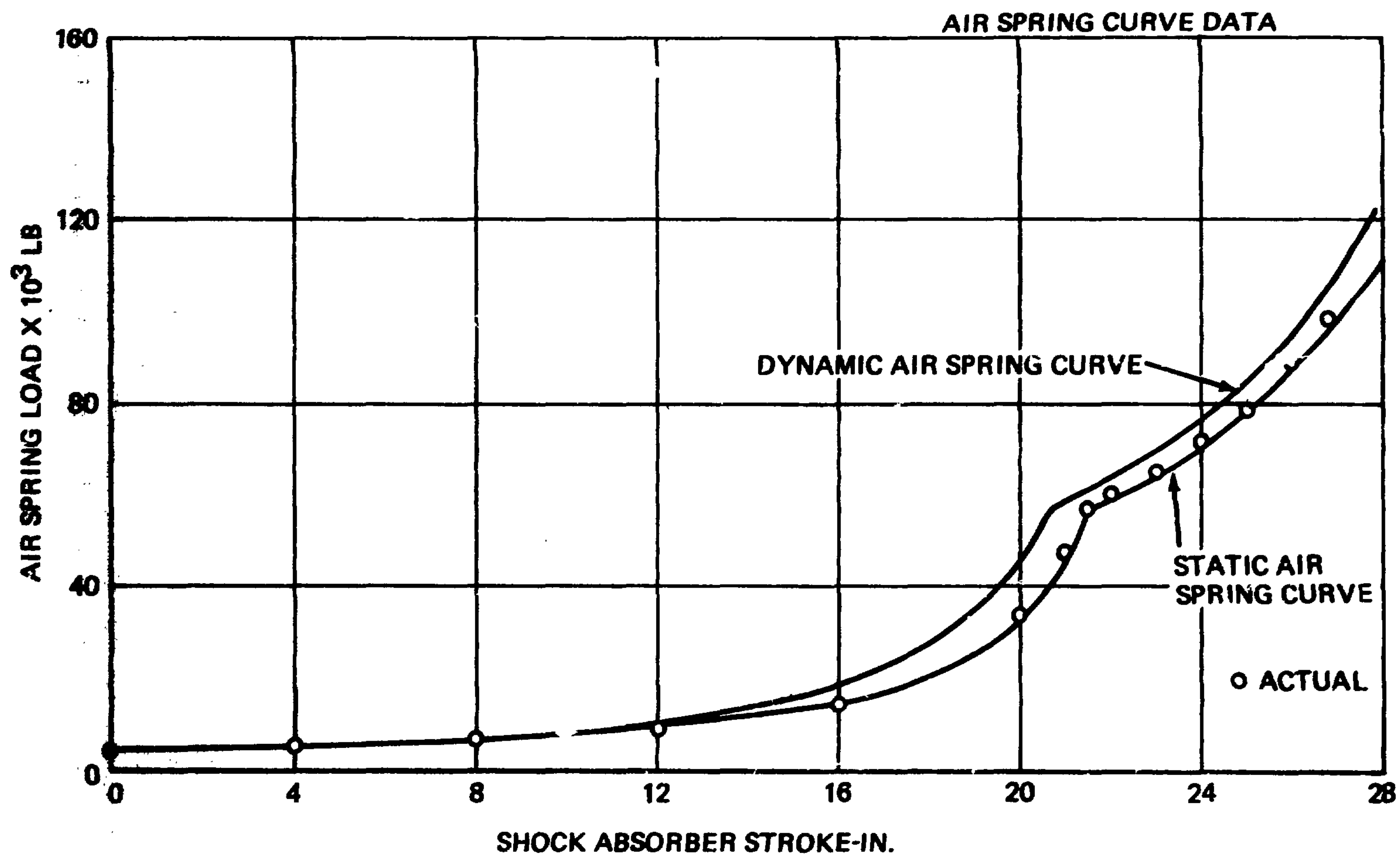

Figure 47. Predicted and actual airspring curves - nose landing gear.

0° wheel position - 500 PSIG; 45° wheel position - 1500 PSIG. The steering unit was operated for approximately 50 such cycles between 45° left steer and 45° right steer position.

Steering Rate. With the strut deflated, dummy wheel connected to hydraulic loading cylinders generating a constant resisting torque of 92,000 lb-in, and the piston collapsed in the static stroke position (axle supported on low friction rotary table), the steering rate was measured through the zero degree position under 3000 PSIG system pressure at the steering actuator in both directions: Clockwise - 10°/sec, Counter-clockwise - 9°/sec.

The total excursion for this test was limited to + 35° by the bottoming of the loading cylinders.

Steering Angle. With the strut deflated, wheels and tires reworked, and the piston held in the static stroke position, maximum steering angle was measured with 3000 PSIG supplied on the steering actuator with the following results:

a. Clockwise - 79.1°

b. Counter-clockwise - 81°

Castoring. The castoring angle was verified with the gear outside the tower by rotating the piston with the steering system and both air chambers depressurized, and the wheels clear of the ground. The castoring angle was found to be 360° clockwise and counter-clockwise.

Centering Time. The centering capabilities of the cams backdriving through the steering system was verified. The gear, with tires included, was installed in a static position at a steering angle of 30° right. The carriage was lifted and the self-centering response time was measured. The test was repeated from steering angle 30° left. The centering times were recorded as follows:

a. From 30° right, 9.4 seconds.

b. From 30° left, 8.4 seconds.

Drop Testing. A summary of drop tests and test conditions that were performed is given in Table 22.

TABLE 22. SUMMARY OF DROP TESTS AND TEST CONDITIONS - NOSE GEAR

TEST NO.	WEIGHT	Vv FPS	VH KNOTS	LANDING ATTITUDE	LIMIT VERT. LOAD spec. req't	LIMIT VERT. LOAD test result
1	BSDGW	12	60	LEVEL 3-Pt	38,400	59,500
2	DAGW	8	60	LEVEL 3-Pt	52,800	42,750
3	BSDGW	12	0	LEVEL 3-Pt	38,400	47,750
4	DAGW	8	0	LEVEL 3-Pt	52,800	45,250
5	BSDGW	12	40	15° NOSE DOWN	96,600	78,500
6	DAGW	8	40	15° NOSE DOWN	70,100	59,250
7	BSGDW	12	0	15° NOSE DOWN	96,600	71,500
8	DAGW	8	0	15° NOSE DOWN	70,100	61,250

In tests 1 and 3 where the specification requirements were exceeded, it was found that these loads were not design conditions. The design condition is the obstruction case which has a V_A=55,700 combined with a D_A=27,850 at fully extended position. It was therefore accepted with no further development to the shock strut.

2.8 AIRCREW SYSTEMS

2.8.1 Crew Seats

A pilot/copilot seat spacing study identified a seat centerline position of 22 inches on either side of the aircraft centerline as optimum for functional reach overlap and ingress/egress area. This is two inches greater than the maximum seat-to-seat centerline spacing allowed by MIL-STD-1333.

Detail requirements for prototype crew seats were reviewed to determine the extent to which anthropometric accomodation, crash survivability, and armor should be furnished or provided. Several combinations of seat buckets and frames were considered and were discussed at the System Requirements Review in March 1973. Based on cost, weight, availability and performance, it appeared that a seat of the UTTAS design type would be the most satisfactory. Consideration was given to the joint Army-Navy (ARA) seat, which appeared to provide less crash survivability than required by TR 71-22, as an alternative. There is no requirement for an armored seat in the prototype but space provisions were allowed to avoid necessity of redesign for production. A fiberglass bucket design with 19.8" seat width was started in the event that the selected seat has only armored buckets available. Since the mounts for the fiberglass bucket would match those for the armored seat bucket, the cost of the seat base should not be affected.

A briefing on crew seat alternatives was conducted at AVSCOM on 10 April 1973. Crash-survivable armored UTTAS seats were selected for the prototype. The installation design included provisions for extended tracks to facilitate ingress/egress.

2.8.2 Crew Vision Study

In an effort to determine helicopter vision requirements by an analytical approach, Boeing Vertol conducted the following study.

First, the flight tasks listed on the information/action analysis sheets which required human vision to accomplish were listed. Then, each of the tasks were correlated with

/1)

the mission segments in which they took place. The flight control tasks then were listed under each mission phase in which they occurred, and columns were allocated (designated left, right, up, and down) in which selected subjects were asked to note their subjective interpretation of the vision requirements (in degrees) necessary to accomplish the function. Seven subjects participated in this study. The survey results were analyzed and the data plotted in rectilinear form using a color coded system of plotting. The color code was based on the priority defined for each visual area.

The top priority vision requirement areas were overlayed on a MIL-STD-8505B vision plot (helicopter). Figure 48 shows them prioritized by both mission segment and functional utilization. The area from 30 degrees to 60 degrees outboard and 20 degrees to 30 degrees down comes out as a prime vision area for hover. It was concluded that vertical posts should be kept out of this area.

As a result of the external vision requirements analysis, the windshield corner post location was moved forward to the 30-degree azimuth, thereby improving downward forward vision. In addition, the browline windshield frame was raised to improve upward vision. These changes permitted the use of flat windshield glass instead of curved glass, which not only reduced glint, but also resulted in an ultimate cost avoidance in production due to simpler windshield fabrication and a less complex washer/wiper scheme.

2.8.3 Flight Engineer Station

A Human Factors crew workload analysis indicated that a flight engineer is not necessary for the production HLH, because there are no flight tasks which cannot be handled by the pilot, copilot, and load controlling crewman. In order to substantiate the analysis during prototype flight test, it was decided that the flight engineer would be located in a forward-facing centerline position just aft of the pilot and copilot. This would permit sharing of the pilot/copilot controls and displays, thereby eliminating the requirement for a separate flight engineer's console. This is the most cost effective approach.

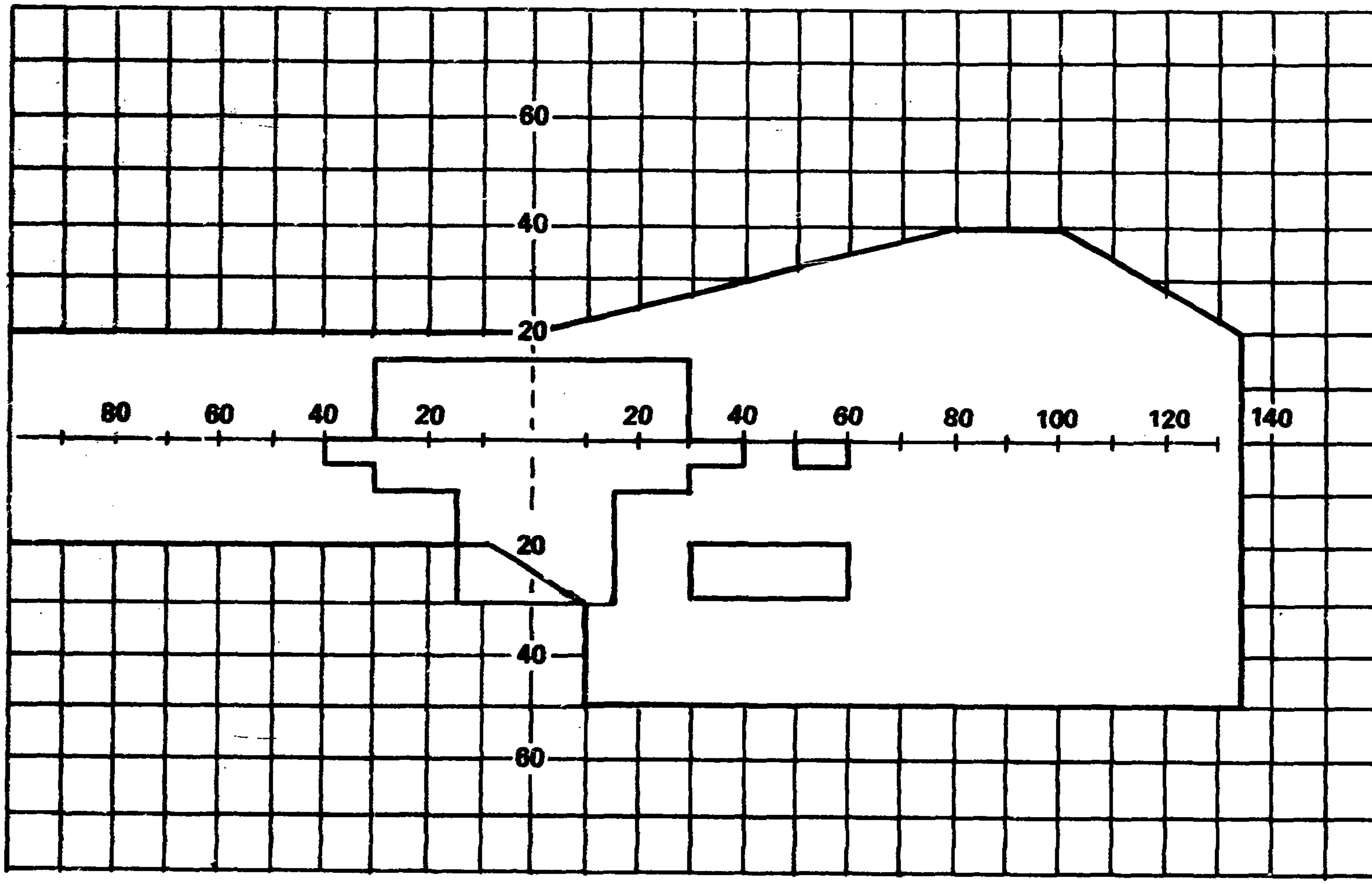

TOP PRIORITY VISION REQUIREMENTS PRIORITIZED BY BOTH MISSION SEGMENT AND FUNCTIONAL UTILIZATION

Figure 48. MIL-STD-850B vision plot.

2.8.4 Crew Compartment Mockup

During September 1973, the crew compartment mockup was completed for an internal Boeing Vertol review. A significant number of change/study requests were generated at the in-house review. Many of these changes were incorporated for the customer mockup review. The review was conducted on October 25-26, 1973 by 48 representatives of the following organizations:

HLH PMO	USAOTEA	USATECOM	USAECOM
USAAMRDL	USAASTA	USAAVSCOM	USAMC
OCRD	USATSCH	USAARL	UTTAS PMO
USABV-PA	USATRADOC	Log Center	USAHEL (APG)
USAAAVS	NAVAISYSCOM	355th Avn. Co.	Allison

Of the 205 change requests submitted, 52 were approved for incorporation into prototype and 60 were disapproved. Eleven were approved for study on the prototype, 4 for study on production, and 10 recommended for incorporation in production. There were 64 duplications and 4 withdrawals.

Approved prototype changes were incorporated into the engineering drawings for the prototype.

Completion of the mockup review marked the successful accomplishment of the contractual milestone. Mockup minutes were submitted by Boeing Vertol letter 8-5100-17-9 dated 16 November 1973, and approved by AVSCOM letter 0840-737L dated 2 January 1974.

The final instrument panel arrangement is shown in Figure 51. Overhead panels and consoles are shown in Figure 52. The LCC station is shown in Figure 53.

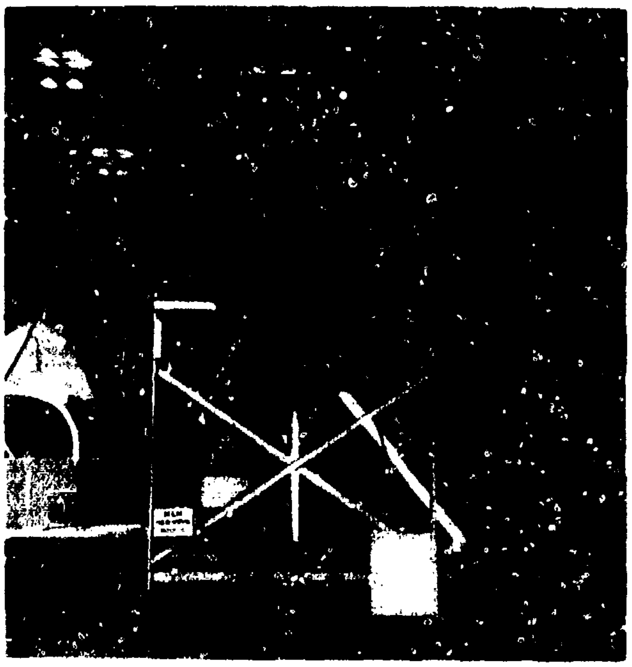

Figure 49. Crew station mockup.

Figure 50. Internal view of crew station mockup.

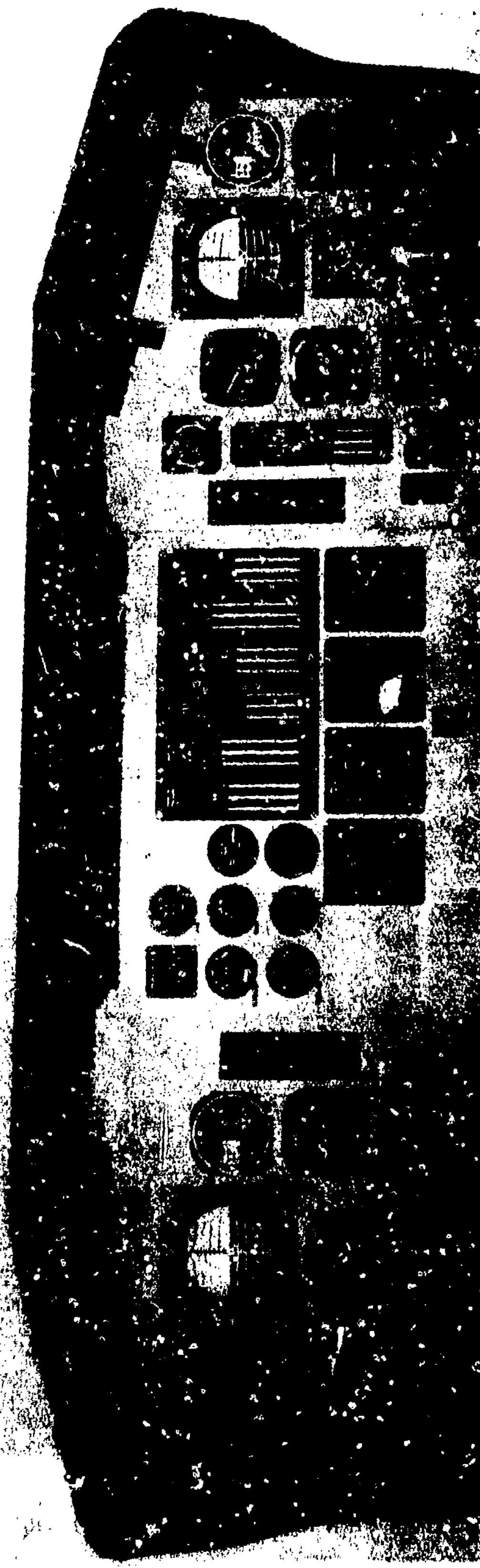

Figure 51. Cockpit instrument panel.

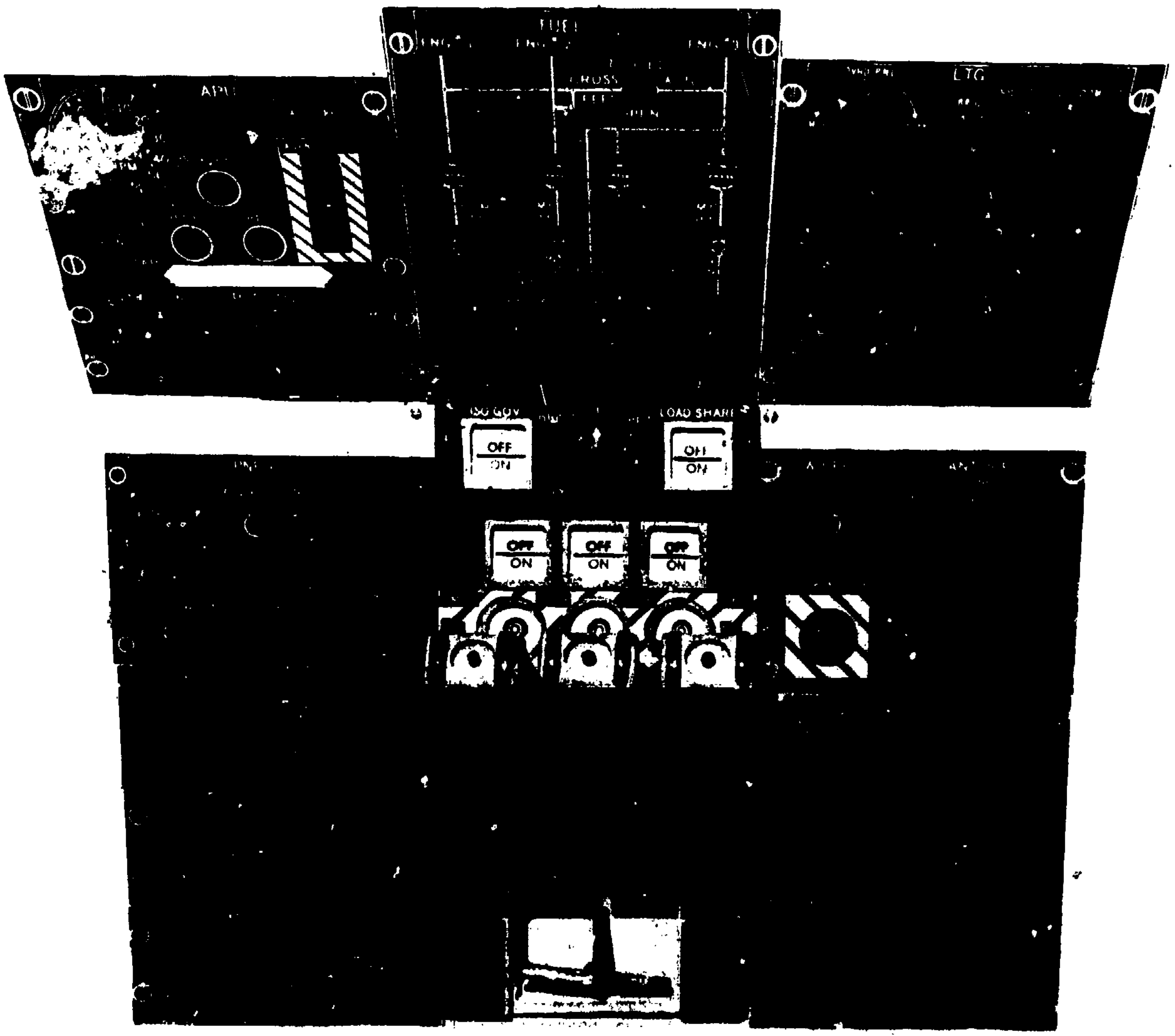

Figure 52A. Cockpit overhead panels.

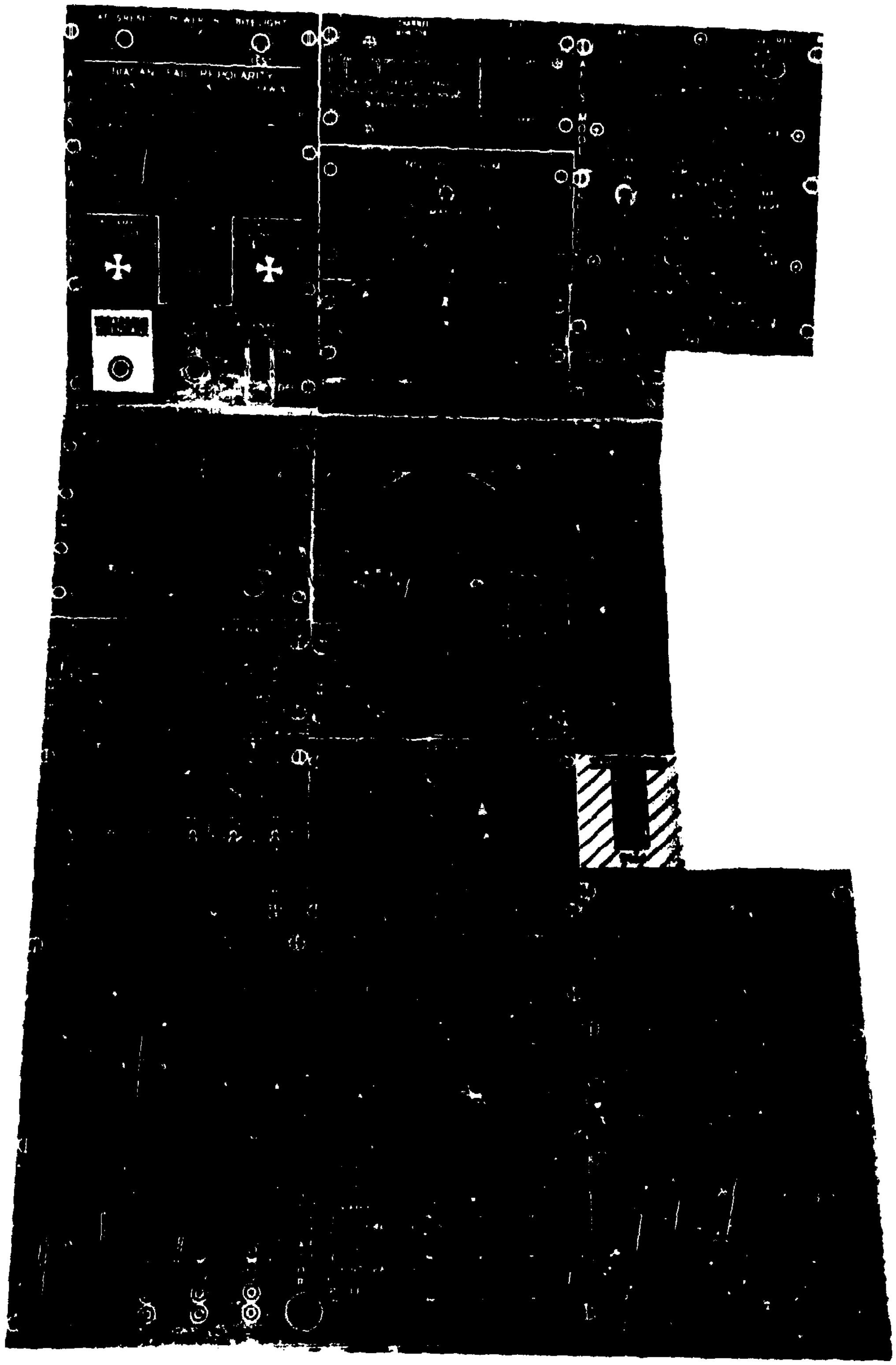

Figure 52B. Cockpit canted and center consoles.

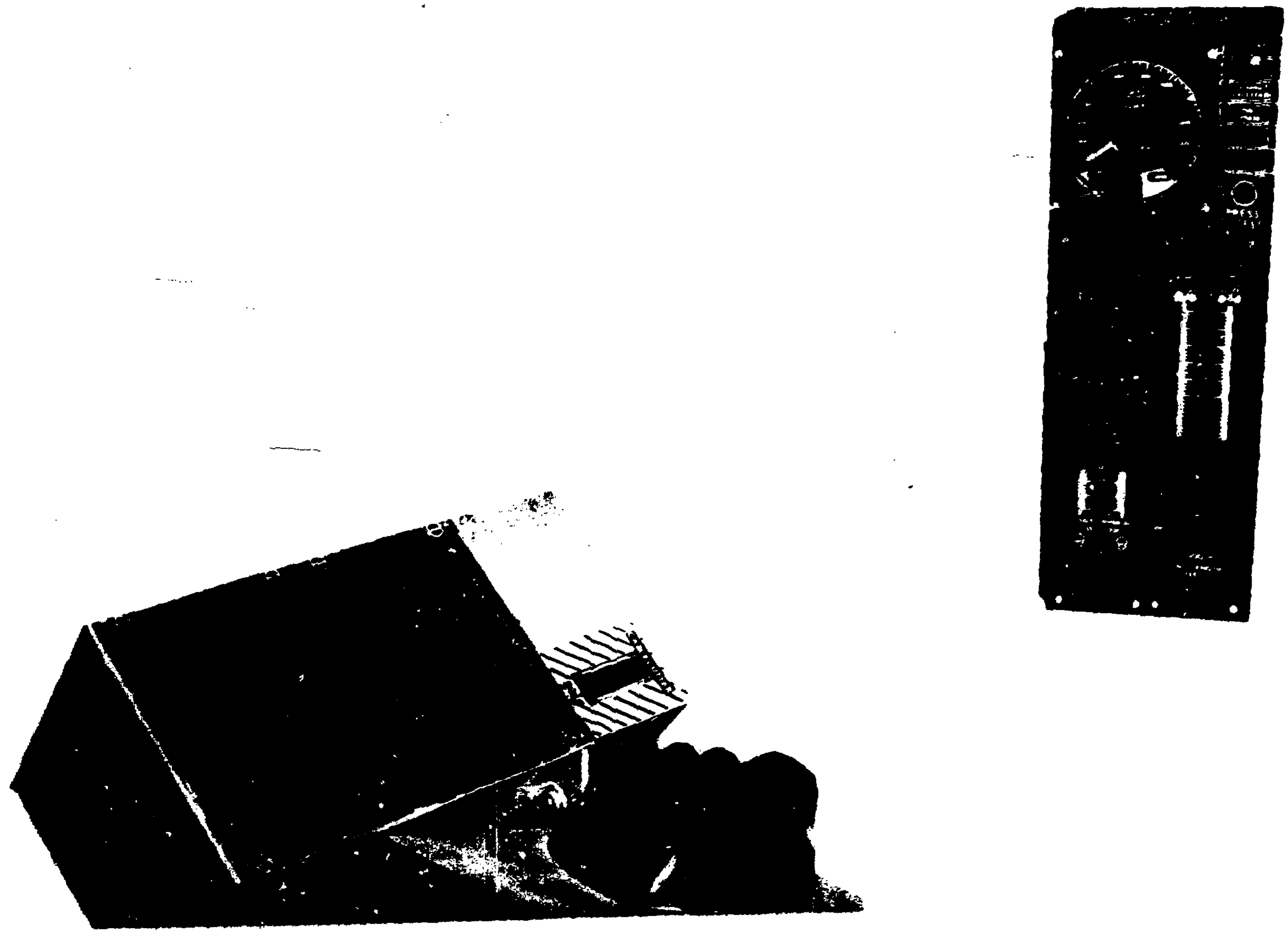

Figure 53. LCC's left console and instrument panel.

2.8.5 Crew Station Vibration Isolation

Dynamic Antiresonant Vibration Isolators (DAVIs) (Figure 54) were installed in the crew support platform shake test rig. Testing was accomplished in the vertical, lateral, and longitudinal excitation modes, both isolated and unisolated, with both ballast and actual crew members. A local lateral resonance of the instrument console was observed and eliminated by the addition of stiffeners to the console structure along with additional fasteners to the crew support platform. Vertical 4/rev vibration transmissibility was reduced to a spread of 15% to 25%, (i.e., isolation of 75% to 85%) at this frequency (10.4 Hz).

The test revealed an unacceptable amplification of 3/rev frequencies (7.8 Hz) by the DAVI units. The effect of additional bar mass on detuning the resonant frequency was investigated. A DAVI modification to reduce the 3/rev amplification was defined and modification was being implemented at program termination.

The test culminated in a demonstration of mixed frequency vertical vibration inputs representative of the anticipated HLH prototype vibration environment and was completed 4 April 1975.

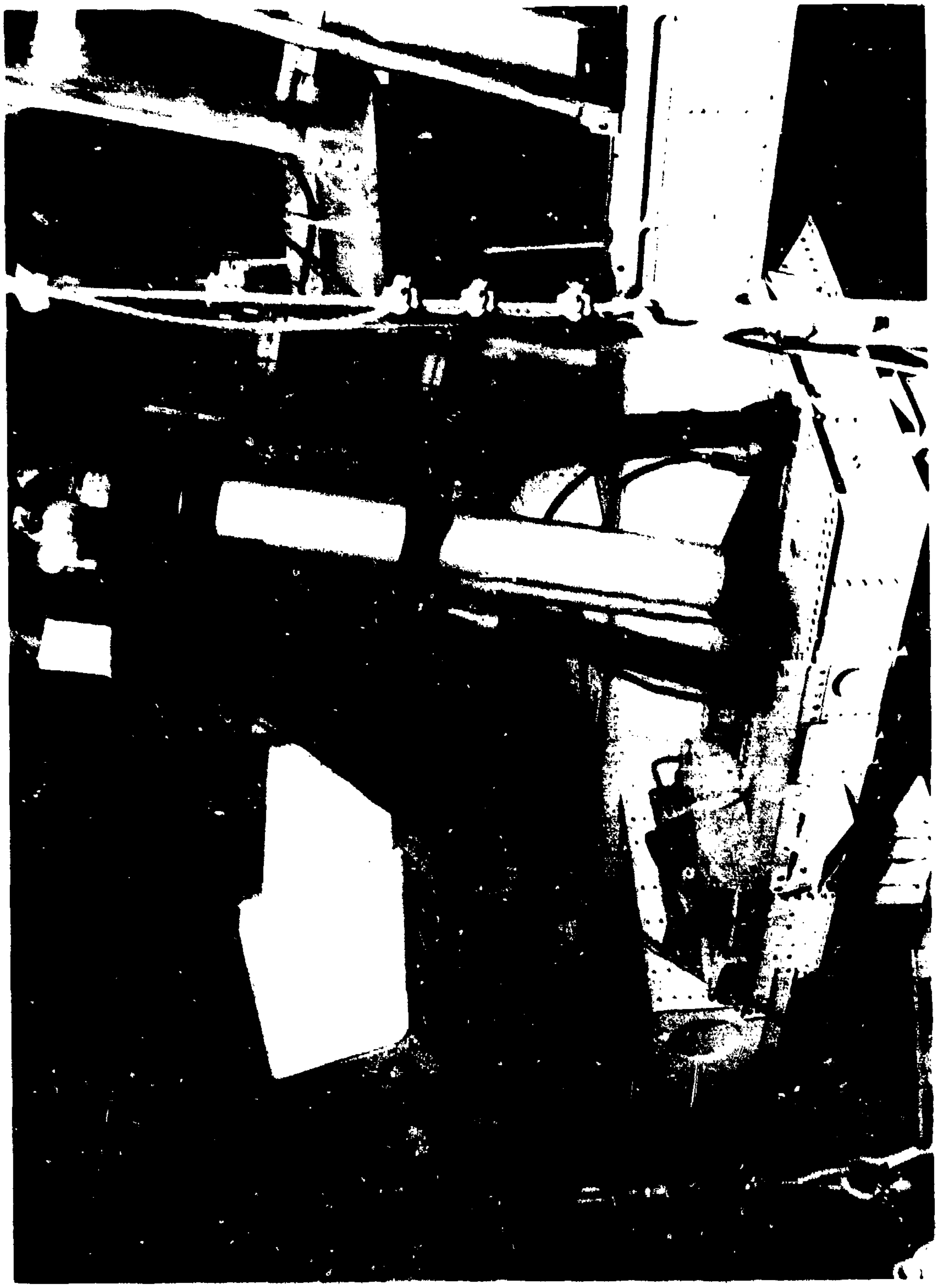

Figure 54. Isolated floor module in test rig.

161

2.8.6 ACOUSTICS

2.8.6.1 External Noise

The PIDS specifies that the external noise of the aircraft during ground running or in hover (10-foot wheel height) at design gross weight shall not exceed that specified in Table I of MIL-A-8806A as shown in Figure 55. The predicted HLH prototype aircraft external noise shown in Figure 55 includes all noise components of the aircraft; rotor rotational and vortex noise, engine noise, and transmission noise. The prediction is based on the latest results from the HLH/ATC improved noise prediction programs.

Rotational noise was estimated using the HLH/ATC modified "Heron" computerized programs. Broadband or vortex noise was estimated using the HLH/ATC improved broadband noise prediction. The engine noise estimate is that predicted by Allison for the HLH engines with the inlet noise becoming the critical component at 4000 Hz (Figure 55). Transmission noise was predicted using the HLH/ATC-developed dynamic analysis (Ref. Report T301-10190-1).

2.8.6.2 Internal Noise

The PIDS specifies that the noise levels within the cockpit during the HLH mission flight profile (design gross weight) shall not exceed the limits described in Tables I, II, and IV of MIL-A-8806A. The most critical of these is Table IV (Cruise Power), shown in Figure 56. This table sets the acoustical design of the aircraft since the allowable noise limits of Tables I and II are much higher in comparison with Table IV than the increase in noise at the higher power settings of Tables I and II.

The crew compartment noise estimate shown in Figure 56 contains:

a. Rotor Transmission Dynamic Analysis (Ref. HLH/ATC Report T301-10190-1 (500 Hz and above)

b. Rotor noise prediction (below 500 Hz)

c. Other source noise predictions (pumps, blowers, etc.)

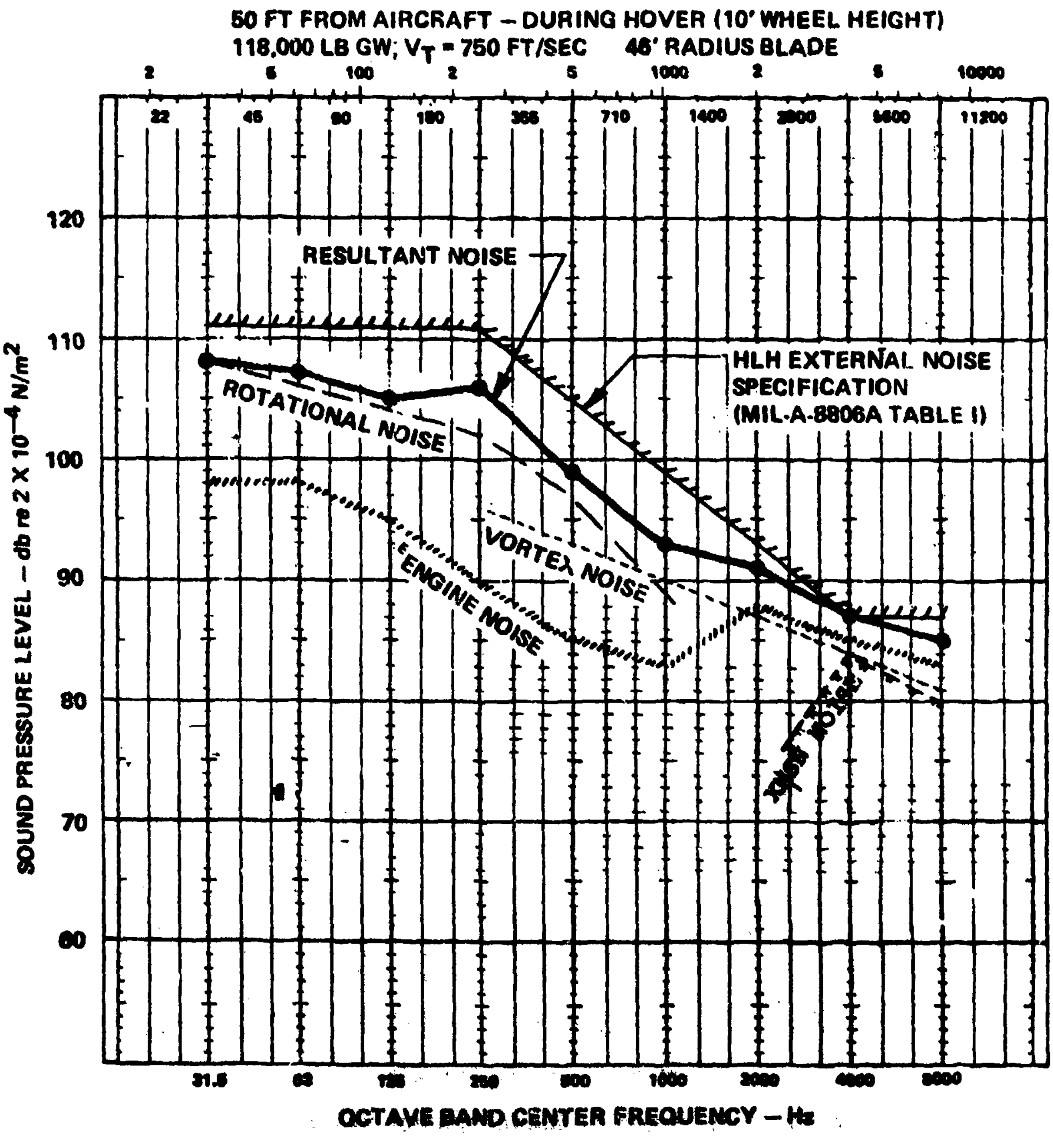

* INLET NOISE SUPPRESSION NOT IN PROTOTYPE S.O.W.

Figure 55. Predicted external noise levels.

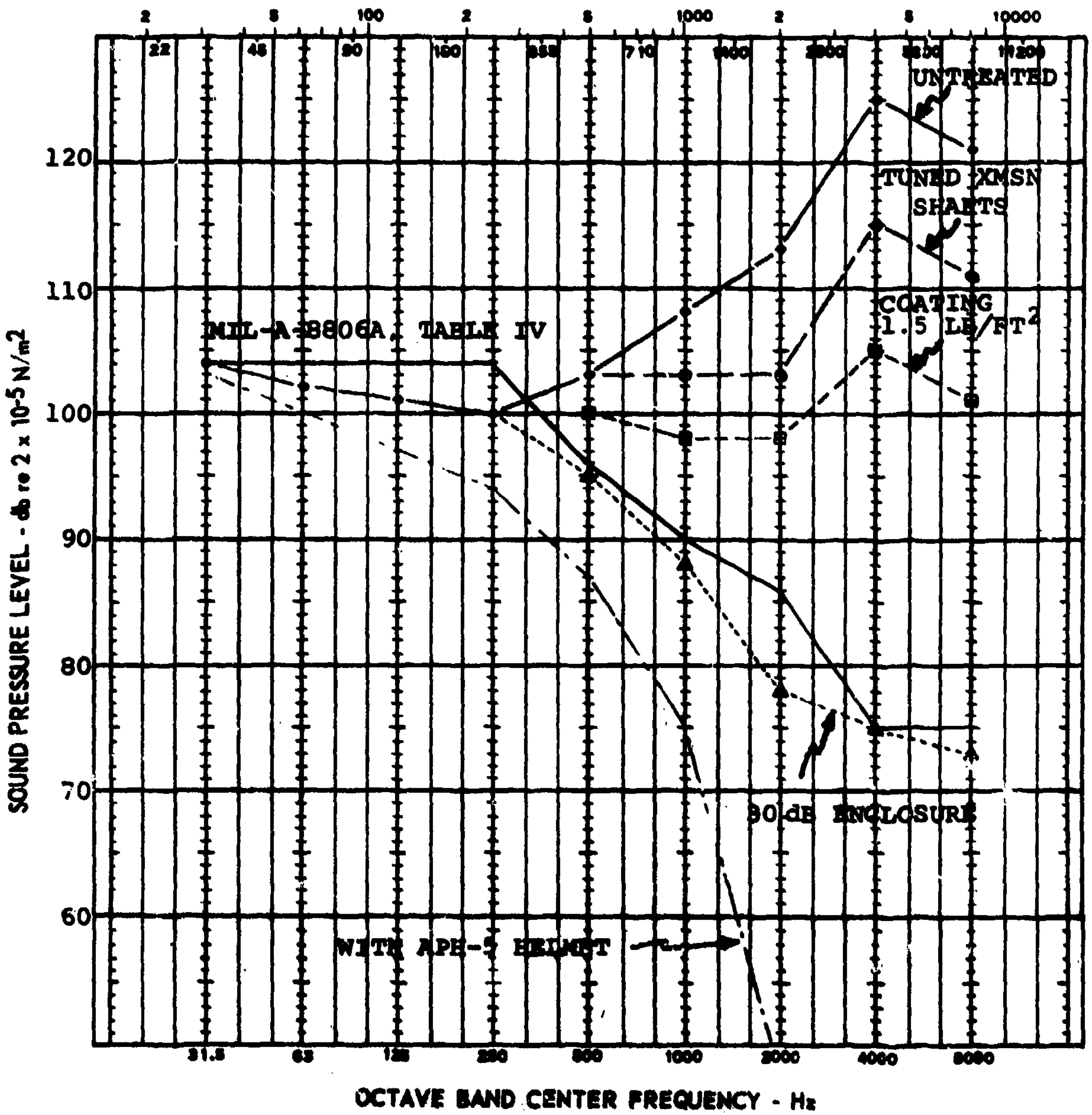

NOTE: SPL AT 2.5 FT. FROM FORWARD TRANSMISSION

Figure 56. Cockpit noise – cruise power.

The sound transmission loss test evaluates the panel for use as a sound barrier between the noise source (rotor transmission, etc.) and the crew, and the sound absorption test evaluates the panel for use as an interior lining to absorb noise within the crew compartment. Both qualities are required in an acoustical panel to provide an acceptable environment which meets the HLH Internal Noise Specification MIL-A-8806A. The five honeycomb panels evaluated are defined in Table 23.

Figure 58 shows the sound transmission loss result of the two best panels, #4 and #5. Also shown is a comparison with the CH-47 type soft fiberglass blanket.

Figure 59 shows the sound absorption results of these same two panels, #4 and #5. These panels exceeded or came quite close to meeting the established goal of 0.6 or 60% acoustical energy absorbed above 1000 Hz. Panels #1 and #2 also had similar satisfactory results, while panel #4 fell far below 0.6 at frequencies above 1000 Hz.

A noise reduction comparison of the panels based on treatment weight was made before selection of the final configuration. Four configurations are compared in Table 24.

Table 24 shows the results of this comparison for the three critical rotor transmission noise frequencies (lower planetary mesh fundamental 1450 Hz, lower planetary mesh second harmonic 2900 Hz, and input spiral bevel mesh fundamental 5000 Hz). By combining the sound transmission loss and sound absorption qualities of the panel configurations, the resultant noise reduction of the treatment can be obtained. The amount of noise reduction also depends on the minimum sound leakage that can be obtained with each configuration. The CH-47 type soft blankets, used as a comparison only, would weigh only 150 pounds but are less serviceable and cannot provide the noise reduction required to meet MIL-A-8806A due to higher sound leakage. Two epoxy panels, #1 and #2, come very close to providing the reduction required by MIL-A-8806A and have good serviceability but cost 450 pounds of treatment weight. The lighter weight rigidized-vinyl panels, #3 and #4, cost 300 pounds, but also fall short of the required reduction. However, the third epoxy panel, #5, combined with the best light-weight rigidized vinyl panel, #4, provides the highest noise reduction for 300 pounds of treatment. Because this configuration meets the reduction required by MIL-A-8806A and is within the current weight allowance for acoustical materials, it was selected as the best configuration.

TABLE 23. ACOUSTIC PANEL EVALUATION

PANEL	SURFACE WEIGHT	FACE SHEET	CORE	BACKING	THICKNESS	TUNING
1	2.1 lb/ft^2	20-ply porous epoxy	4 lb/ft^3	.020-in. Aluminum	1.1 in.	1450 & 5000 Hz
2	1.2 lb/ft^2	9-ply porous epoxy	4 lb/ft^3	.020-in. Aluminum	0.625 in.	2500 Hz
3	1.1 lb/ft^2	Rigidized Vinyl	1.5 lb/ft^3	Fiberglass	0.95 in.	2000 Hz
4	0.7 lb/ft^2	Rigidized Vinyl	1.5 lb/ft^3	Fiberglass	0.47 in.	4000 Hz
5	1.1 lb/ft^2	10-ply porous epoxy	2 lb/ft^3	.020-in. Aluminum	0.43 in.	1450 Hz

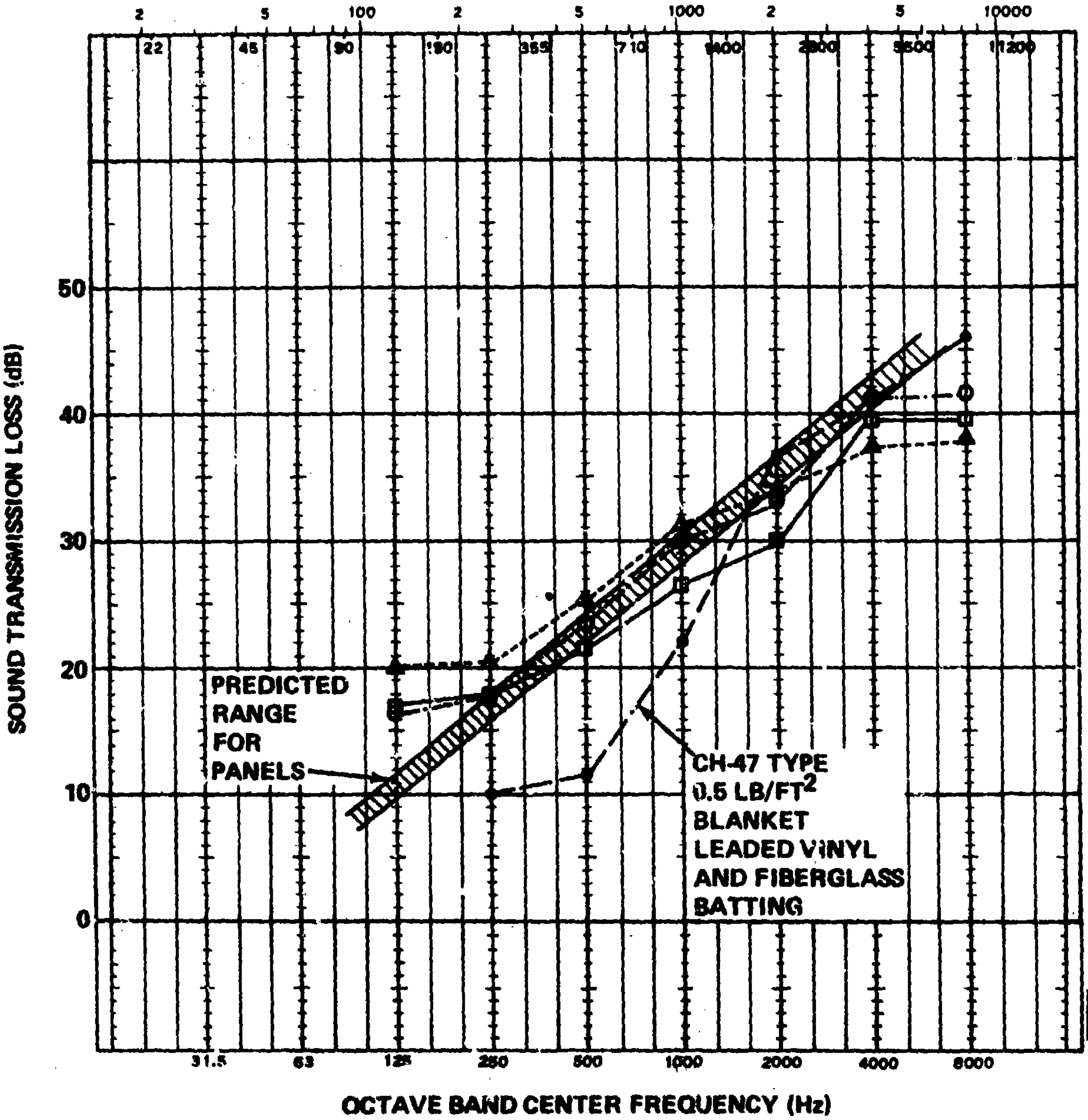

REVERBERATION – ANECHOIC ROOM FACILITY

O-----O 8 PLY POLYIMIDE FACE, 8 PLY FIBERGLASS BACKING
□——□ 8 PLY POLYIMIDE FACE, 0.025 ALCLAD BACKING
Δ-----Δ 6 PLY SOLID FIBERGLASS BOTH SIDES

Figure 57. Acoustic/structural study – sound transmission loss, 38 x 38-inch panels.

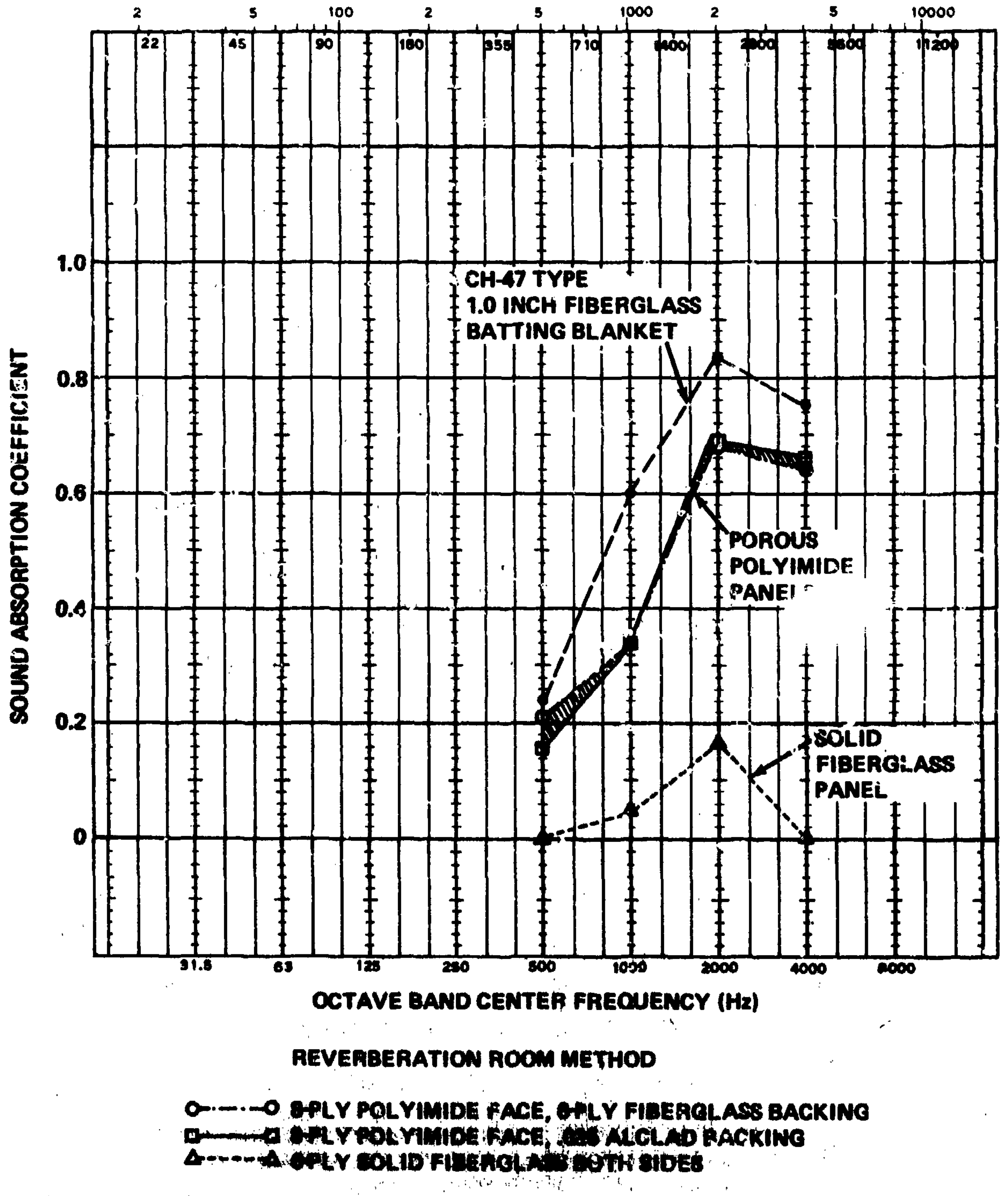

Figure 58. *Acoustic/structural study – sound absorption, 38 x 38-inch panels.*

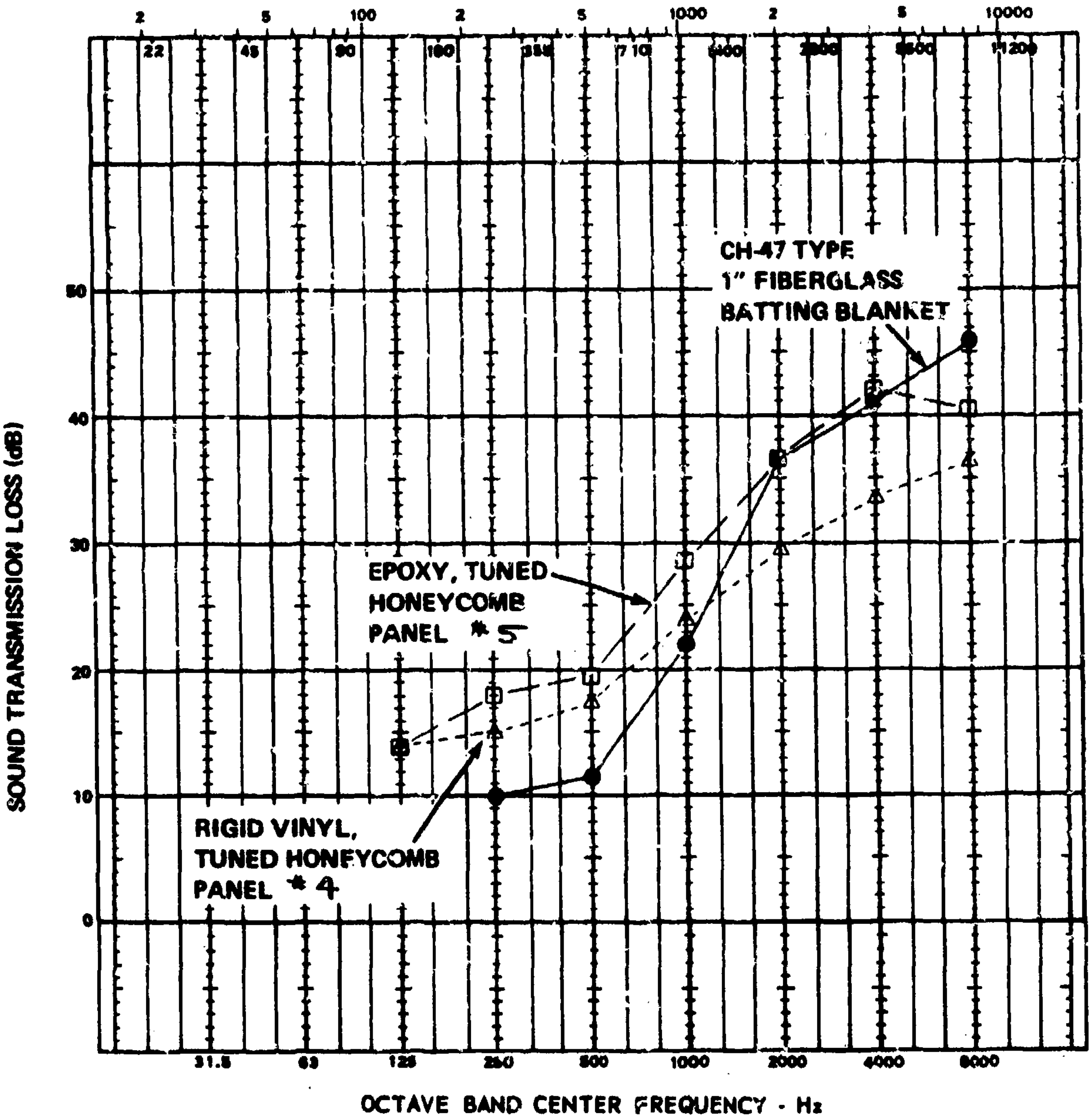

REVERBERATION ANECHOIC ROOM FACILITY

●-----● CH-47 TYPE 0.5 LB/FT^2 BLANKET LEAD VINYL & FIBERGLASS BATTING
□——□ EPOXY, TUNED HONEYCOMB PANEL 1.1 LB/FT^2 OVERHEAD AREAS
△-----△ RIGID VINYL, TUNED HONEYCOMB PANEL 0.7 LB/FT^2 SIDEWALLS

Figure 59. Acoustic/structural study – sound transmission loss, 38 x 38-inch panels.

TABLE 25. ACOUSTIC PANEL COMPARISON

PANEL CONFIGURATION		TOTAL WEIGHT OF TREATMENT	NOISE REDUCTION					
			1450 Hz		2900 Hz		5000 Hz	
OVERHEAD	SIDE WALLS		GOAL	ACHIEVED	GOAL	ACHIEVED	GOAL	ACHIEVED
1	2	450 lb.	25	<u>28</u>	30	<u>31</u>	30	29
3	4	300 lb.	25	<u>26</u>	30	27	30	27
5	4	300 lb.	25	<u>32</u>	30	<u>34</u>	30	<u>32</u>
CH-47 TYPE BLANKETS		150 lb.	25	21	30	27	30	27

- Current HLH Prototype weight allowance for acoustical treatment - 300 lb.
- Treatments which met noise reduction goals are underlined.

The untreated noise level peaks at the 4000 Hz octave band due to the rotor transmission spiral bevel input gear mesh frequency. Consequently, this frequency determines the acoustical treatment of the interior.

To comply with the PIDS specification, a program to achieve an effective noise reduction of 50 dB in the 4000 Hz octave band was established.

2.8.6.3 Acoustical Panels

The acoustical treatment for the crew compartment consists of a rotor transmission enclosure to act as a sound barrier and crew compartment sidewall and bulkhead lining to provide for sound absorption. On the CH-47, this treatment consisted of soft easily-damaged fiberglass batting blankets. Recently, under Boeing Vertol IR&D funding, an evaluation of porous fiberglass (polyimide) acoustical honeycomb panels was completed. These durable panels, which are much more serviceable than the soft blankets, can be acoustically tuned to provide the equivalent sound transmission loss and sound absorption qualities shown in Figures 57 and 58.

Testing was conducted to define the sound absorption and transmission loss qualities of the following panels:

Porous-epoxy, dual-frequency, honeycomb panel tuned for maximum sound absorption at 1500 and 5000 Hz (primary noise frequencies of HLH forward rotor transmission).

Porous-epoxy, single-frequency, honeycomb panel tuned for maximum sound absorption at 2500 Hz.

Rigidized-vinyl, honeycomb panel tuned for maximum sound absorption at 2000 Hz.

Rigidized-vinyl, honeycomb panel tuned for maximum sound absorption at 4000 Hz.

The epoxy-faced panels are the most serviceable but the heaviest of all panels tested. Therefore, further testing was conducted to determine if a lighter-weight epoxy panel can be designed for side wall treatment which is acoustically equal to the best rigidized-vinyl panel.

The fiberglass with epoxy resin test panels initially had a 10-ply porous face surface and a 7-ply impervious backing which could be peeled off one ply at a time. The number of plies on both surfaces was continually reduced, from 10 to 4 on the porous face and 7 to 2 on the impervious back, between acoustical testing. Although various panel configurations were evaluated, the three panels (6, 7, 8) most significant are defined in Table 25. Panel 6 was selected for the HLH prototype overhead areas and panel 9 for the side walls. Panel 9 is identical to the previously tested panel 4 but with only a single-ply backing in order to minimize weight. Figures 60, 61, and 62 show the sound transmission loss and sound absorption results of the selected panels compared with CH-47 type soft fiberglass blankets.

A noise reduction comparison which combines the transmission loss and sound absorption of the panels based on treatment weight is shown in Table 26.

The results indicated that reducing the number of plies of the epoxy panels to reduce the weight below the weight allowance of 300 pounds also decreased the acoustical qualities to a level unacceptable for the crew compartment. However, the combination of an epoxy overhead panel (#6) with good acoustical and limited structural qualities, and a lightweight rigidized vinyl panel (#9) provides the required noise reduction for the minimum weight.

TABLE 25. ACOUSTIC PANEL EVALUATION

PANEL	SURFACE WEIGHT	FACE SHEET	CORE DENSITY	BACKING	THICKNESS	TUNING
4*	0.7 lb/ft^2	Rigidized Vinyl	1.5 lb/ft^3	3-Ply Fiberglass	0.5 in.	2000-4000 Hz
5*	1.1 lb/ft^2	10-Ply Porous Epoxy	2.0 lb/ft^3	.020 Aluminum	0.93 in.	1450 Hz
6**	1.06 lb/ft^2	10-Ply Porous Epoxy	1.5 lb/ft^3	3-Ply Fiberglass	0.92 in.	1450 Hz
7	0.90 lb/ft^2	10-Ply Porous Epoxy	1.5 lb/ft^3	2-Ply Fiberglass	0.46 in.	2500 Hz
8	0.64 lb/ft^2	4-Ply Porous Epoxy	1.5 lb/ft^3	2-Ply Fiberglass	0.43 in.	2500 Hz
9**	0.47 lb/ft^2	Rigidized Vinyl	1.5 lb/ft^3	1-Ply Fiberglass	0.47 in.	2000-4000 Hz

* Panels previously selected for the overhead areas (5) and sidewalls (4) (reference 4th Quarterly Report).

** Final selection for the overhead areas (6) and sidewalls (9).

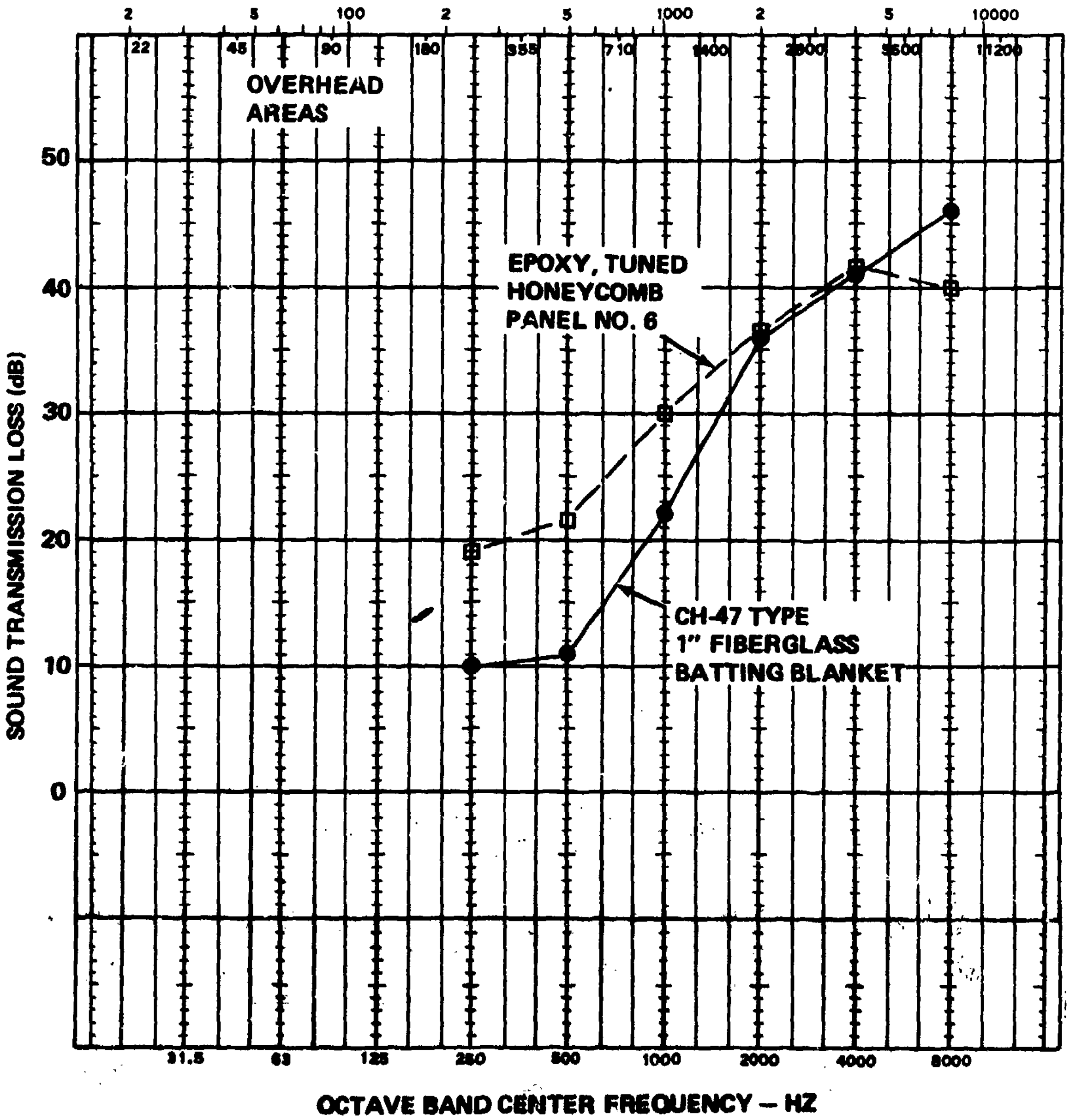

REVERBERATION ANECHOIC ROOM FACILITY

●— · — · —● CH-47 TYPE 0.5 LB/FT² BLANKET LEAD VINYL & FIBERGLASS BATTING
□— — — —□ EPOXY, TUNED HONEYCOMB PANEL 1.1 LB/FT²

Figure 60. Acoustic/structural study – sound transmission loss, 38 x 38-inch panels.

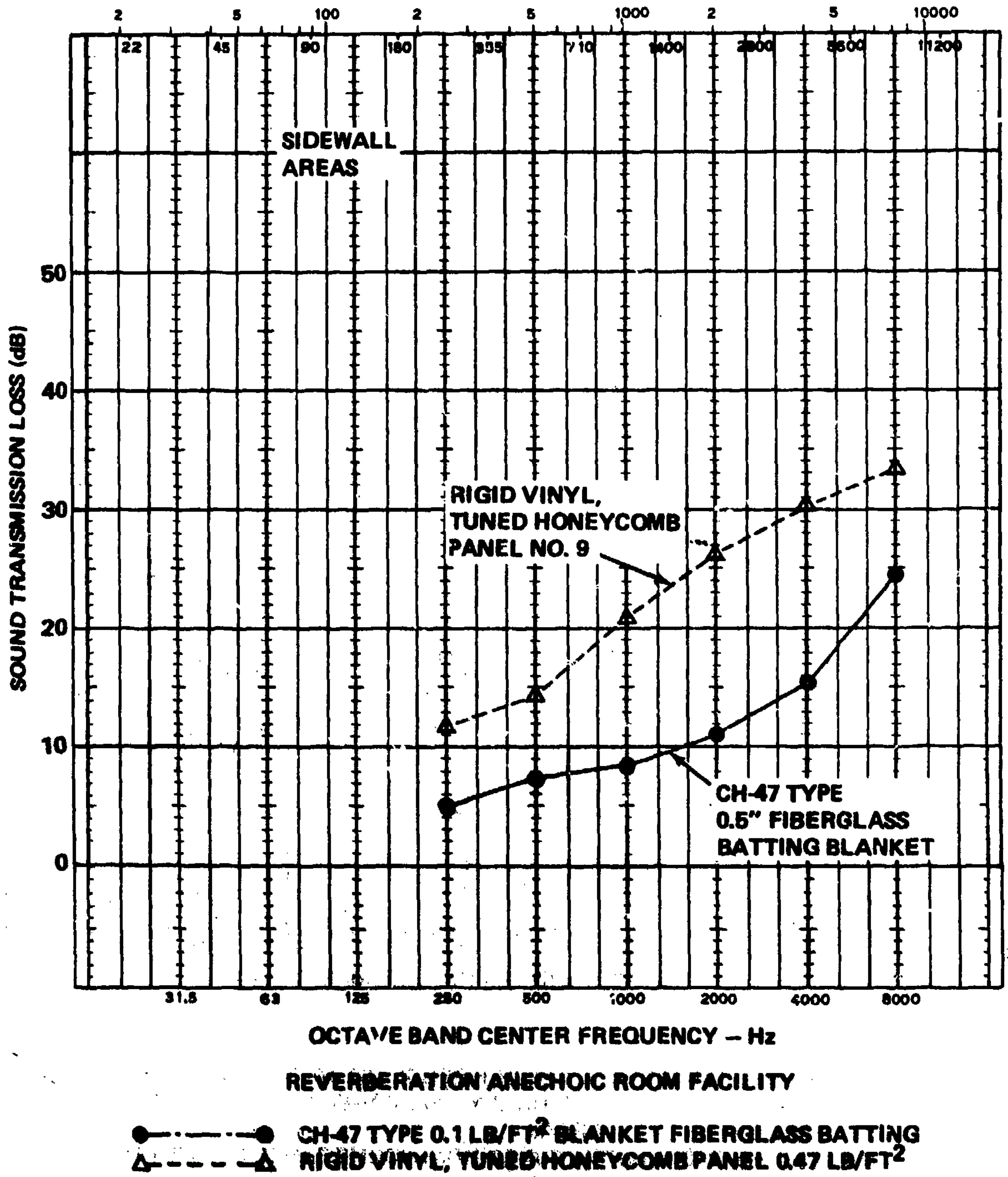

Figure 61. Acoustic/structural study – sound transmission loss, 38 x 38-inch panels.

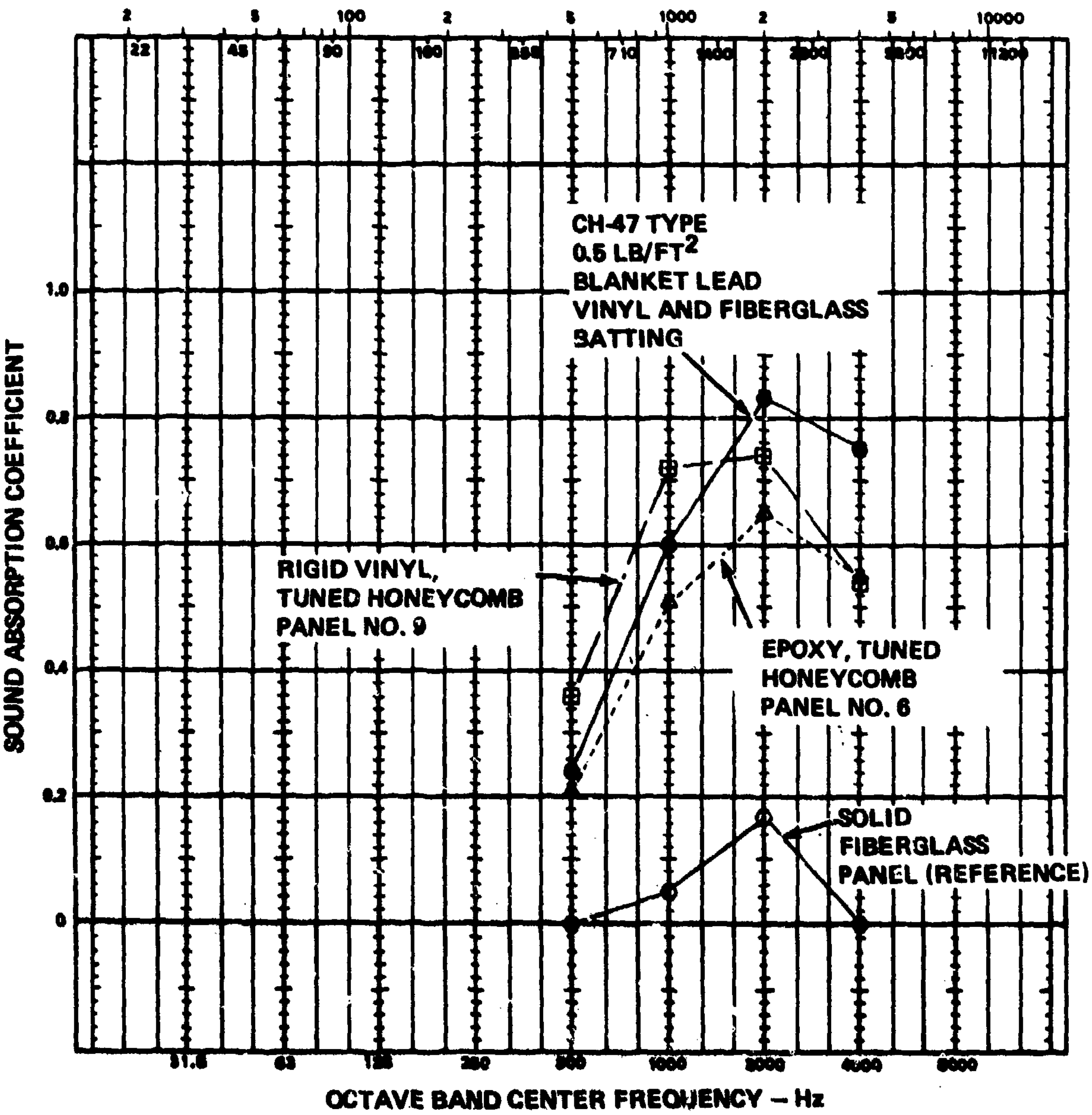

O—·—·—O CH-47 TYPE 1.0 INCH FIBERGLASS BATTING BLANKET
□———□ EPOXY, TUNED HONEYCOMB PANEL 1.1 LB/FT^2 OVERHEAD AREAS
△– – – –△ RIGID VINYL, TUNED HONEYCOMB PANEL 0.47 LB/FT^2 SIDEWALLS

Figure 62. Acoustic/structural study – sound transmission loss, 38 x 38-inch panels – reverberation room method.

TABLE 26. ACOUSTIC PANEL COMPARISON

PANEL CONFIGURATION			NOISE REDUCTION					
OVERHEAD	SIDE WALLS	TOTAL WEIGHT OF TEATMENT (3)	1450 Hz GOAL	1450 Hz ACHIEVED	2900 Hz GOAL	2900 Hz ACHIEVED	5000 Hz GOAL	5000 Hz ACHIEVED
5 (1)	4 (1)	300 lb	25	29	30	34	30	32
6	7	350 lb	25	26	30	35	30	39
6	8	280 lb	25	22	30	32	30	35
6 (2)	9 (2)	230 lb	25	25	30	30	30	32

- Current *HLH* prototype weight allowance for crew compartment acoustical treatment - 300 lbs.
- Treatments which met noise reduction goals are underlined.

(1) Panels previously selected for the overhead areas (5) and sidewall (4) (reference 4th Quarterly Report).

(2) Final selection for the overhead areas (6) and sidewalls (9).

(3) Includes 15% attaching hardware weight.

2.8.6.4 Window Thickness

A test to acoustically determine the crew compartment window thickness was conducted. External noise sources such as rotor, transmission, engine, and boundary layer, if not sufficiently attenuated through the structure and windows, can become the dominating factor in setting the noise level of the crew compartment. It was therefore necessary to measure the sound transmission loss of various thicknesses of plexiglas and determine their critical frequencies. The critical frequency is the point at which the wave length of the incident sound wave coincides with the wave length of the bending wave of the panel, and a maximum amount of acoustical energy is transferred to the panel. At this frequency, the sound transmission loss of the panel drops substantially.

Three different thicknesses of plexiglass (1/8, 1/4, and 1/2 inches) were tested for sound transmission loss properties. Figures 63 through 65 illustrate the measured 1/3 octave band values compared with the predicted values, and identify their critical frequencies.

Figure 66 illustrates all three thicknesses compared with the pre-established test objective, on a full octave band basis. Based on these data, a decision was made to use 3/16-inch thickness.

2.8.6.5 Leakage

To provide an acoustic environment which complies with MIL-A-8806A, a 30 dB noise reduction in the crew compartment is required. To obtain 30 dB noise reduction, 40 dB sound transmission loss barriers with only 0.1% sound leakage will be required. This necessitates a well-sealed, tight-fitted acoustic panel installation. Because sound leakage is a critical factor in providing 30 dB noise reduction, an acoustical test of the joint/seals and access openings of the proposed 40dB sound barriers was conducted. Various types of acoustic rubber and foam seals were evaluated. Results of the test indicated that as long as the seal material was of a soft consistency, the particular material used was less important than the snugness of fit in meeting the 30 dB noise reduction criterial. All the materials tested resulted in noise reductions above 30 dB (4000 Hz octave band) as shown in Figure 67.

2.8.6.6 Transmission Noise

The major noise-producing component, which determines the acoustical treatment of the crew compartment, is the forward rotor transmission. The critical frequency band, or the one

HLH PROTOTYPE – ACOUSTIC TREATMENT

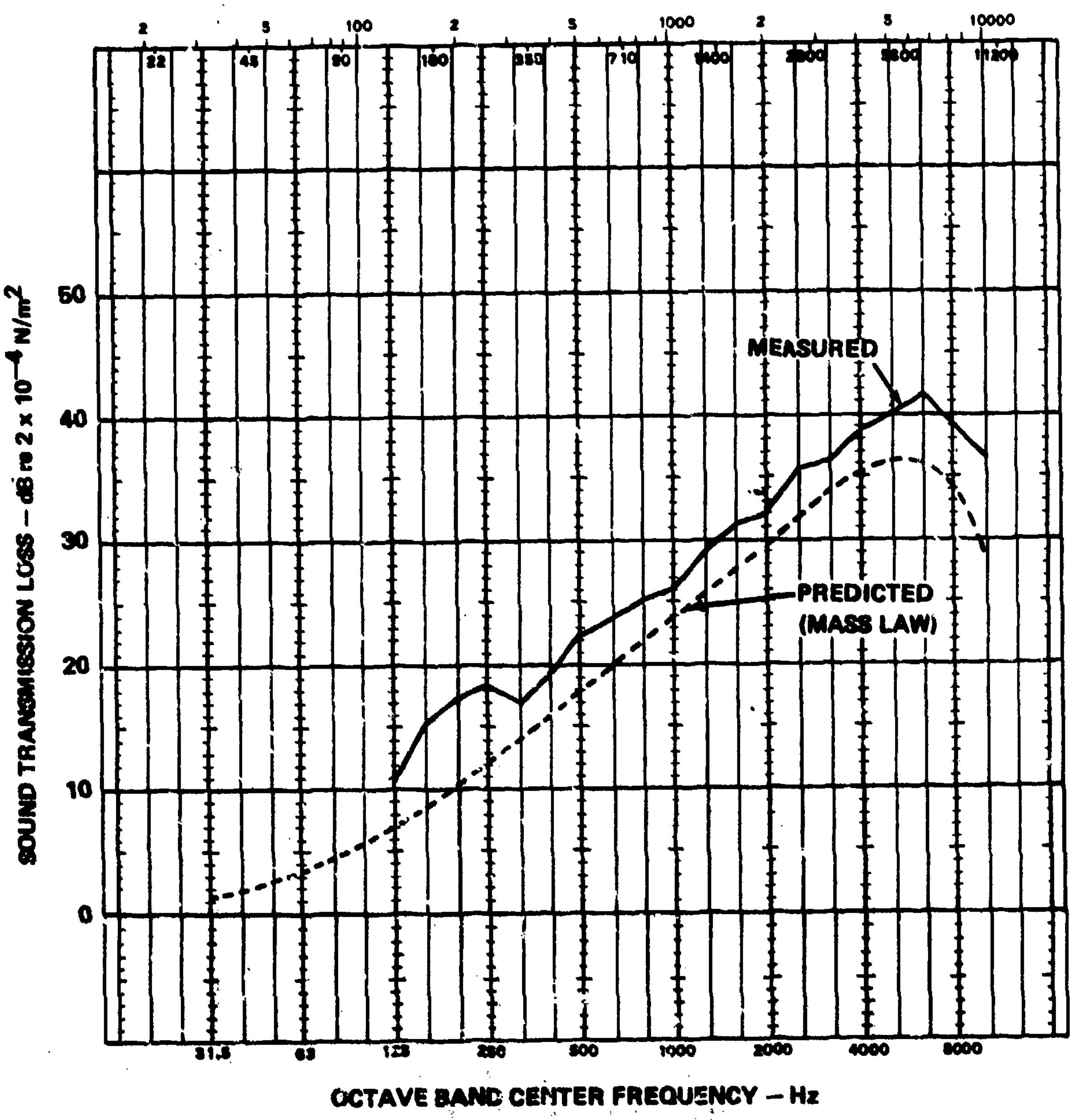

Figure 63. Crew compartment enclosure – sound transmission loss, 1/8-inch plexiglass.

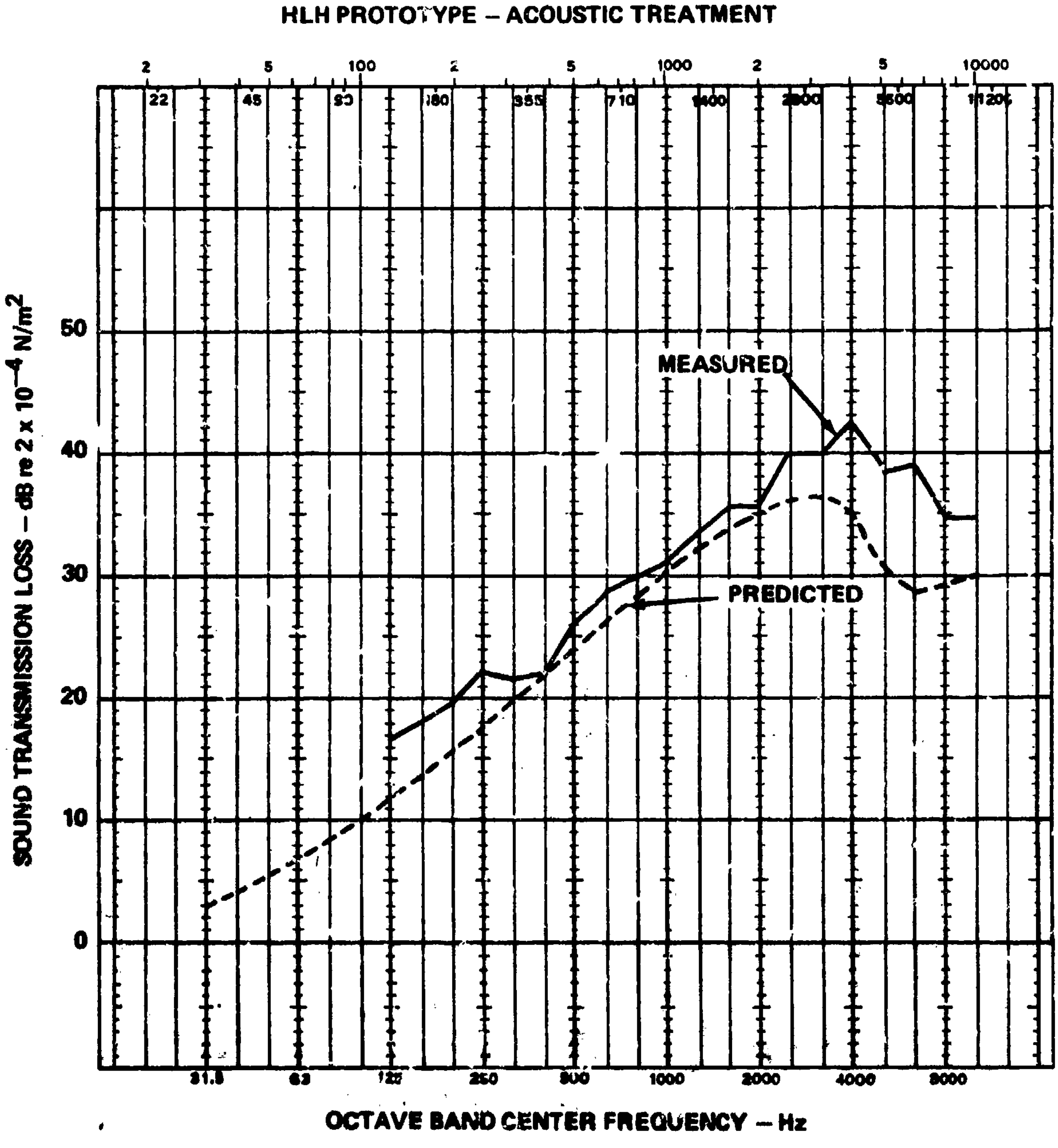

Figure 64. Crew compartment enclosure – sound transmission loss, 1/4-inch plexiglass.

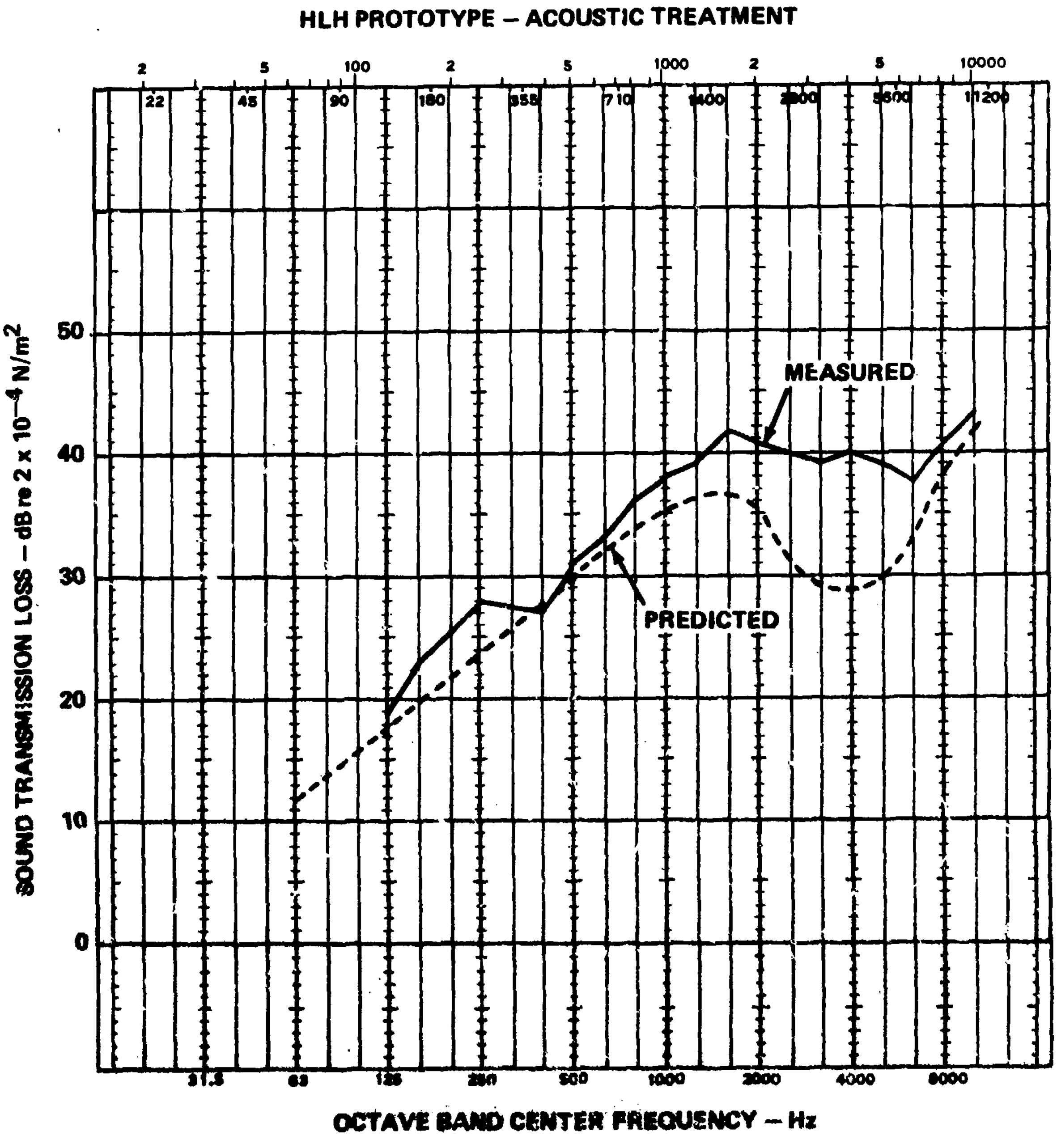

Figure 65. Crew compartment enclosure – sound transmission loss, 1/2-inch plexiglass.

HLH PROTOTYPE – ACOUSTIC TREATMENT

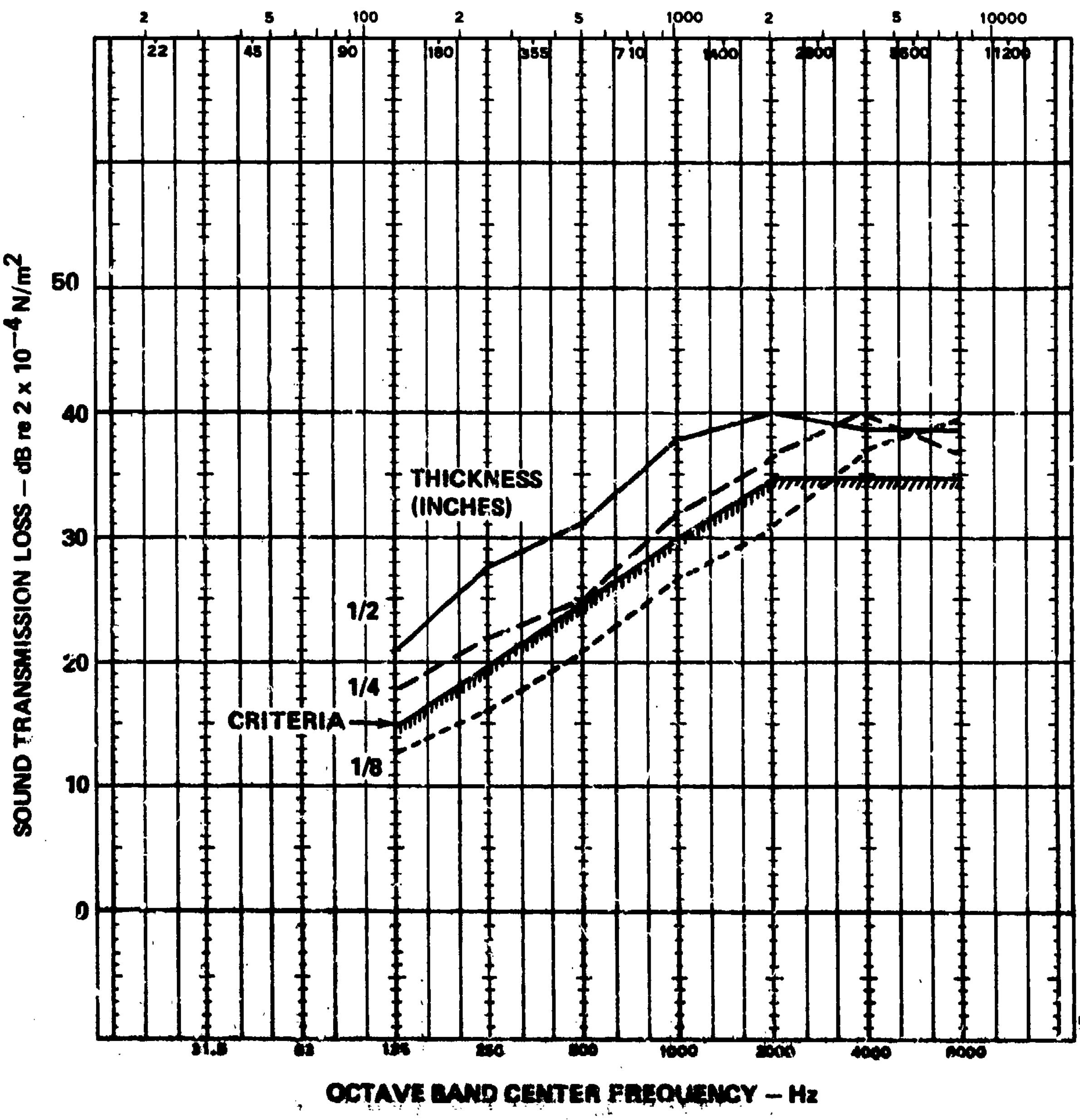

Figure 66. Crew compartment enclosure – plexiglass sound transmission loss.

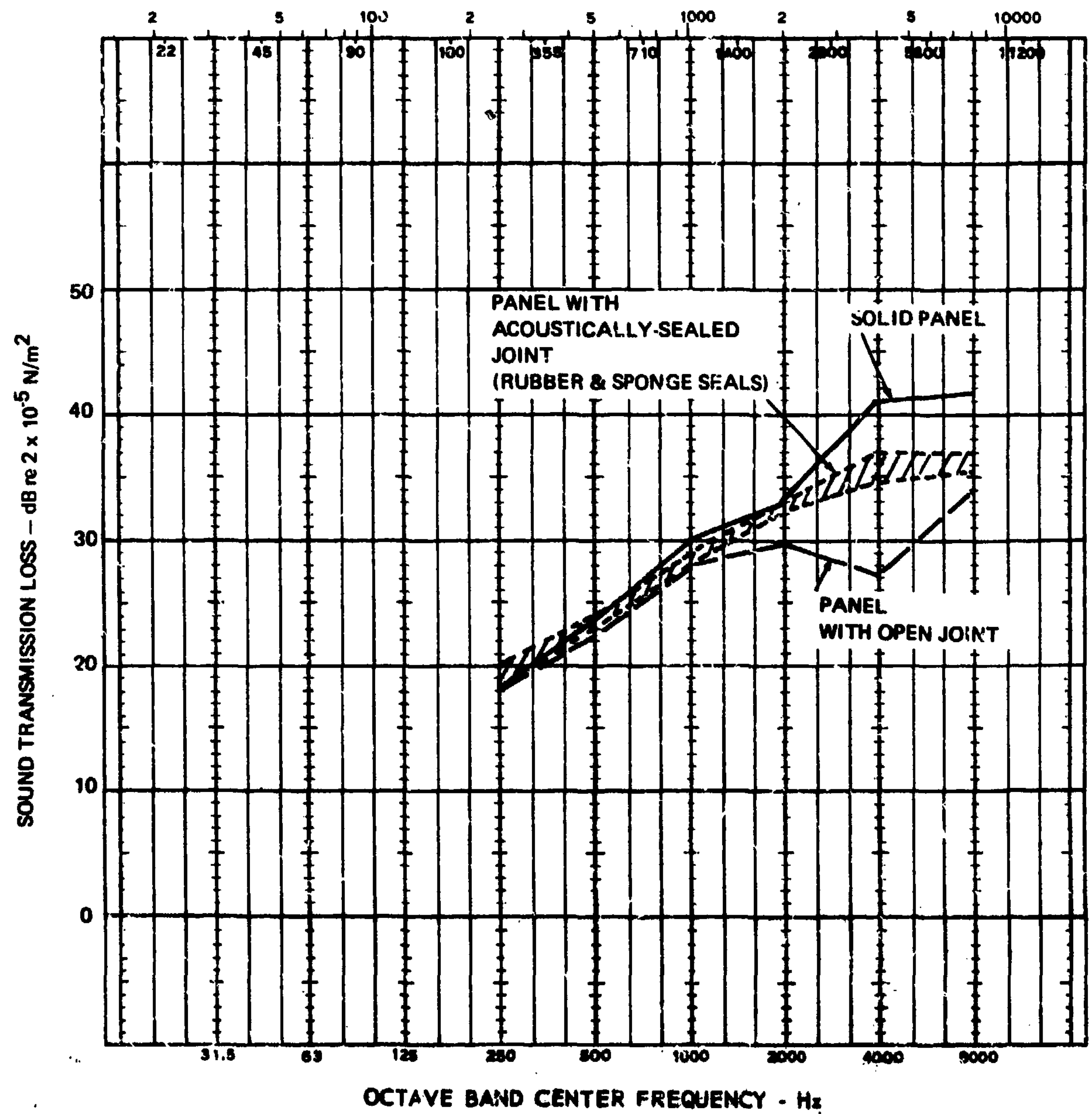

Figure 67. Crew compartment acoustic joint/seal test.

which requires the largest noise reduction, is 4000 Hz. The noise control items that are to be used in achieving a reduction in transmission noise to a level below the MIL-A-8806A level specification are as follows:

Rotor Transmission Dynamic Analysis

The improved dynamic analysis that was developed during the HLH/ATC program (Ref. HLH/ATC Test Report T301-10190-1) to reduce the dynamic response of gears and shafts for minimum noise generation was applied to the HLH transmission.

Using a computer model of the HLH forward transmission, parametric studies were conducted to optimize the dynamic response of the gear shafts for minimum noise. As the dynamic analysis indicated that the baseline configuration did not exhibit any critical frequencies on, or very near, the gear mesh frequencies, considerable effort was required to find a modification which made a significant improvement. Of 15 configurations analyzed, only four configurations appeared to have improved dynamic responses, and two of those configurations were overruled by the strength requirements, as the modifications reduced the wall thickness of the pinion gear shaft.

Results from predicted noise level of the HLH forward transmission indicated that the transmission shafts should be designed for minimum dynamic response to the input bevel mesh frequency (4925 Hz) while not unduly compromising the response to the sun mesh frequency (1436 Hz). An example of this is the input bevel shaft alternate configuration with added material shown by the shaded areas in Figure 68. The reduction in the dynamic response of this shaft as modified, compared to the baseline configuration, minimizes the noise generated by the rotor transmission. The predicted noise reduction due to these modifications is 5 dB at the sun frequency (1436 Hz).

A stationary ring gear modification was also defined, which also could result in an additional noise reduction of 7 dB at the bevel frequency.

Rotor Transmission Case Coating

The application of a vibration damping compound to the transmission case is predicted to reduce the radiated noise an additional 10 dB at 4000 Hz, as shown in Figure 69. This prediction was based on the results of the ATC evaluation of

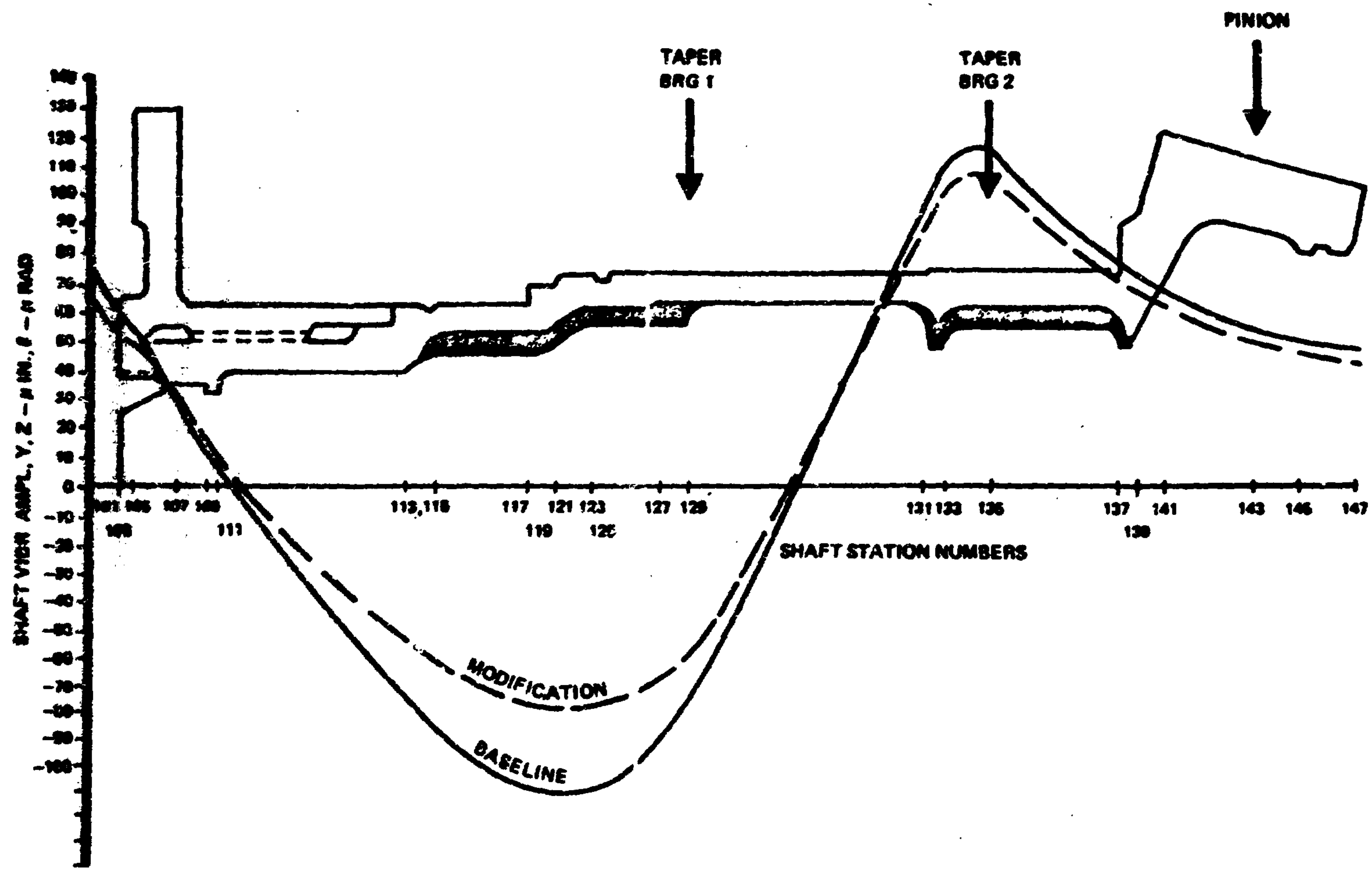

Figure 68. Effects of shaft modification on dynamic response – bevel frequency.

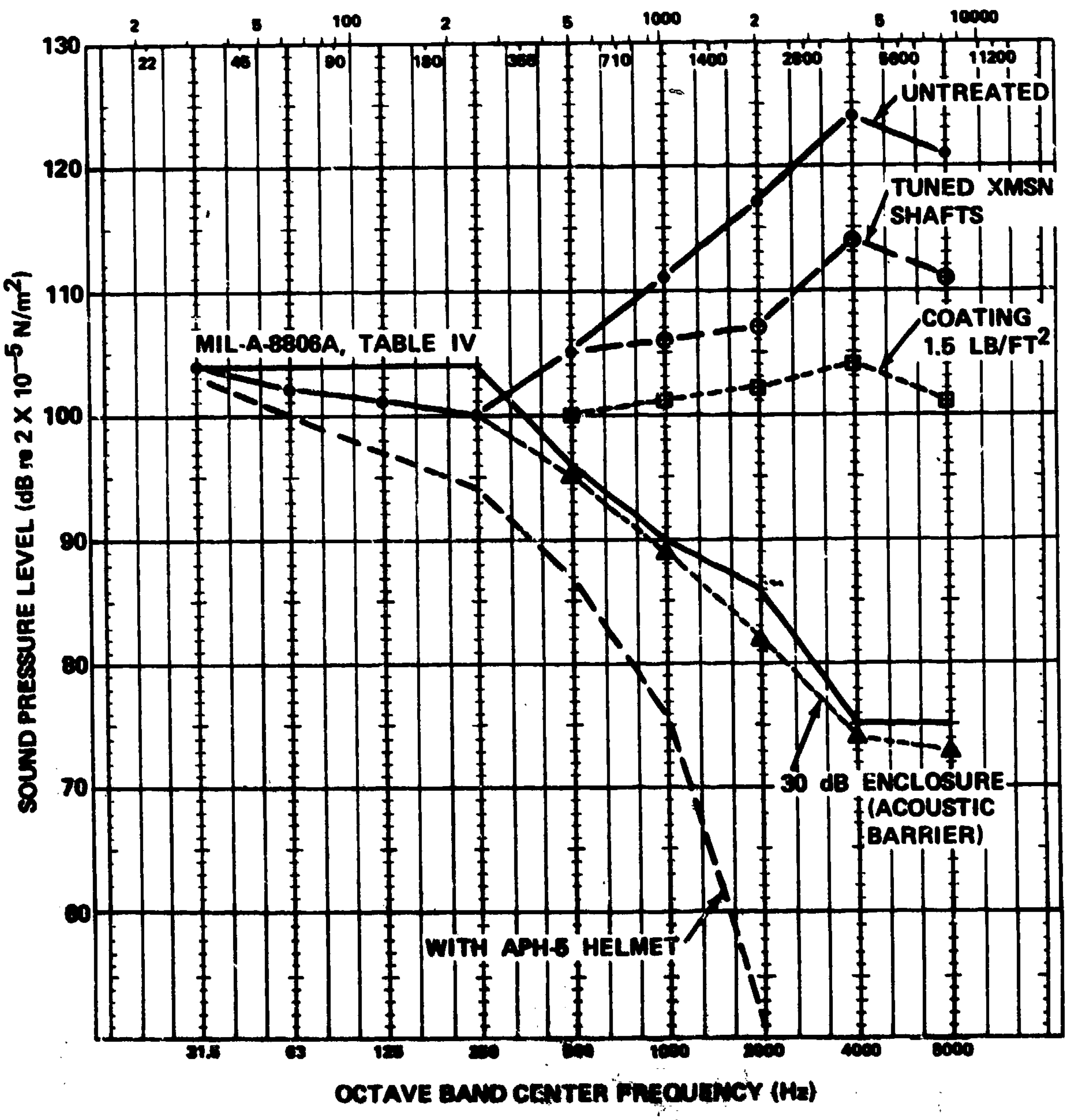

NOTE: SPL AT 2.5 FT. FROM FORWARD TRANSMISSION

Figure 69. Cockpit noise at cruise power.

transmission noise attenuation materials program documented in the HLH/ATC Test Report T301-10176-1. Although the actual noise reduction achieved with a damping compound will depend on the content of resonant and forced vibrations of the case, the 10 dB prediction does not seem unreasonable considering that all of the materials laboratory tested during the program achieved from 10 - 20 dB of reduction in noise and 15 - 25 dB in vibration at the highest resonant frequency reported of 4100 Hz.

Whether or not case coating will be required depends upon the actual noise measured during the aft transmission closed loop bench test. Case coating was not evaluated during the transmission test program.

Rotor Transmission Enclosure

To provide the remaining noise reduction required in meeting MIL-A-8806A, a 30 dB noise reduction acoustic barrier is necessary as shown in Figure 69. The efficiency of an acoustic barrier is determined by a sound transmission loss (TL) laboratory evaluation. However, once a material is installed in the field, the noise reduction achieved will frequently fall short of its TL rating, due to the numerous flanking paths through which the sound waves can circumvent the barrier wall. The most common are sound leaks in seams, perimeter joints, and access doors. As shown in Figure 70 a small leak can seriously jeopardize the acoustical performance of a good barrier.

In the CH-47 type aircraft, the acoustical treatment consisted of soft and loosely-fitted fiberglass blankets. Although their sound transmission loss (TL) rating was excellent for their weight, the actual maximum noise reduction achieved was only 20 dB due to the inability to cover more than 99% of the surface area. The Model 347 transmission treatment had acoustically tuned positive fitting honeycomb panels combined with soft blankets in achieving a 25 dB noise reduction. The HLH crew compartment, consisting of all overlapped tuned honeycomb panels and improved acoustic seals, should provide for a 99.9% coverage and 30 dB of noise reduction. Reductions of 35 dB were consistently achieved in the Acoustical Laboratory with similar panels and seals.

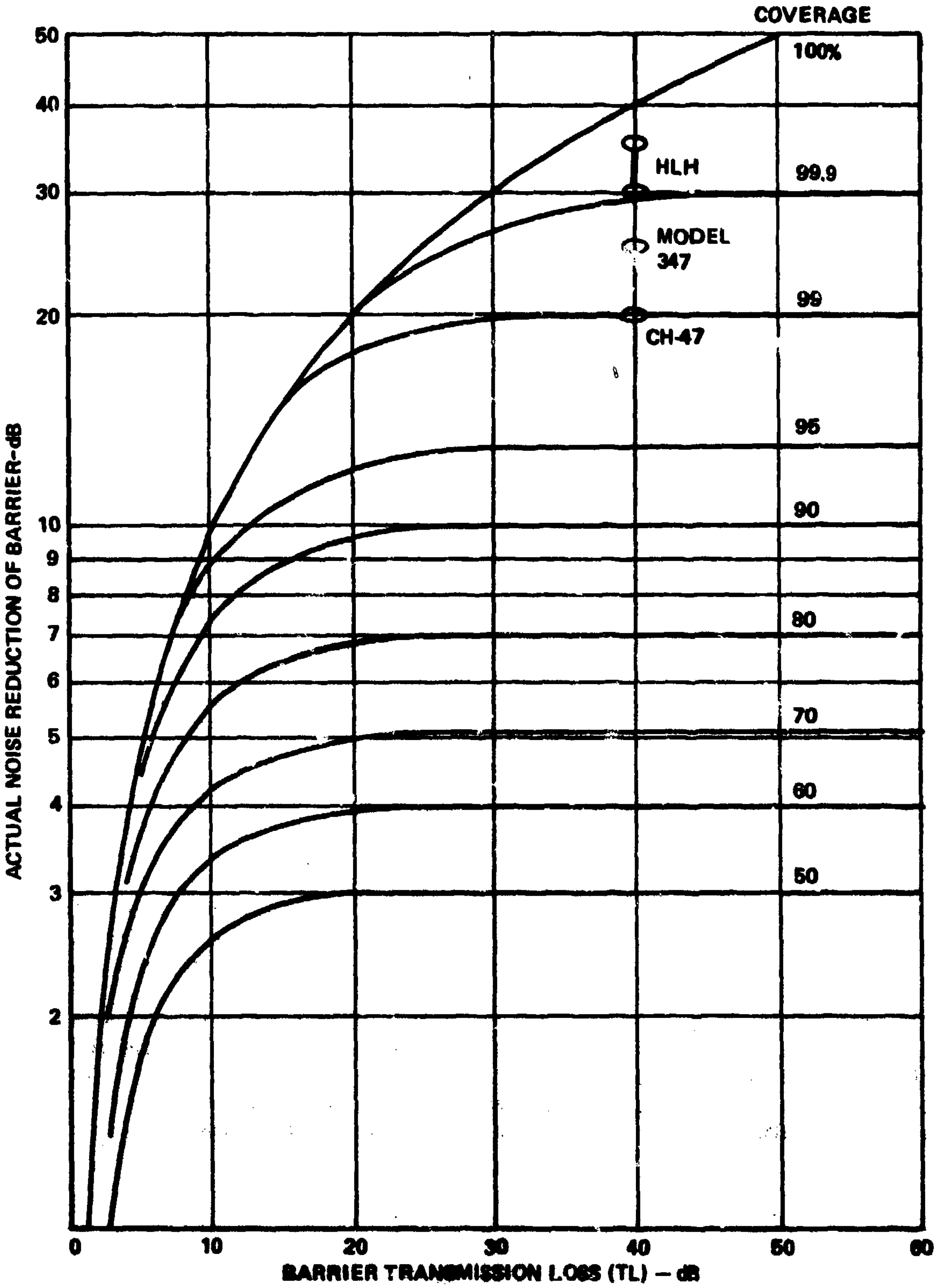

Figure 70. Effect of sound leakage on potential noise reduction.

2.9 PROPULSION SYSTEM

2.9.1 Air Vehicle/Engine Interface

Interface Control Document S301-10026 established and defined procedures, interface areas, and data exchange requirements for a joint air vehicle/engine interface program to identify and resolve problems unique to engine/airframe installations and to initiate design support tests and analysis, as necessary, prior to engine and/or airframe final design and test. It was approved in its entirety by DDA and Boeing Vertol.

Initially, 157 (90 DDA and 67 Boeing Vertol) interface items were identified as a result of a number of coordination meetings and telecons between Boeing Vertol and DDA personnel.

In addition to the interface definition items, 22 interface items were identified in the XT701-AD-700 Engine Model Specification 844 that require resolution. Examples of these items are: starter location and size, bleed port number and location, windmilling capability, noise level, accuracy of torque sensor system, and engine misalignment allowances.

Throughout the program, items were added and resolved. A total of 186 interface items were identified and resolved.

2.9.2 Propulsion System Analyses

Analyses of the engine inlet and exhaust systems, engine compartment cooling, engine control, and fuel and pneumatic systems were conducted.

A trade study of the exhaust system resulted in a straight exhaust and ejector arrangement, rather than the turned-in exhaust which ejected parallel to the direction of flight, as previously shown. The straight exhaust arrangement has lower risk because it provides more predictable ejector performance (and therefore, more predictable temperature distribution), it is more simple (and therefore, costs less to manufacture), it reduces the IR signature detection range of the aircraft by 10%, and it has a negligible effect

on download and drag. Compartment cooling analyses based on this arrangement have resulted in an exhaust ejector with a 29-inch primary diameter and a 33-inch secondary diameter. Ejector flow was determined adequate to meet engine manufacturer's specified operating temperature limits throughout the operating envelope. Analyses of compartment temperatures during soakback were conducted.

Engine compartment cooling analyses resulted in preliminary operating temperature predictions for intermediate power (cooling flow 4.0 lb/sec), very low power - 100% N_{II} (cooling flow 1.1 lb/sec), and soakback (zero cooling flow). Temperatures are predicted to be well below PIDS limits for all of these conditions, based on compartment layouts and engine temperature data current at the time of the analyses. Figure 71 presents the predicted operating temperatures.

In order to proceed with the design of the air induction system components, it was necessary to establish the loads on the system components. Structural loads have been defined for the induction system considering normal engine operation at high power (intermediate power), engine failed at 160 knots, and an engine surge at high power. The data presented in Table 27 are for each of the above operating conditions at those stations in the induction system. The stations considered are the inlet duct (primarily the center engine), the plenum, and the engine inlet bellmouth at the engine flange. Normal operation is characterized by pressure loss and low static pressure in the high velocity flow at engine inlet while pressurization of the inlet by ram at zero flow characterizes operation with the engine shut down.

Surge overpressure predictions are based upon empirical correlation of turbojet and turbofan test data and benefits from analysis performed for the Boeing SST. In addition, the configuration was reviewed by NASA personnel relative to current testing and analysis at the Lewis facility. The overpressure equation is:

$$P = K \times P \times M^{1.26}$$

where K is a function of compressor pressure ratio and bypass ratio (zero for the case considered) and M is the local Mach number prior to engine surge. For this analysis, a high power surge was considered with a pressure ratio of 12:1 resulting in a value of 2 for K. The maximum overpressure is observed at the engine inlet flange where flow area is a minimum and hence velocity is a maximum.

The short length of the bellmouth section minimizes weight penalty associated with designing for this extreme condition.

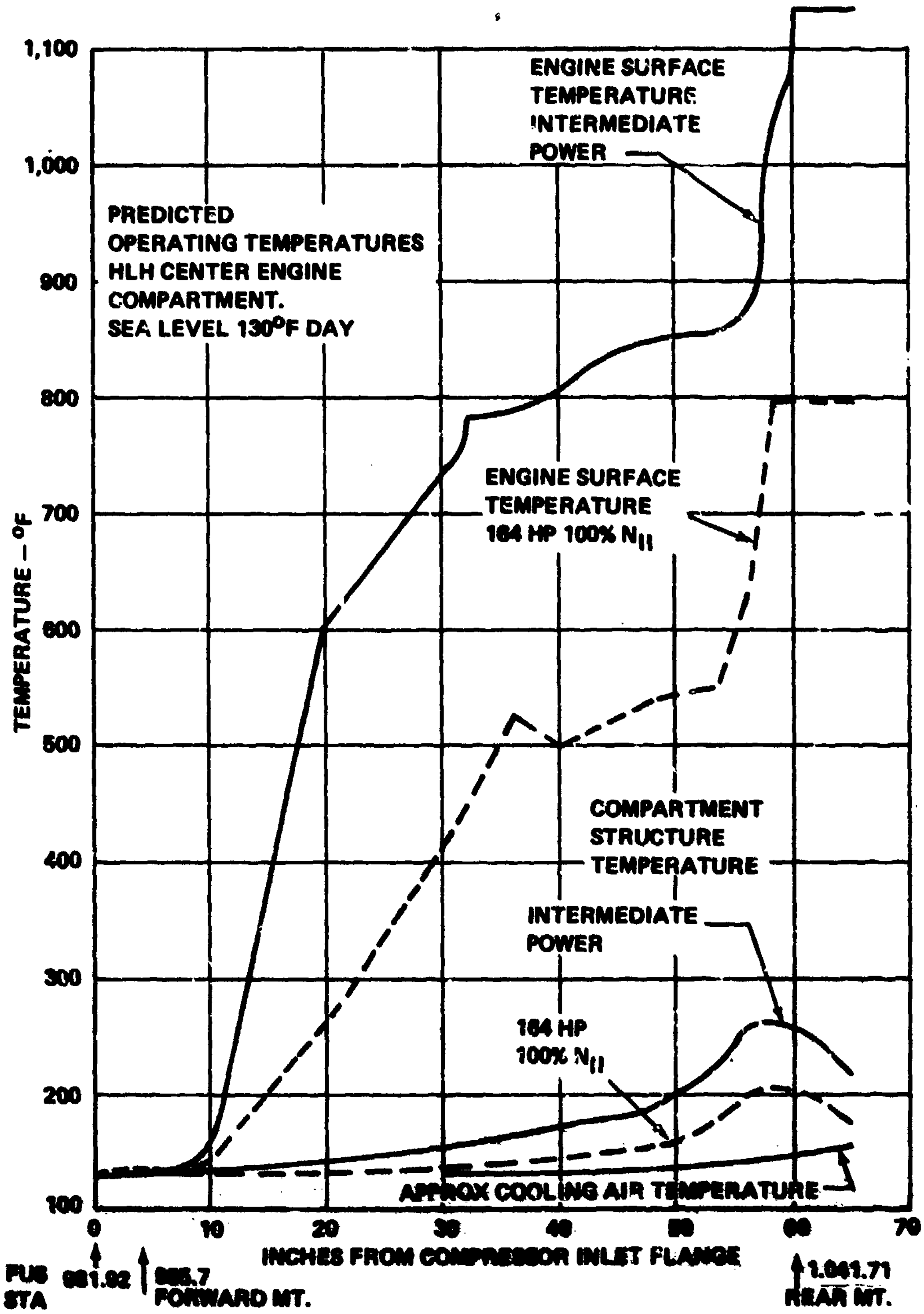

Figure 71. Center engine compartment predicted operating temperature.

191

TABLE 27. DUCT PRESSURES

	FUSELAGE INLET (psi)	PLENUM (psi)	ENGINE INLET (psi)
1. Overpressure as a result of engine surge (assuming P/Pc = 12)	2.1	2.1	12.9
2. Overpressure caused with engine shut down at 160 knots	0.6	0.6	0.6
3. Normal operation at intermediate power S.L. static, std. day	-0.1	-0.1	-1.4

The PIDS required a fuel filter in the airframe portion of the fuel system. The fuel systems performance was therefore evaluated to determine capability under boost pump off conditions. The curve, Figure 72 , shows altitude capability as a function of fuel temperature and aircraft attitude. This curve illustrates the affect of a 2 psi line loss due to a dirty fuel filter (bypassed). These results led to the deletion of the airframe filter from the prototype aircraft. The analysis was based upon meeting the requirements of engine PIDS 844A, paragraph 3.29.1.2, and assumes 3100-2900 lb/hr fuel flow depending on altitude and minimum usable fuel. Head loss together with line and fitting losses are considered. After a review of this data, AVSCOM agreed to deletion of the filter.

2.9.3 Nacelle and Engine Installation

Early studies of the nacelle resulted in the plenum type air induction system in place of the curved duct shown in the proposal configuration (Figure 8).

The location of outboard engines was changed by moving them rearward and outward along the driveshaft centerline by 11.037 inches. This action was taken to remove discontinuities in primary aircraft structure while ensuring adequate

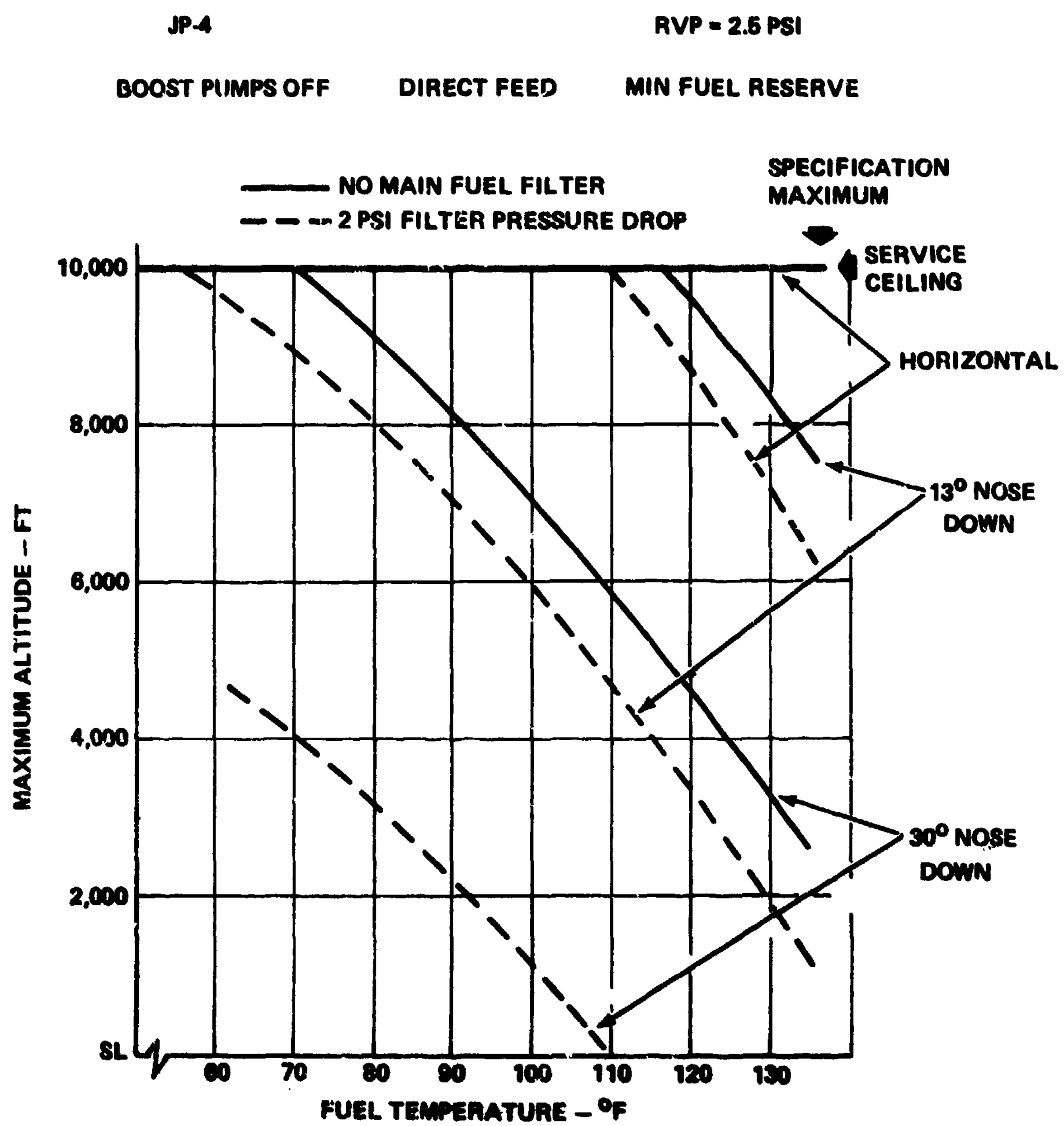

Figure 72. Maximum aircraft operating altitude established by fuel system considerations.

separation between engine bellmouth and induction system plenum wall to promote distortion-free engine airflow. Dynamic analysis of the engine/drive system revealed essentially no change in critical speeds. This was achieved by maintaining the original length of the first shaft section (next to the engine) and accommodating the change in the center shaft section. The mass of the drive system shafting supported by the engine remains unchanged and therefore engine dynamic response was not affected. The final nacelle configuration is shown in Figure 73 and 74 .

The center engine inlet was changed to a simplified duct and plenum arrangement, compared to the previous laterally offset curved duct arrangement.

An exhaust/cooling ejector design was developed which was common to all three engine installations. Final cooling analyses indicated that improvement was required to maintain structure temperatures below 180°F. In order to alleviate this situation, the exaust system outlet areas were reduced by a total of one inch on the diameter which provided the necessary space to add thermal blankets on both the engine tailpipe and ejector for all three engines.

The performance penalties associated with this change were as follows:

> Power loss at intermediate power - 12 shp/engine - equivalent loss of hover capability OEI IGE approximately 132 pounds.
>
> Increased specific fuel consumption at 4000 hp - .0007 lb/hp/hr.
>
> Increased mission fuel - approximately 16.8 pounds.

An engine combustion drain problem was identified. In the event of an engine false start, the fuel would not collect and drain from the combustion chamber but would run out the aft end of the engine into the fuselage thus creating a fire hazard. Since there was no simple modification to the engine to eliminate this discrepancy, the tail pipe was modified to provide a definite draining point. A collector was added to the ejector and appropriate drain lines were attached from this collector to drain the excess fuel overboard. Although this does not provide the required combustion drain, it eliminates the immediate problem of a potential fire hazard.

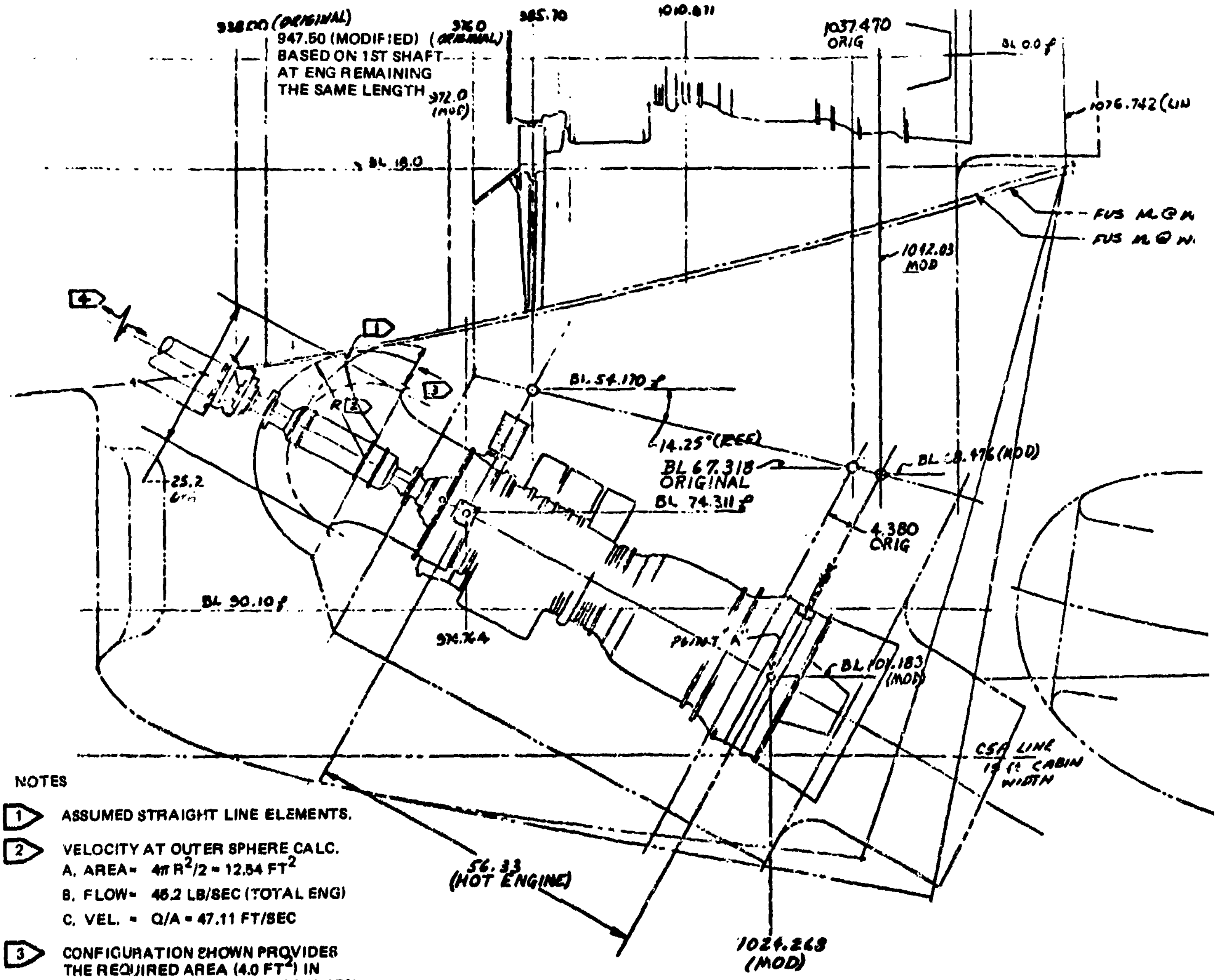

NOTES

1. ASSUMED STRAIGHT LINE ELEMENTS.
2. VELOCITY AT OUTER SPHERE CALC.
   A. AREA = $4\pi R^2/2 = 12.54$ FT^2
   B. FLOW = 46.2 LB/SEC (TOTAL ENG)
   C. VEL. = Q/A = 47.11 FT/SEC
3. CONFIGURATION SHOWN PROVIDES THE REQUIRED AREA (4.0 FT^2) IN ACCORDANCE WITH DESIGN DECISION NO. P-1 (REV A).
4. ADDITIONAL SHAFT LENGTH REQUIRED TO ACCOMMODATE THIS CHANGE IS 11.037 INCHES.
5. THE AFT CG SHIFT IS CONSIDERED TO HAVE A NEGLIGIBLE EFFECT ON THE CG ENVELOPE AND THE ASSOCIATED PERFORMANCE OF THE HLH.

WT CONFIG	PIDS A/C WT	PIDS CG SHIFT	PIDD A/C WT	PIDD CG SHIFT
WT EMPTY	60,603	0.50	62,720	0.60
DGW	118,000	0.26	118,000	0.30
AGW	148,000	0.20	148,000	0.25

Figure 73. Outboard engine/nacelle/fuselage drive system interface.

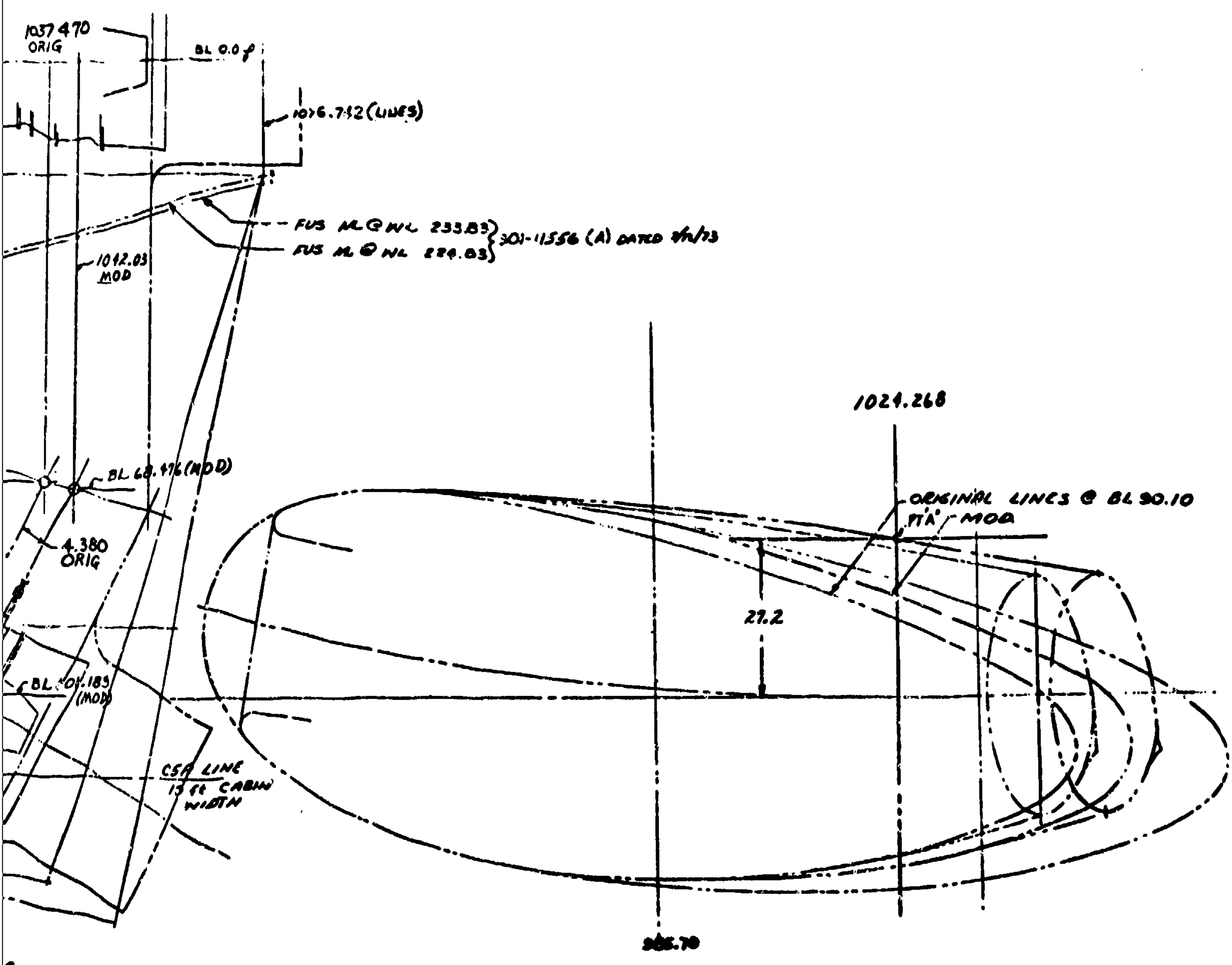

PIDD	
C WT – CG SHIFT	
2,720	0.60
8,000	0.30
8,000	0.25

2

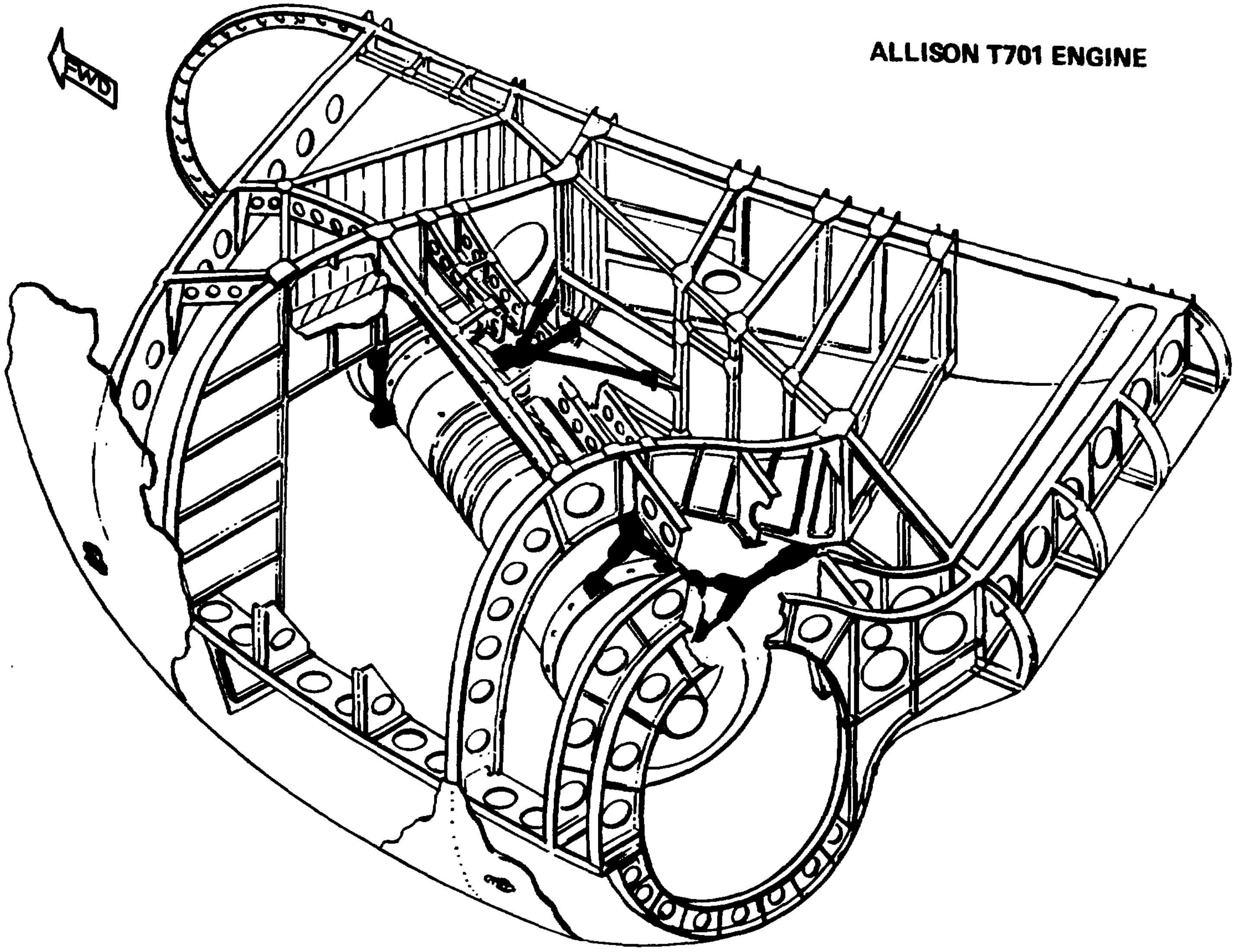

Figure 74. Engine mount installation.

Engine mount vibration isolators were not incorporated in the prototype design. However, in case testing indicated a need for isolators, preliminary design was accomplished, a proposal was obtained from Barry Corporation for the isolators, and space provisions were allowed in the mount design for later installation.

A simulated #1 engine air induction system was fabricated by Kaman and tested by DDA. During the test program, various modifications were made to the nacelle plenum configuration to minimize the possibility of foreign object damage (FOD). Examination of the test data indicated that very low distortion levels were experienced with the incorporation of the FOD modifications, therefore these changes were incorporated into the design of the prototype HLH.

2.9.4 Fuel System

The fuel system schematic is shown in Figure 75.

Two main tanks are installed in each stub wing. Both gravity and pressure fueling are provided. The pressure fueling adapter is located in the right-hand stub wing. Single-point defueling can be accomplished through this adapter.

Each fuel cell is vented independently. Float-operated vent valves with relief capability are provided in each cell to preclude spillage from severe attitude changes. A roll-over anti-spill vent valve is also provided in the vent line. The lines are sized to relieve 75 GPM of fuel in the event of pressure fueling shut-off valve failure in the open position. The vent line terminates through the lower surface of the stub wing between the front and rear spars.

All fuel cells are gaged with conventional capacitor-type transistorized systems. Cockpit displays provide a continuous indication of available fuel in each tank and a digital readout of total available fuel.

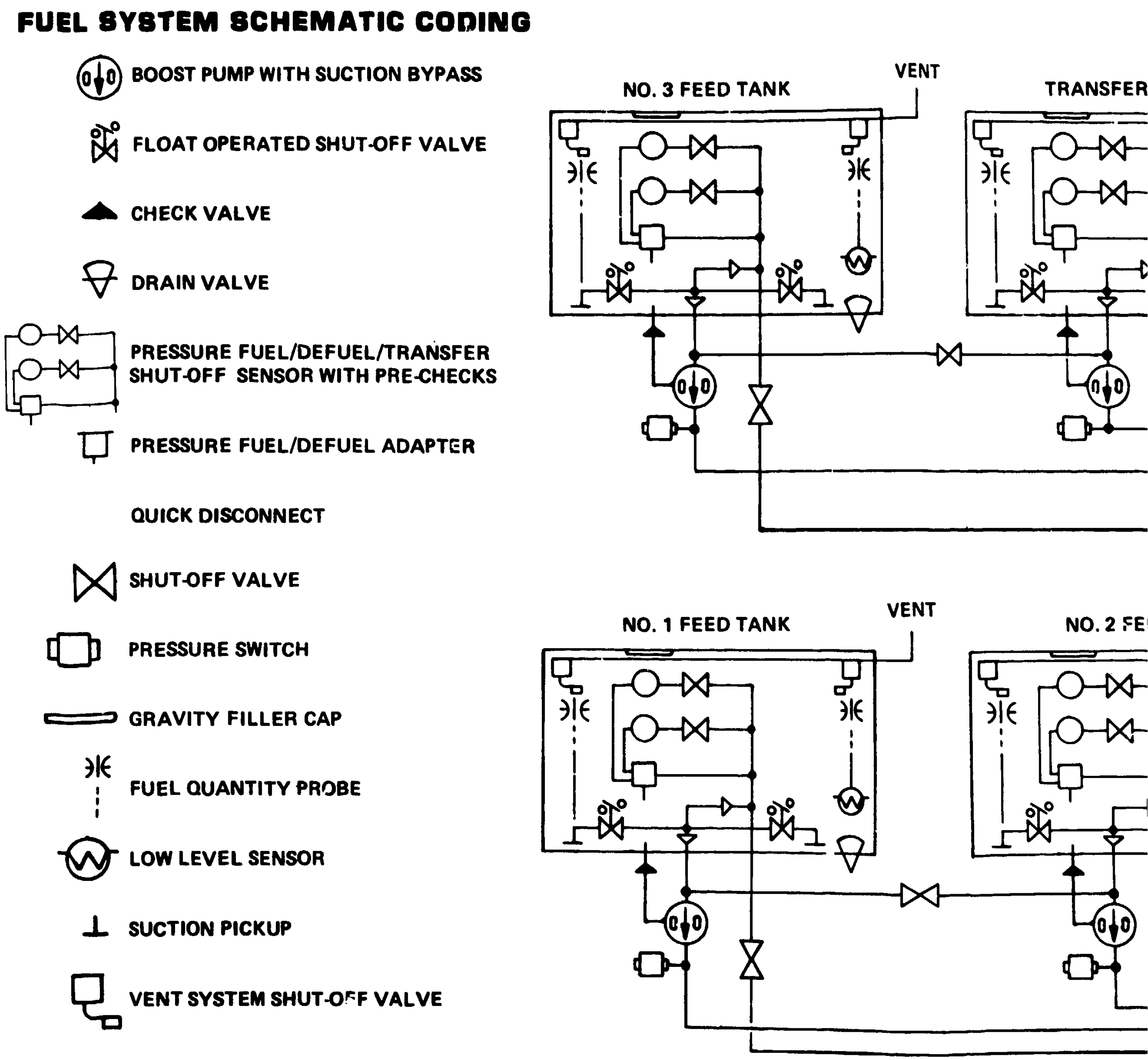

Figure 75. Fuel system schematic.

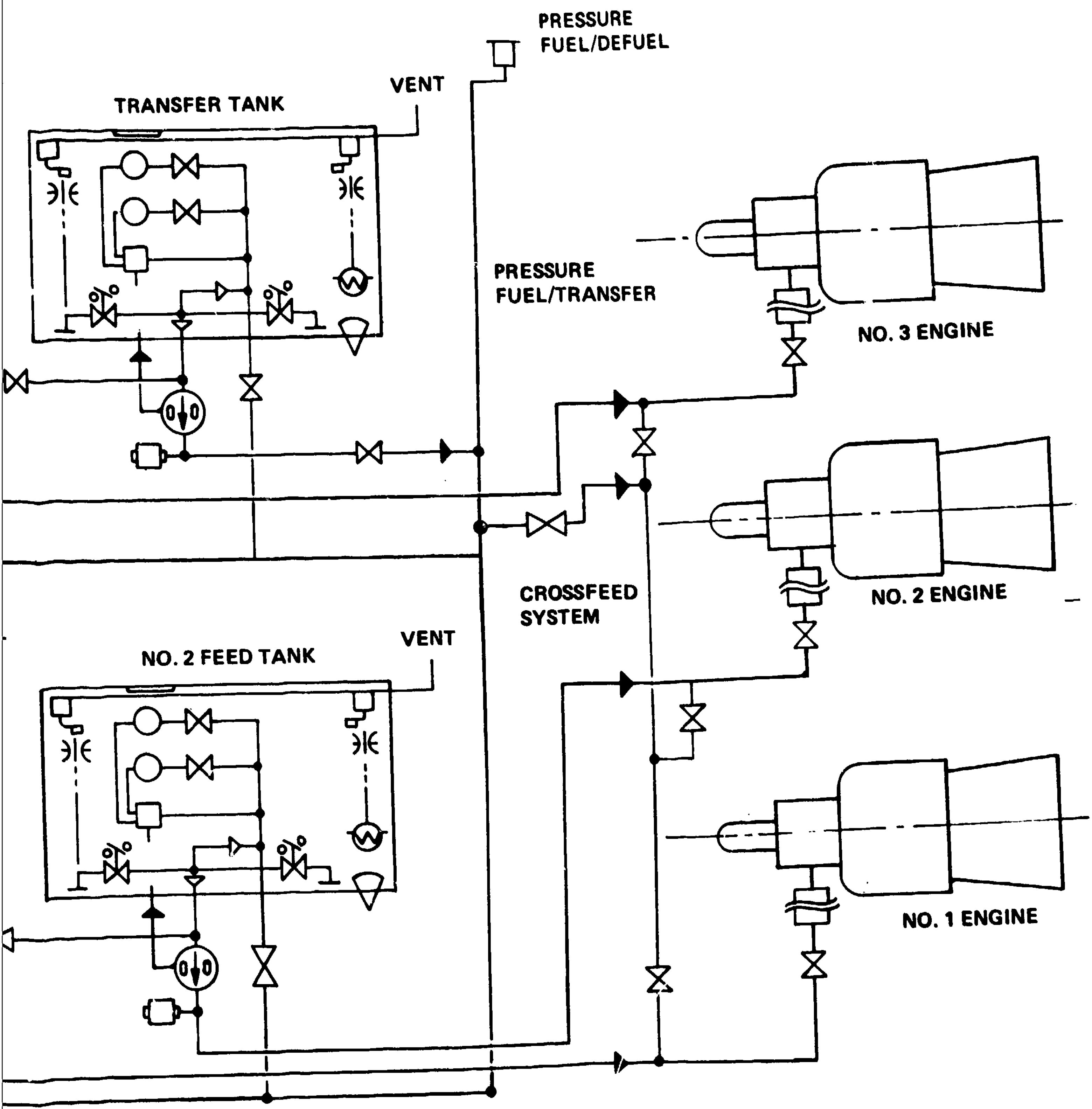
PRESSURE
FUEL/DEFUEL
VENT
TRANSFER TANK
PRESSURE
FUEL/TRANSFER
NO. 3 ENGINE
NO. 2 ENGINE
CROSSFEED
SYSTEM
VENT
NO. 2 FEED TANK
NO. 1 ENGINE

2

The prototype is provided with a positive pressure fuel feed system. The feed system is designed to make all the fuel available, under pressure, to any engine or combination of engines in the event of a boost pump or electrical bus failure.

On August 16, 1974 the fuel cell was prepared for crash impact testing at the Firestone Test Facility, South Gate, California. The cell was filled with 5,025 pounds of water which is equivalent to the weight of 773 gallons of JP4. It was then raised to an elevation of 65 feet where it would be allowed to free fall to the ground. The drop created a fuel cell velocity of 65 feet per second at impact. To meet ASRD requirements, no leakage after impact was permitted. The release mechanism was activated, and the fuel cell successfully completed the test (Figure 76).

During the final testing phase of the crashworthy fuel cell anti-spill rollover vent valve, it was determined that the maximum rate of fuel flow through the unit was 40 gallons per minute; however, the specification requirement for this valve (301-89203) is 75 GPM based on a system malfunction during pressure fueling. These units were returned to the vendor (Hydraulic Research Products Company) for modification. Retesting of modified units produced satisfactory results.

2.9.5 Emergency Equipment

The ASRD specifies a fire and smoke detection system for each engine compartment. Data was submitted to the customer requesting a change from smoke detection to over-temperature detection based on past Boeing experience. This deviation was accepted, but with a continuous-loop-type detection system in lieu of spot thermal detectors.

Due to the volumetric similarity between the HLH nacelle and the Boeing 727 nacelle, it was determined that the Boeing 727 system components could be utilized. This system utilizes two large bottles instead of four, with solenoid valves to provide the dual-shot capability to each engine compartment.

Taking advantage of the large quantity production on the 727 system permits a saving of approximately $1,000/aircraft.

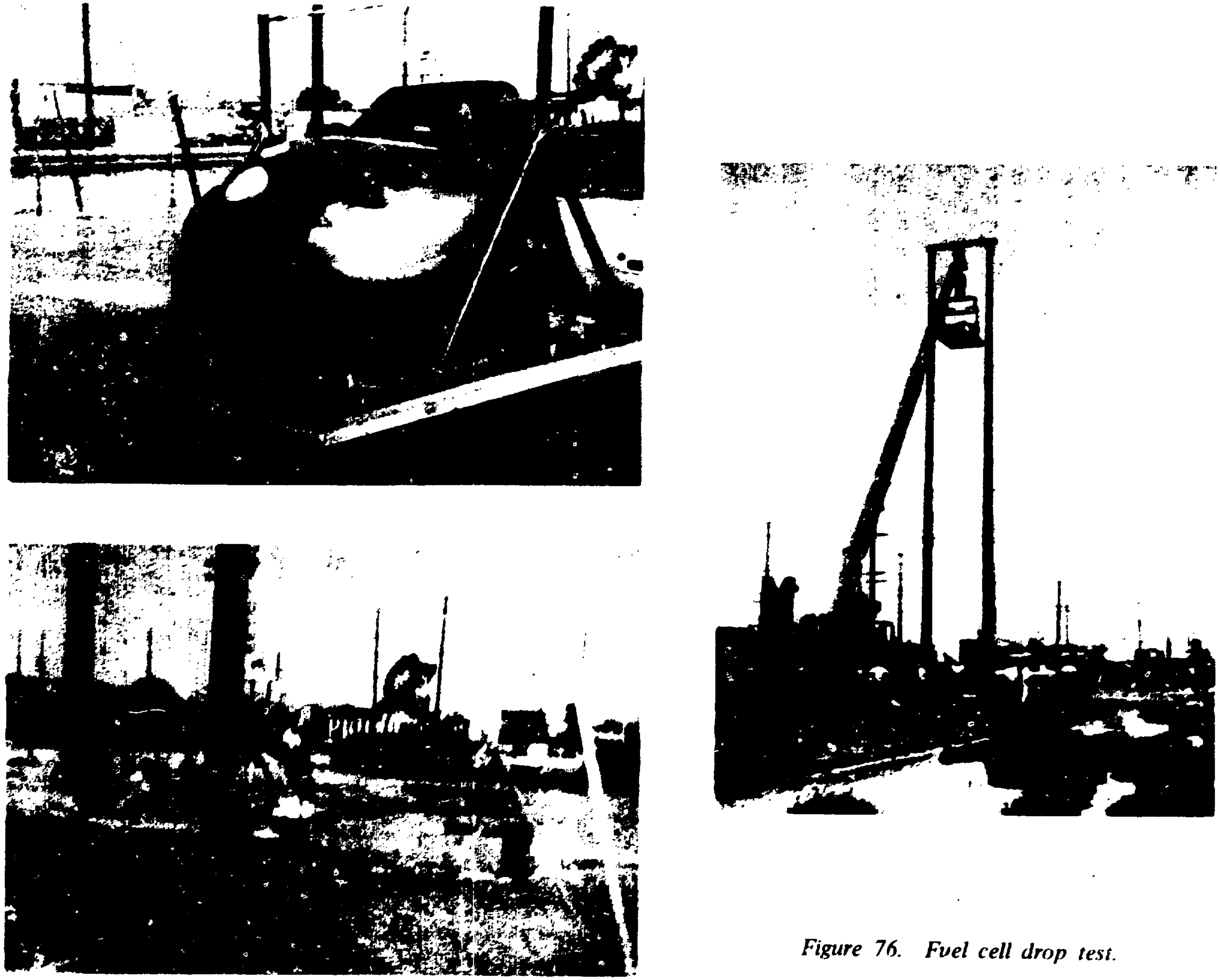

Figure 76. Fuel cell drop test.

A study of areas that have combustible fluids with a possible ignition source, revealed five areas that could be considered serious enough for added fire protection. These were:

a. Aft Transmission Area
b. Forward Transmission Area
c. Electronics Bay Area
d. Rotor Brake Area
e. Rotor Brake Reservoir Area

Installation of fire detection and extinguishing systems in these areas was authorized.

Testing at the DSTR confirmed that optical detectors are sensitive to the light spectrum emitted by the rotor brake during its operation. Based on this data, the supplemental fire detection system was designed for the incorporation of both optical and heat type sensors in the area of the combining transmission.

2.10 ELECTRICAL SYSTEMS

2.10.1 Power Management System

A Systems Requirement Review was held on 20 March 1973. An interface meeting with DDA was held on 23 March 1973 to review power-plant-mounted engine power control actuator types and required airframe interface control signals.

The torquemeter/hydraulic servo system selected provides integrated actuators within the engine's hydromechanical fuel control with an electrical interface with the airframe. This is a departure from current practice where airframe supplied electrical/mechanical actuators were connected to engine controls by levers and rods. Advantages include reduced weight and increased reliability due to simplicity, and the development and qualification of the actuator system in the engine environment. Figure 77 shows the D.C.-powered torquemotor and fuel servo.

The airframe condition lever output signal and collective stick position output interface signal format is as shown in Figure 78.

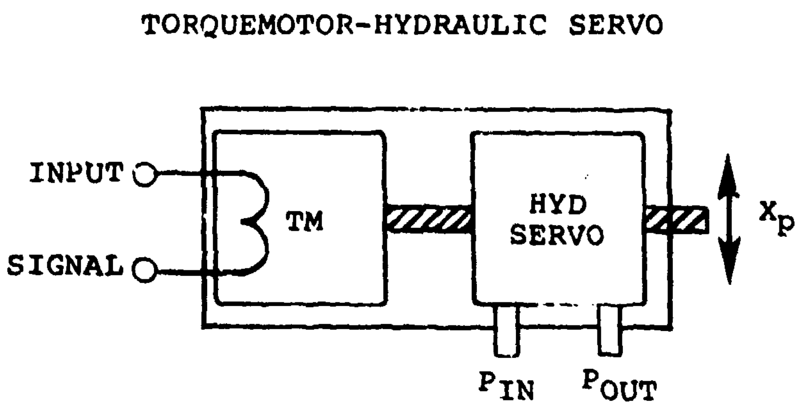

Figure 77. Power management actuator configuration.

1. CONDITION LEVER

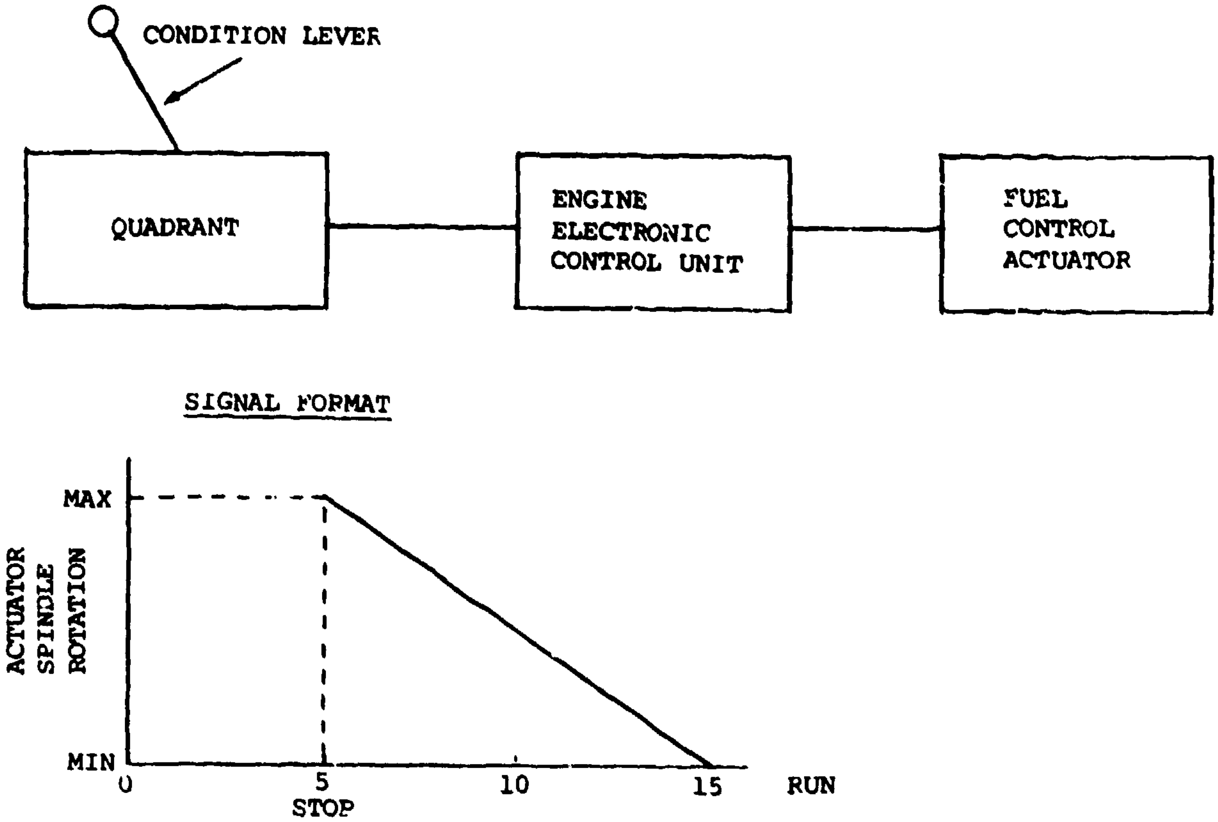

2. COLLECTIVE STICK POSITION

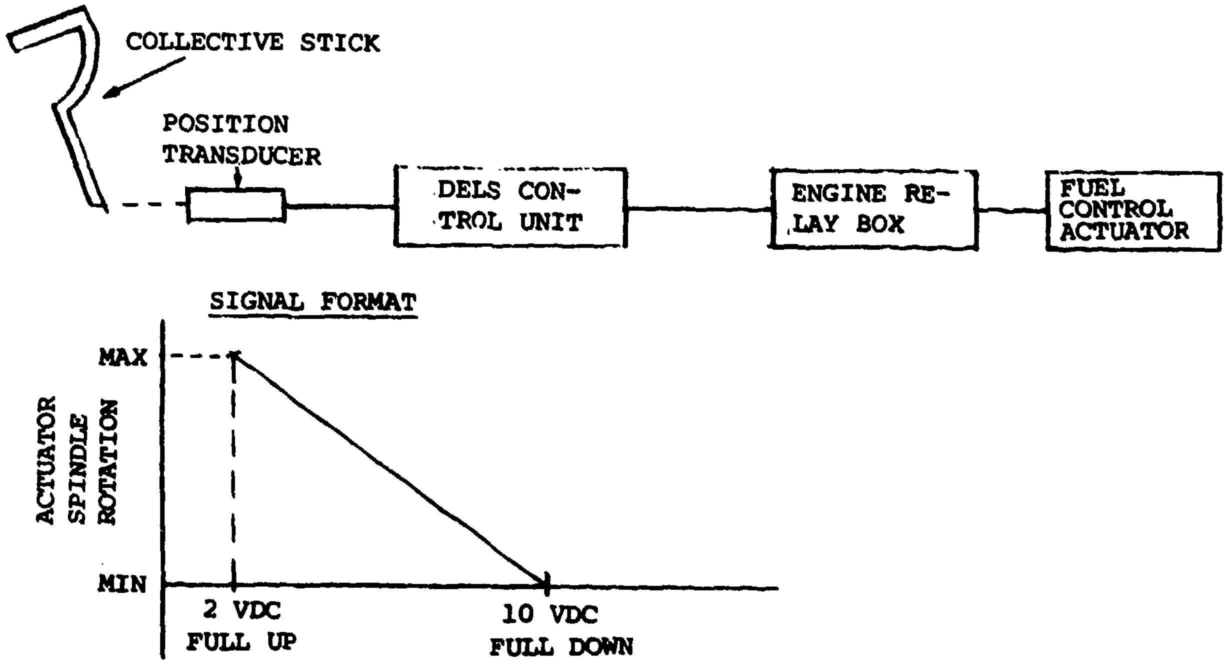

Figure 78. Power management actuator airframe interface schematic.

This selection of actuator and signal format coupled with the actuators supplied by DDA should result in higher reliability, reduced complexity of actuator drive electronic control circuitry, and reduced cost. Open circuit wiring will result in engine power output increase under these fault conditions rather than decrease in engine power output. In addition, with these actuators engine supplied, during the necessary engine development and qualification testing, the actuators will be subjected to real world engine environmental conditions, thus minimizing any unforeseen interface problems which could materially affect the pre-flight system checkout or prolong the flight test program.

Transient analysis of the torsional characteristics of the engines, rotors, and drive train using the digital computer simulation developed by Detroit Diesel Allison was conducted. Large disturbances caused by aircraft maneuvers and collective pitch inputs were investigated with the system exhibiting responsive, well-damped reactions. Typical responses to rotor power decays from cruise to low power, such as experienced during rapid pitch-up maneuvers with no collective input, are illustrated in Figure 79 . The transients describe the satisfactory system response to large, rapid inputs with less than a 4.5% rotor speed overshoot for the 1.0-second maximum to minimum power variation shown. During maneuvers which include collective pitch inputs, the rotor speed deviations are considerably less because of the load anticipation feature of the control system.

An analysis of the condition lever system in support of the engine quadrant design was completed. The original linear quadrant-to-engine schedule, when combined with the engine controls and performance, produced a significant dead band which was especially apparent during rotor start-up. This non-linearity, resulting in no control input effectiveness for more than 60% of the lever travel, is described in Figure 80. Reshaping of the electrical signal output from the quadrant condition lever by nonlinearizing the transducer characteristic has led to the improved lever-to-engine power relationship shown in the figure.

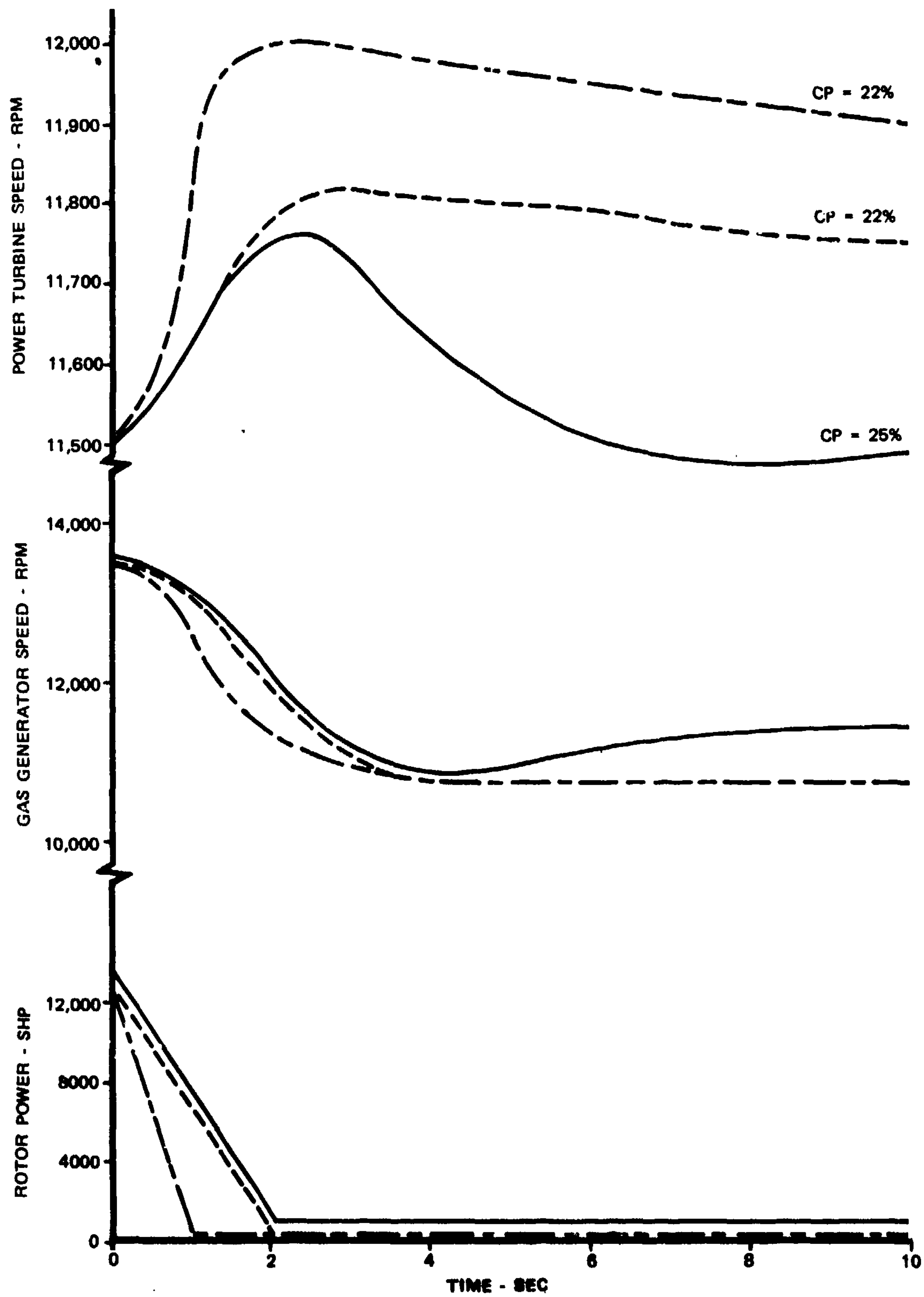

Figure 79. Transient characteristics response to rotor load.

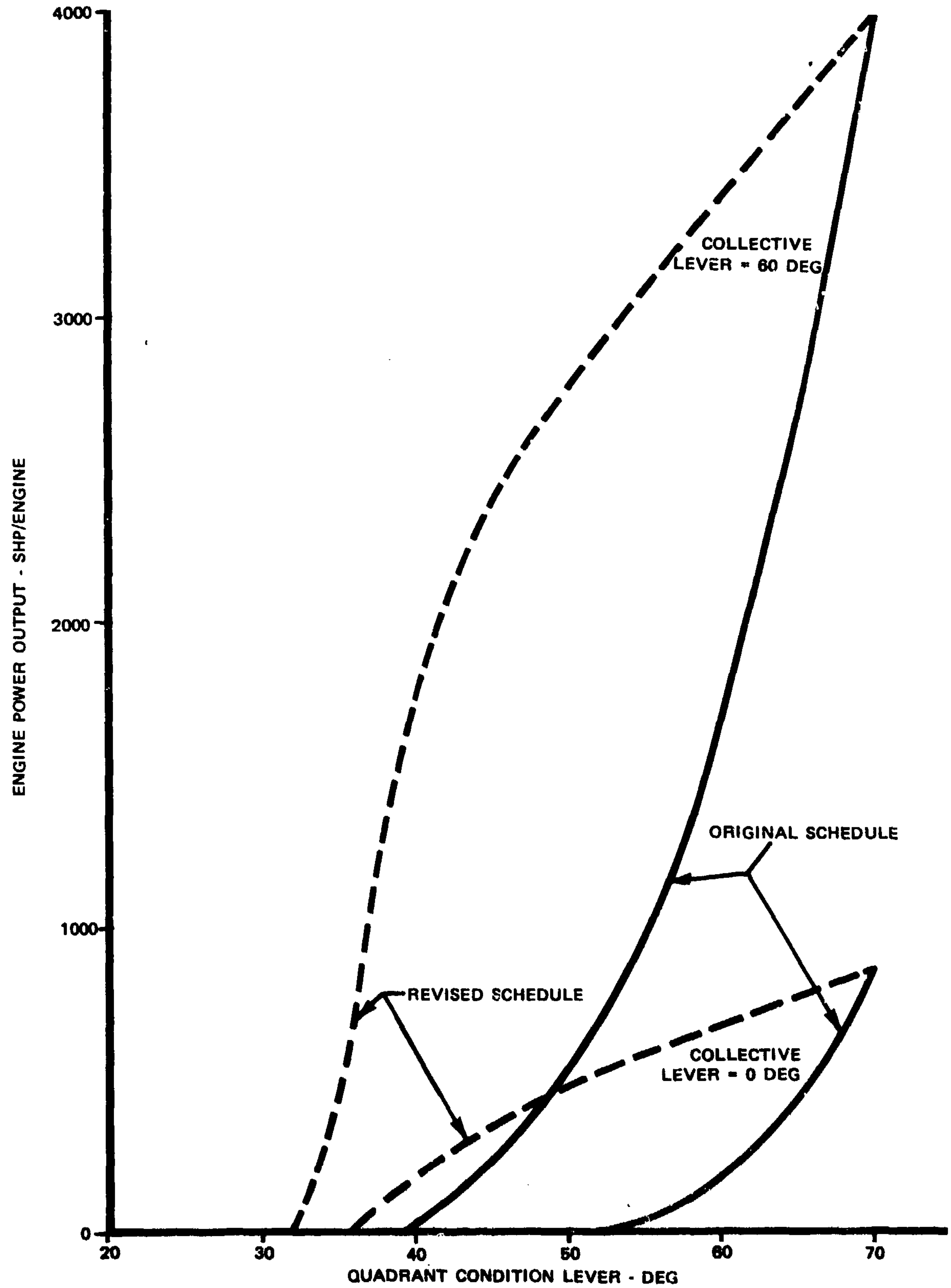

Figure 80. Engine quadrant condition lever/engine power relationship.

The analytical investigation of the power turbine overspeed protection system demonstrated that under no realistic conditions will 115% rotor speed be exceeded with engine power being applied. Therefore, the overspeed switchtrip setting was revised from 110% to 118% rotor speed which will preclude inadventent simultaneous shutdown of three engines. Studies of other schemes for providing required protection, including a cutback to minimum flow rather than shutdown and various logical interlocks, were conducted. The system for providing power turbine overspeed protection was finalized through coordination with Detroit Diesel Allison and completion of analytical investigations. It was concluded that the system configuration which results in engine shutdown following a power turbine overspeed is the best overall solution with the least potential risk. To eliminate the possibility of simultaneous three-engine shutdown while maintaining adequate turbine protection, the overspeed trip setting was raised to 121% power turbine speed. A recommendation has been made to check the system using the engine control test set at normal maintenance intervals. It is not necessary to have a daily check procedure since three malfunctions must occur before flight safety is appreciably affected: a power turbine output drive shaft or clutch must fail; the overspeed protection system must be inoperative; and the third stage turbine blades must fail to shed prior to reaching disc burst speed and therefore prevent containment of the resulting failure.

The dynamic simulation was used in the study of engine control system failure modes to assist in both transient and steady-state analysis of possible failures. An example is illustrated in Figure 81 wherein the power management control (PMC) signal to engine #1 fails to maximum on a cold day (-65°F) at 118,000 pounds gross weight, 100 knots. This causes an immediate uptrim to that engine which begins to pick up power. The other two engines initially follow the power increase, since the load sharing system functions to match the highest engine. However, rotor speed begins increasing, the proportional governors accordingly decrease power, and the speed settles to about 104.5%. The cold day condition maximizes the speed error because large negative trims are required on cold days at a steady state, and therefore, the normal engines saturate their downtrim capability quickly. The PMC trim for these engines goes to zero, since the load sharing positive trim caused by the failure is counteracted by the governed negative trim caused by high rotor speed. Pilot corrective action may be taken by disabling the engine electronic control (EEC) and/or reducing the condition lever of the high power engine. The effectiveness of the gain selection and limited-authority concept is demonstrated by this analysis with a relatively minor transient resulting from a significant control malfunction.

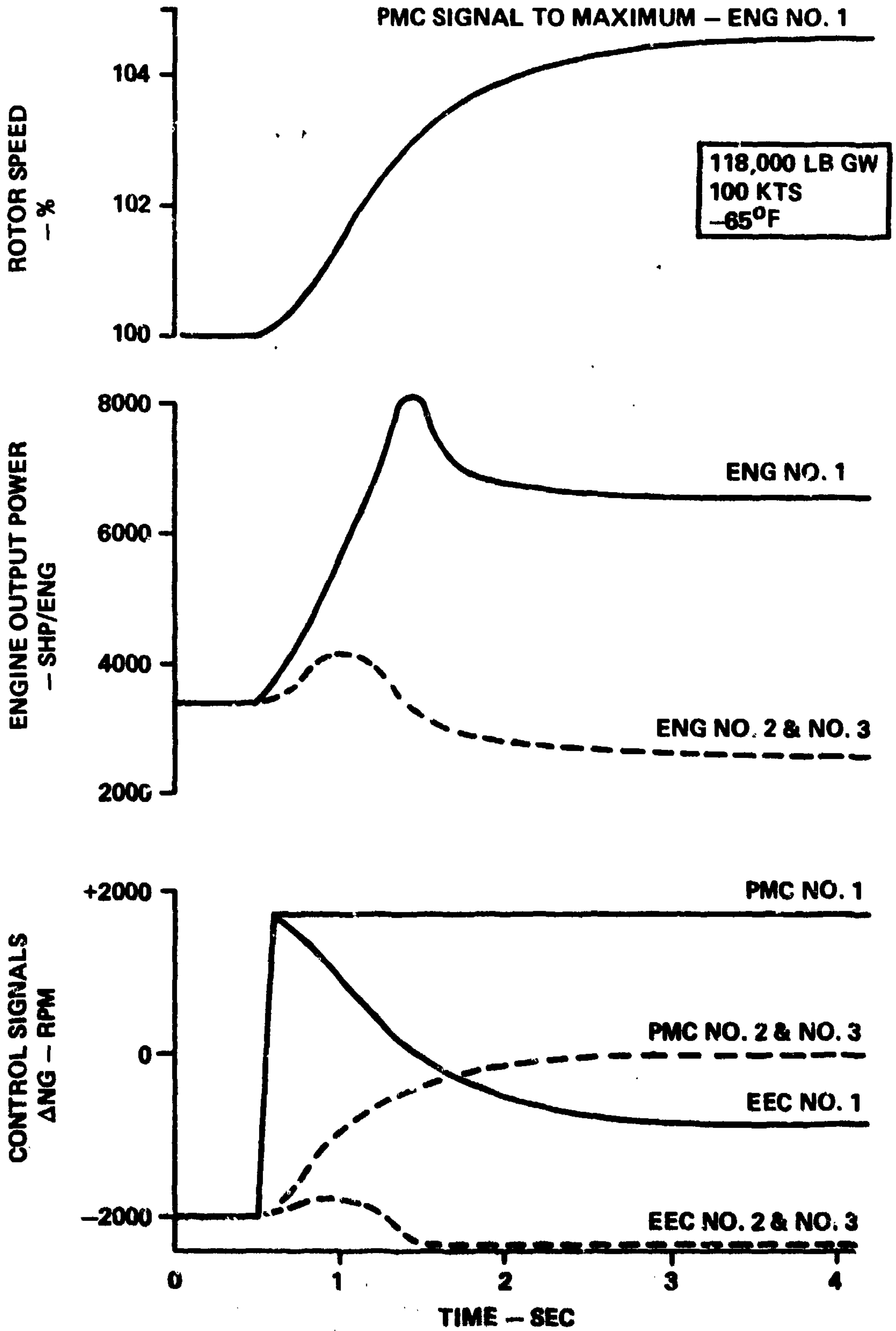

Figure 81. Simulation failure mode analysis.

A detailed nonlinear dynamic model of the lag damper was developed for use in torsional stability analyses of the rotor drive system. This computer program was joined with a simplified engine-control-rotor simulation to provide a preliminary evaluation of the effect of the lag damper and electronic control compensation on power train stability and to provide verification of the large-scale computer simulation being revised at Detroit Diesel Allison.

Results from the analysis demonstrated that the system will have a tendency to dither especially at low oil temperatures because of the low effective damping at low force levels inherent in the current design. A small perturbation transient is illustrated on Figure 82, for a cold day at high power, 100% rotor speed, three engines operating. As shown, stability can be improved by increasing the damper leakage. This modification was recommended.

The program has shown the effectiveness of the notch filter compensation in the engine electronic control power turbine speed loop toward providing stable, rapid transient response. Additional effort is proceeding to verify results through correlation with the DDA program to optimize the compensation considering all operating conditions.

Dynamic analysis continued using a simplified engine/drive/rotor system digital computer simulation in conjunction with a detailed lag damper model. Based on this analysis, specific revisions to the lag damper specification have been effected, resulting in improved drive train stability in the low velocity regime. Flow requirements including suitable tolerances were established by considering cold day operation with 2 and 3 engines on-line. Concurrent analysis at DDA incorporating the large-scale digital simulation has verified these conclusions.

Correlation efforts between the DDA and Boeing dynamic models has demonstrated relatively similar response, with the Boeing Vertol deck exhibiting somewhat less damping.

Dynamic analysis of the engine control rotor drive system resulted in the optimization of engine control parameters to provide suitable torsional stability characteristics. The method of analysis utilized a linearized system model capable of developing power turbine speed loop frequency response for determining the quantitative degree of stability.

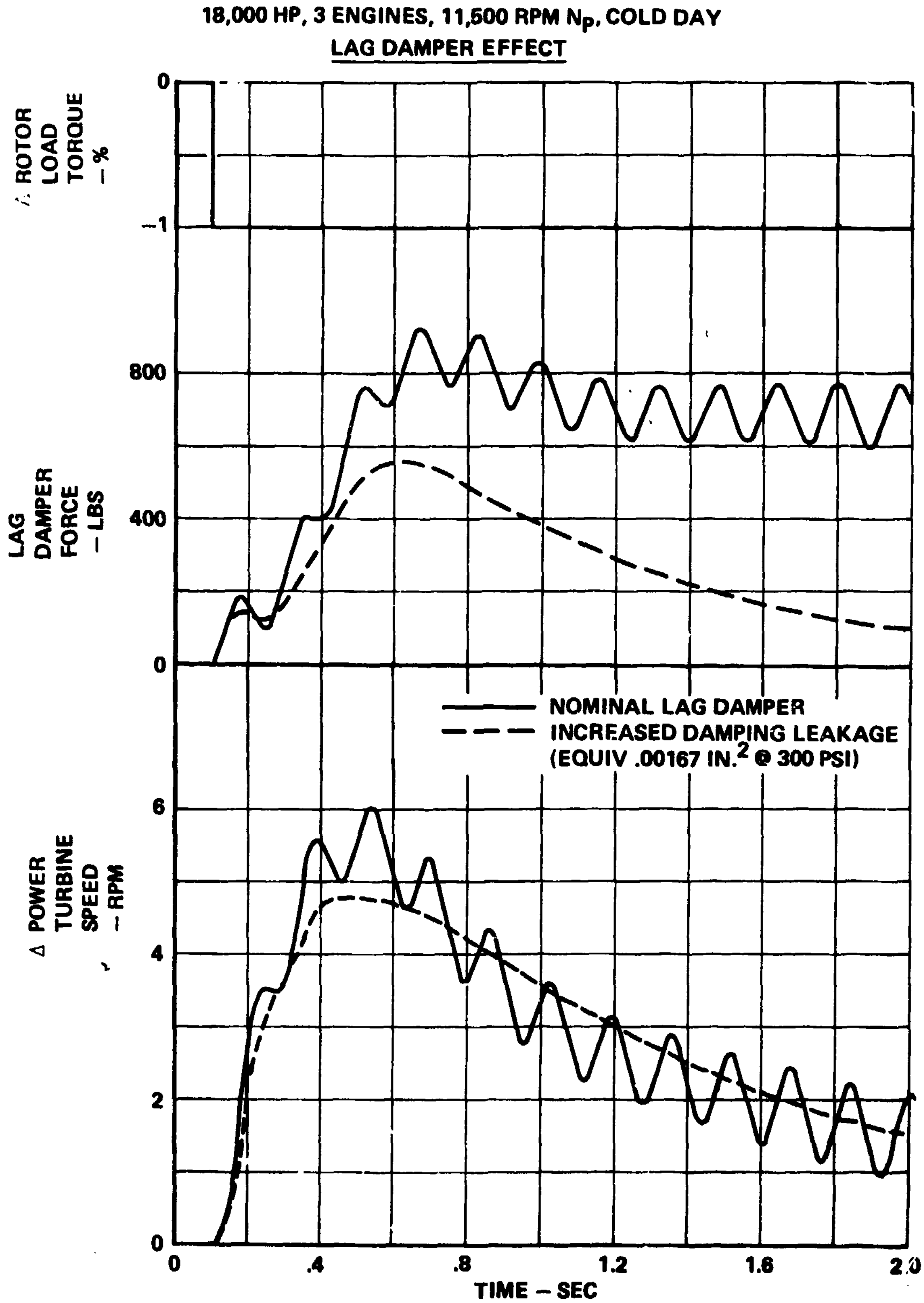

Figure 82. System response to load change.

The frequency response of the nominal system at standard day, high power conditions as given in Figure 83, clearly demonstrates the need for improvement. The basic system exhibits a gain greater than 0 dB at a phase shift of 180° and is therefore unstable. In order to provide stabilization while maintaining good response, a notch-filter type of control compensation (with an anti-resonance at 30 rad/sec) was selected. This compensation reduces the gain in the area of resonance and thereby improves stability as shown in Figure 83. The response characteristics indicate good stability with the gain margin increased to 11 dB and the phase margin to 70°. For comparison, the transient response of the same system is given in Figure 84 and shows good control with minimal speed deviation and tendency to oscillate.

Cold day conditions have been shown to reduce stability by lowering the effective damping of the lag dampers. However, adequate stability margin is present with the selected compensation.

Development of the model used in dynamic analysis of the engine-control-rotor drive system led to refinements in the drive train representation which have some impact on the system response. Correlation with recently available engine test data is underway which may affect engine parameters also used in the analytical model. In order to optimize stability and response, minor revisions to the stabilizing compensation located in the engine electronic control may be required.

Testing was completed using the DSTR to substantiate dynamic analysis and determine rotor/drive train natural frequency. These tests included closed loop operation with reduced engine electronic control stabilizing compensation and several values of notch filter compensation.

Correlation of the overall drive system simulation with this data has led to significant refinements in the drive train model, especially, in reducing the nominal effective spring rate of the lag dampers. Analysis is continuing both at Detroit Diesel Allison and Boeing Vertol to incorporate these results into the prototype similations and optimize the engine control compensation. Preliminary conclusions indicate the necessity to revise the notch filter design frequency to a lower value to provide an adequate stability margin throughout the range of operation.

A review of the DDA power management system EMI/RFI tests accomplished at Elite Electronic Engineering Company, Chicago, Illinois, was conducted and the results approved.

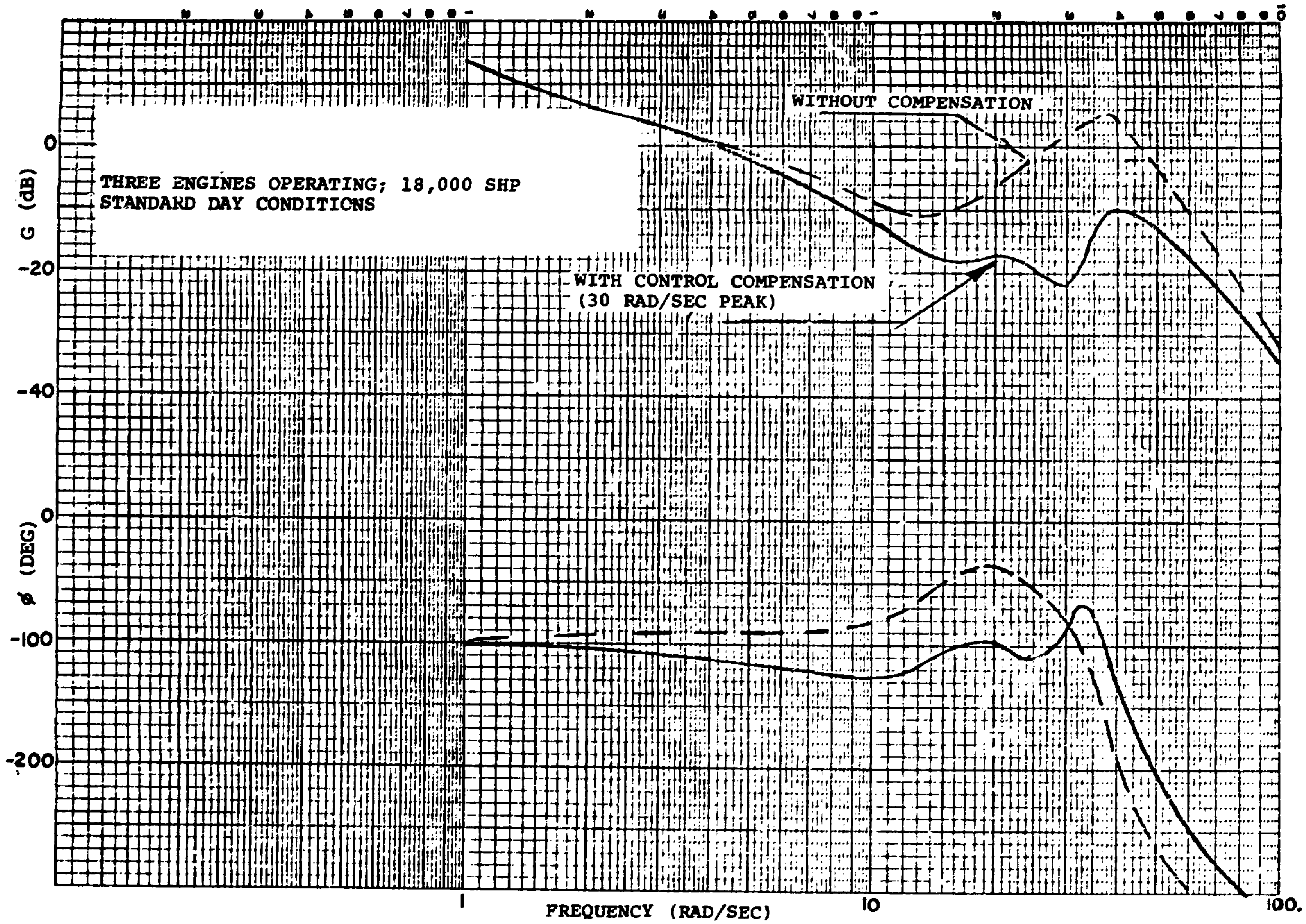

Figure 83. Engine/drive train frequency response.

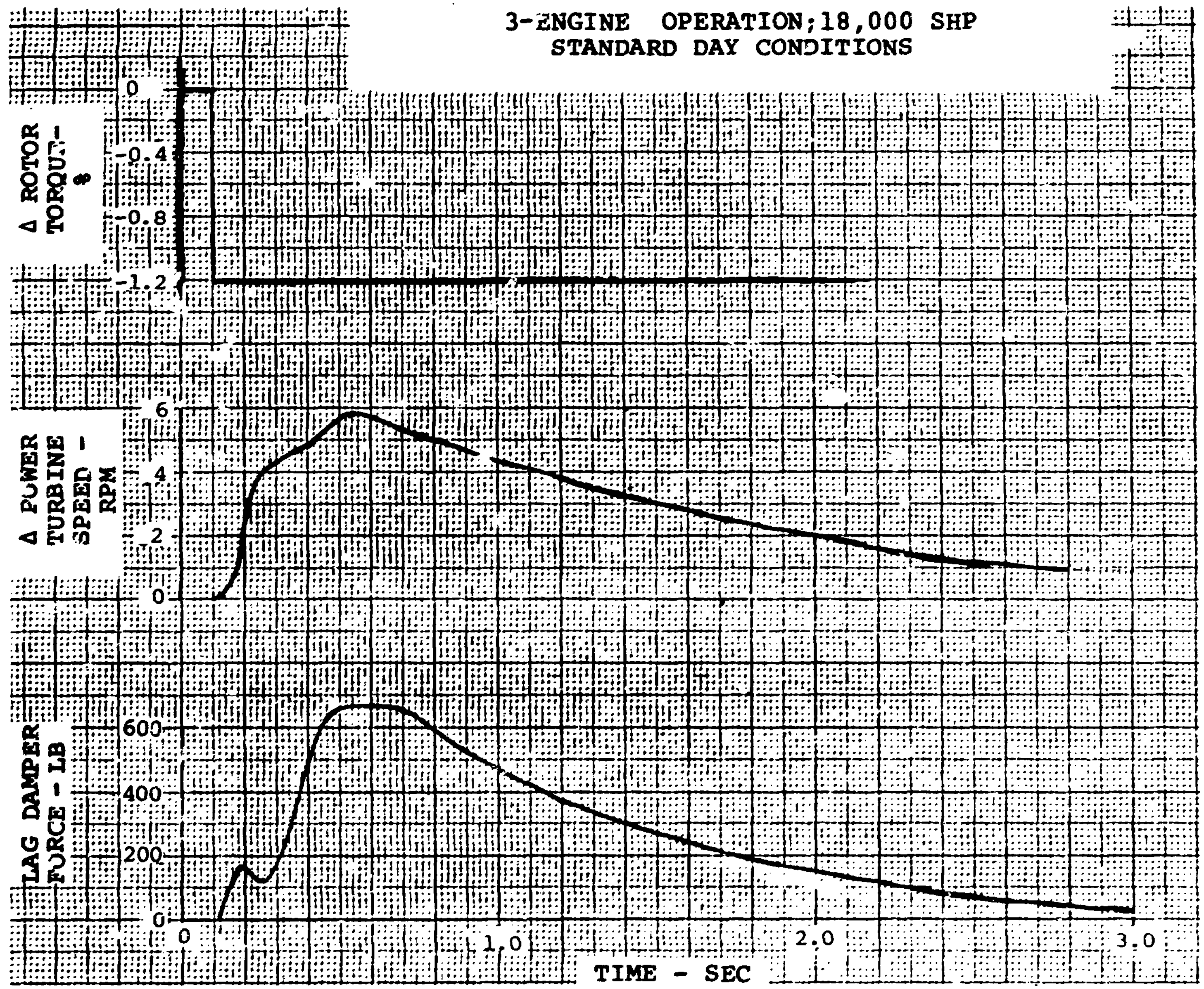

Figure 84. Estimated transient response to rotor torque.

2.10.2 Main Electrical Generation and Distribution System

Initial vendor liaison meetings were held with four generator manufacturers (Bendix, Lear Siegler, Lucas, and Westinghouse) to define HLH requirements for use of oil-cooled 60/90 KVA 12,000 rpm main generators (weight reduction and improved reliability).

Eight alternate candidate distribution systems (four without APU generator, four with APU generator), were revised for safety, reliability, vulnerability, weight, and cost. The systems selected are shown in Figure 85 without APU generator and Figure 86 with APU generator.

A preliminary electrical load analysis was conducted. Maximum 15-minute load is approximately 23 KVA. 60/90 KVA generators will be installed on the HLH prototype.

The Systems Requirements Review was held on 20 March 1973.

Procurement Specification S301-10058 for a 12,000 rpm oil-cooled 60/90 KVA AC generator was prepared and released for supplier proposals and negotiations.

The following source control drawings were prepared and released for supplier proposals and negotiations:

301-70103	Contactor, 3PDT, 50 amp 115/100-volt 400 Hz #3 AC bus
301-70104	Contactor, 3PDT, Center-Off Double-Break; 225 amp 115/200-volt AC, 400 Hz Main Line and Cross Tie
301-70106	Circuit Breaker, 100 amp, 3-phase Toggle AC Bus Tie
301-70107	Circuit Breaker, 150 amp, Toggle DC Bus Tie

A circuit breaker coordination study was conducted to determine the characteristics of the AC bus tie, AC distribution circuit breaker, and generator fault-clearing capacity. From this, it was determined that a 100 amp magnetic-operation circuit breaker of Heinneman AM 1000 series with a Type 2 trip curve would provide the necessary fault-clearing coordination characteristics.

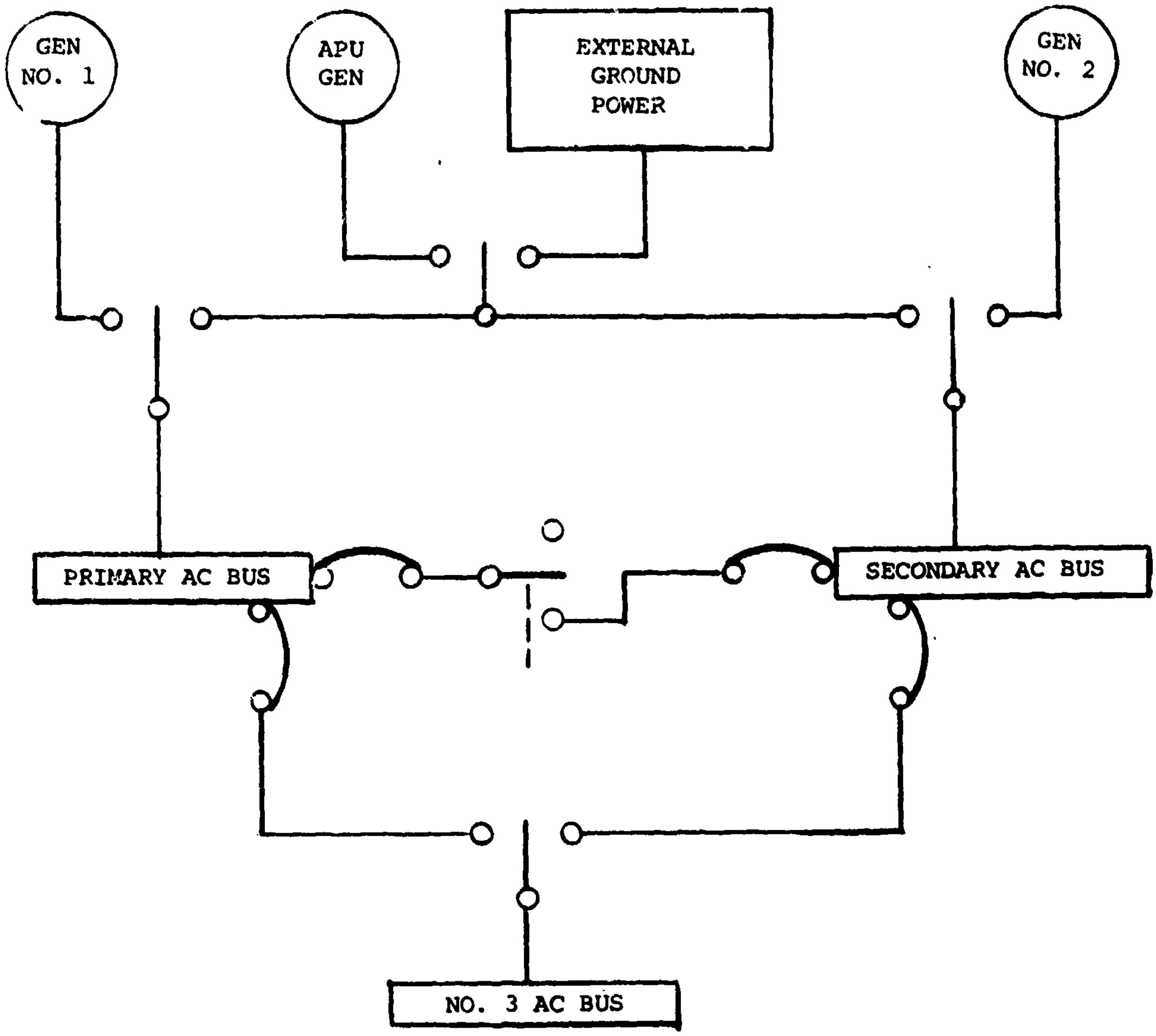

- ALL WIRING SHOWN IS 3 PHASE
- ALL CONTACTORS EXCEPT NO. 3 BUS CONTACTOR ARE CENTER-OFF CONFIGURATION

Figure 85. Selected AC generation and distribution system without APU.

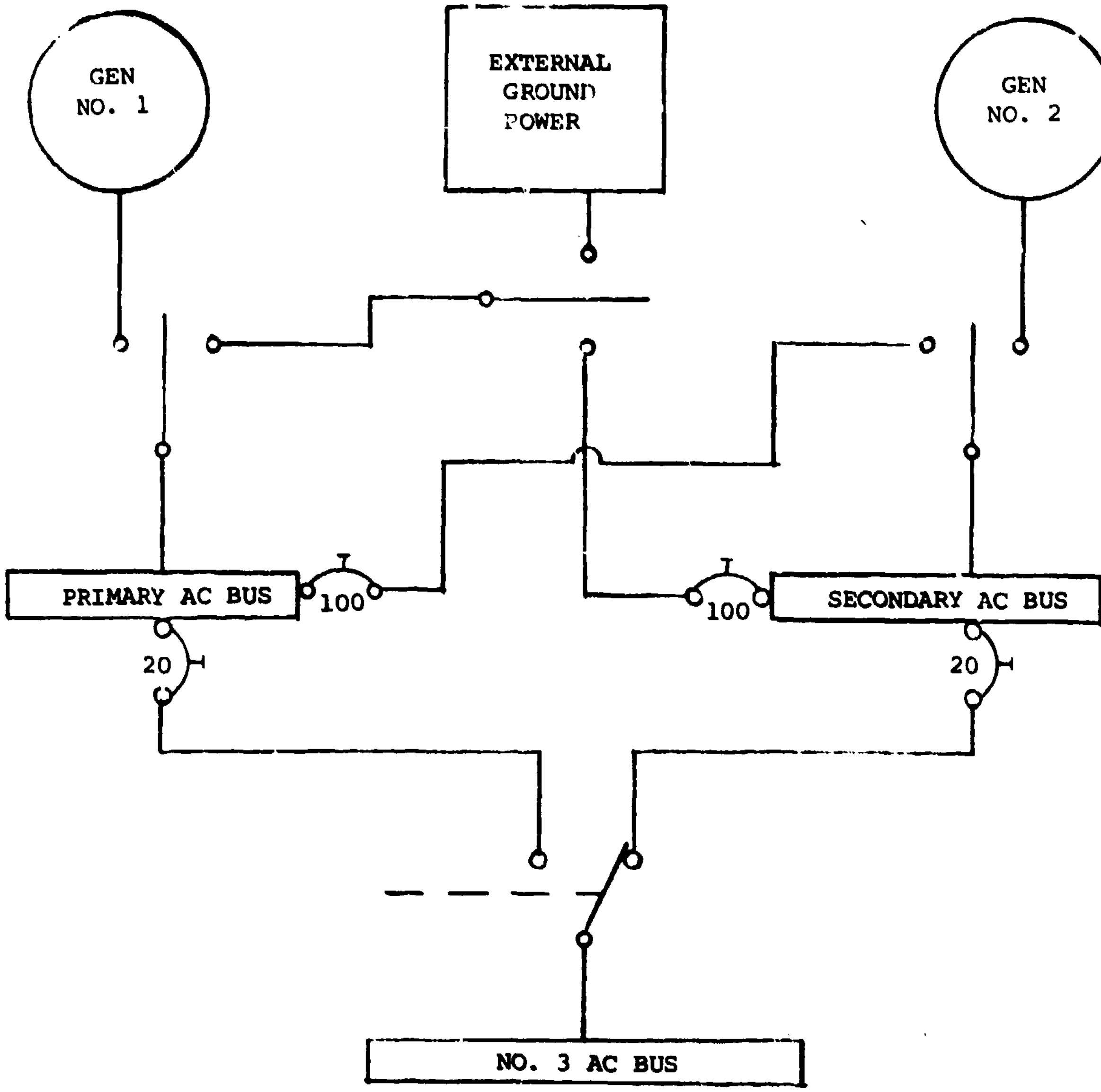

- ALL WIRING SHOWN IS 3 PHASE
- ALL CONTACTORS EXCEPT NO. 3 BUS CONTACTOR ARE CENTER-OFF CONFIGURATION

Figure 86. Selected AC generation system with APU.

Selection of components for the DC system were completed. All components except the reverse current cutout and DC cross tie circuit breakers were standard MS items.

Preliminary layouts of the AC distribution box, DC distribution box, and AC - DC ground power receptacles were completed.

The DC system was simplified from the configuration shown in Figure 87 to the configuration shown in Figure 88. A 29% reduction in component weight with a reduction of 35% component cost was achieved with improved system reliability. The DC ground power receptacle was deleted since DC power can be obtained via the transformer rectifier units when AC ground power is connected.

Suppliers were selected for the engine and transmission triple tape indicators, the engine radiation type fire detection system, and the engine continuous loop overheat detection system (Gull Instruments, Pyrotector, and Fenwall, respectively). Source control drawings for the rotor rpm indicator and rotor rpm zero speed sensor were prepared and released. Electrical schematics were prepared and released.

The Critical Design Review for the AC generator was held at Boeing Vertol on 25 February through 28 February 1974 with Lucas and AVSCOM personnel in attendance.

The generator cooling oil scavenge pump rating was increased from 160% of nominal flow to 200%, with potential growth to 300%. The scavenge pump drive system is now direct from the generator rotor rather than having the speed reduced through helix gears. Increased reliability and maintainability should result due to this change.

Fatigue cracking around the bolt holes in the mounting flange of the main generator occurred during vibration testing at Lucas Aerospace Ltd., Bradford, England. Reinforcing webs have been welded around the flange to stiffen the generator body and flange. The web fix on the generators successfully passed vibration testing. All generators were delivered with machined webs. The quill shafts were machined and aircraft units were delivered with the proper shaft installed. The main generator endurance testing was conducted.

Vibration testing of the generator control units was completed on 12 December 1974. The test results were reviewed and approved. The resonant sweep data was reviewed and dwell frequencies selected. During the dwell testing of the generator, an anti-drive end bearing retaining screw sheared.

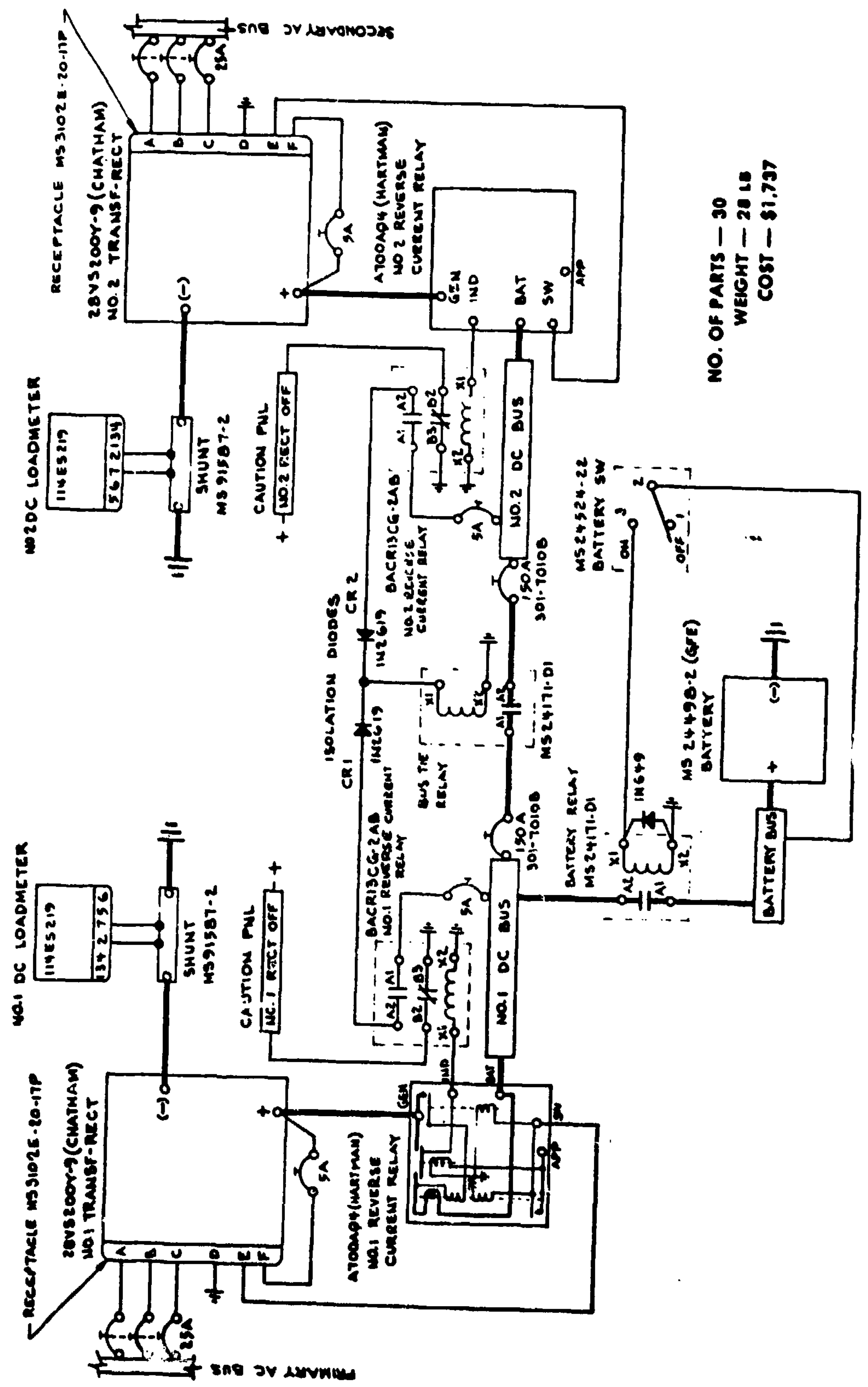

Figure 87. DC power distribution (original).

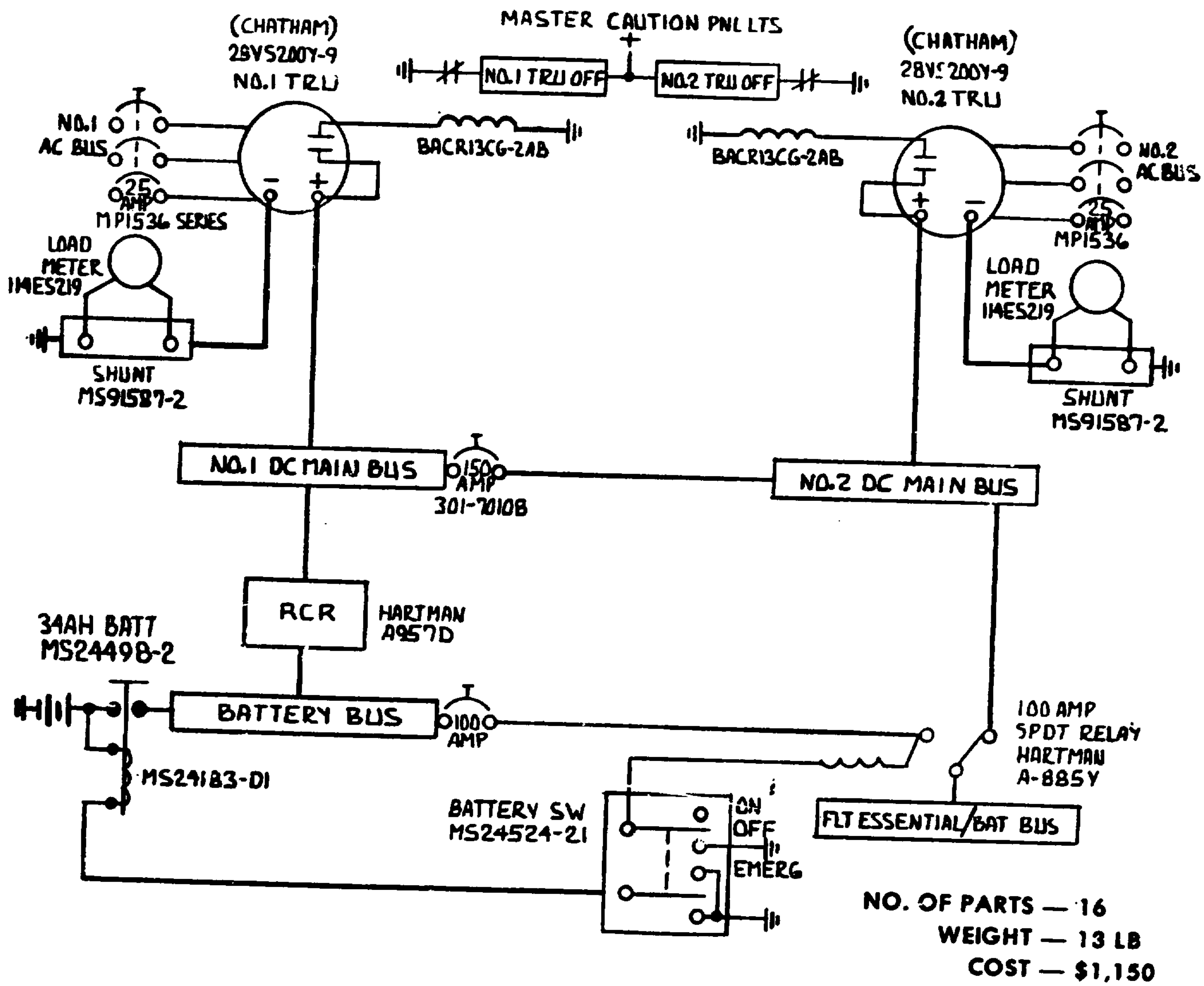

Figure 88. DC power distribution (revised).

Four generators held at Boeing for the aircraft and the forward transmission test stand were returned for rework.

2.10.3 Flight Controls Electrical Generation and Distribution System

The initial vendor liaison meeting with four generator manufacturers was held to define requirements for 28 VDC 1kw air-cooled generators. The System Requirement Review was held on 20 March 1973.

Procurement Specification S301-10059 for a 12,000 rpm air-cooled 0.5/0.75kw DC generator was prepared and released for supplier proposals and negotiations. Lucas was selected to provide the generator.

Source Control Drawing 301-70102, Contactor, 50 amp, 28 Volt, DC Flight Control System Changeover, was prepared and released for supplier proposals and negotiations.

As part of the DELS actuator configuration trade study, candidate generation and distribution systems were developed and analyzed for the DELS driver actuator configuration.

With the selection of DELS driver actuator system, the generation and distribution system was revised to the configuration shown in Figure 89. This system allows the deletion of one flight control system generator, one ground checkout and emergency in-flight power transformer rectifier unit, one distribution box, and the deletion of one circuit breaker from the remaining distribution boxes. The distribution-box layout drawing was revised to reflect this change.

The generator and distribution system, Figure 90, was revised to add battery power supplies and provide for diodes in lieu of contactors. Simplification is accomplished with the diodes, and the batteries provide for safe shutdown in the event ground power should not be available.

The Critical Design Review for the flight control generator was held at the Lucas facility 22-26 May 1974 and design go-ahead was granted.

All flight control generation and distribution wiring diagrams and bundle assembly drawings were completed and released for manufacturing.

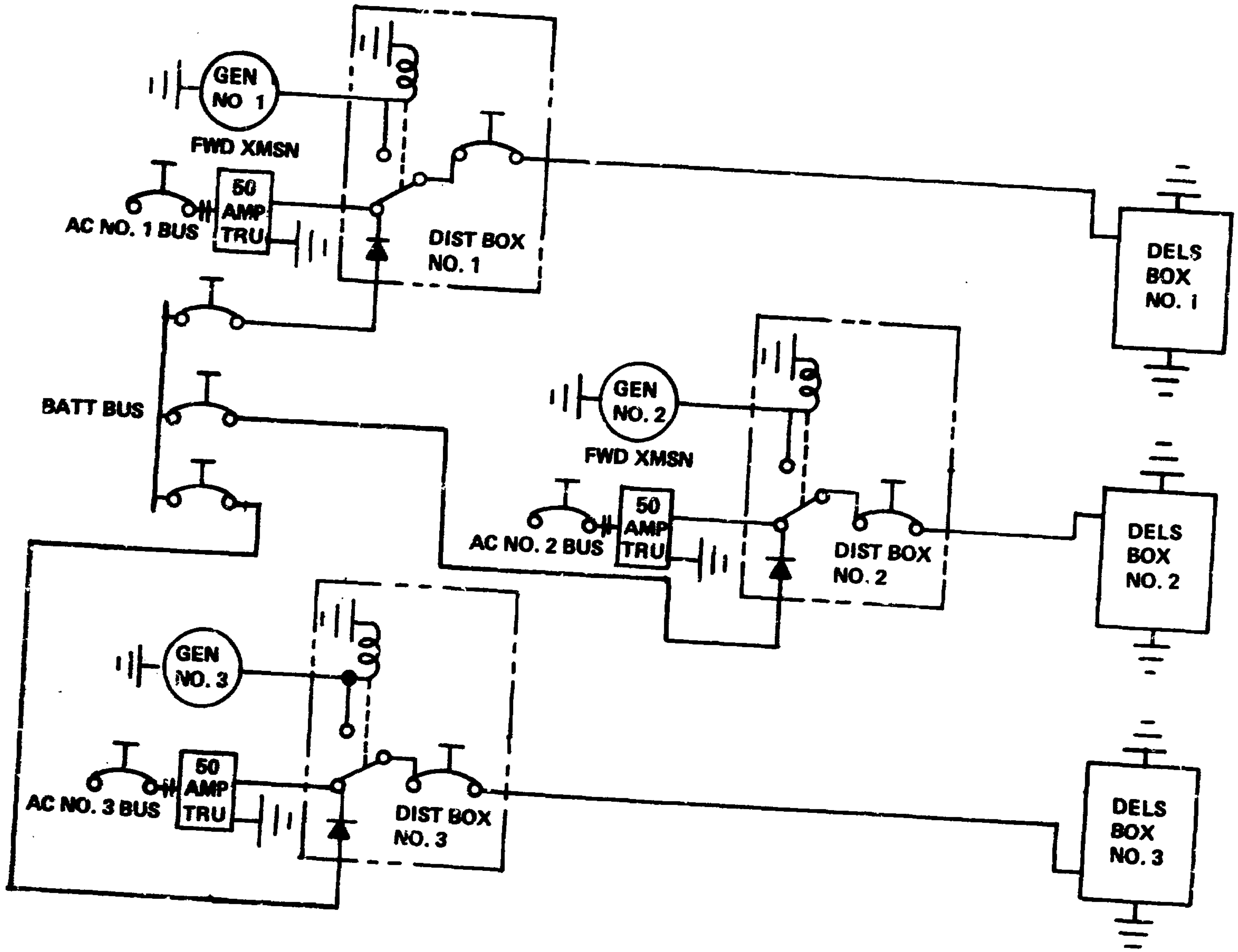

Figure 89. DELS electrical power configuration.

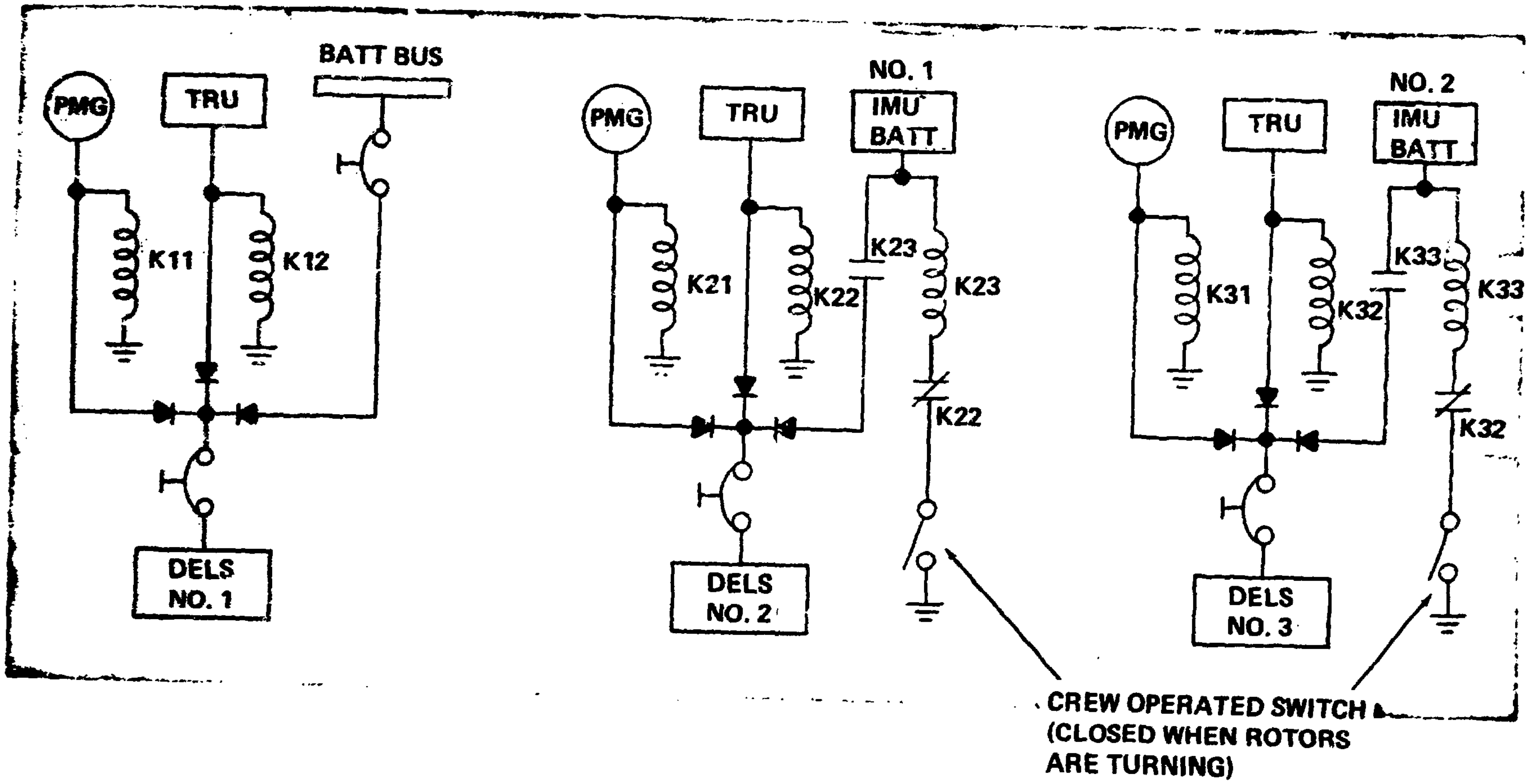

Figure 90. Power supply for DELS.

During the vibration resonant sweep tests of the flight control system generators at the Lucas Bradford, England, facility, a failure of a stud-mounted tantalum capacitor occurred. The failure occurred at the weld of the stud to capacitor case. A revised mounting installation is in preparation to correct this deficiency. The four generators previously delivered to Boeing were returned to Lucas for rework. Vibration testing was completed with satisfactory results in March 1975.

Reworking generators to correct capacitor failure was accomplished and units were shipped. Three units were rejected and returned to the supplier. The supplier shipped three replacement units, with arrival in July 1975.

2.10.4 Electrical Subsystems

Requirements were generated for two candidate engine and transmission cockpit indication systems; a triple nonidentical vertical scale indicator with self-contained conditioning electronics, and a triple identical vertical scale indicator with remote conditioning electronics.

These requirements were submitted to the following potential suppliers for budgetary cost and weight characteristics:

Electro Development Corporation
General Electric
Gull Instruments
Hartmen Systems Division
Simmonds Precision Products

Quotations received from the suppliers revealed no conclusive cost or weight savings advantages between the two systems. Accordingly, the instrument system procurement specification and source control drawing was written for nonidentical triple vertical-scale indicators with self-contained electronics.

Suppliers were selected for all purchased components. The Critical Design Review for the engine and transmission vertical scale indicators was held at the Gull Airborne Instrument, Inc., facility on 15 April 1974 and design go-ahead granted.

Procurement Specification S301-10062 and Source Control Drawing 301-70101 for the engine control quadrant were released and supplier proposals were obtained. Sargent Industries was selected to supply the quadrant (Figure 91).

The control quadrant successfully completed safety of flight testing, including a full vibration qualification (single article). The test article successfully completed the full ATP after testing and was delivered as the flight spare.

Design of the work platform control system was started during the final quarter of the program. Delivery of the caution system was completed and delivery of the engine transmission indicators was started.

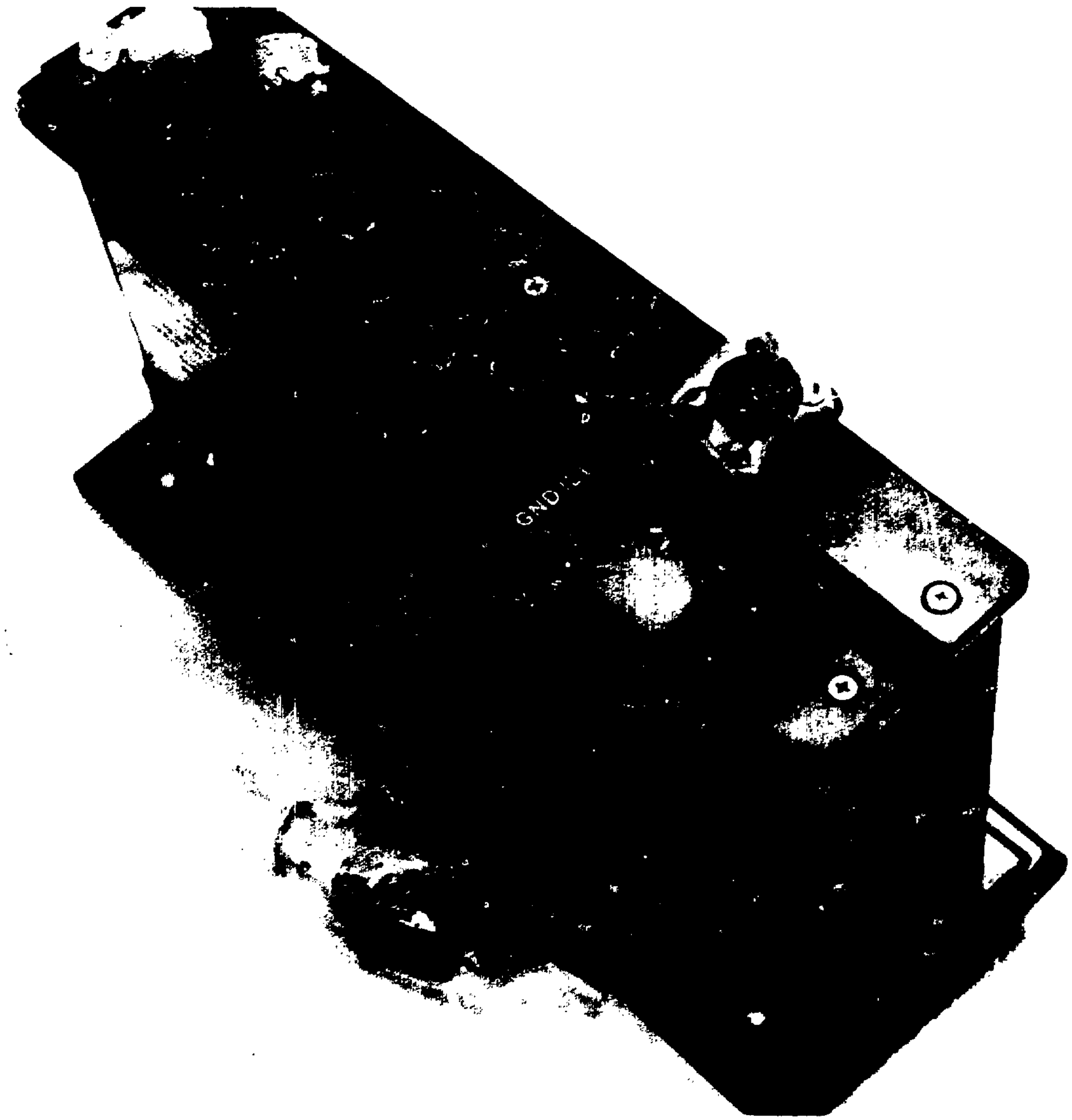

Figure 91. Brassboard control quadrant.

2.11 COMMUNICATIONS/NAVIGATION SYSTEMS

A Systems Requirement Review meeting between Boeing and the Army was held on 20 March 1973 to review and define changes to the PIDS document and GFE list. A preliminary comm/nav configuration was established.

During the second quarter of 1973, preliminary schematics for the UHF, VOR, radar altimeter, interphone, and compass systems were completed. Investigation revealed that the UTTAS interphone function box may be utilized for the prototype HLH. Preliminary layouts of the communications/navigation electronic compartments (right and left sides) were completed. The right-hand electronics shelving layout was completed.

The electronics compartments were relocated fore and aft of Station 236 bulkhead, right- and left-hand side. During the mockup review the Army recommended a fold-down work platform installed in front of the forward L.H. side electronics compartment in order to reach and perform the necessary maintenance on the electronics equipment, or alternatively, to relocate the equipment. To keep cost and weight to a minimum, a decision was made to delete the compartment and reconfigure the remaining electronic compartments to permit installation of the equipment that was removed from the deleted electronics compartment. This resulted in redesign of the shelf details and equipment installation layouts previously completed and released.

The sideslip sensors were mounted in a vertical position with the sensor pressure tube attachments facing downward.

All comm/nav schematics diagrams were completed and released.

UHF/FM and VHF/FM wire bundle assembly drawings were completed and released.

A review of the comm/nav antennas was conducted to verify that the previously selected locations were satisfactory. The review concluded that the existing locations, as shown in Figure 8, are suitable with minor relocation to accommodate the structural design.

The UHF/VHF and radar altimeter installation drawings were released on schedule.

All comm/nav wire bundles and wiring diagrams were released on schedule. The attitude indicator wiring diagram and bundle assembly drawing will be revised to agree with the new requirement for the ARU-18 attitude indicator.

All antenna and electronic compartment equipment installation drawings were completed and released on schedule.

The antenna installation drawing was completed for narrower cone angle antennas. This modification will reduce the probability of the altimeter locking on the external load when conducting cargo handling operations with long cables.

2.12 HYDRAULIC SYSTEM

2.12.1 Utility and Flight Control System

Preliminary descriptions of subsystem/equipment items were sent to vendors and the resultant proposals were reviewed. Flight control system component location layouts were prepared. Design specifications on the flight control hydraulic pump and rotor break control package were released. The flight control hydraulic system schematic was revised to reflect the swashplate actuator arrangement changes. The system consists of two independent transmission-driven hydraulic systems at each rotor swashplate with each system powering one channel of the three dual swashplate

actuators and one channel of the three triple driver actuators. The third driver actuator channels for both rotors are powered by an independent AC-electric-motor-driven hydraulic system. Each of the two mechanically driven hydraulic systems at the forward rotor is connected to each of the aft rotor systems through isolation valves and interconnecting piping normally unpressurized in flight. Upon failure of any of the mechanically driven pumps, the corresponding isolation valves are opened permitting the failed system to be powered from the other rotor system.

Final specifications for the wheel brake and rotor brake control systems, as well as the flight control hydraulic system SCDS, were released. Preliminary layouts for the third channel driver power supply, rotor brake supply, and fill module locations were completed. Actuator planning layouts were completed in support of the integrated flight control actuator envelope studies.

Updated schematic diagrams of the flight control system (301-50001) and the utility system (301-50002) are shown in Figures 92 and 93.

The update on 301-50001 showed integrated swashplate actuators, moved pressure transmitters downstream of accumulators, rerouted bypass return lines through the oil cooler, changed manifolded valve assemblies on interconnect lines to individual valves, removed pressure reducers in driver actuator lines, added brake-by-wire system alternate supply from interconnect lines, added check valve in 3rd channel system return line, removed runaround circuit from interconnect pressure valves, added ground power supply lockout valve in valve packs, and added two relief valves around aft interconnect return valves. These changes resulted primarily from further safety, reliability, and operational study iterations.

Updating of 301-50002 consisted of revising brake-by-wire system to show tie-in to System 1 and System 2 interconnect lines. Nose gear steering system shown is powered by System No. 1 forward only.

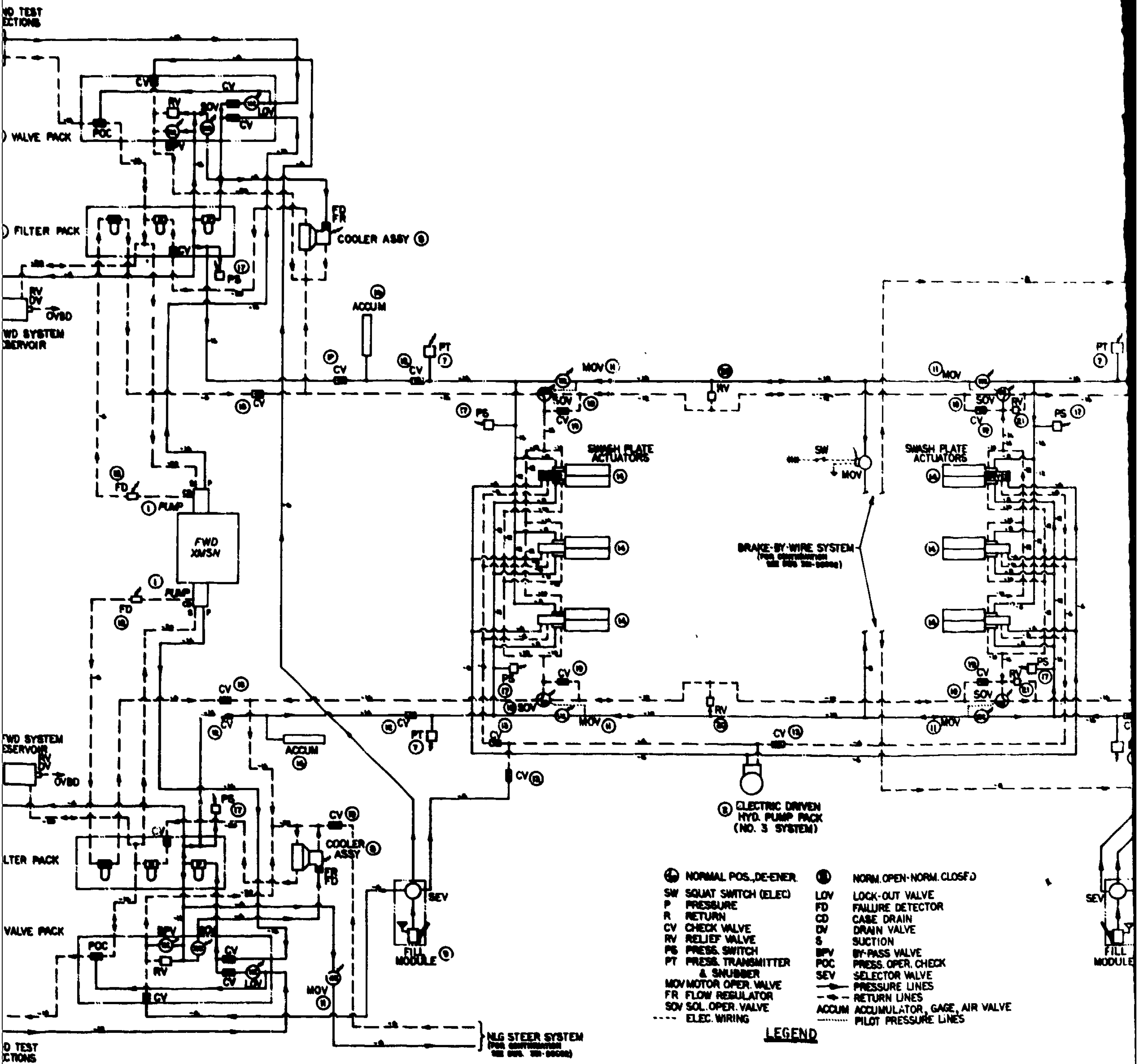

Figure 92. Flight control hydraulic system schematic.

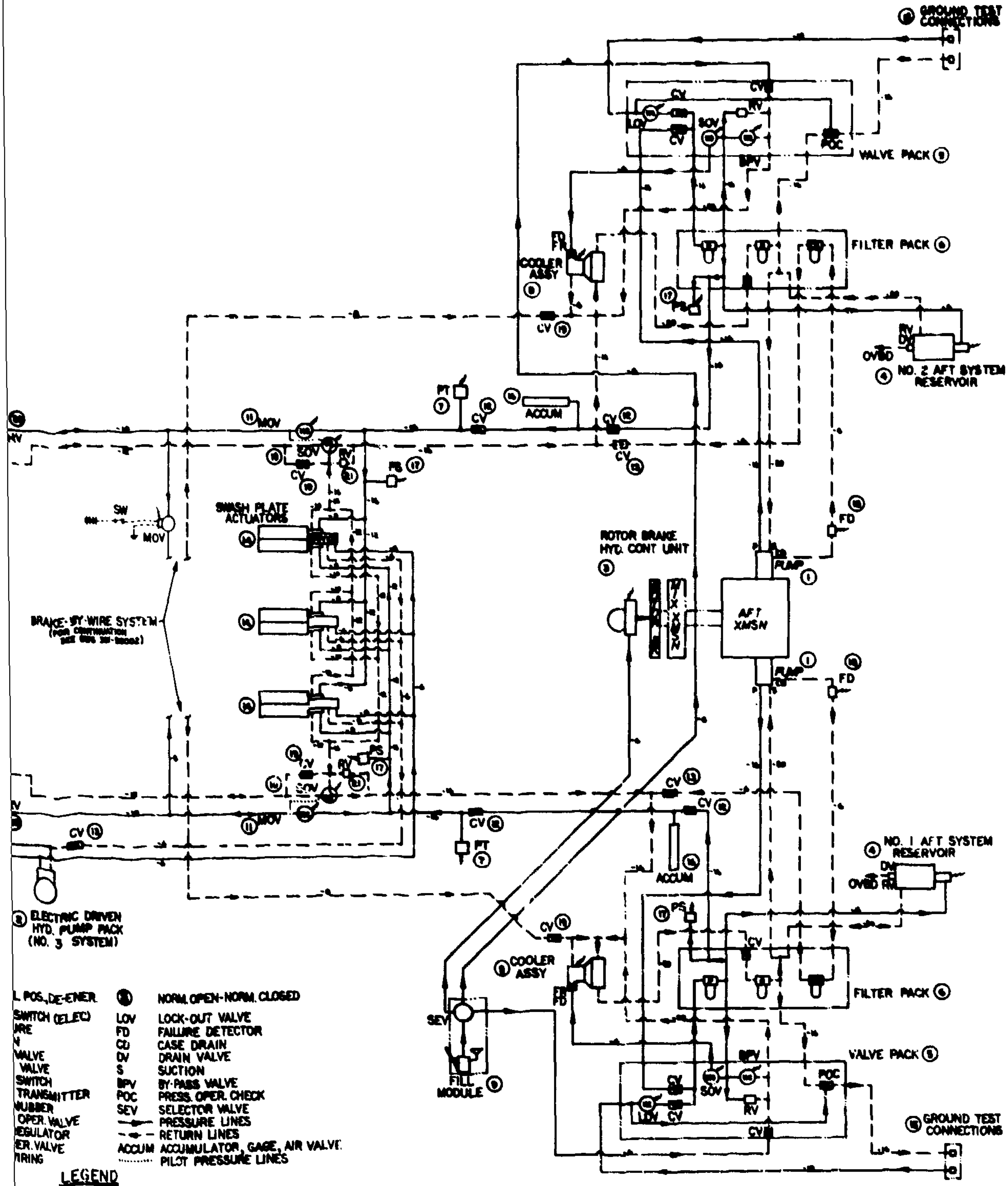
GROUND TEST CONNECTIONS
VALVE PACK
FILTER PACK
COOLER ASSY
NO. 2 AFT SYSTEM RESERVOIR
ACCUM
SWASH PLATE ACTUATORS
ROTOR BRAKE HYD. CONT UNIT
AFT XMSN
PUMP
BRAKE-BY-WIRE SYSTEM
NO. 1 AFT SYSTEM RESERVOIR
ELECTRIC DRIVEN HYD. PUMP PACK (NO. 3 SYSTEM)
FILL MODULE
NORM. OPEN-NORM. CLOSED
LOV LOCK-OUT VALVE
FD FAILURE DETECTOR
CD CASE DRAIN
DV DRAIN VALVE
S SUCTION
BPV BY-PASS VALVE
POC PRESS. OPER. CHECK
SEV SELECTOR VALVE
PRESSURE LINES
RETURN LINES
ACCUM ACCUMULATOR, GAGE, AIR VALVE
PILOT PRESSURE LINES
LEGEND

2

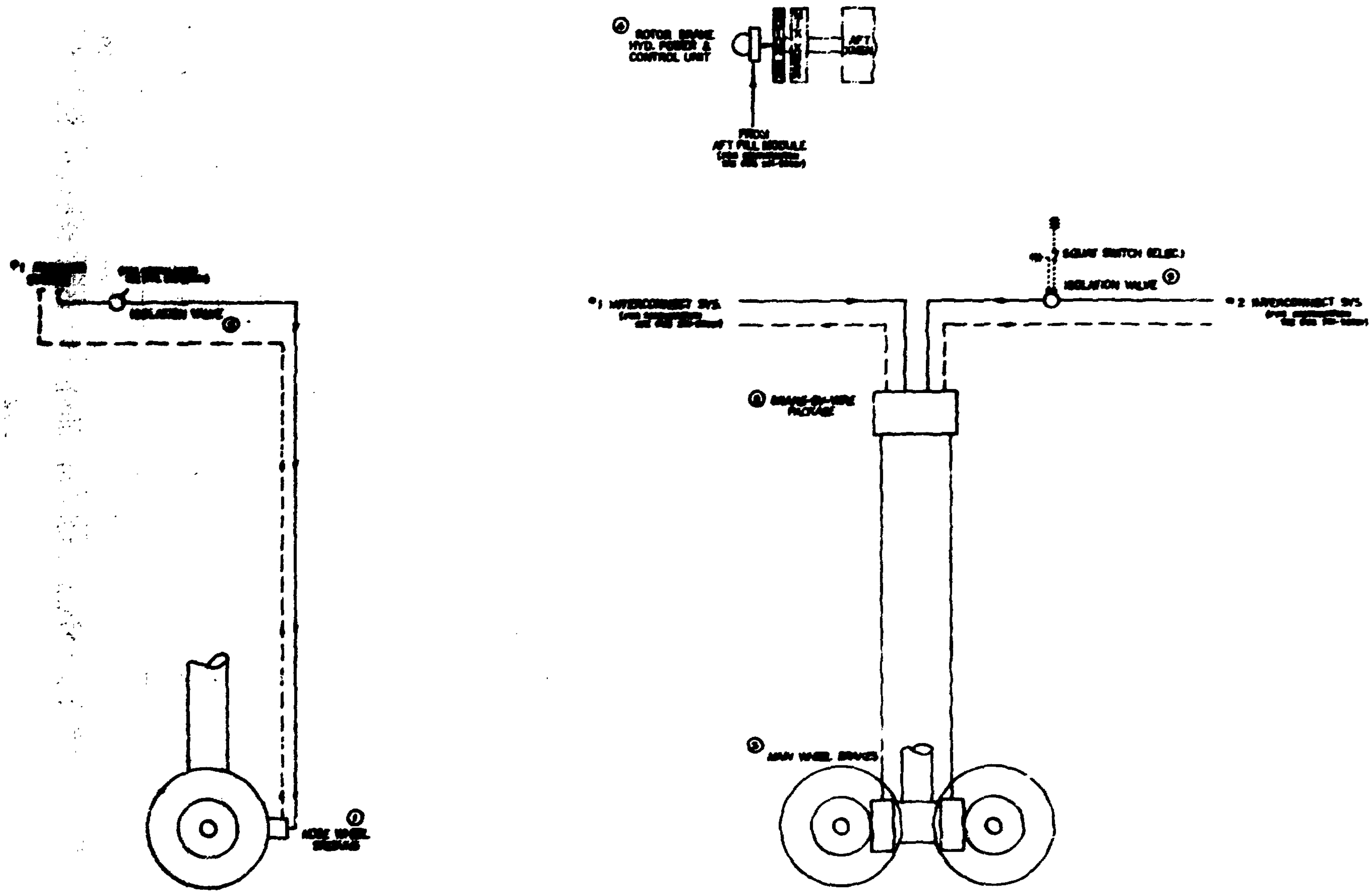

Figure 93. Utility hydraulic system schematic.

Revision A of the "brake-by-wire system" SCD was released. This revision added an alternate hydraulic power system for emergency operation, while eliminating the limited accumulator storage emergency power system. This required associated valve and wiring changes. At the same time, an optional accumulator parking mode was incorporated to allow blocking the return lines, thereby simplifying the system and reducing weight. The original system fed accumulator storage pressure directly into the brake valves.

The brake system changes resulted in a weight saving by reduction in the plumbing and accumulator size while providing unlimited alternate braking capability.

Tube material and sizes, as well as fitting material, was selected as shown in Table 28.

TABLE 28. BRAKE SYSTEM MATERIALS

LINE SIZES (TUBE OD)	FITTINGS		TUBE WALL THICKNESS	
	PRESS.	RET	PRESS. CRES 21-6-9 (BMS 7-185)	RET AL 6061-T6 (MIL-T-7081)
1/4	AL	AL	.020	.035
3/8	AL	AL	.020	.035
1/2	AL (MALE) S (FEMALE)	AL	.026	.035
5/8	S	AL	.033	.035
3/4	S	AL	.039	.035
1	S	AL	.052	.042
1-1/4	S	AL	----	.049

NOTE: ALL HARRISON SLEEVES ARE CRES. DEUTSCH "PERMASWAGE" FITTINGS WILL ALSO BE USED IN SOME LOCATIONS.

Analysis of the No. 3 control channel system (reference Figure 92) shows the need for an oil cooler assembly. This requirement has been transmitted to the supplier who will incorporate the cooler into the package.

Ground test connections will also be added to this system to limit motor/pump operating time during initial system checkout.

Vendor proposals on the rotor brake package and the third channel driver package were received and evaluated. Suppliers have been selected for all major systems and components. They are:

Pumps	- Abex, Oxnard, California
Reservoirs	- Arkwin, Westburg, New York
Flight Control Module	- AiResearch, Torrance, California
3rd Channel Control Actuator Power Supply	- Rexnord, Painesville, Ohio
Rotor Brake Power Supply	- Rexnord, Painesville, Ohio
Brake-By-Wire	- Sundstrand, Rockford, Illinois

The initial operation of the rotor brake pack was witnessed at Rexnord by AVLABS and Boeing Vertol Engineering representatives. Initial tests of the relief valve revealed a chatter condition which was corrected. System temperature during a 10-minute continuous run was satisfactory. No instrumentation was installed at that time, but the technicians present estimated the temperatures to be approximately 160°F.

All planned testing was completed on the rotor brake pack and on the No. 3 system and shipment of these components was made to Boeing Vertol.

2.12.2 Integrated Flight Control Module

At Boeing Vertol request, several suppliers began investigating the possibility of supplying an integrated flight control package consisting of all major components (valves, filters, reservoir, oil cooler) except the pump. By integrating these four major equipments into one unit, it is expected that a more reliable, more compact, and lighter weight installation can be achieved. It appears that the cost of this package is competitive with the multiple component package concept.

A decision was made based on cost, weight, and complexity to proceed with the integrated package concept. This package contains all filters, valves, and the cooler assembly for the main flight control systems. The pump, reservoir, and accumulator are mounted separately. Three vendors sent in proposals: AiResearch, Western Hydraulics, and United Aircraft Products. After evaluation, AiResearch was selected and the design of flight control package is proceeding on schedule. Two PDRs have been held to resolve interface, component, and mounting problems. A new SCD, 301-50150, for the package was prepared.

A re-analysis of the stall flutter damping mode showed a higher heat load into the hydraulic system than had previously been predicted. The increase from 825 to 1125 BTU/min required the cooler fan speed to be increased from 10,000 rpm to 12,000 rpm. This still within the safe operating speed of the fan. The predicted cooler outlet oil temperature increased from 190°F to 225°F during high-speed level flight at high gross weight and a compartment temperature of 135°F. The only hardware change was resizing of the fan flow control valve orifices.

As a result, overtemperature lights were installed in the cockpit and added to the master caution system. These lights were added as development instrumentation in the prototype aircraft.

Development testing of the flight control module in conjunction with the transmission-driven pump and the reservoir was started in September 1974. The purpose of this test was to evaluate the effects of stall flutter damping as well as normal pilot command on the operation of the system, and to evaluate the cooler performance at the higher heat loads.

Initial testing was witnessed by engineering representatives from Eustis Directorate, AVSCOM, and Boeing Vertol during the week of September 9, 1974.

Preliminary temperature data indicated that the cooler was very near the predicted values; that is, at 135°F ambient and 1125 BTU/min, the oil outlet temperature was 222°F. The oil outlet temperature to inlet air temperature ratio is nearly two, so at an ambient of 100°F, we would expect an outlet temperature of approximately 187°F. This is an acceptable condition for the prototype, but a higher capacity cooler would be desirable for production if the predictions prove accurate.

Simulation of the stall flutter mode during initial tests appeared satisfactory.

The flight control module failed in vibration test. The failures were in the mounting feet and their support structure. The configuration of the unit is such that in the fore-and-aft or lateral directions, the mass of the high- and low-pressure manifolds creates a high bending load on the structure.

The original design was a 3-point mounting. After the second failure, a fourth mounting point was added. This configuration failed also. The unit was repaired and another test was conducted utilizing vibration isolators. This was successful; however, the unit failed again when subjected to the required 2g test without isolators.

At a meeting held at Boeing on December 11 and 12, 1974, the decision was made to continue with the isolator testing. A new structure was modified to accept the isolators within the existing envelope.

This modification will reduce the overall height and the resultant bending loads for the non-isolated test. Material thickness was increased in the critical areas to further reduce stress.

This appears to be the most desirable solution for the prototype aircraft; however, repackaging will be considered for follow-on aircraft.

The flight control module successfully passed 10g vibration testing with isolators and the required 2g test without isolators after the modification described above.

The unit was then installed in the endurance test setup for a 100-hour test. The duty cycle was set to include 90 hours of simulated maximum stall flutter damping input. The flow rate was cycled over a delta 12 gpm at a rate of 10.4 Hz.

After 67 hours of testing, a fatique crack appeared in the heat exchanger return end cap weld. The unit was modified to improve the fatique resistance in the weld area. Analysis by AiResearch shows the resulting stress level to be well within the endurance limit.

The test was resumed under the same conditions and at 71.5 hours there was another failure of the heat exchanger. This failure was a separation of the bottom support member of the heat exchanger core. The exact cause of the failure could not be determined without destroying the unit; however, it appeared that the braze in that area was unsatisfactory. The result of this separation was a lack of support of the hydraulic fluid flow tube which expanded and cracked.

In order to confirm the integrity of the basic design of the heat exchanger, the lower 3 flow tubes were sealed and the 100-hour test was completed.

A meeting was held at Boeing Vertol on 9 May 1975 to review the heat exchanger failures and determine a course of action for the prototype aircraft. Representatives from USA Eustis Directorate, AVSCOM, AiResearch, and Boeing Vertol were in attendance.

Stress analysis showed that the heat exchanger had infinite life under the pressure impulses to which it was exposed. The initial damage, therefore, must have occurred during the early vibration testing, before the isolators were installed.

This conclusion was verified by sectioning the unit after completion of the 100-hour test. Fatique damage was evident at the corners where the high vibratory loads would occur. There was no fatique damage in the center portion of the core. Ductile fracture failure occurred in the fins adjacent to the fatigue-damaged pins.

The sequence of failure was: (1) some supporting pins failed during vibration testing, (2) the pressure impulses then completed the fracture of partially damaged fins until, (3) a sufficient number were broken to increase the stress to the tensile failure point.

The conclusion was reached that the unit is acceptable for the prototype aircraft with the isolator mounts. Vibration level will be monitored by roving accelerometers.

As an added precaution, the outer oil flow tube on the top and bottom of the unit will be welded close to give additional strength to the unit. This will have no appreciable effect on oil temperature.

2.13.3 Brake-By-Wire System

Sundstrand experienced a vibration failure of the brake pedal transducer and the accumulator pressure gage and fitting on the hydraulic package. The transducer failure was in a threaded aluminum rod that attaches the sliding core to the external sliding core case member. The rod material was changed to steel.

The failure of the accumulator gauge and fitting appeared to be the result of a defective clamp that attaches the accumulator to the manifold. This allowed high accelerations at the fitting and gage.

The fitting material will be changed from aluminum to steel and redesigned to give greater support to the gage.

If the problem recurs on the aircraft, the accumulator will be removed from the package and will be mounted separately. The failure would not affect braking capability; only the parking brake would be lost.

Performance testing of the brake system was conducted with satisfactory results.

The hydraulic controller was subjected to a vibration re-scan with higher torque on the accumulator clamps and the new air side fitting. There were no significant changes in the resonant frequencies, however, the amplitudes were reduced nearly one-half. No further testing was performed.

One of four transducers failed electrically after 8 hours and 10 minutes of a 9-hour vibration test. The failure was considered an isolated failure and was accepted because three units passed the full vibration test.

This failure was an "open" coil failure which would result in a zero voltage input to the servo valve. Should this failure occur on the aircraft, the result would be a 50% brake pressure application on one wheel at touchdown and closure of the ground contact switch.

This failure mode was introduced because of the unavailability of a small quantity of the proper pedal transducer, and would be eliminated on a production version of the system.

Although this failure mode is considered remote, Boeing Vertol and Sundstrand Engineering have arrived at a tentative means of including this failure mode in the existing brake fault indicating system. Pilot action would be to pull the circuit breaker and land with no brakes.

2.13 PNEUMATIC SYSTEM

The initial pneumatic system consisted of the engine starting system and power to the cargo handling system signal conductor reel. In order to minimize costs of the prototype program, the APU was omitted, the cargo hoists were not powered, and the environmental control system was replaced with a combustion-type cabin heater. During the program, it was decided to make the hoists operable by adding the cargo hoist pneumatic ducting, and to install an environmental control system.

2.13.1 Main Engine Starting

The main engine starting system for the HLH consists of an air turbine starter on each engine and associated ducting and valves. The pneumatic supply is drawn from one of three sources: (1) onboard auxiliary power unit (when installed); (2) pneumatic ground cart; and (3) cross bleed from main engines.

Past efforts directed toward sizing of the main engine starters were based upon the 501-M62 Model Specification (No. 830) and later the XT701-AD-700 Prime Item Development Specification (No. 844). These specifications required a minimum starter power of approximately 33 horsepower. Testing of the 501-M62B DSTR XT engines indicated that higher starter power was required due to the stall margin in the start region being less than predicted. The solution for the DSTR was to substitute a high-pressure nitrogen cart for the gas turbine cart previously identified. It was expected that the compressor rig testing scheduled as part of the XT701 flight engine development program would permit complete solution of the starting problem by means of compressor varible vane schedule changes and other modifications.

Interim testing of a 501-M62B engine modified to include features of the XT701 engine, and incorporating revised compressor vane schedules derived on the compressor rig, showed that despite a significant improvement in compressor characteristics, start power requirements remained high, especially when consideration was given to fuel schedule

tolerances and extreme climatic considerations. This has been partially attributed to the locking of the power turbine during the start, which would be typical of HLH operations.

Boeing requested that DDA provide their best estimate of starter torque requirements. These were needed to facilitate selection of suitable starters and hence sizing of an HLH secondary power system and auxiliary power unit. The DDA estimate was provided by interface memorandum (DDA-053, dated 14 February) and required a starter power of approximately 100 horsepower at cut-out speed. Examination of available test data led Boeing to conclude that the curve provided could be overly conservative and hence it should not be allowed to drive secondary power system weight and cost without further discussion. Subsequent discussion led toward a compromise/risk curve that appeared to be compatible with the available starting data, and in Boeing's opinion, represented minimal risk. The compromise curve approximates a 70-horsepower starter with peak power at starter cut-out speed.

Subsequently, Boeing issued a RFP for an environmental control unit together with the overall secondary power system and APU. This RFP included the Boeing compromise starting torque requirement and also defined a deteriorated A/M32A-60A ground cart. The responses to this RFP included a number of starters sized to meet the HLH requirement, assuming various levels of pneumatic source capability. Figure 94 illustrates starter capability when coupled with the ground cart, which may be considered as the lowest quality pneumatic source. The lower curves show starter flow as a function of inlet pressure as defined by the starter turbine nozzle. The upper curves show the corresponding output torque capability of the starter at 4000 rpm starter speed (approximates cut-out speed).

Also shown are the pressure flow characteristics of a Specification /M32A-60A ground cart and a deteriorated cart with corrections for flexible hose and HLH duct losses included. The specification cart is based upon the requirements imposed on the current cart manufacturer (Hol-Gar Manufacturing Corporation) while the deteriorated cart was biased towards the current USAF T.O. (35C-3-372-13) for this cart. The latter would appear to be unrealistic, based upon more favorable degradation experience with the GTCP85-180 APU installed in the cart and other installations.

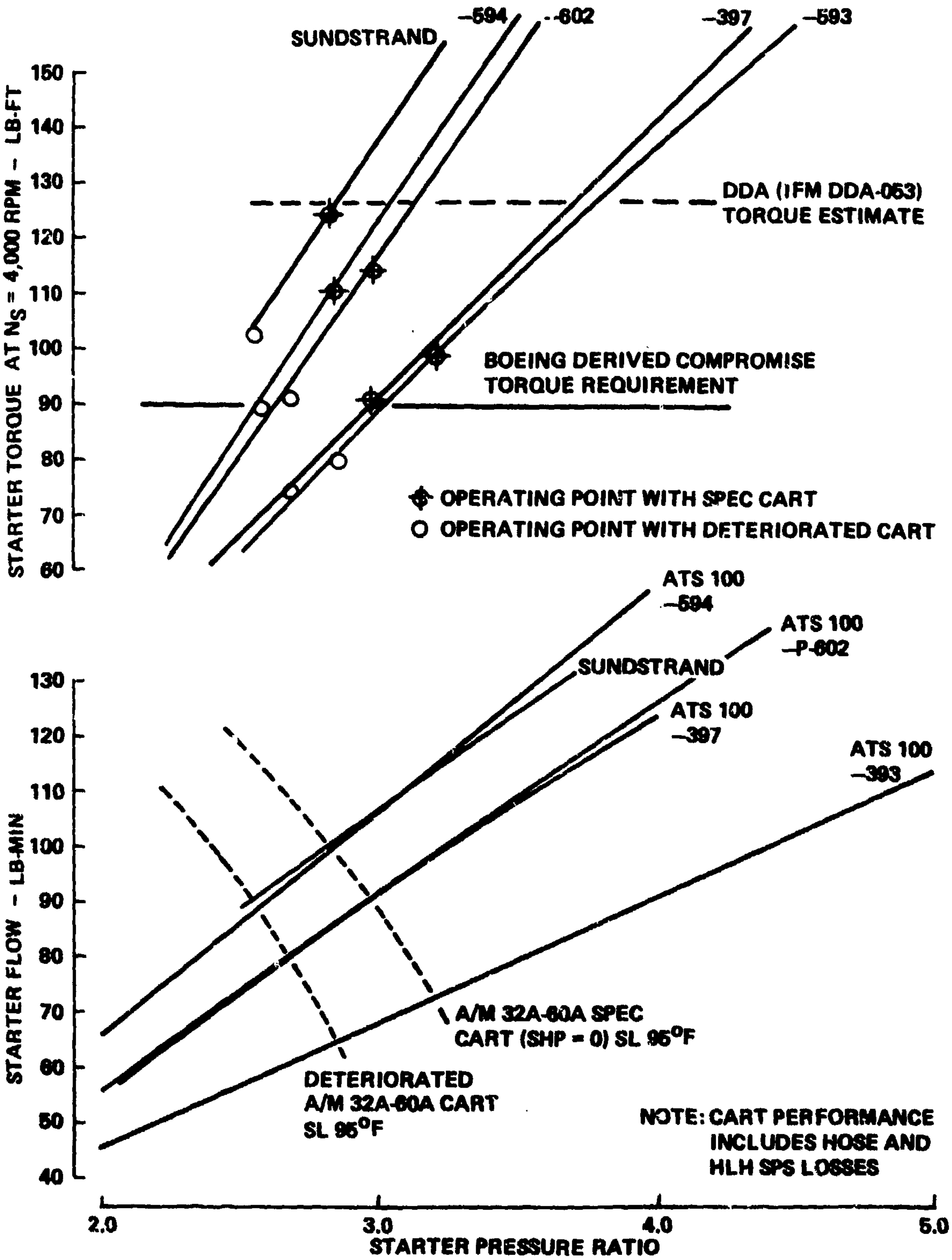

Figure 94. Candidate starters.

Figure 94 shows three starters that meet the 90-pound-feet requirement defined in the Boeing RFP when coupled with the deteriorated cart (Note: the points are shown just below the corresponding line due to a slight deficiency in starter air inlet temperature). Of these, the ATS100-594 is an inefficient unit with excessive flow requirements relative to consideration of an onboard APU. The ATS-100-P-602 is derived from the existing ATS100-294 starter (used on P3B's T56 engines) by introducing the turbine wheel from a commercial JT8-D starter and minor modifications to the output drive. The Sundstrand unit is a modification of a cartridge/pneumatic starter utilizing a turbine wheel derived from the HLH hoist system. The ATS100-397 starter (a further ATS100-294 derivative) as previously designated for the HLH is shown for reference. It is shown to be,at best, marginal.

It may be seen that significant margin is available with the Sundstrand and ATS100-P-602 units when consideration is given to a specification cart, especially when allowance is given to typical new cart characteristics where perhaps two points of additional pressure ratio are available, equivalent to approximately 15 pound -feet of torque.

Based upon these starter characteristics and previous discussions, Boeing prepared an interface memorandum requesting DDA concurrence with the Boeing proposed curve. This is currently under consideration by DDA subject to results of current engine starting tests. In order to facilitate a quantitative evaluation of these recent tests, the starter used will be calibrated by AiResearch to allow determination of actual torque used. It is concluded that the compromise curve is viable for HLH prototype operations, and that starters matched to available ground carts and/or an onboard APU can be identified.

The ATS100-P-602 AiResearch starter and the AiResearch starter regulator valve 392200 were determined to be satisfactory for starting the XT701-AD-700 engine and were procured by AVSCOM.

An engine start test with the starter, start valve, bleed valves, engine-mounted bleed start ducting,and the start cart was conducted. Figure 95 shows the test setup that was utilized to conduct these tests. The pneumatic test equipment was assembled by Boeing Vertol. Its purpose is to provide a connection for the ground cart, provide a valve for start or bleed operation, and provide an orifice to simulate the pneumatic system flow. In operation with the test equipment valve "closed" and the engine bleed valve "closed", the engine would be started utilizing the ground

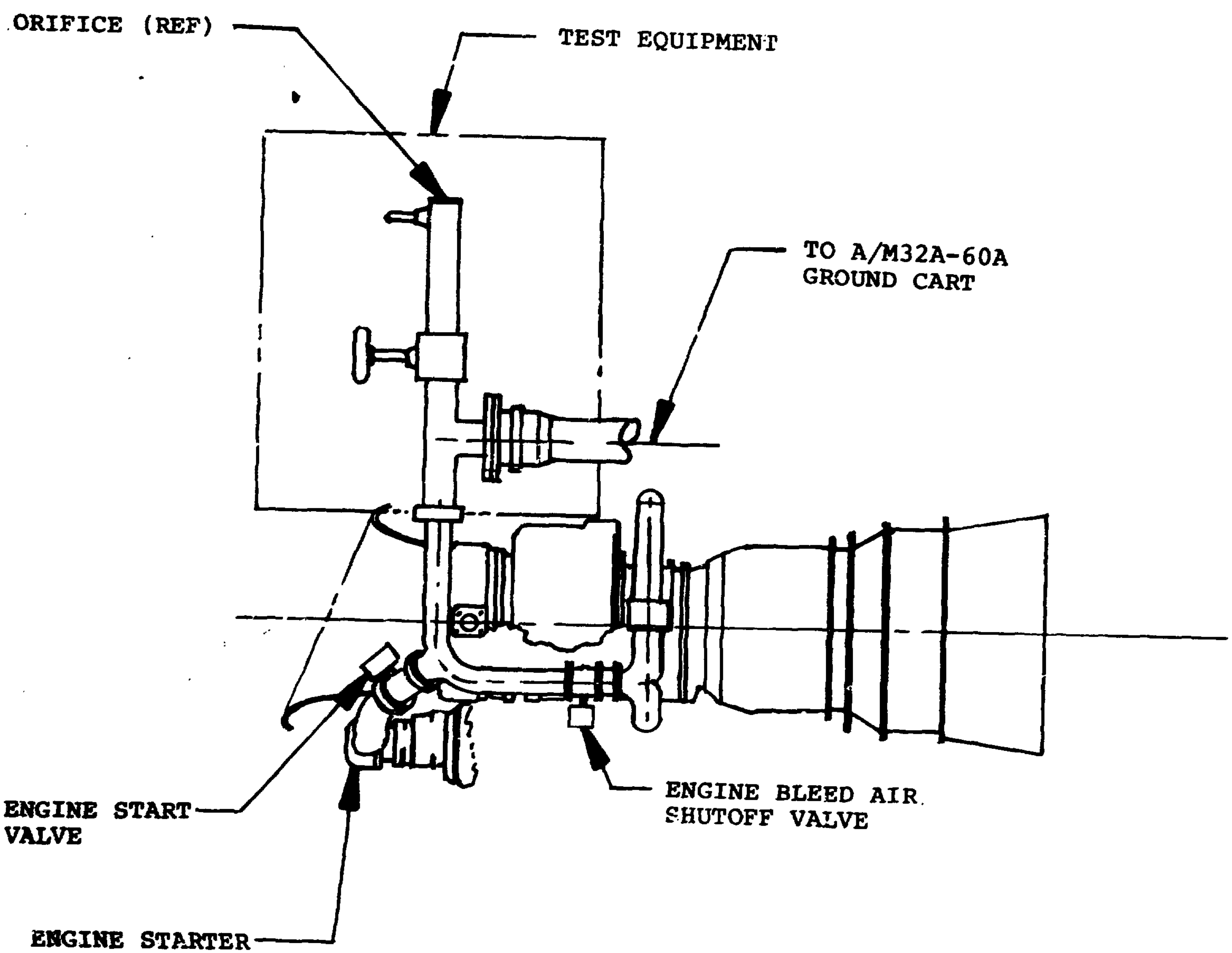

Figure 95. Engine bleed - start test setup.

cart, the start valve, and the starter. As soon as the engine is started, the start cart is turned "off" (a check valve in the nipple will prevent backflow). The test equipment valve is then opened and air flows out through the orifice. Pressure and temperature taps provided data for flow measurement and pressure loss of the engine-mounted ducting. In addition to start and bleed data, information was obtained on the expansion of the bleed/start ducting during engine operation and on vibration of the ducting.

The engine-mounted aircraft pneumatic system, which includes the bleed manifold starting air ducting, starter, and associated valving, was installed on Engine S/N 8 at DDA. Figures 96 and 97 show this installation. The Boeing Vertol design ducting installation was completely compatible with the ending interface. This system was then subjected to a static shaker vibration test to determine its response to low-frequency range excitation. Approximately 50 points (some are indicated by the number on Figures 96 and 97) were probed.

The vibration test data on the Boeing Vertol bleed start manifold mounted on S/N 8 at DDA was delivered and reviewed. The first flight bleed start manifold delivered to Boeing Vertol was checked on the first YT701-AD-700 flight engine. Installation was made easily and fit was excellent.

2.13.2 Engine Mounted Ducting System

The XT701-AD-700 PPFRT engine is designed to provide "customer bleed" simultaneously from two diametrically opposite ports at the tenth stage of the engine compressor. A schematic and assembly design (Figure 98) shows the manifold and components as an integral part of the YT701-AD-700 engine. During conversations with AVSCOM, AMCPM-HLH-T, and AMRDL, it was proposed that the design and installation of the bleed/start engine-mounted manifold system be accomplished by Detroit Diesel Allison. Therefore, Boeing Vertol submitted a proposal for the deletion from the HLH Contract of the requirements to design, fabricate, and install the bleed and start manifold and associated valves. At the Preliminary Mockup Review of the XT701-AD-700 engine on 18 May 1973 at DDA, DDA agreed to submit a similar proposal to add the noted bleed/start manifolds and associated components to the engine.

The design and installation responsibility for the engine-mounted bleed/start system was given to Boeing Vertol. A bleed/start system design for the prototype engine was drawn up and a cardboard mockup was made. The mockup was taken to Allison for fit try. A few minor changes were required, and upon completing the revised design a hard mockup (SK-301-52655) using valve components, bellows, etc. was fabricated for

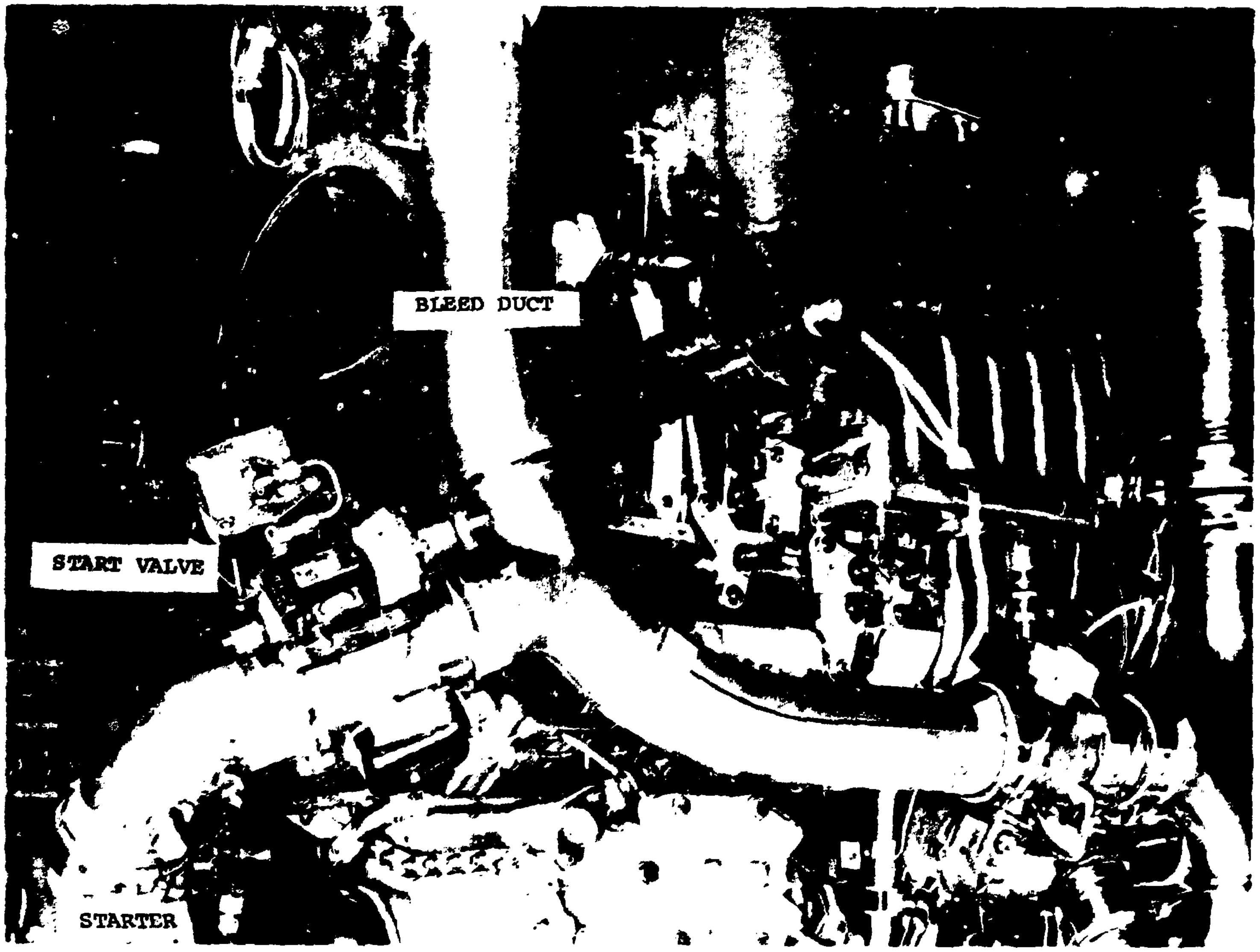

Figure 96. Bleed air manifold.

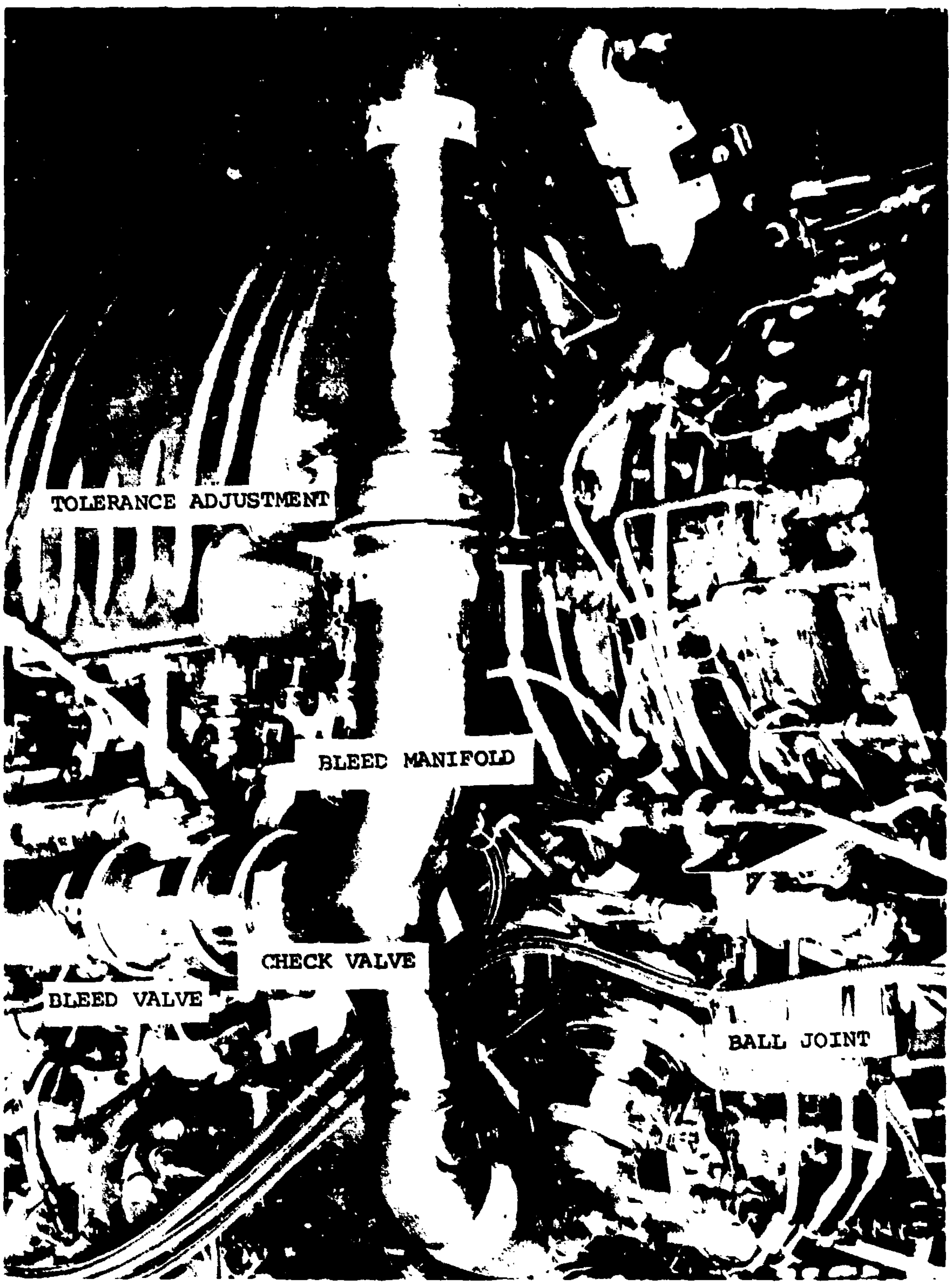

Figure 97. Bleed air manifold.

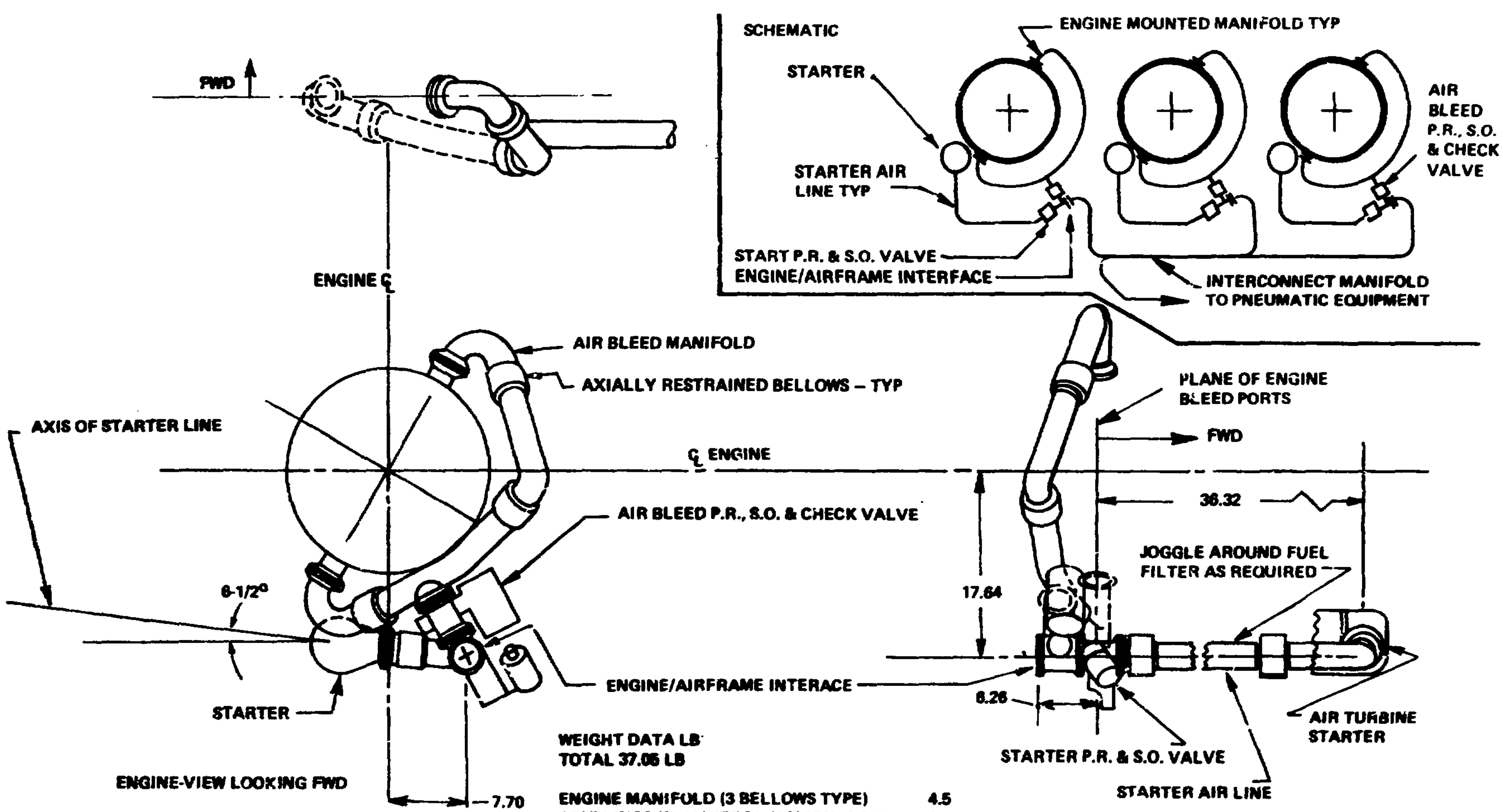

WEIGHT DATA LB
TOTAL 37.05 LB

ENGINE MANIFOLD (3 BELLOWS TYPE)	4.5
COUPLINGS (2) JANITROL (840C58) .3 EACH	0.6
STARTER AR ATS50-H2 WET	15.0
STARTER AIR LINE 301-52652	3.6
TEE 301-52653	0.5
STARTER VALVE AR 392122	5.7
AIR BLEED VALVE AR 398614	5.35
CHECK VALVE SIMILAR TO APCO 325100	0.6
COUPLINGS (4) JANITROL (BNOC53) .3 EACH	1.2
TOTAL	37.05

Figure 98. Sample engine-mounted ducting for bleed air extraction and starter air supply.

installation on the XT701 mockup engine. (See Figure 99). Installation was accomplished on 28 September 1973 at the Allison facility in Indianapolis.

The manifold mockup fitted without any major physical problems. However, the two bleed ports on the engine were sized for 2.50" I.D. which caused Allison to go to a standard flange sized for a 2.75" O.D. tube. Boeing Vertol's ducting is 2.50" O.D. This requires a special flange and elbow, to be designed and manufactured by Boeing Vertol, to accept the transition from 2.50" O.D. tube flange to a 2.75" O.D. tube flange. Since the machining of the engine flanges are underway, it has been agreed (Boeing Vertol IFM 037) that no changes would be made on the prototype engines and that the bleed flange interface for any production engine would be reviewed prior to release. A dynamic analysis of the assembly has been initiated to determine the amount and location of duct support required.

In order to confirm that the engine-mounted bleed/start duct system was satisfactory, the hard mockup of the system was installed on the XT701-AD-700 mockup engine at the formal mockup review (at DDA) on 27 and 28 November 1973. Clearances and fit were reviewed and it was agreed that the installation was satisfactory.

A second review of this installation was held at DDA on 13 December 1973 to determine fit and interface. During this review, in addition to DDA and Boeing Vertol personnel, a representative of Arrowhead Metal Products (the duct manufacturer) was present. In order to obtain more clearance between the bleed start manifold and two oil lines and an electrical fitting in the bottom of the engine oil tank, a slight bend was removed from the portion of the ducting leading forward to the starter. Figure 100 shows a comparison between the original assembly and the modifications being investigated. It should be noted that the three axially restrained bellows have been removed from the bleed manifold connecting the two bleed ports and replaced with two braid-covered bellows. Concern was expressed by the duct manufacturer regarding the bleed and check valve being located unsupported between three axially restrained bellows. It was impractical to support the valve to the engine and the braid-covered bellows will stiffen this assembly and support the valve. It had previously been determined that lateral support of the assembly was required. This is provided (see Figure 100) by a connection from a brace on the tee to the bracket on the engine that supports the engine variable geometry operating cylinder.

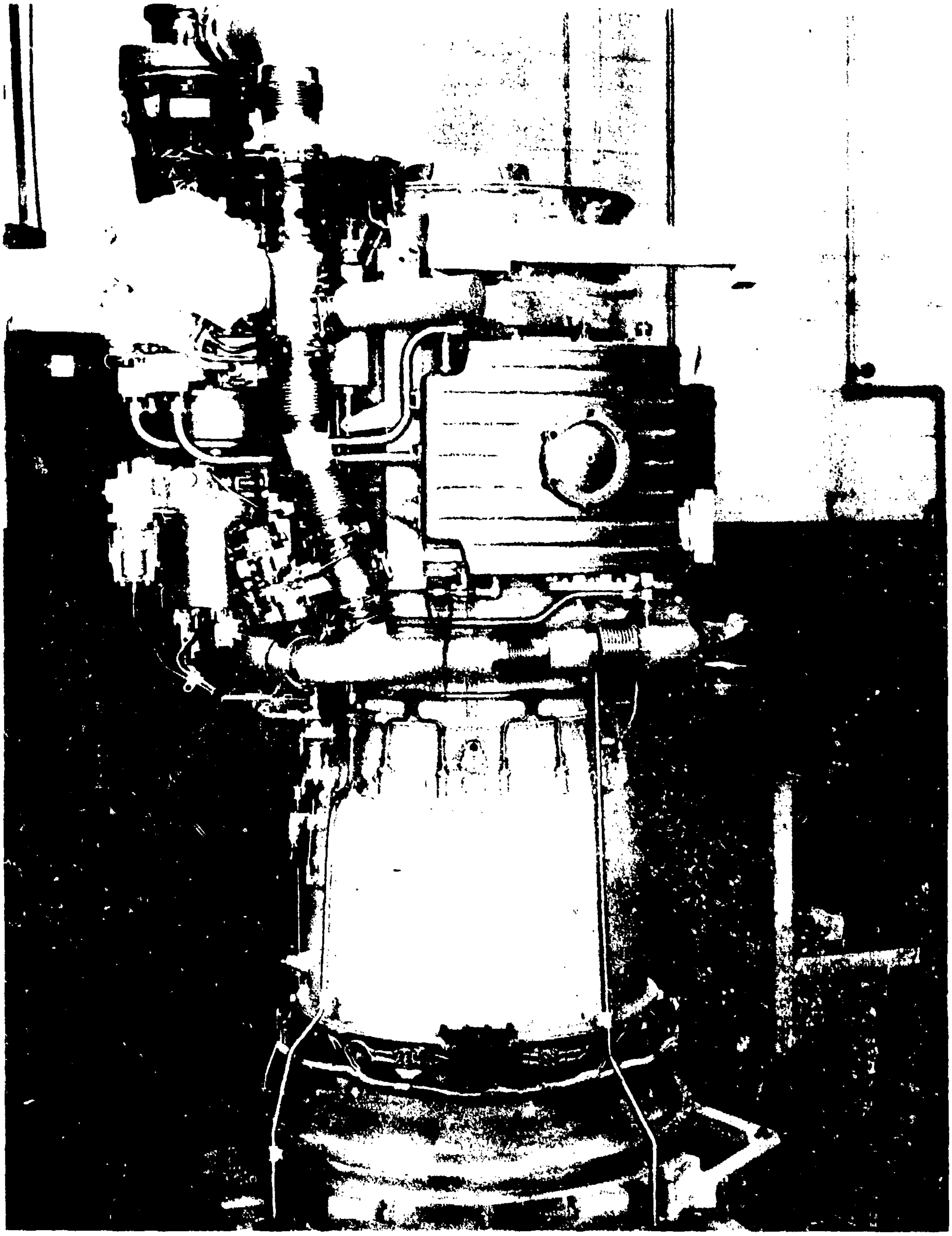

Figure 99. Bleed/start system mockup mounted on engine.

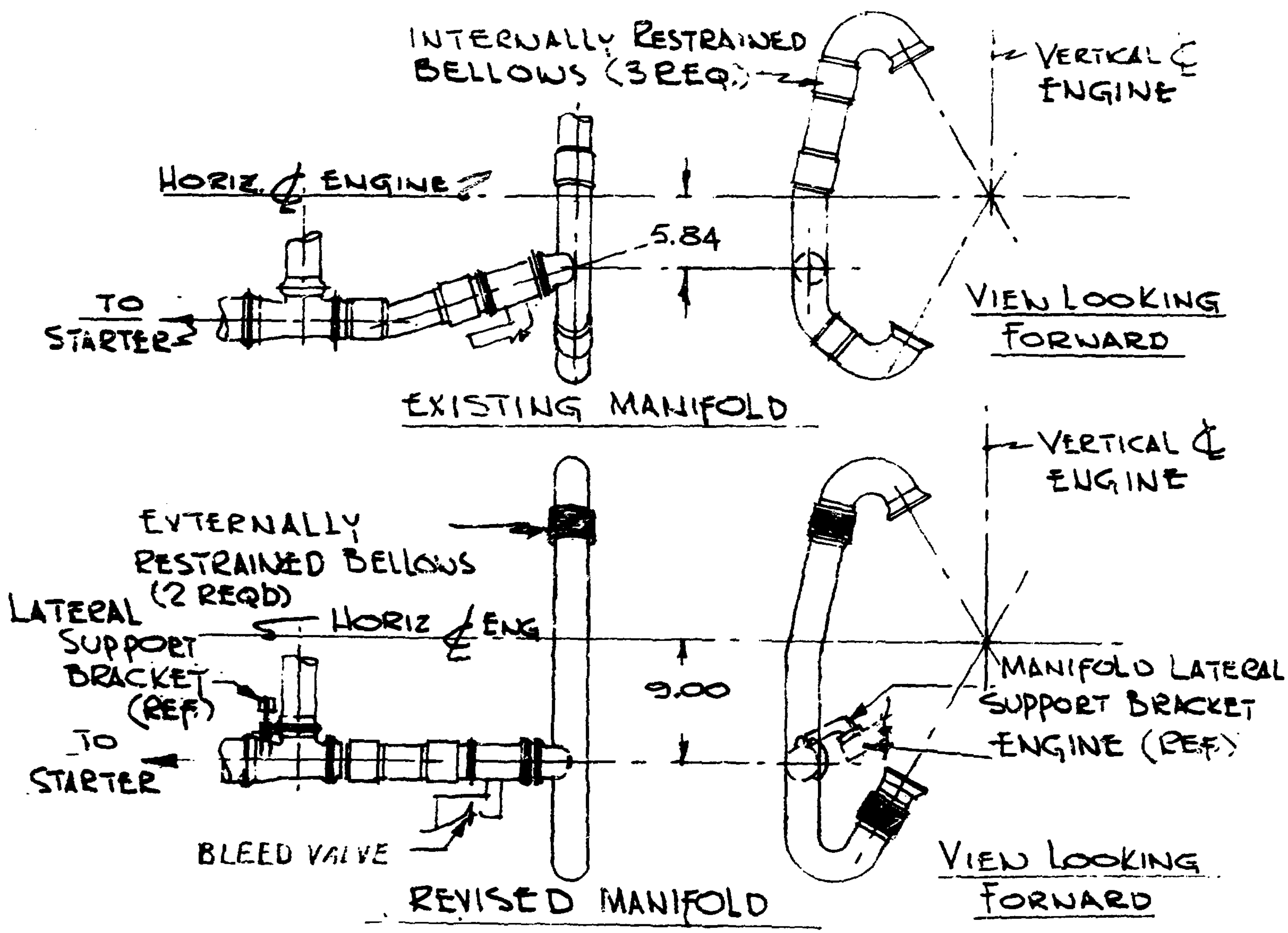

Figure 100. Manifold revision diagram.

It was considered desirable to design without the use of flexible joints (See Figure 101) which are heavy (joint weight, steel ducting), costly, sources of pressure loss, and may require additional support brackets.

In the area of the engine bleed pickup, the load limitations at the connecting flange are:

1000 in.-lb moment
800 lbs shear
800 lbs axial

This limitation is a result of the use of commercially pure titanium in the engine bleed port and scroll (see detail of part on Figure 102). This assembly is welded to the 6AL-4V titanium case.

DDA indicates that commercially pure titanium (lower stress allowables) was used in the scroll detail due to the deep draw operation required for manufacture and for cost.

Two design alternatives were considered:

a. Increase the load capability at the interface flange by redesign of the scroll-flange intersection or by adding strengthening gussets (DDA action).

b. Install flexible joints (U-pin internal tie rod bellows or a bellows sealed ball joint) near the interface flange to minimize bending loads at the joint. Two or three flex joints may be necessary (See Figure 102).

The first alternative would result in a small increase in engine weight, but would allow for a design without flex joints.

The second alternative would require at least two flex joints and the use of steel ducting instead of titanium, since the flexible joint would have to be stainless steel (titanium flexible joints are not recommended due to life limitations, and titanium cannot be welded to steel successfully).

If three flex joints are necessary, additional support brackets would be required (probably to the engine).

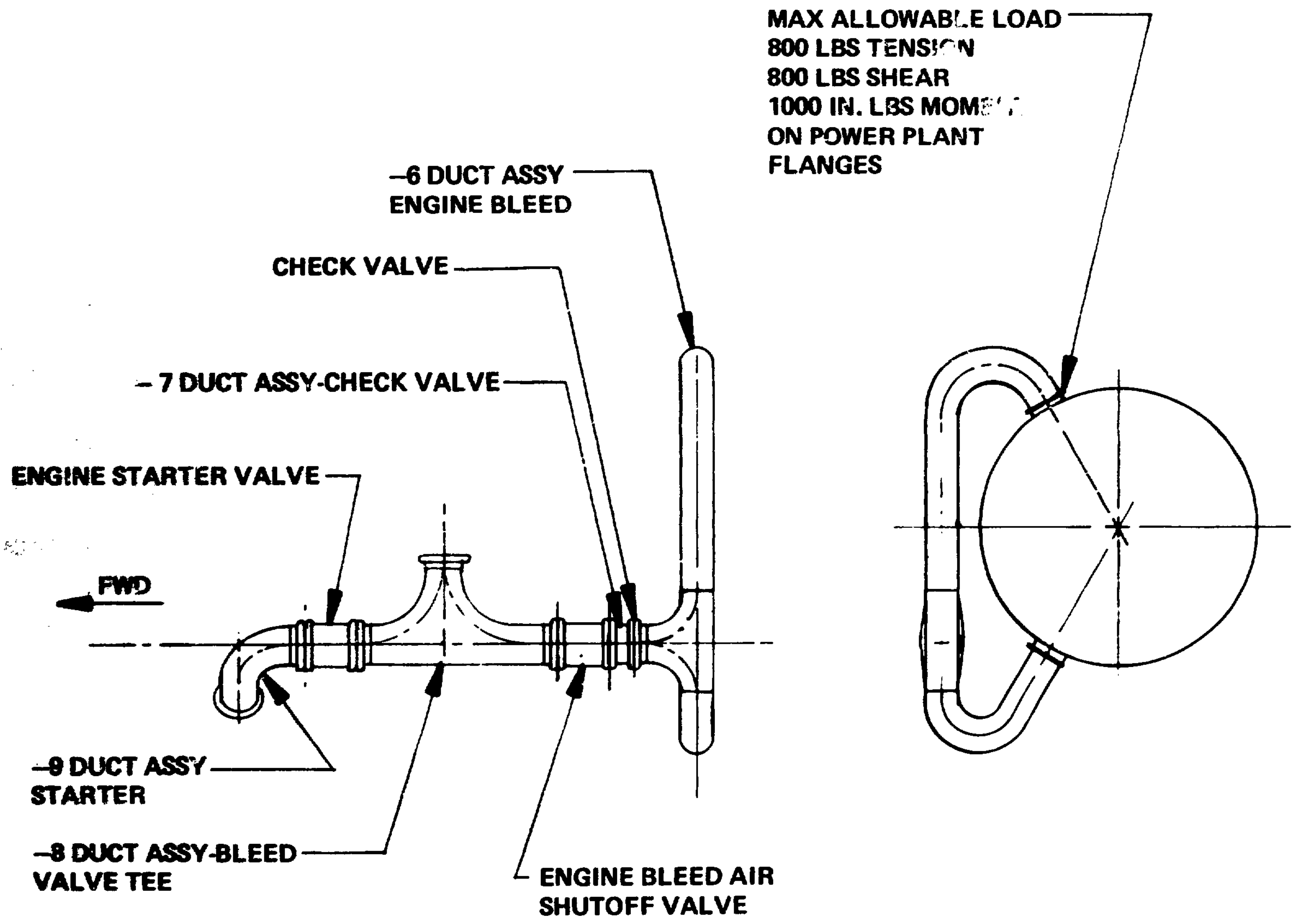

Figure 101. Engine bleed/start manifold.

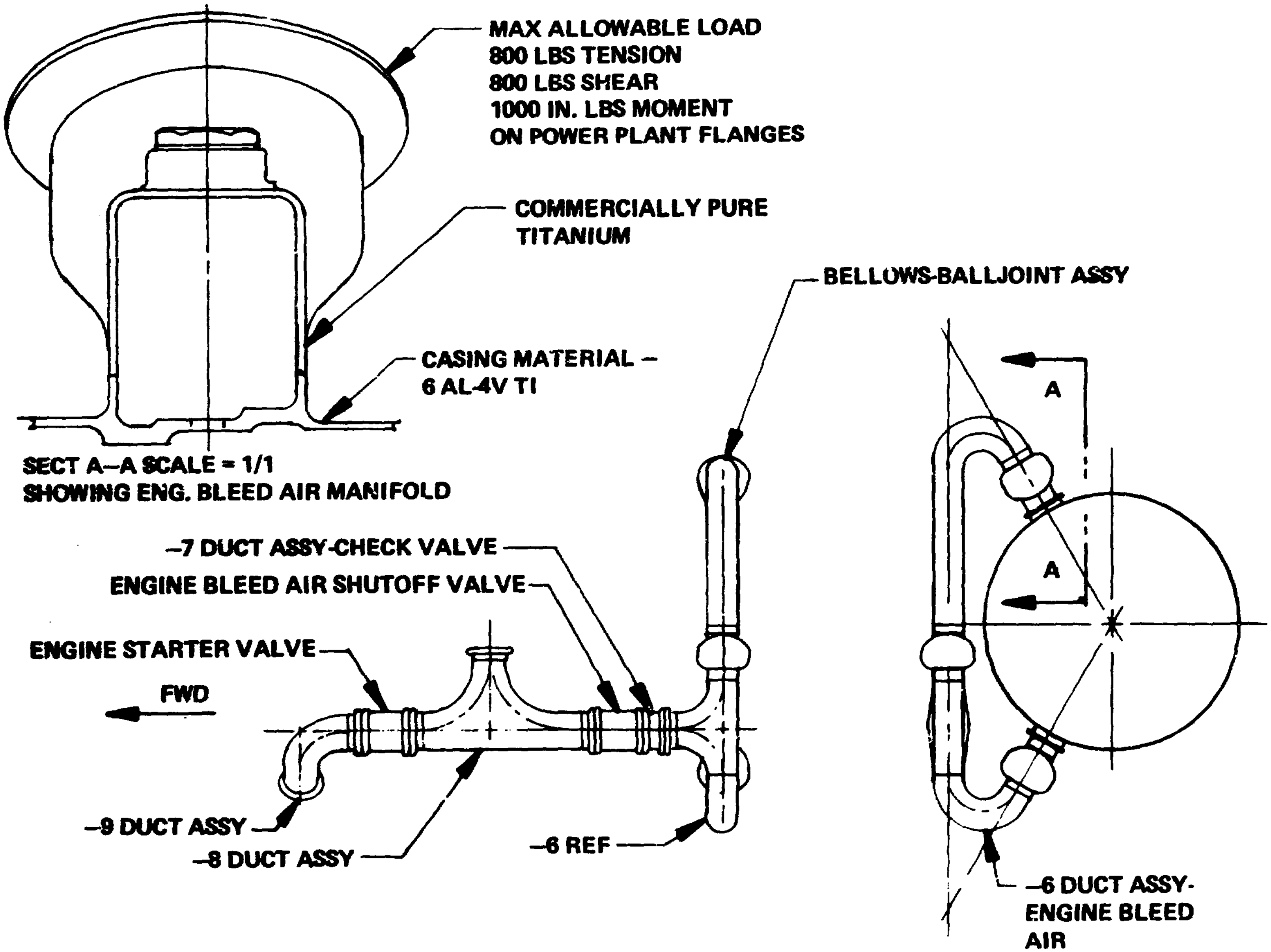

Figure 102. Engine bleed/start manifold with bellows-balljoint assembly.

Design of the engine-mounted ducting system was completed and released for procurement. An additional set was procured for engine testing. Criteria of not imposing more than 1000 in.-lb moment on the engine ports and maintaining pressure drop variations between the two ports to within $\pm10\%$ were imposed.

A photograph (Figure 103) of the bleed start manifold mounted on the XT701-AD-700 engine mockup shows the installation. No supports are required from the bleed/start manifold to the engine other than the normal connections. The final design was accomplished with the use of a tolerance take-up bellows and an externally restrained bellows (not depicted in the photo).

A dynamic analysis was performed using NASTRAN on the final configuration of the pneumatic ducting for the left engine. The model assumed the ducting to be cantilevered at the starter, at the two engine bleed ports, and at the airframe bracket on the transverse manifold assembly. The material modulus at operating temperatures (650°F) was used (80% x 16.2×10^6 PSI).

Table 29 shows the frequencies of the 10 lowest modes. One mode shape is presented in Figure 104. The lowest mode is far above rotor order excitation frequencies (4/rev = 10.4 Hz) and therefore will not be excited. Mode 7 is near the engine operating speed (190 Hz) and may prove troublesome in operation. Its mode shape is shown on Figure 105. This mode can be effectively damped by a duct support at locations A or B in the figure, which are from the duct to the airframe - not to the engine.

TABLE 29. FREQUENCIES OF TEN LOWEST OPERATING MODES

Mode	Frequency (Hz)
1	77.2
2	97.7
3	102.5
4	114.6
5	127.2
6	156.6
7	186.6
8	293.8
9	296.2
10	303.6

A loads analysis was performed on the engine bleed manifold duct for conditions involving thermal expansion, installation

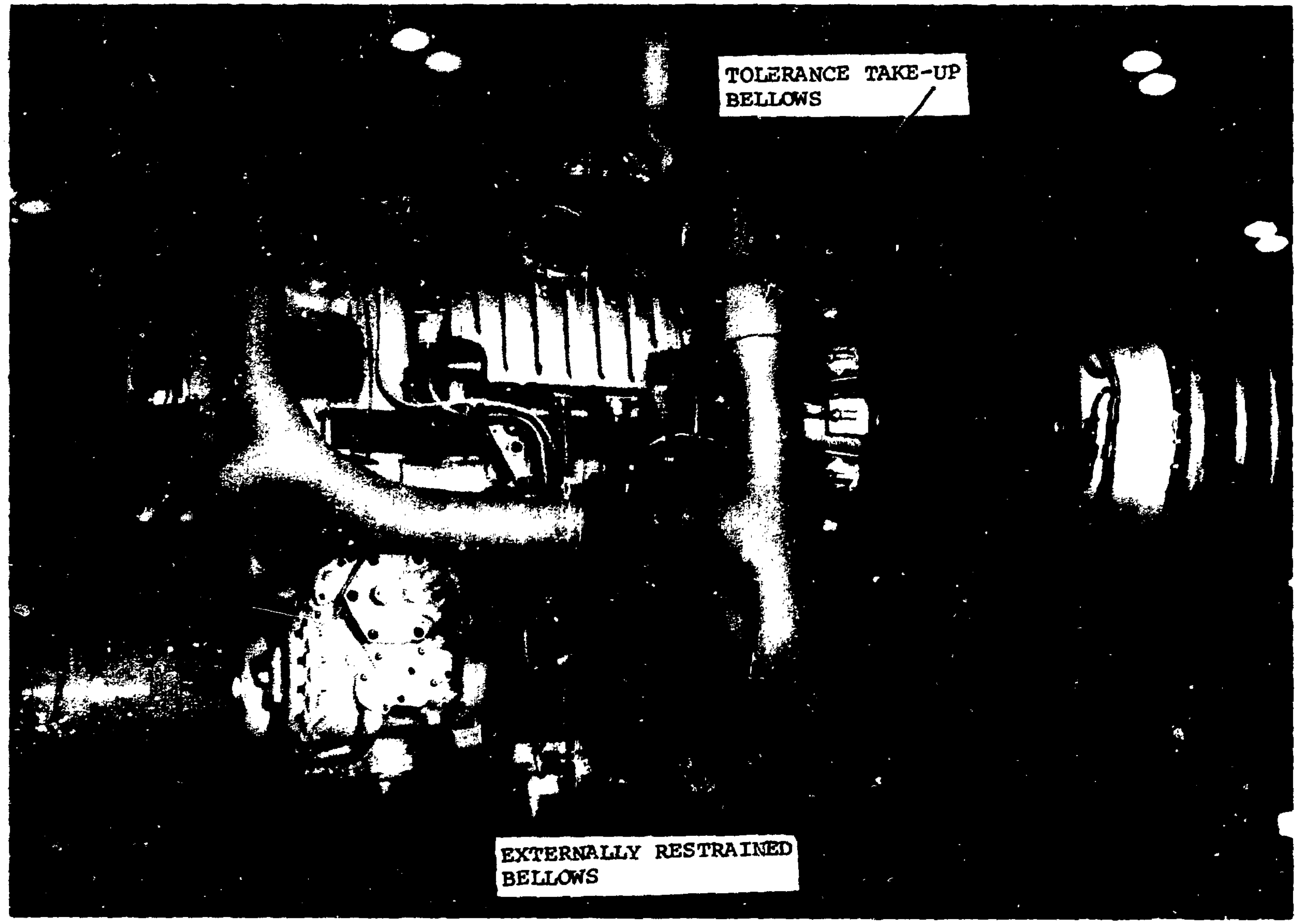

Figure 103. Bleed start manifold mounted on engine mockup.

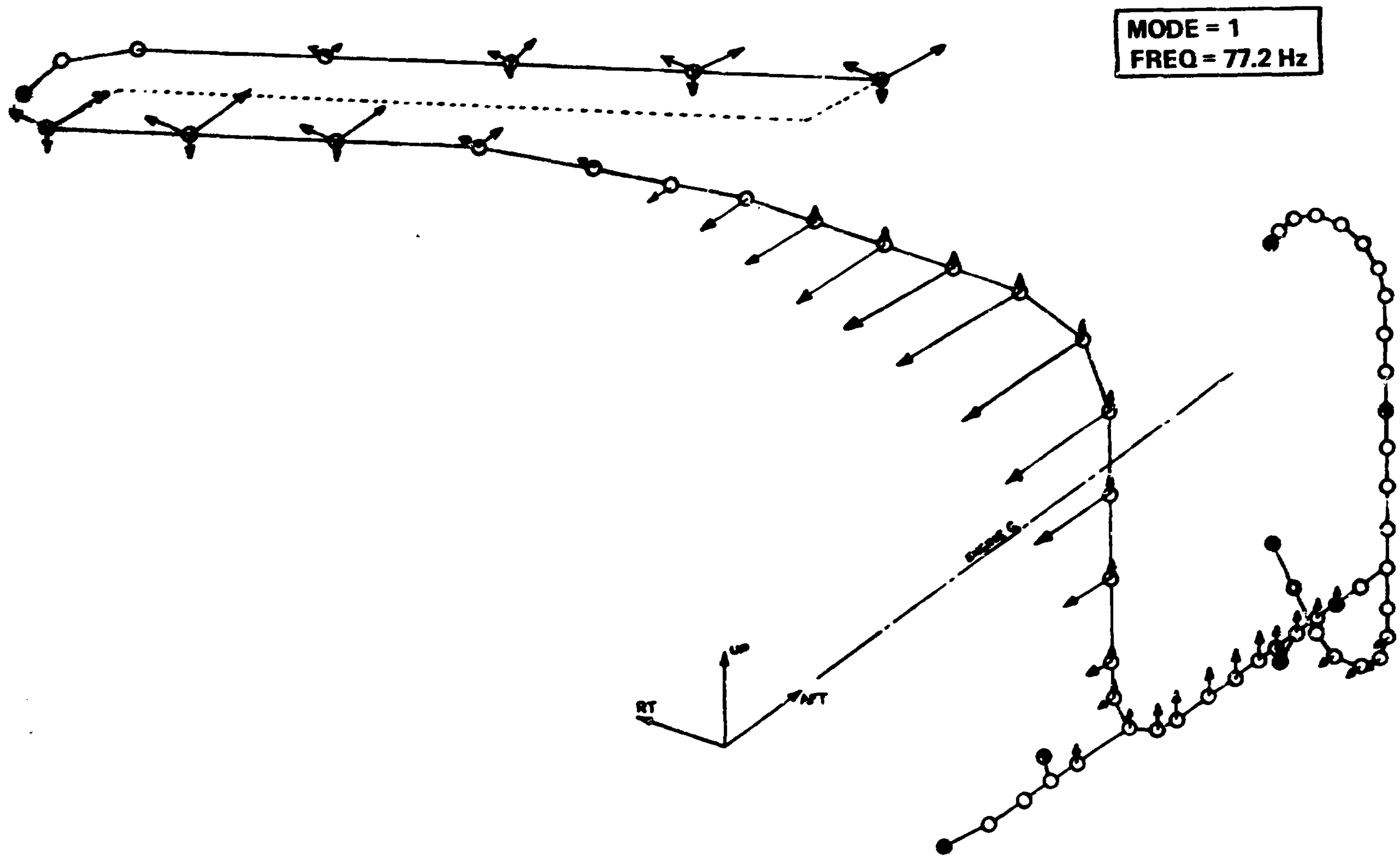

Figure 104. Pneumatic ducting – left engine (mode 1).

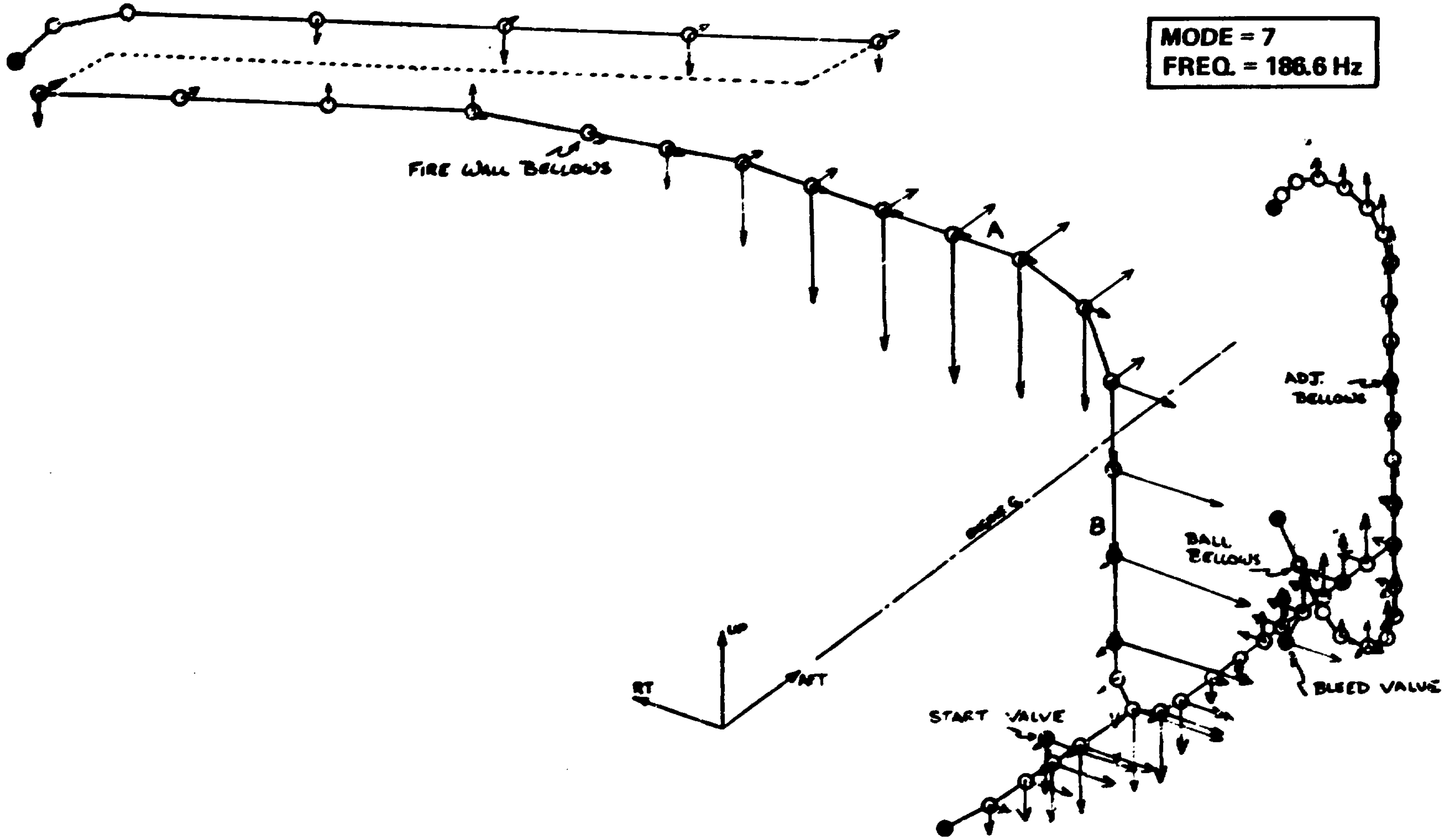

Figure 105. Pneumatic ducting – left engine (mode 7).

tolerances, internal pressure, ground handling, and combinations thereof. The loads on the engine interface flange are summarized in Figure 106. The adjustment device and ball joint have been found to provide the means to keep the interface loads within the limits established on the XT701-AD-700 engine. The loads in the table are defined as ultimate, and for all cases except internal burst, the safety factor used is 1.5.

A pressure drop analysis was conducted on the bleed/start manifold assembly. The study shows that pressure drop variations from .0 to .45 psi can be expected through the duct section for flow ranges between 12 and 76 PPM of bleed through the assembly. The design will permit estimated bleed flow variations of $\pm$5.4% from each of the two 10th stage ports on the engine. This flow split is within the $\pm$ 10% permitted in the Allison Specification 844A, paragraph 3.18.

Analysis of the duct configuration indicated the following flow characteristics, assuming that no balancing orifices are incorporated:

a. Flow distribution from the respective bleed ports on a particular engine will vary approximately 10% because of the difference in resistance in each duct leg to the common junction point. This assumes that the pressure level at each exit port of the particular engine is similar. Tha bottom bleed port which is connected to the duct having the shortest leg to the tee junction will deliver 10% more flow rate than provided by the top bleed port.

b. Assuming all engines provide similar pressure levels at each engine bleed port exit plane , flow distribution characteristics as noted below can be expected.

    (1) Right-hand engine will deliver 9.5% more bleed flow than the left-hand engine, and 1.5% more than the center engine.

    (2) The center engine will provide 8% more bleed flow than the left-hand engine.

The incorporation of any balancing orifices in the duct system will be dependent upon the evaluation of the characteristics of the complete duct system and an analysis of the engine power and/or bleed pressure variations.

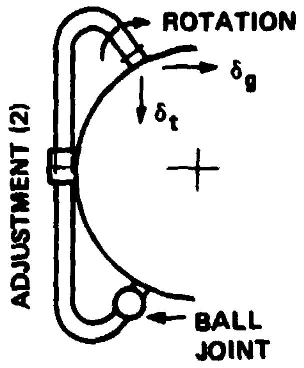

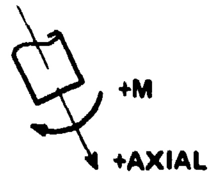

DUCT – 2.5 OD, .020 WALL THICKNESS
MATERIAL TITANIUM, COMMERCIALLY PURE, A70
@ 450° PROPERTIES

CONDITION	SAFETY FACTOR (ULTIMATE)	ULTIMATE DESIGN LOADS		
		BM IN.-LB	AXIAL-LB	SHEAR-LB
① (ENVELOPE) GROUND HANDLING 300 LB ULTIMATE (X, Y, Z)	1.5	±1040	±300	±300
② INTERNAL PRESSURE BURST 100 PSI (425°F)	2.25	0	+1215	0
③ THERMAL @ 131°F S.L. $\Delta T = 160^\circ F$	1.5	+345	−60	22
④ INSTALLATION TOLERANCE	1.5			
a) ROTATION, .125°		±541	–	49
b) δ_y = .01 IN.		± ∓94	–	–
c) δ_z = .01 IN./.005 IN.		−351/−176	–	–
COMBINED Ⓐ ③ ± ④a + ④c (.005) + ④b + $\frac{1.5}{2.25}$ ②	1.5	+779 −441	+750	–
Ⓑ ③ ± ④a + ④b + $\frac{1.5}{2.25}$ ②	1.5	+980	+750	–
Ⓒ (VALVE OPEN) − ④a − ④b + ④c (.005) + $\frac{1.5}{2.25}$ ②	1.5	−811	+810	–

– NEGLIGIBLE VALUES

Figure 106. Summary - interface flange loads with ball joint.

Early in 1974 it was determined that (1) the cargo hoists would be operable in the prototype, and (2) starting the main engine required more pressure and flow than originally anticipated. The pressure drop in the pneumatic system was decreased approximately 50%. This was accomplished by increasing 2-1/2-inch ducts to 3 inches (except for lines connecting the two bleed ports on each engine), increasing 3-inch ducts to 4 inches, and increasing 4-inch ducts to 5 inches. In addition, all tees were streamlined for optimum flow. A preliminary weight investigation indicated an increase of 37 pounds.

All detail ducts of the airframe-mounted duct system were released for procurement to Arrowhead Metal Products. Arrowhead made production-type drawings (included weld designations, etc.) and submitted these drawings for approval.

Figure 107 is the final pneumatic system schematic.

Six of the seven ducts selected for burst testing at temperature (due to complicated shapes) successfully passed proof (105.5 psig at 640°F for 5 minutes) and burst (175 psig at 640°F for 5 minutes). The seventh failed at proof pressure in the weld area where an acute angle tee attaches to the main duct. Refabrication of the duct was completed. The rework included heavier gauge metal in both the basic duct (locally where tee attaches) and in the tee. Gussets holding the tee to the duct were increased in gauge and flanged for extra stiffness to prevent tee flexing.

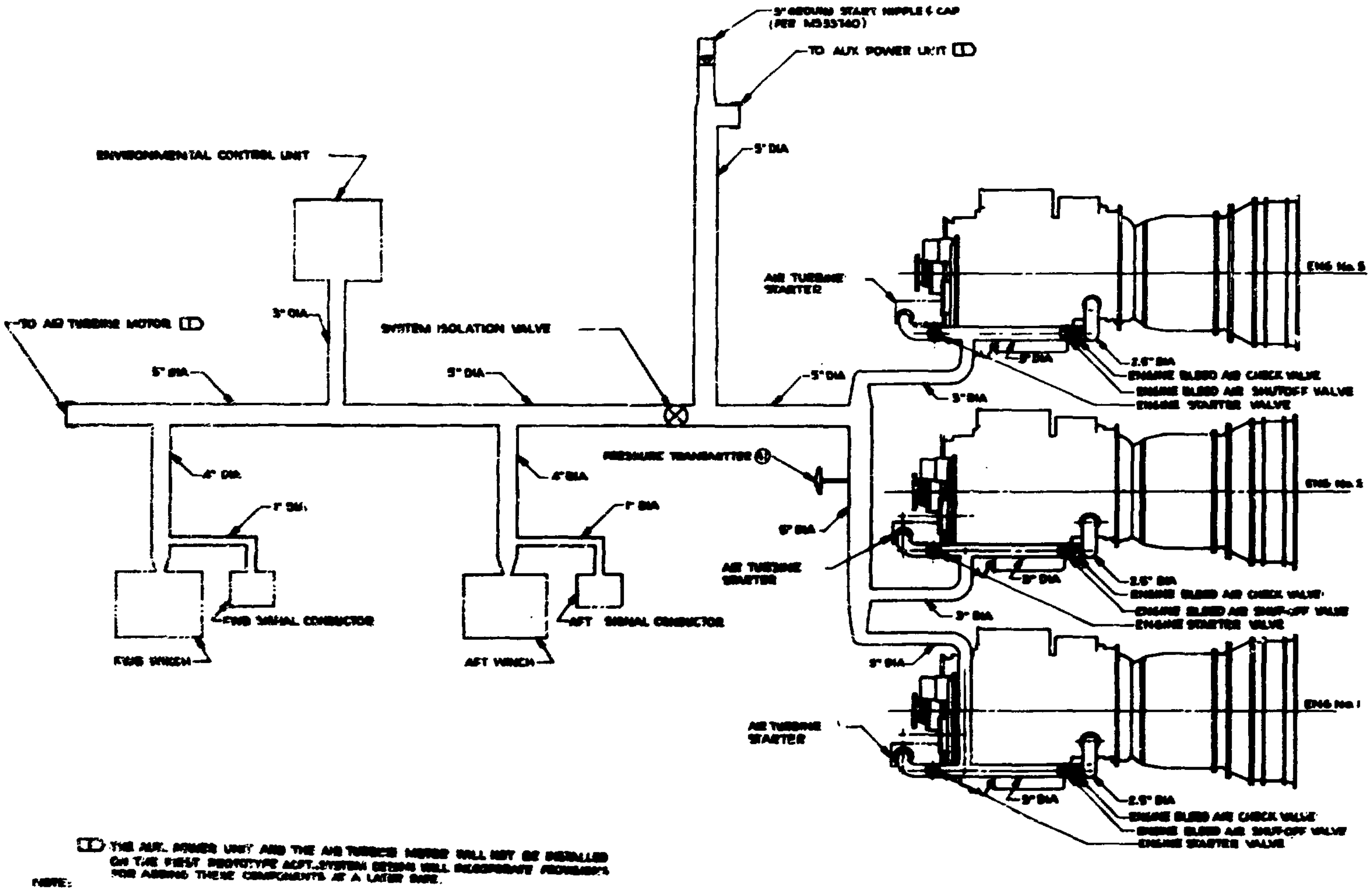

Figure 107. Pneumatic system supply schematic.

2.13.4 Environmental Control System

The HLH prototype contract designated the use of a CH-47 heater to provide heat in the occupied areas. At the Preliminary Design Review meeting 21 March 1973, a suggestion was made to utilize a bleed air heater (engine bleed air mixed with outside air). As an alternative, the installation of an air-cycle environmental control unit utilizing engine bleed air was investigated.

Since two suppliers had offered environmental control units for use in the prototype, a decision was made to incorporate an environmental control unit in the prototype aircraft.

As a result of the decision to install an environmental control unit (providing cooling as well as heating) in the prototype aircraft, various types of units were investigated. Figure 108 is a summary of the flow rate and temperature of the air required to maintain compartment temperatures. Also noted on Figure 108 is a list of eight ECU's investigated. The first six of these units are of the simple cycle, bootstrap or three-wheel cycle. This type of machine utilizes all bleed air. The last two units utilize a different cycle (see Figure 109) in which a portion of the air utilized is bled from the engines, while the remainder is recirculated from the cabin. This cycle will only operate satisfactorily in an unpressurized cabin such as the HLH has. The advantage of this cycle is that the bleed air requirement is greatly reduced. Two companies at present have these machines under development.

– PIDS ECU STATUS –

FLOW RATE/TEMPERATURE REQUIREMENTS

TOTAL AIRCRAFT (COCKPIT + TROOP COMPARTMENT)	COCKPIT ONLY	TROOP COMPARTMENT ONLY
50.5 PPM (1) (35°F)	35.0 PPM (35°F)	15.5 PPM (35°F)

OUTPUT OF UNITS UNDER CONSIDERATION

AIRESCH SABER-LINER UNIT	AIRESCH SABER-LINER UNIT MODIFIED	AIRESCH HUEY COBRA UNIT	AIRESCH GULF-STREAM UNIT	HAM. STD P70-3W CESSNA CITATION	* HAM. STD R72-3W DEHAV. DHC-7	* SUNDSTRAND(2) REVERSE BRAYTON CYCLE	* AIRESCH(2) SHOESTRING CYCLE AAH
26.0 PPM (1) (47°F)	27.5 PPM (35°F)	20.0 PPM (39°F)	58.5 PPM (36°F)	16.5 PPM (36.2°F)	41.0 PPM (42.5°F)	12.7 PPM BLEED + 40 PPM RECIRCULATED AIR (35°F)	15 PPM BLEED + 30 PPM RECIRCULATED AIR (**)

(1) ( ) INDICATES TEMPERATURE OF AIR OUT OF ECU

(2) USES BLEED AIR AND RECIRCULATED CABIN AIR

* MOST LIKELY CANDIDATES

** TO BE DETERMINED

Figure 108. Comparison of outputs from ECU's.

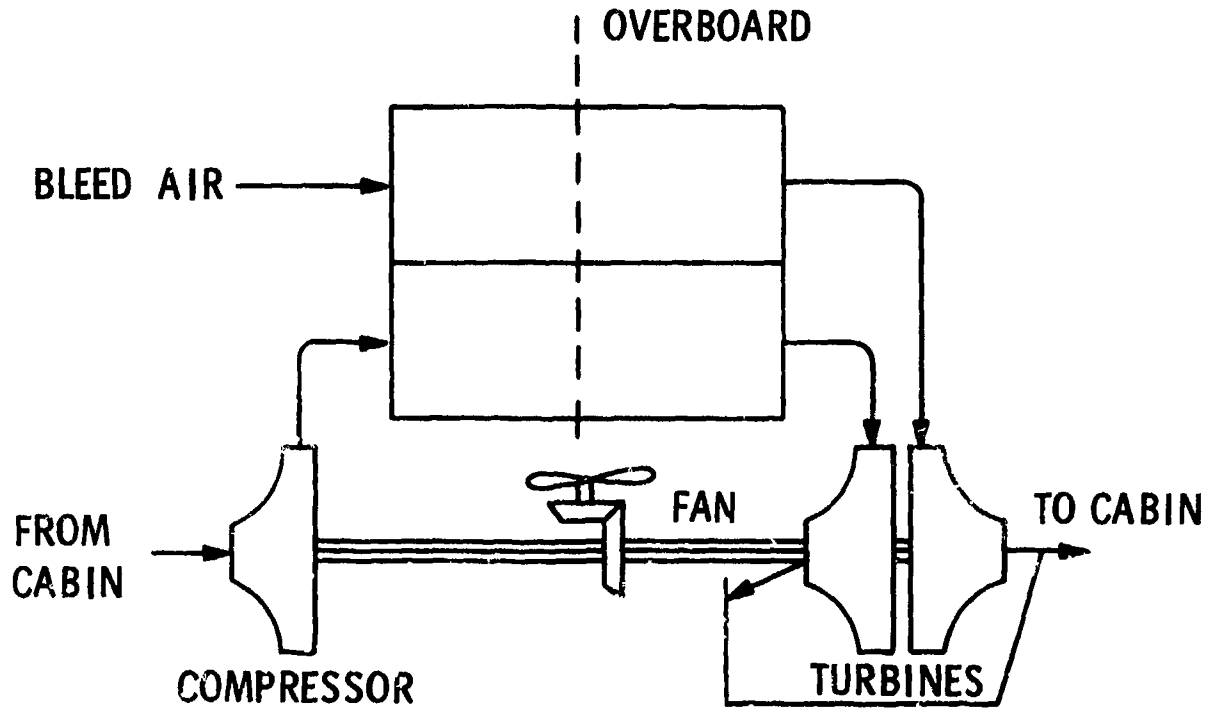

REVERSE BRAYTON CYCLE

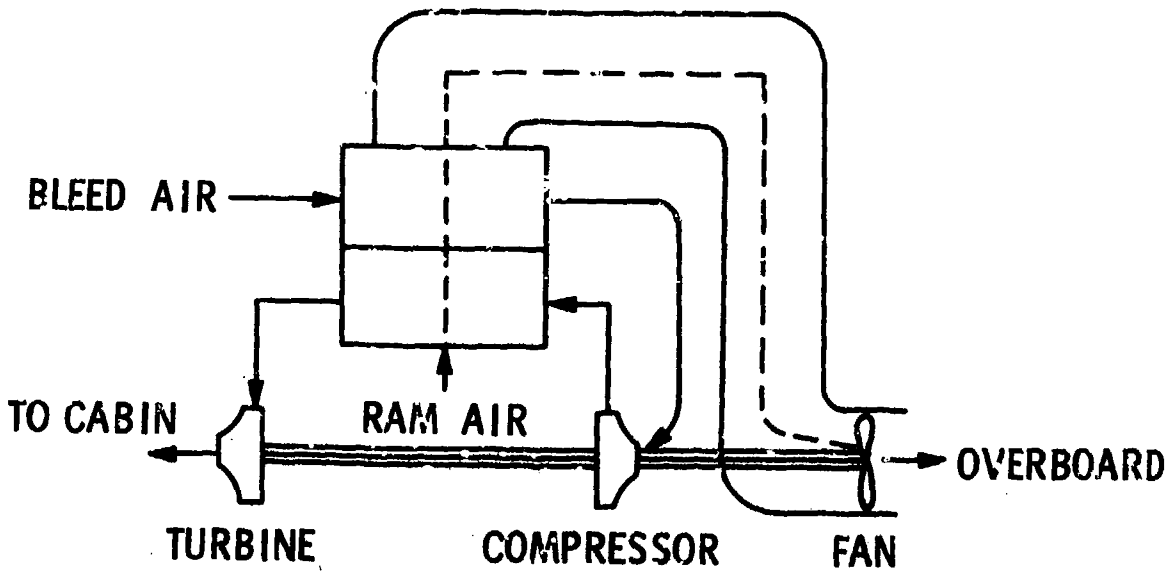

THREE-WHEEL CYCLE

Figure 109. ECU diagrams comparing reverse Brayton cycle with three-wheel cycle.

An RFP was released to three bidders (AiResearch, Sundstrand, and Hamilton Standard) to bid on a complete APU/secondary power system except for ducts and certain valves. The major items in this system are the APU, ECU, ATM, hydraulic pumps, and an electric generator. Two of the companies, AiResearch and Sundstrand, submitted proposals on 21 March 1974. (Hamilton Standard declined to bid.) Both companies bid with the understanding that only the ECU would be purchased for the prototype at this time. An indepth evaluation of these proposals resulted in selection of Sundstrand on 12 April 1974. On 19 April 1974, a no-cost purchase order was issued to Sundstrand for procurement of an ECU.

The pre-prototype unit was assembled in Sundstrand's test cell and testing commenced in April 1974. Design performance is shown in Figure 110 . This unit consists of a turbo-compressor, a turbine tip fan, and heat exchangers which are functionally identical to the prototype design. These components are connected with flexible hoses instead of hard ducting. Testing has been accomplished at laboratory ambient condition with a controlled bleed air supply. Initial testing indicated a problem with the turbine tip fan bearing and the turbo-compressor lube system (oil foaming).

The carbon bearings on the turbine tip fan were replaced with grease-packed ball bearings to facilitate testing were to be replaced with oil-lubed ball bearings in the prototype unit. The unit was run with an external lube system to the turbo-compressor, while the oil foaming problem was addressed. The oil foaming was caused by reservoir size and churning in the gear housing. The prototype reservoir was designed in accordance with Sundstrand constant speed drive practice to preclude this problem.

Initial system testing indicated considerable air leakage, both internal and external. The external leaks were sealed, and the results indicated that the unit was producing about 96% of cooling capacity without moisture separation. These results were reviewed with Boeing Vertol and the Army during the coordination and design review meeting of 3-4 June 1974, and it was agreed that the unit was operating approximately equal to design performance. Those present witnessed the unit in operation. The unit has since been operated with moisture separation, but in the first test it produced an excess of moisture separation. Correction of this data also indicates the unit is near design performance. The unit was reworked to correct internal leakage and retested.

An analysis of the aluminum turbine wheel exducer (curved portion of turbine wheel at wheel discharge) failure which occurred during testing was completed. The mode of failure

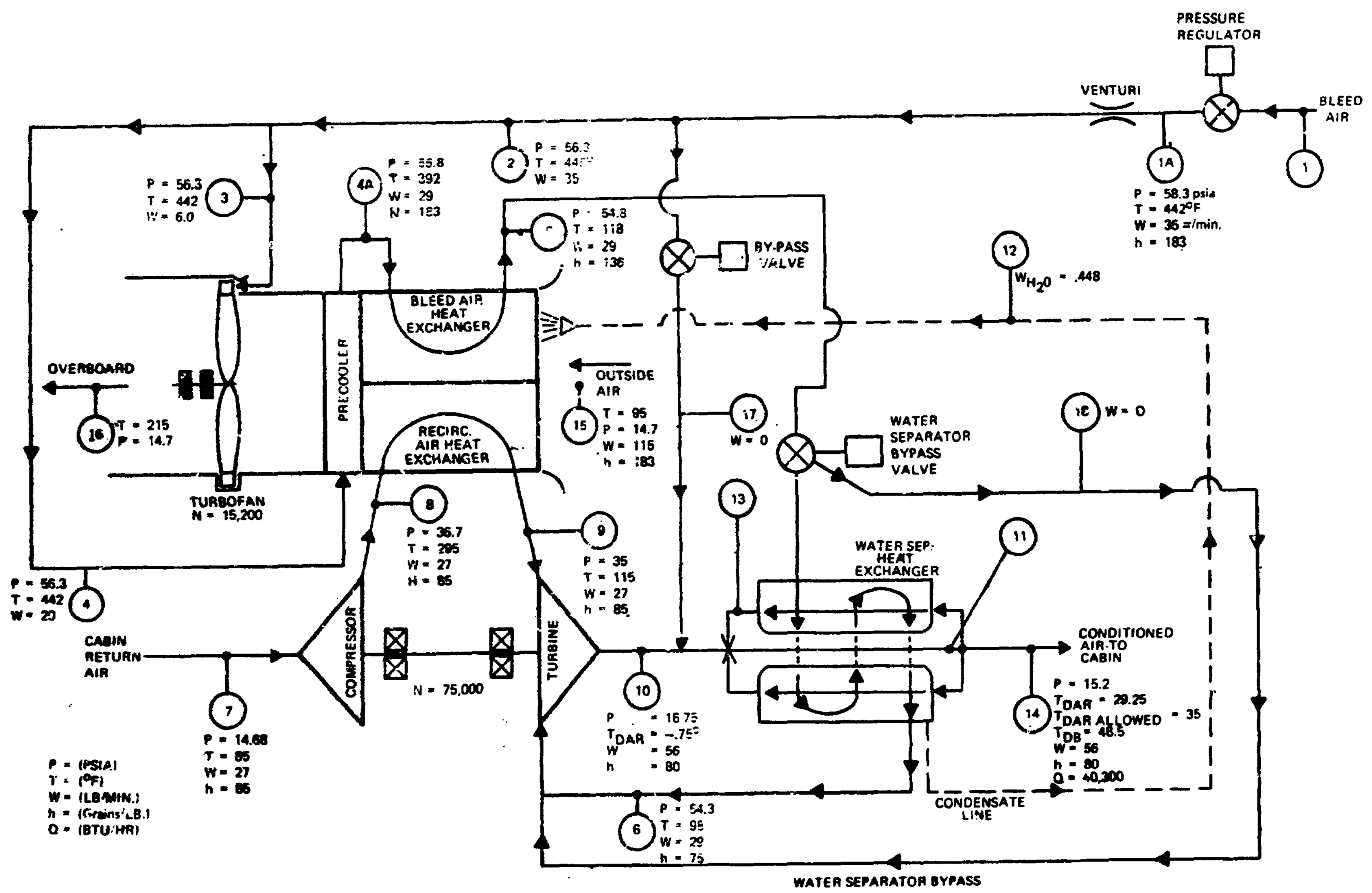

Figure 110. Sundstrand ECU schematic.

was high-cycle fatigue due to reverse bending stresses. The fatigue originated at tool marks along both sides of the blade in the fillet at the blade root. The aluminum material was improperly heat treated, resulting in an overaged material with some reduction in fatigue strength. By the nature of the failure, it was concluded that the nominal stress level in the fillet area was marginally above the fatigue endurance limit, i.e., the material was marginal for this application. Titanium wheel material was selected to solve this problem and to improve corrosion resistance.

During September 1974, a second aluminum turbine wheel (from original order) was put on test, but testing was interrupted when a wheel rub occurred. This was due to unanticipated thrust loads occurring at test conditions. The test rig was modified to prevent recurrence of this problem.

A titanium turbine wheel (replacement for an aluminum turbine wheel) experienced fatigue failure of four of the thirteen exducer blades during a calibration test; two of the blades separated completely. The turbine calibration test does not involve a complete air cycle machine; the turbine wheel, nozzle, and inlet scroll are assembled and run on a testing brake so that turbine output power and speed can be measured.

At the time of the failure, the wheel had been run for a total of eight hours at various speeds up to 75,000 rpm. It was running at 57,000 rpm when the exducer blades failed.

A similar failure occurred in July 1974, when a single exducer blade failed on an aluminum prototype turbine wheel. In that case, the failure occurred at a speed of 62,000 rpm after 15 hours of running at various speeds up to 80,000 rpm.

Aside from the material, the only difference between the two wheels is the blade thickness. The aluminum wheel had a tip thickness of .032 inch and a 1-degree taper; the titanium wheel has a tip thickness of .020 inch and also a 1-degree taper.

A program of analysis and test was conducted to overcome the exducer blade fatigue problem. This program included:

a. Computer modeling of the vibration modes and frequencies of the turbine wheel blades.

b. Analysis of the nozzle and wheel geometries to ascertain the extent of possible excitation modes and forces.

c. Measurement of the blade vibration modes using interferometric holography.

d. A test of a turbine configuration with increased clearance between the nozzles and the wheel tip. The clearance was increased from approximately .030 to .090 inch, to reduce the magnitude of the excitation forces. The effect on turbine performance was measured.

e. A test of a turbine wheel configuration having a shroud around the exducer blade tips. This will provide damping of the blade tips. The effect on turbine performance will be measured.

f. A two-piece turbine wheel was manufactured and tested. In this design the exducer portion of the wheel is manufactured as a separate piece from the inflow portion and the two pieces are tightly clamped together on assembly. This approach provides considerable friction damping for the exducer blades. There is no change in the aerodynamic contour of the wheel and hence, no change in performance.

This program was planned to provide a "quick fix" which would allow ECU development to proceed with minimum delay, and also to establish an analytical basis for a final solution to the problem.

Fabrication of the balance of the ECU components proceeded satisfactorily. A development core for the water separator was delivered from Standard Thompson and assembly of the precoolers and dual heat exchanger was completed.

Calibration of the fan component of the turbofan was completed.

The turbine wheel program of analysis and test was completed early in 1975. The fix was to shrink a steel shroud (1/2" wide x .020" thick) around the tips of the titanium exducer blades. This configuration accumulated 175 hours (operating at 30,000 - 80,000 rpm) with no failures.

The wheel was removed from endurance testing and used in a compressor/turbine assembly test. A prior test of a compressor/titanium wheel and shroud showed rubbing of the shroud. Initial testing of the endurance wheel in the assembly showed no rubbing. This wheel was used in the assembly test until a new wheel was manufactured and then it was returned to endurance testing.

The titanium wheel with the steel shroud accumulated 300 hours of operating time (30,000-80,000 rpm) successfully.

2.14 ROTOR BLADES

The forward and aft rotor blades are identical except opposite hand. Only the aft blade was developed during the ATC program. The prototype blade program included the engineering and tooling releases for the forward blade and for pendulum absorbers.

Geometry, construction, materials, and physical properties of the prototype blade are the same as the ATC blade, as defined in the ATC Program Final Report, Reference 4.

Nine design changes to the ATC blades were identified for the prototype configuration. The changes are a result of full-scale ATC blade test results and cost and manufacturing difficulties identified during ATC blade fabrication. The design changes are shown in Figure 111 . Each of the changes was reviewed and concurred with by the technical divisions of AVLABS AND AVSCOM.

Six of the nine changes required test verification. The changes requiring testing, the test method, and the test hardware are identified in Table 30. The eight-foot tip specimen, which is the hardware source of three of the five tests, is shown in Figure 112 .

2.14.1 Chordwise Airload Specimen Tests

Testing of the six chordwise airload specimens to verify the redesigned aft fairing core was successfully completed. Three outboard sections, with horizontal core splice, and three mid-span sections, no horizontal core splices, were tested. Test results for the mid-span and outboard sections are shown in Figures 113 and 114, respectively. As seen, all specimens, including the ballistically damaged mid-span specimen, fell within or above the scatter of the minimum required strength.

It should be noted that the outboard specimen on the lower side of the scatterband, tested at $\pm$19 psi, slipped in the grips during the test. This slippage may have caused a premature failure. This is supported by the fact that the non-ballistically damaged mid-span specimen, also tested at $\pm$19psi, endured almost twice as many cycles as the outboard specimen (10,000,000 vs. 5,540,000).

The ballistically impacted mid-span specimen was first tested at a shear stress of $\pm$11 psi for 14,342,000 cycles without incurring further noticeable damage. This load level is 15% higher than the design fatigue load of the critical mid-span section and equal to the V_H load level of the critical outboard section. The number of cycles is equivalent to over 1500 flight hours. The specimen was impacted directly, 0°

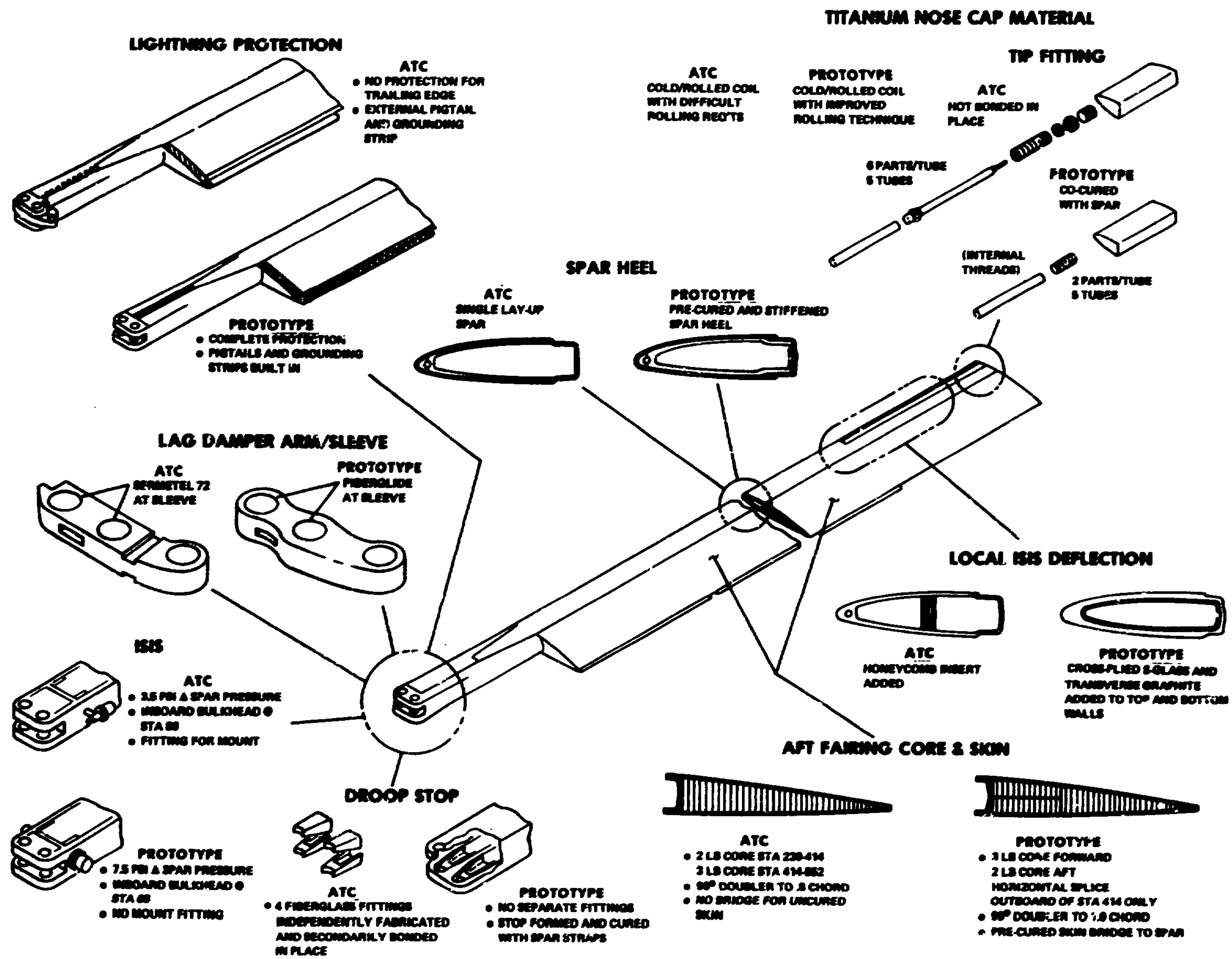

Figure 111. Rotor blade – modifications for prototype.

271

TABLE 30. TESTING OF BLADE MODIFICATIONS

MODIFICATION	TYPE OF CHANGE	TEST NECESSARY	METHOD OF VERIFICATION FOR PROTOTYPE	SOURCE OF TEST HARDWARE
1. AFT FAIRING				
a. NOMEX HONEYCOMB CORE	NECESSARY . STRENGTHEN CORE	YES	TEST OF 4 NEW AIRLOAD SPECIMENS	FABRICATE SPECIMENS AS PART OF NEW 8' TIP SPECIMEN
b. AFT FAIRING SKIN	NECESSARY . ELIMINATE CRACKING DURING FABRICATION	NO	FABRICATION OF A NEW, FULL-SCALE SPECIMEN TO VERIFY SOLUTION	FAIRING TO NEW CONFIGURATION WILL BE FABRICATED AS PART OF NEW TIP SPECIMEN. IT WILL INCLUDE ALL MODIFICATIONS.
	DESIRABLE . COORDINATE SKIN TO MODIFIED CORE	NO	NEW SKINS AND SHIM WILL BE IN NEW AIRLOAD SPECIMENS	
c. CORE TO SPAR BRIDGE	DESIRABLE . ADD SHIM TO ELIMINATE CORE MACHINING PROBLEM	NO		
2. LAG DAMPER ARM AND SLEEVES	NECESSARY . STRENGTHEN ARM	YES	RECONFIGURE #2 ROOT END WITH NEW ARM AND SLEEVES WITH FIBERGLIDE	USE EXISTING #2 ROOT END
	. ELIMINATE FRETTING			NEW SLEEVES & DAMPER ARM TESTED. ELIMINATED FRETTING
3. BEEF-UP OF OUTBOARD SPAR WALL	NECESSARY . INCREASE STIFFNESS OF SPAR WALL AGAINST LOADING	NO	FATIGUE AND STATIC TESTING OF NEW TIP SPECIMEN TO REPLACE #2 TIP SPECIMEN	INCREASED THICKNESS SPAR WALL WILL BE IN NEW TIP SPECIMEN
	. ELIMINATES COST FOR HONEYCOMB BULKHEAD AND SECONDARY INSTALLATION			
4. IMPROVED BONDING OF BLADE DROOP FITTINGS	NECESSARY . PROVIDE A HIGH QUALITY BOND IN A MORE PRODUCIBLE CONFIGURATION	NO	SIMILARITY TO AND IMPROVEMENT OVER PRESENT CONFIGURATION PROVIDES SUFFICIENT VERIFICATION	NONE REQUIRED
5. REDUCED COST TIP FITTING AND IMPROVED ATTACHMENT	DESIRABLE . REDUCE THE NUMBER OF TIP FITTING PARTS	YES	FATIGUE AND STATIC TESTING OF A NEW TIP SPECIMEN TO REPLACE THE #2 TIP SPECIMEN	NEW ATTACHMENT WILL BE FABRICATED IN NEW 8' TIP SPECIMEN (ENCL.
	. DEVELOP A HIGH QUALITY BOND JOINT			

TABLE 30. (Continued)

MODIFICATION	TYPE OF CHANGE	TEST NECESSARY	METHOD OF VERIFICATION FOR PROTOTYPE	SOURCE OF TEST HARDWARE
6. IMPROVED TITANIUM NOSE CAP MATERIAL	NECESSARY . IMPROVES FATIGUE STRENGTH . REDUCES THE COST PER POUND FROM $23/LB TO $16/LB . ORIGINAL MATERIAL NO LONGER AVAILABLE	YES	TEN FATIGUE SPECIMENS FROM NEW COIL WILL VERIFY FATIGUE STRENGTH DETERMINED FROM TI MET LABORATORY COIL FATIGUE TEST OF NEW 180" INTERMEDIATE SPAR SEGMENT	ACTUAL COILS FOR PROTOTYPE FWD AND AFT BLADES NEW 180" INTERMEDIATE TEST SPECIMEN FROM NEW SPAR TO PROTOTYPE CONFIGURATION
7. PRECURED HEEL IN SPAR	NECESSARY . ELIMINATE POSSIBILITY OF SPAR HEEL WRINKLING			72" SPECIMEN OF SPAR WITH PRE-CURED HEEL EXISTS TO EVALUATE EFFECT OF BONDLINES IN SPAR.
	. IMPROVES THE PRODUCIBILITY OF THE BLADE SPAR . INCREASE STIFFNESS OF HEEL TO ELIMINATE EFFECT OF HEEL DEFLECTION ON HONEYCOMB CORE	YES	TEST A 72" SPAR SPECIMEN WITH PRECURED HEEL IN LOADING MODE MOST CRITICAL TO NEW BOND LINE (ALTERNATING TORSION AND ISIS) TO VERIFY THAT ATC TESTING IS COMPLETELY APPLICABLE TEST 72" BLADE SEGMENT IN TORSION (STATIC AND FATIGUE) TEST 180" SPAR SEGMENT IN BENDING AND CF (FATIGUE)	NEW 180" AND 72" TEST SPECIMENS TAKEN FROM NEW SPAR TO PROTOTYPE CONFIGURATION.
8. ISIS PRESSURE IN SPAR AND LOCATION OF INBOARD BULKHEAD	DESIRABLE . TO REDUCE LEAKAGE ACROSS SEALS	YES	REMAINING ATC TEST SPECIMENS WILL BE TESTED AT NEW SPAR PRESSURE (7.5 PSIA)	ATC TEST SPECIMENS EXIST. INDICATORS WILL REQUIRE RESETTING AT VENDORS. NEW SPAR SPECIMENS WILL REFLECT NEW PRESSURE.
	. SIMPLER AND MORE PRODUCIBLE INBOARD BULKHEAD	NO	SIMILARITY TO EXISTING BULKHEAD PROVIDES SUFFICIENT VERIFICATION	
9. LIGHTNING PROTECTION AND PIGTAIL ATTACHMENT	DESIRABLE . PROVIDE PROTECTION FOR GRAPHITE IN T/E WEDGE	NO	SIMILARITY TO ATC TEST CONFIGURATION	NONE REQUIRED

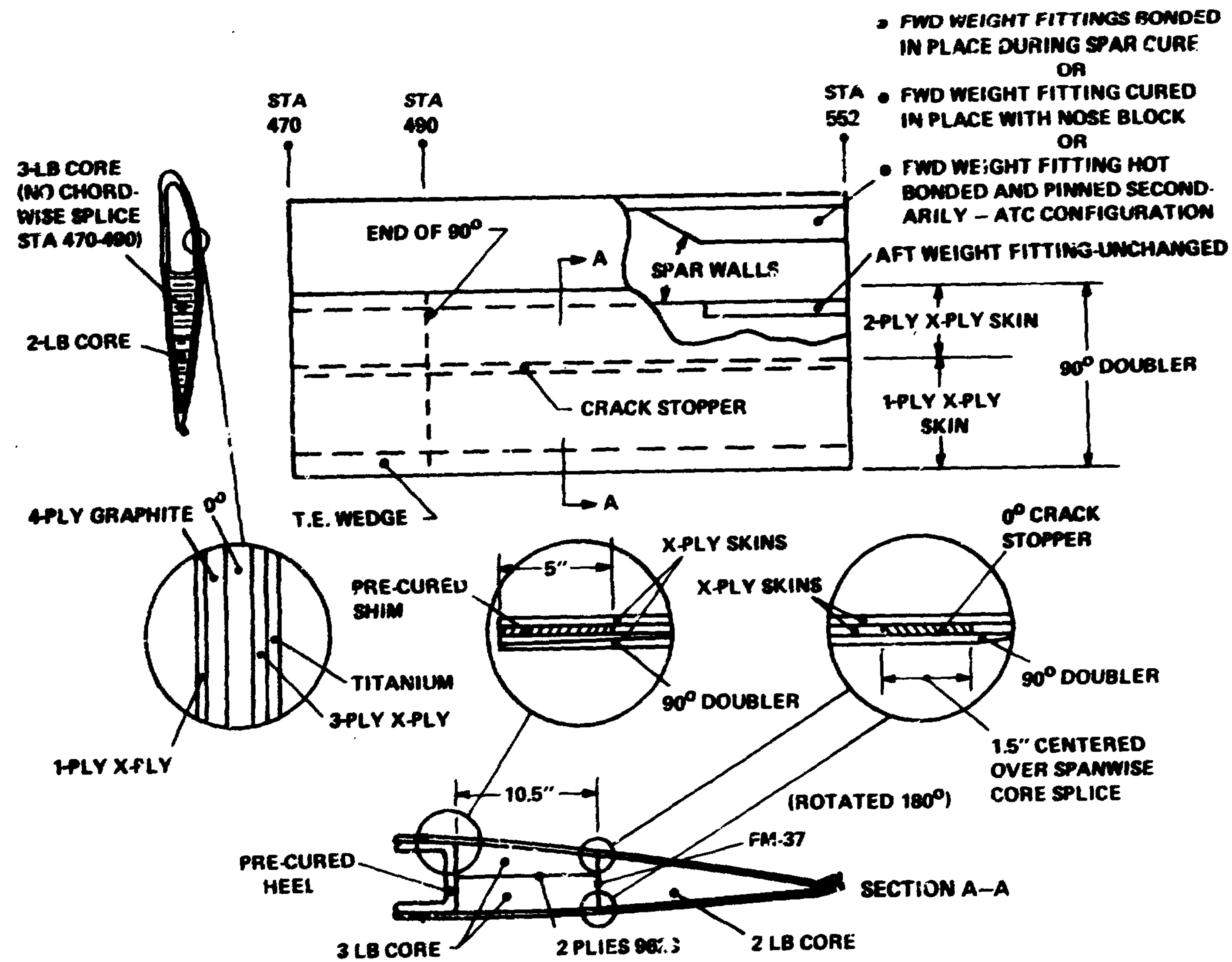

Figure 112. Tip specimen.

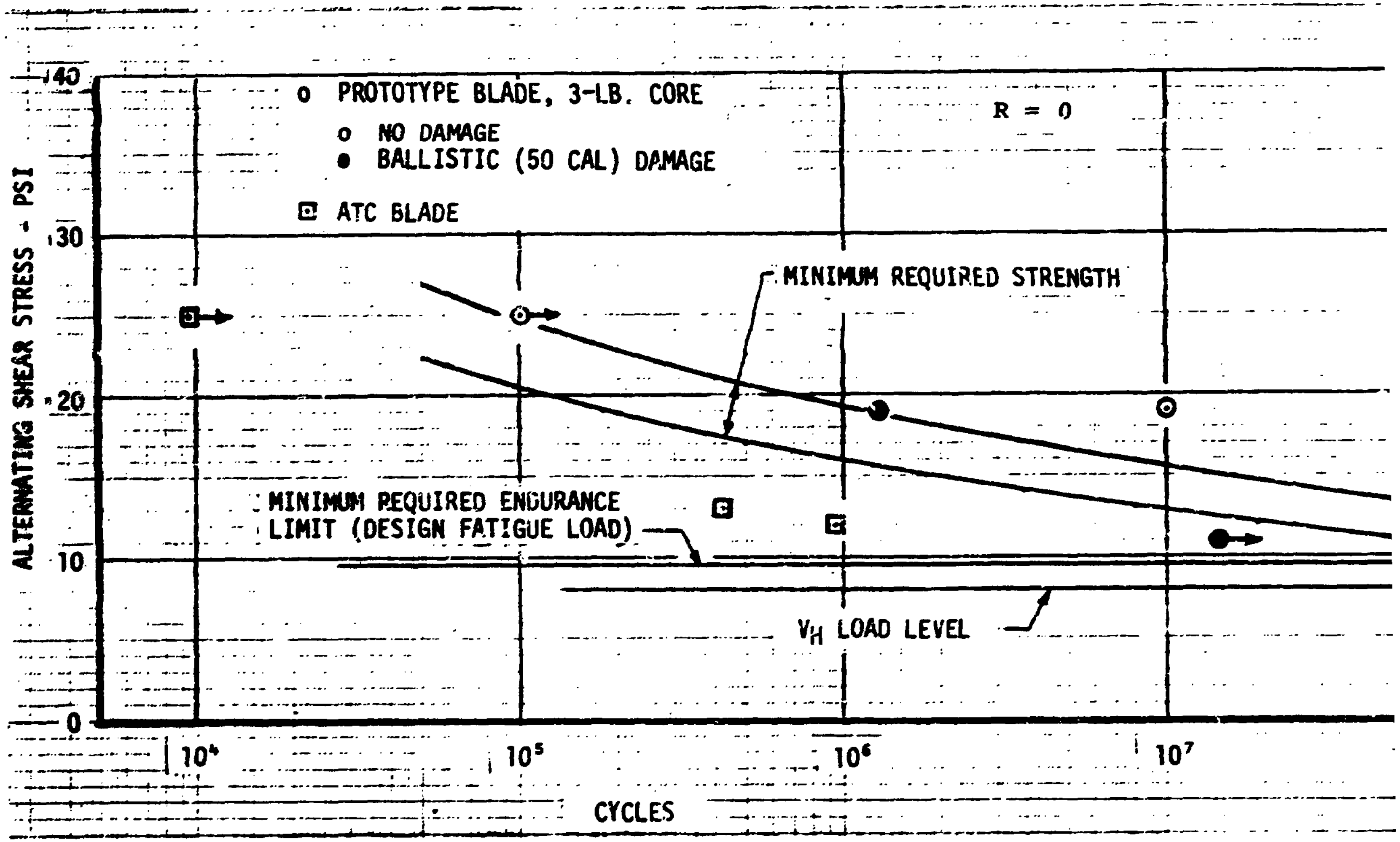

Figure 113. Fatigue strength of Nomex aft fairing core prototype configuration – mid-span section.

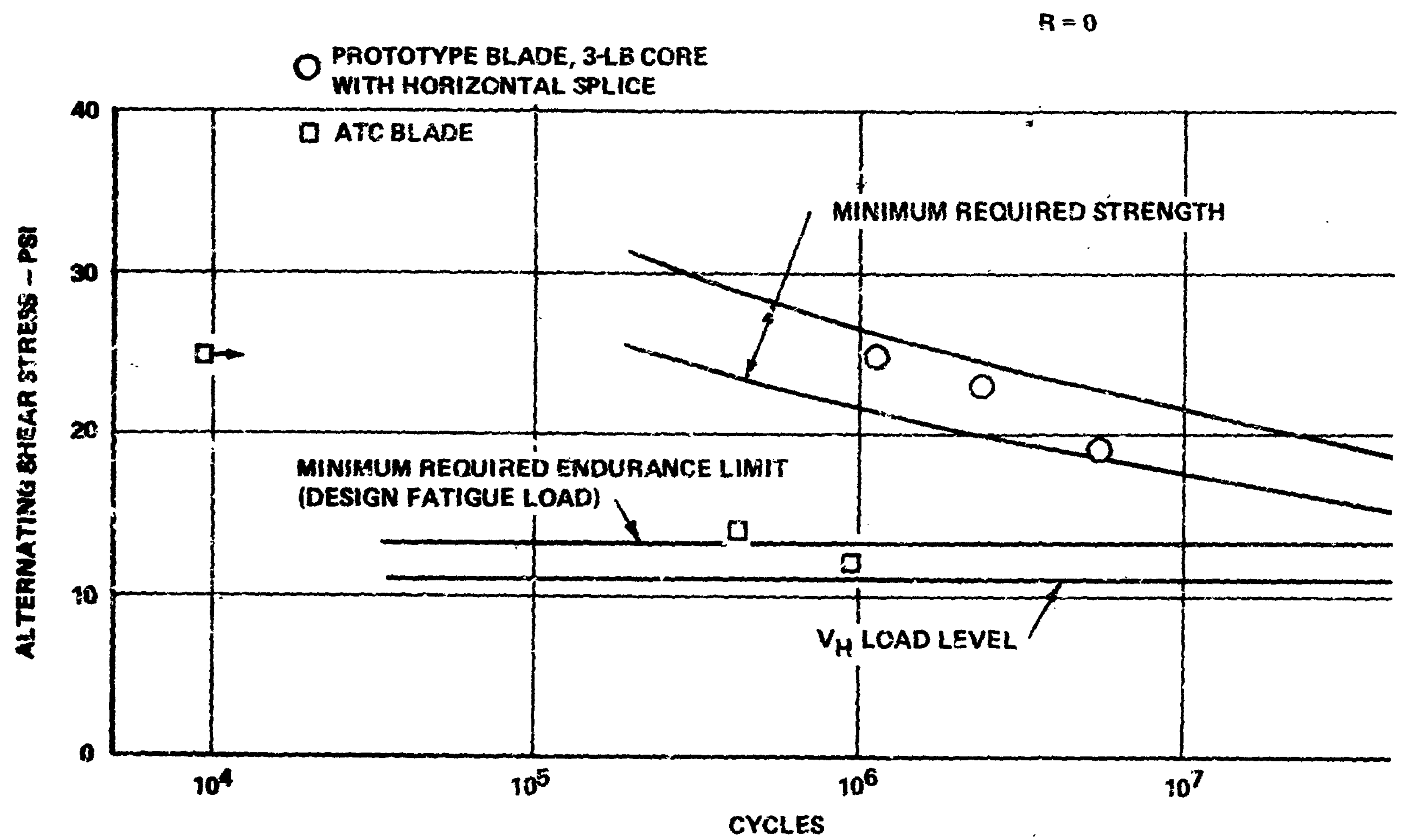

Figure 114. Fatigue strength of Nomex aft fairing core prototype configuration – outboard section.

obliquity, with a .50 caliber ball projectile at a muzzle velocity of 2881 feet per second and then tested without any repair to the core. The external damage at the entrance and exit holes of the projectile are shown in Figures 115 and 116, respectively. These test results verify that the redesigned aft fairing core with a stiffened spar heel increases the shear strength of the core to an acceptable level for the prototype aircraft.

2.14.2 Precured Heel Torsion Test

The torsion test of the precured heel specimen, conducted at Fort Eustis, Virginia, was completed. The specimen endured 5,000,000 cycles at the equivalent 1.5V_H loading without failure to the spar. The aft fairing did debond along the top skin starting at 2,450,000 cycles and completely unbonded at 3,960,000 cycles. The debonding of the fairing caused a loss in stiffness of less than 8%. The debond is attributed to two sources; (1) the configuration of the specimen is such that load is introduced to the aft fairing in an abrupt manner, unlike the root end of the blade fairing, thus causing a stress riser, and (2) ultrasonic inspection of the specimen prior to testing revealed voids in the bond which were considered acceptable for a test specimen but would not be for a blade.

2.14.3 Root End No. 2 Specimen

Testing of the No. 2 root end specimen was successfully completed in late December. Initially the specimen endured 2,400,000 cycles at equivalent V_H loading. The load levels were then increased to the 3.0 V_H level for flap and chord bending, 1.5 V_H for torsion, and 1.14 V_H for lag damper load. The CF loading was maintained constant. An additional 2,500,000 cycles was conducted without any damage. At the conclusion of these safe-life test runs, the limit CF was applied to the specimen and the torsional stiffness was measured. There was no decrease in torsional stiffness from the start of testing.

The highest loaded lug (upper trailing lug) was completely cut through at station 66.0 and fail-safe testing was started at equivalent V_H loading. After 400,000 cycles a second cut was made in the uni straps at station 104.0 under the leading surface. At the conclusion of the testing, 1,600,000 cycles (171 equivalent flight hours), the delamination had propagated outboard 22 inches. The outer torsion wrap also delaminated from each end of the cut at station 104.0. These delaminations propagated at a 45° angle from the cut and were 1.5 and 1.0 inch in

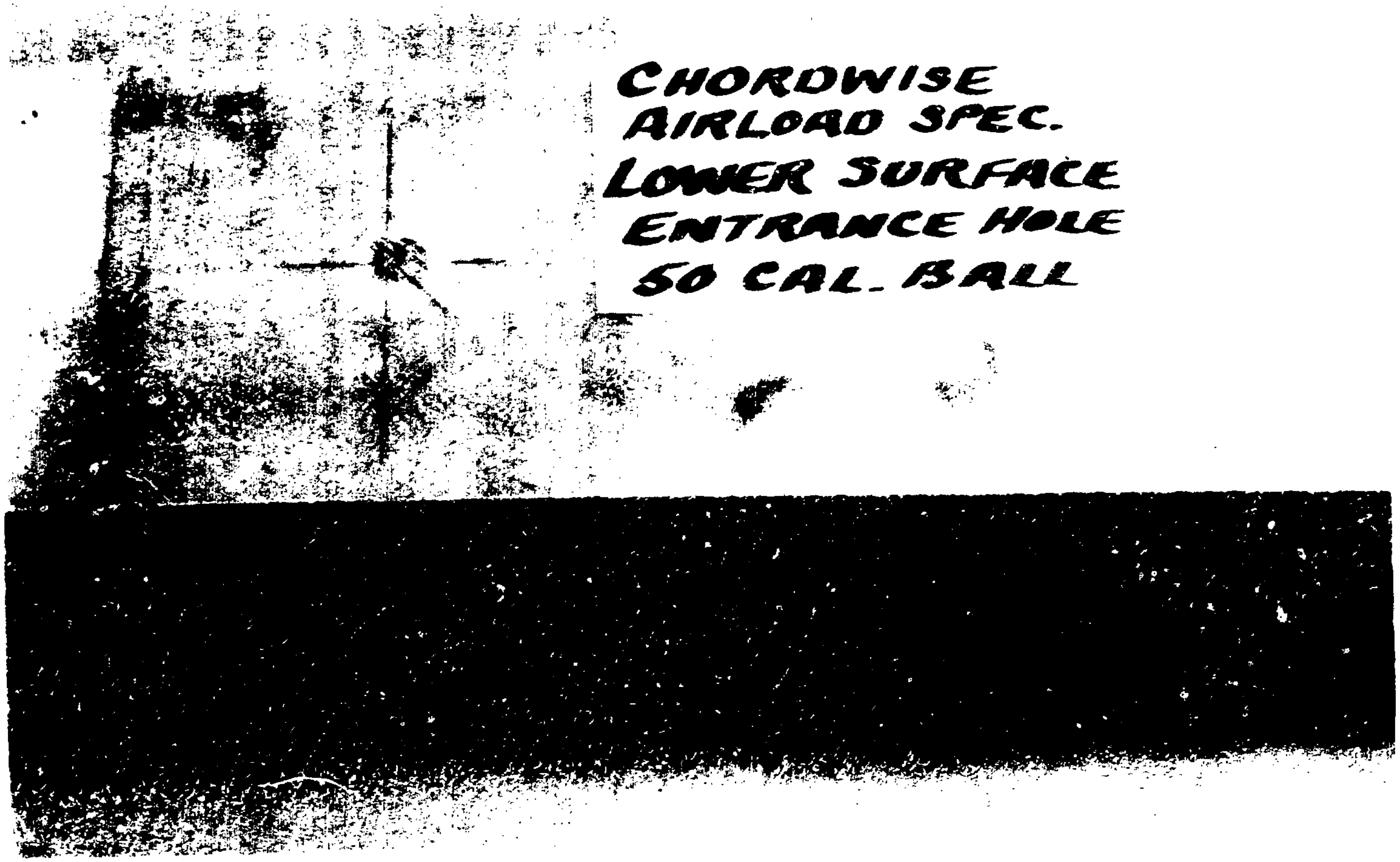

Figure 115. Chordwise airload specimen lower surface entrance hole.

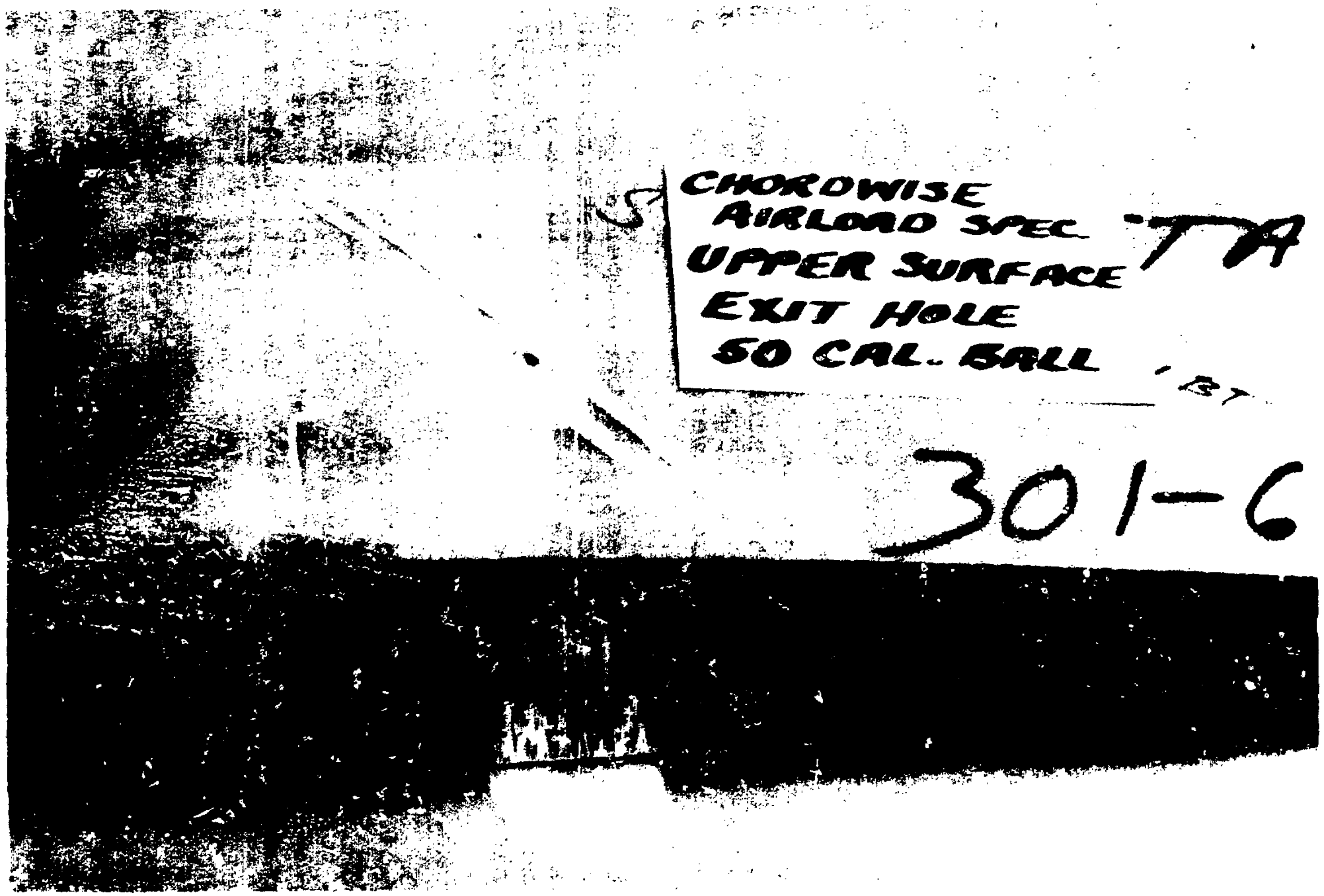

Figure 116. Chordwise airload specimen upper surface exit hole.

length on the upper and leading edge surfaces, respectively. In addition, the uni material appeared to be partially cracked, approximately 2.0 inches spanwise and originating from the upper surface of the cut.

At the conclusion of the fail-safe testing, the limit CF was applied. No further damage was noted from any of the defects. Additional testing of the No. 2 root end specimen was accomplished although the specimen had successfully completed the planned testing. The additional testing raised the total number of hours of the fail-safe test to 200 equivalent flight hours. Prior to the additional 29 hours, the cut in the upper leading edge uni straps at Sta. 104.0 was increased to 12 inches spanwise and a third cut was made in the lower leading edge uni straps, measuring 12 inches spanwise by 6 inches chordwise, and also centered at Sta. 104.0. These cuts are shown in Figure 117.

Before the specimen was fatigued, stiffness measurements were made. Stiffness over the span of the cut was decreased to 44% flapwise, 39.2% chordwise, and 16.9% torsionally.

The specimen was then fatigued at V_H load levels. After 12.7 equivalent flight hours, the torsional load was reduced 50%. (The load actuator bottomed out due to torsional windup of the specimen). The remaining hours were accomplished with no further reduction in loads.

At the conclusion of the test, the lag damper arm was disassembled and inspected. Figure 118 shows the disassembled lag damper arm. Fretting of the lag damper arm has been eliminated by the fiberglide coating on the sleeves. The fiberglide coated sleeves survived the test in excellent condition.

2.14.4 No. 2 Tip Hardware Specimen

Testing of the No. 2 tip hardware specimen was successfully completed in early November. After sustaining the limit CF load, a total of 5,000,000 cycles, half at equivalent V_H loading and half at twice V_H loading, was applied without any degradation of the bond between the tip fittings and the spar.

After fatigue test, a static CF load was applied to the fittings. At 90,000 lbs, a test fixture stud failed. The ultimate design CF load is 58,500 lbs. After repairing the stud, the CF load was applied to the forward and aft tip fittings separately. The tip fittings failed at 61,000 and 82,000 lbs for the forward and aft fittings, respectively. The mode of failure for each was a debonding of the tip weight tubes from the fitting. The failed fittings are shown in Figure 119.

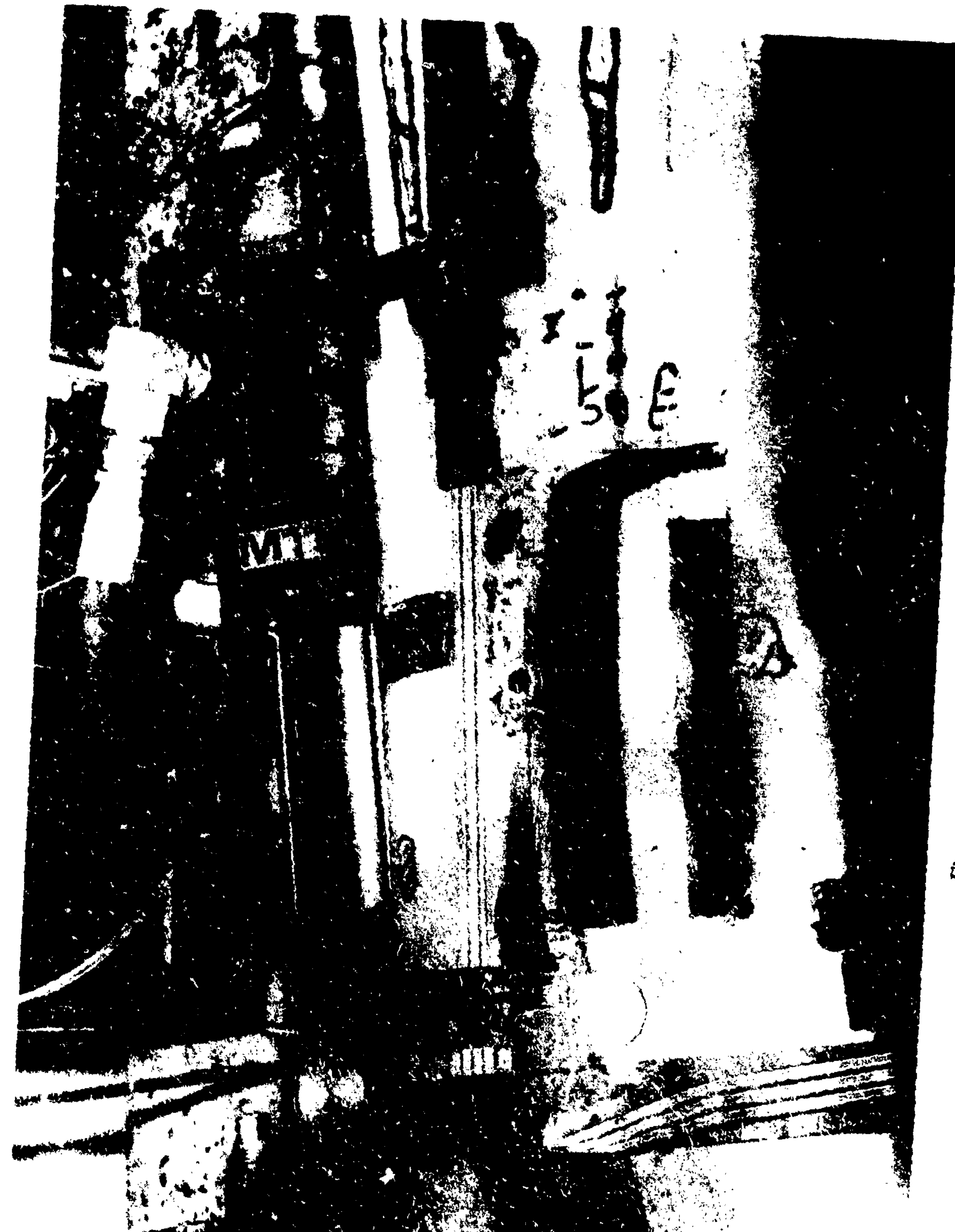

Figure 117. Root end fail-safe test.

Figure 118. Lag damper arm.

Figure 119. Tip hardware test specimen.

2.14.5 Intermediate Bending Specimen No. 2

The spar for intermediate bending specimen and outboard torsion specimens was fabricated and cut into test sections. Both specimens were ultrasonically inspected as well as leak checked. The intermediate bending specimen had the ISIS bulkheads and load plates installed.

Testing of the No. 2 intermediate bending specimen (Sta. 138 to 318) was initiated in late February. The initial load level at the mid-span was 23,200 ± 23,000 psi, equivalent to 1.5 V_H alternating load. After 1,266,000 cycles, a crack in the titanium cap was discovered in the top surface at Sta. 254.

The stress level for this crack is shown in Table 31. Testing was continued at the same load level. Two more cracks were found in the bottom surface of the titanium cap after 1,489,000 and 1,801,000 cycles. The location and stress levels for these cracks are given in Table 31. In addition, the ISIS indicator started to show unsafe at 1,765,000 cycles and was completely unsafe at 1,801,000 cycles. The specimen was leaking at all three cracks.

The vibratory load was reduced to 17,600 psi (1.17V_H) at the initial crack and the fail-safe run of two million cycles was accomplished. During the fail-safe run, seven more titanium cracks were discovered. The test history of these cracks is given in Table 31.

An analysis of the crack surfaces, removed from the specimen, revealed that the cracks originated at local surface burns on the inner surface of the titanium cap on all 10 cracks. The surface burns are generated by abrasive cleaning, power disc sanding of the cap during the post-forming scale removal. The power sanding causes the titanium to spark. The sparks, which are molten titanium, redeposit on the surface of the cap resulting in minute surface cracks.

The local burns were duplicated by subjecting fatigue coupon specimens cut from the selvage area of the prototype caps to power sanding sparks. The results of the coupon tests, Figure 120, verified the strength reduction due to the molten titanium deposits.

A review of the titanium cap fabrication procedure revealed that all the prototype caps were subject to the abrasive cleaning. A life analysis, based on the results of the bending specimen, was presented to AVSCOM personnel in early April. It was recommended that prior to first flight, a life of 1000 hours be established.

TABLE 31. HLH INTERMEDIATE BENDING SPECIMEN NO. 2

CRACK	LOCATION		RUN	STEADY STRESS (PSI)			ALTERNATING STRESS (PSI)	STRESS RATIO R	CYCLES (MILLION)	EQUIVALENT ALT. STRESS @ R=.1 (PSI)
	STA.	SUR-FACE		APPLIED (CF)	RESIDUAL	TOTAL				
1	254	TOP	1	26,900	7,400	34,300	20,640	.249	1.266	22,300
2	228	BOT.	1	23,200	8,200	31,400	20,510	.210	1.489	21,500
3	204	BOT.	1	22,800	8,200	31,000	18,270	.258	1.801	19,500
4	240	BOT.	1	23,200	7,400	30,600	18,400	.249	1.801	19,500
			2	23,200	7,400	30,600	15,690	.322	.858	17,100
5	228	TOP	1	25,840	8,200	34,040	23,040	.193	1.801	24,000
			2	25,840	8,200	34,040	19,650	.268	1.176	21,200
6	208	TOP	1	22,800	8,200	31,000	21,280	.186	1.801	22,000
			2	22,800	8,200	31,000	18,150	.261	1.890	19,400
7	200.5	TOP	1	22,800	8,200	31,000	19,840	.220	1.801	20,500
			2	22,800	8,200	31,000	16,920	.294	1.890	18,300
8	211.5	BOT.	1	22,800	8,200	31,000	19,830	.220	1.801	20,500
			2	22,800	8,200	31,000	16,910	.294	1.890	18,300
9	212.5	BOT.	1	22,800	8,200	31,000	19,970	.216	1.801	21,000
			2	22,800	8,200	31,000	17,030	.291	1.890	18,400
10	193	TOP	1	22,800	8,200	31,000	18,200	.260	1.801	19,500
			2	22,800	8,200	31,000	15,520	.333	2.000	17,000

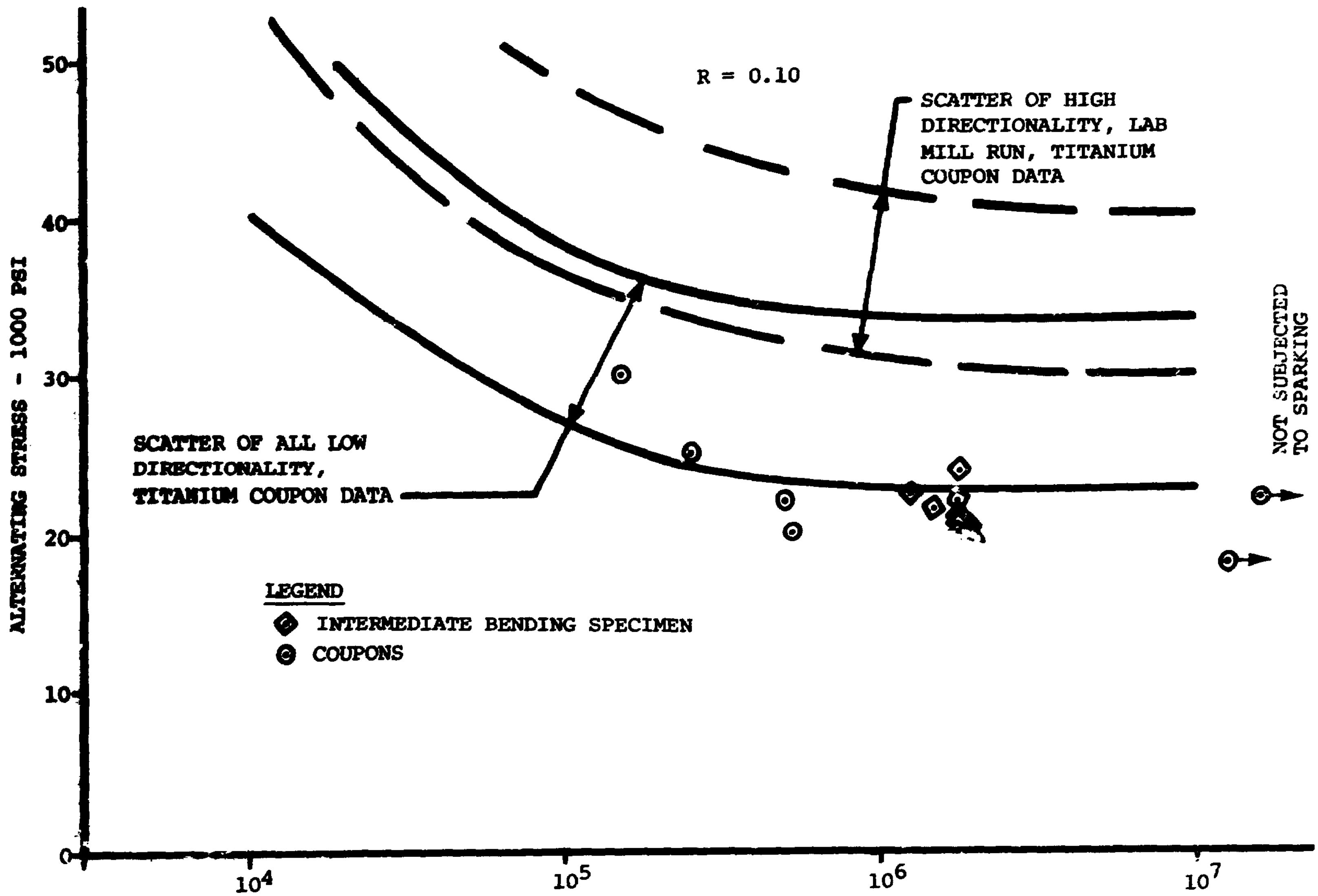

Figure 120. Titanium cap – effect of molten deposits.

It should be noted that since the initial titanium cap crack, over 200 equivalent flight hours at 100% V_H loads have been accrued on the bending specimen with no measurable change in frequency or response, which verifies the predicted fail-safety of the concept. Fail-safe testing of the No. 2 intermediate bending specimen was continued. An additional two million cycles at V_H load level and one million cycles at the 2.0 V_H load were completed. Thus, this specimen accrued over 400 equivalent flight hours at 100% V_H loads and 100 equivalent flight hours at 200% V_H load level with no measurable change in frequency or response.

During the fail safe testing, three additional cracks in the titanium were discovered. The crack locations and time of discovery are; crack no. 11, top surface, Sta. 287, 3,300,000 cycles of V_H loading; crack no. 12 and 13, bottom surface, Sta. 191.5 and 223.5, 160,000 cycles of 2.0 V_H loading.

The only visible discrepancy in the fiberglass was debonding of the outer cross-ply on the top surface adjacent to the crack at Sta. 254, the initial crack in the titanium. (Note: the damage under the titanium cap would not be visible if the section of the cap had not been removed for failure analysis).

Prior to the discovery of the molten titanium deposits, a program was initiated to determine the Goodman effect (steady stress) on the endurance limit and the spanwise and chordwise residual stress levels (due to thermal effects and evacuation of the spar for ISIS). A straight-line Goodman diagram had been assumed for the titanium analysis. Fatigue testing at various stress ratios verified the assumption of the straight-line Goodman diagram as shown by the test results in Figure 121.

During the course of the microstructure analyses of the Goodman effect coupons, small flaws and microstructure variations were identified within the base material. Although neither condition was contributory to the premature cracking, they are considered undesirable effects. Coordination with the titanium producer identified that the two conditions are related and that tighter controls during annealing and a small modification to the rolling schedule would eliminate these conditions.

The coupon program which duplicated the effect of the molten titanium deposits on the fatigue strength of titanium was completed. Test results showed that the high cycle fatigue strength is reduced by the presence of the deposits but the effect is negligible on the low cycle fatigue strength. A

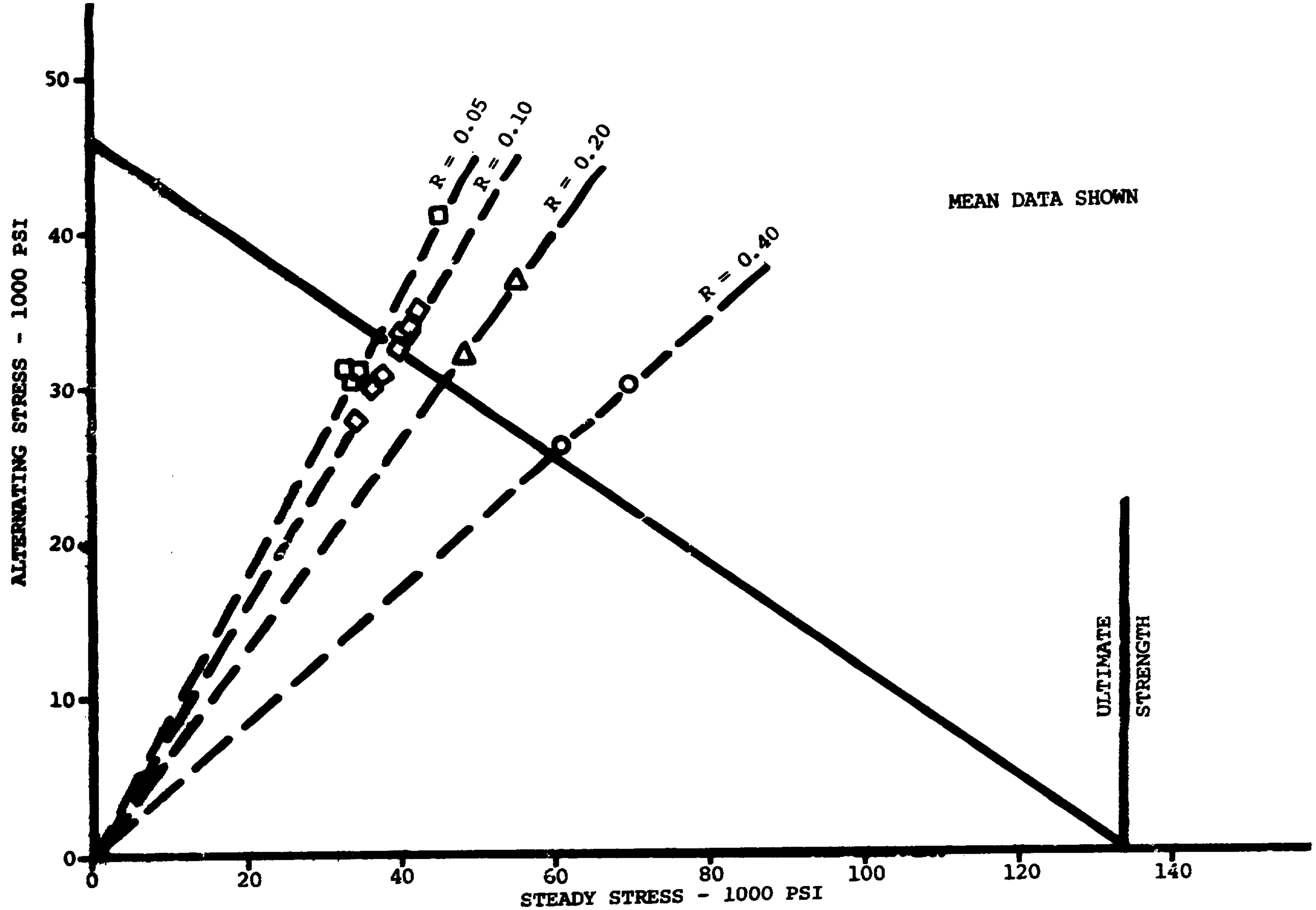

Figure 121. Titanium cap – Goodman diagram.

titanium cap life of 1000 hours was established prior to first flight. The predicted life was based on top-of-scatter loads and the high-directionality titanium with molten deposits curve shape; the mean chance of a cap failure occurring in 100 hours is 0.000024. A comparison of the two curve shapes and the predicted bottom-of-scatter life is shown in Figure 122.

It should be noted that the cracking of the titanium cap is a reliability and maintainability problem and not one of safety. Therefore, the blades will be flown on an "on condition" removal basis.

2.14.6 Outboard Torsion Specimen No. 2

Testing of the second outboard torsion specimen was initiated in early June. The safe life and limit load tests were successfully completed. The safe-life test consisted of three million cycles at 2.0 V_H load level. Prior to the test the aft fairing was impacted at mid-span with a .50 caliber ball projectile. The damage was not repaired. There was no visible damage propagation during the safe-life test. The ability to withstand the limit load proved that the precured heel solved the cross-ply wrinkling problem which caused failure of the initial specimen.

Torsional stiffness measurements of the specimen prior to testing matched the theroretical calculation within 6%. Measurements taken after the safe-life test showed no change in stiffness.

The top surface of the titanium nose cap was cut from its trailing edge to within 1.50 inches of the leading edge. Fail-safe testing of the specimen remained to be accomplished at program termination.

2.14.7 Pendulum Absorbers

The swing testing of the first four-per-rev pendulum absorber was completed. The measured tuning range verified the predicted tuning range. The remaining four-per-rev absorbers and the three-per-rev absorbers were fabricated but whirl and swing tests were not accomplished due to program termination (Figure 123).

2.14.8 Proof Load

Instrumentation of ATC Blade No. 3 for flapwise and chordwise proof load testing was completed. Testing was not accomplished due to program termination.

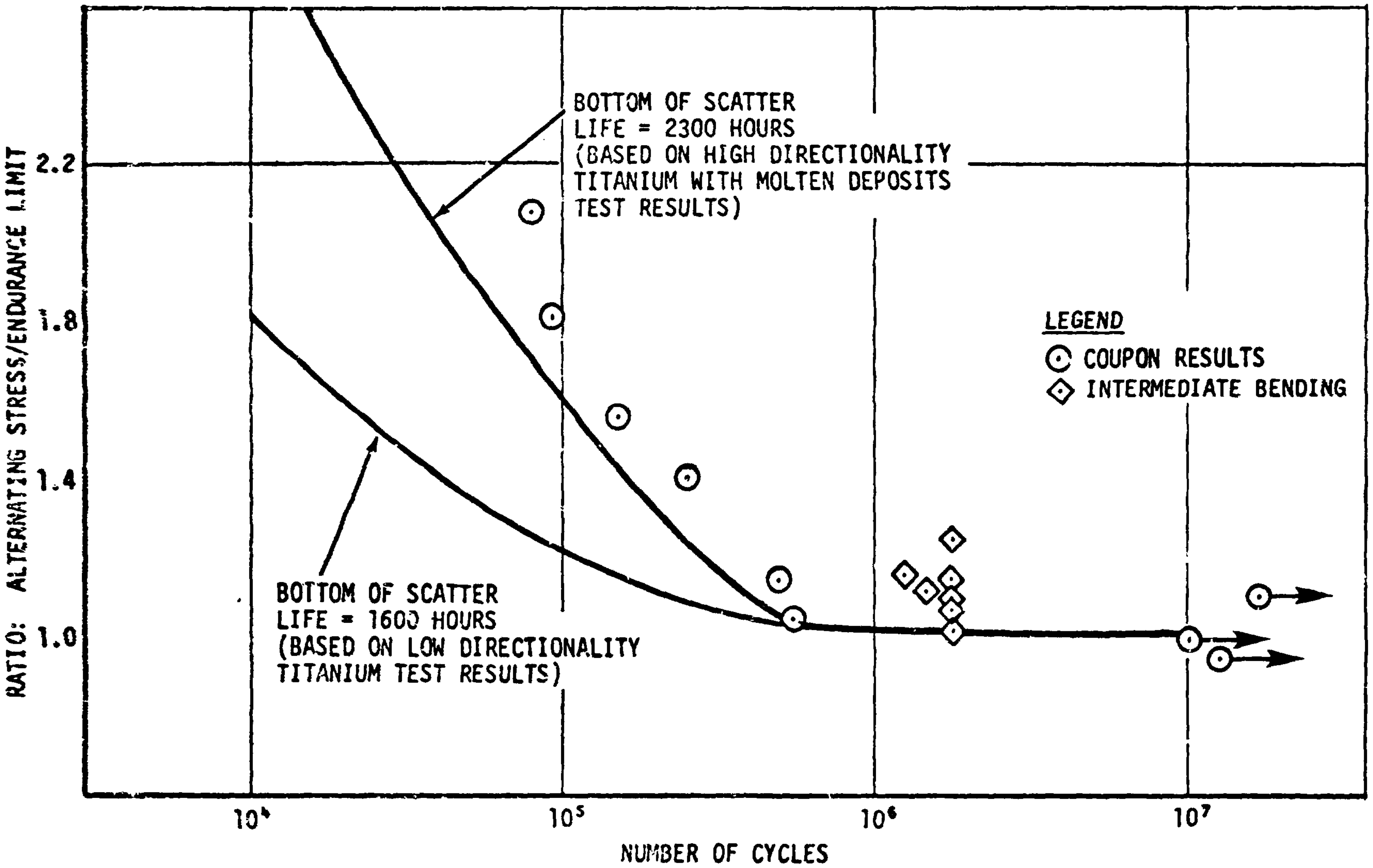

Figure 122. Intermediate bending specimen – predicted life of nose cap.

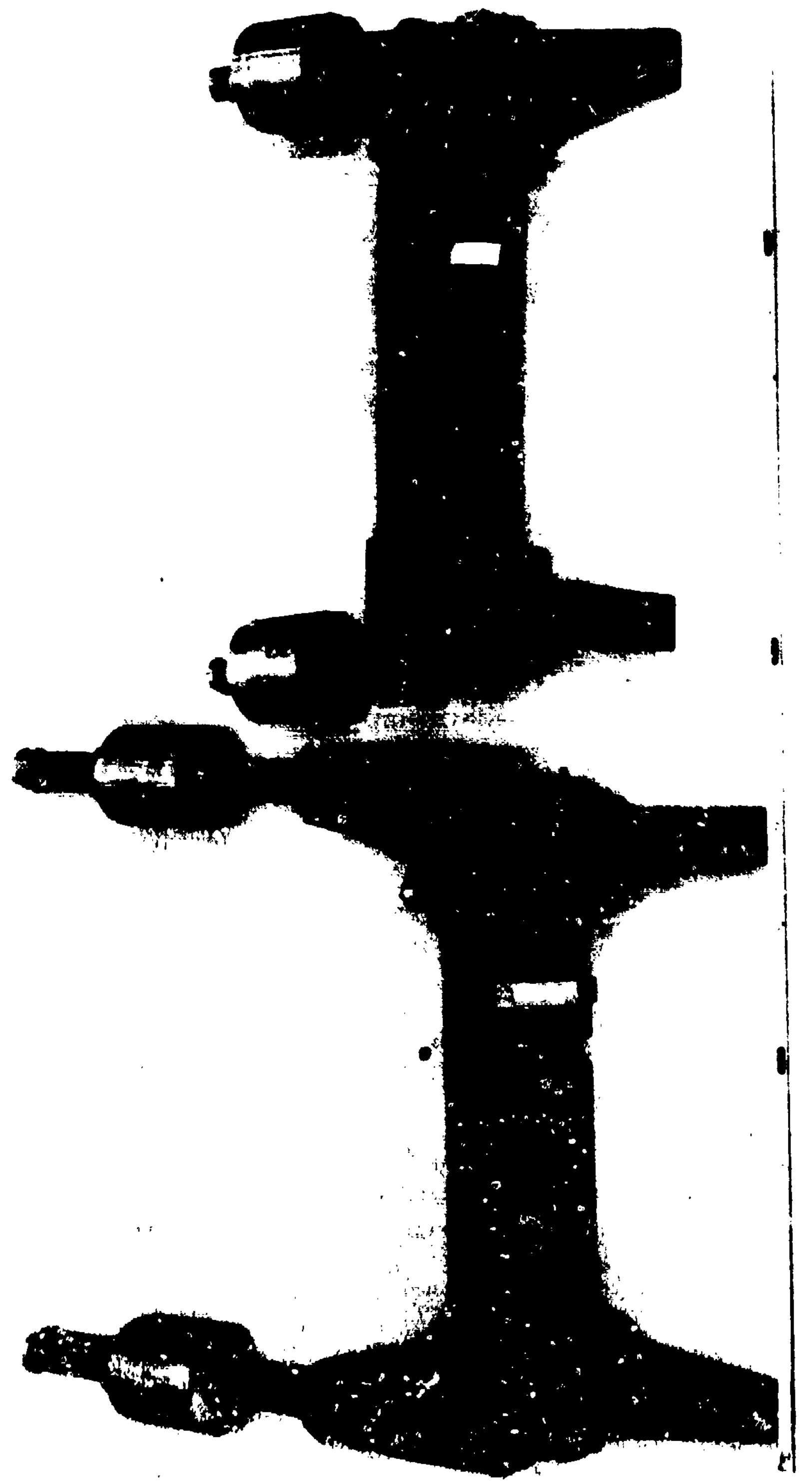

Figure 123. Pendulum absorbers.

2.15 ROTOR HUB AND UPPER CONTROLS

The System Requirements Review meeting held in March 1973 included a review of the applicable ATC design components (Reference 5, ATC Final Report).
Prototype differences and additions include:

Pitch Housing - incorporate delta three

Swashplate rotating ring - incorporate delta three

Droop stop - due to delta three

A layout, weight, and cost savings for a single pitch link in place of the dual pitch link was presented. The single link makes use of fracture mechanics to determine allowable stresses that would provide fail safety by an essentially zero crack growth rate.

The kinematic layout of the forward rotor controls (with delta three) was completed. The layout of the forward pitch housing was completed.

The release to Operations to manufacture those parts designed under the ATC program was accomplished in mid-1973. Long-lead material for the forward rotor swashplate and pitch housing was defined. Parts defined on specification control drawings (such as the lag damper, bearings, etc.) were also released to Materiel for procurement.

Detail drawings for parts comprising the flap stop for the forward rotor were completed and issued. The flap angle limits are different for the two rotors and parts were designed to minimize the possibility of assembling incorrectly.

Design of the swashplate stationary ring for both rotors was completed. The design features three failsafe actuator attaching lugs. All other features of the ATC swashplate stationary ring design are maintained.

Two stationary scissors will be used at each rotor on the prototype. A second scissors assembly will provide fail safety through redundant structures. This precluded the requirement for the actuators to provide restraint for the stationary ring in event of the single stationary scissors failure.

The design of the rotating ring for the forward rotor was completed. The radius of the pitch link attachment is greater because of the delta three in the forward rotor. The box section for the ring was enlarged and three boron stiffening rings were applied to the top and bottom of the ring in lieu of two on the aft rotating ring.

All detail drawings were released for the prototype rotor hub and upper controls by early 1974.

The first rotor hub fatigue test conducted under the ATC phase indicated the need for improved fretting inhibitors in the various joints. Results of the second fatigue test, which incorporated these materials, determined changes to released prototype components.

Deflection tests necessary to evaluate increased stiffness identified in the ATC upper controls endurance test were completed under that program. The data was used to redesign the swashplates. Changes identified include addition of bulkheads to the rotating rings to reduce shear deflections of the ring cross-section and an increase in circumferential bending stiffness of the stationary ring, particularly over the actuator lugs, to reduce local loading of the bearing.

As a result of rotor hub and crossbeam fatigue testing, the design was changed to coat the bushings in the hub and crossbeam attachment with plasma-sprayed aluminum bronze with 10% Ekonol in place of Sermetel 72. The outer faces of the flanges, previously uncoated, were coated with tungsten carbide. The shear pin also had the Sermetel replaced with the aluminum bronze.

Endurance testing of the swashplate has indicated that the bearing would still be expected to ride over the edge of the bearing for the higher design loads. The design of the swashplates was changed for the prototype to increase the thickness of the rings by 0.18 inches on the inside in all places except in the bearing backup walls, where the thickness will be increased 0.23 inches. This beefup dimension was chosen by the status of hardware in process when the change was committed, i.e., rough machined to a nominal 0.25 inch oversize. The 0.18" will allow a finish cut which is expected to clean up the rough-machined and heat-treated surfaces completely. The bearing backup wall is desired to have the maximum smoothness possible and the 0.23" specified may leave a few areas unfinished. The boron rings will increase in dimension to cause the bending stiffness to increase approximately 1.6 times the original design for the aft rotating ring and to approximately twice for the stationary rings. The bearing is now specified to have the race depth 35% of the ball diameter.

The inboard lag damper bracket was found to have interferences with the lag damper when the blade approached extreme permissible angles. This was found in the clearance checks on the whirl tower. While the bracket was adequate for all ground testing, it was redesigned for the prototype.

As a result of experience on the whirl tower and the DSTR, the original conical droop stops were replaced with cylindrical stops. Also, the elastomeric bearing preload button installation for the prototype was completed. It differs from the installation on the DSTR rotor in that the button floats radially, to be located by the elastomeric bearing, and the Teflon/Dacron fabric is on the button rather than on the elastomeric bearing.

All design drawings and changes were completed except one new part which was identified to be designed and fabricated for the prototype. The lag damper is free to rotate about its axis because of the spherical bearings at each end. It is loosely restrained by buttons in the inboard bracket bearing against the damper tailstock. The original installation had nylon buttons. These wore rapidly and were replaced with bronze Oilite. These wore less rapidly, but were still unsatisfactory. The rapid wear occurs because the damper is top heavy and the moment about the damper axis due to centrifugal force put a high load on the button. The solution was to attach a counter balance below the damper to substantially reduce the moment due to top heaviness.

2.15.1 Testing

The testing planned under the prototype program included the following:

- Lag damper fatigue and endurance
- Swashplate endurance
- Swashplate stationary ring fatigue
- Swashplate rotating ring fatigue
- Forward swashplate rotating ring strain survey
- Loop fatigue
- Pitch housing static strain survey
- Actuator gimbal mount fatigue

Major fabrication work was completed for all test specimens. However, due to the program termination, only the lag damper and the swashplate endurance tests were conducted.

2.15.1.1 Lag Damper Fatigue and Endurance Tests

The first fatigue test was interrupted at 34,900 cycles because

of hydraulic fluid leakage. The source of the leak was a crack in the tailstock. Examination of the tailstock showed the crack to have originated in the fillet radius for the bolt head spot-face. The crack had progressed through a hydraulic passage. Revised parts were fabricated for the DSTR rotor and for continuation of the fatigue test. Fatigue testing was resumed with the new tail stock as well as aluminum bronze/Ekonol coated bushings in the outboard end clevis. The latter were included so that the fatigue test configuration would be identical to the prototype aircraft. Testing was interrupted at 147,000 cycles by a split in the aluminum body adjacent to the tail stock. Testing was continued and a failure of the clevis occurred through the threaded piston rod hole. Fretting of the check nut against the clevis was the source of the failure. After failure of another cylinder barrel in pressure pulse testing it was concluded that the barrel is basically under-strength and it was redesigned by thickening the wall. Fabrication of new barrels is approximately 50% complete. The face of the check nut has been coated with aluminum bronze/Ekonol to prevent fretting. Fatigue testing was planned on a rebuilt damper, but was precluded by program termination.

The endurance test specimen completed the required 300 hours of cycling testing. External leakage from the bias piston area was in excess of specification allowables and damper force at low velocities was below specified minimums. Teardown inspection was accomplished and determination of required corrective action was in progress at program termination.

2.15.1.2 Swashplate Endurance Test

The two prototype configuration swashplates with 35% race depth bearings were completed and the test begun, using scissors and pitch links from previous tests. 111 hours of the 250-hour test were completed. All of the high load conditions were completed. All indicators, i.e., pressure indicators for cracks, temperature, and shock pulse, were normal.

2.16 DRIVE SYSTEM

The prototype drive system consists of engine, combining, and aft transmission and drive shafting designed and tested under the ATC program (Reference 6, ATC Final Report) and a forward transmission detail designed under the prototype program.

The forward transmission was identical to the aft in the rotor shaft, upper cover, rotor shaft support bearings, and first and second planetary stages. A new input bevel gear drive was required to accommodate the inclination of the forward transmission; this bevel drive duplicates the 2.86-to-1 ratio of the aft rotor transmission. The bevel drive required a lower case different from the aft to suit the forward shaft angles. The clearance envelope and other considerations also required a blower/cooler position different than the aft. This forced certain changes in the accessory drives. The lubrication and dianostic system was similar in concept and largely identical to the aft transmission. Further study of the forward transmission layout developed under the ATC program resulted in an improved design for the support of the spiral bevel gear. This design provided lower detail weights, improved rigidity in the mounting, and a significant decrease in the velocity of the support bearings.

Other major drive system work under the prototype program included the design and construction of a forward transmission load stand, design and fabrication of a test fixture for the rotor shaft fatigue test, and gear resonance tests.

The System Requirements Review was held on 13 March 1973.

2.16.1 Transmission Design

A change in the ATC transmission upper cover design was required to accommodate the revised swashplate actuator arrangement. This change consisted of providing two independent transmission-driven hydraulic systems at each rotor with each system powering one channel of three dual swashplate actuators instead of the six actuators previously selected. In addition, the ATC transmission design was modified to provide capability for oil-cooling the transmission driven electrical generators, rather than air cooling (ATC design).

Strengthened gears were designed and fabricated for the prototype transmissions. These gears include the following:

301-65004	Forward Bevel Input Pinion
301-65005	Forward Sun/Bevel Gear
301-10428	Aft Bevel/Input Pinion
301-10419	Aft Sun/Bevel Gear
301-10601	Combiner Collector Gear
301-10610	Combiner Slant Shaft Gear
301-10654	Combiner Helical Input Pinion
301-10677	Combiner Bevel Input Pinion

These gears were redesigned as a result of the ATC testing (static deflection, dynamic strain survey, and bench resonance). The new gears were designed to be as rigid as possible with excess material provided wherever practical. These baseline configurations were resonant tested using the air siren technique developed during the ATC test program. This testing was accomplished prior to grinding the gear teeth.

The forward input pinion siren tests and analytical predictions showed extremely good (within 15%) correlation of resonant frequencies. As predicted by analysis, there were no gear resonances in the operating speed range. Therefore, no change to the gear configuration was required.

The aft input pinion was also siren tested. Correlation with calculated frequencies was again excellent and no change in gear configuration was necessary.

The helical input pinion was siren tested for a second time. Results indicate several modes in close proximity to normal operating rpm. These modes involve relatively large displacements of the bearings and should therefore be well damped.

The combiner slant shaft pinion was siren tested. There were no gear resonances in the operating speed range. Correlation between analysis and siren test was extremely good, with an average error of 2.8% between test and analysis.

The combiner spiral bevel input pinion was also siren tested with similar results.

The prototype aft transmission design incorporated upper cover changes and generator oil cooling changes similar to those of the forward transmission.

No changes were necessary in the prototype combiner transmission design over that of the ATC design, except the gears noted above.

Changes in engine drive shaft length were necessitated by the decision to move the engines rearward.

2.16.2 Rotor Shaft Fatigue Test

The rotor shaft fatigue test fixture was designed and fabrication was completed. No testing was accomplished due to program termination.

2.16.3 Foward Transmission Test Stand

A load stand was designed for the forward transmission endurance test. Fabrication assembly and installation of the stand was 90% complete at program termination (Figure 124).

2.16.4 Forward Transmission Static Strain Survey

Bevel gears were instrumented and subjected to a static strain survey during June 1975. The bevel pinion had been used as a trial setup piece for machining and consequently had thin teeth. The measured stresses therefore required adjustment to allow estimation of stresses to be encountered (and remeasured) with full thickness gears. The results indicate that the capability exists to operate safely at 100% torque with the full thickness gears.

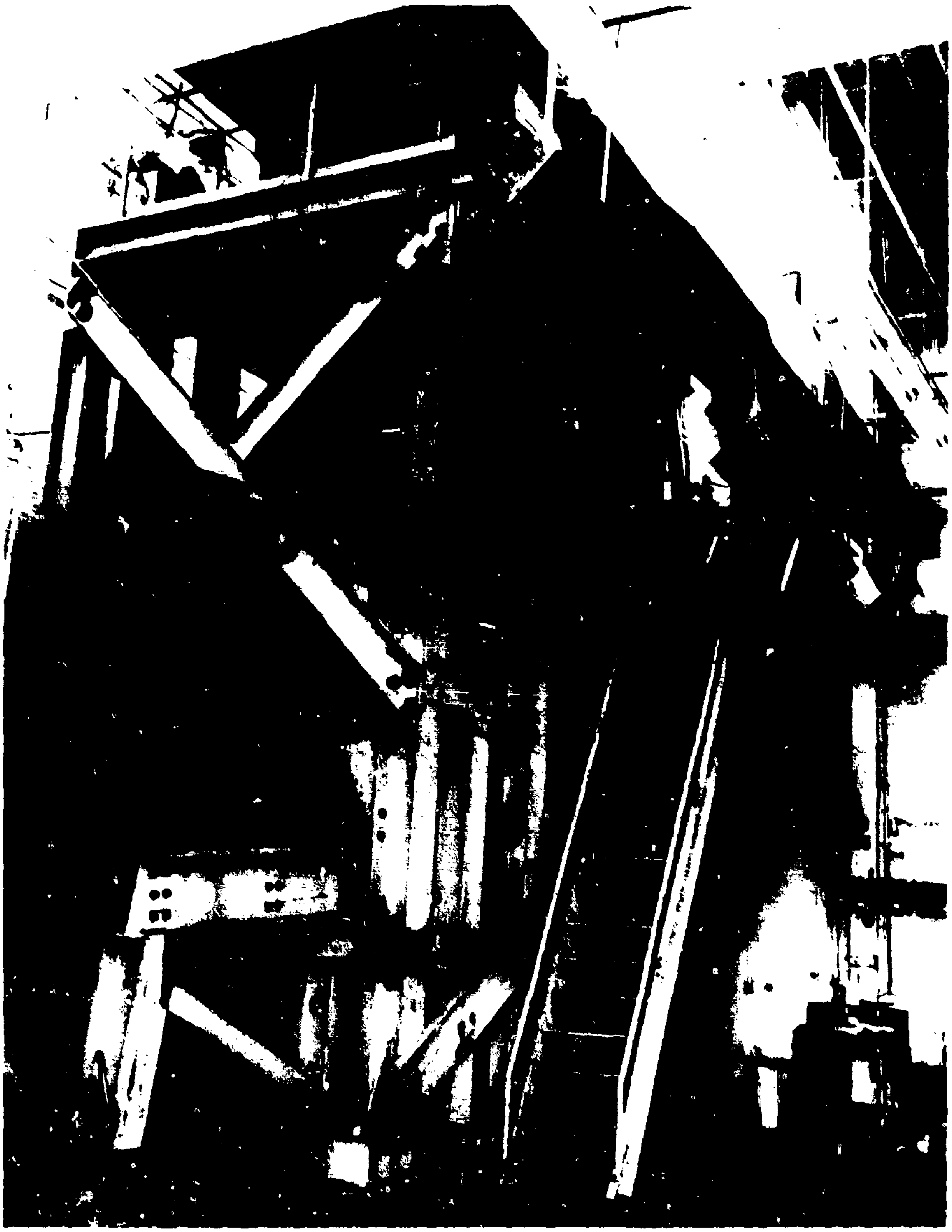

Figure 124. Forward transmission test stand.

2.17 CARGO HANDLING SYSTEM

The ATC-developed tandem dual cargo hook system (Reference 9, ATC Final Report) was provided to allow safe high-speed transport of externally suspended cargo. Load capacity and equipment were provided for 28-ton/2.5g tandem suspensions and 35-ton/2.5g single-point suspensions. Pneumatically powered signal conductor reels were provided to permit remote actuation of the two cargo couplings, by the normal and mechanical backup release modes. Controls and displays were provided for the pilots and load-controlling crewmen, to permit cargo handling operations, hook actuation, and load jettisoning at each cargo coupling independently or in unison, whether loaded or unloaded.

The initial concept omitted the pneumatic power to the hoists, to reduce program costs. Cable lengths were ground adjustable only. Late in the program, it was determined that the cost savings due to omission of power to the winches would be offset by increased flight test costs and operational problems. Therefore, pneumatic ducting was incorporated to power the hoists with engine bleed air.

The longitudinal span positioning system for the hoists was deleted, and a fixed span of 18 feet was selected. The physical ATC program hoists were used for the prototype. No new procurement was required and no testing was necessary.

2.18 FLIGHT CONTROL SYSTEM

2.18.1 Flight Control System Description

The prototype flight control system provides for stabilization and control of the aircraft via a triplex in-line monitored analog fly-by-wire Primary Flight Control System (PFCS) interfaced with a triplex digital Automatic Flight Control System (AFCS)(Figure 125). The PFCS is two-fail operative; the AFCS is fail operative/fail off.

The PFCS is the electrical analog of a conventional mechanical flight control system. The limited-authority AFCS provides for flying qualities enhancement. The helicopter can easily be flown without augumentation; hence the ultimate flight safety is vested in the PFCS. Prototype flight control system concepts have been flight demonstrated on the HLH/347 demonstrator (a modified CH-47 helicopter), as described in Reference 8. The PFCS is composed of conventional cockpit controls and a Direct Electrical Linkage System (DELS). The primary control path originates at the pilot control which drives multi-redundant motion transducers. The pilot control outputs are mixed in the linkage electronics and used to position the swashplates via servoactuators. Three swashplate servoactuators control swashplates at the forward and aft rotor (six actuators in all).

The stiffness of the swashplate actuator is modified by pressure feedback to damp 4/rev loads which occur with the onset of blade stall.

The AFCS consists of airframe motion sensors and processing electronics; its output interfaces with the DELS via a rate- and authority-limiting interface which is analogous to the series stability augumentation and trim actuators found in conventional helicopter flight control systems. The AFCS also provides a path for the aft-facing load-controlling crewman (LCC) to fly the aircraft via a four-axis finger ball controller. The LCC input is limited in terms of authority and rate and may be overridden by the pilot at any time. Finally, the AFCS provides commands to the force feel/control driver actuators. This input is used to position the pilot's control in response to LCC inputs and as an interface for other parallel stabilization inputs (such as altitude hold via inputs to the collective axis). Figure 126 shows the system equipment and interfaces.

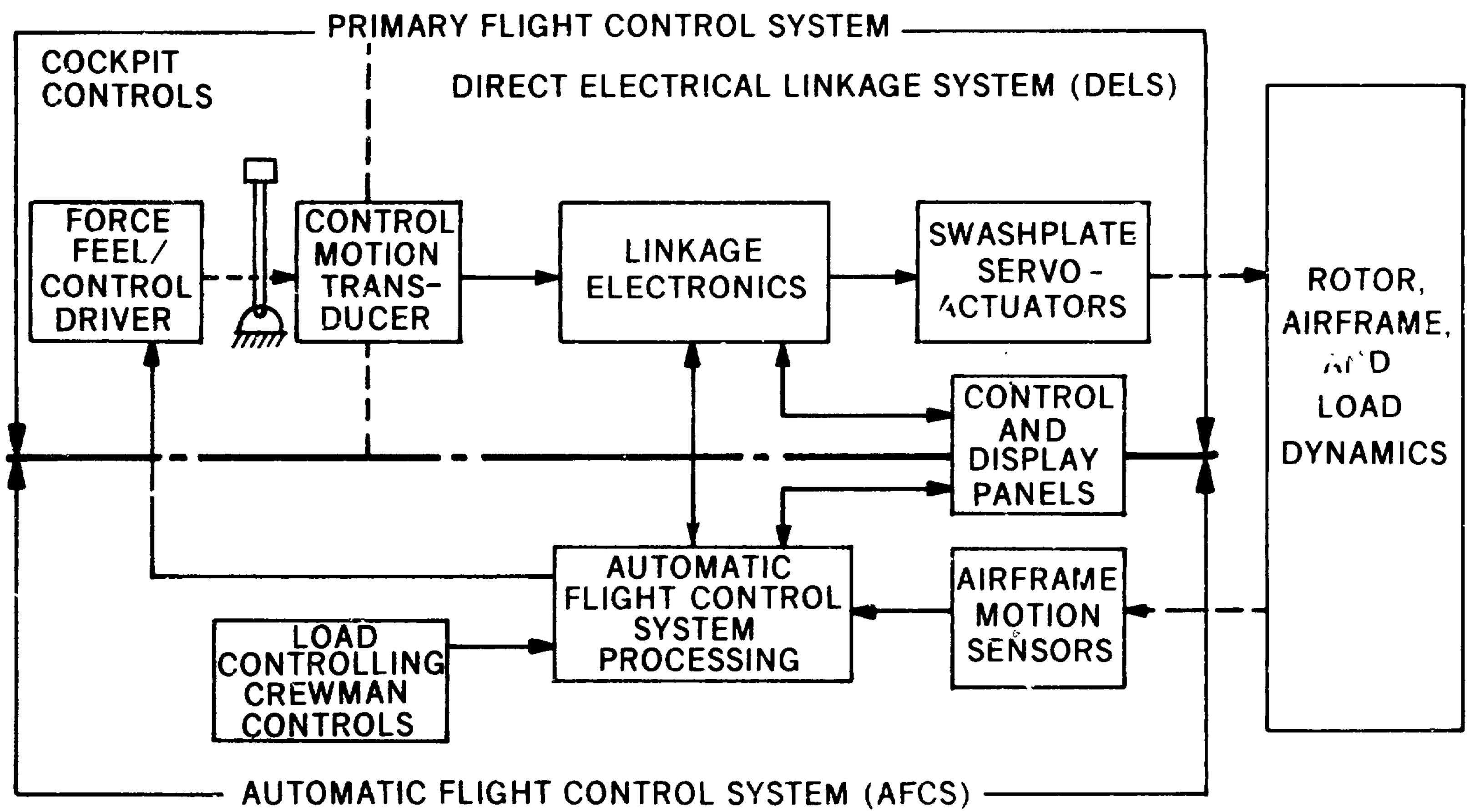

Figure 125. Flight control system schematic.

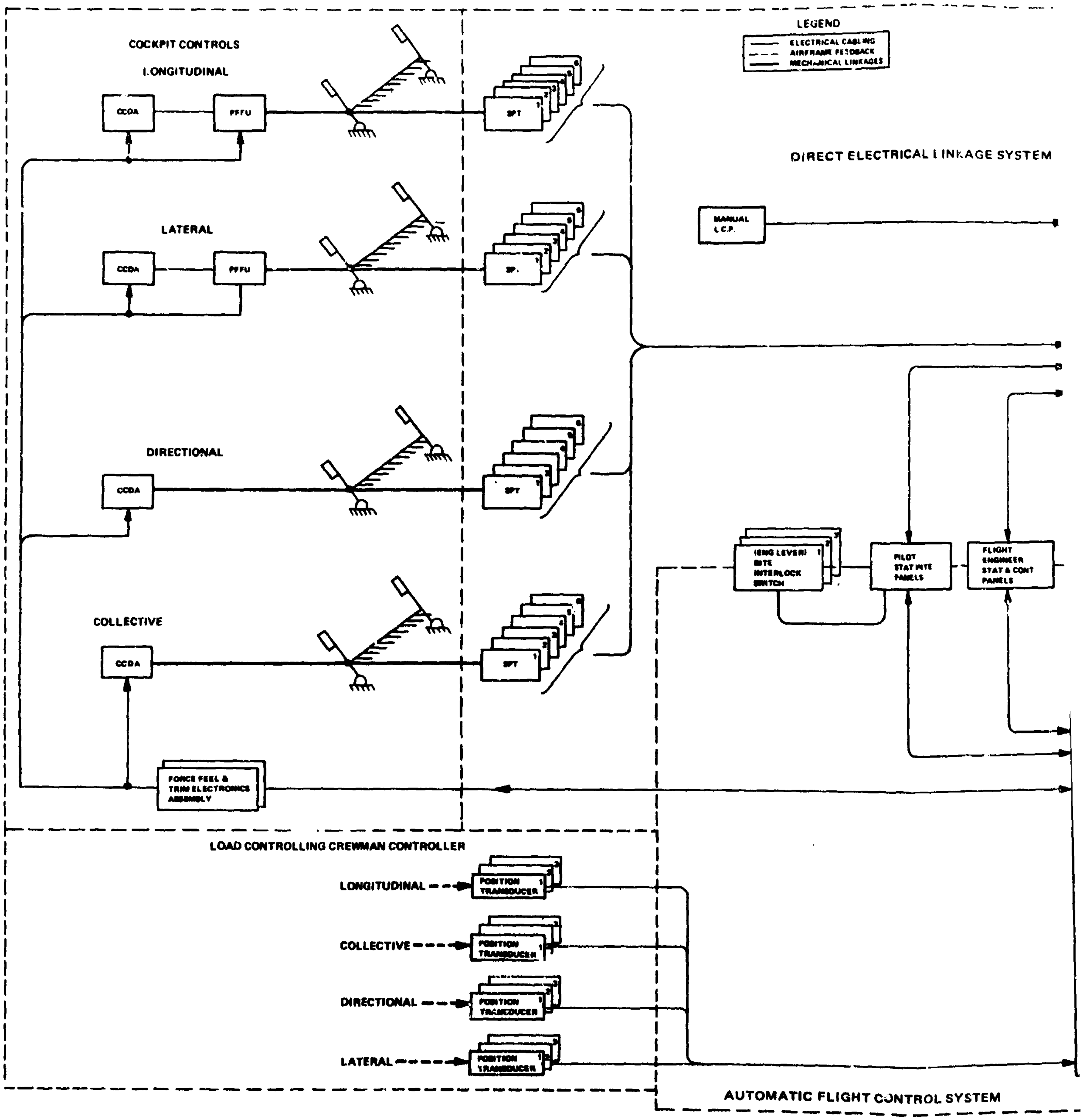

Figure 126. Flight control system equipment block diagram.

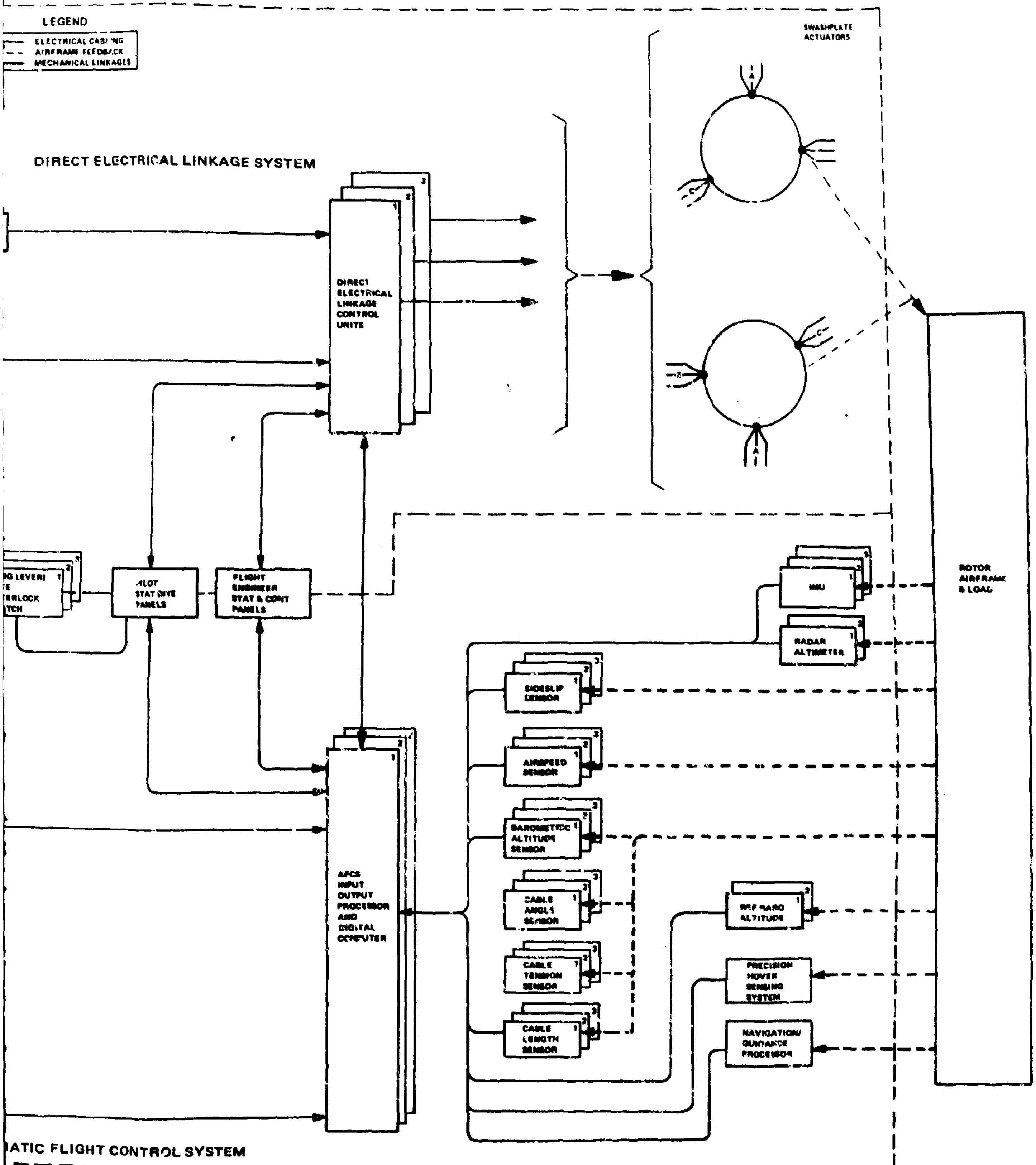
LEGEND
ELECTRICAL CABLING
MECHANICAL LINKAGES
SWASHPLATE ACTUATORS
DIRECT ELECTRICAL LINKAGE SYSTEM
DIRECT ELECTRICAL LINKAGE CONTROL UNITS
FLIGHT ENGINEER STAT & CONT PANELS
ROTOR AIRFRAME & LOAD
IMU
RADAR ALTIMETER
SIDESLIP SENSOR
AIRSPEED SENSOR
BAROMETRIC ALTITUDE SENSOR
CABLE ANGLE SENSOR
CABLE TENSION SENSOR
CABLE LENGTH SENSOR
ALTITUDE
PRECISION HOVER SENSING SYSTEM
NAVIGATION/ GUIDANCE PROCESSOR
AFCS INPUT OUTPUT PROCESSOR AND DIGITAL COMPUTER
ATIC FLIGHT CONTROL SYSTEM

2

2.18.2 Development Approach

A substantial portion of the AFCS equipment developed during the HLH Advanced Technology Component (ATC) program was utilized for the prototype. The PFCS employed cockpit controllers and force-feel actuation developed in the ATC phase and the DELS was based on the ATC concepts. New hardware, in particular integrated swashplate servoactuators, was developed for the prototype.

The emphasis of design activities for the prototype aircraft was placed on the DELS. The AFCS and cockpit controls hardware was modified only to the extent necessary to correct deficiencies found in the ATC phase and to delete functions not required for the austere prototype aircraft. The AFCS software package was modified to reflect the characteristics of the prototype aircraft; since the 347 demonstration characteristics closely match those of the prototype, the changes required were not extensive.

2.18.3 Primary Flight Control System (PFCS)

Figure 127 is a block diagram of a single channel of the primary flight control system. The single channel will be described first and redundancy impacts will be discussed later.

Cockpit Controls. The pilot interface is a set of conventional helicopter controls which have been designed to minimize vulnerability to battle damage and maintenance error. Pilot and copilot controls are coupled directly to large diameter torque tubes which drive dispersed redundant control-motion transducers for each axis. Integrated variable force-feel and control-driver actuators are also connected to the torque tube. Jams of motion transducers or force-feel devices are cleared by shearable connections at the torque tube. Each torque tube has a redundant support so that control is maintained in the event of loss of a support.

The use of separate multiaxis controllers for the pilot and copilot was considered but rejected because of the increased complexity of the system, increased cost, the larger volume required, and the additional weight needed to duplicate input transducers and force-feel and to provide synchronization between pilot and copilot controls. Such controllers are more suitable for a single-pilot vehicle. A four-axis controller is used at the HLH load-controlling crewman's station.

Signal Flow. Both cockpit controls and the AFCS generate command signals in collective pitch, longitudinal, lateral, and directional axis. In addition, the AFCS makes an input to control longitudinal cyclic pitch; this input is programmed with airspeed.

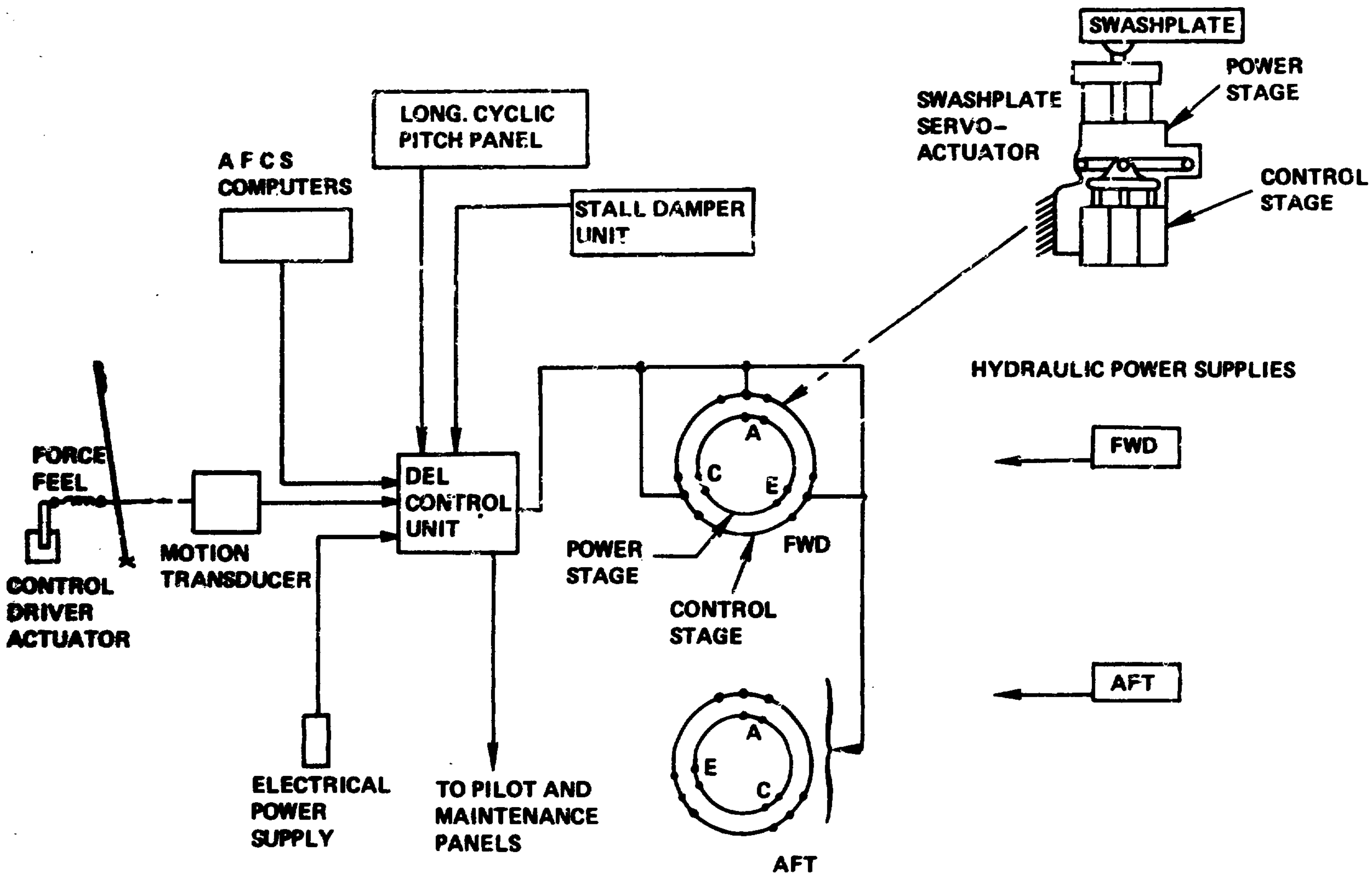

Figure 127. Primary flight control system – simplex block diagram.

The DEL control unit electronically provides for mixing of the axis inputs, signal limiting, and control of the swashplate servoactuator. Figure 128 shows the detail of signal mixing within the control unit.

Control motion transducer signals and AFCS signals are summed. (In the conventional helicopter system this function would be accomplished by a series actuator.) At a second stage of mixing, the axis inputs are summed and limited. This limit fixes the total collective pitch travel and cumulative lateral tilt inputs at the swashplate. Finally, the commands to each actuator are summed through gains and limits appropriate to the actuator azimuth location. The cumulative axis and actuator limits are sized to provide necessary control authority while avoiding overtravel interferences in the rotor controls when the controls are "boxed" on the ground.

Swashplate Servo Actuator. Each swashplate is supported and controlled by three servoactuators which are almost equally spaced in their azimuth locations. Each actuator has a control stage and a power stage which are combined in an integrated design. The following paragraphs discuss the swashplate actuator servo loops and provide details of the actuator configuration.

Figure 129 shows the details of the control unit/actuator interface. When the actuator is at the desired position, the power position motion transducer voltage equals the input command and the control position motion voltage is zero. If the input changes, the control stage piston assumes a position proportional to the error between input and output position. The power stage valve then meters flow to produce the desired velocity, and when the input stops changing, a new equilibrium condition is achieved.

The two-stage design effectively decouples control and power stages so that system redundancy may be achieved without a mismatch in the high force power stage of the actuator.

This configuration was selected after consideration of a separated power actuator concept in which six single actuators were force summed through the swashplate. Three of the actuators would provide support for static loads while the remaining would be on line, ready to assume control in the event of a failure. All six would support the dynamic blade loads. The configuration would allow for open failure of any one actuator without loss of control.

This scheme was rejected because if hardover failure occurs under adverse load conditions, the actuator must be shut down on a timely basis or control will be lost.

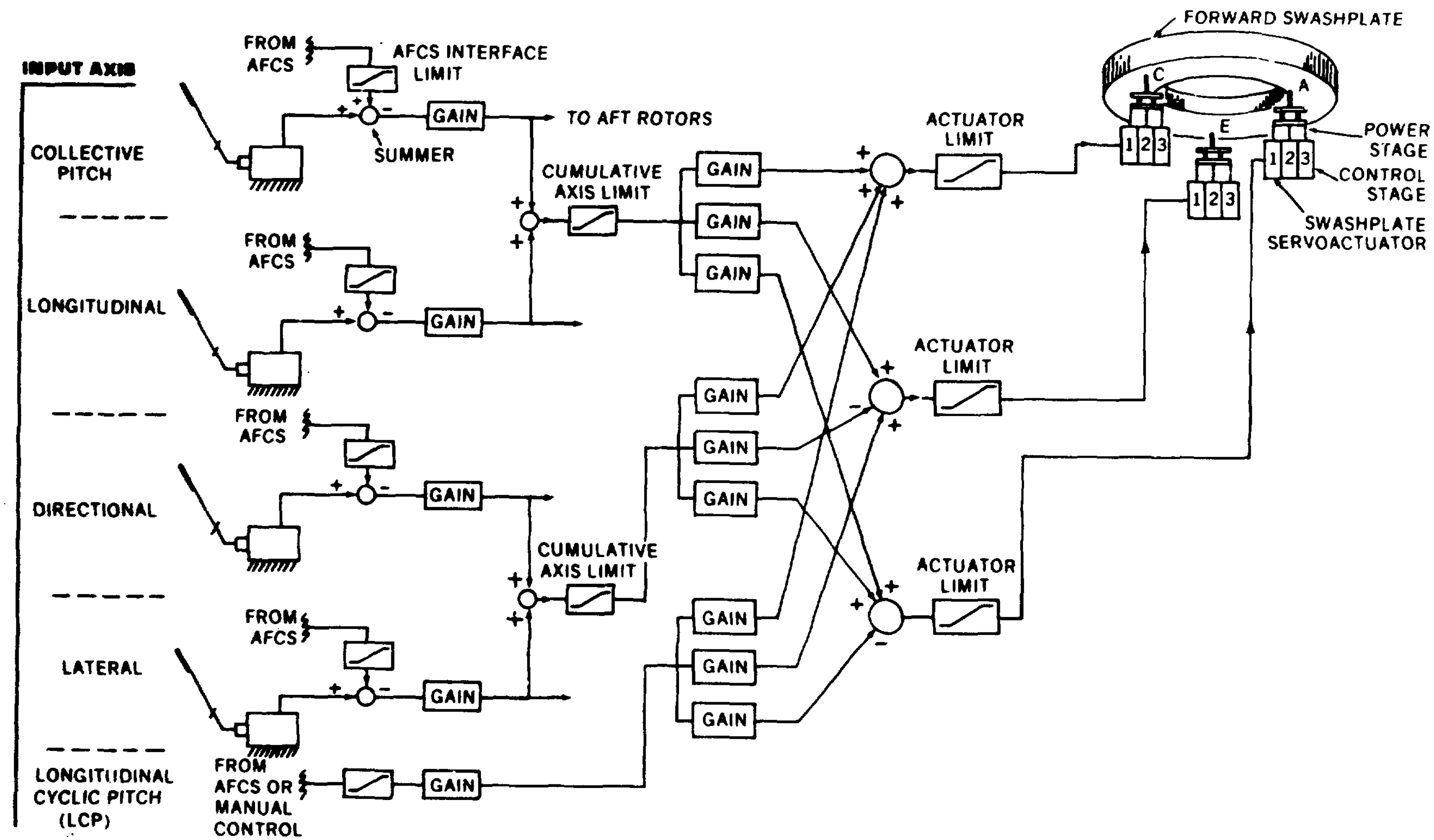

Figure 128. Signal flow to forward rotor head (Channel 1).

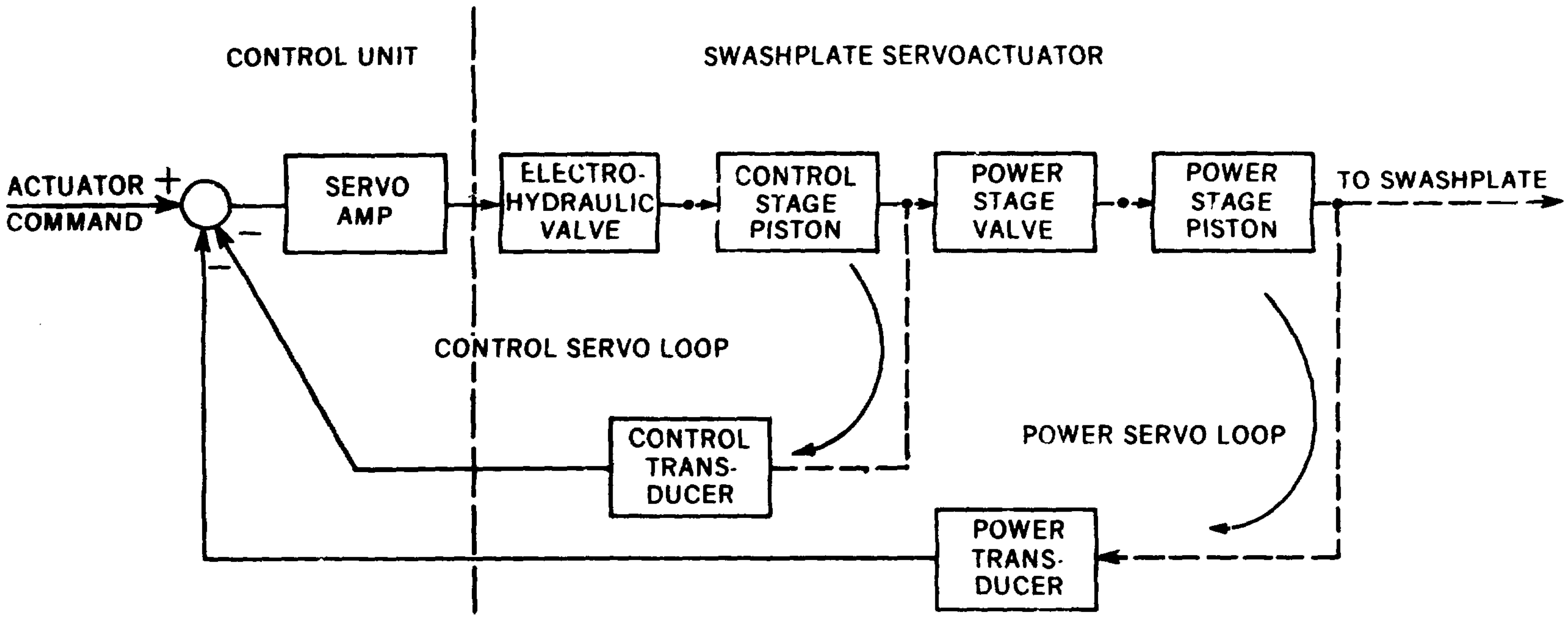

Figure 129. Control unit/actuator interface.

The selected integrated actuator concept allows for electrical compensation of actuator characteristics to modify actuator/rotor system interfaces, if required. It also allows for ready adaption of the scheme to any aircraft having a power-boosted control system.

Figure 130 is a top-level schematic of the swashplate servo-actuator. The dualized power stage is rated at 30,000 pounds stall force, has 15 inches of stroke, and a no-load velocity capability of 10 in./sec. The three-piston design precludes eccentric loading of the remaining channel when one system is shut down.

Velocity of the power stage pistons is controlled by a conventional flow control servovalve. Motion of the power stage servovalve is determined by a linkage which is positioned by control stage pistons; one control stage is normally in command, while the others are ready to assume control in the event of a failure. Management of the three channels is discussed in the following section.

Linear variable differential transformers (LVDT) are provided for measurement of power and control stage motion. These are used to close the power and control position loops. A separate position feedback is provided for each channel. The power stage load transducers are used to produce stall damping inputs. (Details of the stall damper are discussed later).

Figure 131 shows the detail of one of the control stage servos. The electrohydraulic valve (EHV) moves the control piston at a rate proportional to input current. It incorporates a second-stage monitor LVDT for failure detection. The differential pressure/bypass valve measures control stage force output and also provides bypass of the cylinder to minimize loading of the remaining channels when the channel is shut down. The three-way valve removes pressure from the unit at the command of failure detection circuits. DC voltage is applied to the valve to engage the actuator. The check valve in the return passage enables isolation of return passage leakage in the control stage so it does not result in loss of hydraulic fluid.

Power Supplies. Electrical power for the system while inflight is provided by three small dedicated 28-vdc permanent magnet generators. Ground operation is provided by switchable connections to the aircraft buses. Battery backup for startup and shutdown is provided by connection to the aircraft battery and inertial measuring unit batteries. Power conversion units within each control unit produce excitation for transducers and dc voltages for operation of integrated circuit elements.

Dual hydraulic power supplies (Figure 132) are located at each

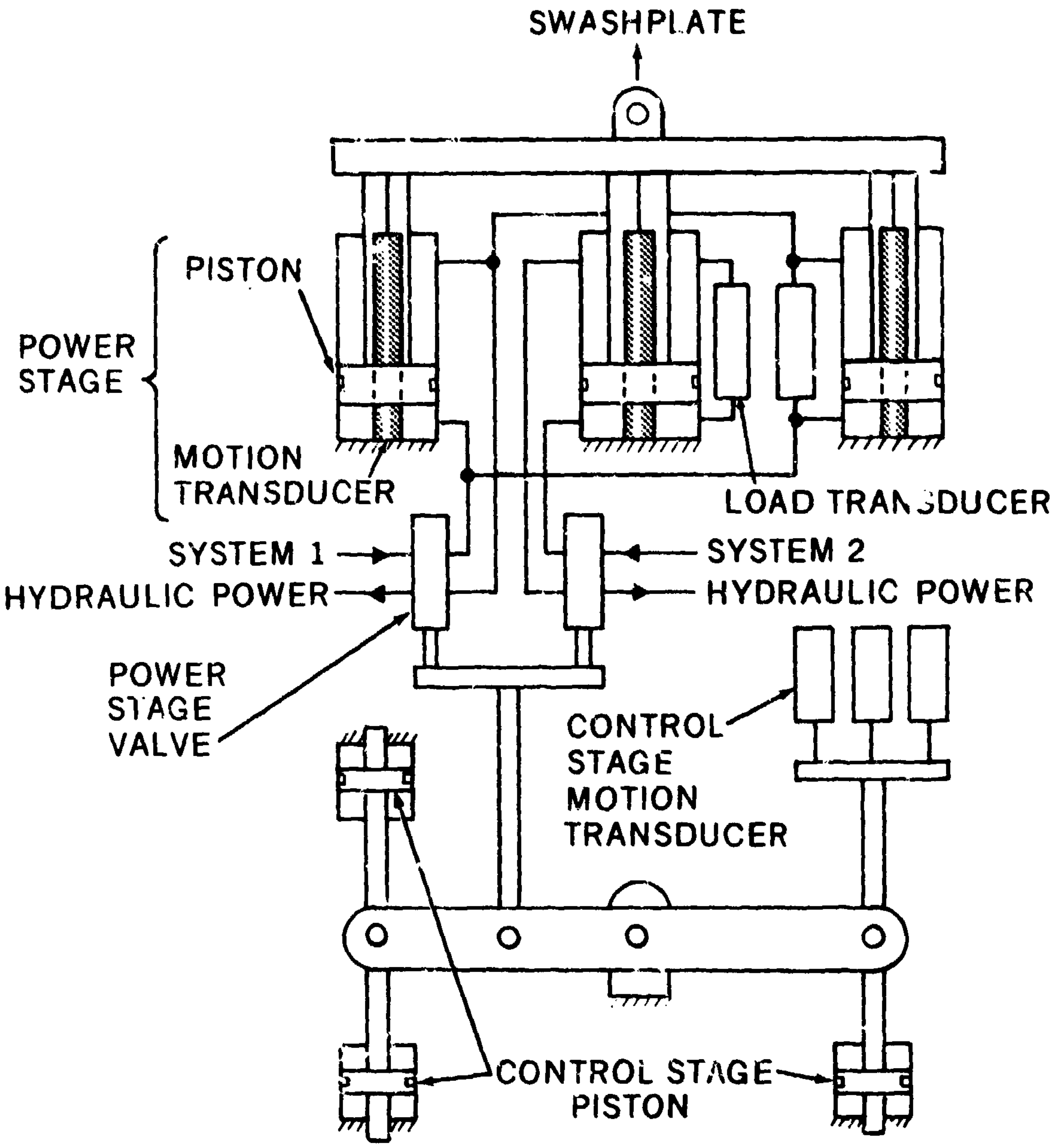

Figure 130. Swashplate servoactuator schematic.

311

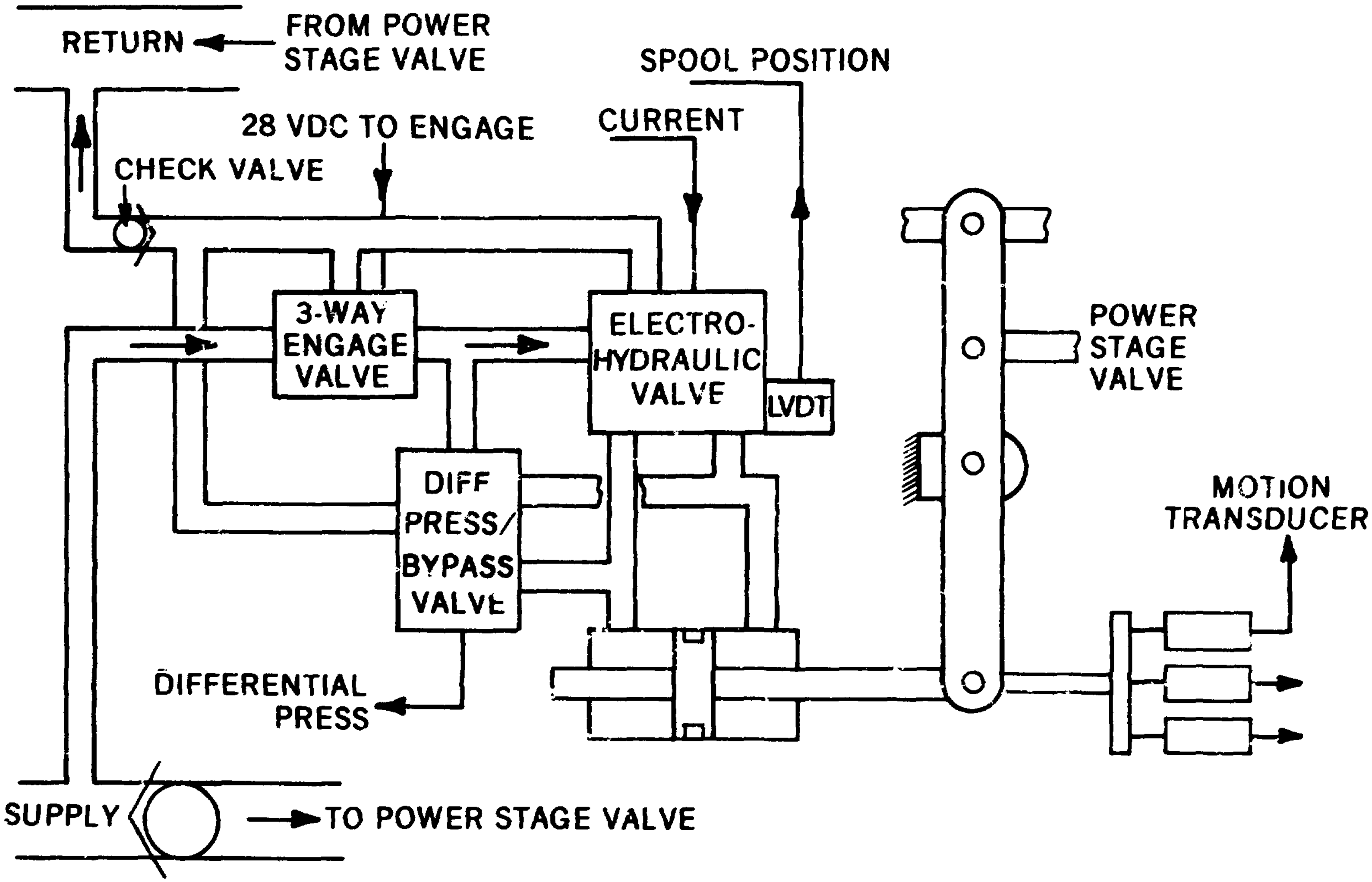

Figure 131. Detail of control stage.

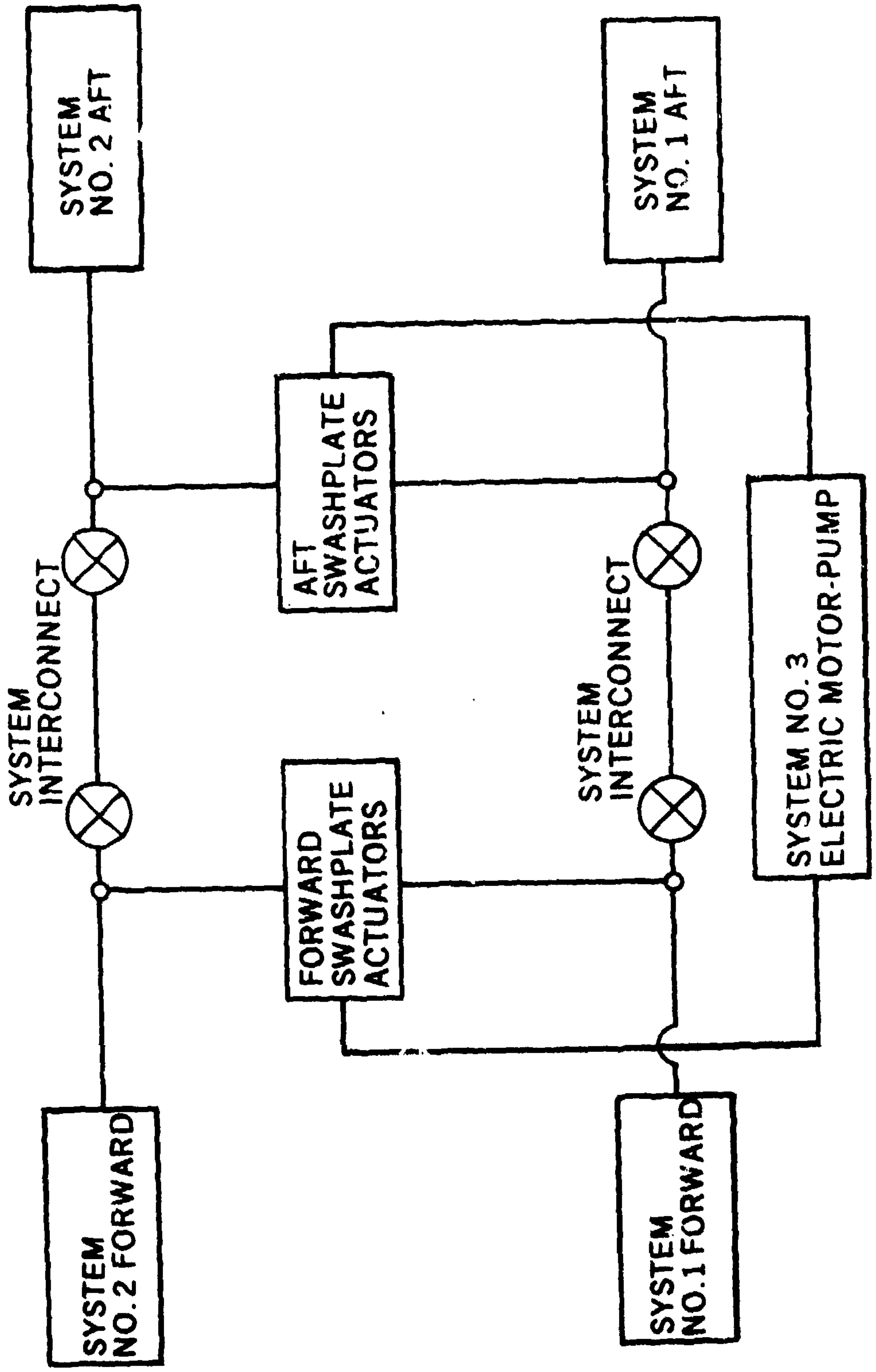

Figure 132. Flight control hydraulics.

rotor, and a motor pump supplies the third control stage. A normally depressurized interconnect between forward and aft hydraulic systems provides backup for supply failures. The aircraft is flyable with any one of the four rotor supplies operational.

2.18.3.1 Redundancy Management

Since no single electrical control path can provide the reliability desired for the primary flight control system, multiple channels must be employed. Success in the management of these redundant channels is the key to success of the fly-by-wire system.

An initial study in the HLH/ATC program resulted in the selection of a triplex, in-line monitored, active/on-line redundancy management mechanization; it incorporates the best features of the two commonly used actuator control concepts, namely, active/standby and force summation.

The means used to detect failures in the system, to compensate for mistrack between the three channels, and to provide protection for AFCS failures are discussed in the following paragraphs.

Failure Detection. The redundant system (Figure 133) is configured with three in-line monitored channels; that is, each channel has two signal paths (called active and model) whose performance is compared at various points to detect failures. After each signal comparison, the outputs of the two paths may be averaged to reduce buildup of tolerances. If the difference between the channels exceeds a prescribed threshold, the control stage section is shut down. Since each channel detects its failures independently, a failure in one cannot affect the others. For example, Figure 134 shows the way that failures at the system inputs are detected.

The dual signal path is carried to the control stage electrohydraulic valve input; thereafter, detection of actuator failures is accomplished by input/output monitoring of the actuator elements. Failures in the control stage electrohydraulic valve are detected by comparing input current to valve spool position. These should be linearly related in the steady state. The difference between these parameters is filtered to account for valve dynamics before input to shutdown logic.

Electrical failures in the control stage motion and differential pressure transducers and in the power stage motion transducer are detected by monitoring the sum of the LVDT secondary voltages. If operation is normal, this sum should be nearly

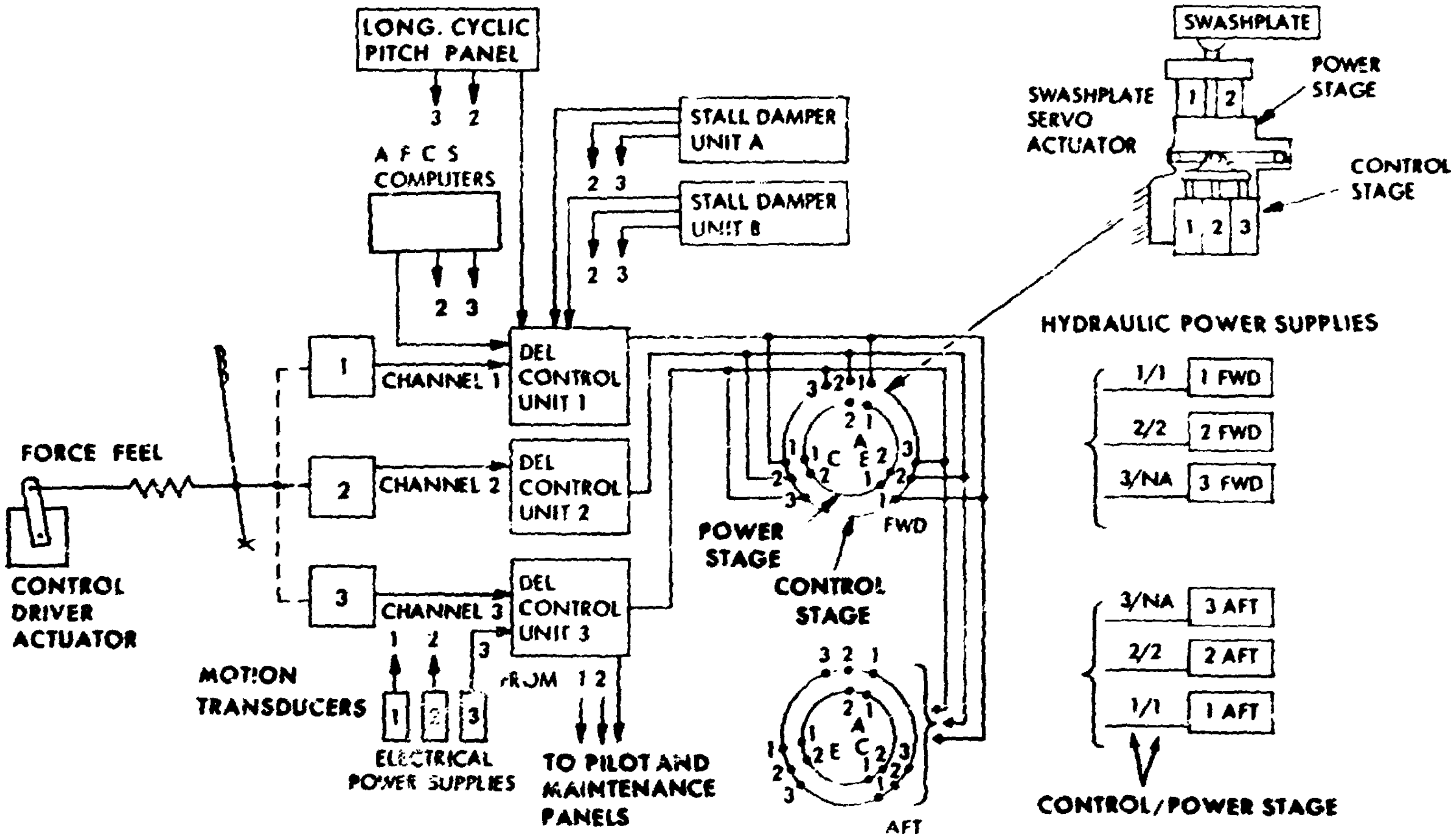

Figure 133. Primary flight control system block diagram.

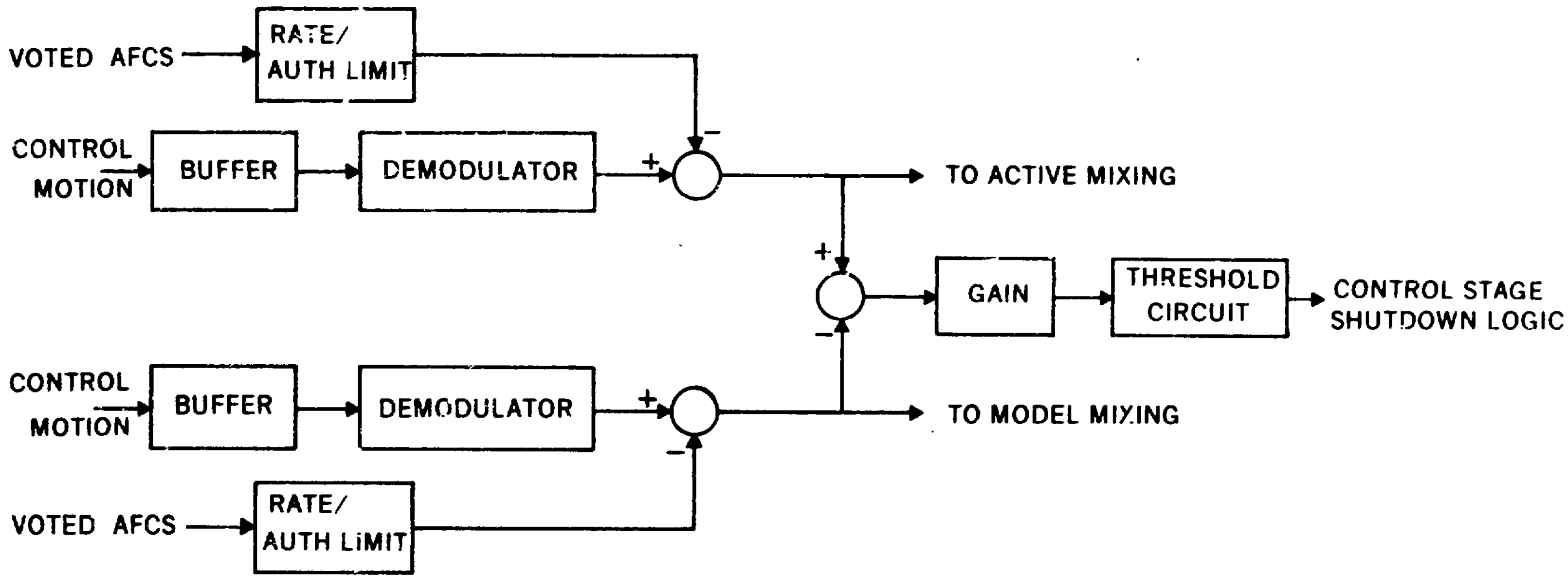

Figure 134. Input failure detection.

constant over the LVDT stroke. If the primary or either secondary is opened, the voltage goes down. If there is a short from primary to secondary, the voltage changes. When the voltage deviates more than the amount allowed by normal tolerances, the associated actuator control stage is shut down.

Electrical power supplies are monitored so that loss of any one will cause shutdown. Failure of a hydraulic supply is detected when the differential pressure/bypass valve goes to the bypass position. At this point, the signal goes beyond its normal dynamic range. This is interpreted as a failure by the electronics.

Interchannel Compensation

This section discusses the methods by which the independent channels are made to work together without a force fight at the actuator.

The force outputs of the three control stage channels come together at a lever which controls the power stage valve. Since each channel has its individual gain tolerance, each would like to position the lever in a slightly different position. If no compensation for this condition is made, the channels would oppose each other, and there would be a hysteresis or dead-band effect in the actuator response. To overcome this condition, two of the three control stages incorporate differential pressure feedback, as shown in Figure 135.

One channel is preprogrammed to be active and to control the actuator response; in the event of its failure, a second becomes active; in the event of its failure, the third channel becomes active. If a channel is not active, it is on-line and has its differential pressure feedback loop closed. Under this condition, the force output of the channel is approximately zero in the steady state. The channel tracks the active channel. (In this respect, the configuration is like an active/standby system.) The limit in the feedback path restricts the amount of compensation allowed to that required for the predicted worst-case mistrack between channels. If the active channel should fail and attempt to move the piston, the on-line channels will fight the motion after the limit is reached. (In this respect, the configuration is like a force-summed system.) In addition, the lag filter is in the differential pressure feedback for abrupt failures of the active channel, so they will fight immediately without any motion of the piston. The force summation provides for arresting a first failure without need to switch out the failed channel. Under normal conditions, however, the failure is switched out by the channel failure detection, as described in the previous section.

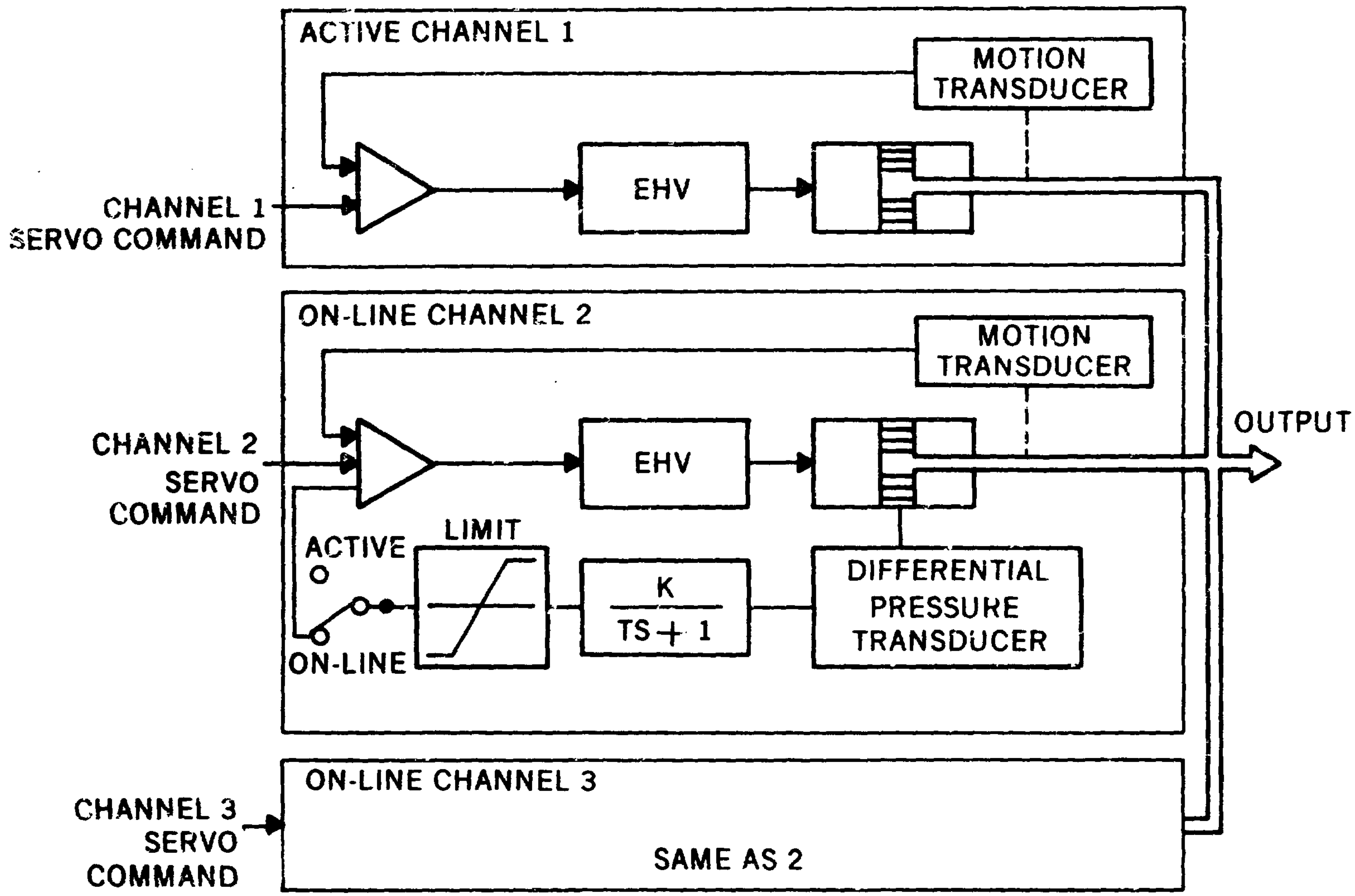

Figure 135. Active/on-line actuator control concept diagram.

Switching of the differential pressure feedback paths is accomplished by exchange of failure information betwe... channels. This is the only electrical connection between the channels. Communication of failure signals is controlled in the interchannel wiring, so that the identical control units assume their active or on-line status as a function of position within the system. Proper communication of failure information is displayed on a status panel.

Coordination of the dual power stage actuator force outputs is achieved by matching of the power valve characteristics. The dual power stages cannot force fight; therefore, only a passive failure such as power-supply loss is possible. With backup for hydraulic supply failures as shown in Figure 132, a dual power stage is adequate to meet the system reliability goals.

2.18.3.2 AFCS Interface

The AFCS interface couples the triplex digital AFCS into the primary linkage and limits response to AFCS failures which occur downstream of the AFCS failure detection, so that the AFCS cannot jeopardize flight safety. Figure 136 is a block diagram of the interface. At the voter, the signals are compared two at a time to detect failures. After a channel has failed, its selection as the voted output is inhibited, and a first failure indication is sent to the caution advisory panel. The voter also selects the median signal as the output. On second failure, the voter commands that a fixed reference voltage be selected as the output and an AFCS off signal is sent to the caution advisory panel.

After voting, the signals are passed to a velocity/authority limit network. This network limits the downstream response to multiple AFCS inputs. Abnormal triplex inputs could occur through error in programming the gain or phasing of the AFCS sensor inputs. In this case, all three computers would have the same response so there would be no voter shutdown. The limit network has a low authority path with direct access to the downstream system; it also has a higher authority path with a rate limit which permits slow input of the signals necessary for trim compensation. The output of the rate limit network is subtracted from the low authority limit input so that the low authority path output is normally at zero in the steady state. The circuit is analogous to the combination of stability augmentation and series trim actuators used in existing helicopters.

First failures are switched out with no transient; on second failure, trim inputs are ramped out at a slow rate. Limits have been established so that the pilot has at least a one-second delay following triplex failures and adequate control margin to fly without switching out the AFCS hardover.

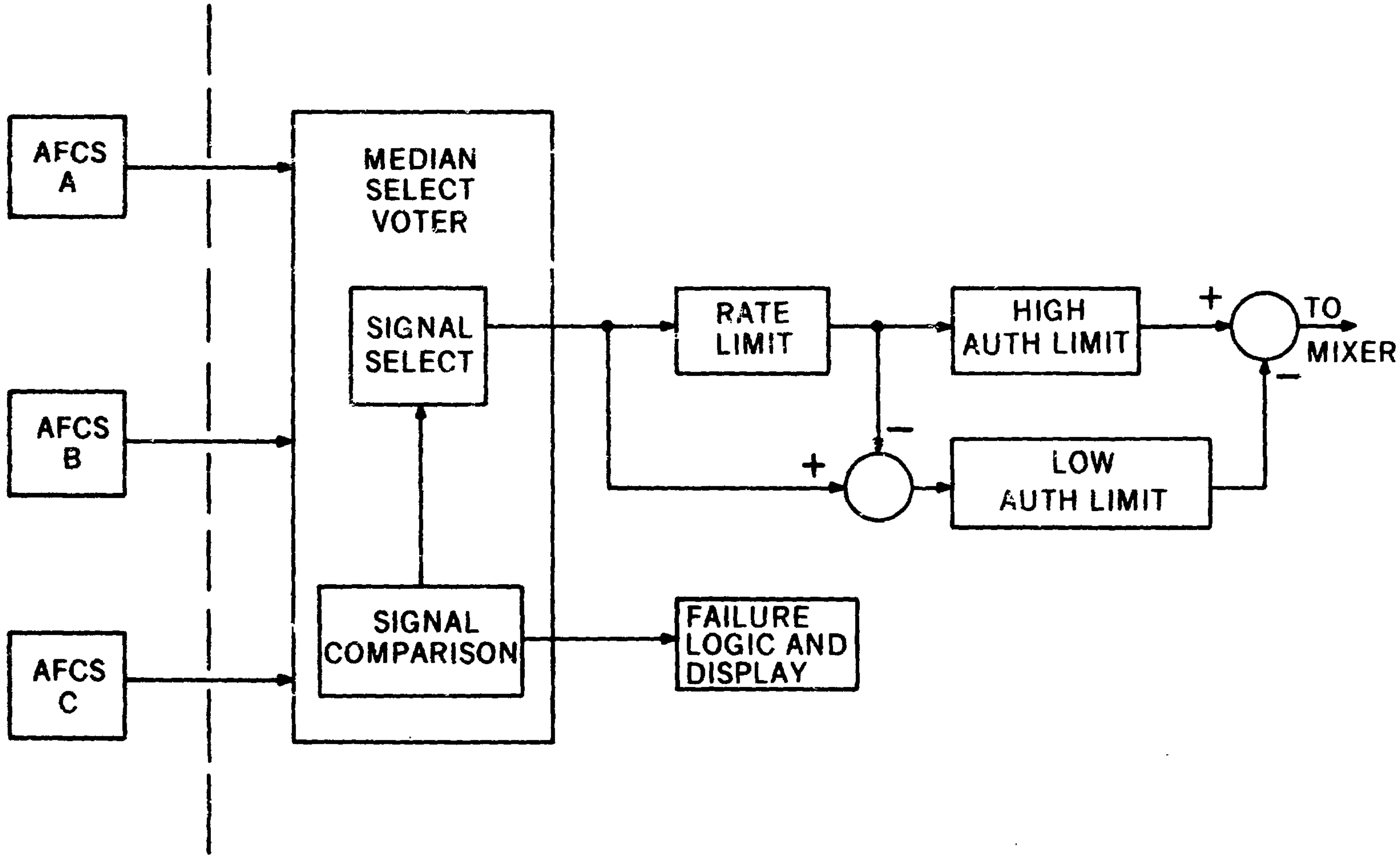

Figure 136. DELS/AFCS interface.

To assure synchronization between the three DELS channels a shutdown command is sent back to AFCS, so that when AFCS is shut down in any one channel, the AFCS initiates shutdown in all channels.

2.18.3.3 Stall Damping

Power stage differential pressure is fed back to the servo input to reduce loads in the rotor system which arise from rotor blade stall-flutter torsional modes. These occur at high airspeeds and in maneuvers. During stall-flutter conditions, alternating loads are transmitted across the swashplates to the supporting actuators at a frequency of four times per rotor revolution.

The 4-per-rev impedances of the actuators are set by networks in the differential pressure signal paths to provide attenuation for the stall-flutter loads. Figure 137 shows the predicted actuator stiffness as a function of frequency. Restricted authority is allocated to the signals to limit hydraulic flow capacity required.

The stall damper is mechanized in duplex form, separate from the DELS. Failures are detected by signal comparison at the DELS interface. A load monitor is incorporated as part of the stall damper electronics. If the load sharing between the two power stage systems differs by more than an allowed threshold, an indicator located on the stall damper control unit is tripped and latched as a maintenance display. This avoids continued operation of an actuator at loading conditions which could affect its fatigue life.

2.18.3.4 Built-In Test

Each control channel contains a preprogrammed built-in test sequence which, when armed and initiated, sequences through thirty tests designed to verify that the failure detection circuits can detect a failure. The automatic sequence takes about 25 seconds per channel. A typical test might be: insert a failure in the active longitudinal input causing a difference between the active and model channels to verify that the actuator shuts down and indicates a failure. During the test, all failure monitors are made to operate. There is no perceptible motion of the actuator during the test.

The second part of built-in test is the boxed-controls test. During this test, the system controls are manually positioned to bring each of the swashplate servoactuators near its full travel. Tracking of the channels is verified by monitoring the control stage differential pressure transducers of the on-line channels. The boxed-controls test provides a comparison across channels as part of the ground check. This test complements the in-line monitoring provided by the fault detection.

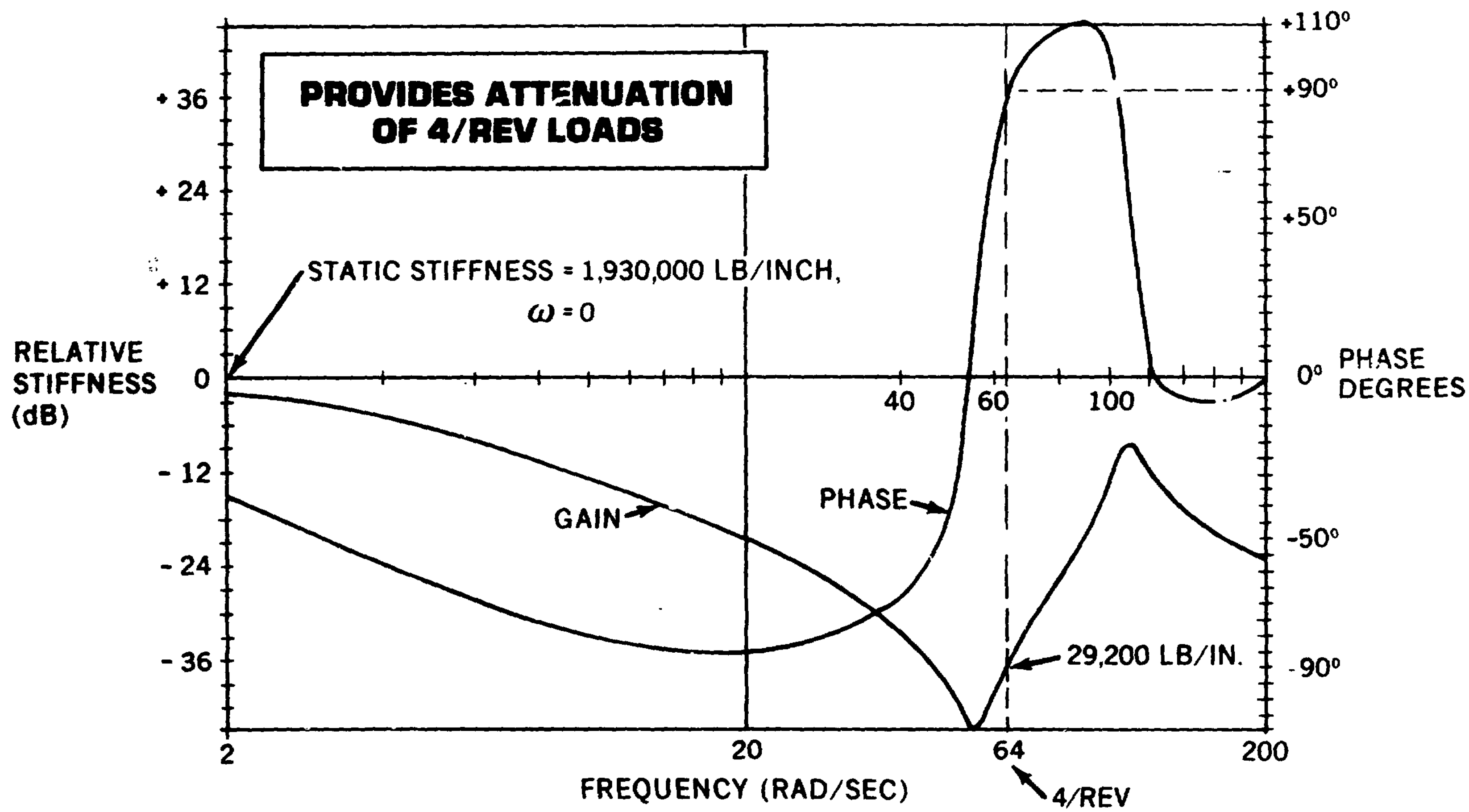

Figure 137. Predicted swashplate servoactuator stiffness.

The final part of the built-in test is a dynamic check of the stall damper function. A simulated 4-per-rev signal is applied to each of the stall damper input circuits. Any failure in the stall damper control units or input circuitry will cause a disagreement at the channel input and a failure indication.

2.18.3.5 System Specifications

Primary flight control system specifications are summarized below. References 21 and 22 give detailed specifications for the DELS and swashplate servoactuator.

• Gain Accuracy	- within 2% of nominal
• Null Offset	- 0.4% of actuator full stroke
• Resolution	- 0.04% of actuator full stroke
• Hysteresis	- 0.08% of actuator full stroke
• Bandwidth	- 48 rad, second order, 0.6 damping factor
• Failure Transient	- 0.1g maximum at cockpit
• Flight Safety Reliability	- 0.9999999 probability of completing a 2-hour mission without loss of function
• Electronic Design	MIL-E-5400P
• Hydraulic Design	MIL-H-5440E, MIL-H-5503C

Gain accuracy and null offset directly affect the match between channels and therefore are strongly related to allowable failure transient. As noted above, the HLH specification limits response to 0.1g at the cockpit. This tight specification results from the need to minimize load disturbance when working in confined areas. If larger disturbances were allowed, gain and null accuracies could be relaxed.

2.18.3.6 Hardware

Electronics

Control units are shown in Figure 138. Both units represent a prototype configuration. They employ relatively large single-side circuit cards which have ample space for modification to suit the developmental program. Circuits are conservatively designed and provide flexibility to change gains easily; they employ circuit and logic elements which have proven reliability. An eventual production unit will employ high density packaging in a hard mount configuration. Size and weight would be reduced accordingly.

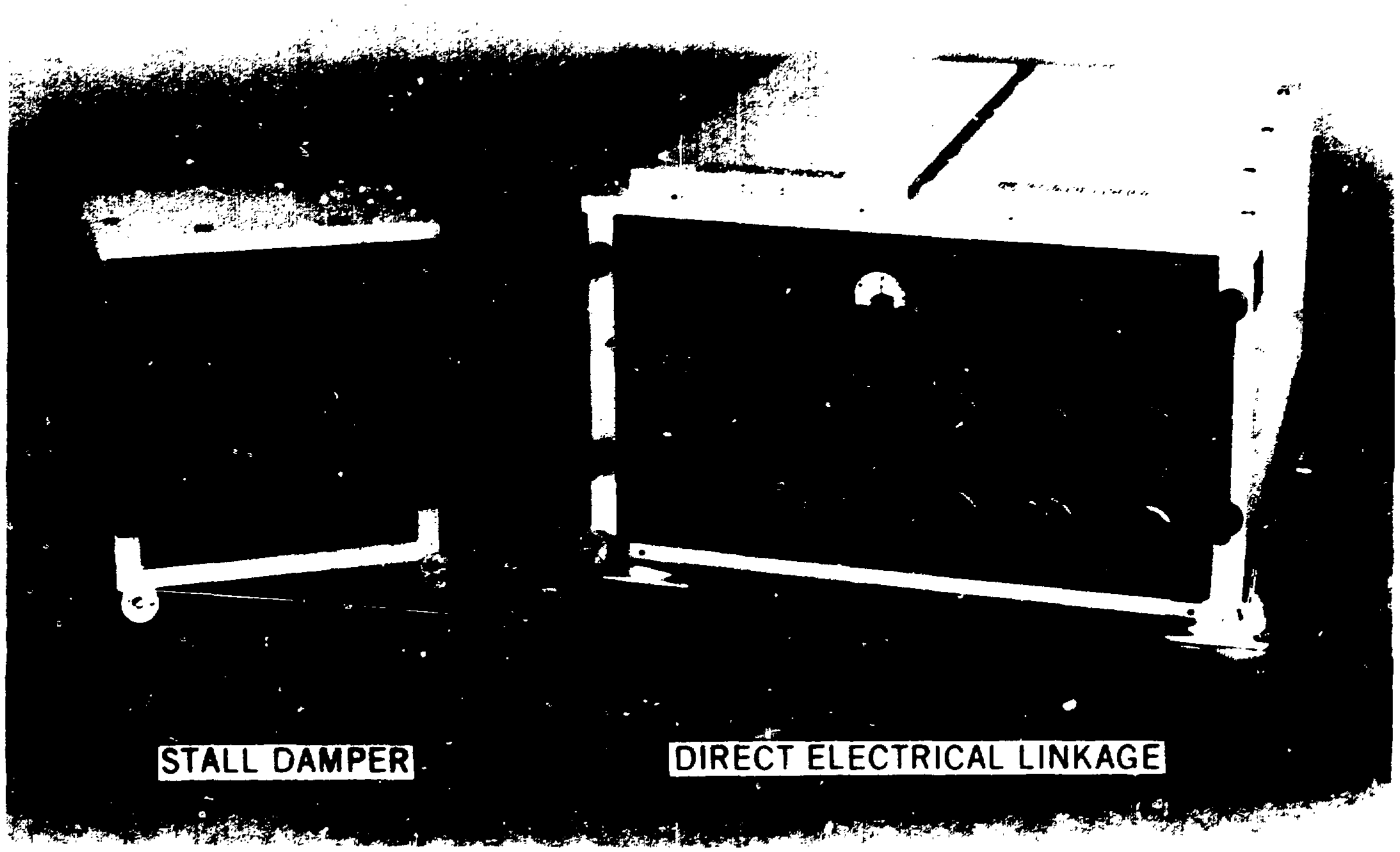

Figure 138. Primary flight control system electronic control units.

The system control panels are shown in Figure 139. The panels perform the following functions:

- Built-in Test - Provides a means for selecting the test to be performed; displays test pass/fail status and test number.
- Failure/Status - Displays detail on failure location and active channel status.
- Monitor Panel - Displays channel failures and provides for channel reset and built-in test arm function.
- Longitudinal Cyclic Pitch Panel - Allows selection of operating mode and provides manual input controls.

These panels represent a prototype approach and are well suited to the technical development stage of the program. In production, these functions will be combined into a single multifunction built-in test/reset panel located in the cockpit. Detail failure enumeration would probably be eliminated in favor of an indication on the control unit displaying the line-replaceable unit to be replaced. The electronic units were designed and built by the Aircraft Equipment Division of General Electric at Binghamton, New York.

Swashplate Servoactuator

The integrated swashplate servoactuator is shown in Figure 140. The pins at each side of the actuator mate with a two-axis gimbal which is attached to the transmission. The actuator is a prototype configuration. A production design would be revised to increase survivability by adding features such as jam-proof power stage valves and shearable piston heads. The swashplate servoactuator was designed and built by the Bertea Corporation, Irvine, California.

Cockpit Controls

The cockpit controls system was developed as part of the HLH/ATC program (Figure 141). Control linkages were designed and built by Boeing Vertol Company. Integrated variable force feel/control driver actuators and the associated electronic units were designed and built by Honeywell, Incorporated, Minneapolis, Minnesota. The variable force-feel actuators for the prototype were based on the ATC design except that the prototype units were designed to have a fixed-feel characteristic. The system was also modified to bring it up to flightworthy status and to correct problems uncovered in the ATC evaluation.

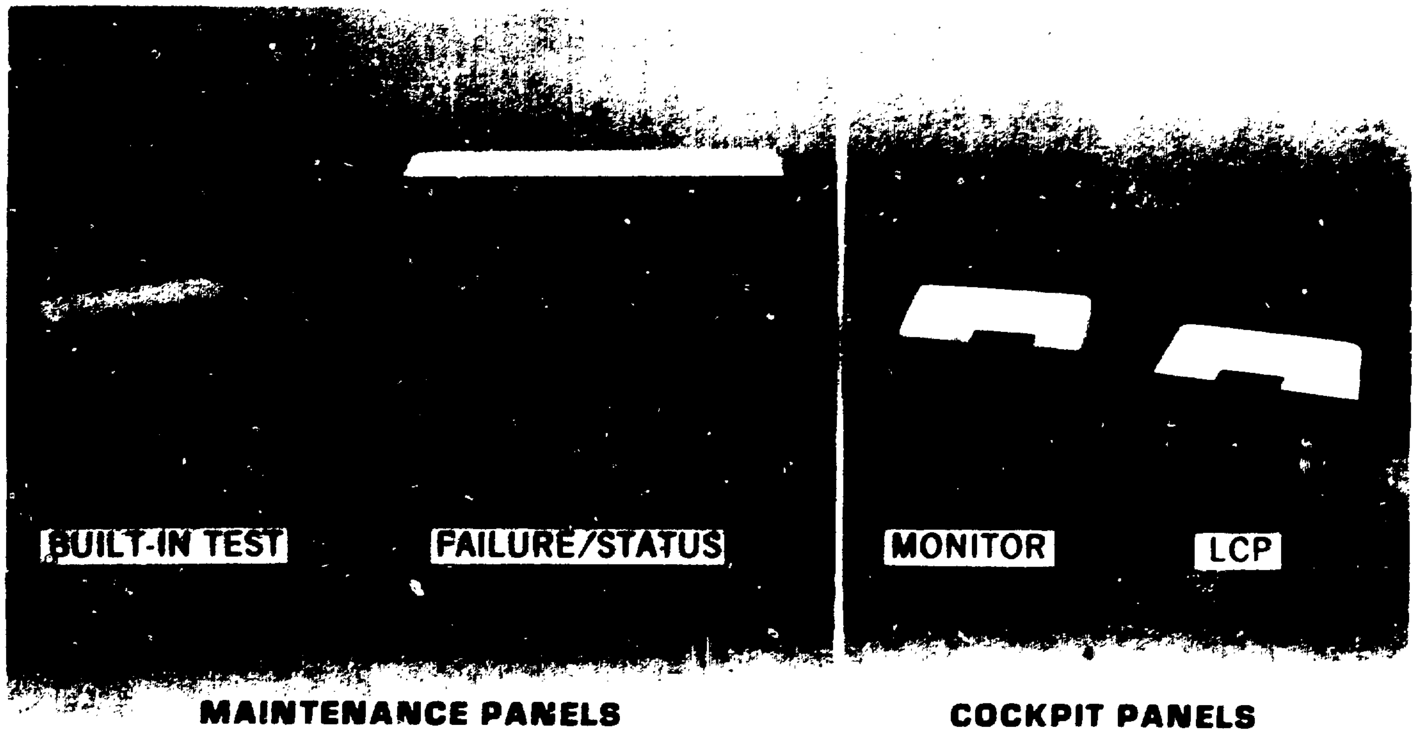

Figure 139. Primary flight control system panels.

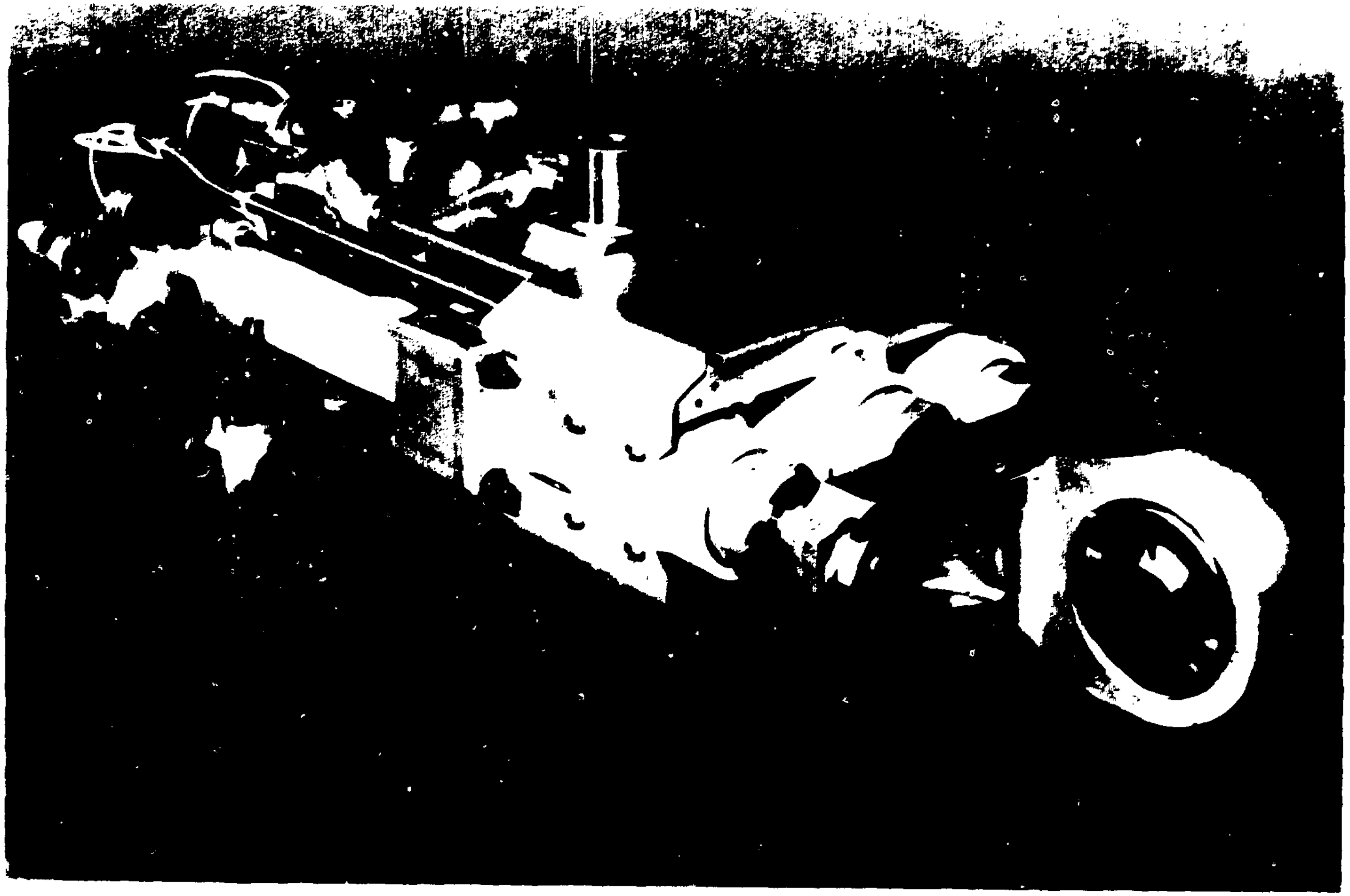

Figure 140. Swashplate servoactuator.

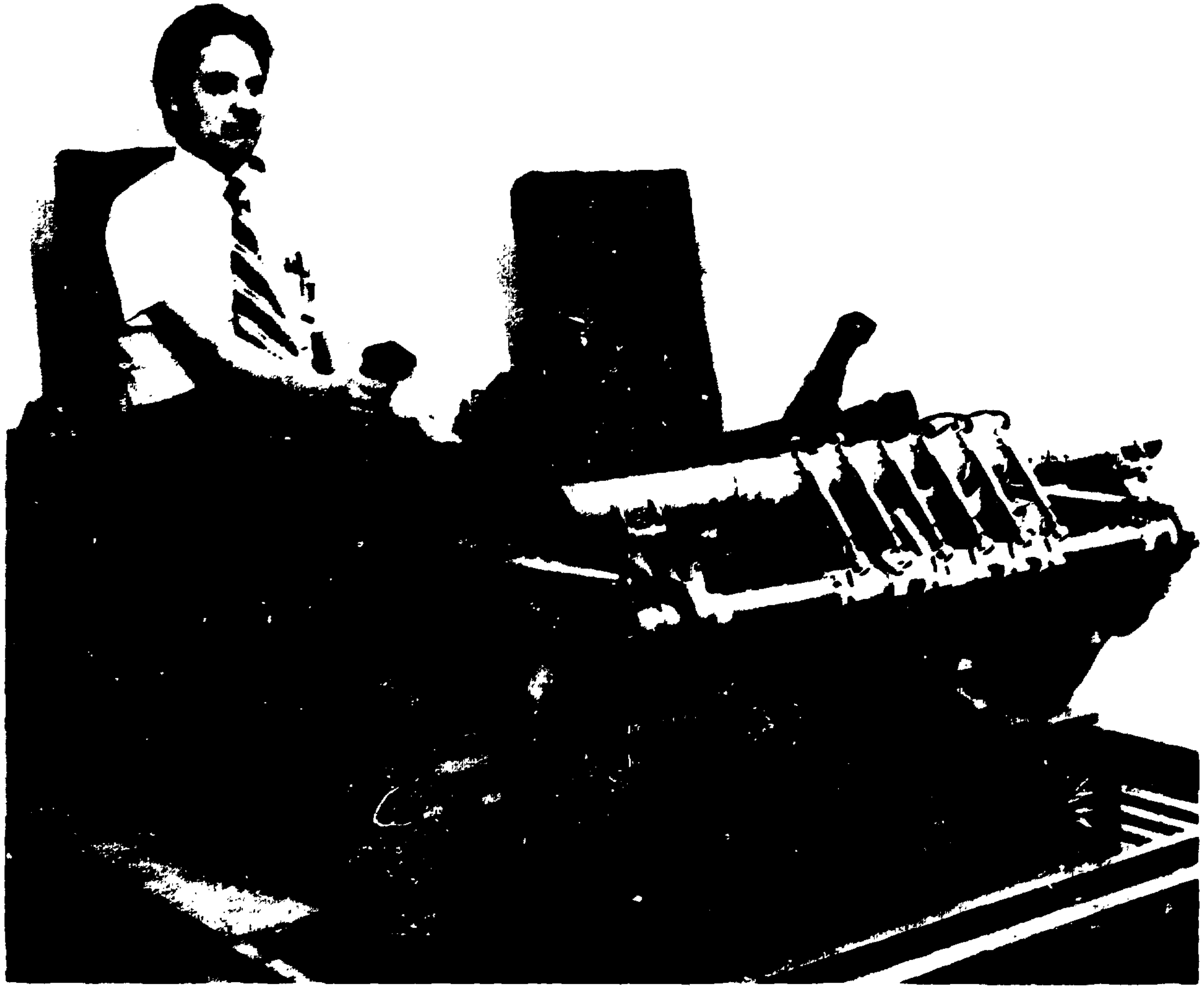

Figure 141. Cockpit control system.

2.18.4 Description of Automatic Flight Control System. The AFCS consists of aircraft motion sensors, a load-controlling crewman (LCC) controller, digital processors, and associated control and display panels to provide stability and control augmentation as well as selectable modes for altitude hold, hover hold, and LCC control. The relationship between the AFCS, the Direct Electrical Linkage System (DELS), cockpit controls, and LCC controls is illustrated in Figure 126.

The AFCS is comprised of the flight control computer subsystem, sensor group, control and display panels, and LCC controller. The computer software conforms to the requirements of the HLH Prototype AFCS functional block diagrams (Drawing No. 301-80060).

2.18.4.1 Functional Description

Flight Control Computer Subsystem (FCCS). The FCCS consists of triple-redundant digital flight control computers (FCC), each with an associated input/output processor (IOP). Each computer is programmed to perform control law, modal logic, and sensor input processing functions. Each IOP provides sensor conditioning, redundancy management, inter-channel communication, modal logic, and Built-In-Test Equipment (BITE) functions.

Sensor Groups. Sensors utilized in the AFCS are:

a. Triple-Redundant Sensors

- Rate Gyros (3-axis)
- Sideslip Measuring System
- Pitot-Static System to sense:
    - Airspeed
    - Barometric Altitude (Total)
- Load-Controlling Crewman Controller LVDT's (4-axis)

b. Dual-Redundant Sensors

- Reference Barometric Altitude
- Inertial Measuring Unit to sense:
    - Velocity (North/South) and Velocity (East/West)
    - Pitch and Roll Attitude
    - Heading
    - Vertical Acceleration

c. Non-Redundant Sensors

- Radar Altimeter
- Radar Rate Adapter
- Attitude/Heading Reference System
- Magnetic Heading Adapter

Control and Display Panels. The AFCS control and display panels include:

- Pilot Station - Mode Select Panel
System Test Function Panel
Caution Indicators
- Flight Engineer Station - Failure Status Panels
BITE Panel
- Flight Test Engineer Station - Parameter Change/ Display Unit
Discrete Signal Status Panel

LCC Controller. The LCC controller is an integrated four-axis finger grip controller to be manipulated by the operator's right hand. This unit is designed in accordance with Boeing Vertol Development Specification S301-10031.

2.18.4.2 External Interfaces. The AFCS is designed to be compatible in interfacing with the following equipment and sub-systems.

a. Cockpit Controls

- Cockpit Control Driver Actuator (CCDA) Engage Discretes (Triplex)
- Parallel Drive into CCDA's - 4-axis (triplex)
- Discrete Signals from Cockpit Controls to AFCS
  - CCDA Shutdown (triplex)
  - Magnetic Brake Control (triplex for each axis)
  - Beep Trim Signals (simplex)
    - Longitudinal - forward and aft
    - Lateral - right and left
    - Directional - right and left

- Control Detent Switches (triplex)

    - Longitudinal Stick Out of Detent
    - Lateral Stick Out of Detent
    - Directional Pedals Out of Detent
    - Vertical Stick Out of Detent

- Selectable Mode Release (For pilot disengagement of Altitude and Hover Hold)

- AFCS Release

b. Direct Electrical Linkage System (DELS)

- Direct Electrical Linkage Control Unit (DELCU) demodulates pilot stick position transducer signals and transmits these signals to the IOP's (triplex).

- AFCS differential commands to DELS Control Units - 6 signals (Triplex): Longitudinal, lateral, directional, vertical, forward rotor LCP, aft rotor LCP.

- Discretes for AFCS 2-fail system level and identification of AFCS second failures by DELCU.

- LCP engage to AFCS.

c. LCC Controller

- Four-axis, linear variable differential transformers (LVDT's) provide signals to the IOP's (triplex).

- Velocity drift clear discrete to IOP's (simplex).

- LCC control enabled discrete from FCCS to LCC station. (triplex).

d. Electrical Power Systems

The AFCS is powered by the aircraft's two-generator, three-bus electrical power supply system.

e. Flight Test Instrumentation

The flight control computers interface with a Digital In-flight Recording System described in Specification S301-10057, through five serial digital data transmission lines.

2.18.4.3 Failure Monitoring and Signal Selection. Failure monitoring and signal selection for the flight control computer subsystem and the triplex sensors associated with the basic AFCS functions utilize majority voting logic and median signal select, respectively, prior to a first failure and automatic shutdown, on an axis basis, upon occurrence of a second like failure. The dual inertial velocity and vertical acceleration signals generated in the IMU's are comparison monitored to provide automatic modal inhibiting of the longitudinal and vertical AFCS, respectively.

The dual-reference baro altitude sensors are comparison monitored to provide automatic disengage of the altitude hold mode upon a sensor failure.

The command outputs for the hover hold mode and LCC control are authority limited to provide flight safety.

Failure status is displayed at the pilot's and flight engineer's stations.

AFCS Performance. AFCS performance is determined by the control laws (defined in Drawing 301-80060) and modal logic (Drawing 301-80061) as implemented in the FCCS, the associated sensors, and command paths to the DELS control units and CCDA's.

The AFCS incorporates single-fail operative digital processing and Stability and Control Augmentation System sensor groups. The interface between the AFCS, Cockpit Control Driver Actuators (CCDA's), and the Direct Electrical Linkage path is shown in Figure 126.

2.18.4.4 Stability and Control Augmentation System (SCAS). Stabilization and control augmentation functions of the AFCS are provided to enhance aircraft handling qualities. The SCAS provides the following functions:

Longitudinal Axis - Longitudinal ground speed control response below and airspeed response above 40 to 45 knots IAS. Automatic longitudinal cyclic pitch (LCP) control for:

- Hover and low-speed command augmentation.
- Air speed plus barometric altitude trim scheduling.

Vertical Axis - Vertical Rate Control Response.

Lateral Axis

- Below 40-45 knots IAS - Lateral ground speed control response.

- Above 40-45 knots IAS - Attitude command for bank angles between ± 10 degrees; for greater bank angles, roll rate command with attitude hold (automatic turn coordination).

Directional Axis - Turn rate response below and sideslip response above 40 to 45 knots IAS. Heading hold capability is provided at all airspeeds.

Longitudinal Cyclic Pitch (LCP). The pilot is provided with manual LCP control which shall individually command forward and aft rotor longitudinal cyclic pitch.

2.18.4.5 Selectable Modes. The AFCS incorporates selectable altitude and hover hold modes and limited-authority LCC control in hover and low-speed flight. The LCC ground taxi mode provides for limited authority control in the longitudinal axis.

Altitude hold capability is provided for operation throughout the flight envelope. Operation in this mode utilizes parallel drive of the pilot's collective stick to maintain the selected altitude.

The hover hold mode provides an inertial-velocity-referenced horizontal, radar-altitude-referenced vertical, and gyro-referenced heading hold capability. Limited-authority LCC control may be enabled with the hover hold mode engaged.

2.18.4.6 Redundancy Management. The computer subsystem provides redundancy management of sensor inputs and computer outputs as follows.

- Triplex Redundant Sensors. The computers each median-vote and select one and the same sensor input channel. Failure in any channel causes a switchover to averaging of the two remaining "good" signals. Failure in any channel is detected, isolated, and reported on the pilot's caution panel and on the Sensor Failure Status Panel.

- Dual Redundant Sensors. Dual sensor inputs are averaged. A failure in either input stores the last valid average output. The failure is reported on the pilot's caution panel and the AFCS Failure Status Panel.

- Single Sensors. Single sensors are interfaced with the triplex system via authority limits. As single sensors are associated with selectable control modes only, the pilot can manually deactivate that mode upon sensor failure.

- Computer Outputs to DELS Control Unit. The redundant computer commands to the DELS Control Unit are majority logic voted in each IOP. Analog outputs from each IOP are input directly to the corresponding DELS Control Unit.

- Computer Output to CCDA. The redundant computer commands to the CCDA's are majority logic voted in each IOP. Analog outputs from each IOP are input directly into the CCDA electronics.

2.18.4.7 Hardware

Hardware for the prototype AFCS was that used during the HLH ATC. In addition, a new air data sensor was procured. Details on changes to the ATC hardware to adapt it to the prototype system configuration are given in the following paragraphs.

Input/Output Processor

- Add CCDA shutdown discrete inputs (one for each axis). Required for synchronization of AFCS parallel drive signals upon CCDA axis failures.

- Add auto/manual LCP select discrete input.

- Replace dual-reference barometric altitude (low gain) sensor inputs with triplex total barometric altitude inputs. Modify failure detect and signal select functions.

- Provide output discretes and system test monitor circuitry for BITE test of dynamic pressure (air speed) and total barometric altitude sensors.

- Add discrete inputs for LCC taxi mode select.

- Modifications for redundancy management loss of AFCS function equipment failures (as defined in S301-10065, Table I).

- Inhibition of modal logic functions associated with those AFCS selectable modes not required in the prototype aircraft, i.e., load stabilization, precision hover trim, and auto approach to hover.

- Added load weight signal.

Flight Control Computer

- Eliminate latch on computer power failure indication LED drive signal.

AFCS Mode Select Panel

- Add LCC taxi select switch in space located on panel face.
- Added CCDA reset capability.

Sensor Failure Status Panel

- Add triplex "total baro" LEDS.

Discrete Signal Status Panel #1

- Add individual landing gear ground contact status LEDS.

Motion Sensors

- Carousel C IV, Inertial Measurement Units - Increased from 1 to 2.
- ASN-76, Attitude/Heading Reference Systems - Decreased from 3 to 1.
- Strapdown Vertical Accelerometers - Decreased from 3 to 0 (replaced by dual outputs available from IMUs).

Air Data Sensor

The units supplied by Rosemount, Inc., provide linear airspeed, total barometric altitude, and reference baro altitude outputs. The single package design, which incorporates the three sensor outputs to AFCS, is a modification of an existing Rosemount, Inc., 542AD-type transducer, which is a proven solid-state design, utilizing a capacitative pressure-sensing capsule designed for precision air data measurements.

The principal features of this unit include:

- Linear dc, single-ended output voltages, proportional to indicated airspeed (IAS) (airspeed shall range from 0 to 200 kts.), geopotential altitude (h), and altitude deviation (Δh) from a commanded reference point within the full range of geopotential altitude.
- Linear dc, single ended ouput voltages, parallel to and buffered from the signal outputs of indicated airspeed (IAS), geopotential altitude (h), and altitude deviation (Δh), for coupling into the flight test instrumentation system.

- Automatic BITE capability to check out the circuitry functions of indicated airspeed (IAS) and geopotential altitude (h). Command signal provisons shall be issued from the AFCS in the form of high-level dc discretes (28 vdc/open) as separate commands for each function. The BITE capability shall check all circuit functions, excluding the capsule, for each of the specified signals.

- Manual BITE capability to check out the circuitry functions of altitude hold. Command signal shall be from a momentary switch located on the unit, initiation of which shall command altitude hold mode followed by a step perturbation in reference altitude, to be held for as long as the switch is depressed.

Radar Altimeter

Analysis indicated that the problems experienced during the ATC flight testing due to radar altitude spiking can be compensated for in computer software processing. The employment of improved complementary filtering on both the radar altitude and altitude rate in conjunction with software rate limiting and increased IOP sensor filtering acting on the altitude input should considerably improve altitude hold over grass and other uneven surfaces in hover flight.

Results of investigations into the feasibility of modifying the APN-194 radar altimeters to compensate for external load interference indicated potential solutions to be beyond the scope of the current prototype program in terms of schedule and cost. Analytical and simulation studies were defined to evaluate complementary filtering and switching techniques to compensate for those dynamic situations where the load intermittently swings into the antenna lobe.

The radar antenna installation on the prototype aircraft was modified to improve altimeter performance while conducting cargo handling operations with long cables. The change included:

a. Replacement of the standard APN-194 circular antennas with the APN-171 rectangular units with more narrow cone angles.

b. Canting the antennas 16.5 degrees, forward edge up, with respect to the reference water line.

AFCS Test Set

Modifications to update the test set to conform to the prototype system requirements include:

- Removal of six switches no longer required and their replacement with four new switch signals on the discrete control panel.
- Revision of the triplex J6 panels to delete the pitch, roll, and yaw rate gyro BITE jacks, to add total baro altitude, and to revise the airspeed jacks (changed from A.C. to D.C. signals).
- Revision of labeling and wiring for 11 jacks on the J9 discrete monitor panel.

2.18.4.8 Software

Flight Control Law Design

The flight control laws for the prototype AFCS are based on the ATC system design as configured at the conclusion of the Task III flight testing. Changes with respect to this base line are dictated on one of two bases:

a. Differences between prototype and ATC system requirements.

   - Deletion of Hover Hold on PHS, Load Stabilization, Auto Hover Trim and Auto Approach to Hover modes.
   - Addition of an LCC Taxi mode and incorporation of LCP speed trim into the digital flight control computers.
   - Added load weight input.

b. A number of problem areas relating to handling qualities were identified during the Task III flight test. Those items which impact on the prototype system are summarized in Table 32 along with the solutions being considered at time of termination.

TABLE 32. AFCS CONTROL LAWS - PROBLEMS/SOLUTIONS CONSIDERED

PROBLEM	SOLUTION
SCAS - Longitudinal	
1. Control margin & outer loop authority limits in steep flares.	Add parallel input thru Cockpit Control Driver Actuator (CCDA) to drive stick forward.
2. Airspeed hold @ 60 kts, level flight & turns.	Adjust velocity feedback gains and airspeed schedule.
	Bank angle cross feed into longitudinal axis scheduled by airspeed and washed out.
3. Trimmability in hover.	Improved CCDA performance.
	Beep trim will be available to pilot thru Hover Hold Mode.
4. Variable beep trim.	Different levels for hover and forward flight switched by airspeed.
SCAS - Vertical	
1. Radar altitude hold inhibit above 45 knots.	Auto switch to baro for A/S >45 kts and modal logic L38BQ true. (Required for hover over a ship where pilot manually selects G/S)
2. Radar altitude and rate spikes.	Signal conditioning filter changed from 4.3 & 21 Hz to 0.5 and 2.1 Hz break points.
	Rate limit on radar altitude (8 fps).
	Improved complementary filter. Change baro sensor filter from 3.12 Hz and 3.21 Hz to 2.2 Hz and 2.1 Hz.

TABLE 32. (Continued)

PROBLEM	SOLUTION
SCAS - Vertical (Cont'd.)	
3. External load interference with radar altimeter operation.	Complementary filter on radar altitude and vertical acceleration.
	Cant antennas further forward.
4. Radar Altimeter failure.	Frequency splitter (software).
	Rate limiter on radar altitude.
	Complementary filter on radar altitude and vertical acceleration.
	Radar and baro altitude comparison & signal selection.
5. Collective pumping in turbulent air.	Rate limiter on altitude error.
	Improved complementary filter.
	Altitude hold thru longitudinal axis.
6. Altitude deviation during low-speed turns.	Increase parallel drive gain, possible with new CCDA hardware.
7. Transmission overtorque.	Dynamic suppression as provided for radar altitude failure.
	Very low frequency suppression in forward flight by altitude hold through longitudinal axis.

TABLE 32. (Continued)

PROBLEM	SOLUTION
SCAS - Lateral	
1. Velocity mode switch during turn maneuver results in lateral differential cmd. loss and control offset.	Inhibit lateral velocity mode transfer when mode transfer threshold exceeded. Limit output from velocity mode transfer switch to provide control margin for damping.
SCAS - General	
1. Control detents - rigging shifts.	Implement detents - 4 axes - in software.
2. Airspeed local flow anomalies.	Signal conditioning filters changed from 13.6/7.9 Hz to 1.3 and 1.2 Hz. Software preprocessing of sensor input.
Hover Hold	
1. Pilot override and beep trim with Hover Hold engaged.	As defined in prototype modal logic, L-11, dated 12/5/74.
2. Drift clear transients and selection.	Latch drift clear operation until G/S errors decay.
3. LCC Lateral Control Response.	Increase controller lateral travel. Modify controller command shaping.
4. LCC control authorities sufficient for shuttle operation.	Longitudinal and lateral - increase to 12 to 15 kn. Vertical - reduce from 320 to 240 ft/min. Directional - remain at 8 deg/sec.

TABLE 32. (Continued)

PROBLEM	SOLUTION
Hover Hold (Cont'd.)	
5. Lateral backdrive hangup during turns.	Improved CCDA performance permits increased parallel drive gains. Feed lateral LCCC as proportional drive into CCDA.
6. Roll oscillations with external load.	Gains as a function of load/gross wt. Manual - set in Δ values prior to flight. Manual input load discrete through PCDU.

Modal Logic Configuration

Ground Contact (L-1). The requirement for the indication of nose gear contact has been deleted, as any operation of the aircraft with the nose gear only in contact requires the AFCS to be in the flight mode. Also, the requirement for all three gear to indicate ground contact in order to enable LCC taxi has been changed to require a single (main) gear only. This simplification is permissible as pilot procedures will preclude selection of this mode until the aircraft is at rest with all gear on the ground.

Hover Hold (L-11). A problem with L-11 has been that the pilot cannot retrim the aircraft without disengaging the hover hold mode. Thus, if he does attempt to retrim in one axis, a transient response or drift may occur in all three axes by the time hover hold is manually re-engaged. The proposed change is to provide individual axis interrupt of the mode when the pilot force-trims or moves his control out of detent. During the interrupt, basic SCAS response is provided and the hover hold is re-synchronized. Also, actuation of the beep trim will provide a series retrim through the hover hold loops. The extent of this change is such that its implementation will require the fabrication of new Mode Logic #3 boards. The impact of this change is presently being evaluated by General Electric.

Longitudinal Cyclic Pitch Engage (L-37E). An output has been added to the Automatic Longitudinal Cyclic Pitch (LCP) engage modal logic function (L-37E) to turn on the LCP OFF light on the pilot's annunciator panel if auto LCP is selected, and either a dynamic pressure or a barometric altitude second failure condition exists.

Redundancy Management Action for Sensor Failures

Automatic shutdown actions to be taken following loss of function sensor failures have been re-evaluated. The following changes have been defined relative to Table I of S301-10065, Rev. A.

REDUNDANCY MANAGEMENT ACTION FOLLOWING FAILURE

COMPONENT	OLD ACTION	NEW ACTION
Airspeed	Ramp to zero last valid longitudinal differential command to DELS.	Store last valid airspeed input to DCP control path.
	Ramp to zero last valid LCP command to DELS.	Store last valid airspeed input to LCP speed trim schedule generation.
Total Barometric Altitude	Ramp to zero last valid LCP command to DELS.	Store last valid altitude input to LCP speed trim schedule generation.

These changes, which tend to minimize the aircraft transients subsequent to the defined failures, can be implemented in the flight control computers with essentially no increase in the software required.

2.18.5 Development Status

This section describes the status of flight control system development when the stop-work order was received.

The system hardware was undergoing preliminary airworthiness substantiation (PASS) testing. The cockpit control system had been installed in the prototype aircraft.

Testing underway included system integration in the integration test facility and environmental testing at vendor facilities. The integration facility is described along with status of each subsystem.

2.18.5.1 System Integration Test Facility

The system integration facility provided for room temperature integration of all system hardware.

Overall Plan

Figure 142 shows a plan of the facility. System electronic control units and panels were arranged into the U-shaped test area shown at the top of the figure. Cockpit controls and the swashplate servoactuator loading fixture were located to provide visual contact between system input and output.

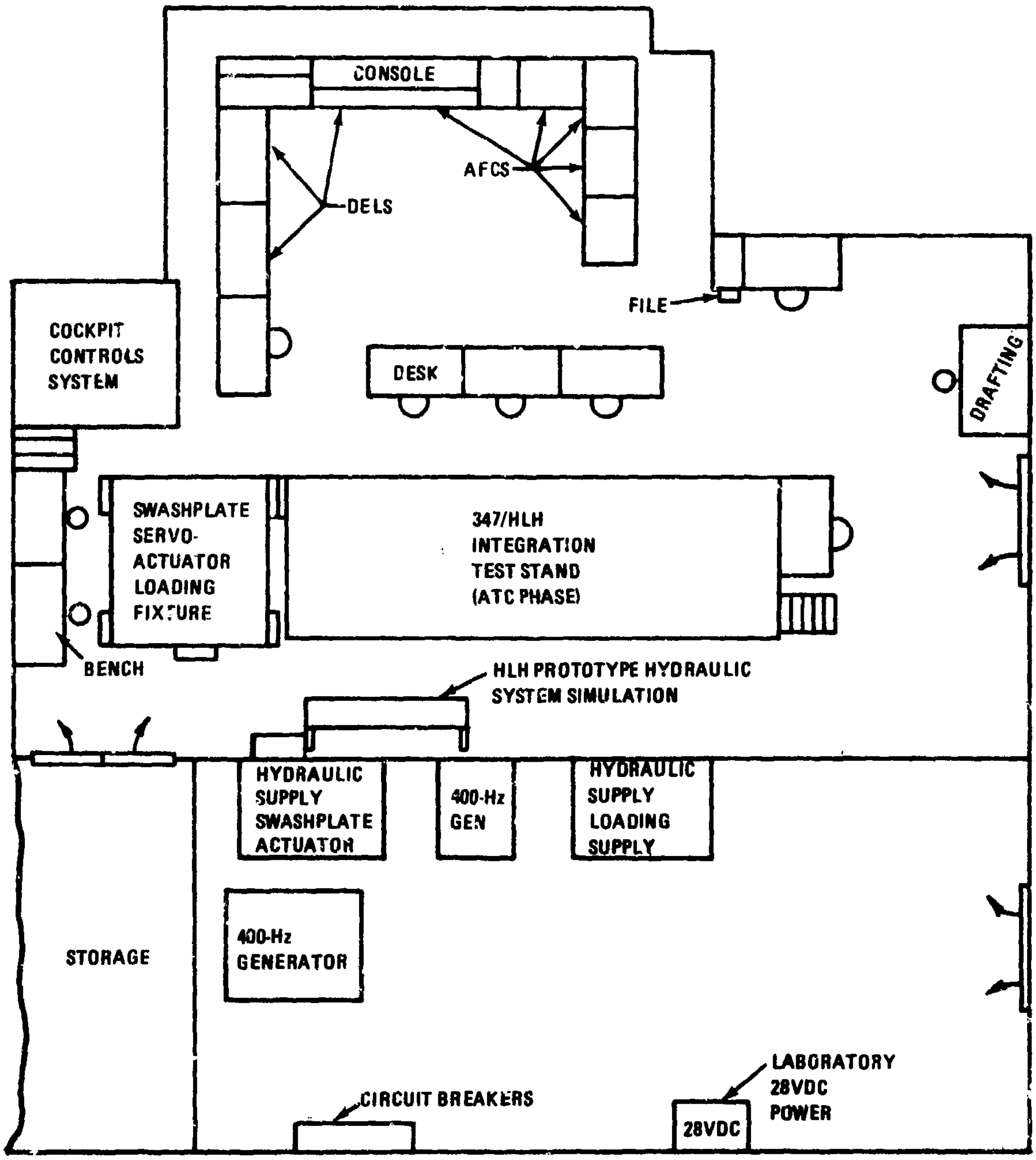

Figure 142. Flight control system integration test facility floor plan.

In addition, the loading fixture was mounted on a dynamic isolator centered over a main structural I-beam to preclude coupling alternating loads into other parts of the building. This location allowed retention of the 347/HLH integration stand in the room.

The flight control hydraulic systems were simulated by a circuit made up of aircraft switching valves and pressure switches and other components necessary to simulate the functions of the real system. Power was supplied from a laboratory source. The system was used to power the single swashplate actuator which was connected hydraulically as an aft actuator. The remaining actuators were simulated electronically.

Verification of the real hydraulic power supply performance was accomplished in a separate integration test conducted by the hardware supplier. In this case the supply powered a dummy load representing three swashplate actuators. Noisy power generating equipment was located in an adjacent room.

Detail Equipment Relationships

Figure 143 shows the relationships of equipment within the test facility. The primary flight control path is shown in the lower portion of the figure.

The cockpit control system is that developed during Phase IV of the HLH ATC program. For the prototype configuration, force-feel/control driver actuators were updated to correct problems found in the ATC program and to make the actuators flightworthy. They had been originally designed for laboratory use only. Also the wiring of components (not shown) on the control test stand was revised to reflect the aircraft configuration. The development of the cockpit controls is described in Volume II of the ATC report (Reference 8). The PRCS electronics includes:

- DELS Control Unit - processes inputs to drive the swashplate actuators

- Stall Damper Unit - processes load feedback from the swashplate actuators to damp 4/rev loads

- Force-Feel/Control Driver Electronics - processes commands to drive the cockpit controls in response to commands from the AFCS

- Hydraulic System Control Unit - controls operation of the hydraulic system interconnect and ground power input valves in response to logic devices within the hydraulic system (including pressure

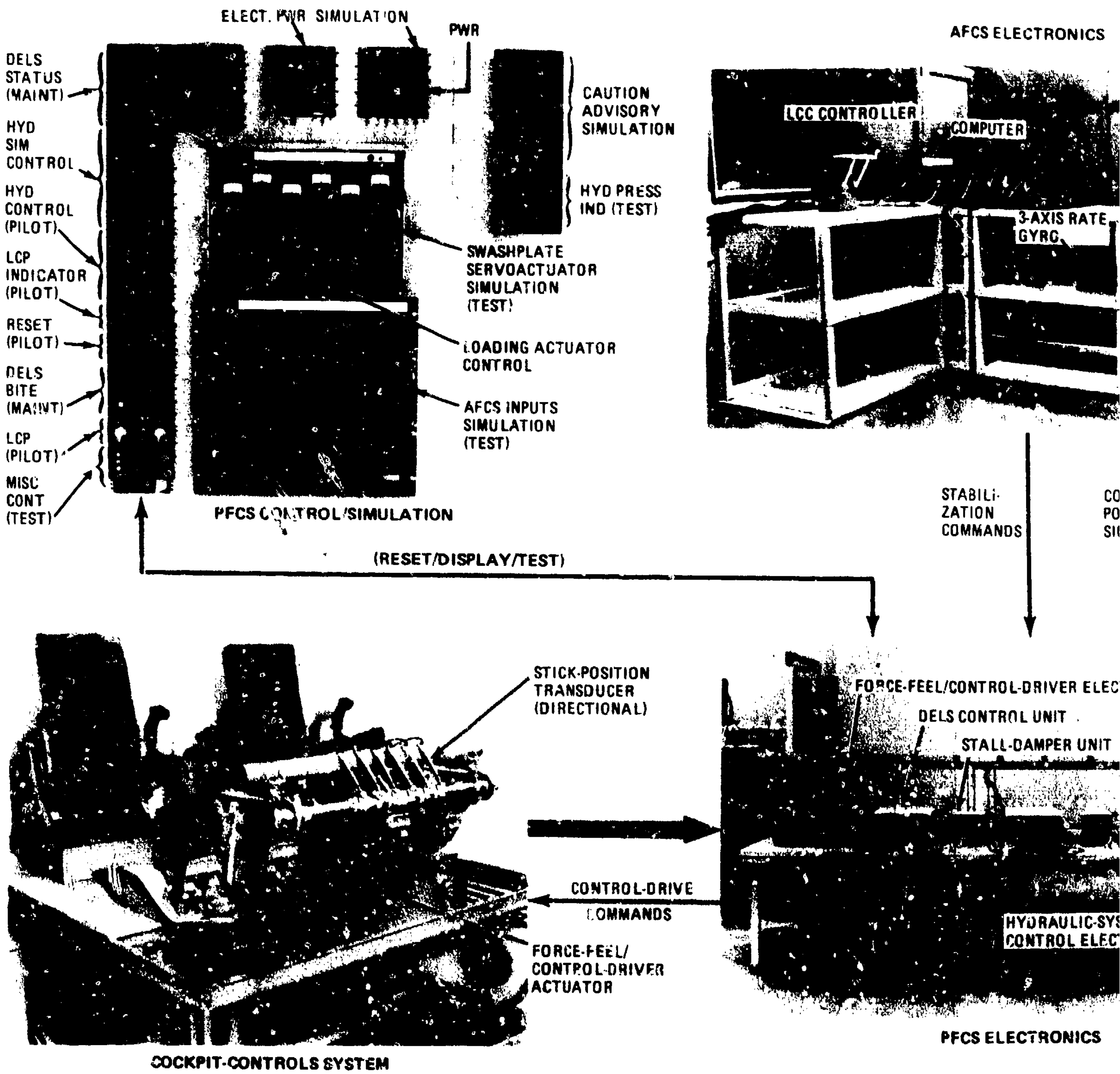

Figure 143. Flight control system integration test facility.

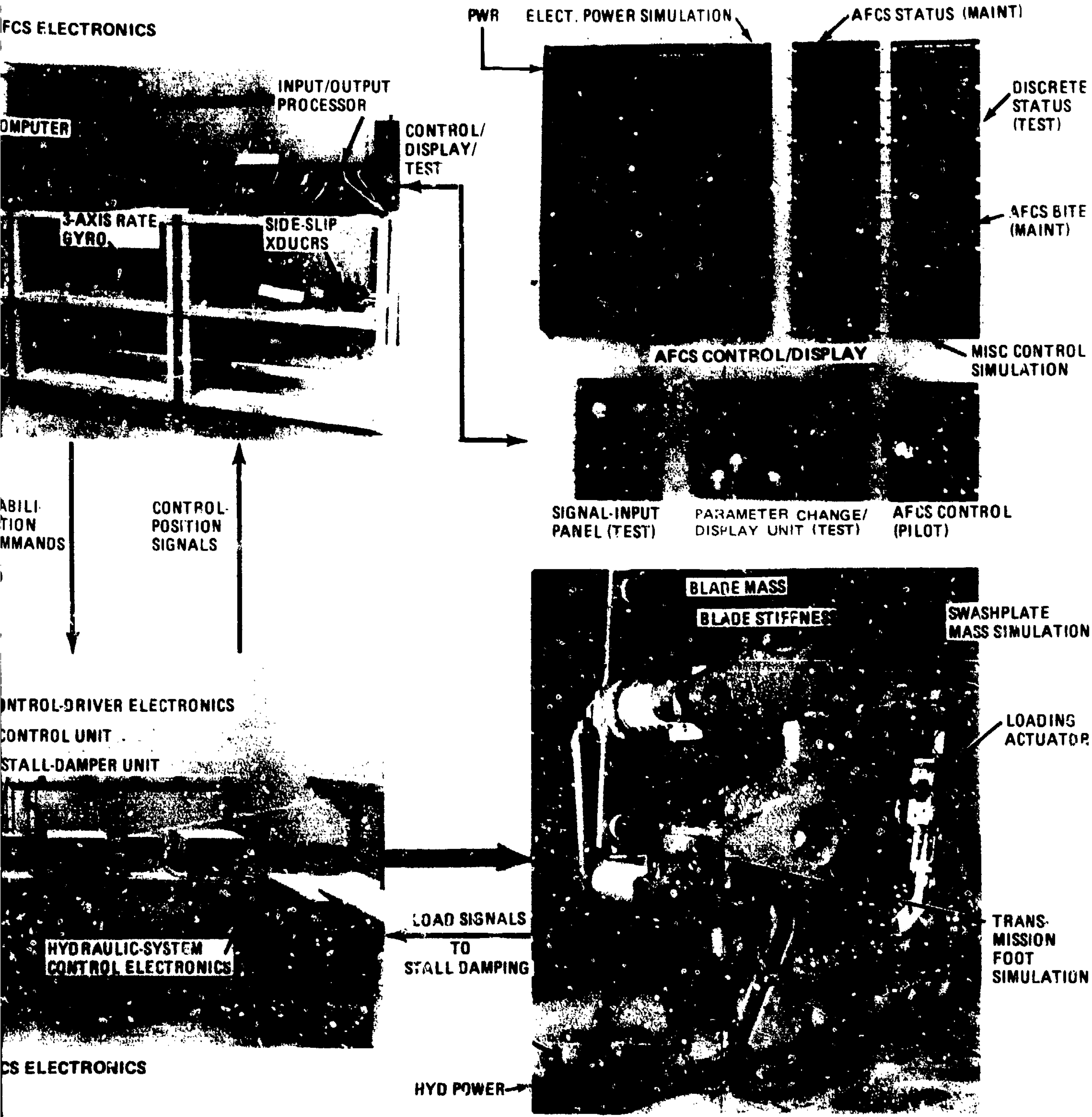

SWASHPLATE SERVOACTUATOR IN LOADING FIXTURE

switching, ground power interlocks).

The swashplate servoactuator loading fixture provides for:

- Simulation of the transmission mounting foot and swashplate interface to allow installation of the swashplate actuator with its gimbol

- Simulation of the actuator dynamic load including:

  a. Swashplate mass

  b. Blade torsional stiffness

  c. Blade mass

  d. Blade damping

  The blade stiffness term is provided by a torque tube which interconnects the swashplate and blade masses. Windup in the torque tube is limited by a mechanical stop which also includes a friction device to vary damping (structural dampening is assumed to exist in the specified actuator model). The friction device assures this level will be available if not provided by lower inherent values in the mechanism.

- Input of dynamic loads via a loading actuator attached to the swashplate mass. This feature was used for evaluation of stall damping function and variation of actuator stiffness as a function of frequency.

The Automatic Flight Control System (AFCS) has access to the PFCS via a rate- and authority-limited interface (reference Section 2.18.3). Stabilization signals are transmitted from the AFCS input/output processors (IOP) to the DELS control unit and force-feel/control driver electronics. The IOP also accepts control position signals from DELS. Other inputs handled by the IOP are as listed in paragraph 2.18.4.1. AFCS control laws are processed in the Flight Control digital computers. The integration test stand has provisions for evaluation of all sensor and discrete inputs. The 3-axis rate gyro packages and sideslip stabilization transducers can be seen in Figure 143.

Controls, display, and test equipment for the systems were located on panels located in the consoles. Equipment used for DELS and AFCS pilot interface and maintenance has been described previously. In addition the test stand included the following facilities:

PFCS Test Provisions

- AFCS Inputs Simulator - allows for control of AFCS inputs to DELS, provides for sinusoidal and bias inputs. It is used to check operation of the interface before integration of DELS and AFCS.

- Swashplate Actuator Simulator - provides for electronic simulation of six swashplate actuators. When the real actuator is operating, the simulator represents the five remaining actuators. The unit also contains electronics to drive the swashplate loading actuator.

- Hydraulic Control Panel - this is the pilot's interface panel found in the cockpit

- Hydraulic Simulation Control - interfaces with hydraulic circuit and allows operation of system discrete inputs such as landing gear switch. Allows simulation of ground power on vs. in-flight power, etc.

- Electrical Power Simulation - allows simulation of various operating modes of the electrical power supplies.

AFCS Test Provisions

- System Test Function Panel - used for in-flight input of step, ramp, and pulse inputs to the AFCS

- Parameter Change/Display Unit

- Discrete Signal Status Panel

- Electrical Power Simulation - contains circuit breakers as provided in the aircraft installation. Allows shutdown of selected portions of the system.

Hardware Status at Stoppage

- Primary Flight Control System

    - DELS Electronics

      Electronics and control panels had completed environmental testing except for salt fog test.

Failures during testing were:

- Light - emitting diodes used for display failed temperature and humidity tests.

- Random failure of an operational amplifier during vibration.

- Component failures on circuit boards of stall damper. Board modified to stiffen, then passed test.

- Wire failures in stall damper during vibration. Added clamp to restrain bundle and passed test.

None of these failures were considered critical to system function. Light-emitting diodes are used for indication only. Must be improved for production.

All hardware had been delivered.

- Force Feel/Cockpit Control Driver System

  - Completed temperature attitude and vibration satisfactorily.

  - ATC actuators had been returned to Honeywell for update to prototype configuration. A program was also established to modify all actuators to mechanically set the force gradient and deactivate the force-feel motors.

- Swashplate Actuator

  - Completed the first phase of fatigue testing. Other tests not started at termination.

  - Low amplitude 13 H_z limit cycle was present in closed loop performance.

Program for actuator modification was underway. Modification included modification of control stage pistons and linkage to reduce friction and backlash.

  - One actuator had been returned for a leak in the control stage piston. An additional test was to be added to check for leakage by measuring control stage force output in response to input

- One actuator had a sheared main ram feedback probe during acceptance test at Bertea. The LVDT body collapsed on the probe. Resolution was not made before stoppage.

- There was a potential difficulty in removal of the actuator. Trial installations were planned to develop a method.

• Integration Testing

  Integration had been completed through evaluation of the actuator with full dynamic model. There were no major problems other than the 13 H_Z limit cycle.

  Selection of stall damper gains was in process.

- Automatic Flight Control System (AFCS)

  • One system of computer IOP and panels had been received and was being checked on the test stand. The second system was at GE ready to ship.

  • The first air data modules were in acceptance test at Rosemont.

3.0 INTEGRATED LOGISTIC SUPPORT SYSTEM DISCIPLINES

3.1 Maintainability

Maintenance Engineering Analyses (MEA's) were prepared throughout the prototype program. A total of 278 MEA's were prepared out of an initial estimate of 293. The MEA's were added to T301-10202-1 "HLH Prototype - Maintenance Engineering Analysis Data Summary Report" which was revised on a quarterly basis.

3.2 Safety

System safety activities were conducted on a continuing basis throughout the duration of the prototype program. Subsystem hazard analyses were conducted and Safety Problem Action Reports (SPAR) prepared. Forty-one SPAR's were issued for identified problems and each was closed out following correction of the problems. Safety statements were issued quarterly, which reported on all system safety activities.

3.3 Reliability

Quantitative reliability objectives established for the ATC components applied to the prototype aircraft. No reliability objectives were established for non-ATC components which were not representative of a production configuration.

3.4 Logistics

The Contractor Recommended Support Plan, S301-10025, described the supply, facilities, test facilities, personnel, and training activities associated with the prototype program.

REFERENCES

1. Boeing Vertol Document S301-10020, Revision B, HLH PROTOTYPE PRIME ITEM DEVELOPMENT SPECIFICATION (PIDS).

2. Boeing Vertol Documents D301-10210 through -6, HLH PROTOTYPE PROGRAM QUARTERLY SUMMARY REPORT.

3. Boeing Vertol Documents D301-10100-13 through -16, HLH ATC/PROTOTYPE PROGRAM QUARTERLY SUMMARY REPORT.

4. Boeing Vertol Document D301-10320-1, HEAVY LIFT HELICOPTER - ADVANCED TECHNOLOGY COMPONENT PROGRAM - ROTOR BLADE FINAL REPORT.

5. Boeing Vertol Document D301-10321-1, HEAVY LIFT HELICOPTER - ADVANCED TECHNOLOGY COMPONENT PROGRAM - HUB AND UPPER CONTROLS.

6. Boeing Vertol Document D301-10319-1, HEAVY LIFT HELICOPTER - ADVANCED TECHNOLOGY COMPONENT PROGRAM - DRIVE SYSTEM FINAL REPORT.

7. Boeing Vertol Document D301-10316-1, FINAL REPORT, DSTR 25-, 50-, AND 30-HOUR TESTS AND 501-M62B ENGINE SUPPLEMENTAL REPORT.

8. Boeing Vertol Document D301-10322, HEAVY LIFT HELICOPTER - ADVANCED TECHNOLOGY COMPONENT PROGRAM - FLIGHT CONTROLS SYSTEM FINAL REPORT, VOLUMES I-III.

9. Campbell, R., et al., HEAVY LIFT HELICOPTER - CARGO HANDLING, ATC PROGRAM, VOLUMES I-III, Boeing Vertol Company; USAAMRDL Technical Reports 74-97A, 74-97B, and 74-97C, Eustis Directorate, U. S. Army Air Mobility Research and Development Laboratory, Fort Eustis, Virginia, January 1976, December 1974, and October 1976, AD A030072, AD A007244, and AD A032129.

10. HLH Advanced Technology Component Phase, DAAJ01-71-Q-0274, Request for Quotation.

11. Aircraft Systems Requirements Document (ASRD), Revision 2, HEAVY LIFT HELICOPTER, 2 June 1972.

12. Boeing Vertol Document S301-10000, Revision F, Prime Item Description Document, VOLUME I - HEAVY LIFT HELICOPTER, 15 November 1974.

13. Detroit Diesel Allison Document 844A, Prime Item Development Specification, MILITARY TURBOSHAFT ENGINE, MODELS T701-AD-700, YT701-AD-700, XT701-AD-700, 27 April 1973.

14. Detroit Diesel Allison Document 845A, Critical Item Development Specification, POWER MANAGEMENT CONTROL, HLH HELICOPTER, 27 April 1973.

15. Boeing Vertol Document T301-10176-1, MODEL 301 HLH/ATC - EVALUATION OF TRANSMISSION NOISE ATTENUATION MATERIALS.

16. Boeing Vertol Document S301-10026, ENGINE-AIR VEHICLE INTERFACE AGREEMENT.

17. Detroit Diesel Allison Document 830D, MODEL SPECIFICATION, 501-M62 ENGINE, 6 July 1973.

18. Boeing Vertol Document T301-10202-1, MAINTENANCE ENGINEERING ANALYSIS DATA SUMMARY REPORT.

19. Boeing Vertol Document S301-10025, CONTRACTOR RECOMMENDED SUPPORT PLAN.

20. Boeing Vertol Document T301-10190-1, MODEL 301 HLH/ATC TRANSMISSION NOISE REDUCTION PROGRAM - TEST RESULTS REPORT.

21. Boeing Vertol Document S301-10064, Critical Item Development Specification, DIRECT ELECTRICAL LINKAGE SUBSYSTEM (DELS) FOR HLH PROTOTYPE.

22. Boeing Vertol Document S301-10063, Critical Item Development Specification, SERVOACTUATOR ASSEMBLY FOR HLH PROTOTYPE.

23. Boeing Vertol Document S301010057, Development Specification, DIGITAL INFLIGHT RECORDING SYSTEM - HLH/ATC FLIGHT CONTROL SYSTEM.

BIBLIOGRAPHY

1. Lenski, J. W., Jr., TEST RESULTS REPORT AND TECHNOLOGY DEVELOPMENT REPORT, HLH/ATC COMPLIANT ROLLER BEARING DEVELOPMENT PROGRAM, The Boeing Company; USAAMRDL Technical Report 72-62, U. S. Army Aviation Systems Command, St. Louis, Missouri, November 1974, AD 755535.

2. Corso, J. M., et al., HLH GROUND SUPPORT EQUIPMENT (GSE) PRELIMINARY INVESTIGATION, Boeing Vertol Company; USAAMRDL Technical Report 73-52, Eustis Directorate, U. S. Army Air Mobility Research and Development Laboratory, Fort Eustis, Virginia, June 1973, AD 768842.

3. Nutley, W., TECHNOLOGY DEVELOPMENT REPORT - MODEL 301 HLH/ATC CARGO HANDLING SYSTEM COUPLING, Boeing Vertol Company; USAAMRDL Technical Report 73-88, U. S. Army Aviation Systems Command, St. Louis, Missouri, January 1974, AD 778770.

4. Lenski, J. W., Jr., TEST RESULTS REPORT AND TECHNOLOGY DEVELOPMENT REPORT, HLH/ATC DRIVE SYSTEM, AFT ROTOR SHAFT BEARING TEST, Boeing Vertol Company; USAAMRDL Technical Report 73-92, U. S. Army Aviation Systems Command, St. Louis, Missouri, January 1974, AD 775897.

5. Lenski, J. W., Jr., HLH/ATC ENGINE SHAFT SUPPORT BEARING DEVELOPMENT PROGRAM, Boeing Vertol Company; USAAMRDL Technical Report 74-16, Eustis Directorate, U. S. Army Air Mobility Research and Development Laboratory, Fort Eustis, Virginia, May 1974, AD 784593.

6. Ayoub, N. J., and Perin, W. G., TEST RESULTS AND TECHNOLOGY DEVELOPMENT REPORT - HLH/ATC TRANSMISSION OVERRUNNING CLUTCH, Boeing Vertol Company; USAAMRDL Technical Report 74-17, Eustis Directorate, U. S. Army Air Mobility Research and Development Laboratory, Fort Eustis, Virginia, April 1974, AD 782814.

7. Solak, J. B., and Wilson, G. J., TECHNOLOGY DEVELOPMENT REPORT - RESULTS OF STATIC ELECTRICITY DISCHARGE SYSTEM TESTS (ACTIVE AND PASSIVE) - HEAVY LIFT HELICOPTER, Boeing Vertol Company; USAAMRDL Technical Report 74-22, Eustis Directorate, U. S. Army Air Mobility Research and Development Laboratory, Fort Eustis, Virginia, May 1974, AD 784130.

8. Hartman, R., and Badgley, R., MODEL 301 HLH/ATC TRANSMISSION NOISE REDUCTION PROGRAM, Boeing Vertol Company; USAARMDL Technical Report 74-58, Eustis Directorate, U. S. Army Air Mobility Research and Development Laboratory, Fort Eustis, Virginia, May 1974, AD 784132.

9. HEAVY LIFT HELICOPTER - ADVANCED TECHNOLOGY COMPONENT PROGRAM - HUB AND UPPER CONTROLS, Boeing Vertol Company; USAAMRDL Technical Report 77-37, Applied Technology Laboratory, U. S. Army Research and Technology Laboratories (AVRADCOM), Fort Eustis, Virginia, September 1977, AD A051348.

10. Mack, J. C., HLH DRIVE SYSTEM, Boeing Vertol Company; USAAMRDL Technical Report 77-38, Applied Technology Laboratory, U. S. Army Research and Technology Laboratories (AVRADCOM), Fort Eustis, Virginia, September 1977, AD A054024.

11. HLH ROTOR BLADE MANUFACTURING TECHNOLOGY DEVELOPMENT REPORT, Boeing Vertol Company; USAAMRDL Technical Report 77-39, Applied Technology Laboratory, U. S. Army Research and Technology Laboratories (AVRADCOM), Fort Eustis, Virginia, September 1977, AD A050592.

12. Niven, A. J., HEAVY LIFT HELICOPTER FLIGHT CONTROL SYSTEM, VOLUME I - PRODUCTION RECOMMENDATIONS, Boeing Vertol Company; USAAMRDL Technical Report 77-40A, Applied Technology Laboratory, U. S. Army Research and Technology Laboratories (AVRADCOM), Fort Eustis, Virginia, September 1977, AD A050618.

13. Saunders, T. H., and McManus, B. L., HEAVY LIFT HELICOPTER FLIGHT CONTROL SYSTEM, VOLUME II - PRIMARY FLIGHT CONTROL SYSTEM DEVELOPMENT AND FEASIBILITY DEMONSTRATION, Boeing Vertol Company; USAAMRDL Technical Report 77-40B, Applied Technology Laboratory, U. S. Army Research and Technology Laboratories (AVRADCOM), Fort Eustis, Virginia, September 1977, AD A049580.

14. Davis, J., et al., HEAVY LIFT HELICOPTER FLIGHT CONTROL SYSTEM, VOLUME III - AUTOMATIC FLIGHT CONTROL SYSTEM DEVELOPMENT AND FEASIBILITY DEMONSTRATION, Boeing Vertol Company; USAAMRDL Technical Report 77-40C, Applied Technology Laboratory, U. S. Army Research and Technology Laboratories (AVRADCOM), Fort Eustis, Virginia, September 1977, AD A050059.

15. HEAVY LIFT HELICOPTER - ADVANCED TECHNOLOGY COMPONENT PROGRAM - ROTOR BLADE, Boeing Vertol Company; USAAMRDL Technical Report 77-41, Applied Technology Laboratory, U. S. Army Research and Technology Laboratories (AVRADCOM), Fort Eustis, Virginia, September 1977, AD A053423.

16. Richardson, D. A., and Alwang, J. R., ENGINE/AIRFRAME/DRIVE TRAIN DYNAMIC INTERFACE DOCUMENTATION, Boeing Vertol Company; USARTL Technical Report 78-11, Applied Technology Laboratory, U. S. Army Research and Technology Laboratories (AVRADCOM), Fort Eustis, Virginia, April 1978, AD A055766.